



Australian Earth Sciences Convention 2021
9–12 February 2021
Core to Cosmos

Geological Society of Australia
Abstract Volume Number #133

www.aesconvention.com.au



Welcome to the AESC 2021

On behalf of the AESC 2021, Hobart Organising Committee, we welcome and thank you for attending the inaugural fully-online **Australian Earth Sciences Convention – ‘Core to Cosmos’** – in **February 2021**.

The online format of the convention allowed us to provide you with **EARLY ACCESS** to the portal so you could explore the online layout and watch the vast array of pre-recorded presentations at your leisure and in the comfort of your own home or office.

The organising committee worked tirelessly to produce an engaging and memorable program which showcased current trends and advances in earth science, including the latest findings on the deep structure and composition of our planet, our diverse crust and surface environments, developments in the energy and resources sectors and critically, the essential role that geoscience plays in our sustainable future. We were amidst challenging yet exciting times and the move to an online format presented us with the opportunity to engage with a new global audience and expand the overall reach of the convention.

The AESC 2021 is eligible for CPD

Attendance at technical geoscientific conferences and learned and professional society technical meetings accrues CPD points.

Members maintain their expertise through ‘Continuing Professional Development (CPD)’, by attending workshops and symposia, participating in courses in developing expertise to keep up with contemporary developments, reading scientific journals, or in organising and contributing to these events.

Do you want recognition and accreditation for your area of expertise?

Visit: [GSA Accredited Geoscientist](#)

The convention included:

- **LIVE-STREAMED** plenary session speakers
- Pre-recorded Presentations – exclusive to you as a delegate, to **watch at your leisure prior to the convention** official start date (9 February 2021) and available after the conference
- **LIVE Q&A** sessions with speakers
- Posters Presentations
- Virtual field trips
- Networking with fellow delegates and direct engagement with industry partners in the online environment

Pre-recorded presentations were available to watch in advance and were also available during the convention (9–12 February), to maximise your experience we suggested watching the presentations during the early access period, which was one week prior to the convention. This allowed delegates to engage with and ask questions during the LIVE Q&A forums that were held during the convention, when presenters were LIVE on screen to answer questions during scheduled times in the program.

Delegates could also connect with presenters, sponsors and exhibitors in the Meeting Hub which is an area of the convention online screen where you can create one-on-one meetings, outside of programmed session and exhibition times.

Convention Organising Committee

CHAIRS	Sebastien Meffre & Andrew McNeill
TECHNICAL PROGRAM DIRECTORS	Karin Orth & Julie Hunt
POSTER DIRECTORS	Claire Kain & Jacqui Halpin
DIVERSITY	Indrani Mukherjee
STUDENT DIRECTOR	Hannah Moore
FIELD TRIPS	Mike Vicary & Grace Cumming
SPONSORSHIP DIRECTORS	Matt Ferguson & Andrew McNeill
SOCIAL MEDIA/OUTREACH/PROMOTION	Indrani Mukherjee, Matt Ferguson & Sue Fletcher
TREASURER	Peter McGoldrick & Sue Fletcher
MEETING SECRETARY	Sue Fletcher

Convention Secretariat

Conference Design www.conferencedesign.com.au

Sponsors and Supporters

Sponsors and Supporters are vital to the success of the AESC. We sincerely thank the following sponsors and supporters for their participation.

Geoscience Australia (Platinum Partner)

Geoscience Australia is Australia's pre-eminent public sector geoscience organisation. We are the nation's trusted advisor on the geology and geography of Australia. We apply science and technology to describe and understand the Earth for the benefit of Australia. <https://www.ga.gov.au/>

Tasmanian Government/Mineral Resources Tasmania (Gold Partner)

Mineral Resources Tasmania (MRT) is a Division of the Department of State Growth. The purpose of MRT is to give effect to government policy in relation to minerals and petroleum resources, and the Division provides essential information for land management in Tasmania. <https://www.mrt.tas.gov.au/home>

MineEx CRC (Silver Partner)

MinEx CRC is the world's largest mineral exploration collaboration bringing together Industry, Government and Research Organisations. <https://minexcrc.com.au/>

CSIRO (Rapid Fire Sponsor)

At CSIRO, we solve the greatest challenges through innovative science and technology. We're Australia's national science agency and innovation catalyst, collaborating to boost Australia's innovation performance. <https://www.csiro.au/>

CODES & TMVC (Poster & Field Trip Gallery Sponsor)

CODES is the Centre for Ore Deposit and Earth Sciences. Formed in 1989 at the University of Tasmania, the Centre has grown substantially over the years and is now widely regarded as a global leader in ore deposit research. <https://www.utas.edu.au/codes/home>

PLENARY SPEAKERS	1
Planetary Geology, Australian's involvement in Moon to Mars <i>Megan Clark</i>	1
Searching for life on Mars in our own backyard, the quest for a second genesis <i>Martin J. Van Kranendonk</i>	1
The Energy Transition: Implications for Geoscience – a View from the North <i>Murray Hitzman</i>	1
Engagement, diversity and interdisciplinarity to tackle future challenges <i>Jessica Melbourne-Thomas</i>	2
From Core to Cosmos in a Post-COVID Earth: our opportunities and roles as geoscientists <i>Hill, Steve</i>	2
ENERGY & RESOURCES	4
Geophysics informing regional tectonic studies and mineral systems analysis	4
The tectonostratigraphic evolution of the South Nicholson region, Northern Territory and Queensland: key discoveries from the Exploring for the Future and implications for resource exploration <i>Carson, Chris, Henson, Paul, Lidena, Carr, Southby, Chris & Anderson, Jade</i>	4
Review of Australian Mesoproterozoic basins: geology and resource potential <i>Anderson, Jade, Carr, Lidena, Henson, Paul, & Carson, Chris</i>	4
Reconstructing the Soldiers Cap Group–Kuridala Group basin: implications for BHT and IOCG mineralisation <i>Connors, Karen</i>	5
Mapping the near surface architecture of the Amadeus Basin using magnetic data: Petrophysical properties and geophysical pitfalls <i>Austin, James, Schmid, Susanne & Foss, Clive</i>	5
Lithospheric-scale magnetotellurics over the Eastern Goldfields Superterrane, Yilgarn Craton <i>Selway, Kate, Dentith, Michael, & Gessner, Klaus</i>	6
Interpreting and validating trans-lithospheric faults in the Central Andes to investigate their control on the localisation of giant porphyry copper deposits <i>Farrar, Alexander, Cracknell, Matthew, Cooke, David, Hronsky, Jon, & Piquer, Jose</i>	6
Mineral systems of the Capricorn Orogen through time <i>Occhipinti, Sandra, Metelka, Vaclav, Lindsay, Mark, & Aitken, Alan</i>	7
Unravelling the “late” evolution of the Gawler Craton: high T/P metamorphism, tectonism and magmatism of the Yorke Peninsula, South Australia <i>Bockmann, Mitchell, Hand, Martin, Morrissey, Laura, Payne, Justin, Teale, Graham, Conor, Colin, & Dutch, Rian</i>	7
How to computationally include regional interpretations into the seismic imaging process <i>Rashidifard, Mahtab, Giraud, Jérémie, Ogarko, Vitaliy, Lindsay, Mark, & Jessell, Mark</i>	8
Au systems: Archean to the modern Earth	9
Controls on gold endowments of porphyry deposits <i>Chiaradia, Massimo</i>	9
Evolution of magmatic fertility for porphyry Au and Cu deposits through the prism of zircon chrono-chemistry, Balkan Peninsula, SE Europe <i>Ireland, Timothy, Bilyarska, Teodora, Bilyarski, Stoimen, Protic, Nenad, & Stefanova, Elitsa</i>	10
Stability of gold nanoparticles in sulfur-bearing hydrothermal fluids: an experimental study <i>Liu, Weihua, Chen, Miao, Yang, Yi, Mei, Yuan, Etschmann, Barbara, Brugger Joël, & Johannessen, Bernt</i>	10
Lifting the cloak of invisibility: Gold in pyrite from the Olympic Dam deposit, South Australia <i>Ehrig, Kathy, Ciobanu, Cristiana, Verdugo-Ihl, Max, Dmitrijeva, Marija, Cook, Nigel, & Slattery, Ashley</i>	10
Do rocks deposited during time periods with high gold in sedimentary pyrite host more gold mineralization? <i>Gregory, Daniel, Lui, Timothy, Wu, Selina, & Large, Ross</i>	11
Source of gold in Neoproterozoic orogenic-type deposits in the North Atlantic Craton, Greenland: Insights for a proto-source of gold in sub-seafloor hydrothermal arsenopyrite in the Mesoproterozoic <i>Saintilan, N. J., Selby, D., Hughes, J. W., Schlatter, D. M., Kolb, J., & Boyce, A.</i>	11
Apatite chemistry indicates that oxidized auriferous fluids along the world-class Boulder Lefroy–Golden Mile fault system were significantly different to fluids from global porphyry systems <i>Bath, Adam, B., Walshe, John, L., Ireland, Tim, Cobeñas, Gisela, Sykora, Stephanie, Cernuschi Federico, Woodall, Katie, MacRae, Colin, Williams, Morgan, & Schmitt, Leanne</i>	12
The unusual Imou porphyry Au–Cu deposit, Western Highlands PNG <i>Ireland, Timothy, Cernuschi, Federico, Sievwright, Robert, Goswell, Hannah, Stefanova, Elitsa, & Dobe, John</i>	13

The Late Archean Au epoch: by-product of Earth degassing <i>Walshe, John L., & Bath, Adam, B.</i>	13
A view of orogenic gold deposits as nonlinear systems: Nonlinear analysis of data <i>Ord, Alison, & Hobbs, Bruce</i>	14
River(ina) of gold – historical activity and structural controls <i>Stuart, Cait, Ricketts, Mel, & Gilmore, Phil</i>	14
Reframing mine wastes as new resources to meet green economy metal	14
Mine Waste as secondary raw material in the framework of mining circular economy: legislation and applicability perspectives <i>Benzaazoua, Mostafa</i>	15
The suitability of Re-mining as remediation method of Be–W skarn tailings in Yxsjöberg, Sweden <i>Hällström, Lina</i>	15
Opportunities for reprocessing polymetallic tailings in western Tasmania <i>Jackson, Laura, King, Lexi, Parbhakar-Fox, Anita, & Meffre, Sebastien</i>	16
Critical metal exploration in Queensland’s mine waste: identifying potential secondary resources <i>Parbhakar-Fox, Anita, Degeling, Helen & Lisitsin, Vlad</i>	16
Critical metals and mine waste across Australia: partners in solutions? <i>Mudd, Gavin M.</i>	17
Application of alkaline industrial wastes in remediation of acid and metalliferous drainage generated by legacy mine wastes <i>Moyo, Annah, Parbhakar-Fox, Anita, Meffre, Sebastien & Cooke, R. David</i>	18
MinEx CRC: National Drilling Initiative frontier precompetitive drilling to support greenfields discovery	18
Mineral and petroleum potential in the South Nicholson region, and the NDI Carrara 1 stratigraphic drill hole <i>Jarrett, Amber, Bailey, Adam, Carr, Lidena, Henson, Paul, Schofield, Anthony, O’Rourke, Angela, Roach, Ian, Budd, Anthony, Munson, Tim, Williams, Ben, Symmons, Jack, & Close, Dorothy</i>	18
The MinEx CRC National Drilling Initiative <i>Budd, Anthony</i>	19
Multicommodity mineral systems analysis for the National Drilling Initiative: The TISA and Delamerian case study <i>Metelka, Vasek, Schofield, Anthony, Wise, Tom, Cole, David, Otto, Alex, Fabris, Adrian, Hong, Wei, & Murr, James</i>	19
Characterising fluid composition and source in a greenfields terrane: west Arunta Orogen, Western Australia <i>Finch, Emily G., & Kelsey, David E.</i>	20
Optimization of sequential drilling locations to reduce geological uncertainty <i>Pirot, Guillaume, Lindsay, Mark & Jessell, Mark</i>	20
Zircon chemistry as an exploration tool for iron oxide–copper–gold deposits <i>Brotodewo, Adrienne, Tiddy, Caroline, Zivak, Diana, Fabris, Adrian, & Giles, David</i>	21
Uncovering the Cobar Basin – new results from the NSW MinEx NDI areas <i>Folkles, Chris, Deyssing, Liann, Trigg, Steven, Carlton, Astrid, & Schifano, Joe</i>	21
Between the Stavely and Koonenberry: a structure with no arc, or an arc hidden in structure? <i>Wise, Tom, Curtis, Stacey, & Robertson, Kate</i>	22
Greening up brownfields: adding new timelines to mineral systems models for the Mesoproterozoic Gawler Craton <i>Morrissey, Laura, Payne, Justin, Hand, Martin, Bockmann, Mitchell, Yu, Jie, & Reid, Anthony</i>	22
Constraining alteration in the buried Benagerie ridge, Curnamona province South Australia <i>Simpson, Alex, Glorie, Stijn, Hand, Martin, Reid, Anthony, & Gilbert, Sarah</i>	23
Hydrothermal alteration and mineralisation characteristics at Anabama Hill: a porphyry Cu–Mo prospect in the Delamerian Orogen, South Australia <i>Hong, Wei, Fabris, Adrian, Curtis, Stacey, & Dutch, Rian A.</i>	24
⁴⁰ Ar/ ³⁹ Ar step-heating geochronology on drill core samples reveals multiple alteration events in the Anabama Hill Cu–Mo prospect, South Australia <i>Goswami, Naina, Forster, Marnie, & Reid, Anthony</i>	24
Hydrothermal-magmatic ore-forming processes	25
Thermodynamic modelling of ore transport and deposition: the good, the bad, and the ugly <i>Brugger, Joël, Etschmann, Barbara, Gonzalez, Christopher, Liu, Weihua, Yuan, Mei, Guan, Qishui, Raiteri, Paolo, Testemale, Denis, & Xing, Yanlu</i>	25
Yttrium speciation in sulfate-rich hydrothermal ore-forming fluids <i>Guan, Qishui, Mei, Yuan, Etschmann, Barbara, Louvel, Marion, & Brugger, Joël</i>	25

Effects of halogen in chemical exchange and porosity evolution during feldspar–fluid reaction interface <i>Duan, Gan, Brugger, Joël, Kontonikas-Charos, Alkiviadis, Ram, Rahul, Etschmann, Barbara, & Guagliardo, Paul</i>	26
Mineral redox buffer in ore forming processes – insights from scapolite <i>Hamisi, Jonathan, Etschmann, Barbara, Micklethwaite, Steven, Tomkins, Andrew, Pitcairn, Iain, Wlodek, Adam, Morrissey, Laura, & Brugger, Joël</i>	26
New insights into gold enrichment process during the growth of chalcopyrite-lined conduits within a modern hydrothermal chimney from PACMANUS Basin <i>Hu, Si-Yu, Barnes, Steve, Pages, Anais, Verrall, Michael, Parr, Joanna, Quadir, Zakaria, Binns, Ray, & Schoneveld, Louise</i>	27
Petrographically constrained in situ sulfur isotopes: why the “SEDEX” can’t be used as model for sediment-hosted sulfide deposits in the 1.6 Ga Edmund Basin, Australia <i>Lampinen, Heta M., LaFlamme, Crystal, Occhipinti, Sandra A., Fiorentini, Marco L., & Spinks, Sam C.</i>	27
Using epidote U–Pb geochronology and multivariate statistics to unravel overprinting propylitic alteration around the Resolution porphyry Cu–Mo deposit: Fingerprinting the fertile porphyry signal <i>Phillips, Joshua, Thompson, Jay, Meffre, Sebastien, Maas, Roland, Danyushevsky, Leonid, & Cooke, David</i>	28
Gold in oil, and its role in the formation of epithermal gold deposits <i>Crede, Lars, Evans, Katy, Rempel, Kirsten, Weihua Liu, Brugger, Joël, Etschmann, Barbara, Bourdet, Julian, & Reith, Frank</i>	28
A morphotectonic analysis of the East Manus Basin, Papua New Guinea <i>Dyriw, Nicholas J., Bryan, Scott E., Richards, Simon W., Parianos, John M., Arculus, Richard J. & Gust, David A.</i>	29
Differentiated Archean dolerites and orogenic gold: influences on fertility <i>Hayman, Patrick, Campbell, Ian, Cas, Ray, Squire, Rick, Douth, David, & Outhwaite, Michael</i>	29
Copper isotope fractionation in volatile-fluxed enclaves: Modern analogues for the genesis of ancient ore deposits <i>McGee, Lucy, Farkas, Juraj, Lowczak, Christopher, Payne, Justin, Wade, Claire, & Reid, Anthony</i>	29
Geochemical and mineralogical signatures of IOCG and affiliated copper deposits in the Mount Isa Province, Queensland, Australia <i>Lisitsin, Vladimir, & Dhnaram, Courteney</i>	30
A manganese oxide discovery, Carrara Range, South Nicholson region, Northern Territory <i>Carson, Chris, Henson, Paul, Huston, David, Jarrett, Amber, Champion, David, & Boreham, Chris</i>	30
Structural evidence for massive sulphide mineralisation during extension, Clarke’s Reef, SE NSW <i>Durney, David W., & Hood, David I. A.</i>	31
Unconventional gas & resources	31
Unconventional gas and resources <i>Garnett, Andrew</i>	31
CO ₂ reduction and fermentation producing in situ CH ₄ in the majority of sampled GAB aquifers and alluvium overlying a coal seam gas field <i>Pearce, Julie, Golding, Sue, Baublys, Kim, Hofmann, Harald, St. John, Herbert, & Hayes, Phil</i>	31
A very unconventional hydrocarbon play: the Mesoproterozoic Velkerri Formation of northern Australia <i>Collins, Alan S., Cox, Grant M., Jarrett, Amber J. M., Blades, Morgan L., Shannon, April, V., Yang, Bo., Farkas, Juraj, Hall, P. Tony, O’Hara, Brendan, Close, David, Baruch, Elizabeth, T., Altmann, Carl, Evans, David, & Bruce, Alex</i>	32
The distribution and origin of hydrogen sulphide gas in the Triassic Montney Unconventional Play, British Columbia and Alberta, Canada <i>Chalmers, Gareth, Bustin, Amanda, & Bustin, Marc</i>	32
Combined petrography and palynofacies study of the Toolebuc hydrocarbon sources <i>Rodrigues, Sandra, Golding, Suzanne, Esterle, Joan, Mendonça Filho, João, Graciano, & Flores, Deolinda</i>	33
Re-evaluation of overlooked petroleum potential in the Powell Depression, southern Galilee Basin <i>Troup, Alison, Esterle, Joan, Rodrigues, Sandra, & Guerer, Derya</i>	33
New geology analytics and machine learning in data-rich and data-poor environments	34
Random forest based mineral potential mapping for porphyry Cu–Au mineralisation in the Eastern Lachlan Orogen <i>Ford, Arianne</i>	34
Are giant ore deposits rogue waves or dragon kings? <i>Hobbs, Bruce, & Ord, Alison</i>	34
Propagating sparse basement markers through inversion volumes using graph convolutional neural networks <i>Gillfeather-Clark, Tasman, Horrocks, Tom, Holden, Eun-Jung, & Wedge, Daniel</i>	35
Extending FaultSeg3D to minerals seismic: Part 1 – a synthetic 3D-seismic training-volume generator for preparing data replicating a hardrock terrane to train an automatic-fault-prediction algorithm <i>Chatterjee, Robindra, Weatherley, Dion, McLachlan, Geoff, & Valenta, Rick</i>	35
Statewide mineral potential mapping of New South Wales using a combined mineral systems and spatial data approach	36

Advancing technologies in mineral exploration	36
Extracting more from exploration soil samples. The evolution of UltraFine+ and next generation analytics <i>Noble, Ryan R. P., Cole, David T., Williams, Morgan J., Lau, Ian C., & Anand, Ravi R.</i>	36
Laser-Induced Breakdown Spectroscopy integrated with multi-variate wavelet tessellation – a new and rapid methodology for lithochemical analysis and interpretation <i>Fontana, F. Fernando, Tassios, Steven, Stromberg, Jessica, Tiddy, Caroline, van der Hoek, Ben, & Uvarova, Yulia</i>	37
Digitalizing the mining industry – core scanner for geochemistry, images, RQD, structures, specific gravity and volume bulk density <i>Arthursson, Mikael, Annelie, Lundström, & Angus, Tod</i>	37
Building a cloud-hosted exploration data platform and its application <i>Kohlmann, Fabian, Noble, Wayne, & Theile, Moritz</i>	38
Multi-scale characterisation of Australia’s deepest drill hole <i>Birchall, Renee, Pearce, Mark, Walshe, John, Powell, Helen, Shelton, Tina, & Woodall, Katie.</i>	38
Better laser focusing on improved reproducibility of U–Pb isotope analysis by LA-ICP-MS <i>Huang, Hui-Qing, Guillong, Marcel, Hu, Yi, & Spandler, Carl</i>	39
dh2loop 1.0: an open-source python library for automated processing and classification geological logs <i>Joshi, Ranee, Madaiah, Kavitha, Jessell, Mark, & Lindsay, Mark</i>	39
New strato-tectonic model and geochemical tool for revitalised IOCG targeting in the Gawler Craton <i>Anderson, John</i>	39
Cr-zoning in pyroxene as a prospectivity indicator for magmatic Ni–Cu sulfide deposits <i>Schoneveld, Louise, Barnes, Steve, Makkonen H. V., Le Vaillant, M., Paterson, D., Taranovic, V., Wang, K-Y, & Mao, Y-J</i>	40
Using gases for mineral exploration through cover: importance of microbial activity <i>Plet, Chloe, Siegel, Coralie, & Noble, Ryan</i>	40
Geophysical data optimisation for modelling: data collection in a value-of-information framework <i>Lindsay, Mark, Pirot, Guillaume, Jessell, Mark, Giraud, Jeremie, Scalzo, Richard, Cripps, Edward, & Aitken, Alan</i>	41
Scale reduction magnetotelluric survey in the East Tennant region, Northern Australia <i>Jiang, Wenping, Duan, Jingming, Schofield, Anthony, Brodie, Ross C., & Clark, Andrew</i>	41
Apatite fission track and U–Pb mapping of the northern Gawler Craton: implications for ore deposit exhumation and preservation <i>Glorie, Stijn, Reid, Anthony, Hall, James, Nixon, Angus, & Collins, Alan</i>	42
Structural data in drill core: methods for analysing anisotropy in core images <i>Hill, June, & Poulet, Thomas</i>	42
Using trace element chemistry of magnetite as an indicator mineral at the Starra iron-oxide copper gold deposits, northwest Queensland <i>Hohl, Max, Barker, Shaun, Cloutier, Jonathan, & Steadman, Jeffrey</i>	43
Automated image analysis for RGB coloured core images <i>Javeed, Umer, Hill, June, & Thomas, Matilda</i>	43
Into the Noddyverse: A massive data store of 3D geological models for application to machine learning and geophysical inversion <i>Jessell, Mark, Guo, Jiateng, Li, Yunqiang, & Lindsay, Mark</i>	43
Applications of spectral geology	44
Characterising the hyperspectral SWIR features of tourmaline from two western Tasmanian granites <i>Harraden, Cassidy L., Hong, Wei, & Deyell-Wurst, Cari</i>	44
HyLogger™ mineralogy from chips: a RoXplorer® pilot study <i>Moltzen, Jake</i>	44
Modelling of petrophysical from hyperspectral drill core data collected from the Osborne Cu–Au deposit, Mount Isa Inlier, Queensland <i>Laukamp, Carsten, Francis, Neil, Gopalakrishnan, Suraj, Hauser, Juerg, & Mule, Shane</i>	45
Deriving quantitative alteration mineralogy from TIR Hyperspectral data in IOCG Systems <i>Stromberg, Jessica, Schlegel, Tobias, Pejic, Bobby, Birchall, Renee, & Shelton, Tina</i>	45
Coal spectral features in the mid-infrared range <i>Rodrigues, Sandra, Fonteneau, Lionel, & Esterle, Joan</i>	46
Tracing mineralogy and alteration intensity using the spectral alteration index and depth ratios at the Northwest Zone of the Lemarchant volcanogenic massive sulfide (VMS) deposit, Newfoundland, Canada <i>Cloutier, Jonathan, & Piercey, Stephen J.</i>	47
Alteration signatures and footprints of the Ernest Henry deposit and camp: Spectral mineralogy and geochemistry	47

<i>Courteney Dhnaram, Vladimir Lisitsin, Suraj Gopalakrishnan, & Daniel Kille</i>	
White mica chemistry from the Vulcan IOCG Prospect, South Australia <i>Gordon, Georgina, Dmitrijeva, Marija, & Berthiaume, Jonathon</i>	48
High resolution vs standard resolution: How an increase in spectral resolution using a field portable spectrometer affects quality of data – a case study on Nickel exploration <i>Shelton Pieniazek, Lori</i>	48
Geomechanics for energy and resources	48
Exploring for the future: New Canning Basin geomechanics and rock property data <i>Bailey, Adam, Jarrett, Amber, Wang, Liuqi, Dewhurst, David, Esteban, Lionel, Kager, Shane, Monmusson, Ludwig, Carr, Lidena, & Henson, Paul</i>	48
Characterising the uncertainty of rock stress and strength estimates <i>Musulino, Matthew, Holford, Simon, King, Rosalind, & Hillis, Richard</i>	49
Re-defining the morphology of the Darling Basin in NSW using 3D modelling and data integration – introducing the Yathong–Ivanhoe Trough <i>Gammidge, Larissa, & Xu, Min</i>	49
Seismic structure of the crust across central Australia from the joint inversion of radial and vertical teleseismic body-wave autocorrelations <i>Tork Qashqai, Mehdi, & Saygin, Erdinc</i>	50
A multi-physics elasto-visco-plastic constitutive framework for geomechanics <i>Sari, Mustafa, Poulet, Thomas, Alevizos, Sotiris, & Veveakis, Manolis</i>	50
Compressional wave velocity estimation using gaussian processes regression <i>Mohammadpour, Mobarakeh, Arashpour, Mehrdad, Roshan, Hamid, & Masoumi, Hossein</i>	50
An improved understanding of the geology and petroleum systems of the southern Canning Basin gained through the acquisition of new seismic and well data <i>Carr, Lidena K., Edwards, Dianne S., Wang, Liuqi., Southby, Chris., MacFarlane, Susannah K., Boreham, Christopher, J., Grosjean, Emma., Khider, Kamal., Henson, Paul., Formin, Tanya., and Geological Survey of Western Australia</i>	51
<i>In-situ</i> stress and geological structure influence on the coal fractures and initial reservoir permeability within Coal Seam Gas reservoirs, eastern Surat Basin <i>Mukherjee, Saswata, Rajabi, Mojtaba, & Esterle, Joan</i>	51
<i>In-situ</i> stress pattern of Australia across spatial scales <i>Rajabi, Mojtaba</i>	52
EARTH STRUCTURE	53
Tectonic and paleogeographic evolution of Mesozoic Eastern Australia	53
Paleozoic and Triassic crustal evolution of the proto-Andes from detrital heavy minerals <i>Bahlburg, Heinrich, & Panca, Fernando</i>	53
Cretaceous evolution of Zealandia dictated by congested subduction <i>Betts, Peter, Moresi, Louis, Whittaker, Joanne, & Miller, Meghan</i>	53
Tectonic evolution and crustal growth processes revealed by detrital zircon petrochronology: Insights from dispersed Paleozoic–Mesozoic sedimentary basins of Zealandia <i>Campbell, Matthew J, Rosenbaum, Gideon, Allen, Charlotte M., & Spandler, Carl</i>	54
Jurassic Arc? Reconstructing the Lost World of eastern Gondwana <i>Foley, Elliot, Henderson, Robert, Roberts, Eric, Kemp, Tony, & Spandler, Carl</i>	54
Jurassic physiography of southeast Australia: evidence from the detrital zircon record of the Nambour Basin <i>Henderson, Robert, Foley, Elliot, & Roberts, Eric</i>	54
Recognition of an Early Cretaceous continental arc in Eastern Australia <i>Spandler, Carl, Henderson, Bob, Foley, Elliot, Roberts, Eric, & Kemp, Tony</i>	55
Raiders of the lost continental arc: deciphering the tectonic regime of eastern Australia during the Jurassic from analysis of tuff beds in the Surat Basin <i>Wainman, Carmine C., McCabe, Peter J., & Reynolds, Peter</i>	56
Mesozoic sedimentary provenance and palaeodrainage evolution of the northeastern Qld: evidence from the northeastern Galilee and Eromanga basins <i>Todd, Christopher N., & Roberts, Eric M.</i>	56
From cratonic assembly to supercontinent cycles	56
Self-consistent geodynamic models through the supercontinent cycle — Testing the introversion and extroversion supercontinent assembly and the stability of LLSVPs <i>Huang, Chuan, Li, Zheng-Xiang, & Zhang, Nan</i>	57

New interpretations of high-resolution aeromagnetic data and implications for stratigraphic correlations in the Tanami Region and northwest Aileron Province <i>Blaikie, Teagan, & McFarlane, Helen</i>	57
Unravelling the Palaeoproterozoic tectonic evolution of the Tanami Region and northwest Aileron Province <i>McFarlane, Helen, & Blaikie, Teagan</i>	58
Assembly of proto-Australia prior to the formation of the Nuna supercontinent in the Paleoproterozoic <i>Kirscher, Uwe, Mitchell, Ross N., Liu, Yebo, Nordsvan, Adam R., Wu, Lei, Pisarevsky, Sergei, & Li, Zheng-Xiang</i>	58
Proterozoic crustal evolution of NE Australia during Nuna assembly: insights from geophysical and radiogenic isotope data <i>Li, Jiangyu, Olierook, H. K. H., Li, Zheng-Xiang, Nordsvan, Adam R., Pourteau, Amaury, Volante, Silvia, Elders, Chris, Collins, William J., & Doucet, Luc S.</i>	59
Palaeomagnetism argue against a stable supercontinent during the Archaean–Proterozoic transition <i>Liu, Yebo, Mitchell, Ross N., Li, Zheng-Xiang, Kirscher, Uwe, Pisarevsky, Sergei A., & Wang, Chong</i>	59
The emergence of eclogites linked to global arc chemistry change at 2 Ga <i>Tamblyn, Renée, Hasterok, Derrick, Hand, Martin, & Gard, Matthew</i>	59
When did Australia’s Cratons come together? <i>Gorczyk, Weronika, Tyler, Ian, Aitken, Alan, & Kohanpour, Fariba</i>	60
Detrital zircon record of Proterozoic strata in the Priest River region of western Laurentia: Evaluating “SWEAT” relationships for supercontinents Nuna and Rodinia <i>Brennan, Daniel T., Li, Zheng-Xiang, Link, Paul K., & Johnson, Tim</i>	60
Review of SHRIMP zircon ages for the Eastern Succession of the Mount Isa and Etheridge Provinces and their provenances <i>Withnall, Ian</i>	61
Partial melting, granulites, retrogression and their control on late orogenic exhumation processes <i>Cenki-Tok, Bénédicte, Rey, Patrice F., & Arcay, Diane</i>	61
Mantle refertilization from 3.2 billion years ago points to an early start of plate tectonics <i>EL Dien, Hamed Gamal, Doucet, Luc-Serge, Murphy, J. Brendan, & Li, Zheng-Xiang</i>	62
The role of isostasy in the evolution and structural styles of fold and thrust belts <i>Ibrahim, Youseph, & Rey, Patrice</i>	62
Structural evolution of a 1.6 Ga orogeny related to the final assembly of the supercontinent Nuna: coupling of episodic and progressive deformation <i>Volante, S., Collins, W. J., Pourteau, A., Li, Z.-X., Li, J., & Nordsvan, A. R.</i>	62
Development of William’s Ridge, Kerguelen Plateau, and Broken Ridge: tectonics, hotspot magmatism, microcontinents, and Australia’s extended continental shelf <i>Coffin, Millard F., Whittaker, Joanne, Daczko, Nathan, Halpin, Jacqueline, Bernardel, George, Picard, Kim, Gardner, Robyn, Gürer, Derya, Brune, Sascha, Gibson, Sally, Hoernle, Kaj, Koppers, Antonius, Storey, Michael, Uenzelmann-Neben, Gabriele, Magri, Luca, Neuharth, Derek, Christiansen, Sascha Høegh, & Easton, Laura</i>	63
Linking supercontinents to a convective mantle framework <i>Martin, Erin L., Cawood, Peter A., & Murphy, J. Brendan</i>	63
Distinct formation history for deep mantle domains reflected in geochemical differences <i>Doucet, Luc S., Li, Zheng-Xiang, EL Dien, Hamed Gamal, Pourteau, Amaury, Murphy, J. Brendan, Collins, William J., Mattielli, Nadine, Olierook, Hugo K. H., Spencer, Christopher J., & Mitchell, Ross N.</i>	64
Coupled evolution of plate tectonics and basal mantle structure <i>Cao, Xianzhi, Flament, Nicolas, & Müller, R. Dietmar</i>	64
What is under the Antarctic ice: An integrated study of U–Pb, O and Lu–Hf isotopes <i>Chen, Bei, & Campbell, Ian</i>	64
Paleomagnetic constraints on formation of the Manning Orocline, far-field effects of Pangea-B to -A transformation and breakup? <i>Klootwijk, Chris</i>	65
Geophysical investigation of the evolution of William’s Ridge and Broken Ridge, Kerguelen Plateau <i>Magri, Luca, Whittaker, Joanne M., Coffin, Millard F., & Gürer, Derya</i>	65
Timescales of continental subduction: Constraints from ultrahigh-pressure metapelites in the Western Gneiss Region, Norway <i>March, Samantha, Tamblyn, Renée, Hand, Martin, Carvelho, Bruna, & Clark, Chris</i>	66
Refining tectonic models of the Rayner Complex in the Rodinia supercontinent <i>Morrissey, Laura, Halpin, Jacqueline, Hand, Martin, & Payne, Justin</i>	66
Understanding continental processes with low temperature thermochronology	67
Thermochronology frontiers in Australia <i>McInnes, Brent I. A.</i>	67

AusGeochem and the future of big data in low-temperature thermochronology <i>Boone, Samuel C., Kohlmann, Fabian, Theile, Moritz, Noble, Wayne, Kohn, Barry, Glorie, Stijn, Danišik, Martin, & Zhou, Renjie</i>	67
Development of a digital apatite fission-track analysis training module <i>Chung, Ling, Boone, Samuel C, Gleadow, Andrew, McMillan, Malcolm, & Kohn, Barry</i>	68
Thermal annealing of implanted ²⁵² Cf fission-tracks in monazite <i>Jones, Sean, Gleadow, Andy, & Kohn, Barry</i>	68
Integrating thermochronology with numerical plate-tectonic models: A case study for Central Asia <i>Glorie, Stijn, Zahirovic, Sabin, & Kohlmann, Fabian</i>	69
Revisiting the break-up evolution of the SE Australian rifted margin: new perspectives from larger data sets <i>Gleadow, Andrew, McMillan, Malcolm, Boone, Samuel, & Kohn, Barry</i>	69
Distal footprints of the Alice Springs Orogeny preserved in Paleoproterozoic northern Australia: An application of multi-kinetic thermochronology in the Pine Creek Orogen and Arnhem Province <i>Nixon, Angus L., Glorie, Stijn, Collins, Alan S., Whelan, Jo A., Reno, Barry L., Danišik, Martin, Wade, Benjamin P., & Fraser, Geoff</i>	70
The uplift history of the Nyika Plateau, Malawi: A long lived paleo-surface or a contemporary feature of the East African Rift? <i>McMillan, Malcolm, Boone, Sam, Kohn, Barry, Gleadow, Andy, & Chindandali, Patrick</i>	70
Detachment fault and metamorphic core complex at the distal continental margin of the northern South China Sea <i>Deng, Hongdan, Ren, Jianye, Rey, Patrice, & McClay, Ken</i>	71
Exhumation of the Indus-Yarlung Tsangpo Suture Zone (NW India): New constraints from low-temperature thermochronology <i>Zhou, Renjie, & Aitchison, Jonathan C.</i>	71
Recent advances in the geology and mineral potential of the eastern Australian Tasmanides	71
New constraints on the tectonic and metallogenic history of Lachlan Orogen <i>Meffre, Sebastien, Leslie, Chris, Wells, Tristan, Habib, Umer, & Schaap, Thomas</i>	71
Devonian–Carboniferous regional deformation in the northeastern Lachlan Orogen, southeastern Australia <i>Fergusson, Chris, & Colquhoun, Gary</i>	72
Substrate of the Macquarie Arc: geophysical evidence and implications for tectonic setting <i>Musgrave, Robert</i>	72
Life cycle of the Ordovician Macquarie Arc, Lachlan Orogen, eastern Australia <i>Zhang, Qing, Nutman, Allen, & Buckman, Solomon</i>	73
Unravelling the Tumut Trough: A Middle Ordovician age for the Brungle Creek Metabasalt, eastern Lachlan Orogen <i>Bruce, Michael, Percival, Ian, Zhen, & Yong, Yi</i>	73
Orogenesis terminated by mafic underplate delamination at prior passive rift margins: The Delamerian-Ross example. <i>Foden, John, Tappert, Ralph, Todd, Angas, & Segui, David</i>	74
Apatite as an indicator of porphyry fertility in the Northparkes district <i>Wells, Tristan, Meffre, Sebastien, Cooke, David R., Steadman, Jeffrey A., & Goemann, Karsten</i>	74
Evolution of the Lachlan Orogen in the East Riverina region, NSW: Insights from 100 new SHRIMP dates <i>Bodorkos, S., Gilmore, P. J., Eastlake, M. A., Bull, K. F., Blevin, P. L., Trigg, S. J., Campbell, L. M., & Waltenberg, K.</i>	75
Structure of the Silurian Quidong Basin: new observations on a microcosm of Eastern Lachlan Orogen tectonic and metallogenic problematica <i>Hood, David I. A., Durney, David W., & Parkes, Ross A.</i>	75
Approaches to structural history in areas of weak to moderate upright folding <i>Durney, David W.</i>	76
Late Cambrian–Middle Ordovician extension of the northern Tasmanides: thinned crust that facilitated intense Silurian (Benambran) shortening deformation <i>Henderson, Robert, Fergusson, Chris, & Withnall, Ian</i>	76
Regional scale folding in the Arthur Metamorphic Complex: structural constraints for the Keith River–Lyons River area, NW Tasmania <i>Cumming, G., Jackman, C., Everard, J. L., & Gray, D.</i>	77
Evidence for fire fountaining at Skillion Hill, southern Tasmania <i>Cumming, G., Orth, K., Bottrill, R., Everard, J., & Vicary, M.</i>	77
Geochronology of various fault bound units at Savage River: a melange of different terranes <i>Cumming, G. V., Bottrill, R. S., Calver, C., & Meffre, S.</i>	78
Early Tasmanides evolution: passive to convergent margin history in New South Wales, Australia	78

CRUST, SURFACE & COSMOS	80
Carbonates as archives of the past	80
Trace element distributions in carbonate rocks: a sedimentologist's perspective on sample targeting versus technique <i>Webb, Gregory E.</i>	80
Neoproterozoic carbonates as archives of paleo-redox conditions on early Earth: Insights from metal isotope analyses of the Tumbiana Formation, Pilbara, WA <i>Farkas, Juraj, Kläbe, Robert, Scarabotti, Liam, Stormberg, Jessica, & Spinks, Sam</i>	80
Descending into the "snowball": Improving interpretations of Tonian palaeoenvironments with multi-proxy elemental and isotopic geochemistry <i>Virgo, Georgina, Collins, Alan, Farkas, Juraj, Blades, Morgan, Amos, Kathryn, & Lloyd, Jarred</i>	81
Deep water cusped stromatolites in the Cryogenian Trezona Formation, South Australia <i>O'Connell, Brennan, Wallace, Malcolm W., Hood, Ashleigh & Rebecchi, Luke</i>	81
Characteristics and diagenesis of the Upper Permian Beekeeper Formation from the Perth Basin, Western Australia <i>Adhari, Muhammad Ridha, & Wilson, Moyra E. J.</i>	81
Quantifying the dolomite problem and its impacts on Mg/Ca change through time <i>Opdyke, Bradley</i>	82
On the foundering of carbonate platforms and reefs <i>Wilson, Moyra E. J., Arosi, Hamed, A., Loche, Marco, & Webster, Jody</i>	82
Rafted benthic microfossils as proxies of Neogene ocean current history in the Bass Strait seaway, southeastern Australia <i>Warne, Mark, & McDonald, Abbey</i>	83
Holocene microbialite records of terrigenous influence on water quality for the offshore southern Great Barrier Reef <i>Salas-Saavedra, Marcos, Webb, Gregory E., Sanborn, Kelsey L., Zhao, Jian-Xin, Webster, Jody M., Nothdurft, Luke D., & Nguyen, Ai</i>	83
Insights into palaeo-hydrology of the Coorong Lagoons, South Australia, based on Strontium Isotope Tracers ($^{87}\text{Sr}/^{86}\text{Sr}$ and $\delta^{88/86}\text{Sr}$) in fossil carbonates <i>Shao, Yuxiao, Woolston, Zara, Farkaš, Juraj, Chamberlayne, Briony, Tibby John, Haynes, Deborah, & Tyler, Jonathan</i>	84
Variations in mid- to late Holocene nitrogen supply to northern Great Barrier Reef <i>Halimeda</i> macroalgal bioherms <i>McNeil, Mardi, Nothdurft, Luke, Erler, Dirk, Hua, Quan, & Webster, Jody M.</i>	84
Solution pipes and focussed vertical water flow in carbonates with matrix porosity <i>White, Susan, Lipar, Matej, Szymczak, Piotr, & Webb, John</i>	85
Quantifying the Dolomite problem and its impacts on Mg/Ca change through time <i>Opdyke, Bradley</i>	85
Paleoatmospheric CO ₂ oscillations through a cool mid-Late Cretaceous recorded from pedogenic carbonates in Africa <i>Orr, Theresa J., Roberts, Eric M., Wurster, Christopher M., Singleton, Russell E., Lawrence, L., & Mtelega, Cassy</i>	86
Sedimentary deposits: Earth and planetary processes	86
Preservation of ancient eolian landscapes beneath flood basalt: an example from the Officer Basin, Western Australia <i>Haines, Peter</i>	86
Correlation of stratigraphic sequences to evaluate downstream transitions within the Wonoka canyon at Umberatana syncline, South Australia <i>Giles, Sarah M., & Christie-Blick, Nicholas</i>	87
Quantifying lateral and distal variability within hybrid beds, case studies from Central and Northern Italy <i>Brooks, Hannah L., & Steel, Elisabeth</i>	87
Reviewing stratigraphic units defined in the ACT <i>Marais-van Vuuren, Christo, Brown, Catherine, & Jarrett, Amber</i>	88
A Pb isotope regolith map of Australia <i>Desem, Candan, Maas, Roland, Woodhead, Jon, Carr, Graham, & de Caritat, Patrice</i>	88
Ediacaran stratigraphy in the western part of the Northern Territory Amadeus Basin, central Australia <i>Verdel, Charles, Donnellan, Nigel, Normington, Verity, & Simmons, Jack</i>	89

Alloccyclic controls on shoreface sedimentation from the Late Cretaceous to Miocene, Gippsland Basin, SE Australia	89
<i>Mahon, Elizabeth, & Wallace, Malcolm</i>	
Paleoflora and environment of the Surat Basin at the time of the JK transition	89
<i>Cooling, Jennifer, Esterle, Joan, & McKellar, Joh</i>	
High-resolution rapid thermal neutron tomographic imaging of fossiliferous cave breccias from Southeast Asia	90
<i>Smith, Holly Ellen, Bevitt, Joseph, Garbe, Ulf, Zaim, Jahdi, Rizal, Yan, Aswan, Puspaningrum, Mika Rizki, Trihascaryo, Agus, Price, Gilbert J., Webb, Gregg, & Louys, Julien</i>	
How the zebra rock got its stripes: origin of hematite banding in East Kimberley siltstones	90
<i>Coward, Andrew J., Slim, Anja C., Brugger, Joël, Wilson, Siobhan A., Pillans, Bradley J., & Williams, Tim</i>	
Understanding the nature transition of the Late Jurassic formations of the Surat Basin through borehole image logs using cumulative dip plots	91
<i>de A V Filho, Claudio Luiz, Sobczak, Kasia, Holl, Heinz-Gerd, Hurter Suzanne, & Vasconcelos, Paulo</i>	
Cryogenian syn-glacial carbonates and implications for a snowball Earth	91
<i>Hood, Ashleigh, Penman, Donald, Lechte, Maxwell, Wallace, Malcolm, Giddings, Jonathan & Planavsky, Noah</i>	
Seismic-scale soft sediment deformation associated with subaqueous dewatering: an example from the continental shelf of the Otway Basin	92
<i>Niyazi, Yakufu, Warne, Mark, & Ierodiconou, Daniel</i>	
Reconstructing environmental conditions in a ca 2.4 Ga microbialite reef using Si isotope and trace element analyses	92
<i>Soares, Georgia, Van Kranendonk, Martin, Scicchitano, Maria, Nomchong, Brendan, & Barlow, Erica</i>	
Using macrofossils to interpret peatland facies of Miocene brown coals, Gippsland Basin, southeastern Australia	93
<i>Tosolini, Anne-Marie P., Korasidis, Vera A., Wallace, Malcolm W., Wagstaff, Barbara E., & Hill, Robert S.</i>	
Investigating the origin of organic matter in Archean chert	93
<i>Zepeda, Vanessa K.</i>	
Understanding basin formation and evolution from a plate-tectonic perspective	93
Mapping and modelling a future passive margin in Afar, East Africa	94
<i>Zwaan, Frank, Corti, Giacomo, Keir, Derek, Sani, Federico, Muluneh, Ameha, Illsley-Kemp, Finnigan, & Papini, Mauro</i>	
Dynamics of arc–continent collision: the role of crustal–mantle dynamics on controlling the formation of basins in continental margins	94
<i>Rodriguez-Corcho, Andres, Móron-Polanco, Sara, Farrington, Rebecca, Beucher, Romain, Moresi, Louis, & Montes, Camilo</i>	
A late Tonian plate reorganization event revealed by a full-plate Proterozoic reconstruction	95
<i>Collins, Alan S., Blades, Morgan L., Merdith, Andrew S., & Foden, John D.</i>	
Reconstructing the Mesoproterozoic palaeogeography of northern Australia through coupled detrital thermo- and geo-chronometers	95
<i>Yang, Bo, Collins, Alan, Blades, Morgan, & Jourdan, Fred</i>	
Reconstruction of the North China Craton within the Meso–Neoproterozoic supercontinents: evidence from large igneous provinces and rift sediments	95
<i>Zhang, Shuan-Hong, Pei, Jun-Ling, Zhou, Zai-Zheng, Yang, Zhen-Yu, Zhao, Yue, Cai, Yuhang, Zhang, Qi-Qi, Hu, Guo-Hui, & Zhuo, Sheng-Guang</i>	
Reconstruction of a Paleoproterozoic greenstone belt and tectonic implications (Toumodi Greenstone Belt, West Africa)	96
<i>Hayman, Patrick, Asmussen, Pascal, Senyah, Gloria, Tegan, Eudes, Coulibaly, Inza, Denyszyn, Steven, & Jessell, Mark</i>	
Building a boundary – processes, products, and consequences of Neogene collisional geodynamics in eastern Indonesia	96
Geology of the Mutis Complex, Miomaffo, West Timor	96
<i>Berry, Ron, Goemann, Karsten, & Danyushevsky, Leonid</i>	
Cenozoic affinity of the Gondwanan rocks of eastern Timor: evidence from geothermo-chronometry	97
<i>Duffy, B., Lew, B., Boland, K., Kohn, B., Matchan, E., Maas, R., Dixon, D., Pedro, L., de Carvalho, P., & Sandiford, M.</i>	
Oblique plate convergence drives deformation, uplift of coral reefs and earthquakes in the eastern Bird’s Head Peninsula, West Papua, Indonesia	97
<i>Saputra, Sukahar Eka, Fergusson, Chris, Dosseto, Anthony, Murray-Wallace, Colin, Nutman, Allen, & Dougherty, Amy</i>	
Seismic Imaging of the subducted Australian continental margin beneath Timor and the Banda Arc Collision Zone	98
<i>Zhang, Ping, & Miller, Meghan S.</i>	
A kinematic model of the northeast Australian Plate boundary zone	98
<i>Zhao, Siyuan, McClusky, Simon, Koulali, Achraf, Cummins, Phil, & Miller, Meghan</i>	
The Proterozoic Earth system and plate tectonics—correlations and causation?	99

Extending whole-plate tectonic models into deep time: linking the Neoproterozoic and the Phanerozoic <i>Merdith, Andrew, Collins, Alan, Williams, Simon, Tetley, Michael, Mulder, Jacob, Blades, Morgan, Young, Alexander, Armistead, Sheree, Cannon, John, Zahirovic, Sabin, & Müller, Dietmar</i>	99
The impact of Snowball Earth Glaciation on ocean water $\delta^{18}\text{O}$ values <i>Defliese, William F.</i>	99
Redefining the basement architecture of the southern Mount Isa Inlier <i>Brown, D. D., Bultitude, R. J., Simpson, J. M., Purdy, D. P., Connors, K. A., & Sanislav, I. V.</i>	99
Detrital zircon age and provenance of the Tonian–Cryogenian of the Adelaide Superbasin <i>Lloyd, Jarred C., Van Der Wolff, Erica, Blades, Morgan L., Virgo, Georgina M., Collins, Alan S., & Amos, Kathryn J.</i>	100
In-situ Rb–Sr dating of Precambrian sediments <i>Subarkah, Darwinaji, Blades, Morgan L., Collins, Alan S., Farkas, Juraj, Gilbert, Sarah, & Lloyd, Jarred C.</i>	100
Did Neoproterozoic (Ediacaran) regional sea-level drawdown trigger extensive allochthonous salt breakout and incision of the Wonoka paleocanyons, Flinders Ranges, South Australia? <i>Giles, Sarah M., Giles, Katherine A., Rowan, Mark G., Christie-Blick, Nicholas, & Lankford-Bravo, David F.</i>	101
Sedimentology and geomorphology of dryland continental systems	101
Australian drylands depositional environments: local news, globally relevant <i>Wakelin-King, Gresley A.</i>	101
Circadian rhythm of dune-field activity <i>Gunn, Andrew, Lancaster, Nicholas, Edmonds, Douglas, Ewing, Ryan, & Jerolmack, Douglas</i>	102
Lacustrine littoral landforms in drylands: diversity and significance with examples from Quaternary megalakes of Africa and Australia <i>Schuster, Mathieu, May, Jan-Hendrik, & Nutz, Alexis</i>	102
Late Holocene landscape dynamics and sediment cycling around Lake Callabonna, Central Australia <i>May, J.-H., Marx, S., Cohen, T., Schuster, M., & May, S. M.</i>	102
Dryland deltas of Western Australia – analogues for mixed-influenced fluvial-deltaic depositional systems <i>Lang, Simon, Paumard, Victorien, O'Leary, Mick, Goodwin, Ian, Cousins, Victoria, Lebrec, Ulysse, Jian, Andy, Holbrook, John, Smith III, Pomeroy, Hasiotis, Stephen, Vakarelov, Boyan, & Krapf, Carmen</i>	103
Cenozoic channel deposits of the Bowen Basin, Queensland <i>Yu, Tianjiao, Dube, Kudzai, Moss, Patrick, Abylgazina, Adiya, Cooling, Jennifer, & Esterle, Joan</i>	103
Sedimentology and geomorphology of Lake Yamma Yamma – a long-lived structurally controlled playa lake of the Lake Eyre Basin <i>Mann, Sandra, & Amos, Kathryn</i>	104
Scientific results of the International Ocean Discovery Program: A decade of success	104
The isotopic footprint of a submarine mineral system: Cr and Sr isotopes in the Iheya North hydrothermal field, Okinawa Trough (IODP expedition 331) <i>McGee, Lucy, Burke, Thomas, Farkas, Juraj, Cave, Bradley, & Yeats, Chris</i>	104
East Antarctic meltwater influx from the Wilkes Subglacial Basin since the Last Glacial Maximum as determined by beryllium isotopes <i>Behrens, Bethany, Miyairi, Yosuke, Sproson, Adam D., Yamane, Masako, & Yokoyama, Yusuke</i>	104
85 000 years of polar front, warm current variability, and ice rafting in contourites off southwest Ireland <i>Westgård, Adele, Gallagher, Stephen J., Monteys, Xavier, Foubert, Anneleen, & Rüggeberg, Andres</i>	105
Hydrocarbons in a new early Paleocene sedimentary section recovered from the Campbell Plateau, south of New Zealand, by IODP Expedition 378 <i>George, Simon C., Ausín, Blanca, Childress, Laurel B., Röhl, Ursula, Thomas, Deborah J., Hollis, Christopher J., and the IODP Expedition 378 Science Party</i>	105
A microbial mayhem in the Chicxulub crater <i>Schaefer, Bettina, Grice, Kliti, Coolen, Marco J. L., Summons, Roger E., Cui, Xingqian, Bauersachs, Thorsten, Schwark, Lorenz, Böttcher, Michael E., Bralower, Timothy, J., Lyons, Shelby, L., Freeman, Kate H., Cockell, Charles S., Gulick, Sean S., Morgan, Joanna V., Whalen, Michael T., Lowery, Christopher, M., & Vajda, Vivi</i>	106
Late Cretaceous turmoil in the southern high latitudes: a story of environmental stress, basin restriction and deltaic sedimentation from IODP Site U1512, Bight Basin, Australia <i>Wainman, Carmine C., & McCabe, Peter J.</i>	107
CORE TO CRUST	108
The Australian Lithosphere in 2021: What do we know and future challenges	108
Geoelectric structure of Tasmania from multi-scale magnetotelluric data <i>Ostensen, Thomas, Reading, Anya, Cracknell, Matthew, Roach, Michael, McNeill, Andrew, Duffett, Mark, Bombardieri, Daniel, Thiel, Stephan, Robertson, Kate, Duan, Jingming, & Heinson, Graham</i>	108
New insight into the Carpentaria Conductivity Anomaly from high resolution MT data in the Cloncurry region	108

<i>Simpson, J. M., Brown, D. D., Duan, J., & Kyi, D.</i>	
Next-generation model of the Australian crust from synchronous and asynchronous ambient noise imaging <i>Chen, Yunfeng, & Saygin, Erdinc</i>	108
Recent progress in laboratory studies of seismic wave attenuation relevant to the Earth's upper mantle <i>Qu, Tongzhang, Jackson, Ian, David, Emmanuel C., & Faul, Ulrich H.</i>	109
Provenance of late Cambrian–Ordovician sedimentary rocks in western, northeastern Tasmania and southern Victoria: constraints from U/Pb dating, zircon geochemistry and ϵ_{Hf} isotope <i>Habib, Umer, Meffre, Sebastien, Kultaksayos, Sitthinon, & Berry, Ron</i>	109
Lapstone Structural Complex and uplift of the Blue Mountains, tectonic backdrop to western Sydney, Australia <i>Fergusson, Chris, & Hatherly, Peter</i>	110
Disorientation control on trace element segregation in fluid-affected low-angle boundaries in olivine <i>Tacchetto, Tommaso, Reddy, Steven, Saxey, David, Fougereuse, Denis, Rickard, William, & Clark, Chris</i>	110
Age constraints on the formation and emplacement of Cambrian Ophiolites along Heathcote, Dookie, and Governor fault zones, Central Victoria <i>Habib, Umer, Meffre, Sebastien, & Bottril, Ralph</i>	111
Lithospheric structure of the Kidson reflection seismic line 18GA-KB1 from 2D multi-constrained gravity inversion <i>Moro, Polyanna, Giraud, Jérémie, Ogarko, Vitaliy, & Jessell, Mark</i>	111
Advances in volcanic and magmatic processes	112
Shallow conduit and vent processes during the 1886 basaltic Plinian eruption at Tarawera, New Zealand <i>Moore, Hannah, Carey, Rebecca, Houghton Bruce, Jutzeler, Martin, & White, James</i>	112
Trace element sector zoning in clinopyroxene as a function of undercooling: an experimental evaluation in trachybasaltic magmas <i>MacDonald, Alice, Ubide, Teresa, Masotta, Matteo, Mollo, Silvio, & Pontesilli, Alessio</i>	112
Timescales of magma ascent recorded by olivine zoning patterns from Mount Leura and Mount Noorat, Newer Volcanics Province, Australia <i>Didonna, Rosa, Handley, Heather, Cas, Ray, Fidel, Costa, & Murphy, Timothy</i>	113
Geophysical and geochemical constraints on the formation of Holocene intraplate volcanism in East Asia <i>Ward, Jack F., Rosenbaum, Gideon, Ubide, Teresa, Wu, Jonny, Caulfield, John T., Sandiford, Mike, & Gürer, Derya</i>	113
Volcanic stratigraphy and eruption mechanisms from the last remaining outcrops at Wiri Mountain, Auckland Volcanic Field, New Zealand <i>Foote, April, Németh, Károly, & Handley, Heather</i>	114
Transitions in Eruptive Style During the 2012 Deep Submarine Silicic Eruption of Havre Volcano, Kermadec Arc, New Zealand <i>Clark, Acacia, Carey, Rebecca, Jutzeler, Martin, & Mitchell, Samuel</i>	114
Zircon trace element geochemistry as an indicator of magma fertility in iron oxide–copper–gold provinces (on the example of Mount Hagen, Papua-New Guinea) <i>Wade, Claire, Payne, Justin, Barovich, Karin, Gilbert, Sarah, Wade, Benjamin, Crowley, James, Reid, Anthony, & Jagodzinski, Elizabeth</i>	115
Newly identified mafic and felsic tuffs of the Shoalhaven and Talaterang Groups, southern Sydney Basin: their volcanic significance and palaeoecological impacts <i>Bann, Glen, Graham, Ian, & Jones, Brian</i>	115
U–Pb ages and aluminium concentrations of colourful sapphire-related zircon megacrysts from Far North Queensland: Merlot, Rosé and Champagne <i>Allen, Charlotte M., Porter, Erica J., & DeBruyn, Mitchell</i>	116
Corundum conundrum <i>Raffan, Nick</i>	116
QEMSCAN and PGE geochemistry to track sulfide saturation, magmatic evolution and fertility of porphyry suites (on the example of Mount Hagen, Papua-New Guinea) <i>Misztela, Monika, & Campbell, Ian</i>	117
Mineralisation around Mount Adrah, New South Wales: new observations by the Geological Survey of NSW <i>Wang, Yamei, Forster, David, Cronin, Dan, Montgomery, Karen, & Blevin, Phil</i>	117
A penecontemporaneous intrusion into marine sediments of the lower Shoalhaven Group and significance to the volcanic history of the southern Sydney Basin <i>Bann, Glen</i>	118
Gem sapphires and zircons in a basalt diatreme, northeastern Tasmania <i>Bottrill, Ralph, Everard, John, Duncan, David, Sutherland, Lin, Meffre, Sebastien, & Matchan, Erin</i>	118
Pompeii to Stabiae: downwind versus substrate-induced variations of the AD 79 Vesuvius fall deposits and their impact on human settlements <i>Chiominto, Giulia, Scarpati, Claudio, Perrotta, Annamaria, Sparice, Domenico, Fedele, Lorenzo, Santangelo, Ileana, Muscolino, Francesco, Rescigno, Carlo, Silani, Michele, & Massimo, Osana</i>	119

Does the St Marys Porphyrite represent a super eruption in eastern Tasmania? <i>Gallagher, Till, Bottrill, Ralph, Carey, Rebecca, Cumming, Grace, & Orth, Karin</i>	119
Magma ascent in Australian Intraplate basaltic volcanic provinces <i>Handley, Heather, Cas, Ray, England, Tom, Didonna, Rosa, & Ezad, Isra</i>	120
Pompeii to Stabiae: downcurrent versus substrate-induced variations of the AD 79 Vesuvius pyroclastic current deposits and their impact on human settlements <i>Santangelo, Ileana, Scarpati, Claudio, Perrotta, Annamaria, Sparice, Domenico, Fedele, Lorenzo, Chiominto, Giulia, Muscolino, Francesco, Rescigno, Carlo, Silani, Michele, & Massimo, Osanna</i>	120
<i>autopew</i> : Microanalytical Coordinate System Transforms <i>Williams, Morgan, & Schoneveld, Louise</i>	121
Where will Australia's next volcano erupt?: wider perspectives <i>Sutherland, Frederick L., & Graham, Ian T.</i>	121
Tracking plumbing system architecture in age-progressive intraplate volcanoes in Eastern Australia. <i>Tapu, Al-Tamini, Ubide, Teresa, & Vasconcelos, Paulo</i>	122
Geochemical data analysis workflows with <i>pyrolite</i> <i>Williams, Morgan, & Schoneveld, Louise</i>	122
Architecture, composition and geo-dynamic history of cratons and craton	122
Contrasting growth of the Pilbara and Yilgarn cratons from hafnium and neodymium isotopes <i>Kemp, Tony</i>	123
Records of the Earth's early crust from apatite inclusions in zircon – development and applications of <i>in situ</i> ⁸⁷ Sr/ ⁸⁶ Sr analysis by SIMS <i>Gillespie, Jack, Kinny, Pete, Martin, Laure, Kirkland, Christopher, Nemchin, Alexander, & Cavosie, Aaron</i>	123
Neodymium and oxygen isotope maps of Western Australia <i>Lu, Yongjun, Smithies, R. H., Champion, D. C., Wingate, M. T. D., Johnson, S. P., Martin, L., Jeon, H., Poujol, M., Zhao, J., Maas, R., & Creaser, R. A.</i>	123
Way out west – does the Arunta Orogen continue westward beneath the Canning Basin? <i>Kelsey, David E., Spaggiari, Catherine V., Wingate, Michael T. D., Lu, Yongjun, Fielding, Imogen O. H., & Finch, Emily G.</i>	124
Multiple ages of rutile from a single sample of granulite <i>Durgalakshmi, Williams, Ian S., & Sajeew, K.</i>	125
Geodynamic influences on volcanological, paleoenvironmental and tectonic evolution of the Archean Kalgoorlie Terrane LIP, Western Australia <i>Cas, R. A. F., Hayman, P. C., Squire, R. J., Campbell, I. H., Wyche, S., Sapkota, J., & Smithies, H.</i>	125
On the destructive tendencies of cratons: 3D geodynamics modelling of cratons and subduction <i>Farrington, Rebecca, Cooper, Katie, & Miller, Meghan</i>	126
An isotopic Atlas of Australia: foundational data for integrated geoscience through time and space <i>Fraser, Geoff, Waltenberg, Kathryn, Jones, Sharon, Huston, David, Champion, David, & Bodorkos, Simon</i>	126
Chasing lower crustal tectonic domains in the Yilgarn Craton <i>Gessner, Klaus, Smithies, R. Hugh, & Lu, Yongjun</i>	126
Archean craton formation and plate tectonics evolution: A new model evoked by discoveries in the Yilgarn Province of Western Australia. <i>Lascelles, D. F.</i>	127
Composition and evolution of the southern African lithosphere from combined xenocryst and magnetotelluric data <i>Özaydin, Sinan, & Selway, Kate</i>	127
Joining the dots: insights into the magmatic nickel sulphide potential of the western Gawler Craton <i>Reid, Anthony, & Pawley, Mark</i>	127
Evidence for a 3.2–3.1 Ga accretionary orogeny along the southeastern edge of the Kaapvaal Craton: a regional setting for late-stage gold mineralisation in Barberton <i>Taylor, Jeanne</i>	128
Crustal-scale controls on the evolution of the Yeneena Basin <i>Tyler, Ian, Kohanpour, Fariba, & Gorczyk, Weronika</i>	129
GEOSCIENCE IN SOCIETY, EDUCATION & ENVIRONMENT	130
Natural hazards and engineering geology	130
Tasmanian landslide fatalities and some implications for landslide risk <i>Roberts, Nicholas</i>	130
Real-time tracking of the 2019 pumice raft in the southwest Pacific <i>Jutzeler, Martin, Van Sebille, Erik, & Marsh, Robert</i>	130

Displacement of mega-boulders across and up coastal rock platforms south of Sydney, Australia, by big storm waves generated by East Coast Lows <i>Bann, Glenn, & Lau, Annie</i>	130
Structural analysis of wavecut platform structures, Shellharbour, New South Wales <i>Lennox, Paul, Goff, James, Edwards, David, & Coates, Ashlie</i>	131
Rock stress in Tasmania <i>Hills, Peter</i>	131
Structural integrity and Liesegang rings <i>Hills, Peter</i>	132
Communication for disaster prevention culture: The Cusco-PATA Case (Cusco, Peru) <i>Piscocoya, Juan Carlos, Reupo, Palmira, & Villacorta, Sandra</i>	133
Natural or green infrastructure to face the effects of extreme events, benefits and proposal of application in Chosica, Lima, Peru <i>Villacorta, Sandra, Evans, Ken, Prendes, Nicanor, Villanueva, Ignacio & Abad, Cesar</i>	133
Geoscience education	134
Coping with COVID – using virtual geological objects for on-line Earth Science Education <i>Roach, Michael, Orth, Karin, & Scott, Robert</i>	134
The real work of virtual teaching: Learnings from EESO Summer School 2021 development <i>McNamara, Greg, Almberg, Leslie, & Carr, Ruth</i>	134
Earth Science Education after 2020 <i>Blewett, Shona & Przeslawski, Rachel</i>	134
100 iconic rocks for a proof-of-concept display at the National Rock Garden <i>Pillans, Brad</i>	135
Geology comes alive for high school students with fieldwork near Yass, NSW <i>Price, Colin, Bradshaw, Marita, & Smith, Mike</i>	135
How do we attract the next generation of Earth Scientists? <i>Selway, Kate, Condon, Jo, Przeslawski, Rachel, Tiddy, Caroline, Underwood, Narelle, & Cohen, David</i>	136
Geoscience education challenges and opportunities – an industry perspective <i>Terry, Jillian</i>	136
Supporting the 3 Rs of earth science education – rocks, relevance and rapture! <i>Meakin, Simone, & Filan, Susan</i>	136
Squiggly lines, mountains, organised chaos or Forrest Gump. What is the image of a geoscience career? <i>Tiddy, Caroline, Andrahannadi, Upekha, Perera, Sanjeewa, & Sardeshmukh, Shruti</i>	137
Gamification – A pathway into Earth Science and Resources career awareness <i>Urbaniak, Suzy</i>	137
Integrative geologic event class activity: a case for Taal Volcano Eruption of 2020 in the Philippines <i>Emralino, Francis & Emralino, Blaisie</i>	138
In Australasia, gender is still on the agenda in geosciences <i>Handley, Heather, Hillman, Jess, Finch, Melanie, Ubide, Teresa, Kachovich, Sarah, McLaren, Sandra, Petts, Anna, Purandare, Jemma, Foote, April, & Tiddy, Caroline</i>	138
Geotourism: enriching the visitor experience	139
Immersive virtual reality in geotourism <i>Raimondo, Tom</i>	139
Augmenting the geotourism experience through new digital technologies <i>Robinson, Angus M., James, Pat, & Ng, Young</i>	139
Geotales and geotrails – collaborative geotourism initiatives and implications for new visitor experiences in regional NSW <i>Fleming, Guy, & Boyd, Ron</i>	140
Building the Darwin City Geotrail. Reflections, experiences and lessons <i>Asendorf, Mark</i>	140
Larapinta Trail, Tjoritja/West MacDonnell National Park, central Australia – a potential geotrail <i>Weisheit, Anett</i>	140
Geological logging of a proposed 305-km recreational geotrail in SE Queensland <i>D'Arcy, Bill, & Winter, George</i>	141
Telling the Earth's stories <i>Boswell, Russell</i>	141
Geotourism in Tasmania <i>Vicary, Mike, Cumming, Grace, & Bottrill, Ralph</i>	142

Driving Australia's National Geotourism Strategy through the AGC <i>Robinson, Angus</i>	142
Myths and perceptions about Geoparks in Australia challenged <i>Briggs, Alan</i>	143
The Murchison GeoRegion – A Potential Aspiring Geopark, Western Australia <i>Dowling, Ross</i>	143
Geoheritage and geoconservation	144
Three decades of geoconservation in retrospection <i>Díaz-Martínez, Enrique, & Brocx, Margaret</i>	144
Geoheritage significance of the deltas of the Pilbara Coast, northwestern Australia <i>Semeniuk, T. A., & Semeniuk, V.</i>	144
Geoheritage significance of the Holocene Yanrey Delta, Pilbara Coast, Western Australia <i>Semeniuk, V., & Brocx, M.</i>	145
Geoconservation of ancient Pilbara stromatolite fossils as a multifunctional landscape <i>Fletcher, Clare, Van Kranendonk, Martin J., Metternicht, G., & Walter, M. R.</i>	145
Geoheritage values of Beenypup Swamp, in the Yellagonga Regional Park, Western Australia <i>Unno, Joy</i>	146
The status of geoheritage and geoconservation in Australia <i>Cresswell, Ian</i>	146
A geoheritage treasure – a case study of the Hornsby Diatrema <i>Semeniuk, T. A.</i>	146
Recognising and preserving mineral diversity: An updated catalogue of type mineral specimens in Victoria's State collections <i>Oskar Lindenmayer</i>	146
Patina: a microscopic feature of palaeo-environmental and geoheritage significance <i>Clifford, Penelope, & Semeniuk, Vic</i>	147
Geoheritage significance of three contiguous Holocene wetlands 161, 162 and 163 in the Becher Wetland Suite, southwestern Australia <i>Semeniuk, Christine, & Semeniuk, Vic</i>	147
Six disused quarries tell of a much earlier Canberra geoheritage story <i>Finlayson, Douglas</i>	148
Geological Surveys now and into the future	148
Mapping the geology that matters – the role of Australia's geological surveys in supporting mineral discovery in the 21st century <i>Yeats, Chris</i>	148
How the GSNSW is helping to preserve data from the NSW infrastructure boom <i>Adewuyi, David</i>	148
Enhancing NSW statewide geophysics with high resolution company data <i>Matthews, Sam</i>	149
The urban geochemical baseline of Canberra: does it provide dirt on criminals? <i>Aberle, Michael, de Caritat, Patrice, McQueen, Ken, & Hoogewerff, Jurian</i>	149
EARTH OBSERVATIONS & MODELS	151
Data-driven and computational methods to reveal hidden or changing surfaces	151
Bayesian inversion of 3D groundwater flow within the Sydney-Gunnedah-Bowen Basin <i>Mather, Ben, Müller, Dietmar, O'Neill, Craig, & Moresi, Louis</i>	151
Mapping subglacial sedimentary basin distribution in Antarctica using Random Forest method <i>Li, Lu, Aitken, Alan, Lindsay, Mark, & Jessell, Mark</i>	151
The AuScope Geochemistry Network and AusGeochem <i>Dalton, Hayden, Prent, Alexander M., Boone, Samuel C., Florin, Guillaume, Greau, Yoann, McInnes, Brent I. A., Gleadow, Andrew, O'Reilly, Suzanne Y., Kohn, Barry P., Matchan, Erin L., Alard, Olivier, Rawling, Tim, Kohlmann, Fabian, Theile, Moritz, & Noble, Wayne</i>	151
Resolving multidisciplinary challenges of seamless integration of data on people, business, and the environment through applying a Discrete Global Grid System Framework <i>Crossman, Shane</i>	152
FAIR Metadata as a tool for consistent data findability and access <i>Bastrakova, Irina</i>	152

Building foundation spatial data <i>Crossman, Shane</i>	153
Digital regolith mapping from integrated sources of LiDAR data and historical imagery – a case study in Hong Kong <i>Hou, Wenzhu, Tsui, Wing Sum Regine, & Hart, Jonathan Roy</i>	153
Parallel coordinate visualisations for knowledge generation in the geosciences <i>Reading, Anya, Morse, Peter, & Staal, Tobias</i>	154
Geophysical inversion through ensemble optimization <i>Scheiter, Matthias, Valentine, Andrew, & Sambridge, Malcolm</i>	154
Data-driven tectonic regionalization of Antarctica: appreciate the similarity <i>Stål, Tobias, Reading, Anya M., Cracknell, Matthew J., Halpin, Jacqueline A., Latto, Rebecca B., Morse, Peter E., Turner, Ross J., & Whittaker, Joanne M.</i>	155
Compressive inversion in an overcomplete basis <i>Turunçtur, Buse, Valentine, Andrew, & Sambridge, Malcolm</i>	155
Detrital zircon facies of the Amadeus Basin, central Australia <i>Verdel, Charles</i>	155
Next generation 3D geological modelling – development and applications	155
LoopStructural 1.0: Time aware geological modelling <i>Grose, Lachlan, Ailleres, Laurent, Laurent, Gautier, & Jessell, Mark</i>	155
LoopResources – reducing the mining footprint <i>Ailleres, Laurent, Grose, Lachlan, Caumon, Guillaume, & Jessell, Mark</i>	156
Reproducible 3D model construction using <i>map2loop</i> <i>Jessell, Mark, Ogarko, Vitaliy, Lindsay, Mark, Joshi, Ranee, Piechocka, Agnieszka, Grose, Lachlan, de la Varga, Miguel, Fitzgerald, Des, Aillères, Laurent, & Pirot, Guillaume</i>	156
Propagation of data and algorithmic uncertainty based on borehole calibration and perturbation – a sensitivity analysis <i>Pirot, Guillaume, Lindsay, Mark, Grose, Lachlan, de La Varga, Miguel, & Jessell, Mark</i>	157
Morphological gravity inversion to refine geological models <i>Giraud, Jeremie Eugene Cyril, Lindsay, Mark, & Jessell, Mark</i>	157
LoopStructural 1.0: Time aware geological modelling <i>Grose, Lachlan, Ailleres, Laurent, Laurent, Gautier, & Jessell, Mark</i>	158
Automated subsampling of geological maps as inputs of 3D geological multiscale modelling: Yalgoo–Singleton Greenstone Belt example <i>Joshi, Ranee, Jessell, Mark, Lindsay, Mark, & Ivanic, Tim, J.</i>	158
The New South Wales 3D wireframe model <i>Spampinato, Giovanni</i>	159
A new approach to integrate passive seismic HVSR depth models in magnetotelluric (MT) 1D inversion to characterize the cover-basement interface <i>Suriyaarachchi, Nuwan, Giraud, Jeremie, Seille, Hoel, Jessell, Mark, Lindsay, Mark, Hennessy, Lachlan, & Ogarko, Vitaliy</i>	159
IAN MCDUGALL SYMPOSIUM	161
Timescale of events around the Cretaceous–Paleogene Boundary: Links between the Chicxulub impact, Deccan volcanism, and the Cretaceous–Paleogene mass extinction <i>Sprain, Courtney J., Renne, Paul R., Clemens, William A., Wilson, Gregory P., Self, Steve, Vanderkluyzen, Loys, Pande, Kanchan, Fendley, Isabel, & Mittal, Tushar</i>	161
Bitterroot and Anaconda Core Complexes: Cretaceous ductile flow and Eocene detachment faulting in the northern U.S. Rocky Mountains defined by Ar/Ar thermochronology <i>Foster, David A.</i>	161
⁴⁰ Ar/ ³⁹ Ar geochronology of syn-kinematic phengite reveals the tectonic history of underthrust European crust (W Alps): a synthesis <i>Yann, Rolland</i>	162
High resolution ⁴⁰ Ar/ ³⁹ Ar geochronology in continental margin settings – the Aegean plate margin as a natural laboratory for subduction processes <i>Wijbrans, Jan, Uunk, Bertram, de Paz Álvarez, Manuel, Huybens, Rosanne, & Brouwer, Fraukje</i>	162
Sub-solidus replacement of rapakivi textures during high-temperature potassium metasomatism of the Mannum Granite <i>Goswami, Naina, Forster, Marnie, Reid, Anthony, & Lister, Gordon</i>	162
The implications of muscovite sub-spectra in phengitic white mica on the theory and practice of argon geochronology	163

<i>Forster, Marnie, & Lister, Gordon</i>	
Hydrous polymetamorphic crustal rocks in an eclogite-bearing terrane record post-peak recrystallisation during arc–continent collision	164
<i>Brown, Dillon, Hand, Martin, & Morrissey, Laura</i>	
Evaluation of the $^{40}\text{Ar}/^{39}\text{Ar}$ technique for kimberlite geochronology: three case studies from Finland	164
<i>Dalton, Hayden, Phillips, David, Matchan, Erin, Giuliani, Andrea, Hergt, Janet, Maas, Roland, Woodhead, Jon, & O'Brien, Hugh</i>	
The KBS Tuff Controversy fifty years on: new ultra-precise ages for the KBS tuff and correlates, Omo-Turkana Basin, Kenya	165
<i>Phillips, David, & Matchan, Erin</i>	
Dating the timing of motion in major ductile shear zones	165
<i>Lister, Gordon, & Forster, Marnie</i>	

ARGA SYMPOSIUM **167**

Regolith and landscape evolution **167**

Australia and Brazil: contrasting weathering and erosion histories but similar cratonic landscapes	167
<i>Vasconcelos, Paulo</i>	
A fresh look at the stratigraphy of the Lefroy Palaeodrainage System, Eastern Goldfields, WA	167
<i>Lynham, Leah</i>	
(U–Th)/He-dating of iron oxides: Towards establishing a temporal framework for landscape evolution and regolith development in southwest Western Australia	168
<i>Wells, M. A., González-Álvarez, I., & Danišik, M.</i>	
Mapping landscape domains in Western Australia: developing a tool to link geology, geochemistry and landscape variability at large scales	168
<i>González-Álvarez, I., Albrecht, T., Klump, J., Pernreiter, S., Heilbronn, K., & Ibrahimi, T.</i>	

Planetary regolith and regolith in mineral exploration **169**

Martian regolith: from cryolithosphere to atmosphere	169
<i>Caprarelli, Graziella</i>	
Inverted Hunder dune swales, Ladakh, India	169
<i>Clarke, J. D. A., & McGuirk, S</i>	
Regolith-hosted ferrihydrite: a forgotten sorbent in the search for REEs?	171
<i>Bamforth, Tobias, Tiddy, Caroline, Gonzalez-Alvarez, Ignacio, Whittaker, Eric, & Faulkner, Leon</i>	
Hydrogeochemistry to explore the Georgina Basin's phosphate potential	171
<i>Schroder, Ivan, & de Caritat, Patrice</i>	

Mineral exploration in and through the critical zone **172**

Application of indicator minerals in mineral exploration	172
<i>Salama, Walid, Le Vaillant, Margaux, Schoneveld, Louise, Schlegel, Tobias, & Anand, Ravi</i>	
Regional cover characterisation of the Central Gawler – clipping regolith–plant associations to better constrain geology and prospectivity	173
<i>Petts, Anna, Noble, Ryan, & Reid, Nathan</i>	
Airborne electromagnetics for regional cover thickness mapping	173
<i>Roach, Ian C., Wong, Sebastian, Ley-Cooper, Yusen, Brodie, Ross C., & Wilford, John</i>	
Soil geochemistry imaging gold prospectivity in the South West Terrane of Yilgarn Craton, Western Australia	173
<i>De Souza Kovacs, Nadir, & Lu, Yongjun</i>	
Understanding the cover in the Gawler Craton, South Australia: combining landscape variability, linear structures, and regolith mapping to assist mineral exploration	174
<i>González-Álvarez, Ignacio, Krapf, Carmen, Kelka, Uli, Martínez, Cericia, Albrecht, Thomas, Ibrahimi, Tania, Pawley, Mark, Irvine, Jonathan, Petts, Anna, & Klump, Jens</i>	

PLENARY SPEAKERS

Planetary Geology, Australian's involvement in Moon to Mars

Megan Clark

Australian Space Agency

The Australian Space Agency was established by the Australian Government in July 2018 to grow and transform the national civil space sector. As outlined in the Australian Civil Space Strategy, the Agency's aim is to triple the size of the sector to \$12 billion and add up to another 20 000 jobs by 2030. Key to achieving this goal is the \$150 million Moon to Mars initiative – a partnership that will open the door for future space cooperation between the Australian Space Agency and NASA. The Moon to Mars initiative focuses on supporting Australian businesses and researchers to grow into national and international space supply chains, build space heritage, and join NASA's inspirational plan to go forward to the Moon and onto Mars. Australia has many unique strengths including exploration foundation services like remote operations and in-situ resource utilisation, advanced communications and remote medicine which puts Australia in a position of strength to apply ingenuity to space exploration in collaboration with NASA and other international counterparts. Dr Clark's presentation will explore Australia's involvement in the future exploration of the Moon and Mars and the path to getting Australian capability into space

Biography: Dr Clark is currently Head of the Australian Space Agency and a director of Rio Tinto and CSL Limited. She is a member of the Australian advisory board of the Bank of America Merrill Lynch. Dr Clark recently chaired the Expert Working Group into the Review of Australia's Space Industry Capability. She was Chief Executive of the Commonwealth Scientific and Industrial Research Organisation (CSIRO) from 2009 to 2014. Prior to CSIRO, she was a Director at NM Rothschild and Sons (Australia) and was Vice President Technology and subsequently Vice President Health, Safety and Environment at BHP Billiton from 2003 to 2008.

Dr Clark holds a BSc from the University of Western Australia and a PhD from Queen's University, Canada and is a Fellow of the Australian Academy of Technology and Engineering, a Fellow of the AusIMM and a Fellow of the Australian Institute of Company Directors. In 2014, she was appointed a Companion of the Order of Australia.

Searching for life on Mars in our own backyard, the quest for a second genesis

Martin J. Van Kranendonk

Australian Centre for Astrobiology, University of New South Wales, Kensington, NSW, Australia

Ancient life thrived on an early Earth that was a very different planet to the one we inhabit today, with green seas filled with dissolved iron, an orange sky rich in CO₂ and other greenhouse gasses, and small black volcanic protocontinents. Yet by 3.5 billion years ago “–only” 500 million years after the end of the heavy meteorite bombardment and in the oldest rocks that preserve widespread primary features at low metamorphic grade

– life had diversified into a variety of niches and employed a variety of metabolisms.

This evidence is preserved in the 3.5 billion-year-old (Ga), shallow water North Pole Chert Member of the Dresser Formation (Pilbara Craton, Western Australia), where putative biosignatures in the form of macroscopic fossil stromatolites, fractionated stable isotopes, and organic matter occurrences are widespread. These have been described from environments that include the shoreline of a shallow water caldera lake, subterranean hydrothermal veins, evaporative barite crystals, and terrestrial hot spring sinter deposits. The discovery of trapped organic matter remnants in columnar Dresser stromatolites that have a similar appearance to extracellular polymeric substances (EPS) of microbial biofilms provide compelling evidence of life. The Dresser stromatolites are unusual in being dominantly composed of nanoporous pyrite, with subordinate sphalerite and dolomite. This assemblage most likely formed via anoxygenic photosynthesis and sulfate reduction, and perhaps also microbes that cycled elemental sulfur and/or sulfide. Putative biosignatures in hot spring deposits on land at this time indicate a microbial community that may have utilised a range of different metabolisms.

The discovery of life on land in the Pilbara 3.5 Ga ago, and in the Barberton Greenstone Belt by 3.2 Ga, changes the way we think about the evolution of life over the course of Earth history and supports recent studies that suggest life may have originated in hot springs on land. Indeed, the Dresser Formation provides a deep-time analogue for better understanding an origin of life on land model.

Additionally, the Dresser Formation provides an important guide in the search for ancient life on Mars. Specifically, the discovery of ancient life signatures preserved in siliceous hot spring deposits from the Dresser Formation, combined with the increasing evidence that life may have originated in hot springs, suggests that these deposits may represent the best chance for success in the search for life on Mars, not only because of the likelihood that hot springs would have been inhabited if life ever got started on Mars but also because of the proven excellent preservation potential of these rocks over billions of years. Stratiform deposits of nodular opaline silica with digitate protrusions that were observed by the Spirit Rover in the Columbia Hills of Gusev Crater, Mars, are of probable hot spring origin and represent a tantalising astrobiological target. A sample return mission to collect these, and other nearby materials, is being developed.

Biography: Professor Van Kranendonk is the Director of the NASA-affiliated Australian Centre for Astrobiology at UNSW. His team investigates the formation mechanisms of ancient crust and the earliest signs of life on Earth and uses this to guide the search for life on Mars, and to understand the origin of life.

The Energy Transition: Implications for Geoscience – a View from the North

Murray Hitzman

Irish Centre for Research in Applied Geosciences (iCRAG)

The plenary will examine the surprisingly rapid

transition from fossil fuels in the North at the end of the first decade of the 21st century and its current and expected impact on geoscientists, geoscience education, and the public perception of geoscience. It will also discuss the potentially important implications of the energy transition for both technology development and raw materials production north and south. Finally, the role of geoscientists in the circular economy will be investigated.

Biography: Murray Hitzman holds an SFI Professorship in the School of Earth Sciences at University College Dublin and is also the Director of the Irish Centre for Research in Applied Geosciences (iCRAG). He served as Associate Director for Energy and Minerals at the U.S. Geological Survey (2016–17) and was the Charles Fogarty Professor of Economic Geology at Colorado School of Mines from 1996–2016 where a primary research focus was the geology of the Central African Copperbelt (Democratic Republic of Congo and Zambia). Dr. Hitzman served in Washington, D.C. as a policy analyst in both the White House Office of Science and Technology Policy (1994–96) during the Clinton Administration and the U.S. Senate (1993–94) for Senator Joseph Lieberman (CT). He worked in the petroleum and minerals industries from 1976 to 1993 primarily conducting mineral exploration worldwide and was largely responsible for Chevron Corporation's Lisheen Zn–Pb–Ag deposit discovery in Ireland (1990). Hitzman has B.A. degrees in geology and anthropology from Dartmouth College (1976), an M.S. in geology from University of Washington (1978), and a Ph.D. in geology from Stanford University (1983). He has previously served on the boards of a number of mineral exploration and mining companies and currently serves as technical advisor for the private company KoBold, focused on utilizing machine learning for cobalt exploration. He has received a number of awards including the Chevron Chairman's award for the Lisheen discovery (1992), the Society of Economic Geologists Silver Medal (1999), the Daniel C. Jackling Award by Society of Mining, Metallurgy, and Exploration and the Des Pretorius Award by the Geological Society of South Africa (both 2015), and the Haddon Forrester King Medal by the Australian Academy of Sciences (2016).

Engagement, diversity and interdisciplinarity to tackle future challenges

Jessica Melbourne-Thomas

CSIRO Oceans & Atmosphere

The future of the Earth and its global population holds significant challenges, particularly with respect to climate change mitigation and adaptation. Indeed, in 2020 we experienced a taste of many of the impacts to come, such as large-scale bushfire events and disruptions associated with the COVID-19 pandemic. Engaging people with science and tackling misinformation will be a key part of finding solutions to the challenges ahead. In this presentation I will discuss approaches to engagement with policy-makers, industry and the general public, including increasing needs for co-design, translation, communication and interpretation of science to tackle complex problems. I will give examples of how inter- and transdisciplinary research approaches can support robust decision-making and will discuss the importance of increased

diversity and equity in STEMM to bring novel solutions for addressing future challenges.

Biography: Dr Jess Melbourne-Thomas is a Transdisciplinary Researcher and Knowledge Broker with CSIRO Oceans & Atmosphere. Her research background is in mathematical modelling and Antarctic climate change science and she was a Lead Author for the recent IPCC Special Report on the Oceans & Cryosphere in a Changing Climate. Jess co-founded the Homeward Bound project, which took the largest ever all female expedition on a leadership journey to Antarctica in 2016. She was one of Australia's first 30 Superstars of STEM and was named Tasmania's Young Tall Poppy of the Year in 2015 for her excellence in research, science communication and policy engagement. Jess was the 2020 Tasmanian Australian of the Year.

From Core to Cosmos in a Post-COVID Earth: our opportunities and roles as geoscientists

Hill, Steve

Chief Scientist, Geoscience Australia, Canberra, Australia

The importance of trusted, high-quality and relevant geoscience to inform and advise governments and our communities is greater now than it ever has been. This is particularly the case for guiding people's connection to the Earth as the place where we live and obtain the resources we use to live our lives.

Our community's recognition of the value of geoscience, ensures the future viability and evolution of geoscience and its ability to contribute to informed impact in our region and its nations. Here we consider some of the societal impacts of the COVID-19 pandemic and the key roles that geoscience plays, in particular how our society can use data, information and knowledge of the Earth to better connect us with the Earth-system and therefore best respond to the impacts of the pandemic. Ultimately, informed decisions utilising the best geoscience data and information provides a key part of our economic, environmental and cultural recovery from the pandemic. The connection to country that comes from personal experience has been especially challenged in 2020. Much of Australia's population have been encouraged to stay in our homes, first because of major fires (the scale and intensity that we have not recorded before) and more recently in response to isolation from the COVID-19 pandemic. This has increased the importance of trusted data and information from across our nation.

This presentation highlights the value of understanding the depths of our planet and ways that geoscience governs our discovery and use of minerals, energy and groundwater resources, as well as builds resilience and adaptation to environmental and cultural change. The broad definition of geoscience here also includes the involvement of geoscience that extends to Australia's space program, including delivery of Earth observations, positioning and location data and information, such as through integrated digital mapping, satellite data and real-time precise positioning. Important here is sharing, with two-way exchange of data, information and knowledge about the Earth, through outreach in geoscience education programs and interactions with communities across Australia. An aspiration here is for geoscience to inform social

licence through evidence-based decisions, such as for land and marine access, for a strong economy, resilient society and sustainable environment.

At Geoscience Australia, we have developed a ten-year strategic plan (Strategy 2028) and Science Strategy that guides us to be a trusted source of information on Australia's geology and geography for government, industry and community decision making. This will contribute to a safer, more prosperous and well-informed Australia.

ENERGY & RESOURCES

Geophysics informing regional tectonic studies and mineral systems analysis

The tectonostratigraphic evolution of the South Nicholson region, Northern Territory and Queensland: key discoveries from the Exploring for the Future and implications for resource exploration

Carson, Chris, Henson, Paul, Lidena, Carr, Southby, Chris & Anderson, Jade

Geoscience Australia, Canberra, Australia

Proterozoic rocks of the South Nicholson region, which straddle the NT and QLD border, are juxtaposed between the Proterozoic Mount Isa Province to the east and the southern McArthur Basin to the north-west. The McArthur Basin and Mount Isa Province are comparatively well-studied and prospective for energy and mineral resources. In contrast, rocks of the South Nicholson region are mostly undercover and, as such, there is incomplete understanding of their geological evolution, relationship with adjacent geological provinces and resource potential. To address this gap, two deep crustal seismic reflection surveys, the South Nicholson and Barkly surveys (completed in 2017 and 2019, respectively), were conducted across the South Nicholson region by Geoscience Australia, under the federally funded *Exploring for the Future* (EFTF) initiative, in collaboration with the Northern Territory Geological Survey, the Geological Survey of Queensland and AuScope (e.g., Carr *et al.*, 2019, 2020). While the Barkly seismic data are still being interpreted, these seismic datasets, together with other complementary regional studies, provides an improved understanding of the geological evolution and resource potential across this poorly understood region.

Both seismic surveys targeted both suspected undercover sedimentary basins and known crustal structures to resolve regional subsurface fault geometry. A key finding from the South Nicholson seismic survey is the discovery of a large concealed sedimentary sag basin that is up to 8 km deep, around 120 km wide and 190 km from north to south, called the Carrara Sub-basin (e.g., Carr *et al.*, 2019). The sub-basin is interpreted to contain Mesoproterozoic to late Paleoproterozoic rocks equivalent to those outcropping in the Lawn Hill Platform and Mount Isa Province. The eastern end of the one of the lines (17GA-SN1), connects with a legacy seismic line that intersects the world class Pb–Zn Century deposit on the Lawn Hill Platform, the late Paleoproterozoic host rocks of which can be traced into the Carrara Sub-basin.

The South Nicholson profiles also reveal a series of ENE-trending, north-dipping half grabens which evolved during two episodes of crustal extension, at ca 1725 Ma and ca 1640 Ma, broadly coinciding with structural and basin forming events identified from the Lawn Hill Platform and the Mount Isa Province. Inversion of the half-graben bounding faults, resulting in south-verging thrusts, probably commenced during N–S crustal contraction characteristic of the early Isan Orogeny at ca 1600–1580 Ma to at least the Paleozoic

Alice Springs Orogeny (ca 400–300 Ma).

Furthermore, our comprehensive regional geochronology program proposes extensive revision of regional stratigraphic relationships. Some successions, previously mapped as Mesoproterozoic South Nicholson Group may instead represent late Paleoproterozoic successions, that form part of the highly prospective Isa Superbasin (and the broadly stratigraphic equivalent McArthur Group in the McArthur Basin), which hosts numerous viable base metal deposits and is prospective for energy commodities (e.g., Jarrett *et al.*, 2020, MacFarlane *et al.*, 2020). Our findings significantly expand the extent of highly prospective late Paleoproterozoic stratigraphy across the South Nicholson region, which, possibly, extends an as yet unknown distance west beneath the Georgina and Carpentaria basins.

Carr, L. K. *et al.*, 2019. Exploring for the Future: South Nicholson Basin Geological summary and seismic data interpretation. Record 2019/21. Geoscience Australia, Canberra. <http://dx.doi.org/10.11636/Record.2019.021>

Carr, L. K. *et al.*, 2020. South Nicholson seismic interpretation. In K. Czarnota *et al.* (Eds), Exploring for the Future Extended Abstracts, Geoscience Australia, <http://dx.doi.org/10.11636/132029>

Jarrett A. J. M. *et al.*, 2020. A multidisciplinary approach to improving energy prospectivity in the South Nicholson region. In K. Czarnota *et al.* (Eds), Exploring for the Future Extended Abstracts, Geoscience Australia, <http://dx.doi.org/10.11636/134164>

MacFarlane, S. *et al.*, 2020. A regional perspective of the Paleo- and Mesoproterozoic petroleum systems of northern Australia. In K. Czarnota *et al.* (Eds), Exploring for the Future Extended Abstracts, Geoscience Australia, <http://dx.doi.org/10.11636/133716>

Review of Australian Mesoproterozoic basins: geology and resource potential

Anderson, Jade, Carr, Lidena, Henson, Paul, & Carson, Chris

Geoscience Australia, Canberra, Australia

Australian cratons underwent substantial tectonism and cratonic reorganisation during the Meso-proterozoic, coinciding globally with the transition from Nuna to Rodinia (e.g., Li *et al.*, 2008, Pisarevsky *et al.*, 2014). The full extent and nature of this tectonism remains contentious (e.g., Bagas, 2004, Betts & Giles, 2006, Cawood & Korsch, 2008, Maidment, 2017).

During the Mesoproterozoic several sedimentary basin systems were deposited, and are now variably preserved, in the Northern Territory, Queensland, Western Australia, South Australia and Tasmania, providing an invaluable indirect record of the evolving Australian lithosphere and tectonic processes. Most of these basins were deposited on or at the margins of Archean to Paleoproterozoic cratons (North Australian Craton, West Australian Craton and South Australian Craton, e.g., see Myers *et al.* 1996, Cawood & Korsch, 2008 for spatial geography and constituents of these cratons). The remnants of these basins vary from weakly-deformed, relatively continuous units, such as the Roper Group of the McArthur Basin in the Northern Territory, to basins that were subsequently deformed and metamorphosed under high grade conditions, such as the Arid Basin of the Albany Fraser Orogen in Western Australia.

Individual basins are typically studied in isolation or in subsets, for which available geological datasets are commonly disparate with markedly different levels of

knowledge. Mineral and energy resources have been identified in some of these basins, including oil and gas resources hosted in the Roper Group in the Beetaloo Sub-basin, manganese deposits in the Collier Basin and Manganese Group (Western Australia), and polymetallic, stratabound, hydro-thermal mineralisation in the late Paleoproterozoic to early Mesoproterozoic Edmund Basin (Western Australia). Typically, these more overtly prospective basins, or groups, have been studied in greater detail than other Mesoproterozoic basins or groups.

This study provides a holistic overview of Australian Mesoproterozoic sedimentary basin systems, integrating geological, geochronological, and publically available resource data. As part of this collated approach, we also discuss potential inter-basin correlations for Mesoproterozoic-aged successions in Australia. This study aims to assist future work targeted at improving the geological understanding of these Mesoproterozoic sedimentary provinces and their resource prospectivity.

- Bagas, L., 2004. Proterozoic evolution and tectonic setting of the northwest Paterson Orogen, Western Australia. *Precambrian Research* 128(3–4), 475–496.
- Betts, P. G. and Giles, D., 2006. The 1800–1100 Ma tectonic evolution of Australia. *Precambrian Research* 144(1), 92–125.
- Cawood, P. A., & Korsch, R. J., 2008. Assembling Australia: Proterozoic building of a continent. *Precambrian Research* 166(1–4), 1–38.
- Li, Z. X., Bogdanova, S. V., Collins, A. S., Davidson, A., De Waele, B., Ernst, R. E., Fitzsimons, I. C. W., Fuck, R. A., Gladkochub, D. P., Jacobs, J., Karlstrom, K. E., Lu, S., Natapov, L. M., Pease, V., Pisarevsky, S. A., Thrane, K., & Vernikovsky, V., 2008. Assembly, configuration, and break-up history of Rodinia: A synthesis. *Precambrian Research* 160(1–2), 179–210.
- Maidment, D. W., 2017. Geochronology from the Rudall Province, Western Australia: implications for the amalgamation of the West and North Australian Cratons. Geological Survey of Western Australia, Perth, 95 pp.
- Myers, J. S., Shaw, R. D., & Tyler, I. M., 1996. Tectonic evolution of Proterozoic Australia. *Tectonics* 15(6), 1431–1446.
- Pisarevsky, S. A., Elming, S.-Å., Pesonen, L. J., & Li, Z.-X., 2014. Mesoproterozoic paleogeography: Supercontinent and beyond. *Precambrian Research*, 244, 207–225.

Reconstructing the Soldiers Cap Group–Kuridala Group basin: implications for BHT and IOCG mineralisation

Connors, Karen

Sustainable Minerals Institute, The University of Queensland, Brisbane, Australia

The vast basin hosting the 1700–1650 Ma Soldiers Cap and Kuridala groups (SCG-KG), eastern Mount Isa Province, NW Queensland, extends >300 km east to include the ca 1700–1610 Ma Etheridge Group, Georgetown Inlier. The present-day extent and thickness represent only part of the original depo-centre following inversion, uplift and erosion (1610–1500 Ma). Whilst the importance of extension has long been recognised, pervasive compression, voluminous 1535–1490 Ma granites, and limited seismic integration, has prevented elucidation of the extensional architecture and its influence on inversion and mineral systems. Integrated interpretation of seismic and potential field data, and review of geochronology has provided a new understanding of the extensional architecture, potential age range and thickness of the basin, and the tectonic evolution.

The preserved thickness, extent, age range, erosion estimates, and the crustal architecture provide first-order constraints on basin reconstruction. The SCG-KG basin overlies several crustal-scale boundaries, including the Gidyea Suture where the thinned eastern margin of the poorly reflective, Mount Isa crust is thrust over the thinner Numil crust. The Numil comprises a series of moderate to low-angle fault blocks, many only 5–15 km thick, and typically has pervasive, dipping reflections.

While outcrop mapping suggests the SCG group is 2–5 km thick, seismic data indicates 3–5 sec TWT, implying 12–15 km preserved thickness. Mapping indicates localised isoclinal folding, nappes and structural repetition within some highly deformed zones. Although regional structural repetition can't be ruled out, the seismic data suggests many areas are dominated by limited repetition and thickening on inverted, normal faults.

The minimum age for the SCG-KG is generally accepted as 1650 Ma. However, the 1650–1610 Ma units of the Tommy Creek Domain and Etheridge Group are likely to have been widespread across the basin. In addition, zircon populations from drainages along the eastern outcrop margin and SCG show peaks in juvenile mafic magmatism at 1630–1625 Ma, as well as 1667 Ma. Although the upper SCG-KG unit (Toole Creek Volcanics (TCV)) is attributed to thermal relaxation from ca 1670 Ma, coeval felsic and mafic magmatism at 1655 and 1625 Ma, and the large volume (20–30%) of high-Fe mafic sills within the TCV suggest extension continued or was episodic.

Prior to inversion and erosion, the 12–15 km SCG-KG basin was thicker as well as wider than the present ~350 km. While the stretching factor and total extension are unknown, the thin low-angle fault blocks of the Numil, are consistent with highly thinned to hyperextended crust (i.e., 10 km thickness or less), and exhumation of lower crust or mantle may have occurred. The resulting high geothermal gradient has implications for BHT mineralisation and raises questions regarding controls on metal deposition.

The extensional fault system and preliminary reconstruction provide insights into the extensional evolution and controls on later inversion. The structural framework and its links to the underlying basement blocks and crustal-scale structures that form the first-order conduits of the plumbing system provide insights for both syn-sedimentary BHT mineral systems and later IOCG deposits.

Mapping the near surface architecture of the Amadeus Basin using magnetic data: Petrophysical properties and geophysical pitfalls

Austin, James¹, Schmid, Susanne² & Foss, Clive¹

¹*Potential Fields Geophysics, CSIRO Mineral Resources, Lindfield, NSW 2070;* ²*Multidimensional Geoscience, CSIRO Mineral Resources, Kensington, WA 6151*

The Amadeus Basin in central Australia is prospective for stratiform base metal deposits and hydrocarbons. The Basin displays subtle magnetic anomalies that trace strata for considerable distance, highlighting complex folding patterns. Magnetic modelling

techniques can be utilised on these stratiform anomalies to extrapolate the near-surface structure of the basin. Generally magnetic anomalies are assumed to have predominantly induced magnetisation, and with this assumption dip can be reasonably estimated using magnetic data alone. However, where the magnetisation is not purely induced (i.e., includes remanent magnetisation) the mathematical trade-off between the dip and magnetisation of bodies means that the dip of a body cannot be known unless the magnetisation is also known. Normally it would be optimal to measure the magnetisation, but this is not always possible or feasible, e.g., due to land access issues. In this study, we investigate the relationships between dip and magnetisation using an approach that would generally be considered a little backward. Rather than constrain structure using petrophysics, we use structural geology to constrain petrophysics. Three study areas were chosen to investigate numerous stratigraphic horizons in three major study areas, the Waterhouse Range, Glen Helen Station and Ross River areas. Modelling results suggest that a paucity of layers retain predominantly induced magnetisation, remanence is dominant in some, but both induced and remanent magnetisation are typically present. Remanence is mainly associated with relatively oxidised units that contain only hematite (e.g., Arumbera Sandstone), and comparisons with known apparent polar wander paths suggest that these magnetisations pre-date major folding in the basin. In some cases, magnetic anomalism reflects redox zonation within units, e.g., the Pertatataka Formation near Glen Helen, where discrete magnetic layers coincide with thin grey (reduced, magnetite-rich) horizons interbedded with more prevalent red (oxidised, hematite-rich) horizons, which are only very weakly magnetised. We also found that where magnetised units are relatively thin and occur near the surface, their magnetic response is sharp. However, in coincident aeromagnetic data, adjacent anomalies commonly overlap to form a single anomaly, thus misrepresenting the magnetic field, and mis-mapping the dip of the magnetic horizons. This study highlights some major pitfalls in attempting to map structure using magnetics. Near surface sedimentary units tend to be variably oxidised, and their petrophysical properties are inconsistent along strike. Their total magnetisation is commonly comprised of a significant component of remanent magnetisation, and therefore due to the mathematical trade-off between dip and magnetisation direction, industry standard inversions will commonly mis-map surface structure. Remanent magnetisation pre-dates major folding in many cases therefore, opposite limbs of the same fold can have completely different magnetic signatures. Our ability to target mineral systems in sedimentary systems is contingent on our ability to map the structure of such systems. This study demonstrates that petrophysical knowledge is a pre-requisite constraint for successfully informing structural and tectonic studies using geophysics.

Lithospheric-scale magnetotellurics over the Eastern Goldfields Superterrane, Yilgarn Craton

Selway, Kate¹, Dentith, Michael², & Gessner, Klaus³

¹Department of Earth and Environmental Sciences, Macquarie University, Australia; ²Centre for Exploration

Targeting, School of Earth Sciences, The University of Western Australia, Crawley, WA 6009, Australia; ³Geological Survey of Western Australia, East Perth, WA 6004, Australia

The Eastern Goldfields Superterrane, in the Yilgarn Craton, Western Australia, is one of the most highly mineralised regions on Earth, hosting world-class orogenic gold and nickel-sulfide deposits. Mineral systems models for both of these deposit types suggest that lithospheric-scale processes are involved in their formation. Therefore, lithospheric-scale geophysical imaging is a promising tool to improve understanding of the formation of the deposits and to aid future exploration.

Long-period magnetotelluric (MT) data were collected over an approximately 250 km x 200 km area covering the western part of the Eastern Goldfields Superterrane and the eastern Youanmi Terrane. The survey region covers the Kalgoorlie and St Ives gold camps and the Kambalda nickel camp, as well as the Ida Fault, a prominent isotopic boundary between the older Nd model ages of the Youanmi Terrane and the younger Nd model ages of the Eastern Goldfields Superterrane. A 3D conductivity model was produced from the data, with good resolution to depths of 150 to 200 km.

Results show that the lithospheric mantle from depths of approximately 100 to 150 km is more conductive (~10 to 100 ohm m) beneath the Youanmi Terrane than the Eastern Goldfields Superterrane (>100 ohm m). Crustal conductivity is more heterogeneous, but most of the strongly conductive regions (<100 ohm m) are located in the Eastern Goldfields Superterrane. The resolution of the model in the near-surface is insufficient to make a detailed comparison with the locations of known deposits, but most upper crustal conductors are spatially correlated with regional-scale faults, which are inferred to be important in the formation of orogenic gold deposits.

Anomalously conductive zones in tectonically stable regions often indicate past metasomatism, either through the hydration of nominally anhydrous minerals or the growth of conductive mineral phases such as amphibole or phlogopite.

Quantitative interpretation of the MT model shows that the mantle conductors in the Youanmi Terrane are too conductive to be explained purely by hydrated peridotite and imply the presence of hydrous metasomatic minerals. The observed patterns of lithospheric conductivity suggest a more complex relationship between mantle metasomatism and gold and nickel mineral systems than expected from previous studies.

Interpreting and validating trans-lithospheric faults in the Central Andes to investigate their control on the localisation of giant porphyry copper deposits

Farrar, Alexander^{1,2}, Cracknell, Matthew¹, Cooke, David¹, Hronsky, Jon^{3,4}, & Piquer, Jose⁵

¹University of Tasmania, Hobart, Australia; ²First Quantum Minerals, Santiago, Chile; ³Western Mining Services, Perth, Australia; ⁴University of Western Australia, Perth, Australia; ⁵Universidad Austral de Chile, Valdivia, Chile

The central Andes (between latitudes of 14°S and 35°S)

accounts for approximately 40% of the world's annual copper production and is the most important copper province on the planet. However, since 1998, just one giant porphyry copper greenfield discovery has been made in the central Andes. Post-mineralisation cover consisting of transported gravels and young volcanics make up at least 50% of the surficial outcrop of the central Andes and of the 60 or so known giant Cu ±Au ±Mo deposits, only three giant ore deposits have been discovered beneath these surficial materials in the greenfields domain. Therefore, it is likely that many concealed, undiscovered giant porphyry copper deposits are waiting to be discovered. However, no proven effective exploration process exists that enables explorers to consistently achieve economic greenfield discoveries through cover.

Giant porphyry copper deposits tend to cluster in discrete geographic “camps” of a similar age. This indicates that exceptional transient geologic processes have affected localised regions of the crust prior to and during the age of mineralisation and that the formation of giant porphyry deposits is non-random. Key predictive geological features of giant porphyry Cu deposits are the structural pathways (basement faults) that focus fluid and magma flow from the mantle to upper crust. Nevertheless, these so called trans-lithospheric faults (TLFs) are notoriously difficult to identify in the field due to their subtle surficial characteristics, complex multi-stage reactivation history and continental-scale. As a result, the notion of TLFs has, until recently, been treated with scepticism by many in the geologic community.

This research focuses on identifying and mapping the continental-scale trans-lithospheric structural architecture of the central Andes through the integration and interpretation of multiple geoscience datasets supported by field observations. Datasets used in this analysis include geophysical inputs such as airborne magnetics, regional gravity, magnetotellurics and seismic epicentres as well as geologic reconstructions through time from the Proterozoic to present, which map out inherited basement architecture as well as regions of rapid crustal thickening or thinning. Fieldwork undertaken in the regions of the interpreted TLFs demonstrates that on the surface they are expressed as linear zones of brittle faulting, tens of kilometres wide and hundreds of kilometres long, consisting of thousands of individual fault planes. This is interpreted to reflect the upper crustal propagation of the underlying zone of basement weakness through younger sequences in the geologically active convergent plate margin.

A map of the TLFs across the central Andes shows that the TLFs have a fractal distribution with N, NW and NE strikes. A prominent relationship exists with the location of known giant porphyry deposit camps occurring where two or more TLFs meet. Such regions are inferred to have been loci of deep-seated strain-anomalies which have localised dilation and increased permeability, during transient changes to the regional stress field. Regions adjacent to the intersection of two or more TLFs that overlap with the magmatic arc during metallogenic epochs (themselves transient geodynamic anomalies) are deemed to represent valid exploration targets in this model.

Mineral systems of the Capricorn Orogen through time

Occhipinti, Sandra¹, Metelka, Vaclav¹, Lindsay, Mark², & Aitken, Alan²

¹CSIRO, Kensington, Australia; ²Centre of Exploration Targeting, University of Western Australia, Crawley, Australia

Opening up greenfields regions for minerals exploration programs is best facilitated through the understanding of regional minerals prospectivity. The Capricorn Orogen is a greenfields-dominated region, for which a multicommodity mineral systems analysis has been completed forming the basis for new prospectivity analysis and mapping. Known mineral occurrences or deposits in the region formed between the Paleoproterozoic and Neoproterozoic. Mineralisation can be related to basin development and orogenesis in the region, in turn related to periods of supercontinent assembly and breakup. These were manifested in the region through the contractional 2005–1950 Ma Glenburgh, 1830–1780 Ma Capricorn, and ca 1030–950 Ma Edmondian and 920–850 Ma Kuparr orogenies. These periods of orogenesis were preceded and interspersed with periods of subsidence, perhaps including the 1680–1620 Mangaroon Orogeny, which led to the development of volcanosedimentary and sedimentary basins throughout the region. Prospectivity models were generated for several commodity groups of various ages and ore genesis mechanisms, including combinations of Ni, Cu, PGEs, V, Ti, Au, Pb, Zn, channel Fe and U. The work has found a link between key mineral systems and a spatial relationship between disparate styles of mineral deposits in the region. Crustal-scale tectonic architecture was analysed by allying a 2D map view geological-geophysical interpretation with 2.5D magnetic and gravity joint inversions of selected profiles, a 3D Moho model, and by inference from 2D and 3D magnetotelluric models, 2D reflection seismic images and 3D passive seismic models from the region. This work clearly illustrates that different ‘zones’ of the Capricorn Orogen are prospective for different commodity groups due to the tectonic environment in which they developed. Major crustal-scale deformational zones intrinsically control the location of known ore deposits in the area and are inferred to be sites of fluid migration associated with ore deposition. Of these, some are considered to be of Archean origin, whereas others are thought to have first developed during the early Paleoproterozoic. In both cases, many structures have been re-activated through time, influencing the formation of basins over them and perhaps the formation of ore deposits.

Unravelling the “late” evolution of the Gawler Craton: high T/P metamorphism, tectonism and magmatism of the Yorke Peninsula, South Australia

Bockmann, Mitchell^{1,2}, Hand, Martin^{1,2}, Morrissey, Laura^{3,1}, Payne, Justin^{4,3,1}, Teale, Graham⁵, Conor, Colin⁴, & Dutch, Rian^{6,2}

¹Departments of Earth Science, University of Adelaide, Adelaide, Australia; ²Mineral Exploration Cooperative Research Centre, University of Adelaide, Adelaide, Australia; ³Mineral Exploration Cooperative Research

Centre, Future Industries Institute, University of South Australia, Adelaide, Australia; ⁴UniSA STEM, University of South Australia, Adelaide, Australia; ⁵Teale and Associates Pty Ltd, Prospect, Australia; ⁶Department for Energy and Mining, Geological Survey of South Australia, Adelaide, Australia

The early Mesoproterozoic is a geologically active time in the Gawler Craton, recording widespread magmatism, deformation, metamorphism and mineralisation. Much of this activity occurs within the time period of 1600–1575 Ma, during the Hiltaba tectonothermal event and associated the worldclass Iron-oxide–Copper–Gold (IOCG) mineralisation, which has focussed attention on this timeline. This event has often been considered the timing of ‘cratonisation’ as there was perceived to be little tectonic activity that post-dates this timeline. However, sporadic evidence across the Gawler Craton for metamorphism, deformation and minor magmatism post-dating this major event has indicated tectonic activity extends beyond this age. This study further highlights the importance and extent of post-1575 Ma activity in defining the modern-day structural and metamorphic architecture of the Gawler Craton.

The Yorke Peninsula in the southern Gawler Craton is a highly prospective region for IOCG mineralisation, as it hosts the historically significant Moonta and Wallaroo mines and more recently discovered Hillside deposit. Despite extensive evidence for early Mesoproterozoic hydrothermal fluid activity and great potential for mineralisation, the Yorke Peninsula is incredibly understudied with modern analytical techniques.

Here we present evidence for high T/P metamorphism from the Yorke Peninsula at ca 1555 Ma, with peak metamorphic constraints of ~ 3.5 kbar, 660 °C and ~4.2 kbar, 700 °C from two samples taken approximately 35 km apart. In addition, monazite U–Pb geochronology also provides evidence for shear zone activation at this time, along with possible evidence for re-activation of the Pine Point Fault as young as 1500 Ma, significantly post-dating mineralisation at the Hillside deposit. Apatite U–Pb cooling ages from these rocks provide relatively young ages between 1460–1400 Ma, indicating that these rocks remained at elevated temperatures for an extended period following the metamorphic peak, supporting a long-lived thermal driver for metamorphism. The record of this post-Hiltaba event is also manifest in published monazite and zircon ages from the Barossa Complex on the Fleurieu Peninsula, signifying that this event impacted the entire southeastern Gawler Craton. The metamorphic conditions and prolonged time at depth indicated by relatively young apatite U–Pb cooling ages from the Yorke Peninsula are consistent with thinned continental crust, implying that the southeastern Gawler Craton was in an extensional setting after the Hiltaba Event. Post-Hiltaba activity is distinct from metamorphism and deformation associated with the Hiltaba Event, which is also recorded within the southeastern Gawler Craton, but typically with lower thermal gradients. The metamorphism reported in this study has long been assumed to be linked to the Hiltaba Event, along with much of the Mesoproterozoic magmatism, deformation and mineralisation on the Yorke Peninsula. This study reveals that the ca 1515 Ma Spilsby Suite is not the only expression of post-Hiltaba activity on the Yorke Peninsula and

demonstrates that the thermal and tectonic footprint of post-Hiltaba events is much greater than previously interpreted, suggesting that some of the mineralisation hosted within the region (e.g., Moonta-Wallaroo) may also be post-Hiltaba, with evidence for potential thermal drivers, fluid sources and deformation in operation after this time.

How to computationally include regional interpretations into the seismic imaging process

Rashidifard, Mahtab^{1,3}, Giraud, Jérémie^{1,3}, Ogarko, Vitaliy^{1,2}, Lindsay, Mark^{1,3}, & Jessell, Mark^{1,3}

¹Centre of Exploration Targeting (School of Earth Sciences), University of Western Australia, 35 Stirling Highway, Crawly, WA 6009, Australia; ²International Centre for Radio Astronomy Research (ICRAR), University of Western Australia, 7 Fairway, Crawly, WA 6009, Australia; ³Mineral Exploration Cooperative Research Centre, School of Earth Sciences, University of Western Australia, 35 Stirling Highway, WA Crawley 6009, Australia

Understanding the regional evolution of the Earth and subsurface processes is a key for mineral exploration. Crucial to this understanding is accounting for geoscience knowledge obtained from integrated interpretation of geological and geophysical data. Reflection seismic data, although sparsely distributed due to the high cost of acquisition, is the only data that gives a high-resolution image of the crust to reveal deep subsurface structures and the architectural complexity that may vector attention to minerally prospective regions. Without an iterative depth migration and a depth conversion step, seismic images remain in time domain and are totally data-driven. However, for reconstructing the architecture and history of the area it is necessary to have these images in depth. To obtain the depth of seismic events, depth correlations need to be applied to them from other sources of information. The limitation here is that existing depth conversion methods rely on borehole information which is rarely available for deep crust studies.

We introduce a new methodology which allows inclusion of deep regional interpretations from potential field and geological sources of information in depth migration of seismic data. This fast algorithm aims at reducing the ambiguity in time-to-depth conversion and reduce the time spent on depth migration of seismic data by numerically including geologists’ interpretations.

A modelling-ray approach, not dependent on borehole information and accounting for lateral variations in velocity models, is used for switching from a time-migrated to depth-converted domain. An imagery approach is used for the reverse process to move from a depth-migrated to a time-converted domain. On the other hand, primary geological models are directly used in potential field inversion algorithms without reparametrization of the model using an existing generalized level-set algorithm. Integrating solutions of the Eikonal equation in the form of Hamilton-Jacobi for both potential-field level-set inversion and seismic migration leads to a simultaneous modelling through which seismic, potential field, and geological data mitigate each other’s limitations. An investigation of the proposed methodology and a proof-of-concept using a

fairly advanced realistic synthetic dataset are presented.

The proposed workflow is a novel approach for questioning the geological meaning of the sparsely distributed seismic sections and to integrate them in a 3D volume following the regional geological data and potential field results. The primary outcome of this study is a step toward adding equal weight to geological data not only as primary models, but also as additional quantitative information within geophysical modelling and seismic imaging algorithms.

Our results lead to a significant improvement in the final model consistency with available sparsely distributed data sets. As a result, seismic migration is influenced by complementary information from potential field inversion results while simultaneously respecting sparse seismic sections in the 3D model obtained from regional interpretation and potential field inversion.

We acknowledge the support of the MinEx CRC and the Loop: Enabling Stochastic 3D Geological Modelling (LP170100985) consortia. The work has been supported by the Mineral Exploration Cooperative Research Centre whose activities are funded by the Australian Government's Cooperative Research Centre Programme. This is MinEx CRC Document 2020/44.

Au systems: Archean to the modern Earth

Controls on gold endowments of porphyry deposits

Chiaradia, Massimo

Department of Earth Sciences, University of Geneva, Geneva, Switzerland

Porphyry deposits are natural suppliers of ~75% copper and ~20% gold to our society. Nonetheless, gold endowments of porphyry deposits are characterized by a wide range going from a few tons to >2500 tons of gold. Here, I propose a model to explain the reasons of the large variations in metal endowments of porphyry Cu–Au deposits.

Porphyry Cu–Au deposits define two distinct trends in Au versus Cu tonnage plots: Cu-rich ($Au/Cu \sim 4 \cdot 10^{-6}$) or Au-rich ($Au/Cu \sim 80 \cdot 10^{-6}$). Cu-rich porphyry deposits are related to Andean-type subduction and typical calc-alkaline magmatism in thick continental arcs. In contrast, Au-rich porphyry deposits are associated with high-K calc-alkaline to alkaline magmatism in late to post-subduction or post-collision and extensional settings, and also with calc-alkaline magmatism. The largest Au-rich porphyry deposits are associated with high-K calc-alkaline to alkaline magmatism. Geochronological data at individual porphyry deposits suggest that gold endowments for both trends grow larger the longer the mineralization process is. However, Au is precipitated at much higher rates in Au-rich (~4500 tons Au/Ma) than in Cu-rich porphyry deposits (~100 tons Au/Ma).

Monte Carlo modelling of petrologic processes suggests that the different rates of gold precipitation in Cu-rich and Au-rich porphyry deposits most likely result from a 5–12 times better efficiency of gold precipitation in Au-rich than in Cu-rich deposits. The reason of the different efficiencies of gold precipitation is the different depths of formation of Cu-rich and Au-rich porphyry deposits which favour (deep level) or not (shallow level) a decoupling of Au and Cu precipitated from the magmatic-hydrothermal fluids. Interestingly, Au-rich porphyry deposits formed at shallower levels are also associated with magmatic rocks that have evolved at average shallower levels than Cu-rich deposits, as suggested by systematically lower Sr/Y values of the former (Au-rich systems) with respect to the latter (Cu-rich systems). Monte Carlo modelling shows that the higher gold endowments of Au-rich porphyry deposits associated with alkaline magmas require higher gold contents in the parental magmas such as those that are typical of alkaline magmas, but not of calc-alkaline ones. This suggests an additional petrogenetic control in the formation of the Au-richest porphyry deposits associated with variably alkaline magmas.

Whereas depth of porphyry formation and chemistry of magmas (alkaline versus typical calc-alkaline) seem to control the Au-rich versus Cu-rich nature of porphyry Cu–Au deposits, the correlation of the Cu and Au endowments with ore deposition duration suggests that the final Cu and Au endowments of these deposits are determined by the cumulative number of mineralizing steps that are ultimately controlled by magma volume and ore process duration. The difference is that variably alkaline systems and shallow crustal calc-alkaline

systems are inherently associated with magmas, whose fluids are tectonically (i.e., shallow emplacement) and chemically (alkaline magmas) optimized for high gold precipitation efficiency. In contrast, typical calc-alkaline (high Sr/Y) magmas form in a geodynamic context that favours enormous magma accumulations, which are necessary to produce behemothian Cu-rich deposits but are emplaced at depths at which the exsolved fluids are less efficient for gold precipitation.

Evolution of magmatic fertility for porphyry Au and Cu deposits through the prism of zircon chrono-chemistry, Balkan Peninsula, SE Europe

Ireland, Timothy¹, Bilyarska, Teodora², Bilyarski, Stoimen¹, Protic, Nenad¹, & Stefanova, Elitsa³

¹First Quantum Minerals Ltd, Vancouver, Canada; ²St Kliment Ohridski University of Sofia, Sofia, Bulgaria; ³Bulgarian Academy of Science – Geological Institute, Sofia, Bulgaria

The accreted arc terranes of the Balkan western Tethyan host a complex metallogeny that includes almost all Cu and Au mineralisation styles typical of subduction-related arcs and post-collisional settings. Broadly, magmatism in the belt began as a series of submarine arcs constructed on thinned continental basement and evolved to subaerial post-collisional magmatism during and after arc–continent collisions in the Late Cretaceous and Eocene. Each collisional event is associated with a phase of metallogenesis that changes in terms of metal budget and deposit style as collision occurs and then collapses, e.g., in the Timok and Panagjurishte districts, three phases of magmatism, each lasting 5–10 my. record a transition in space and time from sub-volcanic diorites associated with porphyry Cu–Au deposits, to more voluminous effusive andesites associated with epithermal deposit styles, and then monzonitic intrusions with a Au-dominant metal budget. The rocks from all of these three phases are the products of hydrous, intermediate magmas that yield equivalent ‘fertile-looking’ results in terms of whole rock magma chemistry proxies such as Sr/Y that explorers may use for area selection in arc environments.

A similar metallogenic progression occurs among less well-documented magmatism that occurred subsequent to the Alpine orogeny. In this case the main, early metallogenic phase is represented by porphyry and epithermal Cu–Au deposits associated with trachyandesite and monzonitic volcano-plutonic complexes. As post-collisional extension comes to dominate the regional tectonic environment the metallogeny becomes dominated by Pb–Zn in a series of ‘ore fields’ that we infer to be genetically related to syn-extensional granitoids, and thereafter by epithermal gold deposits in terrestrial grabens.

In this study we compiled all the available published whole rock chemistry and zircon chronology and chemistry for magmatic rock units associated with each of these metallogenic stages and collected new complementary data from rock samples and stream sediments. The result is a coherent record of the temporal evolution of magmas associated with each of these metallogenic stages. We observe that the detrital zircon populations are closely related to the results from

rock samples, however, we contend that the detrital record is a superior medium as it avoids sampling bias and undersampling. These detrital results were interpreted as a holistic record of the magmatism in each district. There are patterns among this zircon chronochemical evolution that correspond to consistent aspects of regional metallogeny. Short periods of zircon crystallisation (i.e., <3 my) in which zircons span a wide range of compositions suggesting both primitive and enriched or evolved source contributions tend to characterise the metallogenic events in which Au is the primary economic commodity. In contrast, more protracted zircon crystallisation history and slower evolution to fertility implied by proxies such as Eu/Eu* characterises the major porphyry Cu camps. This approach may be applicable in other terranes wherein the magmatic-metallogenic history is not well constrained.

Stability of gold nanoparticles in sulfur-bearing hydrothermal fluids: an experimental study

Liu, Weihua¹, Chen, Miao¹, Yang, Yi¹, Mei, Yuan¹, Etschmann, Barbara¹, Brugger Joël¹, & Johannessen, Bernt¹

¹CSIRO Mineral Resources, Melbourne, Australia; ²Monash University, Melbourne, Australia; ³Australian Synchrotron, Melbourne, Australia

Current theories of the gold deposit formation from hydrothermal fluids have been challenged by recent field and laboratory observations, suggesting that gold nanoparticles/colloids could be important in gold transport/deposition in ore fluids. In this study, the stability of gold nanoparticles (colloidal gold) in sulfur-bearing and citrate-bearing solutions was investigated at temperatures up to 225 °C using Synchrotron X-ray Near-edge Spectroscopy (XANES), and up to 350 °C with a visual check of colour change. The citrate-based colloidal gold solutions, with or without colloidal silica in the solution, are only stable up to 225 °C. In contrast, the gold colloids in Na₂S solutions are not stable upon heating to 150 °C, but stable up to 300 °C when 0.5–1.5 wt% of colloidal silica is present in the solution. The colloidal gold particles started to aggregate and deposit from the solution with the aggregation and growth of silica particles at 350 °C. The concentrations of gold as colloids in the solutions are up to 0.5 mmol (~95 ppm), more than three orders of magnitude higher than gold solubility as aqueous complexes under the same condition calculated based on available thermodynamic data. These results provide the first evidence that high concentrations of gold nanoparticles are stable in sulfur-bearing fluids at elevated temperatures (~300 °C). This implies that the formation of gold nanoparticles is an effective way to concentrate gold in hydrothermal sulfur-bearing fluids to form high-grade gold ores.

Lifting the cloak of invisibility: Gold in pyrite from the Olympic Dam deposit, South Australia

Ehrig, Kathy^{1,2}, Ciobanu, Cristiana³, Verdugo-Ihl, Max³, Dmitrijeva, Marija³, Cook, Nigel², & Slattery, Ashley⁴

¹BHP Olympic Dam, Adelaide, Australia; ²School of

Civil, Environmental and Mining Engineering, University of Adelaide, Adelaide, Australia; ³*School of Chemical Engineering and Advanced Materials, University of Adelaide, Adelaide, Australia;* ⁴*Adelaide Microscopy, University of Adelaide, Adelaide, Australia*

'Invisible gold' in pyrite refers to gold either present within the sulfide lattice or as discrete nanoparticle (<100 nm-diameter) inclusions (NPs), making it undetectable by conventional optical and scanning electron microscopy. Investigation of "invisible gold" in chalcopyrite-pyrite ores from the Olympic Dam Cu-U-Au-Ag deposit (one of the world's largest Au deposits) confirms the presence of Au in some arsenic-bearing pyrites at concentrations measurable by laser ablation inductively coupled-plasma mass spectrometry (LA-ICP-MS). Arsenic-bearing pyrite in the studied sample shows As-Co-Ni-oscillatory zoning patterns with variable complexity suggesting grain recrystallization during replacement by chalcopyrite. LA-ICP-MS data obtained from 164 pyrite grains plot below the Au and As solubility limit empirically defined from studies of epithermal and Carlin-type deposits.

Several As-rich pyrite grains were analyzed using Scanning Transmission Electron Microscopy (STEM) and EDX-STEM analysis of foils obtained by Focused Ion Beam methods. Micron-scale, oscillatory zoning patterns observed on back-scattered electron (BSE) images and LA-ICP-MS element maps extend down to the nanoscale. Decoupling between trace elements is common, for example Ni depletion wherever As and Co are enhanced, with nucleation of discrete Co-As-bearing NPs (cobaltite/safflorite?)

Importantly, Au-bearing NPs are identified in all cases, in intimate association with other (sulpho)tellurides. In addition, abundant cassiterite and rare chalcopyrite NPs are also identified. Some of the largest Bi-Ag-telluride NPs contain electrum as tiny pore-attached NPs within the larger telluride. Nanometer-size electrum NPs were also identified in association with chalcopyrite. Silver-Au-telluride NPs form mono- or bi-component NPs. These NPs occur along trails displaying As-Co-enrichment, or formation of nm-wide lamellae of Bi-Pb-sulpho-tellurides marking pyrite twin boundaries. One wider lamella was identified from the layer stacking as a strongly disordered member of the aleksite series. Coarser tellurobismuthite (Bi₂Te₃), a few μm-wide, is associated with altaite (PbTe) at pyrite-chalcopyrite boundaries.

Pyrite displays kink- and screw-dislocations associated with trace element remobilization or NPs nucleation. These defects can be associated with either 'marcasitization' or loss of Fe (formation of pyrrhotite), within nanoscale domains affected by fluid percolation and pyrite recrystallisation. Twin planes in pyrite enriched in heavy elements (Bi-Pb-Te) represent zones of weakness and assist element exchange between host mineral and percolating fluids during coupled dissolution reprecipitation reactions (CDRR), analogous to those known for hematite from Olympic Dam.

Nanoscale textures in pyrite allow for interpretation of Au-NPs as Au released from solid solution in pyrite during CDRR associated with marginal chalcopyrite replacement. Nanoscale analysis lifts the cloak of invisibility for Au in pyrite at Olympic Dam. These results show that confirmation of whether gold occurs as NPs or in solid solution based solely on position above or

below the solubility limit of Au in pyrite on a plot of Au vs As is impossible without corroborative studies at the nanoscale.

Do rocks deposited during time periods with high gold in sedimentary pyrite host more gold mineralization?

Gregory, Daniel¹, Lui, Timothy¹, Wu, Selina¹, & Large, Ross²

¹*University of Toronto, Toronto, Canada;* ²*ARC Centre of Excellence in Ore Deposits (CODES), School of Physical Sciences, University of Tasmania, Hobart, Australia.*

Over the past 10 years it has become increasingly common for people to view host rocks, often sedimentary rocks, to be a source of metals for orogenic gold systems. For sediment hosted deposits it has been proposed that syngenetic and/or diagenetic pyrite may be an important source of the gold. This model states that the gold is released during metamorphism, after which it migrates with metamorphic fluids and is deposited in trap sites. During the same time period it was shown that pyrite trace element content, including gold, varies significantly through geologic time. Thus, it stands to reason that an initial step to finding new gold districts may be to identify basins / periods of time when gold is elevated in sedimentary pyrite. Databases of trace element content of sedimentary pyrite show that gold was elevated at approximately: 3 Ga, 2.5–2.7 Ga, 1.9 Ga, 0.9 Ga, 550 Ma, 450 Ma and 300 Ma (Precambrian ages ±100 Ma, Phanerozoic ±50 Ma to encompass the length of time that sedimentary pyrite is generally elevated in gold). These are also the ages of the host rocks for many important gold districts (for example, the Superior and Yilgarn craton orogenic gold deposits, the Witwatersrand deposits, the Sukoi Log deposit, the Bendigo district, and the Carlin district). In this study we went to an area where gold deposits occur but is not one of these more famous districts where gold is well established to be hosted by sediments the same age as those with elevated gold in pyrite: Queensland Australia. Approximately 8658 known gold deposits or occurrences are present in Queensland. Of these 3023 (35%) are host by the stratigraphy of the ages given above, a further 898 (10%) are within 1 km and 1579 (18%) are within 5 km. Furthermore, the geologic units of prospective age encompass less than 5% of the land area of Queensland. This suggests that indeed gold deposits are more likely to form in areas that are likely to have elevated gold in sedimentary pyrite and these stratigraphic packages should be prioritized when searching for new gold districts.

Source of gold in Neoproterozoic orogenic-type deposits in the North Atlantic Craton, Greenland: Insights for a proto-source of gold in sub-seafloor hydrothermal arsenopyrite in the Mesoproterozoic[†]

Saintilan, N. J.^{1,7}, Selby, D.^{1,2}, Hughes, J. W.^{1,3}, Schlatter, D. M.⁴, Kolb, J.⁵, & Boyce, A.⁶

¹*Department of Earth Sciences, University of Durham, Durham DH1 3LE, United Kingdom;* ²*State Key Laboratory of Geological Processes and Mineral Resources, School of Earth Resources, China*

University of Geosciences, Wuhan, China; ³Bluejay Mining Plc, 2nd Floor, 7–9 Swallow Street, London, W1B 4DE, United Kingdom; ⁴Helvetica Exploration Services GmbH, Carl-Spitteler-Strasse 100, 8053 Zürich, Switzerland; ⁵Institute of Applied Geosciences, Department of Geochemistry and Economic Geology, Karlsruhe Institute of Technology, Adenauerring 20b, 76131 Karlsruhe, Germany; ⁶Isotope Geoscience Unit, SUERC, Rankine Avenue, East Kilbride, Glasgow G75 0QF, United Kingdom; ⁷Present address: Institute of Geochemistry and Petrology, Department of Earth Sciences, ETH Zürich, Clausiusstraße 25, 8092 Zürich, Switzerland

Given that gold (Au) mostly remained in the incipient Earth mantle until ca 3.9–3.8 Ga, a “proto-source” of gold may have been present in the dominantly mafic crust precursor born through first-stage melting of the early Earth mantle. In south-westernmost Greenland, a fragment of the North Atlantic Craton is characterised by greenstone belts comprising mafic volcanic and magmatic rocks, and harzburgite cumulates that were emplaced at ca <3.19–3.01 Ga (e.g., Tartoq greenstone belt). Here, combining detailed sulphide petrography with rhenium–osmium–sulphur (Re–Os–S) isotope geochemistry of individual mineral separates of arsenopyrite from gold–sulphide mineralised shear zones, we pinpoint the precipitation of ca 3.18–3.13 Ga (Re–Os model ages) hydro-thermal arsenopyrite associated and coeval with arc-related magmatism of the Tartoq Group. We consider sub-seafloor hydrothermal alteration of the oceanic crust and magmatic activity to have supplied arsenic (As), Re, and Au, to result in the precipitation of the ca 3.18–3.13 Ga arsenopyrite with primary invisible gold. Additionally, in major shear zones in a rigid juvenile continental crust, retrograde greenschist-facies metamorphism overprinted the ca >3.0 Ga prograde amphibolite-facies metamorphic assemblages and caused local dissolution of arsenopyrite. During this retrograde tectono-metamorphic stage, in gold-rich shear zones, the Re–Os geochronometer in arsenopyrite was reset to a Neoproterozoic age while invisible gold was liberated and deposited as free gold with 2.66 Ga pyrite (Re–Os isochron ages). The initial Os isotope ratios of Neoproterozoic arsenopyrite ($^{187}\text{Os}/^{188}\text{Os}_i = 0.13 \pm 0.02$) and gold-bearing pyrite (0.12 ± 0.02) overlap with the estimated $^{187}\text{Os}/^{188}\text{Os}$ ratio of the Mesoarchean mantle (0.11 ± 0.01) and preclude contribution of radiogenic crustal Os from evolved lithologies in the accretionary arc complex but instead, favour a local contribution in Os from basaltic rocks and serpentinised harzburgite protoliths by metamorphic fluids. Thus, the ca 2.66 Ga lode gold mineralisation identified in the North Atlantic Craton may illustrate a gold endowment in shear zones in Earth’s stabilizing continental crust at the time of the 2.75–2.55 Ga Global Gold Event, through metamorphic upgrading of bulk gold which had originally been extracted from the Mesoarchean mantle and concentrated in hydrothermal arsenopyrite deposits in oceanic crust beneath the overall reduced Mesoarchean ocean.

*Santilan et al. (2020) Source of gold in Neoproterozoic orogenic-type deposits in the North Atlantic Craton, Greenland: Insights for a proto-source of gold in sub-seafloor hydrothermal arsenopyrite in the Mesoarchean. *Precambrian Research* **343**, 105717.

Apatite chemistry indicates that oxidized auriferous fluids along the world-class Boulder Lefroy–Golden Mile fault system were significantly different to fluids from global porphyry systems

Bath, Adam, B., Walshe, John, L., Ireland, Tim, Cobeñas, Gisela, Sykora, Stephanie, Cernuschi Federico, Woodall, Katie, MacRae, Colin, Williams, Morgan, & Schmitt, Leanne

CSIRO Mineral Resources, PO Box 1130, Bentley, WA 6102, Australia, First Quantum Minerals Ltd, 1/24 Outram St, West Perth WA 6005, Lundin Mining, El Bosque Norte 500, piso 11, Of. 1102, Las Condes, CP 7550092, Santiago, Chile

The Boulder Lefroy–Golden Mile (BL–GM) fault system contains >70 Moz of gold and accounts for more than a quarter of the known gold mineralization in the Archean Yilgarn Craton, Western Australia. Alteration along the BL–GM fault system shows a wide range of redox conditions (hematite/anhydrite- to pyrrhotite-stable), and this range in many cases can be linked to mineralization. Oxidized fluids have been linked to adakitic magmas or more generally, Au fluids linked with sub-arc mantle wedges. However, invariably in Archean Au systems there is a lack of evidence of causative intrusions at the time of oxidized alteration and mineralization, leading numerous authors to reject the possibility that magmas were a major source of auriferous fluids. Despite this, oxidized fluids derived from deeper concealed intrusions cannot be ruled out, particularly given the length and breadth of anhydrite alteration can be spatially significantly large (km-scale). Here we present mineral and isotopic datasets on oxidized fluids from the BL–GM fault system with the aim to view these datasets in comparison to those from porphyry systems. Porphyry Cu–Au systems are associated with oxidized magmatic fluids generated in arc environments, and here we test if apatite chemistry can be used to make any links between oxidized fluids in Archean Au systems and global porphyry systems. Close to 1000 apatite analyses were obtained on the electron microprobe. The apatite crystal formula is $\text{Ca}_5(\text{PO}_4)_3\text{X}$, where X represents the channel volatile site that runs parallel to the crystallographic c-axis, occupied by OH, F, and Cl. Results from our dataset show that apatite from gold-bearing oxidized alteration assemblages in Archean Au system have variable amounts of F (2.5 to 4.1 wt%), whereas Cl values remain low (<500 ppm) over the wide range of F values. In contrast, apatite from porphyry Cu–Au deposits with anhydrite have a wide range of F values (2.2 to 4.8 wt%) and show a significant linear increase in Cl (<300 ppm to 1.7 wt%) with decreasing F. The stark difference in the X-site substitution appears the main variance between the chemistry of apatite from the two environments. In hydrothermal Archean Au and porphyry Cu–Au systems, higher amounts of F tend to correspond to lower temperatures (based on biotite–apatite thermometer). Also, previous experimental studies show that relatively low Cl and F concentrations in acidic (H_2O –HCl) fluids result in high ratios of $\text{XCl}_{\text{Ap}}/\text{XOH}_{\text{Ap}}$ and $\text{XF}_{\text{Ap}}/\text{XOH}_{\text{Ap}}$ in apatite, whereas much higher abundances of Cl and F are required in basic fluids to achieve the same result. Data from previous studies also show that the dilution of aH₂O with higher aCO₂ results in apatites with higher ratios of

XCl_{Ap}/XOH_{Ap} and XF_{Ap}/XOH_{Ap} from fluids with comparatively lower levels of Cl or F. Our data shows no evidence of these processes. The most plausible explanation for the comparatively low XCl_{Ap}/XOH_{Ap} apatites from Archean Au systems is that the fluids were comparatively low saline compared to those from oxidized alteration assemblages in porphyry Cu–Au systems. Furthermore, results of this study show that apatite from oxidized and reduced alteration assemblages of Archean Au systems across the Yilgarn Craton plot along the same trend on the Cl versus F diagram. One notable difference between the two populations is that those forming part of reduced alteration assemblages have lower F values (1 to 3.3 wt%) and appear to be associated with hotter fluids.

The unusual Imou porphyry Au–Cu deposit, Western Highlands PNG

Ireland, Timothy¹, Cernuschi, Federico², Sievwright, Robert¹, Goswell, Hannah¹, Stefanova, Eliisa³, & Dobe, John⁴.

¹First Quantum Minerals Ltd, Vancouver, Canada; ²Eclectic Rock Ltd, Punta del Este, Uruguay; ³Bulgarian Academy of Science – Geological Institute, Sofia, Bulgaria; ⁴Footprint Resources Pty Ltd,

Imou (4.944°S, 142.806°E) is a porphyry gold–copper deposit located western Papua New Guinea along structural strike between the deposits at Frieda River and Yandera. The area was highlighted during systematic geochemical exploration in the mid-1970s, when five porphyry centres were identified in a camp covering ~30 x 30 km. The Imou target was delineated in the 1990s as a stream sediment and soil Cu anomaly of >500 ppm coincident with Au anomalism >0.2 ppm and associated with a magnetic polyphase porphyritic intrusive complex. Two holes drilled in 1999 discovered the deposit, and a dozen recent holes permit this first attempt at geological description.

Magmatic rocks comprise equigranular and lesser porphyritic diorites that belong to the Nekiei intrusive suite, which was emplaced into a thrust duplex of obducted siltstone and oceanic crust. New zircon–U–Pb geochronology records at least 700 ky, but less than 2.1 my of Late Miocene magmatic evolution. The intrusions are low to mid-K calc-alkaline series rocks composed primarily of calcic plagioclase and hornblende with rare biotite and quartz, and accessory titanomagnetite. Whole rock chemical proxies for porphyry fertility are comparable to causative suites in other deposits (Sr/Y up to 65 and V/Sc up to 16), but zircon in these rocks has relatively low concentrations of U, Th, LREE and Hf. The intrusions manifest in airborne magnetic surveys as discrete high amplitude magnetic ‘bullseye’ features, but no cogenetic large plutons are observed at surface, nor can be inferred from the magnetic response.

The outcropping manifestation of the porphyry deposit at Imou is in many ways typical: within a geochemical footprint of ~2 km² there are domains of A-family quartz veins that sometimes contain Cu–Fe-sulphides and/or magnetite, the distribution of which broadly coincides with the occurrence of hydrothermal magnetite, feldspar, anhydrite and muscovite. These quartz vein domains reach 50 vol% quartz in the vicinity of the magnetite-bearing assemblage. There are structurally controlled domains of late D-veins and phyllic

alteration, followed by post-mineral porphyritic dykes. However, there are numerous differences with economic PCD described elsewhere. Cu–Au grade is not associated with the abundance of A-family quartz veins. Further, there is no petrographic nor bulk chemical evidence for large volumes of potassic alteration. Observed feldspars are albite and sporadic hydrothermal biotite represents only remobilisation of local potassium. There is little disseminated sulphide associated with this alteration, instead, grade development is associated with chalcopyrite–pyrite–(magnetite) fracture paints, and sulphide–anhydrite veins that cross-cut the quartz vein stages. These paragenetically late brittle veins are widely distributed at low frequency but are associated with best Cu–Au grades. These late hydrothermal features are not systematically associated with a particular wallrock alteration assemblage, although chlorite–montmorillonite is the dominant alteration assemblage outboard of localised sericite- and albite-bearing assemblages.

We advance several working hypotheses for why Imou differs from other porphyries, and especially why metals did not precipitate efficiently with the early high temperature alteration and quartz veining. We speculate that many barren or subeconomic porphyries may have inferior Cu–Au grade development for similar reasons.

The Late Archean Au epoch: by-product of Earth degassing

Walshe, John L., & Bath, Adam, B.

CSIRO Mineral Resources, PO Box 1130, Bentley, WA 6102, Australia

It is possible to think of the mineral systems that created the Earth’s major mineral deposits and provinces as volatothermally driven chemical engines with roots deep in the mantle. It may be argued that the chemical potential of systems was linked to this degassing history and reflects the interplay of deep-Earth anhydrous fluids with the Earth’s hydrous outer layers. Metal transport and deposition capacity was closely linked to propagation of redox and related physicochemical gradients through systems. Such arguments imply quite specific links between the formation of the Earth’s resources across time and space, secular changes in architecture and geochemistry of the planet over some 4.5 billion years of evolution and Earth phenomena such as mass extinction events, global anoxia and atmospheric evolution. Conceivably a better understanding of large-scale linkages may lead to better techniques for differentiating productive terrains and epochs of Earth history as well as the links between metallogenesis and other Earth processes.

The Late Archean Au deposits, at ca 2.7 to 2.63 Ga, can be interpreted as one manifestation of planetary degassing of highly reduced and oxidized volatiles. The Late Archaean gold deposits are known from five continents, are hosted within supra-crustal volcano-sedimentary sequences and are spatially associated with trans-crustal structures, 100s of kilometres in length, as exemplified by the deposits of the eastern Yilgarn Craton, Western Australia. All the productive gold camps of the eastern Yilgarn gold province show evidence of deposit to district scale mineral zoning and

systematic patterns in $\delta^{13}\text{C}_{\text{carbonate}}$ and $\delta^{34}\text{S}_{\text{sulfide}}$ that can be related to chemical gradients sustained by fluxes of reduced (H_2 , CH_4) and oxidized volatiles (SO_2) of mantle origin, triggered by tectonic events and related magmatism. Gold transport and deposition was favoured by chemically zoned volatothermal plumes with an inner core of reduced, alkaline and quartz undersaturated fluids and outer zones of oxidized fluids. Gradients in activity of H_2O were sustained by pulsed injection of anhydrous mantle-volatiles into pre-existing crustal hydrothermal systems. Local electrical discharges occurred over distances of ~10 to 100 m, coupled to rock fracturing in the anhydrous parts of systems. Gold deposition was controlled by water activity gradients, coupled with pH and redox gradients. Sustaining these gradients was key to sustaining gold transport and formation of high-grade resources. Collapse led to dispersion of the gold \pm low grade mineralization.

It is hypothesized that the ultimate driver of the Late Archean Au epoch was an electron flux from the core-mantle boundary that released H from the mantle ($\text{e} + \text{OH}^- = \text{O}^{2-} + \text{H}$), drove redox reactions and sustained the volatile flux of the late Archean.

A view of orogenic gold deposits as nonlinear systems: Nonlinear analysis of data

Ord, Alison¹, & Hobbs, Bruce²

¹The University of Western Australia, Perth, Australia;

²CSIRO, Perth Australia

Despite many studies of orogenic gold systems, the underlying processes involved in their formation and in defining their location remain enigmatic. This arises because such processes are multiscale and nonlinear so that patterns of alteration and mineralisation are apparently irregular and unpredictable. The goal of a nonlinear dynamical analysis of spatial data is to extract the dynamics of the underlying nonlinear and multiscale physical and chemical processes that produced these data. We review nonlinear analysis methodology and explore hyperspectral and gold assay data for a drill-hole in an orogenic gold system. The analysis is non-parametric and purely data driven. We use recurrence, cross- and joint-recurrence plots to extract the invariant measures of the system including the embedding dimension, the first positive Lyapunov exponent and the entropy and construct the attractor for the mineral distributions. The resulting dynamical model is tested using nonlinear prediction algorithms. Cross recurrence analysis shows strong spatial correlations of gold with carbonates and weaker correlations with phengitic micas and chlorite. Joint recurrence analysis reveals that all parts of the system are part of the same dynamical attractor and hence parts of the same physical-chemical system. We speculate on the coupled processes, compatible with the nonlinear analysis, responsible for the mineralising system. The overall aim is to constrain the structure and organisation of the coupled non-equilibrium dynamics that define this system. We propose that autocatalytic reactions associated with quartz and carbonate deposition control pH variations responsible for gold deposition and present a new view of mineralising systems.

River(ina) of gold – historical activity and structural controls

Stuart, Cait, Ricketts, Mel, & Gilmore, Phil

Geological Survey of New South Wales, Department of Regional NSW, Maitland, Australia

The Riverina region of New South Wales is well known for agriculture, but the region also has a long history of gold mining, dating back to the late 19th century. The Riverina has seen relatively little modern mineral exploration. The five-year (2014 to 2019) East Riverina Mapping Project undertaken by the Geological Survey of NSW has highlighted the prospectivity of the region for structurally controlled, low-sulfide (orogenic) gold, as well as intrusion-related gold and porphyry copper-gold mineralisation.

Structurally controlled, low-sulfide gold mineralisation within the eastern part of the Riverina region, which extends from West Wyalong to Albury, is hosted by Ordovician to Devonian units and largely located adjacent to the Gilmore Fault Zone. The area has a current endowment (past production and identified resources) of 33.45 t (1.4 M ounces) of gold in 23 identified goldfields situated along the Gilmore Fault Zone and other major, parallel structures.

For each goldfield, a review of historical data, host lithologies, endowment, structural setting, style and timing of mineralisation was undertaken. Each goldfield was considered in a regional structural context. In particular, the structural setting and timing of mineralisation were related to movement along the Gilmore Fault Zone and associated structures.

Structurally controlled, low-sulfide gold mineralisation was found to occur in three main settings:

1. In narrow vein arrays in orientations that fit within a Riedel shear model. Veins are typically found in more competent rock types adjacent to second or third order splay faults of the Gilmore Fault Zone or major parallel structures. Mafic dykes are commonly associated with shear zones and may have caused desulfidation of gold-bearing fluids, resulting in mineralisation. Examples of this setting include Adelong, West Wyalong and Sebastopol.
2. Along the contacts between intrusions and metasedimentary country rock, or in pressure shadows of intrusions. Competency contrast between intrusions and metasedimentary rocks is thought to have focussed fluids along these contacts or around competent bodies. Pressure changes during fluid migration likely played a role in gold mineralisation. Examples include Yalgogrin, Weethalle and Grong Grong.
3. Gold found in fold hinges and fold limbs adjacent to the Gilmore Fault Zone. Barmedman is the only recognised example of this style in the area.

Geochronological data for gold mineralisation in the project area are rare and further work is required. However, field relationships indicate the majority of structurally controlled, low-sulfide gold mineralisation occurred during the Devonian, in the Bindian Event or the Tabberabberan Contraction, with minor mineralisation also potentially occurring during the Ordovician Benambran and Carboniferous Kanimblan contraction events.

Reframing mine wastes as new

resources to meet green economy metal

Mine Waste as secondary raw material in the framework of mining circular economy: legislation and applicability perspectives

Benzaazoua, Mostafa

Research Institute of Mining and Environment (RIME) – University of Quebec UQAT, Canada

Worldwide, the mining industry during the previous century played a so important role in the first industrial revolution, but at the same time mine operators increasingly suffered from a very bad image related to important environmental liabilities and difficult societal acceptance. In fact, mine exploitations that still follow the linear economy scheme extract finite ore resources and generate high volume of solid wastes (“Take-make-dispose”), where the only profits are those of the valuable minerals. For this reason, legislations and policies nowadays keep evolving to become increasingly binding regarding mine wastes management practices and rules and towards waste preservation from weathering and pollution release.

Mine waste management strategies remain complex to achieve effectively and very cost consuming. This is why the environmental management is becoming increasingly integrated in the mine life cycle, instead of being a late expenses after mine closure. More and more countries around the world privilege other actions that tend to reduce the amount of wastes to be deposited within mine site surfaces. Among actions already used, the mine industry proceeds with (i) upstream geometallurgical modelling, (ii) smart and rational extraction of ores in underground or open pit mines, (iii) maximisation of in situ reuse of mine wastes with or without reprocessing for novel practices like underground backfilling, and (iv) waste reuse in the reclamation process (covers construction, once the mine wastes are proven clean, or after waste reprocessing for decontamination).

Presently, the main challenge of the mine of future consists of developing more symbiotic strategies that include more circular economy (“make-use-recycle”), to be able to valorize and recycle mine wastes outside of mining sites in other industrial sectors like geo-materials and infrastructures construction for civil engineering. This strategy depends on many factors that could be conditioned by at least four conditions: (1) adequate legislative arsenal, including incentives, (2) geometallurgical integrated waste management strategy, including on-site ore/waste sorting, reprocessing and in-situ reuse, (3) an efficient environmental prediction tool for mine wastes all along mine cycles and once within their recycled state, and finally (4) the possibility as well as the acceptance of reusing mine waste out of mining site. As a finality, this philosophy may allow transforming wastes into secondary raw materials for other industrial sectors, such as in civil engineering.

Mine wastes metal revalorization or reuse in situ and out of mine sites as sands and/or aggregates for roads, concretes, bricks manufactures ... represent promising ways that might help in reducing the environmental impacts of mining activities. Some examples from works undertaken at RIME-UQAT or in Morocco around

the phosphate mining industry will be presented in this presentation. A focus on the legislation and its importance, as the one in force in Quebec province (Canada), will be detailed as an example that encourages mining circular economy. Then, examples will be presented to illustrate the main challenges that have to be taken up in this field.

The suitability of Re-mining as remediation method of Be–W skarn tailings in Yxsjöberg, Sweden

Hällström, Lina

Luleå University of Technology, Luleå, Sweden

The development of green technology increases the cycling of several more “unusual” elements in society, e.g., Be and W. They are unusual in the sense that the geochemical knowledge of the mobility, transport and environmental impact are limited. At the historical Yxsjö mine site (W–Cu–CaF₂) in Sweden, the geochemical behaviour of Be and W were studied from both (1) tailings open to the atmosphere (Smaltjärnen Repository), and (2) covered and water saturated tailings (Morkulltjärnen Repository). Several state-of-the-art findings were found by combining geochemistry with mineralogy within the Smaltjärnen tailings and by taken monthly water samples from the groundwater in the tailings and surface water downstream the tailings. Furthermore, re-mining was evaluated as a possible remediation method for the Smaltjärnen Repository.

In Smaltjärnen, pyrrhotite oxidation and too low calcite neutralization had decreased pH from 8 to 4 in the upper-parts of the tailings and formations of secondary gypsum [CaSO₄] and hydrous ferric oxides (HFO) had occurred. Beryllium leached from the unusual mineral danalite [Be₃(Fe_{4.4}Mn_{0.95}Zn_{0.4})(SiO₄)₃.2S_{1.4}] due to oxidation and slightly acidic pH conditions. Released Be had temporarily been scavenged by precipitation with secondary Al(OH)₃ and CaSO₄ within the tailings and at the shore of the tailings. In the groundwater, Be was detected in one of the highest groundwater concentrations worldwide (average 4.5 mg/L). Beryllium released to the surface water had formed complexes with F⁻ and was transported >5 km from the mine site. This is interesting since pH in the both the groundwater and the surface water was around 6, in which Be usually precipitates as insoluble Be(OH)₂.

Tungsten has previously been considered as an immobile element. In the Smaltjärnen tailings, W had partly been mobilized from scheelite [CaWO₄] by anion exchange with CO₃²⁻ released from the calcite neutralization. Released W had adsorbed to HFO within the Smaltjärnen tailings and only low concentrations of W leached to the surface water. There it adsorbed on particulate Fe and settled to the sediments a few 100 m from the tailings. Contradictory, high concentrations of dissolved W was found downstream the Morkulltjärnen tailings, which were covered and water saturated. The concentrations of particulate Fe were low, and W was transported several km with the surface water.

A first step to evaluate the environmental impact of the surface water downstream the tailings was to study silican algae growing on rocks. Preliminary results show that the water quality had a negative impact on them compared to a reference stream.

These findings show that remediation of the

Smaltjärnen tailings is necessary. The release of contaminated neutral mine drainage will be ongoing for hundreds of years because only a minor part of the tailings in Smaltjärnen have been weathered during the 50–100 years of storage. The results from Morkulltjärnen Repository showed that the traditional technique with cover and water saturation was not suitable for scheelite. Instead, Re-mining could be beneficial from both an economic and environmental perspective since Be and W mainly were found in their primary minerals.

Opportunities for reprocessing polymetallic tailings in western Tasmania

Jackson, Laura¹, K ng, Lexi², Parbhakar-Fox, Anita¹, & Meffre, Sebastien³

¹The W.H. Bryan Mining & Geology Research Centre, Sustainable Minerals Institute, The University of Queensland, Brisbane, Australia; ²RGS Environmental, Brisbane, Australia; ³The School of Natural Sciences, The University of Tasmania, Hobart, TAS

The Rosebery Pb–Zn–Cu–Ag mine, 3 km north west of Rosebery, Tasmania, Australia has been in operation since 1936. During this time >17 Mt of tailings were deposited in Bobadil Tailings Storage Facility, which opened in 1974 and reached capacity in 2018. Historically the materials contained in the Bobadil tailings are known to be endowed in ecotoxic metals including Pb, Zn, Cu, As and Mn, as would be expected based on the ore mineralogy (i.e., sphalerite, galena, pyrite). To assess the risks posed, samples were collected from 10 trenches (52 samples) and 4 cores the upper 2 m across the accessible parts of the TSF and detailed geochemical and mineralogical studies (e.g., acid base accounting (ABA), X-ray diffractometry, sulphide alteration index (SAI), mineral liberation analysis (MLA), scanning electron microscopy, laser ablation ICPMS) undertaken to assess the viability of reprocessing as a means to reducing environmental risks associated with the facility, and extend the mine life.

Eleven facies (A to K) were visually defined in these sampled tailings, ranging from oxidised hardpan (i.e., Facies K) to fresher sulphide dominated tailings (Facies A). Despite this visual heterogeneity, ABA results classified all samples as potentially acid forming (PAF) with total sulphur ranging from 3.8 to 13.8%. The inherent acid neutralising potential (ANC) was low across all facies (0.5 to 1.9% carbon) and is complimentary to the measured tailings mineralogy which reported a low abundance of carbonates (<2% calcite). Sulphide alteration index (SAI) values confirm most tailings as un-oxidised to partially armoured. When SAI values are screened against paste pH values, these materials classified as PAF with a lag time to AMD generation anticipated. MLA results reported >89% of pyrite as liberated and where locked, mineral associations were dominantly with muscovite and quartz. To determine the tenor and deportment of precious, base and critical metals in the pyrite and sphalerite LA-ICP-MS analysis reported trace metals (e.g., Co, Ni, Cd and Bi) in pyrite were considered low, whilst in sphalerite bivalent metals including Cd and Mn were notably high. Only two Au inclusions were identified in MLA-SEM images. Due to the homogenous, trace element free and highly liberated

pyrite particles these tailings could be amenable to reprocessing and desulphurisation. The remaining gangue tailings have the potential to be reused into products such as ceramics, road base and industrial building materials. With additional analysis of tailings at depth, a robust retreatment framework could be redeveloped to help remove the requirement to maintain and manage a large tailings facility in perpetuity.

Critical metal exploration in Queensland's mine waste: identifying potential secondary resources

Parbhakar-Fox, Anita¹, Degeling, Helen² & Lisitsin, Vlad²

¹W. H. Bryan Mining and Geology Research Centre, Sustainable Minerals Institute, 40 Isles Road, Indooroopilly, Qld 4068, Australia; ²Geological Survey of Queensland, Department of Natural Resources, Mines and Energy, Level 4, 1 William Street, Brisbane, Qld 4002, Australia.

The global response to climate change, initiated by the Paris Agreement, has been to encourage transition to low-carbon economies. Technologies such as electric vehicles, low-emission power sources and products for the medical and defence sectors are required to support this. The manufacture of these products requires resources of 'new economy metals' including cobalt, tungsten, rare earth elements (REEs), indium, gallium and germanium. Traditionally, these metals were considered unwanted by-products of base metal and precious metal mining operations, and consequently are concentrated in mine waste.

Mine waste reprocessing is a business proposition that is increasingly being adopted in many countries, with at least 75 active projects, including one in Queensland at the Century Mine. Whilst the concept of remediating sites through removing and reprocessing mine waste is being considered to extend the life-of-mine at operational mines and to rehabilitate abandoned and legacy wastes, these materials are mineralogically heterogeneous thus, a 'one approach-fits all' will not optimise value-recovery or indeed, guarantee that the waste is environmentally de-risked. Further, as these wastes are superficially deposited in different climatic zones, metal cycling can be a more dynamic process in for example, sub-tropical to tropical climates than when compared to temperate or Mediterranean climates. Thus, geochemical processes, as related to mineralogy, must be studied at each.

This research focusses on secondary prospectivity in Queensland, where there are at least 40 significant metalliferous mining operations producing mine waste streams containing unknown quantities of new economy metals. Additionally, there are 120 state-managed abandoned mines. Many of these sites contain reactive sulphide-rich mine waste with associated acid and metalliferous drainage risks. The ongoing management of these sites is costly, but their potential new economy metal content – as yet uncharacterised – presents a unique opportunity to economically rehabilitate these sites through reprocessing waste.

In this research, the new economy metal fertility of reactive mine waste (tailings, waste rock, spent heap leach) at nine sites (Capricorn Copper, New Century,

Osborne, Selwyn, Lady Annie, Wolfram Camp, Baal Gammon, Mt Oxide, Pindora) was examined. For each site, geometallurgical assessments were undertaken using bulk geochemical, mineralogical (X-ray diffractometry, mineral liberation analysis) and mineral chemistry (LA-ICPMS) tools. Integration of these data allowed for a first-pass assessment of metal fertility. In terms of Co, the greatest tenor was reported at Osborne (TSF 1 = 856 ppm, TSF 2 = 582 ppm data from Chinova Resources) and is refractory in pyrite. Waste rock at Capricorn Copper was also endowed (273 ppm, n = 20) and associated with Mn and Fe oxides, but the sampled tailings were less endowed (63 ppm, n = 79), however, only the upper 1.5 m was sampled and it is postulated that grade will increase with depth. Several waste rock samples from Baal Gammon reported > 500 ppm indium (93 ppm, n = 41) in chalcopyrite whilst at Pindora, REE's were endowed in iron oxides contained in heap leach (n = 17) and waste rock (n = 8) (e.g., Ce 200 ppm and 1374 ppm, respectively, La 123 ppm and 884 ppm, respectively). Detailed investigations for critical metal recovery at these four sites is ongoing.

Critical metals and mine waste across Australia: partners in solutions?

Mudd, Gavin M.

Environmental Engineering, School of Engineering, RMIT University

Australia has had a long history of mining and continues to enjoy a robust and extensive mining industry – albeit with a much greater environmental (and social / cultural) footprint. One of the principal environmental legacies of mining is mine waste: specifically, tailings left over from processing ores and waste rock from the mining stage (especially open cut mines). Poorly managed, mine wastes can lead to the formation of acidic and metalliferous drainage (AMD), catastrophic failures or impact on rehabilitation objectives and post-mining land-use. The world, however, still needs the metals provided by mining – many of which are not the primary target of mines but are often extracted as by-products in smelters or refineries, such as indium, tellurium, selenium, gallium and others. These metals are crucial for the transformation of the world's energy infrastructure to renewable energy (solar photovoltaic panels, wind turbines) and energy storage batteries as well as the electrification of transport (electric vehicles). Other metals of great need include rare earths, which can be mined on their own or as by-products from a variety of mineral deposit types (e.g., monazite from heavy mineral sands, iron oxide copper–gold). Collectively, these metals are often referred to as 'critical metals', due to their fundamental importance to modern technology and the risks that a major supply disruption could have on global development needs. Although there are examples of reprocessing tailings to extract additional metals (principally in the gold sector), this practice still focusses on the primary metals – leaving behind untapped potential to extract critical metals. In order to assess this potential, the first starting point is working out how much tailings Australia has stored and where, assigning mineral deposit types and then adding in geochemical assessments to explore potential critical metals which might be present. Despite the lack of data for critical metals, given they are often substitute elements in primary economic minerals (e.g., indium in sphalerite or stannite), concentration data for

primary metals can be combined with statistical models used to estimate critical metals. This research presents the first ever national database of mine tailings around Australia, covering most mines and production since the 1970s (and some historical sites) combined with preliminary findings from geochemical assessments for critical metals in those tailings. The approach is a significant advance on understanding the potential for critical metals from tailings in particular

Application of alkaline industrial wastes in remediation of acid and metalliferous drainage generated by legacy mine wastes

Moyo, Annah¹, Parbhakar-Fox, Anita^{1,2}, Meffre, Sebastien¹ & Cooke, R. David¹

¹ARC Research Hub for Transforming the Mining Value Chain & Centre for Ore Deposit and Earth Sciences, University of Tasmania, Hobart, TAS 7001, Australia; ²WH Bryan Mining and Geology Research Centre, The University of Queensland, Indooroopilly, QLD 4068, Australia

Alkaline industrial by-products are increasingly used in the remediation of acid and metalliferous drainage (AMD). AMD remediation occurs via acid neutralisation by the carbonate and hydroxide fraction and immobilisation of metals through precipitation and sorption. In this study, green liquor dregs (GLD), wood ash, coal ash and red muds, as well as scallop, mussel and oyster shells were co-disposed with acid-generating mine wastes from six abandoned sites in Tasmania. Initial geochemical static tests classified the mine wastes as potentially acid forming with NAG pH ranging between 1.9–5.0. The acid neutralizing capacity of the industrial wastes ranged between 35.3–1017.2 (kg H₂SO₄/ton) with shells having the highest and wood ash the lowest capacity. A new bench-scale accelerated kinetic leach test was developed using 55 mm diameter Buchner funnels for subsequent tests on combinations of mine wastes with industrial wastes. 82 cells were established with each funnel filled with milled (< 75 µm) native mine waste (i.e., controls) and 7:3 weight ratio of mine to industrial wastes (both blended and as cover layers). These were irrigated with deionized water every second day for 1 month and after every 10 days thereafter until 100 days had elapsed. Blending of the industrial and mine wastes achieved the greatest neutralization, however, the pH difference when compared to multi-layering and the top covering was mostly < 1.0 pH unit. GLD showed the greatest capacity for neutralising AMD, whilst the wood ash was least effective. Metal analysis of leachates showed that the mine waste controls leached toxic levels of Al, As, Cd, Cr, Cu, Ni, Pb and Zn. The application of industrial wastes inhibited the leaching of these metal(oids) except for wood ash. These results indicated that the metal(loid)s leachability was mostly influenced by pH, but the leachability of As increased with increasing pH. This work demonstrated that industrial wastes are potentially a cheaper and environmentally sustainable alternative for AMD remediation.

MinEx CRC: National Drilling Initiative frontier precompetitive drilling to support greenfields discovery

Mineral and petroleum potential in the South Nicholson region, and the NDI Carrara 1 stratigraphic drill hole

Jarrett, Amber^{1,2}, Bailey, Adam¹, Carr, Lidena¹, Henson, Paul¹, Schofield, Anthony^{1,2}, O'Rourke, Angela^{1,2}, Roach, Ian^{1,2}, Budd, Anthony^{1,2}, Munson, Tim³, Williams, Ben³, Symmons, Jack³, & Close, Dorothy³

¹Geoscience Australia, Canberra, Australia; ²MinEx CRC, Canberra, Australia; ³Northern Territory Geological Survey, Darwin, Australia

The MinEx CRC-led National Drilling Initiative (NDI) is the world's largest mineral exploration collaboration designed to undertake precompetitive geoscience research in under-explored, but potentially prospective regions. One of the first NDI projects is being undertaken in the South Nicholson region of the Northern Territory (NT) as a collaboration with Geoscience Australia and the Northern Territory Geological Survey.

The South Nicholson Basin, and underlying Lawn Hill Platform region, have the potential for sediment-hosted base metal mineral deposits including critical minerals and hydrocarbons. The region is poorly understood compared with the neighbouring resource-rich areas of the McArthur Basin and the Mount Isa Province. Providing baseline data in frontier basins is essential as legacy data coverage can often be inadequate for making investment decisions, particularly with new commodities where exploration may not yet have provided the required information.

In 2017, Geoscience Australia acquired the L210 South Nicholson Deep Crustal Seismic Reflection Survey. This survey demonstrated the existence of an approximately 1550 km² sedimentary depocentre underlying the surface sedimentary rocks of the Georgina Basin, and coincident with a prominent gravity low. This depocentre has been termed the 'Carrara Subbasin' and its successions may host a continuation of the resource-rich rocks located on the northern Lawn Hill Platform of northwest Queensland, in addition to South Nicholson stratigraphy that has never been sampled by drill core.

MinEx CRC and its partners seek to better understand the geology and resource potential of the Carrara Subbasin through the drilling of the first deep vertical stratigraphic borehole in the region –the NDI Carrara 1 stratigraphic borehole. This borehole has been designed to answer key scientific questions suggested by Geoscience Australia and the Northern Territory Geological Survey including determining geological and geochemical characteristics of sedimentary units from fresh drill core, identifying any evidence of alteration or fluid flow, and finally determining whether there are favourable indicators for the presence of mineral or petroleum systems. To address these questions, both physical samples (e.g., drill core and cuttings) and downhole data (e.g., wireline geophysical data) will be acquired over the entire borehole interval, to a depth of about 2000 m.

Drilling of NDI Carrara 1 is set to be completed by the end of 2020. This presentation will provide a rationale for drilling the NDI Carrara 1 stratigraphic borehole and will present preliminary data generated through drilling. The South Nicholson NDI has already provided and integrated new geoscience data and knowledge in the region, and NDI Carrara 1 will allow for direct testing of resource potential. This precompetitive data is fundamental to underpinning increased industry investment and sustainable economic development in this greenfield region of northern Australia.

The MinEx CRC National Drilling Initiative

Budd, Anthony^{1,2}

¹Geoscience Australia, Canberra, Australia; ²MinEx CRC, Canberra, Australia

Approximately 80% of Australia has some form of cover rocks obscuring potentially mineralised geological regions. In order to remain internationally competitive for exploration investment, government geoscience agencies around Australia provide pre-competitive geoscience data to lower exploration risk. Mostly this has been geophysical data to see through cover – MinEx CRC is developing new tools and opportunities to sample bedrock directly by drilling.

MinEx CRC was established in 2018 under the Australian Government's Cooperative Research Centre program (www.minexcrc.com.au). MinEx CRC has three Programs: Program 1 is developing new drilling technologies, Program 2 is developing new ways of gaining data from drilling, and Program 3 is the National Drilling Initiative (NDI).

The NDI is conducting drilling campaigns in selected areas as determined by each sponsoring geological survey. During September–November 2020, two campaigns are underway on behalf of Geoscience Australia (GA) with the Northern Territory Geological Survey in the Barkly region of the Northern Territory. A program of 10 holes of depths between ~300–500 m is designed to test a range of stratigraphic and mineral system targets in the East Tennant region. The East Tennant area was selected during GA's Exploring for the Future Program (<https://www.ga.gov.au/efft>) as a possible extension to the Tennant Creek mineralised region. A single deep stratigraphic borehole (~2000 m) is underway to test the Carrara Sub-basin recently identified in the Barkly Seismic Program of the EFTF (<https://www.ga.gov.au/efft/energy/barkly-seismic-survey>) in the South Nicholson area. Both of these campaigns are being conducted using conventional drilling methods.

In 2021 two campaigns are expected to be conducted utilising the RoXplorer Coiled Tube drilling rig undergoing further development by MinEx CRC Program 1 (<https://minexcrc.com.au/program-one-drilling-technologies/project-2-coiled-tubing-drilling-for-definition-of-mineral-deposits/>). MinEx CRC will conduct drilling on behalf of the GSWA in the East Yilgarn, and in two areas of the Delamerian for the GSSA. Further campaigns are planned for the North and South Cobar, Mundi, Dubbo and Forbes areas for the GSNSW, and the Tabberabberan for the GSV. Additional drilling campaigns are likely to be undertaken in other areas later in the life of the MinEx CRC.

MinEx CRC picks up from three previous CRCs: DET CRC for the RoXplorer and associated technologies, CRC LEME for exploration through cover using cover materials, and the pmd*²CRC for mineral systems analysis. Taking a mineral systems approach, the *Geological Architecture and Evolution* project provides new data and interpretations in the drilled areas to underpin mineral systems analysis and develops new technologies and methodologies for acquiring and interpreting this data.

The *Targeting Mineral Systems in Covered Terranes* project deploys fit-for-purpose data and geoscience analytical techniques designed to identify and map mineral system footprints within cover and underlying basement and apply a suite of mineral systems mapping tools designed to identify and prioritise areas of high prospectivity.

The *Maximising the Value of Data and Drilling Through Cover* project provides the tools and data infrastructure to facilitate upload and management of legacy and NDI drilling data delivered to stakeholders and researchers in near real-time, and to the broader geoscience community in efficient time frames.

Multicommodity mineral systems analysis for the National Drilling Initiative: The TISA and Delamerian case study

Metelka, Vasek¹, Schofield, Anthony², Wise, Tom³, Cole, David⁴, Otto, Alex¹, Fabris, Adrian³, Hong, Wei⁵, & Murr, James²

¹CSIRO Mineral Resources, Perth, Australia; ²Geoscience Australia, Canberra, Australia; ³Geological Survey of South Australia, Adelaide, Australia; ⁴CSIRO Data 61, Melbourne, Australia; ⁵University of Adelaide, Adelaide, Australia

The National Drilling Initiative (NDI) and MinEx CRC research activities aim at providing new data that will drive our understanding of geological processes and mineral systems in key underexplored areas of the Australian continent. Ultimately, the newly acquired knowledge will underpin the future of the exploration industry as we push for discoveries under deeper cover.

Prospectivity analyses were conducted to aid with drill targeting for the NDI. These analyses were performed for two regions of interest: The East Tennant Creek–Mount Isa Area (TISA) of Northern Territory and Queensland and the Delamerian Orogen (Delamerian) Area of South Australia. Both regions, albeit with a different geological setting, were primarily omitted from substantive exploration efforts either due to thick regolith or younger sedimentary cover or lacking knowledge and missing significant discoveries. On paper, however, the geological settings and the proximity to known mineralisation suggest a high potential for discovery of new deposits under younger sedimentary/ regolith cover or deposits that formed mineral systems that were not considered previously.

We employed a multicommodity knowledge-based mineral systems analysis approach to identify critical components and model the overall propensity to mineralisation. Theoretical gold and copper–gold mineral systems models were established first. The models were then converted to geospatial representations, and quantitative prospectivity maps were created utilising fuzzy logic inference and

compared to weighted overlay as well as data-driven methods (logistic regression, random forest), where training data could be applied from adjacent uncovered regions.

The results show several zones of interest that can serve the researchers and stakeholders as first-pass information for drill targeting. The approach also highlighted the importance of primary input data. It helped focus on areas where data quality or discrepancies existed as well as identified data sets that were crucial for mapping the components of a mineral system more accurately. When compared to the data-driven methods, which showed good classification accuracy metrics, the knowledge-driven results open up more space and enable conceptual, regional targeting.

Characterising fluid composition and source in a greenfields terrane: west Arunta Orogen, Western Australia

Finch, Emily G.^{1,2,3}, & Kelsey, David E.^{1,3}

¹*Mineral Exploration Cooperative Research Centre;*

²*The University of South Australia, Adelaide, Australia;*

³*The Geological Survey of Western Australia, Department of Mines, Industry Regulation and Safety, Perth, Australia*

Discovering major mineral deposits is increasingly difficult because easily findable deposits located at Earth's surface have already been discovered. Exploration focus has now consequently shifted to relatively unexplored regions where basement rocks are commonly obscured by sedimentary cover. Exploration success in covered regions requires understanding of whole mineral systems. Fluids are crucial to understanding hydrothermal mineral systems, because fluids are present during all stages of ore formation: in the source region, throughout transport, and in deposition of metals.

The Arunta Orogen is one such underexplored and largely covered terrane and is a key focus for the Geological Survey of Western Australia in the National Drilling Initiative. It is comprised of two Paleoproterozoic provinces overlain by sedimentary basins, and spans east–west across the Northern Territory, with the westernmost extent crossing into Western Australia. The Northern Territory component of the Arunta Orogen contains several mineral prospects and deposits, but the Western Australian component (the west Arunta) is one of the continent's least explored regions for mineral deposits due to its remoteness, paucity of outcrop, and lack of detailed study aimed at constraining key geological factors such as litho-stratigraphy and age. Limited work on the west Arunta indicates the region is prospective for copper, gold, uranium and sedimentary-exhalative base metal deposits, but little to no analysis of alteration signatures or fluid source has been undertaken there to date.

Basement rocks of the west Arunta have undergone multiple high-temperature metamorphic and deformation events, most of which appear to postdate fluid infiltration events of interest, making these rocks unsuitable for fluid inclusion studies. Instead, minerals such as apatite can preserve information about fluids they have formed from or interacted with and can be used to infer fluid characteristics such as composition and potential source. Additionally, apatite can be used

as an exploration tool because it is an indicator mineral for different rock types and mineralisation styles.

A suite of samples with varying degrees of fluid infiltration and mineralisation were collected from co-funded Exploration Incentive Scheme diamond drillcores from the west Arunta. Petrography of the drillcore samples indicates fluid infiltration is widespread, demonstrated by pervasive sericite, chlorite, epidote, magnetite and hematite alteration, commonly associated with veins and felsic intrusive rocks. The halogen, major element, trace element, and Cl isotope composition of apatite in these samples was determined using electron probe microanalysis. Samples were selected to reflect a range of apatite compositions: those affected by fluids but with no associated mineralisation, those affected by fluids associated with mineralisation, and samples relatively unaffected by fluids, thus representing the baseline chemistry. The composition of apatite from these samples provides insights into the composition, possible sources of the fluid, and influence of the host rock on apatite chemistry.

Optimization of sequential drilling locations to reduce geological uncertainty

Pirot, Guillaume, Lindsay, Mark & Jessell, Mark

Centre for Exploration Targeting, The University of Western Australia, Crawley, Australia

In a context of early-stage exploration, geological modelling relies heavily on sparse surface and drill - hole geological observations. These data allow us to develop interpretations of the stratigraphy, organizing identified lithological formations. Though the data may provide local estimations about the thickness and depth of some formations, geological uncertainty away from the observations may be huge. One way to reduce this geological uncertainty is to acquire more data by drilling. However, given the associated costs and risk to the project, the next drilling location is carefully selected. This is difficult as the next location for drilling is often decided under uncertainty due to a dearth of supporting information and knowledge.

Here, we explore different strategies to optimize the selection of successive drilling locations. The first strategy relies on the volume of influence around the borehole design, acting as a moving window filter, and on the value of new information, that is assumed proportional to the current state of geological uncertainty. The second exploration strategy aims at reducing the geological misfit with a Bayesian Global Optimizer.

We test the different strategies on a synthetic case based on a Precambrian basin setting. The initial geological knowledge is composed of surface data and five initial boreholes, whose locations are determined by Latin Hypercube Sampling. At each iteration, an ensemble of geological realizations is generated by stochastic perturbation of the current geological knowledge. Geological uncertainty is summarized from different indicators based on the cardinality, entropy, connectivity, topology and geostatistics of both lithological formations and their underlying scalar-fields.

Preliminary results show that the first strategy allows a decrease of both the mean and ninetieth percentile of the geological uncertainty. The Bayesian Global

Optimisation approach reduces locally the geological misfit. A third strategy combining the first two approaches gives a good compromise to reduce both the geological uncertainty and the geological misfit and shows promise to support decision-making in practical regional geological exploration scenarios.

This work is supported by the ARC-funded Loop: Enabling Stochastic 3D Geological Modelling consortia (LP170100985) and DECRA (DE190100431) and by the Mineral Exploration Cooperative Research Centre whose activities are funded by the Australian Government's Cooperative Research Centre Programme. This is MinEx CRC Document 2020/45.

Zircon chemistry as an exploration tool for iron oxide–copper–gold deposits

Brotodewo, Adrienne^{1,2}, Tiddy, Caroline^{1,2}, Zivak, Diana³, Fabris, Adrian⁴, & Giles, David^{1,2}

¹*Future Industries Institute, University of South Australia, Adelaide, Australia;* ²*Mineral Exploration Cooperative Research Centre (MinEx CRC), Adelaide, Australia;* ³*Department of Earth and Environmental Sciences, The University of Adelaide, Adelaide, Australia;* ⁴*Geological Survey of South Australia, Adelaide, Australia*

Zircon preserves chemical signatures that reflect crystallisation environments and post-crystallisation modification (e.g., Belousova et al., 2002). Typically, zircon is used to study petrogenesis and evolution of rocks due to its robustness during surficial, metamorphic and igneous processes, as well as its affinity for rare earth elements (REE), U and Th. Recent research has focused on understanding and characterising the geochemical composition of zircon. However, this has been met with many challenges as REE and trace element compositions can be highly variable in zircon from the same lithological unit, and within a single grain itself as a result of micro inclusions, metamictisation, strong differences in compositional zoning and recrystallisation (Nardi et al., 2003). Despite this, zircon has successfully been used as a provenance tool to discriminate between igneous, metamorphic and sedimentary source rocks (Belousova et al., 2002). Zircon has also been demonstrated to preserve a geochemical signature that can be related to porphyry Cu mineralisation (Lu et al., 2016). However, the use of zircon as a pathfinder for other commodities, such as iron oxide–copper–gold (IOCG) deposits, is limited (Courtney-Davies et al., 2019).

The Gawler Craton, South Australia, preserves a complex geological history dating back to the late Archean. The craton preserves multiple igneous units that each have their own unique geochemical characteristics and some of which are associated with IOCG mineralisation. IOCG mineralisation occurred during a major period of mineral genesis, magmatism, deformation and metamorphism at ca 1600–1580 Ma (e.g., Tiddy & Giles, 2020) and includes the Olympic Dam, Prominent Hill and Carrapateena deposits along the eastern Gawler Craton. Within the Gawler Craton, zircon has commonly been used for dating or isotopic purposes. However, limited research has focused on the geochemistry of zircon, its variability between igneous suites and its use as a pathfinder mineral towards IOCG deposits.

In this study, new zircon geochemical data is presented on samples from the ca 1850 Ma Donington Suite, ca 1600–1575 Ma Hiltaba Suite and ca 1594–1587 Ma Gawler Range Volcanics. Samples from all three suites preserve evidence of variable potassic and hematite alteration associated with hydrothermal activity during IOCG mineralisation at ca 1600–1580 Ma. Assessment of zircon chemistry within each of the three igneous units shows that there are characteristic enrichments and depletions in trace and REE chemistry in samples that have undergone variable degrees of alteration. The variations in zircon chemistry between unaltered and altered samples is attributed to chemical modification by F-rich hydrothermal fluids that altered the host rocks and was associated with IOCG mineralisation. These distinct geochemical characteristics recognized in zircon suggests the potential of zircon as a pathfinder for IOCG deposits in the Gawler Craton.

Belousova et al. 2002: *Contrib. Min. Pet.* 143, 602–622
Courtney-Davies et al. 2019: *Min.* 2019, 9, 364
Lu et al. 2016: *Soc. Eco. Geo.* Vol 19
Nardi et al. 2013: *Chem. Geo.* 335, 1–7
Tiddy & Giles, 2020: *Ore Geo. Rev.* 122, 103–483.

Uncovering the Cobar Basin – new results from the NSW MinEx NDI areas

Folkes, Chris¹, Deyssing, Liann², Trigg, Steven², Carlton, Astrid¹, & Schifano, Joe³

¹*Mineral Exploration Cooperative Research Centre, Geological Survey of New South Wales, Department of Regional NSW, Maitland, NSW, Australia;* ²*Mineral Exploration Cooperative Research Centre, Geological Survey of New South Wales, Department of Regional NSW, Orange, NSW, Australia;* ³*Mineral Exploration Cooperative Research Centre, University of New South Wales, Sydney, NSW, Australia*

The Cobar region of central-western New South Wales hosts numerous precious and base metal mineral systems, many exploited by active and historical mine workings. These are mostly located around rock outcrops and under shallow cover sequences of the Cobar Basin. The North Cobar and South Cobar MinEx CRC National Drilling Initiative (NDI) areas were selected by the Geological Survey of New South Wales (GSNSW) to improve the understanding of the geology, mineral systems and groundwater in basement and regolith profiles that extend away from the margins of these known mineralised areas.

Understanding the prospective basement geology in the Cobar region is complicated by variations in the depth and nature of the weathering profiles through the region. A mix of transported and in situ weathering reflects a complex palaeolandscape.

Recent activities by the GSNSW are designed to map the thickness and character of the weathering profile and increase our knowledge of basement geology. This work will inform and complement proposed drilling in the NDI areas to further investigate the geo-chemical and petrophysical signatures of basement geology and mineral systems. The activities also have implications in understanding groundwater resources.

Comprehensive audit and gaps reports were published in 2020 for the North Cobar and South Cobar NDI areas. These reports reviewed existing data, provided recommendations for new sampling and data capture, and prioritised the scientific questions that should be

addressed. Recent mineral potential mapping and mineral-systems studies identified new prospective areas and provided a better understanding of the main controls on, and timing of mineralisation for the Cobar region.

An airborne electromagnetic (AEM) survey was flown in the region in 2019, comprising 116 east–west lines spaced at 2.5 km and 5 km, totalling approximately 11 000 line km. Ongoing modelling and interpretation of the data have enhanced knowledge of depth and nature of the cover, groundwater systems, structural geology (e.g., fault locations and geometry), mineral systems and stratigraphy. The AEM data, with other datasets such as fault attribution, NSW Seamless Geology, and crustal-scale fault models, are being integrated into a new 3D model of the region that will benefit mineral explorers and hydrogeologists.

The AEM data have also been integrated with drilling, hydrogeochemical, biogeochemical and spectral surveys. Downhole lithology and assay information from legacy drilling has been imported into 3D viewable datasets. Hydrogeochemical analyses from water bores in the Cobar region were completed by CSIRO and GSNSW and highlighted new areas for potential exploration. Researchers from UNSW analysed Cypress Pine needles to provide a regional biogeochemical dataset with focus areas over known mineralisation. Spectral scanning of legacy drill core using the HyLogger™ has provided useful constraints on the depth and nature of weathering, and alteration of basement rocks.

These activities build on recent mineral system studies to advance the understanding of the geology, and mineral and groundwater resources in the North Cobar and South Cobar NDI areas. This has greatly helped to inform the site selection and scientific questions to be answered with future MinEx CRC drilling in these NDI areas.

Between the Stavely and Koonenberry: a structure with no arc, or an arc hidden in structure?

Wise, Tom^{1,2}, Curtis, Stacey^{1,2,3}, & Robertoson, Kate^{1,2,4}

¹*Geological Survey of South Australia, Adelaide;*

²*Mineral Exploration Cooperative Research Centre;*

³*University of South Australia;* ⁴*University of Adelaide*

Late Cambrian volcanic arc segments are recognised in the Stavely and Koonenberry belts, whilst the presence or absence of a similar segment in the South Australian section of the Delamerian Orogen has been debated. Regional scale geophysical imagery has been re-interpreted to suggest that the Mount Wright Volcanics, part of the calc-alkaline volcanic arc in the Koonenberry Belt, likely extends into South Australia beneath the central Murray Basin. This continuation into South Australia may link to fore-arc style magmatism near Keith (Foden *et al.*, 2020), rendering a temporal-spatial link between the Stavely and Koonenberry belts unlikely due to the parallel nature of the potential arc segment near Keith with the Stavely Belt.

A potential volcanic arc/subduction system positioned along the eastern margin of South Australia has direct implications for the porphyry-epithermal potential of the Delamerian basement to the Murray Basin, but also prompts a re-evaluation of the regional effects of the Delamerian Orogeny. Province-wide magneto-telluric models provide information about the nature of the middle crust down to the lithospheric mantle and reveal highly resistive zones associated with rift axes of the middle Cambrian Kanmantoo Group, whilst further east, where potential arc crust may reside, the crust and lithospheric mantle is less resistive.

If volcanic arc rocks in South Australia represent the earliest subduction products along the east Gondwana margin (Foden *et al.*, 2020) prior to roll-back and subsequent subduction in the Stavely zone, post-tectonic intrusives in a belt from the Padthaway Ridge to Anabama can be re-examined in the context of regional extensional episodes. Foden *et al.* (2020) attribute post-tectonic magmatic suites to delamination and asthenospheric upwelling. However, the geometry of the post-tectonic belt may imply that a crustal tear was developed earlier during rollback-induced extension and exploited favourable original Kanmantoo rift structures. Potential field interpretation/modelling tests this hypothesis, whilst drilling as part of the MinEx CRC National Drilling Initiative will provide greater constraint for the proposed geologic framework of the region.

Greening up brownfields: adding new timelines to mineral systems models for the Mesoproterozoic Gawler Craton

Morrissey, Laura^{1,2,4}, Payne, Justin^{3,2,4}, Hand, Martin^{4,2}, Bockmann, Mitchell^{4,2}, Yu, Jie^{4,2}, & Reid, Anthony⁵

¹*Future Industries Institute, University of South Australia, Adelaide, Australia;* ²*Mineral Exploration Cooperative Research Centre;* ³*UniSA STEM, University of South Australia, Adelaide, Australia;* ⁴*Department of Earth Science, University of Adelaide, Adelaide, Australia;* ⁵*Department for Energy and Mining, Geological Survey of South Australia, Adelaide*

The Gawler Craton is commonly considered to record a complex tectono-metamorphic and magmatic history from the Archean to the Mesoproterozoic, culminating in voluminous magmatism of the Hiltaba Suite and the Gawler Range Volcanics (GRV) between 1600–1570 Ma. Although there is widespread evidence for tectono-metamorphic and magmatic events younger than 1570 Ma, these commonly receive little attention because they are enigmatic, occur in poorly outcropping parts of the craton and are difficult to correlate regionally. In addition, because the Hiltaba–GRV event was associated with the development of large Iron-Oxide–Copper–Gold (IOCG) and Au deposits it holds the most interest for mineral exploration, with the younger events considered to be of little importance. However, these younger events have potential for both new addition of metals and remobilisation of existing deposits, and therefore understanding their character and expression is vital to create a holistic mineral systems framework for the Gawler Craton.

Reanalysis of legacy drill holes using modern geochronologic and metamorphic techniques has led to the identification of younger metamorphic events between ca 1570–1550 Ma, ca 1530–1520 Ma and 1500–1400 Ma in the northern Gawler Craton. In the Mount Woods region, monazite age populations of ca 1570 Ma and ca 1550 Ma are interpreted to record a phase of high thermal gradient metamorphism, deformation and mafic magmatism that post-dates Hiltaba-aged granitic magmatism in this region. Similar metamorphic ages between ca 1570–1550 Ma elsewhere in the northern Gawler Craton, Yorke Peninsula and Barossa Complex suggests that this event is widespread across the Gawler Craton. In the Peake and Denison Inlier, calcic alteration has been dated at 1530 Ma, and is approximately coeval with migmatitisation and metamorphism in the Nawa Domain at ca 1520 Ma. Magmatic rocks with inferred ages of ca 1520 Ma in the northern Gawler contain marialitic cavities, suggesting that they intruded at relatively shallow depths. Post 1500 Ma, the Gawler Craton is thought to record only minor sedimentation such as the intra-continental Pandurra Formation. However, A-type magmatism and high thermal gradient metamorphism occur at ca 1450 Ma in the Nawa Domain, and reactivation of lithospheric-scale shear zones occurs between 1470–1450 Ma. The crustal-scale Karari Shear zone and Cairn Hill Fe–Cu deposit also record monazite growth at ca 1490–1480 Ma.

The high thermal gradients recorded in the metamorphic rocks, combined with a lack of evidence for significant exhumation or dissection of the GRV in the central Gawler Craton, suggests that all these younger events record periods of extension. The locus of extension and shear zone reactivation may have migrated through time, leading to apparently discrete zones of reworking. These extensional events have the potential to drive fluid flow events along reactivated shear zones (derived from overlying sediments such as the Pandurra Formation, or from magmas intruded at depth), as well as add new metals to the crust. This, with the evidence for young metamorphism/alteration at Cairn Hill, suggests that the Hiltaba Event may not be the final mineralising event in the Gawler Craton.

Constraining alteration in the buried Benagerie ridge, Curnamona province South Australia

Simpson, Alex¹, Glorie, Stijn¹, Hand, Martin¹, Reid, Anthony², & Gilbert, Sarah³

¹Mineral Exploration Cooperative Research Centre, School of Earth & Environmental Sciences, University of Adelaide; ²Mineral Exploration Cooperative Research Centre, Geological Survey of South Australia; ³Adelaide Microscopy, University of Adelaide

The Curnamona province, situated at the border between SA and NSW is a piece of Paleoproterozoic crust that is separated from the Gawler craton by the Adelaide Rift Complex. This geological region is highly prospective for a variety of mineralisation types, including the Pb–Zn–Ag (e.g., the world class Broken Hill deposit), and iron-oxide copper gold (IOCG) (e.g., Kalkaroo and Portia deposits) [Conor and Preiss, 2008]. The Benagerie ridge volcanic suite (BVS) sits in the centre of the province and is a correlative of the Gawler Range Volcanics (GRV), host of the world class Olympic Dam IOCG deposit [Wade *et al.*, 2012]. The province has undergone multiple episodes of deformation, with the most important events considered to be the ca 1600 Olarian Orogeny and the ca 500 Delamerian orogeny [Conor and Preiss, 2008], with some evidence for ca 830 Ma dyke emplacement [Wingate *et al.*, 1998]. Additionally, multiple episodes of alteration and mineralisation have occurred, particularly regional scale albitisation [Skirrow *et al.*, 1999]. Limited direct constraints exist on the timing of these episodes, with most thought to have occurred prior to the Olarian Orogeny.

LA ICP MS elemental and isotopic mapping, combined with LA ICP MS U–Pb geochronology, and geochemistry provide insight into multiple episodes of post-Olarian fluid alteration, including ca 820 Ma albitisation and mineralisation in the BVS. We further demonstrate the utility of U–Pb geochronology applied to hydrothermal apatite, titanite, calcite and magnetite to constrain the timing of episodes of fluid alteration.

Conor, C. H. H., & W. V. Preiss (2008). Understanding the 1720–1640 Ma Palaeoproterozoic Willyama Supergroup, Curnamona Province, Southeastern Australia: Implications for tectonics, basin evolution and ore genesis. *Precambrian Research*, 166(1–4), 297–317.

Skirrow, R., R. Maas, & P. M. Ashley (1999). New age constraints for Cu–Au(–Mo) mineralisation and regional alteration in the Olary–Broken Hill region. *AGSO Research Newsletter*, 31.

Wade, C. E., A. J. Reid, M. T. D. Wingate, E. A. Jagodzinski, & K. Barovich (2012). Geochemistry and geochronology of the c. 1585 Ma Benagerie Volcanic Suite, southern Australia: Relationship to the Gawler Range Volcanics and implications for the petrogenesis of a Mesoproterozoic silicic large igneous province. *Precambrian Research*, 206–207, 17–35.

Wingate, M. T. D., I. H. Campbell, W. Compston, & G. M. Gibson (1998). Ion microprobe U–Pb ages for Neoproterozoic basaltic magmatism in south-central Australia and implications for the breakup of Rodinia. *Precambrian Research*, 87, 135–159.

Hydrothermal alteration and mineralisation characteristics at Anabama Hill: a porphyry Cu–Mo prospect in the Delamerian Orogen, South Australia

Hong, Wei^{1,2,3}, Fabris, Adrian^{2,3}, Curtis, Stacey^{2,3}, & Dutch, Rian A.^{2,3}

¹Department of Earth Sciences, School of Physical Sciences, The University of Adelaide, Adelaide, SA 5005, Australia; ²Geological Survey of South Australia, Department for Energy and Mining, 11 Waymouth Street, Adelaide, SA 5001, Australia; ³Mineral Exploration Cooperative Research Centre (MinEx CRC)

The Delamerian Orogen is the oldest component of the Phanerozoic Tasmanides and is argued to have constituted a Proterozoic continental rift margin overprinted by convergent, west-dipping subduction since the Cambrian (Foden et al., 2020). It has experienced a complex geological history that includes deformation, metamorphism and magmatism from the middle Cambrian (ca 520 Ma) to early Ordovician (ca 480 Ma), involving of the emplacement of a series of I-type, S-type and A-type granitoids. Magmatic-hydrothermal Cu–Mo mineralisation in the Delamerian Orogen was first identified in the 1970s, and related Cu–Mo occurrences include the Anabama Hill, Blue Rose, Netley Hill, Cronje Dam-Oak Dam, and Bendigo, situated along the eastern margin of the Adelaide Fold Belt. This belt forms part of a Cambro-Ordovician arc that extends southeast into Victoria (e.g., Thursday's Gossan Cu deposit) and northeast into New South Wales (e.g., Loch Lilly-Kars Cu prospect), respectively.

The Anabama Hill Cu–Mo prospect is located in the northeast part of the Delamerian Orogen and associated with the Anabama Granite that has limited surface outcrop. Recent geophysical investigations shows that it is a NE-trending large batholith, with an estimated subsurface area > 50 km². A granodiorite pluton is the major component of this batholith, which was intruded by quartz diorite and monzogranite. Minor components include microgranodiorite, dacite porphyry, and lamprophyre dikes as identified in seven legacy diamond drill cores. These magmatic facies were emplaced into a Neoproterozoic sedimentary sequence composed of mica schists, tillites, quartzites, and siltstones. Only a Pb–Pb plateau zircon age of 485 ± 4 Ma is currently available for the granodiorite (Nasev, 1998). Extensive pyrite–muscovite–quartz alteration prevails in the granodiorite, diorite and monzogranite, which is capped by a 50 m-thick weathering zone consisting of kaolinite, montmorillonite, jarosite and goethite. The pyrite–muscovite–quartz zone extends intermittently downwards for more than 700 m and occurs commonly as multiple veins and veinlets. Epidote–quartz–magnetite–pyrite veinlets contain chalcopyrite and/or molybdenite disseminations and are overprinted by the pyrite–muscovite–quartz veins. Euhedral, coarse-grained molybdenite, pyrite and muscovite typically occur along fractures or as disseminated patches within massive quartz (> 1 m wide). Narrow K-feldspar–quartz veinlets (several cm in width) cut the diorite porphyry and equigranular granodiorite and generally occur below the intense muscovite-dominated alteration zone. Copper grade in the muscovite-rich altered zone range from 0.17% to 0.38%, whereas Mo contents increase from 2–10 ppm

in the granodiorite up to 620 ppm in the muscovite-rich assemblages. Epidote–chlorite alteration generally develops in a peripheral domain, extending a few hundred metres laterally from the Cu and Mo anomalies. The granodiorite, monzogranite and diorite have mostly undergone selective epidote–chlorite replacement. Locally, epidote, chlorite, pyrite and minor quartz and magnetite assemblage develop intensely and occur as thick veins (1 to 30 cm wide) that truncate the intrusive facies. Epidote and chlorite mineral chemistry are used to further characterise alteration patterns and assess mineralisation fertility of the Anabama Hill prospect and broader Cu–Mo porphyry-style mineralisation potential of the Delamerian Orogen, which forms part of ongoing research of the Mineral Exploration Cooperative Research Centre and Geological Survey of South Australia.

⁴⁰Ar/³⁹Ar step-heating geochronology on drill core samples reveals multiple alteration events in the Anabama Hill Cu–Mo prospect, South Australia

Goswami, Naina^{1,2}, Forster, Marnie^{1,2}, & Reid, Anthony³

¹Research School of Earth Sciences, Australian National University, Canberra ACT 2601; ²MinEx CRC, Canberra ACT 2601; ³Geological Survey of South Australia, Adelaide SA 5001

⁴⁰Ar/³⁹Ar ultra-high-vacuum (UHV) step-heating experiments can routinely provide key data using small samples taken from drill core, in this case revealing the timing of the evolution of alteration zones, in the Anabama Granite. ⁴⁰Ar/³⁹Ar geochronology was conducted in conjunction with ³⁹Ar diffusion experiments on K-feldspar, white-mica, and biotite from different depths from seven core samples and provided evidence for alteration in what appeared to be unaltered host rocks. This is because potassium feldspar can grow and regrow during periods of alteration and metasomatism, with the timing of these events constrained precisely by the ages of the high retentivity-core domains. White-mica and biotite behave differently to K-feldspar due to their hydrous nature, crystal structure and chemical composition, but nevertheless can still preserve important age information and retentivity data that helps constrains the evolution of temperature with time, as extracted by conjoint inversion of the data from ³⁹Ar UHV diffusion experiments and ⁴⁰Ar/³⁹Ar geochronology.

The Anabama Granite is hosted within weakly metamorphosed metasediments in the Adelaide fold belt. The proposed early Ordovician age of ca 468 Ma is based on a Rb/Sr isochron, implying emplacement at the climax of the Delamerian Orogeny. The granite shows progressive stages of alteration grading from fresh granitic rocks to greisen envelopes hosted in variety of lithologies (granite, granodiorite and adamellite). The region is host to variety of alteration styles introducing secondary minerals such as quartz–sericite–pyrite (phyllic alteration), epidote–chlorite–albite (propylitic alteration), fleshy-pink K-feldspar (potassic alteration), kaolinite–illite (argillic alteration) and precious metals such as Cu, Mo in various sulfide-bearing phases (sulfide-mineralisation) which are indicative of existence of different environments and range of temperature conditions during these

process(s). A Cu–Mo prospect has been identified, but its geological history is yet to be completely deciphered.

Our results show younger ages of ca 375–371 Ma preserved within the retentive cores of K-feldspar domains that otherwise show slow cooling from a minimum age of ca 380 Ma with growth of highly retentive new K-feldspar at ca 360 Ma. The co-existing white-micas when analysed, reflect an older age of ca 457 Ma, thus in agreement with previously determined K–Ar ages for muscovite in greisen from alteration zones, at ca 455 Ma. However, since microstructural analysis demonstrates the presence of K-feldspar overgrowing previously crystallised white-mica, we suggest the presence of an as yet unrecognised alteration event. This later-stage potassic alteration did not exceed temperatures required (or was not of sufficient duration) to reset argon-systematics in mica. These ages can be correlated with ages of thermal perturbations in the Lachlan Fold Belt (LFB) to the east, in which case Anabama Granite represents a western extent of the metamorphic and deformation imprint.

This work has been supported by the Mineral Exploration Cooperative Research Centre (MinEx CRC) whose activities are funded by the Australian Government's Cooperative Research Centre Program.

Hydrothermal-magmatic ore-forming processes

Thermodynamic modelling of ore transport and deposition: the good, the bad, and the ugly

Brugger, Joël¹, Etschmann, Barbara¹, Gonzalez, Christopher¹, Liu, Weihua², Yuan, Mei², Guan, Qiushi¹, Raiteri, Paolo³, Testemale, Denis⁴, & Xing, Yanlu⁵

¹School of Earth, Atmosphere and Environment, Monash University, Clayton, VIC 3800, Australia; ²CSIRO Mineral Resources Flagship, Clayton, VIC 3168, Australia; ³Department of Chemistry, Curtin University, Perth, WA 6845, Australia; ⁴CNRS, Université Grenoble Alpes, Institut Néel, F-38000 Grenoble, France; ⁵University of Minnesota, Department of Earth and Environmental Sciences, 116 Church St. SE, Minneapolis, MN 55455, USA

Ore deposit formation and the associated fluid-induced alteration require effective advective mass transfer of fluids, volatiles, and metals over length scales of meters to hundreds of kilometres. Over the past 20 years, our understanding of the geochemical aspects of ore transport and deposition has seen major advances driven by revolutions in theoretical, experimental, and characterization capabilities. This has improved our ability to *predict* metal behaviour at scales ranging from the ore system to the hand specimen, but this new knowledge raises also important new challenges.

1. Thermodynamic modelling enables prediction of the metal-carrying capacity of geological fluids and mapping the distribution and efficiency of metal-precipitating processes through time and space. In the past 20 years a large amount of *in situ* spectroscopic data complemented by increasingly accurate *first principle* molecular dynamic simulations have dramatically improved our understanding of the molecular-level nature of the

hydrothermal reactions that are responsible for metal transport in the mid-to upper-crust. This underpins the development of more accurate models of reactive transport over wide ranges in pressure, temperature, fluid composition, and physical states.

2. Supercritical aqueous fluids link subducting plates and the return of water, carbon, sulfur, and metals to the Earth's surface. Innovative theoretical thermodynamic extrapolations have extended our capacity to model the role of aqueous fluids in the deep Earth. These new predictions suggest a rather more profound role for deep fluids than originally thought: for example, dissolved organic carbon species stable at high pressure recycle large amounts of carbon out of the subduction zone and into the atmosphere, and polysulfide species, stable at high pressure, may form Au deposits rather than the reduced sulfur species stable at lower pressure. With regard to metal complexes, these extrapolations are ultimately based on a large body of experimental studies, the vast majority were conducted at near ambient temperature and pressure, a reasonable number investigated solutions to ~300 °C, $P \leq 300$ bar, but few experimental data are available at pressures above 1 kbar, and hardly any reliable data is available beyond 10 kbar for any metal complex. Molecular dynamics can be used to address this fundamental limitation. The data produced by MD provide realistic properties in PT space that underpin accurate simulations of element transfer by fluids expelled from subducting slabs and their contributions to the deep Earth's volatile, redox and metal budgets.
3. Finally, the role of fluids in controlling both the kinetics and pathways of mineral replacement reactions is now firmly established. The positive feedback between these reactions and porosity creation is one of the key mechanisms that explains the pervasive nature of many alteration reactions. On-going experiments demonstrate the important role of trace elements in controlling the fate of fluid-driven reactions. For example, we discovered that the presence of trace amounts of dissolved cerium (Ce) increases the porosity of hematite (Fe_2O_3) formed via fluid-induced replacement of magnetite (Fe_3O_4), thereby increasing the efficiency of coupled magnetite replacement, fluid flow, and element mass transfer.

Yttrium speciation in sulfate-rich hydrothermal ore-forming fluids

Guan, Qiushi^{1,2}, Mei, Yuan¹, Etschmann, Barbara², Louvel, Marion³, & Brugger, Joël²

¹CSIRO Mineral Resources, Kensington, WA 6151, Australia; ²School of Earth, Atmosphere and Environment, Monash University, Clayton, VIC 3800, Australia; ³Institute for Mineralogy, WWU Muenster, D-48149 Germany

Rare earth elements (REE) have in high demand due to their nearly unsubstituted applications but limited production, and their use as geochemical tracers. REE form strong complex with sulfate and these complexes in hydrothermal fluids are responsible for REE transport and deposition in a wide variety of geological

environments, ranging from sedimentary basins to magmatic hydrothermal settings. However, the thermodynamic properties of most REE–sulfate complexes are derived from extrapolation of ambient temperature data. The direct information on REE–sulfate complexing under hydrothermal conditions is limited to a single study that derived formation constants for Nd, Sm and Er in sulfate solutions to 250 °C (Migdisov & William-Jones, 2008).

In this study, we employ *ab initio* molecular dynamics (MD) simulations to calculate the speciation and thermodynamic properties of yttrium(III) in sulfate solutions at temperatures and pressures up to 500 °C and 800 bar. The calculated formation constants of Y–SO₄²⁻ complexes are employed to fit the modified Ryzhenko–Bryzgalin (MRB) model, which enables the extrapolation of the formation constants to a wider temperature and pressure. The MD results were complemented by the *in-situ* X-ray absorption spectroscopy (XAS) measurements. Our results show that yttrium(III) forms complexes with sulfate with both monodentate and bidentate structures over the investigated temperature range (200 °C to 500 °C). The thermodynamic properties for yttrium(III) sulfate complexes derived from MD enable a better modelling of REE transport in hydrothermal systems.

Effects of halogen in chemical exchange and porosity evolution during feldspar–fluid reaction interface

Duan, Gan¹, Brugger, Joël¹, Kontonikas-Charos, Alkiviadis², Ram, Rahul¹, Etschmann, Barbara¹, & Guagliardo, Paul³

¹School of Earth, Atmosphere and Environment, Monash University, Clayton, VIC 3800, Australia; ²School of Chemical Engineering and Advanced Materials, The University of Adelaide, Adelaide, SA 5005, Australia; ³Centre for Microscopy, Characterisation, and Analysis, University of Western Australia, 35 Stirling Highway, Crawley, WA 6009, Australia

Interface coupled dissolution–reprecipitation (ICDR), through which dissolution of the parent phase produces is coupled to the precipitation of the product phase(s), is a widespread mechanism for this fluid-driven mineral replacement. The mode(s) of ion transport in ICDR and the nature of the mineral–fluid interface at the micron- to nanometer- scale are fundamental controls on the coupling between mass transfer, fluid flow, porosity creation/destruction, and mineral replacement that is responsible for large-scale fluid–rock interaction.

In this work, the effect of halogen (chlorine and fluorine) in alkali exchange during the mineral fluid reaction interface was investigated on a model system wherein sanidine (K,Na)AlSi₃O₈ was reacted with a combination of NaCl, NaF or FeF₂ and ¹⁸O-enriched solutions at 600 °C and 2 kbar, leading to replacement by albite and/or K-feldspar. Nanoscale secondary ion mass spectrometry (Nano-SIMS) of oxygen isotopes (¹⁶O vs ¹⁸O) in the parent and product phases at high-spatial resolution, showed that Al–O and Si–O bonds in the sanidine tectosilicate framework were broken during replacement. Transmission electron microscopy (TEM) of “foils” cut across the reaction boundary indicated a sharp reaction boundary and interfacial zone between reactant and products, consistent with

the ICDR mechanism. Based on its morphology (distinct stress-induced S-shape distortion), the results suggest that the interfacial zones consist of an amorphous hydrosilicate colloid or gel rather than a fluid or solid phase. The ion diffusion occurs horizontally in this dynamic interfacial layer, with exchanges between interface and bulk solution occurring along cracks/defects in the product, this is further indicated by the absence of connected porosity in the bulk newly precipitated phases. Compared to chlorine-bearing solutions, in fluorine-bearing solutions, element diffusion in the interfacial zone is likely enhanced by the formation of Na–Si–Al–fluoride complexes, which results in more extensive reaction progress. The presence of fluoride also influenced the fate of minor amounts of Ti in subsequent mineral replacement.

These results reveal that the nature of the reaction interface depends on both the nature of the mineral and on solution chemistry, this directly affects porosity evolution and chemical exchanges between the reaction front to the bulk solution. Altogether these results can further help explain why the sodic and potassic alteration associated with metal and fluid transport in some of the world’s largest ore deposits can develop extensively and access the metals locking in silicate mineral assemblages.

Mineral redox buffer in ore forming processes – insights from scapolite

Hamisi, Jonathan^{1,2}, Etschmann, Barbara¹, Micklethwaite, Steven¹, Tomkins, Andrew¹, Pitcairn, Iain², Wlodek, Adam³, Morrissey, Laura⁴, & Brugger, Joël¹

¹School of Earth, Atmosphere & Environment, Monash University, Melbourne, Australia; ²Department of Geological Sciences, Stockholm University, Stockholm 106-91, Sweden; ³Department of Mineralogy, Petrography and Geochemistry, AGH-University of Science and Technology, Kraków 30-059, Poland; ⁴School of Natural and Built Environments, University of South Australia, Adelaide, Australia

Metal transports in ore forming fluids is highly dependent on pH, ligands species (S, Cl, F) and redox conditions. The scapolite group is a family of tetragonal aluminosilicate consisting of meionite (Me, Ca₄Al₆Si₆O₂₄CO₃), marialite (Ma, Na₄Al₃Si₉O₂₄Cl) and silvialite (Si, (Ca,Na)₄Al₆Si₆O₂₄(SO₄,CO₃), respectively rich in [CO₃]²⁻, Cl⁻, and [SO₄]²⁻. During fluid/rock interaction occurring during mineralising process of scapolite bearing terranes, scapolite breakdown or crystallization releases into the fluids its volatile components. We analysed a set of 17 scapolite samples sourced from various geological context (metamorphic terranes hosting iron-oxide copper and gold deposits (IOCG), skarns deposits, and scapolite placers). Scanning Electron Microscope and Electron Probe Micro Analyser results show that our sample set contains S as SO₃ up to 1.29 wt% (n = 215) and Cl up to 3.68 wt% (n = 215). In Ca-rich pelite scapolite coexists with graphite and in lesser extent traces of pyrite and has typically a low S concentration. Scapolite hosted in calcsilicates rocks has typically higher S concentration and coexists with pyrite minor chalcopyrite, hematite and/or magnetite and little to no graphite. Sulfur K-edge (2472 eV) X-ray Absorption Near Edge Structure (XANES) spectra collected on the

samples provided evidence of the coexistence of several forms of S species in scapolite in the form of oxidized S (S^{6+} , S^{4+}) and reduced S (S^{2-} , S^{-} , as well as polysulfides). Using the spectra intensity, we evaluate qualitatively the ratio ΣS oxidized/ Σ total S (ΣS oxidized + ΣS reduced). Our results show that variation of the ΣS oxidized/ Σ total S ratio can be used to trace redox conditions prevailing during scapolite breakdown or crystallisation. Ca-rich graphite bearing-pelite have a lower ΣS oxidized/ Σ total S ratio compared to calcsilicates rocks providing evidence that Ca-rich graphite bearing-pelite will typically produce a reduced fluid during devolatilization while calcsilicates rocks will produce a more oxidized fluid as it contains a higher content of oxidized S. As scapolite crystallizes (sink for S) or devolatilizes (source for S) depending on whether it contains more reduced S than oxidised S or vice versa, the volatile released to the fluids will buffer the redox conditions of the fluids, in the case of mineralising brines, this will result in changes of the fluids chemistry to ideal composition for metal transport, given that the fluids will be very reactive. Therefore, scapolite may act as a buffer for redox conditions of the fluids.

New insights into gold enrichment process during the growth of chalcopyrite-lined conduits within a modern hydrothermal chimney from PACMANUS Basin

Hu, Si-Yu¹, Barnes, Steve¹, Pages, Anais², Verrall, Michael¹, Parr, Joanna³, Quadir, Zakaria⁴, Binns, Ray³, & Schoneveld, Louise¹

¹CSIRO Mineral Resources, Kensington, WA 6151, Australia; ²Department of Water and Environmental Regulation, Joondalup, WA 6027, Australia; ³CSIRO Mineral Resources, Lindfield, NSW 2070, Australia; ⁴Microscopy and Microanalysis Facility, John de Laeter Centre, Curtin University, GPO Box U1987, Perth, WA 6102, Australia

Seafloor hydrothermal systems are modern analogues of ancient volcanogenic massive sulfide deposits. The hydrothermal chimneys above the seafloor from back-arc basins are important hosts for metals, such as Cu, Zn, Pb, Ag and Au. Although the general growth history of chimneys has been well acknowledged, recent studies have revealed that the fine-scale mineralogy formed from variable physicochemical conditions can be highly complex. Knowledge of detailed mineralogy and formation process in complex chimney structure helps us better understand the spatial distribution and enrichment mechanisms of precious metals. This study utilized a novel combination of scanning electron microscopy (SEM)-based electron backscattered diffraction (EBSD) and synchrotron x-ray fluorescence microscopy (SXFM) to investigate the mechanism of native gold precipitation during the growth of multiple chalcopyrite-lined conduits as part of a modern chalcopyrite-sphalerite chimney. A thin tubular conduit of fine-grained (< 1 μm) sphalerite was initially precipitated under super-saturated conditions when hot hydrothermal vent fluids mixed with surrounding low temperature fluids within an already formed chimney structure. Accretionary growth of chalcopyrite onto this substrate thickened the chimney walls by bi-directional growth inward and outward from the original sphalerite tube wall. A group of similar conduits, but with slightly different mineral assemblages, is interpreted to

continue to form in the vicinity of the main conduit during the further fluid mixing process. Four distinct gold-sulfide associations were developed during the growth process, including associated to triangular tennantite in coarse chalcopyrite, thin sphalerite layer, euhedral pyrite, and in cavities of chalcopyrite. The gold is thought to precipitate from various mechanisms, including fluid mixing, sphalerite replacement by chalcopyrite, and the dissolution and re-precipitation of chalcopyrite. A previously unobserved paragenesis of gold nanoparticles occurs as chains at the boundary of early sphalerite and chalcopyrite, distinct from gold observed in massive sphalerite as identified in previous studies. These observations provide baseline data in a well-preserved modern system for studies of enrichment mechanisms of native gold in hydro-thermal chimneys. Furthermore, this study provides significant implications that (1) native gold is closely associated to chalcopyrite-line conduits but not necessarily occurs along with tennantite, Bi-rich minerals and bornite as reported before, and (2) the broad spectrum of gold occurrence in chalcopyrite-line conduits is likely to be determined by the mixing process between hot hydrothermal fluids with various surrounding fluids.

Petrographically constrained in situ sulfur isotopes: why the “SEDEX” can’t be used as model for sediment-hosted sulfide deposits in the 1.6 Ga Edmund Basin, Australia

Lampinen, Heta M.^{1,3}, LaFlamme, Crystal^{1,2}, Occhipinti, Sandra A.¹, Fiorentini, Marco L.³, & Spinks, Sam C.¹

¹CSIRO Mineral Resources, 26 Dick Perry Avenue, Kensington, WA 6151, Australia; ²Département de Géologie et de Génie Géologique, Université Laval, Pavillon Adrien-Pouliot 1065, av. de la Médecine, Québec, QC G1V 0A6, Canada; ³Centre for Exploration Targeting, ARC Centre of Excellence for Core to Crust Fluid Systems (CCFS), School of Earth Sciences, University of Western Australia, 35 Stirling Highway, Crawley, WA 6009, Australia.

A common foundation for sediment-hosted massive sulfide (SHMS) deposit sulfur isotope data interpretation is the assumption of sedimentary exhalative “SEDEX” model. The model presumes syndimentary sulfide precipitation and the sulfur mainly sourced from the contemporaneous ocean via bacterial sulfate reduction, which can be further interpreted to reflect the evolution of ancient hydrosphere. However, syndimentary SEDEX model has been challenged or disproven for many SHMS deposits, including ones in the McArthur Basin, Australia. Many SHMS deposits also contain multiple coexisting sulfide generations and/or express geospatial associations between the isotope signature and distance from the hydrothermal vent. Due to the internal complexity of SHMS systems, unravelling their sulfur isotope architecture requires both a robust paragenetic framework and a well-known geological context for the data. In situ secondary ion mass spectrometry (SIMS) sulfur isotope analysis has this capability.

Petrographically constrained in situ sulfur isotope SIMS analysis was applied to pyrite and chalcopyrite (n=135) to investigate the spatial and temporal sulfur isotope architecture of replacement and syndimentary-style

SHMS deposits at four sites (including the Abra deposit) in the ca 1680–1455 Ma Edmund Basin, Western Australia. From this data, the sulfur isotope fractionation associated with the hydrothermal mineral systems, and representativeness for the secular evolution interpretations of the seawater sulfate through the Proterozoic Eon was evaluated.

The epigenetic replacement-style SHMS systems in the Edmund Basin yield $\delta^{34}\text{S}$ from +24 to +54‰ from pyrite and chalcopyrite. The relatively ^{34}S depleted pyrite were associated with ore fluid composition in main hydrothermal channels. The bulk isotopic composition of the ore fluid can be used as proxy for sulfate in the underlying sediments. The extremely ^{34}S enriched were found in pyrite in distal parts of the deposit hydrothermal footprint. This ^{34}S enrichment was possibly caused by deficiency of iron relative to sulfur in low permeability rocks, which decelerates the formation of pyrite allows the mass-dependent Rayleigh distillation of sulfur isotopes to reach extreme residual fraction. The systems with syn-sedimentary sulfide precipitation yield $\delta^{34}\text{S}$ from +1 to +22‰, which can be associated with seawater sulfate and bacterial activity in the basin.

In situ sulfur isotope analysis offered the capacity to link isotopic data to a comprehensive spatially and temporally constrained framework representative of the stratigraphic and geodynamic context. The results of this study also highlight the importance of using tailored geological constraints and a mineral system model as a framework for isotope chemistry – not a generic SEDEX. Tailored geological constraints and deposit model are particularly important for the data are intended for evaluation of hydrosphere over time.

Using epidote U–Pb geochronology and multivariate statistics to unravel overprinting propylitic alteration around the Resolution porphyry Cu–Mo deposit: Fingerprinting the fertile porphyry signal

Phillips, Joshua^{1,2}, Thompson, Jay^{1,2}, Meffre, Sebastien^{1,2}, Maas, Roland³, Danyushevsky, Leonid^{1,2}, & Cooke, David^{1,2}

¹Australian Research Council (ARC) Research Hub for Transforming the Mining Value Chain (TMVC), University of Tasmania, Hobart, Australia; ²Centre for Ore Deposits and Earth Sciences (CODES), University of Tasmania, Hobart, Australia; ³School of Earth Science, University of Melbourne, Melbourne, Australia

The Laramide aged Resolution porphyry Cu–Mo deposit, located within the Superior mining district, Arizona, has a resource of 1787 Mt at 1.53% Cu and 0.035% Mo, making it one of the largest and highest grade porphyry Cu deposits in North America. Tertiary gravels and volcanic rocks related to Basin and Range extension buried all but the most distal epithermal veins and propylitic alteration under approximately 1.5 km of post-mineralisation cover. Identification and mapping of the distal propylitic alteration at surface is itself hampered by a diverse range and multiple generations of epidote–chlorite alteration assemblages observed within the district that could be related to multiple orogenic and/or hydrothermal events that have affected the area over its ca 1650 m.y. history.

Here we present the development of a LA-ICP-MS method for U–Pb geochronology applied to epidote to

aid in resolving multiple epidote-forming events.

Our results demonstrate the presence of at least three spatially coincident but temporally distinct epidote-bearing alteration assemblages within the Superior district of Arizona. The first of these formed yielded a U–Pb LA-ICPMS age of 1183 ±23 Ma, broadly coeval with the emplacement of ca 1100 Ma dolerite sills temporally associated with the Midcontinent rift. The second event was related to the emplacement of a 74 Ma early Laramide weakly mineralized intermediate stock. The final phase of epidote alteration had insufficient U for high-precision dating but is temporally constrained through cross-cutting field relationships and relates to the 65 Ma distal propylitic halo surrounding the Resolution porphyry Cu–Mo deposit.

By constraining the relative ages of epidote-bearing alteration, it is possible to isolate the Laramide signal using LA-ICPMS mineral chemistry trace element data. Multivariate statistical classification demonstrates that the Laramide epidote and chlorite are chemically distinct from, but in some cases overgrow the Proterozoic epidote throughout the Resolution propylitic alteration halo. LA-ICPMS mapping of epidotes reveals complex growth and sector zoning within Proterozoic epidotes (enriched in As, Bi, P, REE), overgrown by a much later Laramide epidote strongly enriched in Pb and Sr.

This development in understanding between local background epidote compositions and Laramide hydrothermal epidote gives explorers new tools to more fully understand the alteration geochemistry observed within Proterozoic rocks in the SW US porphyry province and, ultimately, better target undiscovered porphyry systems.

Gold in oil, and its role in the formation of epithermal gold deposits

Crede, Lars^{1,2}, Evans, Katy¹, Rempel, Kirsten^{1,3}, Weihua Liu⁴, Brugger, Joël⁵, Etschmann, Barbara⁵, Bourdet, Julian⁶, & Reith, Frank^{7*}

¹School of Earth and Planetary Sciences, Curtin University, Perth, Australia; ²Germany; ³McGill University, Montreal, Canada; ⁴CSIRO Mineral Resources, Clayton, Vic 3168, Australia; ⁵School of Earth, Atmosphere and the Environment, Monash University, Clayton, VIC 3800, Australia; ⁶CSIRO, ARRC, 26 Dick Perry Avenue, Kensington WA 6151, Australia; ⁷School of Biological Sciences, The University of Adelaide, Adelaide, SA 5005, Australia; * Passed away in 2019.

Gold can be associated with hydrocarbons in hydrothermal gold deposits, but the near-absence of experimental data on gold–hydrocarbon interactions at hydrothermal conditions prevents a quantitative interpretation of the significance of the observed textural relationships. We present the results of hydrothermal two-phase experiments that investigate Au partitioning between aqueous and organic liquids, and a petrographic and synchrotron investigation of samples from the McLaughlin epithermal Au deposit, USA. Carbonaceous material from McLaughlin contains Au concentrations of up to 18 ppm. We conclude that remobilisation and/or transport of Au by hydrocarbon-rich liquids cannot be excluded.

A morphotectonic analysis of the East Manus Basin, Papua New Guinea

Dyriw, Nicholas J.^{1,2}, Bryan, Scott E.¹, Richards, Simon W.³, Parianos, John M.², Arculus, Richard J.⁴ & Gust, David A.¹

¹*School of Earth and Atmospheric Sciences, Queensland University of Technology, Brisbane, QLD, Australia;* ²*Nautilus Minerals Ltd (now Deep Sea Mining Finance Ltd), Brisbane, QLD, Australia;* ³*Independent research geologist, Brisbane, QLD, Australia;* ⁴*Research School of Earth Sciences, Australian National University, Canberra, ACT, Australia.*

Backarc basins develop through a continuum of evolutionary phases. Surface morphology, magmatism and associated volcanism are key indicators of the various stages of development. The East Manus Basin, Papua New Guinea, is a young (<1Ma) rapidly rifting system on the eastern flank of the larger Manus Basin. Like many other backarc systems of the Southwest Pacific, numerous volcanic centres in the East Manus Basin are associated with active, Cu–Au mineralized hydrothermal systems known as seafloor massive sulfide deposits. However, not all the hydrothermal systems host significant Cu–Au mineralization and the link between the location of these seafloor massive sulfide deposits and the stages of basin evolution are unclear. Here we present the first morphotectonic description and interpretation of the East Manus Basin. Multi-resolution, multibeam echosounder seafloor data and derivatives were used in combination with the Benthic Terrain Modeler for ArcGIS to investigate seafloor characteristics, including volcano morphology and structural lineaments, and define three evolutionary phases for the East Manus Basin. Phase 1 is a period of incipient extension of existing arc crust. Phase 2 evolves to incipient crustal rifting and a transition to effusive volcanism. Phase 3 progresses to nascent organized half-graben system with axial volcanism. Intersecting rift-parallel and rift-oblique structures are important extension accommodation zones and, at the transition between Phase 1 to Phase 2, host the most significant Cu–Au seafloor massive sulfide system within the East Manus Basin. This relationship suggests the accommodation structures developed during early basin evolution may be critical to focus fluid and magma for seafloor massive sulfide formation. Furthermore, the morphotectonic features and relationships associated with modern backarc basin evolution will help to improve interpreting fossilized backarc systems around the world.

Differentiated Archean dolerites and orogenic gold: influences on fertility

Hayman, Patrick¹, Campbell, Ian², Cas, Ray³, Squire, Rick³, Douch, David³, & Outhwaite, Michael⁴

¹*Queensland University of Technology, Brisbane, Australia;* ²*Australian National University, Canberra, Australia;* ³*Monash University, Clayton, Australia;* ⁴*Lithify Pty Ltd, East Victoria Park, Australia*

Granophyre and quartz dolerite are the evolved fractions of differentiated dolerite (diabase) sills and are an important host to Archean gold deposits, in part because accessory magnetite acts as a chemical reactant for orogenic fluids. Despite their economic importance, the understanding of processes leading to

enhanced formation of these favourable rock types is poor. Drill core logging, whole rock geochemistry, magnetic susceptibility, gold assay and thermodynamic modelling data from eleven mineralized and unmineralized ca 2.7 Ga differentiated dolerites in the Eastern Goldfields Superterrane (Yilgarn Craton, Western Australia) are used to better understand the igneous and emplacement processes that increase the volume of host rock favourable for gold precipitation during orogenesis. Orogenic gold favours differentiated dolerites, derived from iron-rich parental magmas, that crystallize large volumes of coarse quartz (magnetite) dolerite (>25% total thickness). Mineralized sills are commonly >150 m thick and hosted by thick sedimentary sequences. Sill thickness is likely the most important factor as it largely controls cooling rate and hence fractionation. The parental melts must have fractionated large amounts of clinopyroxene and plagioclase (possibly up to 50%) before emplacement in the shallow crust. A second fractionation event at shallow levels (<3 km) operated both vertically and laterally, resulting in an antithetic relationship between quartz (magnetite) dolerite and cumulates (pyroxenites and peridotites). By comparison with younger mafic sills emplaced in syn-sedimentary basins, we argue that the geometry of these high-level sills was more irregular than the often-assumed tabular form. Any irregularities in the lower sill margin act as traps for early formed (dense) ferromagnesian minerals, now represented by pyroxene and peridotite cumulates, while irregularities in the upper sill margin trap the buoyant fractionated liquids when the sill is mostly crystalline, through magma flow on the scale of <1 km. Late formation of magnetite (F>50%) is critical to produce disseminated texture and increase the volume of magnetite-bearing quartz dolerite, thus dry magmas are more prospective. Less Fe-enriched melts are known to host orogenic gold, but these are less common, and probably only become good hosts for economic gold when sufficiently thick to fractionate large volumes of magnetite. We summarize the characteristics of the most prospective hosts relevant for exploration of differentiated dolerites hosting orogenic gold.

Copper isotope fractionation in volatile-fluxed enclaves: Modern analogues for the genesis of ancient ore deposits

McGee, Lucy¹, Farkas, Juraj¹, Lowczak, Christopher¹, Payne, Justin², Wade, Claire^{1,3}, & Reid, Anthony^{1,3}

¹*Department of Earth Sciences, University of Adelaide, Adelaide, Australia;* ²*University of South Australia, Adelaide, SA;* ³*Geological Survey of South Australia, Adelaide, SA*

Mafic enclaves are a common feature of volcanic deposits and provide some of our best estimates of the material entering the plumbing system beneath volcanic edifices. Geochemical studies of enclaves in modern volcanic settings can be compared to ancient volcanic deposits where little is known about the tectonic history and magmatic inputs of the system. When applied to a region rich in critical minerals, such studies may provide important links between magmatic processes and genesis of economic deposits.

Mafic material has the potential to carry volatiles to the surface which may transport metal elements. Deep volatiles driven from the subducting slab also provide

elemental enrichment to the mantle wedge beneath areas of potential magmatism, which could be an important precursor to ore forming magmas [1]. We compare the $\delta^{65}\text{Cu}$ values of mafic material from ancient, mineralised terranes with modern active volcanic settings where processes and inputs are less ambiguous. We focus on the Mesoproterozoic Gawler Range Volcanics (GRV) of Southern Australia, a voluminous Silicic Large Igneous Province which contains mafic material in the form of minor basaltic lava flows and enclaves dispersed within dacites and rhyolites which range from $\delta^{65}\text{Cu}$ -0.73 to $+0.61 \pm 0.05$. Importantly, one of the world's most valuable Iron Oxide Copper Gold (IOCG) deposits, Olympic Dam, is associated with GRV magmatism at ca 1590 Ma [2]. We compare these new isotopic data with analyses of mafic enclaves erupted within andesitic material between 1995 AD and 2010 AD from Soufriere Hills Volcano, Montserrat. Volcanic material from this eruption has chemical signatures suggestive of recent volatile fluxing from mafic recharge material which correlate with extremely light $\delta^{65}\text{Cu}$ values extending to -2.4 suggesting volatile transport of Cu on rapid timescales [3].

[1] Skirrow, R., *et al.*, 2018, *G-cubed*, 19(8), 2673–2705.

[2] Reid, A., 2019, *Minerals*, 9(6): p. 371.

[3] McGee *et al.*, 2019, *Earth Planet. Sci. Lett.*, 524, 115730

Geochemical and mineralogical signatures of IOCG and affiliated copper deposits in the Mount Isa Province, Queensland, Australia

Lisitsin, Vladimir, & Dhnam, Courtney

Geological Survey of Queensland, Brisbane, Australia

Geological Survey of Queensland (GSQ) has undertaken systematic geochemical and mineralogical characterisation of numerous Iron-oxide copper-gold (IOCG) and affiliated copper \pm gold deposits in the Cloncurry district of the eastern Mount Isa Province. This work contributes to and expands a current collaborative project between GSQ and CSIRO, focusing on characterisation of key mineral systems and deposits in the region. The geochemical and mineralogical dataset is based on >1000 of individual samples from multiple deposits, including Ernest Henry, E1, Great Australian, Mount Elliott - SWAN, Eloise, Little Eva, Blackard, Kalman, Osborne and Starra. Samples from each deposit were generally collected from multiple boreholes, at a spacing from 15 m to 50 m, to characterise the range from high-grade mineralisation to proximal alteration zones and further to relatively distal samples, hundreds of metres away from visible mineralisation. More extensive sampling and analytical work was undertaken around the Ernest Henry and Mount Elliott-SWAN deposits, aiming to better characterise geochemical and mineralogical zonation at a scale of hundreds to thousands of metres.

Major and trace element geochemistry (for up to 67 elements) was consistently characterised using a combination of digestion methods and analytical techniques. All samples were analysed using four-acid digestion and ICP-MS / OES (48 elements), with the majority also analysed by lithium metaborate fusion and ICP-MS / OES (31 elements, to ensure near-total digestion of Ba, REE, Sn, W, U), fire assay and ICP-MS (Au, Pt, Pd), Leco furnace (C, S), KOH fusion – ion chromatography (F) and Aqua regia – ICP-MS (Hg, Se, Te). Prior to geochemical sampling, drill core samples

(and often – entire drill cores) were scanned using GSQ's HyLogger-3 to characterise spectral mineralogy.

Exploratory statistical data analysis (principal component and clustering analyses) highlight a multi-element geochemical signature common for almost all of the sampled copper-gold deposits – Cu–Au–Ag–S–Te \pm Co–Bi–Se. There are also significant differences between signatures of individual deposits (and their spatial clusters). In particular, the Ernest Henry and several nearby deposits are characterised by a particularly complex multi-element geochemical signature – **Cu–Au–Ag–S–Te–As–Bi–Mo–W–Co–Se–Re** \pm Pb–Ba–In–U–Sb–Sn–Hg.

In addition to copper and gold, IOCG deposits in the district are also significantly enriched in several critical metals, most notably, Co (commonly hundreds ppm, with smaller deposits and parts of orebodies averaging >0.1% Co), REE (locally >0.5% total REE) and Re (particularly in Mo-rich deposits and orebodies affiliated with IOCG deposits *sensu stricto*), which could become potentially economically extractable by-products.

A manganese oxide discovery, Carrara Range, South Nicholson region, Northern Territory

Carson, Chris, Henson, Paul, Huston, David, Jarrett, Amber, Champion, David, & Boreham, Chris

Geoscience Australia, Canberra, Australia

Proterozoic rocks of the South Nicholson region, northeastern Northern Territory, are juxtaposed between the Mount Isa Province and the McArthur Basin. Whereas the latter two provinces are well-studied and prospective for energy and mineral resources, the geological evolution and resource potential of the South Nicholson region is not well understood. Geoscience Australia, under the *Exploring for the Future* (EFTF) initiative, in collaboration with State and Territory Geological Surveys, conducted a range of regional geoscience investigations to better understand the resource potential across the region, encouraging greenfield resource exploration.

Here we discuss preliminary findings on an unreported manganese oxide (MnO) occurrence in the Carrara Range in the South Nicholson region. The occurrence is hosted by north-dipping quartz sandstones of the ca 1640 Ma Plain Creek Formation (McNamara Group), in the hanging wall of the south-verging, east-west-trending Wild Cow Fault zone. The Plain Creek Formation conformably overlies the Shady Bore Quartzite, and conformably underlies shales and carbonaceous siltstones of the Lawn Hill Formation. The Plain Creek Formation is stratigraphically equivalent to the Riversleigh Siltstone in the Lawn Hill Platform.

The MnO body is almost entirely comprised of pyrolusite (MnO_2) and cryptomelane ($\text{KMn}_8\text{O}_{16}$), surrounded by a halo of partially MnO altered host sandstone, crosscut by numerous 1–5 mm wide zoned 'feeder' veinlets. Veinlets consist of quartz, pyrolusite and cryptomelane with euhedral wall quartz projecting into the veinlets and Mn minerals infilling the centre of the veins. The MnO body is ~20 m wide across strike. The lateral and depth extent of the occurrence is unknown, but satellite imagery indicates that MnO mineralisation is visible, along strike, for at least several

hundred metres. These observations suggest that the Carrara Range MnO occurrence is likely an epigenetic replacement stratiform body.

Geochemistry on the MnO body return 49.8 wt% MnO with appreciable (~450 ppm) Zn, the host sandstone return 10.8 wt% MnO and ~25 ppm Zn. Reconnaissance fluid inclusion analysis on quartz–MnO veinlets reveals both brine + vapour aqueous inclusions and hydrocarbon + vapour inclusions. Coexisting aqueous and hydrocarbon were not observed. Homogenisation temperatures are 90–180 °C for aqueous inclusions and 60–140 °C for hydrocarbon inclusions. Fluid salinities are 10–23 wt% (NaCl equivalent), which may suggest interaction with evaporites. Decrepitation of the fluid inclusions yielded CO₂ with no accompanying hydrocarbon gases, suggesting an oxidising fluid. The $\delta^{13}\text{C}$ of the released CO₂ is –22.96‰, consistent with a biogenic source, possibly from hydrocarbon oxidation.

The mineralising fluids were high salinity and low temperature (~120 °C) brines, typical of mineralising fluids for Mississippi-Valley and/or Mount Isa style base-metal deposits. The host Plain Creek Formation is broadly stratigraphically equivalent to units that host world-class regional Pb–Zn deposits such as Century, McArthur River (HYC) and Lady Loretta and others of northwestern Queensland and northeastern Northern Territory. This correlation, together with the knowledge that many Pb–Zn deposits across the region are associated with manganese enrichment, increases the potential of a base-metal resource in the South Nicholson region and the discovery of the Carrara Range Mn occurrence may help stimulate regional base-metal exploration.

Structural evidence for massive sulphide mineralisation during extension, Clarke's Reef, SE NSW

Durney, David W¹, & Hood, David I A²

¹Earth & Environmental Sciences, Macquarie University, Australia; ²R&D Dept., ARDEX Australia, Sydney, Australia

Different explanations have long been given for the formation of base-metal massive sulphide mineral deposits in the Lachlan Orogen of New South Wales. (1) One holds that combined syngenetic and epigenetic mineralisation is associated with either sedimentation (SedEx) or volcanism (VMS) during basin formation. (2) An alternative, sometimes labelled “epigenetic”, suggests that the mineralisation forms syn-deformationally from fluids released by orogenic regional metamorphism (Metamorphogenic) during thrusting and basin inversion. In the first, the tectonic environment is generally considered extensional while, in the second, it is necessarily convergent. Examples where these explanations have been suggested to include the Cobar, Woodlawn and Clarke's Reef sulphide deposits. The outcome has been either a lack of consensus or a tendency for Metamorphogenesis to be a partial or dominant paradigm.

New observations are reported which throw further light on the origin of the Clarke's Reef Pb–Zn–Cu deposit and associated occurrences of massive sulphides in the Silurian Quidong Basin of far southeastern New South Wales. These are part of a broader series of conclusions drawn from field observations of structures

in the Quidong Basin by Hood and co-workers at this Conference, highlighted here as an example of how structural data may assist in resolving questions of this kind.

As the Quidong sulphides occur partly in pyritic sediments at the unconformable base of the Basin and partly on faults and veins which extend into the overlying limestones and mudstones, a key question is the nature of the faulting and whether it pre-dates, syn-dates or post-dates the folds. In agreement with earlier unpublished work, the observed faults within the Basin reported by Hood and co-workers are all normal, with or without a wrench component. This places them either before or after the convergent fold deformation which also affected the Basin. A newly recognised structure called *incoherent fault-related minor folds*, where subhorizontal thinly layered rocks show localised buckling against steep faults, provides, for the first time, clear structural evidence that the faulting occurred before folding in this area.

The observations therefore support a combined syngenetic–epigenetic origin for the Clarke's Reef deposits, contemporaneous with extension during basin formation.

Unconventional gas & resources

Unconventional gas and resources

Garnett, Andrew¹

Centre for Natural Gas, The University of Queensland, Brisbane, Australia

Primary energy demand is set to grow significantly over the next few decades. There is an increasing realisation that natural gas has several critical, complex and, to some extent, counter-intuitive roles in pursuing a “less than 2 deg C” scenario. With reference to the IEA's Sustainable Development Scenario, natural gas will need to remain abundant and affordable and socially and environmentally acceptable in order to fulfil these roles. However, the proportion of gas that is traded as LNG looks set to grow, at least for a while, and importantly, the proportion of gas that comes from unconventional sources is also forecast to grow. This has significant implications, for example, for the confidence needed in sub-surface prediction of resources and their flow behaviour, as well as for the technologies and technical costs by which they are developed. The challenges of the future are harder than those of the past. There will be significant, new trials which only geoscientists and petroleum engineers can resolve. This presentation will highlight the main technical challenge areas and the contribution that earth science professionals will have to make within the complex and wicked energy trilemma.

CO₂ reduction and fermentation producing in situ CH₄ in the majority of sampled GAB aquifers and alluvium overlying a coal seam gas field

Pearce, Julie^{1,2}, Golding, Sue², Baublys, Kim², Hofmann, Harald², St. John, Herbert³, & Hayes, Phil¹

¹UQ Centre for Natural Gas, University of Queensland, Brisbane, Australia; ²School of Earth and Environmental Science, University of Queensland,

Brisbane, Australia; ³Arrow Energy, Brisbane, Australia

Understanding the origin and source of gas in aquifers with multiple users is of increasing importance. The Walloons coal seams are a major coal seam gas (CSG) resource in Queensland, where various shallower and deeper aquifers are part of the Great Artesian Basin (GAB). Dissolved gases and waters were sampled from water bores in the Gubberamunda, Mooga, Orallo, Hutton, Precipice and Springbok Sandstones, the Condamine Alluvium, Walloons bores, and also CSG wells. The majority of $\delta^{13}\text{C}$ and $\delta^2\text{H}$ of CH_4 and CO_2 sampled from shallow aquifer bores indicated in situ primary microbial CO_2 reduction, with three water bores in the Gubberamunda, Mooga, and Walloons plotting in the fermentation pathway region. CSG wells and a gassy Springbok bore however plotted in the secondary microbial region, typical of biogenic CSG. The majority of the Condamine Alluvium bores sampled had very low CH_4 concentrations, with $\delta^{13}\text{C}\text{-CO}_2$ in the range -17 to -21 ‰, and $\delta^{13}\text{C}\text{-DIC}$ $+2.2$ to -13 ‰. The range of $\delta^{13}\text{C}\text{-DIC}$ from CSG wells ($+16$ to $+19$ ‰) was typical of methanogenesis. Stable isotopes of water encompassed a wide range, with Alluvium samples and one Walloons water bore more enriched. A gassy Springbok bore, CSG wells, and deeper bores had depleted values consistent with recharge during colder climates or greater impact from microbial-water-rock reactions. Strontium isotopes of aquifer waters were mainly more radiogenic and distinct from CSG waters indicating disconnectivity in the majority of cases. Results so far suggested that CH_4 was formed in situ (rather than leakage) in the majority of our samples, however in a few cases sources could not be determined. Analysis of a subset of samples for $\delta^{14}\text{C}$, ^{36}Cl , ^{34}S , and CH_4 clumped isotopes are also in progress.

A very unconventional hydrocarbon play: the Mesoproterozoic Velkerri Formation of northern Australia

Collins, Alan S.¹, Cox, Grant M.¹, Jarrett, Amber J.M.², Blades, Morgan L.¹, Shannon, April, V.¹, Yang, Bo.¹, Farkas, Juraj¹, Hall, P. Tony¹, O'Hara, Brendan³, Close, David³, Baruch, Elizabeth, T.⁴, Altmann, Carl⁴, Evans, David⁵, & Bruce, Alex⁵

¹Tectonics and Earth Systems (TES), MinEx CRC, Department of Earth Sciences, The University of Adelaide, Adelaide, SA 5005, Australia; ²Geoscience Australia, P.O. Box 378, Canberra, ACT, 2601, Australia; ³Santos Limited, Santos Centre, 60 Flinders Street, Adelaide, SA 5000, Australia; ⁴Origin Energy Ltd, Level 25, 180 Ann St, Brisbane, QLD 4000, Australia; ⁵Empire Energy, Empire Energy Group Limited, Level 19, 20 Bond Street, Sydney NSW 2000

The ca 1.5–1.3 Ga Roper Group of the greater McArthur Basin is a component of one of the most extensive Precambrian hydrocarbon-bearing basins preserved in the geological record, recently assessed as containing 429 million barrels of oil and eight trillion cubic feet of gas (in place). It was deposited in an intracratonic sea, referred to here as the McArthur-Yanliao Gulf.

The Velkerri Formation forms the major deep-water facies of the Roper Group. Trace metal redox proxies from this formation indicate that it was deposited in stratified waters, in which a shallow oxic layer overlay

suboxic to anoxic waters. These deep waters became episodically euxinic during periods of high organic carbon export. The Velkerri Formation has organic carbon contents that reach ~10 wt%. Variations in organic carbon isotopes are consistent with organic carbon enrichment being associated with increases in primary productivity and export, rather than flooding surfaces or variations in mineralogy.

Although deposition of the Velkerri Formation in an intracontinental setting has been well established, recent global reconstructions show a broader mid to low latitude gulf, with deposition of the Velkerri Formation being coeval with the widespread deposition of organic rich rocks across northern Australia and North China. The deposition of these organic-rich rocks may have been accompanied by significant oxygenation associated with such widespread organic carbon burial during the Mesoproterozoic.

The distribution and origin of hydrogen sulphide gas in the Triassic Montney Unconventional Play, British Columbia and Alberta, Canada

Chalmers, Gareth¹, Bustin, Amanda², & Bustin, Marc²

¹University of the Sunshine Coast, Sippy Downs, Australia; ²University of British Columbia, Vancouver, Canada

The distribution and origin of hydrogen sulphide (H_2S) within the Triassic Montney Formation of the western Canadian sedimentary basin (WCSB) were investigated in British Columbia and Alberta, Canada. Hydrogen sulphide is a toxic gas that can be co-produced with hydrocarbons and impacts well economics and the environment. Even small amounts of H_2S can impact hydrocarbon operations by depositing 'elemental sulphur' within pipelines and compressors as observed in Australia and overseas.

This study has mapped the H_2S concentration in the Upper, Middle and Lower sections of the Montney Formation as operators are drilling multi-directional well pads within three zones of a 200 m reservoir. The Montney Formation has tested or produced H_2S gas at concentrations between 0.001% and 22%. The stratigraphic and lateral variation in the H_2S concentration can be inexplicable.

Sulphur available to generate H_2S includes sulphide oxidation, decomposition of well-completions surfactants, bacterial sulphide reduction, kerogen cracking or fluid migration of sulphate ions from sulphur-rich evaporites. The isotopic ratios of sulphur and oxygen will depend on the source and the formation pathway of the H_2S gas and these ratios can be used to help model H_2S gas generation. Samples were collected from the Triassic Charlie Lake, Doig, Montney formations and the Devonian Nisku, Elk Point and Muskeg formations within areas of sour wells. Organic matter, sulphate and sulphide minerals were isolated using chemical and physical mineral separation techniques. These samples were analysed for sulphur and oxygen isotopes at the Jan Veizer Stable Isotope Laboratory, University of Ottawa (Ontario, Canada). Sulphur and oxygen isotopic ratios from sulphate minerals within the Montney Formation and the Charlie Lake Formation have a range between 9.0 to 18.0 ‰ V-CDT and -5.0 to 19.0 ‰ V-SMOW, respectively. These

isotopic ratios differ from the sulphur and oxygen isotopic ratios from sulphate minerals sampled from Devonian rock sources which vary between 18.0 to 30.0 ‰ V-CDT and 12.0 to 30 ‰ V-SMOW, respectively. The sulphur isotopic ratio measured from H₂S gas of producing Montney Formation wells varies between 9.3 and 20.9 ‰ V-CDT.

Preliminary results from isotopic analyses suggest that the sulphur that generated H₂S in the Montney Formation is from Triassic sulphates or a mixture of Triassic and Devonian sources and not solely from Devonian rocks as first expected. It is postulated that the sulphate ions have migrated through localised fractures into the Montney Formation and then the sulphate is used to generate H₂S. Another possibility is the H₂S gas formed in the Charlie Lake Formation and/or Devonian rocks and then migrated into the Montney Formation. Textural relationships between the reservoir rock and the sulphate minerals is currently being examined which will provide key data for creating a H₂S generation model for the Montney Formation.

Combined petrography and palynofacies study of the Toolebuc hydrocarbon sources

Rodrigues, Sandra¹, Golding, Suzanne¹, Esterle, Joan¹, Mendonça, Filho², João, Graciano, & Flores, Deolinda³

¹The University of Queensland, School of Earth and Environmental Sciences, St Lucia, Australia; ²Laboratório de Palinofácies & Fácies Orgânica (LAFO), Departamento de Geologia (DEGL), Instituto de Geociências (IGEO), Universidade Federal do Rio de Janeiro (UFRJ), Brazil; ³The University of Porto, Department of Geosciences, Environment and Spatial Planning, Porto, Portugal

This research provides new insights into the petrology of the organo-facies of the Cretaceous marine Toolebuc Formation, Eromanga Basin. One well from the deep section of the Toolebuc Formation in the most prospective southern part of the basin in Queensland was used for this study. The core section is a 20 m thick carbonate-mud shale with poor expression of the conquinite section often associated with this formation at other locations in the basin. Around 26 polished blocks cut perpendicular to the stratification were used for maceral analysis and 7 slides were prepared for palynofacies analysis. Telalginite represents the structured components. In the samples studied, *Tasmanite* (green algae) is easily recognised in most of the samples. Its original spherical cyst (phycoma) is flattened along the bedding plane during sediment compaction. Other alginite are present but their identification is difficult. However, the palynofacies showed the presence of dinoflagellates and acritarchs, which may correspond to some of the alginite observed in the petrographic blocks. Furthermore, organic matter with a concentric arrangement of walls is also observed. It has been described in the literature as “organic matter of unknown affinity” and sometimes sporangia (term associated with terrestrial material). However, given the good preservation of this material in this well, this component actually suggests different stages of a life cycle, possible from the *Tasmanite*. Other organic components include lamalginite and liptodetrinite, probably derived from the algae materials. Bituminite was identified as one of the major organic

components in the petrographic blocks, it presents very low fluorescence and is often micritized, and corresponds to the amorphous organic matter in the palynofacies slides. In part, bituminite could be derived from the algal components, however, no direct association between the two components was found. The micritization of the bituminite indicates that hydrocarbons were generated from this maceral. Other petrographic evidence for the production of hydrocarbons is the occurrence of solid bitumen. Although not often described in the literature, solid bitumen occurs filling the cavities of the foraminifera fossils as well as in the rock matrix of the Toolebuc samples. The origin of these solid bitumens might be different as they have distinct optical properties. Live oil was also observed in some samples during microscopic analysis. There is no direct petrographic evidence of hydrocarbon migration in the samples studied, as solid bitumen was not observed in the fractures, therefore, it might be assumed that hydrocarbons were produced within the Toolebuc Formation and not migrated from the underlying formation.

Re-evaluation of overlooked petroleum potential in the Powell Depression, southern Galilee Basin

Troup, Alison^{1,2}, Esterle, Joan¹, Rodrigues, Sandra¹, & Guerer, Derya¹

¹School of Earth and Environmental Sciences, University of Queensland, Brisbane, Australia; ²Queensland Department of Natural Resources, Mines and Energy, Brisbane, Australia

Extensive sedimentary basin development occurred in eastern Australia during the late Carboniferous to Triassic. The Cooper and Bowen basins are both part of productive petroleum systems, with source rocks and reservoirs found in late Permian and Triassic units, as well as Jurassic and Cretaceous units in the overlying Surat and Eromanga basins. No corresponding discovery has been made in the Galilee Basin. Partially as a result of perceived prospectivity, the Galilee Basin is under-studied and under-explored.

The Galilee Basin is a large late Carboniferous to Triassic aged sedimentary basin in central Queensland, extending across an area of approximately 247 000 km², though most of this extent is under the cover of the Triassic to Cretaceous Eromanga Basin. It is divided into four main regions: the Lovelle Depression in the north west, the Koburra Trough in the north east, the Springsure Shelf in the south east and the Powell Depression in the southwest. It overlies meta-sedimentary rocks and remnant sedimentary basins of the Thompson Orogen, including the early to middle Carboniferous Drummond Basin in the north east, underlying the Koburra Trough and the Devonian Adavale Basin in the southwest, underlying the Powell Depression.

Recent projects have re-evaluated the late Permian units of the Koburra Trough, which examined the sequence stratigraphy, palaeogeography, age dates, provenance and lithostratigraphic correlation with the Bowen Basin and past projects have evaluated the petroleum potential of the Lovelle Depression. However, the Powell Depression has been overlooked in previous regional studies, potentially due to the effect of perceived prospectivity or a relatively lower number

of wells available for interpretation.

By proxy to the Cooper Basin and Bowen Basin, the Galilee Basin should be expected to have a late Carboniferous to Permian sourced petroleum system. Age-equivalent rocks of the major source rock bearing units in the Cooper and Bowen basins are present in the southern Powell Depression, though controls on the source rock quality and maturity in the Powell Depression are scarce. Coal seams are present in the late Permian Bandanna Formation, though the coal seam distribution in the Powell Depression is uncertain. For a conventional petroleum system, reservoirs and traps are likely to be channel sandstones associated with late Carboniferous to early Permian glacial outflow channels or late Permian fluvial channels. The major regional seals in the Bowen and Cooper basins are a thick Triassic aged sequence of terrestrial mudstones in the Moolayember and Tinchoo formations. Thus, the Moolayember Formation should also provide a regional seal in the Powell Depression

Historical exploration in the Powell Depression region primarily targeted structures in the Adavale Basin. As these structures form basement highs to the Galilee Basin, a thinner sequence was drilled, which has formed the perception of limited exploration potential. Seismic reflection survey data show thickening of the Galilee Basin sequence off these basement structures, which suggests potential in this region may have been overlooked.

New geology analytics and machine learning in data-rich and data-poor environments

Random forest based mineral potential mapping for porphyry Cu–Au mineralisation in the Eastern Lachlan Orogen

Ford, Arianne

Kenex Ltd., Lower Hutt, New Zealand

Random forests represent a machine learning implementation of a decision-tree algorithm that can be applied to data-driven mineral potential mapping. Most published studies using random forests include relatively small numbers of input maps that are typically pre-classified by an expert familiar with the mineral system being targeted. The aim of this study was to investigate how random forests performed using different input parameters in terms of the individual predictive maps and training data. Four different implementations of the random forest algorithm were produced based on a case study using data from the eastern Lachlan Orogen in NSW for the purposes of targeting porphyry Cu–Au mineralisation related to the Macquarie Arc: (1) using a large number of multi-class categorical or non-thresholded predictive maps that have had no favourability criteria applied, (2) using a large number of binary predictive maps that have had statistically valid and geologically meaningful thresholds determined through weights of evidence analysis and expert review, (3) using a subset of the binary predictive maps that were used in a weights of evidence mineral potential mapping study, and (4) using this same subset of binary predictive maps with weighted training data. These results were then compared to the results of an existing weights of

evidence mineral potential mapping study.

The results of the random forest analysis demonstrate how both the ranking of the input maps and subsequent mineral potential varies considerably depending on the degree of intervention from an expert in the modelling process. The first approach produced a prospective area that covered 47.7% of the study area, the second approach 6.5%, the third approach 23.4%, and the final approach with the weighted training data 40.4%. In comparison, the weights of evidence study produced a prospective area that covered 15.2% of the study area, however failed to predict one of the training points within this prospective area. Increasing the complexity of the input data improved the predictive capacity of the mineral potential maps for targeting the porphyry Cu–Au mineralisation when expert review was used to determine meaningful thresholds and classifications for the input predictive maps. However, when a large number of multi-class categorical or non-thresholded predictive maps were used as input to the random forest (i.e., no favourability criteria were applied, so the algorithm determined the thresholds rather than an expert), a poor result was obtained. The results also highlight that the main limitation of using random forests (and other machine learning approaches) for mineral potential mapping is the lack of a sufficient number of economically significant deposits which can be used to train a large number of input predictive maps.

The random forest study clearly demonstrates that the use of predictive maps that have statistically valid, geologically meaningful, and practically useful thresholds and reclassifications assigned produce more robust mineral potential maps that can be used for exploration targeting.

Are giant ore deposits rogue waves or dragon kings?

Hobbs, Bruce¹, & Ord, Alison²

¹CSIRO, Perth Australia; ²The University of Western Australia, Perth, Australia

We address the question: *Does the formation of giant ore hydrothermal deposits involve different process to the formation of average sized ore deposits?* We draw analogies with the processes involved in mineralising systems with those used to explain the formation of rogue waves in oceanography and nonlinear optics and of tropical cyclones. Giant ore bodies constitute the tails of “fat tailed” distributions, or lie off the end of such distributions. It is important to distinguish between deposits that belong to a self-similar system (referred to as *black swans* by Sornette), and those that exceed what is expected from such a distribution (Sornette’s *dragon-kings*). It is proposed that similar processes operate for all members of a black swan distribution, and different processes operate via a phase transition for those that differ from the rest of the distribution. The nonlinear coupling between chemical reactions, deformation and permeability generation is discussed as a mechanism for forming regions of the Earth’s crust with anomalously high permeability. This nonlinear coupling between chemical reactions and deformation is identical to the physics used to explain rogue waves, tropical cyclones and dragon-kings. Thermodynamic arguments suggest the probability distributions for ore bodies at regional and microstructural scales should be fat tailed Fréchet distributions and it is shown that

examples from natural mineralising systems conform to these distributions at a range of spatial scales. The implications for mineral deposit prediction and assessment using log-normal distributions and Zipf's law are discussed together with the implications for kriging.

Propagating sparse basement markers through inversion volumes using graph convolutional neural networks

Gillfeather-Clark, Tasman, Horrocks, Tom, Holden, Eun-Jung, & Wedge, Daniel

Centre for Exploration Targeting, School of Earth Sciences, The University of Western Australia, Perth, Australia

A common problem in geoscience is spatially extrapolating sparse data, such as drill core logs or geochemical assays, in the presence of larger encompassing datasets such as inversion volumes. For example, a seismic-derived basement surface may be refined using a collocated physical model in which the basement and regolith are in high contrast, for example, an airborne electromagnetic (AEM) inversion volume. What makes this integration challenging for an interpreter or a machine learning approach is relating different datasets in a way that is both robust and scalable. While co-kriging is a scalable approach for this problem it requires variables to be consistently correlated, where graphs can address changing relationships. We propose the usage of graphs to understand the relationships between multiple datasets in 3D space.

A graph is a data structure comprised of entities (nodes) and connections between them (edges). Nodes can have attributes like values and labels, while edges can be directional or bidirectional, and weighted or unweighted. Graphs are underutilized in geosciences due to a lack of inherently graph structured data and relatively recent development of Graph Neural Networks. Our work shows the potential for graphs and graph neural networks to be applied to geoscience problems, as well as a general workflow to successfully implement a graph structure on 3D geoscience datasets.

We focus on basement delineation over a detrital iron deposit of the Fortescue valley in the Pilbara. Detrital iron deposits are accumulations of detritus eroded from a primary deposit (Koodaideri Iron) and trapped in basement depressions. Thus, the paleo-basement surface is crucial to the formation of the deposits. We use two key datasets: an AEM laterally constrained inversion volume (LCI) and a basement surface. This surface is produced using interpretation of: AEM inversion data, drilling, and seismic data.

Graph Neural Networks (GNNs) are powerful neural network architectures designed for graph data. The central paradigm of GNNs is called message passing, where prediction is made by 'passing' the embedded state of a node to its neighbours. This means that classification is controlled by the edges, we define instead of the attributes of the nodes. Further this allows us to connect nodes from different datasets that do not have common attributes, but that occupy the same space.

The nodes of our network come from the AEM LCI point

cloud, where conductivity and uncertainty are discrete points in 3D space. We use the basement surface to label our nodes as either cover (above) or basement (below). The edges of the graph are generated using an adjacency matrix calculated by thresholding a cosine-similarity matrix, based on the z-score of the similarity value. Cosine similarity is a measure used to compare any two vectors. These vectors are generated based on relationships we consider important within our data such as spatial relationships (X, Y, Z), or conductivity depth relationships (COND, Z). We can combine and weight these matrices using the dot product for any number of similarity matrices.

Our preliminary results predicted with 93.5% accuracy if an inversion point was basement or cover in the 4200-point line using only 200 labelled points. The points that were misclassified, were mainly along the basement interface where the greatest uncertainty of label quality exists, based on conflicting interpretations. This represents a preliminary examination of our research problem and future work includes increasing the number of survey lines in the graph, different labelling regimes, the integration of additional datasets (drilling), and the propagation of more challenging labels (lithology).

Extending FaultSeg3D to minerals seismic: Part 1 – a synthetic 3D-seismic training-volume generator for preparing data replicating a hardrock terrane to train an automatic-fault-prediction algorithm

Chatterjee, Robindra¹, Weatherley, Dion², McLachlan, Geoff³, & Valenta, Rick^{1,2}

¹The University of Queensland, Sustainable Minerals Institute, W.H. Bryan Mining and Geology Research Centre, Brisbane, Australia; ²The University of Queensland, Sustainable Minerals Institute, Julius Kruttschnitt Mineral Research Centre, Brisbane, Australia; ³The University of Queensland, School of Mathematics and Physics, Brisbane, Australia

Automatic seismic interpretation of 3D volumes used in minerals exploration is an under researched topic. We are conducting a three-part investigation to extend the state-of-the-art in automatic fault interpretation methods based on the FaultSeg3D algorithm developed by Wu *et al.* (2019, 2020). This approach has demonstrated superior performance in automatic fault and horizon picking on: (i) synthetic seismic volumes created to emulate the geological complexity for petroleum targeting present in sedimentary terranes, and (ii) publically available field surveys that were part of a petroleum exploration program. Our hypothesis is that training FaultSeg3D on this style of data leads to poor prediction performance of fault locations in 3D-seismic datasets surveyed over hard-rock terranes that typically exhibit greater geological complexity. This is referred to as a model generalisation issue, that occurs when the joint distribution of the data present in the synthetic volumes used for training a machine-learning-based, fault-prediction algorithm is significantly different from that present in the field survey used for prediction. A 3D seismic volume from an operating gold mine in Queensland was provided for this study courtesy of Evolution Mining Ltd. (ASX: EVN) along with the 3D geological model and drilling database to validate results.

This research has developed a flexible, synthetic-seismic-volume generator that will be used to create more representative training data for a machine-learning-based, fault-prediction algorithm. Geological folding, faulting, post-process-filtering and acquisition noise are modelled via successive image-processing convolutions. The first feature of the model is the ability to accommodate a user-specified degree of geological complexity by adjusting the level of geological folding and faulting present in the target field-survey's terrane for any size cube. The second feature of the model is a more physically realistic way to model three major kinds of faults based on elastic dislocation theory. The third feature of the model is the addition of multifractal fault and vein population characteristics that further impart geological realism. In the next phase of the research, we will train a deep-learning algorithm on several hundred synthetic-seismic volumes, that emulate the geological complexity at the gold mine, to produce an automatic-fault-surface prediction tool that could aid the targeting of fault-constrained mineralisation.

Statewide mineral potential mapping of New South Wales using a combined mineral systems and spatial data approach

Blevin, Phillip¹, Downes, Peter¹, Fitzherbert, Joel¹, Ford, Arianne², Peters, Katie², & Greenfield, John¹

¹*Geological Survey of New South Wales, Department of Regional NSW, Maitland, Australia;* ²*Kenex Ltd, Wellington, New Zealand*

The Geological Survey of New South Wales (GSNSW) has completed a four-year mineral potential mapping project across the major metallogenic provinces of NSW. These include the New England, eastern and central Lachlan and Delamerian orogens as well as the Curnamona Province. Mineral system models, specific to each province/event, were prepared for orogenic Au and Au–Sb, polymetallic volcanic associated massive sulfide, Broken Hill Pb–Zn–Ag, Cobar Pb–Zn and Cu–Au, Macquarie Arc porphyry Cu–Au and intrusion-related Au and Sn–W systems. Modelling of the skarn potential of the eastern Lachlan Orogen was also undertaken to test the intersection between granite fertility with structural and reactive rock data to potentially model fluid flow and traps using essentially 2D data.

In excess of 10 million drill hole assays, 152 000 attributed faults, 31 190 mineral occurrences, 197 754 field observations and 883 967 surface geochemical assays were used in addition to the NSW Seamless Geology, and statewide geophysical and metamorphic datasets.

Where possible, a weights-of-evidence approach was used. Typically, over 100 valid predictive maps were generated for each mineral system to model source, transport, trap and depositional characteristics. Spatial relationships were tested with between 8 to 28 training points. Between 8 to 18 predictive maps were selected for each final model. The efficiency of classification for most models was better than 95%, with the prospective areas covering 3% to 16% of the relevant province and the highly prospective areas being significantly smaller. Importantly, measures of data confidence were captured, and all polygons have attached metadata indicating the predictive layers used in their construction. There was interactive feedback at all

stages between the Kenex spatial analysts and GSNSW mineral system specialists. The final reports, primary datasets, spatial data tables and data, including thousands of intrinsically useful predictive maps, are freely available for download from DIGS, with key spatial layers also accessible on the MinView platform. The prepared data outputs provide an ideal opportunity for testing revised and new mineral system models, or to add new data and explore alternate methodologies.

In areas under cover, geophysical mapping of secondary structures and intrusions was key in compensating for a lower data density. The associations of many mineral systems with gravity and magnetic worms at various depths is also intriguing, although the reason for this association is not yet clear. The correlation and understanding of these linkages through the crust will be a focus for future mineral potential mapping studies in areas devoid of relevant surface data.

A key learning from the project is the need to ensure that all datasets are in usable formats and fit-for-purpose prior to spatial modelling. This includes the standardisation of geological drill logs, stratigraphic unit descriptions and attributes in mineral occurrence and petrological databases. In the future, rock reactivity and permeability values, petrophysical data and magmatic fertility parameters combined with seamless geology, and fully attributed fault and metamorphic layers will allow for the construction of on-demand mineral potential maps viewable on MinView and permit the data to be exported into machine learning packages for real-time modelling on online platforms.

Advancing technologies in mineral exploration

Extracting more from exploration soil samples. The evolution of UltraFine+ and next generation analytics

Noble, Ryan R. P., Cole, David T., Williams, Morgan J., Lau, Ian C., & Anand, Ravi R.

CSIRO Mineral Resources, Kensington, Perth, Western Australia

Continued exploration success requires consistent innovation. While large geochemical surveys conducted by mining companies are common, the suite of data we collect beyond standard soil chemistry has remained stagnant. A novel integration of analytical methods known as UltraFine+™ extracts the “standard soil chemistry” of the <2 µm soil clay fraction, which is combined with soil VIS-NIR and FTIR spectral mineralogy proxies and physicochemical properties to improve interpretation of soil chemistry leading to better targeting for gold and base-metal exploration.

At numerous study sites across Australia, we demonstrate how the integration of spectral mineralogy proxies and particle-size variation can assist in understanding landscape processes and anomaly formation, and in some settings provide explanations for false positives. Through providing uncertainty estimates on spatial geochemical predictions and reducing the influence of explainable false positives, key information is communicated to decision makers for more confident targeting. A marked decrease in censored results using UltraFine+™ for gold (from 63%

to 10% below detection limit) is a major improvement over historical techniques. Automated analytics pipelines using a variety of unsupervised machine learning techniques (e.g., dimensionality reduction, clustering) ensure the rapid interpretation of survey datasets, and accelerate the path to discovery.

Laser-Induced Breakdown Spectroscopy integrated with multi-variate wavelet tessellation – a new and rapid methodology for litho-geochemical analysis and interpretation

Fontana, F. Fernando^{1,2}, Tassios, Steven^{2,3}, Stromberg, Jessica^{2,4}, Tiddy, Caroline^{1,2}, van der Hoek, Ben^{1,2}, & Uvarova, Yulia^{2,4}.

¹Future Industries Institute, University of South Australia, Mawson Lakes, Australia; ²Mineral Exploration Cooperative Research Centre – MinEx CRC; ³CSIRO Mineral Resources, Clayton, Australia; ⁴CSIRO Mineral Resources, Kensington, Australia.

Rock classification and discrimination is commonly performed by geologists through visual inspection of rocks in the field or by geological logging of drill cores. However, this visual interpretation of rock lithology is notoriously subjective and inconsistent. The utilisation of handheld and core scanning instruments for collecting standardized data coupled with rapid and consistent methods for extracting geological information (e.g., clustering algorithms and boundary detection techniques) is gaining popularity for supplementing traditional geological classification. Such techniques are objective and reduce inconsistencies, improving rock classification and geological logging outputs. Laser-Induced Breakdown Spectroscopy (LIBS) is an emission spectroscopy technique of interest for litho-geochemical analysis due to its sensitivity to light elements common in geological materials (e.g., Li, Be, Na, Mg), that are difficult to quantify using other techniques such as X-ray fluorescence (XRF). The wavelet tessellation method utilises the wavelet transform for edge detection in spatialized data and can be used for determination of boundaries in downhole geochemical data which may represent lithological contacts. Wavelet tessellation can be applied to raw LIBS data outputs (counts vs wavelength) with no requirement for data filtering or manipulation. In this study we demonstrate the application of wavelet tessellation for rapid analysis of LIBS geochemical data to produce pseudo-logs that are representative of a test-block geological stratigraphy. A test-block stratigraphy was created using 22 rock slabs glued together to produce a block ~16 cm in length. The samples were chemically (XRF) and mineralogically (XRD) characterised and selected to represent two discrete and geochemically distinct rock types (granitoid and marble). LIBS spectral data for nine major elements (Al, Ca, Fe, K, Mg, Na, Si, Ti and Mn) was generated along a continuous line at a constant speed of 10 mm/min at 5 Hz in which every group of 10 spectra were averaged into 1 spectrum, creating 460 spectra that each correspond to an interval of ~0.35 mm. Clustering algorithms were used to separate the samples into groups reflective of rock-types based on the LIBS outputs for those 9 elements. Wavelet tessellation was undertaken to produce pseudo-logs of the test-block stratigraphy. Comparison of the known

test-block stratigraphy from laboratory XRF and XRD data with the wavelet tessellation pseudo-logs generated from the LIBS data shows the potential application of multi-variate wavelet tessellation analysis for rapid interpretation of stratigraphic boundaries and rock-type from LIBS geochemical data. The discrete lithological groups of marble and granitoid were effectively separated, and less obvious distinctions between Ca and Mg-rich and Ca-rich marble slabs, and mafic to alkali-rich granitoids were also successfully made. The methodology presented here highlights how a workflow using LIBS coupled with wavelet tessellation can be used for rapid litho-geochemical interpretation to produce reliable and objective litho-geochemical pseudo-logs to supplement subjective visual drill core logging. Moreover, the sensitivity of LIBS analysis for light elements provides the opportunity for the development of new litho-geochemical interpretation workflows for exploration campaigns and characterisation of alteration halos.

Digitalizing the mining industry – core scanner for geochemistry, images, RQD, structures, specific gravity and volume bulk density

Arthursson, Mikael², Annelie, Lundström¹, & Angus, Tod²

¹Minalyze AB, Gothenburg, Sweden; ²Minalyze Pty Ltd, Perth, Australia.

Minalyzer CS is a scanner which in a contactless and non-destructive way generates geochemistry, high-resolution images, rock quality designation (RQD), structures, specific gravity and bulk density for drill cores and other drill samples.

The patented scanner is designed for handling large volumes of drill samples and is capable of scanning drill cores directly in core trays. A laser (LiDAR) generates a 3D-model of the topology of the core and trays, which enables the control and precision of the continuous XRF scanning. RQD and structures are also derived based on the 3D-model.

The objective, continuous and consistent nature of the datasets as well as the high but compact data density generated by the scanning technology is paramount in machine learning and deep learning applications and approaches to geology. Machine learning and deep learning have been demonstrated to be effectively used, based on the data from the scanning, for prediction of host rock lithologies.

A cloud-based software www.minalogger.com for visualisation and generation of datasets through digital tools facilitates remote access to a digital version of the drill sample. Remote access to data has become critical in order to keep project and operations moving forward when travel has become impossible and/or risky due to the pandemic.

The bulk density can be derived based on measured volume from LiDAR scan of the Minalyzer CS, combined with the weight of the core tray. The method is suitable for friable sediment core where a true representation of the friable or heavily fractured sample through manual measurements and estimates can be error prone. The new method has been tested and applied in live application by Iron ore companies in Western Australia where extensive comparisons

between the new method and the traditional have been made. The method has also been tested on known volumes and densities for verification and demonstrate both a high level of repeatability and accuracy. Other benefits with the method are that it can be automated to a high degree and provides a non-subjective measurement. Due to its implementation the bulk density value derived would represent a conservative measurement of the bulk density.

Building a cloud-hosted exploration data platform and its application

Kohlmann, Fabian, Noble, Wayne, & Theile, Moritz
Lithodat Pty. Ltd., Melbourne, Australia

Well-managed, standardized data is vital for the exploration industry as it currently undergoes an intense digitalization phase. As most available geoscientific datasets are regionally bound and have bespoke implementations, it is challenging to merge all data into a consistent global framework. Lithodat's vision is to provide geoscientists with global geoscientific databases and analytics to decrease the time taken to gain new insights about regions of interest. Currently, LithoSurfer offers the largest global, standardised thermochronology and geochronology repository available. The detailed analytical data and advanced analytical tools allow the options to query data and thermal histories through time, or even rerun thermal history models.

To achieve this Lithodat has developed LithoSurfer, an online platform for viewing, analysing and extracting data. LithoSurfer gives quick access to a wealth of information (analytical details, lab information, literature etc.) across multiple analytic techniques and localities. Lithodat's team of experts 'extract, validate and integrate data in our cloud-hosted database. This consolidation opens up the full potential that spatial geoscience data has to offer and is a vast improvement on storing data in separate spreadsheets and folders as often happens within laboratories and research projects. LithoSurfer makes disperse and complicated research datasets understandable and usable for the wider geoscience community.

Lithodat's strong links with academia and industry help bring the geoscience community together with a consistent platform for their global geospatial research data. LithoSurfer allows academic communities to enter, organize and analyse their data and collaborate with researchers and industry. Data owners have the opportunity to share their published data with the entire global research community or with just selected co-researchers or customers. Unpublished data or data which needs to be kept private is only accessible to authorized researchers. Although protected, this data can still be integrated with other already published data. In addition, LithoSurfer also details the analytical origin and techniques to enable users to filter the data they want and trust.

Using the right tools means researchers can help to solve scientific questions and industrial demands. With LithoSurfer researchers can now visualize, combine and export data from areas of interest including diagrams, graphs and auto generated reports on the fly. However, LithoSurfer does not constrain the researcher to its tools, and data can be extracted in multiple formats to take full advantage new techniques such as

machine learning (ML) and artificial intelligence (AI).

Multi-scale characterisation of Australia's deepest drill hole

Birchall, Renee, Pearce, Mark, Walshe, John, Powell, Helen, Shelton, Tina, & Woodall, Katie.

CSIRO Mineral Resources, Kensington, WA, Australia.

The Jundee Gold Camp (Jundee), located in the northern Yandal Greenstone Belt of the Yilgarn Craton, is relatively understudied compared to the adjacent historic Wiluna Gold Camp. In 2018, Northern Star Resources drilled an Australian-record-breaking 3217 m drill hole through Jundee's Zodiac Discovery to complement a recently acquired 3D seismic dataset. In this study, the entire stratigraphy of this world-class gold camp was characterised by combining 3.2 km of continuous chemistry measurements made using the Minalyze X-ray Fluorescence (XRF) Core Scanner and over 400 mineral maps acquired using a Tescan Integrated Mineral Analyzer (TIMA) scanning electron microscope. The Minalyze XRF dataset was used to inform the sampling for mineral maps and additional portable X-Ray Fluorescence (pXRF) measurements were taken, to allow the XRF data to be used to benchmark future pXRF analyses on site. The high-spatial resolution of the Minalyze XRF enabled the lithogeochemistry of the 3.2 km of stratigraphy to be characterized in detail. Locally, the Jundee stratigraphy consists of two Archaean basalt-sediment sequences that have been intruded by multiple dolerites and later by lamprophyres, porphyries, granodiorites, granites and further, Proterozoic dolerite dykes. The dolerite and basalt units in the stratigraphy were classified using spatial patterns of elemental variations resulting from igneous fractionation, which can be used to fingerprint individual dolerites in the stratigraphy. Comparison of the Minalyze XRF and pXRF datasets support using immobile elements (Zr, Cr and Ti) to classifying the lithostratigraphy at Jundee. The automated mineralogy data were integrated with the Minalyze XRF and concurrent pXRF lithogeochemical datasets to discriminate between spatial variations in mineralogy caused by lithological changes and those associated with alteration. Interrogation of textural information available in the automated mineralogy phase maps is critical in underpinning the key metamorphic and hydrothermal alteration assemblages in the stratigraphy. The primary gold-bearing mineral assemblage at the Zodiac Discovery is summarised by chlorite (clinocllore and chamosite), calcite, pyrite, titanite, actinolite ±arsenopyrite ±scheelite ±tourmaline (dravite and schorl). Quantifying changes in mineral assemblages and their paragenetic relationships provides information on fluid compositions and pressure-temperature conditions during metamorphism, hydrothermal alteration and mineralisation events. At Jundee, four events were defined through the TIMA SEM method, which may or may not be temporally continuous: Stage 1a: Metamorphic assemblage (greenschist to amphibolite facies), Stage 2a: Alteration assemblages from K-rich fluids, Stage 2b: Alteration assemblages from CO₂-bearing fluids (±Au), and Stage 2c: Assemblages from late, low-CO₂ fluids. Further, fluid pathways and during mineralisation are easily identified because of the high spatial resolution, and quantitative nature of the techniques used.

Better laser focusing on improved reproducibility of U–Pb isotope analysis by LA-ICP-MS

Huang, Hui-Qing¹, Guillong, Marcel², Hu, Yi³, & Spandler, Carl¹

¹*Economic Geology Research Center, Division of Tropical Environments and Societies, James Cook University, Townsville, QLD 4811, Australia;* ²*Department of Earth Sciences, ETH Zurich, 8092 Zurich, Switzerland;* ³*Advanced Analytical Centre, James Cook University, Townsville, QLD 4811, Australia*

Spatial resolution and precision of U–Pb isotope analysis by LA-ICP-MS has been greatly improved in the last two decades. However, reproducibility of this most widely used in situ technique is still relatively poor, and error sources remain challenging to determine. Factors such as matrix composition, air, laser fluence have been systematically examined. Here we evaluate a previously underappreciated source of error on U–Pb isotope determination associated with laser focus. Using two different LA-ICP-MS systems but similar ablation parameters (a circular spot of ~20 µm and a final depth of ablation of ~10 µm only with a laser fluence of 2 J/cm², an ablation time of 30 seconds and a repetition rate of 4 and 5 Hz), we show that sole variation of laser focus by 30 µm can lead to a systematic offset in ²⁰⁶Pb/²³⁸U of ~4–6% for zircons. Focus position variation led to change of laser irradiance on sample surface and shape of ablation craters. The degree of age offset is controlled by the final depth of ablation and crater aspect ratios (depth to diameter). We demonstrate further that the impact of focus variation on U–Pb isotope fractionation is matrix dependent. Using same conditions, defocus of laser beam by 30 µm can cause an offset in ²⁰⁶Pb/²³⁸U by <1% for NIST610 glass, ~3% for titanite, and up to 12% for rutile. The uncertainty related to laser focus appear random. We suggest that enhanced repeatability of laser focusing is required for improved uncertainty and better reproducibility in the determination of elements and particularly high precision U–Pb isotopes by LA-ICP-MS.

dh2loop 1.0: an open-source python library for automated processing and classification geological logs

Joshi, Ranee^{1,2}, Madaiah, Kavitha^{1,2}, Jessell, Mark^{1,2}, & Lindsay, Mark^{1,2}

¹*Centre of Exploration Targeting, School of Earth Sciences, University of Western Australia, 35 Stirling Highway, Crawley 6009 Western Australia;* ²*Mineral Exploration Cooperative Research Centre (MinEx CRC), School of Earth Sciences, University of Western Australia, 35 Stirling Highway, Crawley 6009 Western Australia*

Exploration and mining companies rely on geological drill core logs to target and obtain initial information on the composition and size of mineralized zones and/or a potential ore deposit. The drilling data is also used as inputs to 3D geological modelling to allow better visualization and understanding of the geology in a local and/or mine scale. With the amount of legacy drilling data available in geological surveys, extraction and processing of these data will allow for better

shallow subsurface constraints for semi-regional and regional 3D geological models. These models will be helpful in designing mapping programs and more efficiently targeting sustainable new discoveries.

In this contribution, we focus on the processing and classification of lithological logs from the Geological Survey of Western Australia Mineral Exploration Reports Database in the Yalgoo-Singleton Greenstone Belt (YSGB) region. We refer to lithological logs as the component of a geological log that contains the dominant rock type in a specific downhole interval. Inevitably, lithological drill core logging is subjective and plagued with uncertainty, particularly as at a regional scale it is likely to have been conducted by tens to hundreds geologists, all of whom would have their own personal biases. It can also be difficult to recognize lithology with confidence and to establish subtle variations or boundaries in apparently homogeneous sequences. Given that we are dealing with geological legacy datasets, a large amount of important data are recorded in an unstructured textural form using varying geological drill core logging forms and formats depending on the company, logging geologist, investigation method, investigated materials and/or drilling campaign.

To resolve these challenges and unlock the vast information store in legacy drilling datasets, we developed dh2loop ([github.org/Loop3D/dh2loop](https://github.com/Loop3D/dh2loop)), an open-source python library that provides the functionality to extract and standardize drill hole data and export it into readily importable interval tables (collar, survey, lithology). dh2loop addresses the subjective nature and variability in nomenclature of lithological descriptions within and across different drilling campaigns by integrating published dictionaries, glossaries and/or thesaurus that were built to improve resolution of poorly defined or highly subjective terminology and idiosyncratic logging methods. Furthermore, lithological data is classified into multi-level groupings that can be used to systematically upscale and downscale drill hole data inputs for multiscale 3D geological modelling. dh2loop also provides drill hole desurveying and log correlation functions so that results can be plotted in 3D for analysis and comparison. dh2loop formats legacy data bridging the gap between utilization and maximization of legacy drill hole data and drill hole analysis functionalities available in existing python libraries (lasio, welly, striplog).

We acknowledge the support of the MinEx CRC and the Loop: Enabling Stochastic 3D Geological Modelling (LP170100985) consortia. The work has been supported by the Mineral Exploration Cooperative Research Centre whose activities are funded by the Australian Government's Cooperative Research Centre Programme. This is MinEx CRC Document 2020/41.

New strato-tectonic model and geochemical tool for revitalised IOCG targeting in the Gawler Craton

Anderson, John

Austrike Resources Pty Ltd, Principal, Glenalta, SA

The combination of a new strato-tectonic model for the Olympic Metallogenic Event (OME) and zircon-based geochemical tool is a significant step-change for ore vectoring for a spectrum of IOCG and coeval deposit

styles in the Gawler Craton.

Minerals exploration by Aberfoyle Resources, MIM Exploration and Investigator Resources resulted in the recognition of the Nankivel advanced argillic cap in the nineties and resulting discovery of the 42 Moz Paris silver deposit in 2011. Paris is interpreted as an intermediate sulphidation epithermal associated with Nankivel and Helen copper gold silver magnetite skarn, all within a 100 km² sericite pyrite lithocap. The mineralisation is hosted in part by 1620 Ma subduction monzodiorites with the Paris-Nankivel mineralisation dated within 2 Ma of the 1590 Ma Olympic Dam mineralisation.

The revised model proposes the Paris-Nankivel epithermal-porphyry belt is formed at the same time as Olympic Dam on the margins of a super caldera filled with upper Gawler Range Volcanics (GRV). Prior subduction tectonics produced precursor epithermal-porphyry conditions on the southern shoulder of the caldera, whereas IOCGs formed on the northern and eastern margins with haematite- or magnetite-dominated systems respectively forming on the shoulder or in hotter more reduced conditions under the GRV blanket within the caldera.

The epithermal/porphyry and IOCG belts are both fluorine-anomalous and connected by a conductive magneto-telluric (MT) corridor possibly representing a fossil transfer fault and metal source along the mantle interface.

Variations of a mid-GRV stratigraphic marker of the caldera collapse and OME are interpreted as the Bitalli Rhyolite at Paris, Nankivel palaeosurface and as lateral ferruginous sediments and volcanogenic conglomerate facies that collapsed into the IOCG systems preserved under the Stuart Shelf. Drill logs indicate the overlying Pandurra Formation is transitional in places with the mid-GRV marker, so the cover role of that unit needs reassessment with implications for deposit preservation and exploration.

The Zircon Alteration Index (ZAI = 40–Zr/Hf) is a robust search tool that is universally applicable to the OME spectrum of deposit styles and hosts. Compared with other pathfinder applications, ZAI is a simpler, more reliable and far-seeing proximity tool requiring less assay samples in less drill holes for future targeting. The exclusive association of Hf with Zr in zircon enables whole-rock analysis of the Zr/Hf ratio to measure the amount of hydrothermal overprinting of the inherited volcanic or detrital zircon in a host rock and hence proximity to a mineral target. Downhole variations of ZAI and comparisons with lithologies enables lateral or vertical target vectors to be often added to the proximity measure.

The ZAI tool and stratotectonic vectoring have been validated for the Stuart Shelf IOCG systems with a comprehensive study of 35 holes with the requisite Zr and Hf analyses in varying proximities to known IOCG deposits. Preliminary target ranges are assigned to the ZAI values. Combined with the approach of structural and MT targeting, ZAI identified ten drilled prospects recommended for reconsideration by the tenement holders. The mineral systems targeting approach is also recommended to select areas else-where in the Gawler Craton for ZAI target analysis.

Cr-zoning in pyroxene as a prospectivity indicator for magmatic Ni–Cu sulfide deposits

Schoneveld, Louise¹, Barnes, Steve¹, Makkonen H. V.⁵, Le Vaillant, M.¹, Paterson, D.⁶, Taranovic, V.¹, Wang, K-Y^{2,3}, & Mao, Y-J⁴

¹Mineral Resources, Australian Resources Research Centre, CSIRO, Kensington, WA, Australia; ²State Key Laboratory of Ore Deposit Geochemistry, Institute of Geochemistry, Chinese Academy of Sciences, Guiyang 550081, PR China; ³University of Chinese Academy of Sciences, Beijing 100049, PR China; ⁴Key Laboratory of Mineral Resources, Institute of Geology and Geophysics Chinese Academy of Sciences, Beijing 100029, China; ⁵Boliden FinnEx Oy, Finland; ⁶Australian Synchrotron, ANSTO, Clayton, VIC, Australia

Small intrusions dominated by olivine- and pyroxene-rich cumulates are common in a variety of settings around the world, but only a very small proportion contain economically exploitable sulfides. We aim to provide a new tool for distinguishing these fertile intrusions from sparse exploration drilling.

Cumulate and poikilitic pyroxenes in strongly mineralised intrusions have complex grain-scale Cr zonation. We separate the zonations into three distinct types: (1) abrupt zoning, (2) sector zoning, and (3) oscillatory zoning. This combination of zoning patterns is likely to indicate high magma flux and fluctuating cooling rate that accompanies wall rock assimilation in the dynamic conduits where sulphide liquid forms and accumulates. As the diffusion of chromium is extremely slow, these zoning patterns can last thousands of years within hot terranes.

We have investigated pyroxene-bearing samples from small intrusions containing magmatic sulphide deposits including the Noril'sk-Talnakh camp in Siberia, the Kotalahti Nickel Belt in Finland, Ntaka Hill in Tanzania, Nova-Bollinger in the Albany-Fraser Orogen and Savannah in the Halls Creek Orogen of Australia, Jinchuan in central China, Xiarihamu in Tibet and Huangshanxi in the east Tianshan Ni province of NW China. To compare, we analysed samples from the weakly mineralised or barren intrusions in four of these regions along with four mafic intrusions that are not associated with any economic sulfide mineralisation.

Cumulus orthopyroxene with a combination of abrupt zoning, sector zoning and resorbed olivine inclusions has so far only been detected in mineralised intrusions. Desktop XRF mapping instruments easily image this distinctive zoning pattern in large pyroxenes, which provides a useful fertility indicator for exploration of new magmatic Ni–Cu–(PGE) deposits.

Using gases for mineral exploration through cover: importance of microbial activity

Plet, Chloe, Siegel, Coralie, & Noble, Ryan
CSIRO Mineral Resources, Kensington WA 6151, Australia

In Australia, the presence of a thick transported cover on ~70% of the continent has hindered the discovery of new world-class mineral deposits. To overcome this challenge, novel approaches are developed. Gases, with their high mobility, are thought to hold great

potential as pathfinders for mineral exploration through cover. Previous investigations of gases detected at the soil surface have shown varying degrees of success in revealing the presence of buried mineralisation.

Here we investigate gases produced during laboratory weathering of sulfides. The experiments were run under sterile and non-sterile conditions. Carbon dioxide (CO₂) and carbon disulphide (CS₂) were the most abundant gases detected in all experiments. Non-sterile experiments produced more abundant gases than their sterile equivalents highlighting the importance of microbes in the weathering of sulfides.

In addition, the results of sterile experiments were compared to equilibrium thermodynamic predictions. In all experiments, as predicted, CO₂ was the most abundant gas detected. However, some sulfur gases predicted by thermodynamic modelling were not detected in the laboratory (e.g., S₂, H₂S, CH₃SH and C₂H₆S). Moreover, the most abundant sulfur gas predicted, carbonyl sulfide (COS) was only detected at trace levels. These results indicate that the experiments did not reach equilibrium.

Further soil gases experiments should include characterisation of the microbial communities. These would permit to gain a better understanding of the processes by which microbes impact the gases and improve the reliability of both techniques in the search for buried mineral deposits.

Geophysical data optimisation for modelling: data collection in a value-of-information framework

Lindsay, Mark^{1*}, Pirot, Guillaume¹, Jessell, Mark^{1*}, Giraud, Jeremie¹, Scalzo, Richard^{2*}, Cripps, Edward^{3*}, & Aitken, Alan¹

¹Centre for Exploration Targeting, School of Earth Sciences, The University of Western Australia, Perth, Australia; ²School of Mathematics and Statistics, The University of Sydney, Sydney, Australia; ³Department of Mathematics and Statistics, The University of Western Australia, Perth, Australia; *ARC Centre for Dare Analytics for Resources and Environment

Crustal 3D models provide an understanding of the tectonic history of a region and its mineral endowment. As mineral resources are now mostly discovered under sedimentary cover, geophysical data are necessary to guide exploration. Recent developments in modelling 3D uncertainty with optimisation techniques are combined to guide data acquisition to image mineral systems and identify prospective regions. Most mineral systems are difficult to image with individual geophysical techniques so it is important to understand which data combinations are most effective for each system component (architecture, fertility, depositional trap, geodynamic throttle, preservation). In the course of these model-driven studies, there are often competing choices to be made around which data should be collected in order to reduce geological uncertainty. The “GDOM” project “–Geophysical Data Optimisation for Modelling” – seeks to determine what and how much geophysical data is worth collecting, the best processing methods and application in the most economically efficient manner. The intention here is to guide government policy and industry data collection practices. The workflow aims to inform how geophysical datasets can be best used to constrain geoscientific

concepts and models to reduce uncertainty and more reliably answer geological questions. Recent advances in 3D model analysis helps to place focus where required and be used within a value-of-information (Vol) proposition to help us decide where and what data to collect. Two important parameters used in a Vol calculation are the estimate of “gain” from data collection and the probability of that gain. “Gain” may be the increase in value through deposit discovery, or finding prospective mineralisation amongst a portfolio of prospects and results. Both gain and its dependence on critical system parameters are also uncertain, and have a large influence on the Vol analysis and estimating the risk involved in an exploration project. The cost of data collection is likewise critical information for decision-makers, especially if hierarchical scenarios where additional data reduces the cost of drill targeting are considered. We propose a method that places these parameters into a hierarchical Bayesian framework to give us a clearer understanding on the uncertainties around Vol analyses and helps us to determine the relative utility of collecting different geophysical data.

We acknowledge the support of the MinEx CRC and the Loop: Enabling Stochastic 3D Geological Modelling (LP170100985) consortia. The work has been supported by the Mineral Exploration Cooperative Research Centre whose activities are funded by the Australian Government’s Cooperative Research Centre Programme. This is MinEx CRC Document 2020/xx.

Scale reduction magnetotelluric survey in the East Tennant region, Northern Australia

Jiang, Wenping, Duan, Jingming, Schofield, Anthony, Brodie, Ross C., & Clark, Andrew

Geoscience Australia, Canberra, ACT, Australia

Geoscience Australia has undertaken a series of integrated studies to identify prospective regions of mineral potential using new geological, geophysical and geochemical data from the Exploring for the Future (EFTF) program, together with legacy datasets. Data from the Australian Lithospheric Architecture Magnetotelluric Project (AusLAMP) have been used as first-order reconnaissance survey to resolve large-scale lithospheric architectures for mapping areas of mineral potential in northern Australia. The resistivity model derived from the newly acquired AusLAMP data has mapped deep lithospheric-scale conductivity anomalies in highly endowed mineralised regions and in greenfield regions where mineralisation was not previously recognised. For example, the model reveals a conductivity anomaly extending from the Tennant Region to the Murphy Province, representing a potential fertile source region for mineral systems. This conductive feature coincides with a broadly northeast–southwest-trending corridor marked by a series of large-scale structures identified from preliminary interpretation of seismic reflection and potential field data. This under-explored region, referred to as East Tennant, is, therefore, considered to have significant mineral potential.

We undertook a higher-resolution infill magnetotellurics survey to investigate whether the deep conductivity anomaly is linked to the near surface by crustal-scale fluid pathways. Broadband MT (BBMT) and audio-MT (AMT) data were acquired at 131 stations

with station spacing of ~2 km to ~15 km in an area of approximately 90 km x 100 km. The 3D resistivity model revealed two prominent conductors in the resistive host whose combined responses result in the lithospheric-scale conductivity anomaly mapped in the AusLAMP model. The resistivity contrasts coincide with major structures preliminarily interpreted from seismic reflection and potential field data. Most importantly, the conductive structures extend from the lower crust to the near surface. This observation strongly suggests that the major faults in this region are deep-penetrating structures that potentially acted as pathways for transporting metalliferous fluids to the upper crust where they could form mineral deposits. This result indicates high mineral prospectivity for iron oxide copper–gold deposits in the vicinity of these major faults. We then used AMT data to estimate cover thickness to assist with drill targeting for the stratigraphic drilling program which, in turn, will test the models and improve our understanding of basement geology, cover sequences and mineral potential. This study demonstrates that integration of geophysical data from multiscale surveys is an effective approach to scale reduction during mineral exploration in covered terranes with limited geological knowledge.

This abstract is published with the permission of the CEO, Geoscience Australia.

Apatite fission track and U–Pb mapping of the northern Gawler Craton: implications for ore deposit exhumation and preservation

Glorie, Stijn¹, Reid, Anthony^{1,2}, Hall, James¹, Nixon, Angus¹, & Collins, Alan¹

¹The University of Adelaide, Department of Earth Sciences, Adelaide, Australia; ²Geological Survey of South Australia, Department for Energy and Mining, GPO Box 320, Adelaide, Australia

The formation of major Palaeoproterozoic and Mesoproterozoic (Cu)–Au deposits at the metal-rich margins of the Gawler Craton, South Australia, has received a lot of attention, however, the relationships between metal occurrences, the exhumation level of the crust and the structural architecture of the craton margins are less clear. Here, we present results from apatite fission track and U–Pb thermochronology applied to basement rocks at the northern margin of the Gawler Craton. Resulting age interpolation maps reveal differential cooling histories with respect to major structures such as the Karari Shear Zone. Further-more, the extent of Phanerozoic exhumation shows a spatial relation with the location of Au (and/or Cu, Fe) mineralization in the northern Gawler Craton. Areas that were significantly modified by Mesoproterozoic mineralizing events, such as the Olympic IOCG province and the Central Gawler Gold Province, record post-Silurian exhumation histories related to the Alice Springs Orogeny. To the west of these two major mineral provinces, Archaean–early Palaeoproterozoic terranes in the northwestern Gawler Craton with abundant Au (and Cu, Fe) mineral occurrences were not affected by Phanerozoic exhumation and denudation. These relations suggest that Mesoproterozoic fluids might have weakened the Gawler Craton, making the mineralized terranes more susceptible to Phanerozoic deformation compared to the Archaean–Palaeoproterozoic terranes within the stronger parts of the Gawler Craton. Hence,

understanding the timing of fault reactivation and the associated relative exhumation level may provide valuable constraints for ore deposit preservation and mineral exploration within the Gawler Craton.

Structural data in drill core: methods for analysing anisotropy in core images

Hill, June, & Poulet, Thomas

MinEx CRC, CSIRO Mineral Resources, Kensington, WA, Australia

The collection and analysis of structural data is an important part of exploration for structurally controlled mineral deposits. For mineral deposits under cover, drill core is the main source of structural information. Methods for collecting high density structural data from core images are being investigated to complement traditional geology logging with data that is non-subjective and rapid to collect. Automated measurement of anisotropy can be used to quantify scale, intensity and orientation of vein networks, compositional layering and grain fabrics, these are key components of structural analysis. We have explored two published measures of anisotropy for rock images (1) variogram maps and (2) inertia tensor analysis to assess their practicality and usefulness for collecting continuous structural data from core images.

The variogram is a popular method of texture analysis. It measures the spatial continuity of the input variables. If the spatial continuity is stronger in one direction than another, then the fabric can be considered to be anisotropic. Variograms result from comparing the values of two points in the image at increasing distances from each other (lag). When the direction of the measured lag is included, this produces a 2D variogram map. Diaz *et al.* (2019, *Mathematical Geosciences*) tested the variogram map method for a set of rock images and demonstrated its ability to detect anisotropy. In this study, the Diaz method has been modified for continuous testing along the core image. A threshold is applied to the variogram map and an ellipse is fitted to the resulting data points. Varying the threshold provides results for different scales. The relative length of the ellipse axes provides a measure of anisotropy and the orientation of the principal axis provides the direction of maximum spatial continuity, i.e., the direction of the anisotropy. Prior to analysis the core photo is segmented into overlapping square images and the algorithm is applied to each image. The result is a continuous downhole measurement of anisotropy and angle.

The inertia tensor analysis provides a simple and general approach to quantify anisotropy in terms of position, direction and scale. We use the method described by Lehoucq *et al.* (2015, *Frontiers in Physics*), where an image is partitioned into analysis boxes at a chosen scale, with an ellipse being fitted in each box to determine the prevalent direction of the signal. This allows the user to determine an anisotropy measure with orientation at all scales up to the image size and the resulting signal provides useful information about the original image. This approach reproduces some results of the variogram method and also captures the variation of anisotropy and orientation with scale. In this study we investigated the signature of conceptual scenarios as well as real vein networks at different scales to understand how this quantitative

measure can be used to characterise vein arrays on drill core images, including characteristic lengths and orientation. The variability of anisotropy as a function of scale allows us to identify different characteristics of vein arrays.

Using trace element chemistry of magnetite as an indicator mineral at the Starra iron-oxide copper gold deposits, northwest Queensland

Hohl, Max, Barker, Shaun, Cloutier, Jonathan, & Steadman, Jeffrey

CODES – Centre of Ore Deposits and Earth Science, University of Tasmania, Private Bag 79, Hobart, TAS 7001, Australia

Iron Oxide–Copper–Gold (IOCG) deposits are hydrothermal ore deposits that occur worldwide and globally account for significant amounts of copper, gold, and uranium. They are defined by large scale potassic, sodic and iron alteration that often extend several kilometres from the mineralised centre, making it difficult to differentiate between fertile and barren alteration systems. In recent years, it has been suggested that trace element chemistry of alteration minerals may be used to discriminate fertile from barren hydrothermal systems. This aims to test the discrimination potential of magnetite at the Starra Au–Cu system which is hosted in the Eastern Fold Belt of the Mount Isa Inlier in Northwest Queensland (Australia). Five deposits occur along a circa 6 kilometres long interval. The mineralisation is spatially associated with magnetite–hematite dominated ironstones along the Starra shear, which are focused at the contact between the Answer Slate to the west and the Staveley Formation to the east. Magnetite is the dominant iron oxide mineral in the ironstones and define a strong magnetic anomaly that can be detected for more than 20 kilometres. Incorporation of trace elements in magnetite is influenced by physicochemical parameters at time of precipitation such as temperature and redox, making it ideal to record process-based information. In addition, the extensive nature of the ironstones at Starra makes it an ideal location to study the trace and major elements variations in magnetite with increasing distance to the ore bodies.

At Starra, mineralisation zones are associated with variable magnetite overprinted by hematite. New laser ablation ICP-MS of magnetite from distal, proximal, and mineralised setting reveals that magnetite spatially associated with the mineralisation contain lower V content compared to distal magnetite, suggesting higher fO_2 conditions in mineralised areas. Hematite within ironstones replaced the pre-existing sedimentary lithology retains the original texture as shown by different crystal orientation and distinct trace element concentrations in hematite. Scheelite inclusions in magnetite support reduction of hematite to magnetite due to relative incompatibility of W in magnetite compared to hematite. Together, these indicate a complex evolution of prevailing redox conditions during formation of the IOCG system.

Our findings support previous formation models that suggest the main controlling factor on the Cu–Au precipitation in IOCG systems is the oxygen fugacity fO_2 of the hydrothermal fluid. At Starra, previous genetic model suggested that oxidized fluids interacted with

magnetite and were reduced, leading to reduction of sulphates to bisulphides and precipitating Cu.

Automated image analysis for RGB coloured core images

Javeed, Umer^{1,2}, Hill, June^{1,2}, & Thomas, Matilda^{1,3}

¹MinEx CRC; ²CSIRO Mineral Resources, Kensington, WA, Australia; ³Geoscience Australia, Canberra, Australia

Rapid and reliable core logging plays a vital role in the discovery of ore deposits. Drilling operations produce large repositories of rock core, which are used to determine the lithology, mineralogy, structure and alteration zones of the core. Geologists have a limited time to analyse the core and the logging process is subjective and may vary depending upon the experience of the geologist. In mineral exploration the identification of veins and characterisation of their form is important for prediction of the presence of vein-hosted mineral deposits and understanding the mineralisation processes. Therefore, the collection of vein information which is accurate and consistent is critical. Red Green Blue (RGB) coloured core images are routinely collected but are mostly used only for visual inspection and record keeping. Automated core analysing systems have the potential to provide rapid and consistent quantitative assessment of core. In this paper, a methodology to detect the veins and fractures by using computer vision techniques is proposed. In this method a simple approach is used to separately define the core from the core tray material. Undesired objects or material are removed from core images by using intensity transformation and morphological image processing operations. If the input image has poor contrast, then contrast stretching techniques are used to enhance the texture of the core. The performance of individual or combined edge detection filters have been analysed to detect veins and fractures in core. The results and effectiveness of these workflows are visually compared with the original core images. The proposed workflows will provide an effective solution to pre-processing of core images prior to the application of sophisticated machine learning techniques to quantify and categorize structural information.

Into the Noddyverse: A massive data store of 3D geological models for application to machine learning and geophysical inversion

Jessell, Mark¹, Guo, Jiateng², Li, Yunqiang², & Lindsay, Mark¹

¹Mineral Exploration Cooperative Research Centre, Centre for Exploration Targeting, School of Earth Sciences, UWA, Perth, Australia; ²College of Resources and Civil Engineering, Northeastern University, Shenyang, China

Although both machine learning (ML) and geophysical inversion techniques have been applied to the challenge of characterising 3D geology from available data, they each suffer from many of the common challenges facing the application of ML to geoscientific models: a spatiotemporal structure, heterogeneity of information in space and time, interest in rare phenomena (such as ore deposits or earthquakes), uncertainty in the data and a lack of ground truth (Karpatne *et al.*, 2017). We present an open resource

consisting of 1 million 3D geological models and corresponding gravity and magnetic fields, all labelled by the simplified geological history that defines the model and use realistic density and magnetic susceptibility properties. The models were constructed by randomly perturbing the model parameters (including fold wavelength, fault offset, dyke thickness etc.) and order of predefined kinematic 'events' using the Open Source Noddy modelling engine (Jessell, 1981, Jessell & Valenta, 1996). The first two events are predefined as a stratigraphy and a TILT of the model, and the subsequent three events can be any from the following list of seven events: TILT, FOLD, SHEAR-ZONE, FAULT, PLUG, DYKE, UNCONFORMITY with a total of 343 possible model label combinations (e.g., FOLD FAULT UNCONFORMITY). A model label such as TILT->FOLD->DYKE, has many parameters associated with the event, such as tilt angle (TILT), fold wavelength (FOLD) and dyke position (DYKE) which all modify the resulting geology. The density and magnetic susceptibility of each unit in the model are perturbed around idealised distributions for specified lithologies. Each model represents a 4 km cube in the Earth divided into 20 m voxels, making 8 million voxels per model. These models, which can be accessed programmatically via a small python jupyter notebook, together with the full description of the parameters needed to reconstruct the model, and the gravity and magnetic fields, forms the basis for training a ML model, or used to benchmark new geophysical inversion schemes. This poster presentation will explain the methodology used and will provide access to the models via a dedicated website.

We acknowledge the support of the MinEx CRC and the Loop: Enabling Stochastic 3D Geological Modelling (LP170100985) consortia. The work has been supported by the Mineral Exploration Cooperative Research Centre whose activities are funded by the Australian Government's Cooperative Research Centre Programme. This is MinEx CRC Document 2020/47.

Applications of spectral geology

Characterising the hyperspectral SWIR features of tourmaline from two western Tasmanian granites

Harraden, Cassady L.¹, Hong, Wei^{2,3}, & Deyell-Wurst, Cari¹

¹Corescan Pty Ltd, Vancouver, BC, Canada, V6E 2E9;

²Centre for Ore deposit and Earth Sciences (CODES), University of Tasmania, Hobart, TAS 7001, Australia;

³Department of Earth Sciences, School of Physical Sciences, The University of Adelaide, Adelaide, SA 5005, Australia

Western Tasmania is one of the most important resource suppliers for Sn and W production in Australia and is host to numerous world-class high-grade deposits. The Heemskirk Granite, a highly productive batholith in this terrane, is associated with numerous skarns and greisens, which together have yielded a total of more than 104 000 tons of Sn. The nearby Pieman Heads Granite is of similar age (365–360 Ma; Hong *et al.*, 2017) and has similar geochemical and mineralogical characteristics, but has not been associated with any known mineralisation. Both plutons contain abundant tourmaline in a variety of forms

including magmatic hydrothermal veins, cavities, orbicules. This study compares the geochemical and spectral features of the tourmaline in both plutons to identify potential indicators of fertile magmatic systems.

Tourmaline samples were previously analysed by Hong *et al.* (2017) using Electron Microprobe (EMPA) and Laser-Ablation Inductively Coupled Mass Spectrometry (LA-ICP-MS) to quantify the major and minor element compositions. Results showed that tourmalines are dominated by schorl varieties with a narrow range of chemical compositions (enriched in Fe and Al, moderately enriched in Mg, and poor in Ti, Li and Zn). Some systematic increases in Fe, Al and Li, and decreases in Mg and Ti are recognised from early- to late-stage tourmaline occurrences.

These analysed samples were also scanned using the Corescan Hyperspectral Core Imaging (HCI-3) system to obtain high resolution hyperspectral imaging data between 450 nm and 2500 nm (representing the visible to near-infrared (VNIR) and short-wave infrared (SWIR) regions). Characteristic absorption features in the SWIR are attributed to BOH, AIOH, and MgOH stretching vibrations: ~2200 nm (AIOH), ~2250 nm (BOH), ~2320 nm (MgOH), and ~2360 nm (BOH) (Hunt *et al.*, 1973; Clarke *et al.*, 1990; Bierwirth, 2004). Results show very little variation in individual wavelength values across samples for all four major SWIR absorptions. However, using combination of spectral features and specialised imaging capabilities, differences in tourmaline spectra between the two plutons are apparent. Tourmaline from the Pieman Heads Granite has relatively high ~2375 nm wavelength positions while the ~2200 nm and ~2250 nm wavelengths are shifted to lower wavelengths. The Heemskirk Granite tourmalines display mid-range wavelength positions for all three absorption features. Additionally, variations in specific reflectance ratios in the SWIR region highlight zoning patterns that could reflect small-scale Fe variations.

Distinguishing between the barren Pieman Heads and fertile Heemskirk Granites has implications for Sn exploration activities in Western Tasmania. The major-element compositions of the tourmalines in these two granites are very similar but discrete variations in key SWIR absorption feature relationships are apparent using high resolution hyperspectral imaging. This demonstrates the potential to apply hyperspectral imaging techniques to differentiating compositionally similar intrusive bodies with different mineral potential for mapping and exploration activities in the region and beyond.

HyLogger™ mineralogy from chips: a RoXplorer® pilot study

Moltzen, Jake

Geological Survey of New South Wales, Department of Regional NSW, Londonderry, Australia

The RoXplorer® coiled tube drilling system is scheduled to be used for MinEx CRC drilling activities in New South Wales (NSW) from 2022 for National Drilling Initiative (NDI) areas South Cobar, North Cobar, Mundi, Forbes and Dubbo. This recently developed system provides a faster and more cost-effective alternative to conventional diamond and reverse circulation drilling, while also offering safety advantages and reduced environmental impacts (Hillis *et al.*, 2014). Ongoing

technology development within MinEx CRC will maximise RoXplorer® production during MinEx CRC drilling campaigns, with 5 km spaced holes planned throughout NDI areas to better understand basement and cover sequence geology and the potential for undiscovered ore deposits buried beneath cover.

In this pilot study, two trial drillholes from the RoXplorer® system were scanned using the HyLogger-3™ instrument to determine the best method for scanning RoXplorer® chips and to assess the quality of visible-near infrared to shortwave infrared (VNIR-SWIR) and thermal infrared (TIR) spectra for routine interpretation. Downhole chip samples produced by the RoXplorer® range in size from ~10 µm to ~4 mm (Tiddy *et al.*, 2019), however a separated coarse fraction with sizes ranging from ~1 mm to ~4 mm was used for both drillholes. Outcomes from this study included:

1. VNIR–SWIR and TIR spectra were found to be reliable for routine mineral identification, tracking mineral chemistry and identifying lithological variations downhole.
2. Black plastic chip trays produced better spectral results than clear or white trays.
3. Larger 50 mm x 50 mm chip compartments produced better spectral results than standard 25 mm x 50 mm chip compartments.
4. Regular linescan mode produced spectra with higher reflectance and therefore better sensitivity, than chip scanning mode.
5. Rinsing chips with water to remove clinging fines increased TIR reflectance by up to 40% and reduced volume scattering effects.

The findings of this work will be used to help develop a consistent approach to scanning future RoXplorer® drillholes across the state and territory Geological Survey HyLogger™ nodes.

Hillis R. R., Giles D., Van Der Wielen S. E., Baensch A., Cleverley J. S., Fabris A., Uvarova Y. (2014). Coiled tubing drilling and real time sensing – enabling prospecting drilling in the 21st Century? Society of Economic Geologists Special Publications, 18, 243–259.

Tiddy C. J., Hill S. M., Giles D., van der Hoek, B. G., Normington V. J., Anand R. R., Baudet E., Custance K., Hill R., Johnson A., McLennan S., Mitchell C., Zivak D., Salama W., Stoate K. Wolff K. (2019). Utilising geochemical data for the identification and characterisation of mineral exploration sample media within cover sequence materials, Australian Journal of Earth Sciences, <https://doi.org/10.1080/08120099.2019.1673484>

Modelling of petrophysical from hyperspectral drill core data collected from the Osborne Cu–Au deposit, Mount Isa Inlier, Queensland

Laukamp, Carsten¹, Francis, Neil¹, Gopalakrishnan, Suraj², Hauser, Juerg¹, & Mule, Shane¹

¹CSIRO Mineral Resources; ²Geological Survey of Queensland

The combination of magnetic susceptibility and density allows identification of iron oxide copper–gold (IOCG) mineralisation by estimating proportions of magnetite, sulphide and hematite alteration which can be indicative of IOCGs. In the frame of the National Virtual Core Library project, hyperspectral reflectance spectra acquired from drill core of the Osborne Cu–Au deposit, Mount Isa Inlier, Queensland using a HyLogger3 at GSQ's Exploration Data Centre were compared with

magnetic susceptibility and density measurements. In this study we explore the feasibility of inferring the petrophysical data from the (1) visible-near (VNIR), shortwave (SWIR) and (2) thermal (TIR) infrared wavelength regions. Specifically, we seek to predict magnetic susceptibility and density values in drill core sections where petrophysical data are not available and potentially extrapolate these to other hyperspectral data sets, such as those acquired by field or Earth Observation instruments.

Using The Spectral Geologist (TSG™) software, partial least squares (PLS) was employed to derive predictive models using 23 unique magnetic susceptibility and density measurements, that were assigned to all nearby spectral measurements (\pm ~10 cm). The values of the input magnetic sustainability and density values ranged from 0 to 2.3 K (Si) and 2.7 to 4.9 g/cm³, respectively. The hyperspectral data were not spatially re-sampled to fit with the drill core interval measured for petrophysical data. Instead, the original 1 cm spatial resolution was used to evaluate the variability of hyperspectral data within the petrophysical sample intervals. The correlation between the 23 measured and corresponding modelled magnetic susceptibility ($n = 157$) for the same 23 depth intervals was high for the VNIR-SWIR ($r^2 = 0.95$) and the TIR ($r^2 = 0.969$), but the PLS-modelled magnetic susceptibility values showed a large variance (± 0.8 and ± 0.5 , respectively). Similarly, the correlation between the measured and modelled density was high for the VNIR-SWIR ($r^2 = 0.958$) and the TIR ($r^2 = 0.989$), with the PLS-modelled density values showing a large variance (± 0.4 g/cm³ for both wavelength ranges). However, HyLogger3 high-resolution RGB imagery showed that the predicted value ranges were sufficiently different to discriminate drill core intervals dominated by magnetite-rich rocks, from magnetite-rich breccia and least-altered (non-mineralised) rocks. PLS models based on the VNIR-SWIR wavelength ranges were mainly driven by depth changes of electronic transition absorption features related to iron and copper in the VNIR, which are most intense in the highly altered, magnetite- and/or sulphide rich rocks. PLS models based on the TIR wavelength ranges were highly influenced by the thermal background typically associated with iron oxides and sulphides. Density values modelled from VNIR-SWIR compared to those modelled from TIR showed a good correlation ($r^2 = 0.729$), whereas the correlation between magnetic susceptibility modelled from VNIR-SWIR and TIR was comparably low ($r^2 = 0.518$). While the small amount of data used to infer the models discussed here means that their predictive power needs to be assessed comprehensively, our results nevertheless indicate a high potential for successfully inferring petrophysical from hyperspectral data and cost-effective mapping of IOCG-related alteration.

Deriving quantitative alteration mineralogy from TIR Hyperspectral data in IOCG Systems

Stromberg, Jessica, Schlegel, Tobias, Pejic, Bobby, Birchall, Renee, & Shelton, Tina

CSIRO Mineral Resources, Kensington, WA

Identifying alteration mineral zonation around hydrothermal ore systems is critical to the mineral exploration process. Hyperspectral methods are commonly used to map alteration because they are

fast, inexpensive, and require little to no sample preparation compared to other mineralogical techniques such as scanning electron microscope (SEM) based mineral mapping, for example. The visible-near and shortwave infrared (VN-SWIR, 350–2500 nm) spectral regions are most used as they are sensitive to hydrated mineral phases including chlorite and white micas. However, in mineral systems which are iron oxide-rich or where key alteration assemblages include abundant anhydrous phases, such as in iron oxide–alkali–calcic alteration systems, using this spectral range can be problematic. In this case, the thermal-infrared (TIR) spectral range (6000–14500 nm) may be more appropriate as it is sensitive to anhydrous silicates such as quartz and feldspars. However, there are inherent challenges in unmixing hyperspectral data for deriving quantitative mineral abundances. In particular, when the quantification of minor or spectrally similar phases are key to the alteration assemblages, such as in the quantification of different feldspars. This can be overcome with the use of a calibration dataset such as quantitative X-ray diffraction or SEM-based quantitative mineralogy in combination with Partial-Least Square (PLS) regression methods. In developing such models, scale is of critical importance. Variability in the sampling area and volume between datasets is one of the greatest challenges in validating hyperspectral data with quantitative mineralogy, and in integrating any geoscience datasets. In this work, we used several hyperspectral and spectroscopic instruments (HyLogger, Agilent 4300 FTIR, Bruker Vertex FTIR, ASD Fieldspec Pro) to evaluate the impact of scale on hyperspectral data validation in IOCG systems. In this process we developed a methodology for creating the first scale-consistent dataset of VNIR-SWIR, TIR, and SEM-based quantitative mineralogy data on drill core samples. This dataset comprises 250 samples from a world-class IOCG deposit in which the key mineral phases, assemblages, and alteration patterns were identified using the SEM-based quantitative mineralogy. Hyperspectral data was processed using The Spectral Geologist Software (TSG™) software and even with a scale consistent dataset, and a constrained mineral library based on the SEM-based mineralogy, conventional unmixing methods such as the The Spectral Assistant (TSA™) were unable to reproduce key alteration patterns for vectoring towards ore. Using the SEM-based mineralogy data, PLS modelling was applied to derive predictive models for key mineral phases from the TIR hyperspectral data. The resulting models produced quantitative mineralogy with $r^2 > 0.94$ for key phases including quartz, K-feldspar, albite, calcite, and >0.80 for magnetite, biotite, and plagioclase. More importantly, the key mineral assemblages change with distance to ore and the relative abundance feldspar species (albite, K-feldspar, plagioclase) identified by the SEM-based mineral mapping were reproduced using PLS-derived mineral abundances in a validation drill core. This method and the models generated will provide a framework for improving the application of hyper-spectral data for mapping alteration in IOCG systems.

Coal spectral features in the mid-infrared range

Rodrigues, Sandra¹, Fonteneau, Lione², & Esterle, Joan¹

¹The University of Queensland, School of Earth and Environmental Science, St Lucia, QLD 4069, Australia;

²CoreScan Pty Ltd, 1/127 Grandstand Road, Ascot WA 6104, Australia

An increasing rank coal suite (from subbituminous to low volatile bituminous coal, LVB) was used to investigate the spectral features of the organic matter in coal in a wide spectral range from 450 nm up to 14 300 nm. Different sensors and equipment were used, covering the visible-near and -shortwave infrared (VNIR-SWIR, 450–2500 nm), the mid-infrared (MIR, 2000–8000 nm) and the thermal infrared (TIR, 6000–14 300 nm) regions. The MIR and a small portion of the TIR holds the fundamental vibrations for organic materials, while the SWIR only exhibit the overtones and combinations of those fundamental vibrations. Consequently, spectral features (absorption bands) are better defined in the MIR. The 2900 nm absorption feature is attributed to the fundamental –OH stretch in organic materials. This feature is more prominent in the low rank coal and tends to disappear with increasing rank. Therefore, it must be related with the moisture content in the coal samples. The 3280 nm band corresponds to CH stretch in the aromatic fraction. This band develops with increasing coalification, appearing as a deep absorption feature in the LVB coal. A doublet occurs at 3380 nm and 3420 nm, corresponding to CH₃ and CH₂ asymmetric stretches, respectively, in the aliphatic fraction. In the subbituminous coal sample, these two bands are hard to decouple appearing as an intense absorption band around 3420 nm. In the medium volatile bituminous coal, these bands are clearly separated but become shallower when the LVB coal rank is reached. The 3500 nm absorption band is attributed to CH₃ symmetric stretch in the aliphatic fraction and becomes shallower with increasing rank. In the region between 3280 nm up to 3500 nm the absorption bands seem to be related with the increasing of the aromaticity in the coal, with the loss of the aliphatic components favouring the development of the aromatic. The absorption features described above are the most prominent bands recognised in the MIR region in the coal samples available for the project (ACARP C28045). Other minor bands also occur in the MIR, including the band at 5250 nm, which is an aromatic related feature that does not occur in the subbituminous coal sample. The 6200 nm absorption band is possibly related to the CC aromatic bonding and it is a deeper feature in the LVB coal. On the other hand, the band at 6860 nm correspond to CH₂ asymmetric bending and becomes shallower with increasing rank. The results showed that the MIR spectral range has the potential to characterise the rank of the coal though the development and/or disappearance of the spectral absorption features by evaluating the variations in their area, depth and position.

Tracing mineralogy and alteration intensity using the spectral alteration index and depth ratios at the Northwest Zone of the Lemarchant volcanogenic massive sulfide (VMS) deposit, Newfoundland, Canada

Cloutier, Jonathan^{1,2,3}, & Piercey, Stephen J.¹

¹Department of Earth Sciences, Memorial University of Newfoundland, St. John's, Newfoundland and Labrador, Canada, A1B 3X5; ²School of Earth and Environmental Sciences, University of St Andrews, Scotland, United Kingdom; ³Centre for Ore Deposit and Earth Sciences, University of Tasmania, Hobart, TAS, Australia

The use of hyperspectral reflectance in mineral exploration has been steadily increasing in recent decades. This study presents a novel approach that integrates geochemical and spectral proxies to delineate ore formation and alteration processes, which provide new spectral-based exploration parameters that can be used in real time. The precious metal-bearing, bimodal-felsic Northwest Zone of the Lemarchant VMS deposits, Newfoundland, Canada is used as a case study.

Alteration associated with the Northwest Zone includes intense and localized sulfide (pyrite, chalcopyrite, sphalerite and galena) and barite enrichment, and quartz, white mica and chlorite alteration. Zones of elevated Zn (>5000 ppm) are associated with high chlorite carbonate pyrite index (CCPI), Ishikawa alteration index (AI), Ba/Sr, and low Na₂O values and elevated SiO₂ and K₂O, Fe₂O₃, Na₂O, and BaO contents, similar to global alteration signatures in VMS deposits. Mineralized areas contain phengitic white micas with 2200 nm absorption features longer than 2215nm and Mg-rich chlorites with 2250 nm absorption features shorter than 2252nm. Together, these data are consistent with the Northwest Zone having experienced intense hydro-thermal alteration during the mineralization event.

A new lithology normalized spectral alteration index (SAI) for white mica and chlorite was developed in order to map and characterize the alteration intensity surrounding the deposit. In addition, depth ratio parameters (2200D/2340D vs 2250D/2340D) were used to characterize mineralogical changes and zonation. Together, these features document a paleo-fluid pathway with Mg-chlorite alteration extending to at least 300 m away from the mineralization, outside the study area, within the andesitic and dacitic units.

This study demonstrates that the use of VSWIR spectral reflectance data coupled with geochemical alteration proxies (i.e., AI, CCPI, Ba/Sr, Na₂O) and litho-geochemical mass balance changes can identify and characterize alteration haloes and paleo-fluid pathways in the vicinity of VMS deposits. More specifically, hyperspectral reflectance can identify and quantify areas of intense alteration using spectral alteration indexes (SAI), estimate the relative abundances of white mica and chlorite using depth ratios, and characterize the chemical composition of the mineral phases, and relate them to specific alteration processes, which is not possible using only geochemistry. One of the main advantages of this method is that hyperspectral reflectance can be rapidly achieved on drill core at a high resolution for a relatively low cost, minimal sample preparation and results are

available instantly, compared to a longer wait time for geochemical results, greatly enhancing decision making processes during drilling exploration programs, allowing vectoring and rapid decisions making during exploration programs.

Alteration signatures and footprints of the Ernest Henry deposit and camp: Spectral mineralogy and geochemistry

Courteney Dhnaram, Vladimir Lisitsin, Suraj Gopalakrishnan, & Daniel Kille

Geological Survey of Queensland, Brisbane, Australia

The Ernest Henry Cu–Au deposit is the best-known – and the most economically significant to date – example of Iron-oxide copper–gold (IOCG) deposits in the Cloncurry district of the eastern Mount Isa Province in Queensland, Australia. Geological Survey of Queensland (GSQ) has undertaken systematic sampling and mineralogical and geochemical analyses of drill core samples to characterise geochemical and mineralogical zonation of hydrothermal alteration associated with the Ernest Henry deposit, at a scale of hundreds to thousands of metres.

Short-wave infrared (SWIR) and thermal infrared data was collected using the GSQ's HyLogger-3 machine across 19 drill holes (9 continuous drill holes and 10 sub-sampled drill cores), with >200 samples collected across these drill holes analysed for multi-element geochemistry (four-acid digestion - ICP-MS / OES, lithium metaborate fusion, fire assay – Au, Pt, Pd, Leco furnace – C, S, KOH fusion - ion chromatography – F, and Aqua regia – ICP-MS, Hg, Se, Te, 48–67 elements).

Multi-element geochemistry from samples within the orebody identified a Cu–Ag–S–Te–As–Bi–Mo–W–Co–Se–Re (Pb–In–U–Sb–Sn) signature of the main phase of copper mineralisation. This signature is mostly seen within and near the orebody (up to 100 m) and shows a strong association with potassic alteration.

Chlorite composition within both SWIR and TIR spectra varied from Mg-rich chlorite to Fe-rich chlorite with increasing distance to Ernest Henry orebody. This trend was seen both along the NE- and NW-trending drill holes up to a distance of ~1 km. Both SWIR and TIR spectra were used to discriminate early regional Phlogopite from pre-ore Biotite within the Dark Mica mineral group, with Biotite alteration extending to ~2 km NE of the deposit and only 500 m to the NW.

Potassic alteration from both geochemistry and mineralogy was identified ~1 km outwards of the deposit (within the proximal zone). K-feldspar group compositional variations were identified using TIR, with potassic alteration consisting of microcline within the proximal to ore zone and orthoclase associated with copper mineralisation.

Multiple phases of the same mineral were identified in the hyperspectral data across the study area, specifically minerals previously thought to be only associated with early regional alteration (actinolite, albite, epidote etc). Understanding which phases of these minerals are associated with pre-ore and ore mineralisation for similar Cu–Au systems will hopefully aid exploration in the future.

White mica chemistry from the Vulcan IOCG Prospect, South Australia

Gordon, Georgina¹, Dmitrijeva, Marija², & Berthiaume, Jonathon²

¹*Geological Survey of South Australia, Adelaide, Australia;* ²*Fortescue Metals Group Ltd., Keswick, Australia.*

The Vulcan iron-oxide copper gold (IOCG) deposit in South Australia lies 30 km northeast of the world class Olympic Dam deposit. Three drill holes (VUD009, VUD015, VUD017), were chosen to examine the prospect scale alteration of white micas, across differing geophysical domains of the Vulcan IOCG prospect. A variety of breccias host mineralisation, including massive hematite and hematite-sericite-chlorite. The breccias are hosted within altered quartz-feldspar rock varying granitic to gneissic in texture. Dating of the host rock (VUD007) using zircon U–Pb geochronology showed that hematite–sericite–chlorite altered and brecciated granite was dated to 1.743+–Ma.

A spectral index for the AlOH – 2200 nm white mica wavelength was plotted for the three drill cores (VUD009, VUD015, VUD017) showing excellent correlation with the aluminium assay values and iron oxide content. Sericite present in less altered, barren rocks was found to have longer wavelengths (2214–2218 nm) and transgressed to shorter wavelengths (2208–2212 nm) – approaching iron enriched intervals. High aluminium content corresponded to longer wavelength sericite, opposite to iron content and differing from sericite wavelengths in the Olympic Dam deposit. A direct correlation between elevated copper and white micas was not observed.

High resolution vs standard resolution: How an increase in spectral resolution using a field portable spectrometer affects quality of data – a case study on Nickel exploration

Shelton Pieniazek, Lori

Spectral Evolution, United States

Standard resolution of a field portable spectrometer at 3 nm (UV), 8 nm (VIS) and 6 nm (NIR) has been used successfully in the geological remote sensing and mining industry for a variety of applications. Alteration mapping has been key for finding different mineral assemblages that indicate an area of interest. Using a higher resolution field spectrometer has proven to be beneficial in understanding and identifying new features in a variety of different mineral groups and subgroups.

A study was conducted using three different field spectrometers, each with different resolutions. As you increase resolution, features that are not visible with a standard resolution spectrometer appear in all three ranges (UV, VIS, NIR) thus yielding a better understanding of alteration changes and geochemical conditions

Geomechanics for energy and resources

Exploring for the future: New Canning Basin geomechanics and rock property data

Bailey, Adam¹, Jarrett, Amber¹, Wang, Liuqi¹, Dewhurst, David², Esteban, Lionel², Kager, Shane², Monmusson, Ludwig², Carr, Lidena¹, & Henson, Paul¹

¹*Geoscience Australia, Canberra, Australia;* ²*CSIRO Energy, Perth, Australia*

Exploring for the Future (EFTF) is an Australian Government initiative focused on gathering new data and information about potential Northern Australian mineral, energy and groundwater resources. Northern Australia is generally under-explored yet offers enormous potential for industry development, as it hosts many prospective regions and is located close to infrastructure and major global markets. In June 2020, a four-year extension to the EFTF program was announced, expanding the scope to include the whole of Australia.

The energy component of EFTF aims to improve our understanding of the petroleum potential of Australian frontier basins. The Kidson Sub-basin, located within Western Australia's Canning Basin, is an EFTF primary area of interest. A large, underexplored depo-centre, it is likely that the proven petroleum systems of the Canning Basin extend into this frontier region. Geoscience Australia and partners recently acquired significant new data over the Kidson Sub-basin, including the L211 Kidson Sub-Basin 2D Seismic Survey and the deep stratigraphic borehole, Waukarlycarly 1.

This study brings together the geomechanical studies undertaken in the Canning Basin, including the Kidson Sub-basin, as part of EFTF. This includes interpretation of the regional stress regime and its context within the Australian continent, detailed analysis of present-day stress magnitudes, and geomechanical rock testing undertaken by CSIRO-Energy on samples recovered from Waukarlycarly 1.

Wireline log data, including wellbore image logs, were interpreted from open-file petroleum and stratigraphic wells to define stress orientations and magnitudes across the Canning Basin. A NE–SW regional present-day maximum horizontal stress orientation is interpreted from observed wellbore failure in image logs and is in broad agreement with both the Australian Stress Map and previously published earthquake focal mechanism data. A strike-slip faulting stress regime is interpreted through the basin, however, when analysed in detail there are three distinct stress zones identified: (1) a transitional reverse to strike-slip faulting stress regime in the top ~1.0 km of the basin, (2) a strike-slip faulting stress regime from ~1.0 km to ~3.0 km depth, and (3) a transitional strike-slip to normal faulting regime at depths greater than ~3.0 km. Detailed mechanical earth models demonstrate a variable present-day state of stress within the Canning Basin. Significant changes in stress within and between lithological units, due to the existence of discrete mechanical units, form numerous inter- and intra-formational stress boundaries that are likely to act as natural barriers to fracture propagation.

Rock testing targeted potential reservoir–seal pairs and intervals with identified unconventional hydro-carbon potential, characterising mechanical and petrophysical properties through unconfined compressive stress (UCS) tests, desktop ultrasonic testing, mercury

injection capillary pressure (MICP), road-ion-beam milling and scanning electron microscopy (BIB-SEM), and gas porosity and permeability experiments. Hence, conventional and unconventional reservoir rock properties are characterised.

These data provide geomechanical and petrophysical insights into intervals with identified or potential hydrocarbon prospectivity and allow for extrapolation of rock properties. Although the Kidson Sub-basin is underexplored, these results demonstrate that should Canning Basin petroleum systems extend into the Kidson Sub-basin, geomechanical properties are likely to be favourable for the development of shale resources.

Characterising the uncertainty of rock stress and strength estimates

Musolino, Matthew, Holford, Simon, King, Rosalind, & Hillis, Richard

The University of Adelaide, Australian School of Petroleum and Energy Resources, Adelaide, Australia

Accurate estimates of in-situ stresses and rock strengths are required for multiple practical applications during petroleum exploration and development, such as ensuring wellbore stability, minimising breakouts, and the design of hydraulic fracturing treatments. Issues regarding the aforementioned practices cost operators about US\$8 billion globally each year. However, when predictive geomechanical models are constructed, both rock stress and strength are typically estimates rather than fully quantified, and their uncertainties are rarely examined. Based on data from the Cooper Basin in South Australia, this presentation examines uncertainty relating to estimates of the three principal stresses (vertical stress and minimum and maximum horizontal stress) and rock strength as a result of (a) available data inputs and (b) methodological approaches. We show that the magnitude of vertical stress at depths of ~3 km can vary up to 6 MPa depending on the methodologies employed when integrating and processing density logs and sonic transit time data. Minimum horizontal stress magnitudes are commonly estimated using leak-off tests (LOTs). We demonstrate that accurate interpretation of LOTs is challenging due to factors such as the presence of pre-existing fractures, cement channelling, non-linear pressure build-up, and plastic and elastic leak off. Based on the choice of interpretation technique and calculations based on the assumption of tensile or shear failure, estimates of minimum horizontal stress may also vary by up to 6 MPa at depths of 3 km. The maximum horizontal stress magnitude is typically considered to be the most difficult to quantify, and we compare five methods (frictional limits, presence of drilling induces tensile fractures, presence of wellbore breakouts, wellbore breakout width, and shear plane failure). We show that at depths of ~2.5 km, estimates of maximum horizontal stress magnitude determined using these approaches can vary between 18–40 MPa. Finally, we compared empirical approaches for estimating rock strength using sonic velocity data with laboratory uniaxial compressive tests for a variety of stratigraphic units in the Cooper Basin. We show that, depending on the empirical correlation being used, rock strengths may be underestimated by 25–43% when comparing sonic velocity log derived rock strength to physical

compression testing. In summary, our investigation into the uncertainty in principal stresses and rock strength estimation leads us to propose enhancements to methodologies concerning density log preparation and filtering, check-shot calibration, low data density leak-off interpretation, and rock strength-sonic transit time relationships. Our results provide end-users with a better understanding of the uncertainties associated with stress and strength estimates that can be factored into geomechanical risk assessments.

Re-defining the morphology of the Darling Basin in NSW using 3D modelling and data integration – introducing the Yathong–Ivanhoe Trough

Gammidge, Larissa, & Xu, Min

Geological Survey of New South Wales, Department of Regional NSW, Maitland, Australia

The late Silurian to Devonian Darling Basin in western New South Wales is one of the least explored sedimentary basins in the state and is prospective for petroleum. It comprises many sub-basins that share, or partially share, a similar depositional history. The location of the boundaries of some of the sub-basins have recently been revised as more data have been acquired and new modelling completed.

Limited seismic and drilling data across the Darling Basin, particularly near the margins of the sub-basins, and extensive shallow cover required a reliance on gravity and aeromagnetic data to interpret the boundaries of the sub-basins. The most widely used dataset to interpret sub-basin boundaries is the 2006 Murray-Darling-Eromanga SEEBASE™ model, created by Frogtech.

The SEEBASE™ model for the Yathong and Ivanhoe troughs shows that they are contiguous, but they were interpreted as two troughs based on their different orientations and slightly different structural histories. However, the interpretation and modelling of seismic survey data acquired in 2009 and 2013 show that there is continuity of strata across the Yathong and Ivanhoe trough boundaries. Therefore, there is no justification for two separate troughs and a single trough is more consistent with the current data. The revised trough is named the Yathong–Ivanhoe Trough.

The Yathong–Ivanhoe Trough boundary has been defined based on the extent of outcropping Devonian sedimentary rocks and the interpreted pre-Devonian basement rocks. Additionally, the SEEBASE™ and aeromagnetic data were used to define the boundary in areas of no outcrop. The former Yathong Trough has been shortened in the north–south direction by almost half. In contrast, the former Ivanhoe Trough is revised to be larger.

The revised boundary for a combined Yathong–Ivanhoe Trough is a more geologically robust interpretation than previous ones. This has implications for petroleum exploration targets within the trough. Recent work has highlighted areas where petroleum systems may be located and gives a greater understanding of the development of the Darling Basin over time.

Seismic structure of the crust across central Australia from the joint inversion of radial and vertical teleseismic body-wave autocorrelations

Tork Qashqai, Mehdi, & Saygin, Erdinc

Deep Earth Imaging Future Science Platform, CSIRO, Perth, WA

Teleseismic body-waves coda recorded on the radial and the vertical components of a seismogram have been used for decades to image the local structures below a seismic station through the inversion of P-to-S receiver functions (RFs). It has been shown that the observed response of the subsurface structure to a seismic wave, generated by a deep source, can be converted to a zero-offset reflection response by autocorrelating the recorded signals. Recently, the autocorrelation of the teleseismic P-wave coda or its inversion (Tork Qashqai *et al.*, 2019) has emerged as a powerful tool to obtain complementary constraints on subsurface structures. Compared to the RFs, the autocorrelations of the teleseismic P-wave coda recorded on the radial and vertical components of a seismogram contain additional information. They include both P- and P-to-S converted phases, whereas the RFs mainly contain P-to-S phases as the P-waves are attenuated by the deconvolving the vertical component (P) from the radial (S_v) component. Therefore, one can account for the variability of both the V_p and V_s structures if the radial and vertical component autocorrelations are jointly inverted. Here, we present a new approach which can simultaneously estimate the crustal V_p , V_s , and V_p/V_s ratio structures below a seismic station by jointly inverting the vertical and radial component autocorrelations of the teleseismic P-wave coda. This has significant implications for characterizing the V_p/V_s ratio, which can be a good indication of the crustal composition. Our synthetic inversion tests showed substantial improvements in the estimation of the crustal properties (especially the V_p/V_s ratio) compared to the inversion of either the teleseismic RFs or the autocorrelation of the vertical component. The application of this method on passive seismic data recorded by a north-south-oriented passive seismic experiment in central Australia (BILBY) provided the first comprehensive joint estimates of all crustal properties (V_p , V_s , and V_p/V_s ratio) for this experiment. We imaged crustal structures across the transition between the northern and southern Australian cratons which includes east-west-trending geological domains of central Australia (the Gawler Craton, Eromanga and Officer Basins, Musgrave Province, Amadeus Basin, Arunta Block and the Georgina Basin). The comparison of the Moho estimates from the previous studies with our velocity and Moho models indicates that they might have imaged the top of a high-velocity lower crust in some regions. The overall trend of our Moho model follows the long-wavelength pattern of the Moho structure interpreted from the deep seismic reflection method along the GOMA seismic line that is parallel to the BILBY profile. It is also closer to the change of the reflectivity seen at the base of the crust in the GOMA migrated seismic section. Our approach is cost-effective and can be used in conjunction with the deep active seismic reflection profiling to obtain additional information, especially at depths where the deep seismic reflection method has penetration problems.

Tork Qashqai, M., Saygin, E., & Kennett, B. L. N. (2019). Crustal imaging with Bayesian inversion of teleseismic P wave coda autocorrelation. *Journal of Geophysical Research: Solid Earth*, 124, 5888–5906.

A multi-physics elasto-visco-plastic constitutive framework for geomechanics

Sari, Mustafa¹, Poulet, Thomas², Alevizos, Sotiris², & Veveakis, Manolis³

¹CSIRO, Mineral Resources, WA, Australia; ²National Technical University of Athens, Athens, Greece; ³Civil and Environmental Engineering, Duke University, Durham, USA

Abstract: Understanding and improving the performance as well as the productivity of reservoirs at extreme conditions (high pressure and high temperature) is a big challenge in Geomechanics. This is particularly important for the operation of unconventional shale gas reservoirs, but also applies to other areas like geothermal or deep conventional formations. Other applications include environmental remediation around nuclear waste disposal sites, as well as deep underground storage of energy resources. In order to meet such a formidable challenge, constitutive modelling is required that can span the temperature and pressure range of the Earth's upper crust and offer possibilities for long-term forward modelling at such extreme conditions. The main requirement is to formulate a plasticity theory which helps describe and even predict long-term behaviour, at conditions where materials are frequently well beyond their initial yield, in environments where rocks may experience extreme temperatures, pressures, as well as internal transformations. To model such multi-physical processes, we suggested a multi-physics elasto-visco-plastic constitutive framework including the effect of interface processes, whereby the hardening law of plasticity is a function of the global and internal state variables of the problem (temperature, pressure, density, chemical potentials). The evolution of the laws of the state variables are therefore obtained from the governing laws of physics for mass and energy balance. We included the effect of interface processes at the grain contacts and surface, through an energy upscaling of the internal enthalpy of the system. The framework was validated against a suite of multi-physical tests in different materials, showing good agreement for a realistic range of material parameters. The analysis also showed that simulation results contain enough information to constrain the parameter space for the definition of the mechanical enthalpy, providing insights to develop further the underlying theoretical model and emphasizing the complementarity of data-driven and physics-based approaches.

Compressional wave velocity estimation using gaussian processes regression

Mohammadpour, Mobarakeh¹, Arashpour, Mehرداد¹, Roshan, Hamid², & Masoumi, Hossein¹

¹Department of Civil Engineering, Monash University, Melbourne, Australia; ²School of Mineral and Energy Resources Engineering, UNSW, Sydney, Australia

Geophysical logs have been routinely performed in coal mines for many years. Compressional velocity is one of the important characteristics which can be measured using sonic log. Despite importance of P-wave velocity

and its application in geophysical and geomechanical studies, some boreholes in coal mines do not have P-wave velocity or sonic log in their log suits, as a result, empirical correlations were commonly used to estimate P-wave velocity. However, these models are mostly local correlations which were derived for specific areas.

In this study Machine Learning based Gaussian Processes Regression was used to predict the P-wave velocity. Gamma, two density logs with different resolutions (Long Spaced Density and Short Spaced Density) and depth were applied as the input parameters. These three logs are the most common ones which are extracted from the coal mines. The model was generated using the data obtained from six boreholes in one of the Australian coal mines in Queensland. The data were divided into two groups including 35382 points for the training of the model and 11794 points for the testing. Root mean square deviation (RSME) and coefficient of determination (R^2) were calculated to evaluate the accuracy of the proposed model.

An improved understanding of the geology and petroleum systems of the southern Canning Basin gained through the acquisition of new seismic and well data

Carr, Lidena K., Edwards, Dianne S., Wang, Liuqi., Southby, Chris., MacFarlane, Susannah K., Boreham, Christopher, J., Grosjean, Emma., Khider, Kamal., Henson, Paul., Formin, Tanya., and Geological Survey of Western Australia

Geoscience Australia, Canberra, Australia

Geoscience Australia's Exploring for the Future (EFTF) program has used new and established techniques to collect onshore pre-competitive datasets over northern Australia. The Exploration Incentive Scheme (EIS) is a Western Australian Government initiative that aims to encourage exploration for the long-term sustainability of the state's resources sector. Integration of EFTF and EIS datasets has improved our understanding of the northern part of Western Australia, and the associated energy, mineral and groundwater resources across northern Australia

The onshore Canning Basin covers approximately 530 000 km², and has proven prospectivity for conventional oil and gas, mainly in the northern part of the basin. Unconventional resources remain largely unexplored and untested. Gas resource assessments indicate that the basin has potential for recoverable shale gas and tight gas. Canning Basin remains one of the least explored Paleozoic basins in the world (DMIRS, 2020).

Australia's longest onshore seismic line, 18GA-KB1, was acquired in the southern Canning Basin to address a long-standing data gap across the Kidson Sub-basin and Waukarlycarly Embayment that informs with the resource evaluation of this frontier region. The Kidson Sub-basin covers 91 000 km² and has a sag basin architecture. Preliminary interpretation of the seismic data indicates that the sedimentary succession is approximately 6 km deep and includes a conformable package of Ordovician–Devonian siliciclastic, carbonate and evaporite facies of exploration interest. Located on the western end of the seismic line, the newly drilled deep stratigraphic well Waukarlycarly 1 penetrated 2680.53 m of Cenozoic and Paleozoic strata and provides stratigraphic control for the geology

imaged in the Waukarlycarly Embayment. A comprehensive elemental and $\delta^{13}\text{C}$ isotope chemostratigraphy study assists with strati-graphic correlations within Ordovician sedimentary strata across the region (Forbes *et al.*, 2020a, 2020b).

Canning Basin oil and gas discoveries throughout the Canning Basin were generated from Paleozoic marine source rocks, deposited under stratified oxic to euxinic water columns. Three distinct petroleum systems, the Ordovician (Larapintine 2), Late Devonian (Larapintine 3) and latest Devonian–early Carboniferous (Larapintine 4), are recognised based on the geochemical character of their associated fluids (Carr *et al.*, 2020). Widespread generation of gas from Paleozoic sources is evident from molecular analyses of gases recovered from petroleum wells and fluid inclusions (Boreham *et al.*, 2020). Currently the Larapintine 2 Petroleum System is regarded as the most prospective system in the Kidson Sub-basin based on interpretations from new and existing well and seismic data.

Black Mountain Energy, 2020. American giant announces Canning Basin exploration. Energy News Bulletin, 7/16/2020.

Boreham, C. J., Edwards, D. S., Sohn, J. H., Palatty, P., Chen, J. H., Mory, A. J. 2020. Gas systems in the onshore Canning Basin as revealed by gas trapped in fluid inclusions. Geoscience Australia, Canberra. <https://ecat.ga.gov.au/geonetwork/srv/eng/catalog.search#/metadata/135207>

Carr, L. K., Edwards, D. S., Anderson, J. R. & MacFarlane, S., 2020. Exploring for the future: Canning Basin. Seismic survey and geological interpretation. Geoscience Australia Record 2020/XXX, in prep.

Department of Mines, Industry Regulation and Safety (DMIRS), 2020. Canning Basin. <https://www.dmp.wa.gov.au/Petroleum/Canning-Basin-10989.aspx>

Forbes *et al.*, 2020a. Chemostratigraphy of Waukarlycarly-1, Canning Basin, Western Australia. Report CAu50017 prepared for Geoscience Australia.

Forbes *et al.*, 2020b. Chemostratigraphy of Kidson-1, Willara-1 and Samphire Marsh-1, Canning Basin, Western Australia. Report CAu50022 prepared for Geoscience Australia.

In-situ stress and geological structure influence on the coal fractures and initial reservoir permeability within Coal Seam Gas reservoirs, eastern Surat Basin

Mukherjee, Saswata^{1,2}, Rajabi, Mojtaba¹, & Esterle, Joan^{1,2}

¹*School of Earth and Environmental Sciences, University of Queensland, Brisbane, Australia;* ²*Centre for Natural Gas, University of Queensland, Brisbane, Australia*

The development of Coal Seam Gas (CSG) reservoirs in the Surat Basin has highlighted the basin as a prolific gas province and one of the significant economic successes in eastern Australia. An improved understanding of the controls on CSG reservoir behaviour contributes to better reservoir management for determination of production area targets. *In-situ* stress patterns and subsurface fractures within CSG reservoirs control the reservoir permeability and, hence, comprehensive studies are required for better exploration and development of these unconventional reservoirs. This is particularly important for the Surat Basin, where significant stress variations have been reported due to local geological structures. However, a detailed and systematic analysis of localised stress

perturbations within the basin and their impacts on reservoir permeability have not been presented thus far in the published literature. Herein, we combine different sets of data including conventional log data, wellbore image logs, 2D seismic lines and interpreted permeability (from well test data) in order to characterise the role of geological structures in the fracture character and subsurface fluid flow of the Walloon Coal Measures in eastern Surat Basin.

Analysis of 8.4 km of borehole image log in 33 vertical wells revealed a regional ENE–WSW orientation of the maximum horizontal stress (S_{Hmax}) in the study area. However, there are massive stress rotations, spatially and with depth. Analysis of 2D seismic data highlights the role of geological structures in stress perturbation. In addition, the interpretation of natural fractures using image logs show that most of the open fractures are oriented sub-parallel to the acute angle of local S_{Hmax} orientation. Herein, we show some examples of the complexity of major deformation underlying the Surat Basin and the controls on later fracture development in the Walloon Coal Measures. The greater concentration of net negative graben features recognized as “keystone structures” in the eastern part of the Surat Basin, significantly influenced fracture development within the Walloon Coal Measures. Interpreted well test data in the study wells demonstrates that most of the high permeability data points are located where *in-situ* stress rotation is observed. This indicates the influence of local S_{Hmax} orientation responding to geological structures on the subsurface fluid flow in the eastern part of the Surat Basin. In addition, the connection between different structural domains and the *in-situ* stress and/or fracture relationship, in previously unidentified areas of oblique-slip faulting is discussed.

In-situ stress pattern of Australia across spatial scales

Rajabi, Mojtaba

*School of Earth and Environmental Sciences,
University of Queensland, QLD 4072, Australia*

Present-day stresses are of extreme importance for understanding both natural processes (e.g., neotectonics deformation, earthquake cycle and seismic hazard assessment) and anthropogenic activities of underground usage (e.g., petroleum exploration and production, geothermal energy extraction, CO₂ sequestration, and mine stability).

This paper presents the updated version of the Australian Stress Map that includes over 2500 *in-situ* stress data records in >20 sedimentary basins across Australia. Analysis of stress provinces throughout the continent reveals four major trends for the orientation of maximum horizontal stress, including NE–SW in northern, northeastern Australia as well as Bonaparte and Canning basins in northwestern Australia, E–W in most part of Western Australia and South Australia, ENE–WSW in most parts of eastern Australia and NW–SE in southeastern Australia. In addition, high density datasets in several sedimentary basins of eastern Australia reveal substantial stress perturbations at both basin (10–200 km) and field (0.1–10 km) scales owing to the influence of various geological structures, including basement structures, faults, fractures and lithological contrasts.

Large scale geomechanical-numerical models for the

Australian continent reveals that all the stress sources, acting from the tectonic plate to the wellbore scales, are inter-related to each other, so that the *in-situ* stress at any given point is the resultant of all these different stress sources. However, it should be noted that large scale stress analyses do not necessarily represent the *in-situ* stress pattern at smaller scales. Similarly, the analyses of just a couple of borehole measurements in one area might not be a good representation of the regional stress pattern.

EARTH STRUCTURE

Tectonic and paleogeographic evolution of Mesozoic Eastern Australia

Paleozoic and Triassic crustal evolution of the proto-Andes from detrital heavy minerals

Bahlburg, Heinrich, & Panca, Fernando

Institut für Geologie und Paläontologie, Westfälische Wilhelms-Universität, Münster, Germany

The central Andean margin of South America evolved as an external accretionary orogen since the Late Neoproterozoic. During the Paleozoic and Triassic evolution, the evolution of the margin and its orogenic basins was linked to alternating extensional and compressional states. The most prominent arc system is the Late Cambrian–Ordovician Famatinian arc which extended along the entire margin. The Devonian is here a time of tectonic, magmatic and metamorphic quiescence allowing for the steady accumulation of shallow marine facies on a stable platform west of the Ordovician orogen. This setting appears like a passive margin but in the geologic context has to be considered enigmatic.

Connected to the Gondwanide Orogeny, a Late Carboniferous to Triassic arc system with episodic activity was present in northern Chile and absent from Bolivia. In southern Peru it is preserved as Late Carboniferous to Early Permian backarc magmatic rocks.

In the late Permian and Triassic, extensional alluvial basins hosting within-plate magmatic rocks developed here. The latter evolution is represented by the Mitu Group. Its depocenters are considered rift and not backarc basins, mainly because a contemporaneous magmatic arc is nowhere exposed and unknown.

Accretionary orogens are considered to be the sites of the production of juvenile continental crust. The Famatinian and Late Carboniferous to Early Permian magmatic arcs, however, are characterized by a marked scarcity of mafic intrusive and extrusive rocks. The detrital heavy mineral spectra reflect this with Nb/Cr ratios in detrital rutiles, for example, indicating predominant input from felsic rocks. Detrital zircon U–Pb age distributions denote the arcs as prolific zircon sources. The $\epsilon_{\text{Hf}(t)}$ isotope values of the zircons derived from the arcs, and the Famatinian arc in particular, are strongly negative. In both cases a pronounced recycling of older continental crust is indicated. Detrital zircons of Devonian age are very scarce.

The late Permian and Triassic Mitu Group basin system extends for 1500 km in NW–SE orientation along the length of Peru. It is characterized by highly variable alluvial facies with angular unconformities at base and top. The group appears to be arranged in several subbasins. Mafic alkaline and calc-alkaline lavas, and felsic ignimbrites are intercalated episodically. U–Pb zircon ages of the latter allow for a stratigraphic subdivision of the subbasin fills.

Detrital zircon age distributions of the Paleozoic central Andes show a typical South American, Amazonian provenance, with ages ranging from the Archean to the

maximum ages of deposition. In the Mitu Group, maximum depositional ages indicate a variable onset of deposition between 260 and 216 Ma, locally continuing into the Jurassic. The $\epsilon_{\text{Hf}(t)}$ isotope values of late Permian and Triassic zircons form vertical arrays between ca –10 and +6 and indicate a significantly more pronounced juvenile component in Mitu rocks than in the older arc rocks.

Considering the effects of Cenozoic subduction erosion at the Chile–Peru margin it may be possible that the Mitu age magmatic arc west of the basin has been lost. If that turns out to be the case the Mitu Group formed in a backarc rift basin.

Cretaceous evolution of Zealandia dictated by congested subduction

Betts, Peter¹, Moresi, Louis², Whittaker, Joanne³, & Miller, Meghan²

¹School of Earth Atmosphere and Environment, Monash University, Melbourne, Australia; ²Research School of Earth Sciences, Australian National University, Canberra, Australia; ³Institute for Marine and Antarctic Studies, University of Tasmania, Hobart, Australia

Congested subduction occurs when buoyant lithosphere within the down-going plate interacts with the convergent margin trench and prevents the slab from subducting in the region of collision. This can trigger several dynamic behaviours in the slab including slab tearing beneath the congestion and roll back of the trench away from the collision zone. Congested subduction also drives contemporaneous shortening and extension along different parts of the overriding plate and has the potential to dismember and segment subducting slabs.

During the Cretaceous collision of the Hikurangi Plateau with the east Gondwana margin triggered a major re-organisation of the margin culminating in the opening of the Tasman Sea and separation of Zealandia from Gondwana. Tectonic models for this plateau accretion have proposed collision between the plateau and Campbell Plateau (South Island of New Zealand) at ca 100 Ma, which triggered the opening of the Tasman Sea at ca 84 Ma. These models are appealing because they explain the present-day relationship between the Hikurangi Plateau and the New Zealand along the Pacific–Australia plate margin.

In this abstract, we provide an alternative model for the collision of the Hikurangi Plateau and Gondwana that is informed by numerical modelling of congested subduction. We present this alternative tectonic model as a series of G-plates reconstructions. Our new model requires collision of the Hikurangi Plateau with the Gondwana along the North Island of New Zealand, rather than the South Island. Suturing of the Hikurangi Plateau with the North Island resulted in crustal shortening in front of the collision zone and triggered collapse of the Gondwana margin to the south and north. Initiation of asymmetric trench roll back to the south is evidenced by the ubiquitous extension in the overriding plate, affecting the Campbell Plateau and Chatham rise. Asymmetric opening of Tasman Sea and opening of the Bounty Trough at 84 Ma. Counter-clockwise rotation of the Chatham and Campbell plateaus segmented the slab along the Gondwana margin. Soft collision of southern Zealandia (Chatham

and Campbell Plateau) along the southern margin of the Hikurangi Plateau occurred at ca 70 Ma and stable subduction was established outboard of this accreted margin. In this model, the Alpine fault initiated as a sinistral fault at the transition between trench advance in the North Island and trench roll-back to the south.

Tectonic evolution and crustal growth processes revealed by detrital zircon petrochronology: Insights from dispersed Paleozoic–Mesozoic sedimentary basins of Zealandia

Campbell, Matthew J¹, Rosenbaum, Gideon¹, Allen, Charlotte M.², & Spandler, Carl³

¹*School of Earth and Environmental Sciences, The University of Queensland, Brisbane, QLD, Australia;*

²*Institute for Future Environments, Queensland University of Technology, Brisbane, QLD, Australia;*

³*Geosciences, James Cook University, Townsville, QLD, Australia.*

Paleozoic–Mesozoic supra-subduction units, which originally formed along the paleo-Pacific margin of east Gondwana, are now preserved in eastern Australia, Antarctica and Zealandia. Previous works have characterized the temporal and geochemical history of magmatism within this broad accretionary orogenic system but the Zealandia continent remains a problematic piece of the Gondwana puzzle due to (1) 94% of the continent being submerged beneath the southwest Pacific Ocean and (2) a number of major phases of deformation that culminated in the oceanward dispersal of continental fragments of Zealandia. Here we reconstruct the Paleozoic and Mesozoic evolution of the active continental margin of Zealandia (eastern Gondwana), using a combination of detrital zircon geochronology, trace-element geochemistry, and Hf isotope data from several Paleozoic–Mesozoic terranes in New Zealand and New Caledonia. We find that zircon grains dated 360–160 Ma from New Zealand are characterized by ϵHf_i (+15 to +2) and trace-element compositions typical of predominantly juvenile magmatic sources. In contrast, the ϵHf_i (+15 to –5) and trace-element compositions of detrital zircon grains dated 245–140 Ma from New Caledonia reflect a mix of juvenile and evolved crustal sources. Secular trends in trace-element and Hf isotope compositions of zircon grains suggest that magmatism and continental crustal growth in Zealandia during the Devonian–Cretaceous were controlled by switches from trench advance to trench retreat. Orogenesis and crustal growth were controlled by a long-lived westward-dipping subduction system, which during the Permian–Triassic, was intermittently affected by distinct phases of arc accretion (e.g., of the Brook Street intra-oceanic arc) and orogenesis (e.g., driven by trench advance). These phases of orogenesis coincided with the Gondwanide Orogen (265–230 Ma), which might have been controlled by a plate-scale reorganization event following the final assembly of Pangea supercontinent.

Jurassic Arc? Reconstructing the Lost World of eastern Gondwana

Foley, Elliot¹, Henderson, Robert¹, Roberts, Eric¹, Kemp, Tony², & Spandler, Carl³

¹*James Cook University, Townsville, QLD 4811;* ²*The*

University of Western Australia, Perth, WA 6009; ³*The University of Adelaide, Adelaide SA 5005*

The tectonic setting of the east Gondwana margin during the Jurassic and Early Cretaceous is an enduring geological unknown. Whereas Paleozoic to early Mesozoic (ca 520 to 220 Ma) accretionary orogenic domains in eastern Australia are considered an exemplary record of convergent margin processes, the Late Triassic to Cretaceous represents an enigmatic gap in this record due to the paucity of exposed igneous and metamorphic rocks. This latter witnessed the deposition of vast quantities ($>1.5 \times 10^6$ km³) of sediment into the Great Australian Superbasin, including Jurassic silicic tuff horizons and a substantial Cretaceous component identified as volcanogenic.

The nature of magmatism that provided this volcanogenic material is debated, with two principal hypotheses posited. One suggests a continental magmatic arc enduring from the Carboniferous to mid-Cretaceous. The second model favours intraplate, rift-related magmatism unrelated to subduction, exemplified by the early–mid Cretaceous Whitsunday Igneous Province, a silicic large igneous province (SLIP) generated in the prelude to rapture of east Gondwana in the Late Cretaceous. Resolution of this question has been hampered by the sparse Jurassic–Cretaceous igneous record for eastern Australia. To overcome this deficiency, we investigated detrital zircon from the Great Australian Superbasin as a proxy record for subjacent igneous activity, employing U–Pb geochronology and Hf isotopic analysis to evaluate Mesozoic magmatism and clarify this enigmatic episode of east Gondwana crustal evolution.

Detrital zircon ages indicate that magmatism along the east Gondwana margin continued into the mid Cretaceous, with short-lived (ca 10 Myr) pulses of Mesozoic magmatic activity indicated by peaks at ca 160, ca 140, and ca 100 Ma. A trend of increasing igneous activity, from the Jurassic towards eventual Late Cretaceous continental rapture of east Gondwana, as predicted by the SLIP hypothesis, is not supported by the detrital zircon record. Hf isotopic analysis of dated zircons shows a strongly positive ϵHf signature (+8 to +12) throughout the Mesozoic to ca 95 Ma indicative of juvenile sources for the original igneous parent rocks. Similar positive ϵHf signatures are characteristic of Permian–Triassic granitic rocks of the New England Orogen for which a continental magmatic arc setting has been long accepted.

A potential Australian igneous source for Cretaceous zircon, the Whitsunday Igneous Province, is of limited aerial extent and a Jurassic source is unknown. Northern Zealandia, now submerged, formed the eastern borderland of east Gondwana prior to the Late Cretaceous, and must have been the main locus of Jurassic and Cretaceous magmatism.

Jurassic physiography of southeast Australia: evidence from the detrital zircon record of the Nambour Basin

Henderson, Robert, Foley, Elliot, & Roberts, Eric
James Cook University, Townsville, QLD 4811

Jurassic fluvial infill of the Nambour Basin consists largely of quartzose sandstone of the Myrtle Creek and Landsborough formations and succeeding heterolithic

sandstone, shale and coals of the Tiaro Coal Measures. Detrital zircon age spectra for representative sandstone samples constrain the ages and sediment sources of these units. Maximum depositional ages from zircon, broadly consistent with published biostratigraphic age determinations, assign this succession as Early to Middle Jurassic (195–163 Ma). With a coastal location in southern Queensland, these units represent the easternmost record of Jurassic sedimentation for Australia.

Zircon age spectra from Early Jurassic samples of the Myrtle Creek Formation are dominated by a 650–500 Ma (Pacific-Gondwana) age cluster, with a Grenville age cluster (1300–950 Ma) also showing prominence. Detrital zircon of these ages is characteristic of Cambro-Ordovician metasediments of the Tasmanides as widely represented in southeastern Australia. Rocks of this Tasmanide assemblage stood as epeirogenic Jurassic upland, shedding sediment northwards and eastwards across southeast Queensland. Transport vectors obtained for the Myrtle Creek Formation fluvial sandstone horizons support this conclusion. Devonian–Triassic ages of detrital and igneous zircon characteristic of the New England Orogen, which abuts the Nambour Basin and forms a broad crustal tract to its west, are sparingly represented in these samples.

Relief across the orogen in southeastern Australia, as generated by the Permo-Triassic (260–230 Ma) Hunter Bowen Orogeny, had therefore been reduced towards base level, with little contribution to ongoing erosion and sediment production, by the Early Jurassic (*ca* 190 Ma). By implication, the base level surface forming the floor to the Great Artesian Basin, marking a unconformity of remarkable extent, continued eastwards as a surface of low relief across much of the New England Orogen. Detrital zircon from sandstone samples of the Middle Jurassic Tiaro Coal Measures indicates a continuing provenance contribution from Cambro-Ordovician Tasmanide metasediments but also from a more pronounced New England Orogen source, suggesting some physiographic rejuvenation of this crustal sector subsequent to the Early Jurassic.

Jurassic aged zircon is scarce in most samples. However, it is well represented in a sample from the Myrtle Creek Formation and dominates the detrital zircon age spectrum of an arkosic sample from the Tiaro Coal Measures. As no source terrain for Jurassic zircon is known for the crustal fabric of eastern Australia, it must have been derived from igneous assemblages on continental crust to the east, now represented by submerged northern Zealandia, which rifted from the Australian continent during Late Cretaceous–Paleocene. An eastern source is supported by westerly paleocurrent directions measured for the sandstone intervals from which these samples were obtained.

Recognition of an Early Cretaceous continental arc in Eastern Australia

Spandler, Carl¹, Henderson, Bob², Foley, Elliot², Roberts, Eric², & Kemp, Tony³

¹The University of Adelaide, Adelaide SA 5005; ²James Cook University, Townsville, QLD 4811; ³The University of Western Australia, Perth, WA 6907

The Phanerozoic tectonic setting of eastern Australia involved two separate regimes. The older setting was a

Cambrian to Triassic active convergent margin as registered by a succession of orogenic systems collectively grouped as the Tasmanides. The younger setting was a passive margin, driven by plate divergence that initiated in the Cretaceous, and continues to characterize eastern Australia. The tectonic setting of eastern Australia during the gap between these contrasting tectonic regimes (approx. 130 m.y. from the late Triassic to Cretaceous) has been poorly documented and remains open to question. While extensive continental detritus of this age is preserved in the Great Artesian Basin, recognized igneous activity is restricted to the Whitsunday Igneous Province that formed from 132 Ma to 95 Ma.

Here we investigate a suite of igneous rocks/units that includes the Grahams Creek Formation (>0.25 M km³) and a series of small plutons and volcanic units that are exposed in the region between the Sunshine Coast and Maryborough in SE Queensland. The plutonic rocks range from I-type, hornblende-rich gabbros and diorites, to granodiorites, and quartz syenites, while the Grahams Creek Formation consists of a thick sequence (up to 1200 metres) of volcanic to volcanoclastic rocks of basaltic to dacitic composition. Both plutonic and volcanic components have distinctive subduction-related trace element compositions, including relative depletion in Ti, Nb and Ta, and enrichment in Pb, Sr, K, Rb, Th, U, Ba and Cs. These compositions are typical of hydrous magmatic rocks from continental arc settings. Uranium–Pb dating of magmatic zircons from these samples returned ages between 145 and 140 Ma, an age range that is distinctly older than the Whitsunday Igneous Province. The initial Hf and O isotope composition of these zircons ($\epsilon_{\text{Hf}} = +8$ to $+12.5$, $\delta^{18}\text{O} = +5.7$ to $+6.5$) is consistent with a juvenile mantle source for these magmas.

The recognition of this new suite of magmatic rocks, together with new chemical analyses of mafic rocks from the Whitsunday Igneous Province and detrital zircon records of quartzo-feldspathic sedimentary sequences of the Great Artesian Basin (see Foley *et al.*, 2020, this session), allow a re-evaluation of the tectonic setting of eastern Australia across the Mesozoic. We propose that the plate convergence regime along eastern Australia that formed the New England Orogen persisted across the Triassic, Jurassic and into the Cretaceous, with the newly recognised arc rocks representing the youngest episode of continental arc magmatism recorded on the Australian continent. Eastwards rollback of the slab in the Early Cretaceous led to continental extension and opening of a continental back-arc (analogous to the present-day Okinawa Trough) that formed the Whitsunday Igneous Province. Continued slab rollback and extension of the overlying plate in the late Cretaceous and Cenozoic lead to rifting and fragmentation of the eastern continental margin to form the current configuration of the eastern Australia–Zealandia, where large tracts on thinned continental crust remain submerged.

Raiders of the lost continental arc: deciphering the tectonic regime of eastern Australia during the Jurassic from analysis of tuff beds in the Surat Basin

Wainman, Carmine C., McCabe, Peter J., & Reynolds, Peter

Australian School of Petroleum and Energy Resources, University of Adelaide, Adelaide, Australia

Volcanogenic rocks are important components of the Late Triassic to Early Cretaceous infill of the Great Australian Superbasin, including the widespread deposition of air-fall volcanic ash (tuff) preserved in the Jurassic Walloon Coal Measures (WCM) of the Surat Basin. With the paucity of known igneous bodies in eastern Australia, these tuff beds provide important clues on the tectono-magmatic environment of eastern Gondwana during the Mesozoic. To better understand the source and character of the volcanic province, age-constrained tuffs (168 to 148 Ma) were analysed in detail. Bed thickness, petrography (supported by XRD data), zircon crystal size and their geochemistry were documented. New datasets reveal these buff-coloured tuffs, mostly preserved within coal seams, are between 0.01 and 2 m thick with sharp lower and upper contacts. They are dominated by splintery, angular quartz clasts (approx. 10–100 µm in diameter) supported in an amorphous, white-buff coloured matrix consisting of clay minerals (predominantly smectite). The same beds are poorly sorted, lightly compacted and lack any structure. Tuff isopach maps from the WCM show elongate lobes that thin from current day northeast to southwest (5 m to <1 m). Dated zircon crystals average 170 µm in size, are euhedral to tabular in shape, and have moderate U values (100 to 1000 pm) and elevated Y values (>500 pm). Integrating these datasets demonstrate that these tuffs were (1) produced from volcanoes fed by intermediate to felsic magmas, (2) that the prevailing paleowind direction was from east-southeast to west-northwest and (3) sourced from volcanoes approximately 280 to 1000 km away which erupted with a volcanic explosivity index (VEI) of approximately 8. We infer that these tuffs originated from a long-lived (late Palaeozoic to Cretaceous) continental arc related to the westward subduction of the paleo-Pacific oceanic crust beneath eastern Australia. These tuffs were most likely derived from the Whitsunday Igneous Association as supported from similar studies from Early Cretaceous strata of the Eromanga Basin. These previous findings will help better constrain the timing of when eastern Gondwana transitioned from a convergent to a divergent margin and define future targets for ocean drilling to locate the parent igneous bodies in the Tasman Sea.

Mesozoic sedimentary provenance and palaeodrainage evolution of the northeastern Qld: evidence from the northeastern Galilee and Eromanga basins

Todd, Christopher N.¹, & Roberts, Eric M.¹

Geosciences, James Cook University, Townsville, QLD 4811, Australia

The Phanerozoic tectono-sedimentary evolution of Eastern Australia is generally well understood, with considerable agreement on the plate dynamics and

basin development during the Paleozoic to early Mesozoic and from the late Mesozoic to Cenozoic. However, basin development and plate tectonic patterns during the mid-Mesozoic, particularly for northeastern Australia, remain enigmatic due to the scarcity of well-preserved magmatic rocks of this age along the continental margin. To decipher the tectonic framework and drivers of basin development during this time, sedimentary provenance analysis, involving palaeocurrent measurements, pebble counts, sandstone petrography, and U–Pb detrital zircon geochronology, was conducted on upper Paleozoic to late Mesozoic strata of the northeastern Galilee and Eromanga basins. The results establish the presence of syn-depositional magmatism along the eastern margin of northeastern Queensland during the Triassic and Jurassic, however, sandstone petrography and detrital zircon geochronology indicate that these were distal sources that account for only a small proportion of the total sediment input into the study region during this time. Sandstone petrography points towards a recycled orogenic source for the Triassic samples, whereas the Jurassic samples suggest a cratonic source signature, indicating that most of the syn-depositional volcanic input into the basin during this time was likely through distal airfall ash deposits. However, it is also possible that minor erosion of intrusive, arc-related rocks may have intermittently entered the basin from the east. Palaeocurrent and detrital zircon provenance analysis demonstrates that fluvial drainage patterns during the late Permian to Middle Jurassic were dominated by south to southwest palaeoflow with sediment sourced from the Etheridge Province and the Kennedy Igneous Association to the north. A significant Late Jurassic palaeocurrent reversal (flow to the north/northeast) is documented in the upper Blantyre Sandstone, which is interpreted to reflect an uplift event on the eastern Australian margin. This drainage reversal is confirmed by a change in the detrital zircon provenance evidenced by input of zircon populations eroded from the Anakie Inlier, located to the southeast of the study area. These populations are characterised by polyphase zircons that were likely recycled from the central Australian Musgrave Complex, the Ross-Delamerian Orogen, and Patterson-Petermann Orogen. As the basin filled, palaeoflow shifted to west-southwest in the Early Cretaceous, with the dominant detrital zircon population returning to Kennedy Igneous Association sources. Lower Cretaceous strata also yield significant syn-depositional detrital zircons, with a range of 135–120 Ma grains that are interpreted to be sourced from the Whitsunday Igneous Province. This study not only demonstrates that sediments for the northern Galilee and Eromanga basins are primarily sourced from Paleozoic terranes to the north-northeast, but also documents the presence of a continuum of Mesozoic magmatic zircons whose sources lie somewhere to the east of the present coastline of northeastern Australia, which most likely entered the basin as airfall deposits.

From cratonic assembly to supercontinent cycles

Self-consistent geodynamic models through the supercontinent cycle — Testing the introversion and extroversion supercontinent assembly and the stability of LLSVPs

Huang, Chuan¹, Li, Zheng-Xiang¹, & Zhang, Nan²

¹*Earth Dynamics Research Group, ARC Centre of Excellence for Core to Crust Fluid Systems and The Institute for Geoscience Research (TIGeR), Department of Applied Geology, Curtin University, Perth, Western Australia, Australia;* ²*Key Laboratory of Orogenic Belts and Crustal Evolution, School of Earth and Space Sciences, Peking University, Beijing, China*

We developed a series of new dynamic models aiming to more realistically model the full supercontinent cycle, testing parameters critical for introversion vs extroversion assembly, and mantle response to the alternative supercontinent evolution paths. The numeric simulations allow for self-generated subduction and supercontinent break-up during the supercontinent cycle. Subduction within the oceanic realm is implemented by considering plastic yielding in the oceanic lithosphere, through which rapid viscous weakening occurs when convection stress is larger than the yield strength. For subduction along continental margins, weak zones are introduced in oceans near the continental edge when the age of oceanic lithosphere is greater than a certain value (e.g., 180 Ma). Under such a model setup, our models are able to naturally generate Earth-like ocean–ocean and ocean–continent subductions.

By simulating the mantle evolution from the breakup of a supercontinent to the formation of the next one, we found that heat distribution (monitored by mantle temperature) between the mantle domains under either the supercontinent or the surrounding super-ocean, divided by the subduction girdle, provides an important control on how the next supercontinent forms. During the breakup stage, the average mantle temperature beneath the supercontinent (here denoted by T_c) is higher than that under the super-ocean (T_o) partially due to thermal isolation by the supercontinent. After the breakup, T_c decreases with the vanish of the thermal isolation effect, but T_o maintains at a similar level. It causes T_o shifts to a value slightly larger than T_c in the time soon after the breakup. Despite the limited higher energy level in the superocean-side, subduction/girdle retreat maintains the continuous drift of continents. After that, dispersing continents will reach their maximum distance from each other. The relative value of T_c and T_o after the time that greatest distance is reached determines whether the next supercontinent assembles through introversion or extroversion. Generally, models with a dense chemical layer above the core–mantle boundary tend to have introversion cycle, due to the much higher heat level (~50 K) in the superocean-side reserved by its larger chemical layer volume than the continent side. Two LLSVPs formed in our models during the full cycle locating in the ocean and continent sides, respectively. However, migrations up to several thousand kilometres for the two structures can be also observed.

New interpretations of high-resolution aeromagnetic data and implications for stratigraphic correlations in the Tanami Region and northwest Aileron Province

Blaikie, Teagan, & McFarlane, Helen

CSIRO Mineral Resources, Perth, Australia

The Tanami Region, located 600 km to the northwest of Alice Springs, preserves an important record of basin development, deformation, magmatism, and the assembly of the North Australian Craton during the Paleoproterozoic. The region comprises extensive polydeformed metasedimentary and volcanic rocks, preserved as the ca 1885–1840 Ma Tanami Group and the ca 1824–1816 Ma Ware Group. The Lander Rock Formation of the adjoining Aileron Province represents a comparably aged metasedimentary package that is considered to be laterally equivalent to the Killi Killi formation in the upper part of the Tanami Group. These metasedimentary packages were extensively intruded by 1825–1790 Ma granites and dolerite dykes, and deformed during the ca 1840 Tanami Event, and the 1825–1790 Ma Stafford Event.

Extensive cover makes geological studies in this region challenging, but newly acquired 200 m line spaced aeromagnetic data and previously acquired gravity and seismic data offers valuable information on the underlying geology. These data were interpreted to produce a solid geological map and develop a new cohesive structural framework. This aimed to test the different stratigraphic, structural and tectonic models that presently exist for the region. The interpretation initially focussed on mapping the fault architecture and lithological units under cover and was constrained by the petrophysical characteristics of each unit and correlation of outcropping geology with distinct geophysical features.

Results of the interpretation led to revision of the extent of previously mapped or interpreted units, and recognition of potential correlative units across the two terranes. In the northwest Aileron Province, the extent of the Archean inlier known as the Billabong Complex was revised based on correlation of outcrop with a distinct geophysical response characterised by a variable moderate to high amplitude magnetic intensity and featuring strong magnetic lineaments. The complex is now defined as a fault bounded arcuate belt flanked by granitic units. A continuous geophysical signal, defined by a moderate to low gravity response, and low magnetic intensity with a smooth texture was also recognised between the Killi Killi and Lander Rock formations. Magnetic units with a moderate magnetic intensity and strong linear fabric, which are very similar in character to the Dead Bullock Formation were also noted within the northwestern Aileron province and may represent a previously unrecognised lateral equivalent of the Dead Bullock Formation in this area. These observations support previous interpretations of the deep crustal seismic data which suggest stratigraphy is continuous and drapes the crustal boundary between Tanami Region and Aileron Province. This implies the two terrains were joined together prior to deposition of the Tanami Group and Lander Rock Formation and the onset of deformation and magmatism related to the Stafford Event.

Unravelling the Palaeoproterozoic tectonic evolution of the Tanami Region and northwest Aileron Province

McFarlane, Helen, & Blaikie, Teagan

CSIRO Mineral Resources, Perth, Australia

Stradling the Northern Territory–Western Australia border approximately 600 km to the northwest of Alice Springs, the Tanami Region comprises regionally expansive, polydeformed metasedimentary and volcanic rocks (Tanami and Ware groups: ca 1885–1816 Ma). Recording a protracted and complex tectonic history, the sequences are extensively intruded by 1825–1790 Ma granites and dolerite dykes. To the southeast, the adjoining Aileron Province is comprised largely of metasedimentary and magmatic rocks of a comparable age. The region is highly prospective for gold, and preserves several deposits including the world class Callie deposit. Geological studies of the region are made challenging by extensive Mesoproterozoic to Cenozoic sediment-ary cover and Early Cambrian basalt flows, with most geological information derived from sporadic outcrop and drill core. Geophysical data is therefore critical in this region and is relied upon to understand the structural architecture and extent of potential gold-bearing metasedimentary and volcanic rocks under cover.

Newly acquired and legacy government and industry aeromagnetic data available across the Tanami Region and northwest Aileron Province were reprocessed and interpreted for this work to produce new seamless solid geological and structural maps. This new interpretation attempts to resolve inconsistent geological correlations in the Northern Territory and develop a new cohesive structural framework for the entire region.

Deformation is typically best resolved in the magnetic stratigraphy of the Tanami Group which preserve several styles of fold interference patterns. The earliest deformation event (D₁) is characterised by isoclinal folding and low angle thrust faulting. D₁ structures are extensively overprinted by subsequent deformation events, however, evidence suggests it is associated with an episode of SW-directed tectonic vergence. D₂ deformation is characterised by the refolding of D₁ structures by tight to isoclinal NNE- to NE-striking F₂ folds, associated with WNW–ESE to NW–SE shortening. Both D₁ and D₂ are attributed to the ca 1830 Ma Tanami Event which also involved regional greenschist to amphibolite facies metamorphism and early gold mineralisation. This was followed by an episode of sedimentation and volcanism, preserved as the Ware Group. The oldest recognised deformational structures in the Ware Group are attributed to NE–SW shortening during D₃ as evidenced by NW- to NNW-striking chevron folds. The overprinting relationship of D₃ on D₁ structures generated a Type-2 fold interference pattern in the magnetic stratigraphy of the Tanami Group. The localised development of tight, E–W striking chevron folds is attributed to D₄ N–S shortening and is associated with comparatively weaker deformation compared to earlier events. The final folding event (D₅) generated long wavelength, open, NE-striking F₅ folds during NW–SE shortening. Deformation events D₃–D₅ are interpreted as polyphase deformation during the 1810–1790 Ma Stafford Event and was coeval with widespread felsic magmatism. The transition to brittle-ductile deformation (D₆) is

associated with the development of the regionally prominent WNW–ESE to NW–SE striking dextral and sinistral shear zones, associated with the major period of gold mineralisation in the region.

Assembly of proto-Australia prior to the formation of the Nuna supercontinent in the Paleoproterozoic

Kirscher, Uwe^{1,2}, Mitchell, Ross N^{3,1}, Liu, Yebo¹, Nordsvan, Adam R^{4,1}, Wu, Lei^{5,1}, Pisarevsky, Sergei¹, & Li, Zheng-Xiang¹

¹*Earth Dynamics Research Group, School of Earth and Planetary Sciences, The Institute for Geoscience Research (TIGeR), Australian Research Council Centre of Excellence for Core to Crust Fluid Systems (CCFS), Curtin University, Perth, WA, Australia;* ²*Department of Geosciences, Eberhard Karls University of Tübingen, Tübingen, Germany;* ³*State Key Laboratory of Lithospheric Evolution, Institute of Geology and Geophysics, Chinese Academy of Sciences, Beijing, China;* ⁴*Department of Earth Sciences, University of Hong Kong, Pokfulam, Hong Kong;* ⁵*Department of Earth & Planetary Sciences, McGill University, 3450 Rue University, Montréal, Québec H3A 0E8, Canada*

The paleogeography, chronology and importance of the Paleoproterozoic assembly of the supercontinent Nuna are still debated. To further test the paleo-geographic evolution of the Australian cratons in the leadup to Nuna formation, we present new paleomagnetic results from two Paleoproterozoic rock formations in North Australia. First, we obtained paleomagnetic directions from the 1825 ± 4 Ma, bimodal Plum Tree Creek Volcanics sequence of the North Australian Craton (NAC). Second, we studied the 1855 ± 2 Ma layered mafic–ultramafic ‘Toby’ intrusion from the Kimberley Craton (KC). Samples from both study areas reveal high quality, stable, magnetite related characteristic remanent magnetization directions. Combining within-site clustered mean directions, we obtained two paleo-poles, which plot proximal to each other in the present day central Pacific Ocean, off the east coast of Australia. These results agree with previous interpretation that the Kimberly Craton was amalgamated with the rest of the NAC prior to ca 1.85 Ga. Comparing these new results with slightly younger poles from the NAC and slightly older, rotated poles from the West Australian Craton (WAC) reveal a high degree of similarity suggesting minimal absolute plate motion between ca 1.9 and 1.65 Ga. All available paleomagnetic poles agree with an assembly, or close juxtaposition, of the two major Australian cratons (NAC and WAC) before 1.8 Ga. Furthermore, the individual virtual geomagnetic poles from the potentially slow cooled Toby intrusion show a non-fisherian distribution along a great circle. This spread might be related to previously interpreted major true polar wander events based on data from Laurentian cratons, which would be global if such an interpretation is correct. The assembly of proto-Australia prior to ca 1.85 Ga roughly 250 to 300 Myr before the final stage of super-continent Nuna’s amalgamation ca 1.6 Ga suggests that assembling of major building blocks, such as Australia and Laurentia for the supercontinent Nuna and Gondwana for the supercontinent Pangea, is an important step in the formation of supercontinents.

Proterozoic crustal evolution of NE Australia during Nuna assembly: insights from geophysical and radiogenic isotope data

Li, Jiangyu¹, Olierook, H. K. H.^{2,3}, Li, Zheng-Xiang¹, Nordsvan, Adam R.^{1,4}, Pourteau, Amaury¹, Volante, Silvia^{1,5}, Elders, Chris², Collins, William J.¹, & Doucet, Luc S.¹

¹Earth Dynamics Research Group, The Institute for Geoscience Research (TIGeR), School of Earth and Planetary Sciences, Curtin University, Perth, WA, Australia; ²Faculty of Science and Engineering, The Institute for Geoscience Research (TIGeR), School of Earth and Planetary Sciences, Curtin University, Perth, WA, Australia; ³Timescales of Mineral Systems, Centre for Exploration Targeting – Curtin Node, and John de Laeter Centre, Curtin University, GPO Box U1987, Perth, WA 6845, Australia; ⁴Department of Earth Sciences, University of Hong Kong, Pokfulam, Hong Kong; ⁵Institute of Geology, Mineralogy and Geophysics, Ruhr-Universität Bochum, Bochum, Germany

The final assembly of the Proterozoic supercontinent Nuna occurred via a collisional event between Australia and Laurentia in NE Australia at ca 1.60 Ga [1]. However, detailed collisional processes and the resulting orogenic architecture in NE Australia remain elusive. Here, we combine aeromagnetic [2] and gravity data [3] with surface geological data and a reinterpretation of seismic profiles [4–5] to depict the deep crustal structure that developed during this collisional event. Neodymium and hafnium isotopic data from Proterozoic mafic and felsic intrusions [6] were also compiled to investigate the crustal evolutionary processes. A N–S-trending, distinctive terrane boundary is recognized on the eastern margin of the Mount Isa Inlier from the filtered aeromagnetic and gravity grid, coinciding with the Gidyea Suture Zone previously recognised from the seismic reflection data. Between the Mount Isa and Georgetown inliers, a west-dipping, crustal dissecting fault is interpreted as another suture zone with additional smaller-scale thrusts that are antithetic to the main suture. The duplexed crustal architectures between the Mount Isa and Georgetown inliers are interpreted to have formed during a crustal thickening event associated with the docking of the Georgetown Inlier along a west-dipping subduction zone. The Georgetown Inlier is isotopically distinguishable from the Mount Isa Inlier at ca 1.68 Ga but shares the same isotopic history after ca 1.60 Ga. Subduction may have initiated at ca 1.64 Ga but ceased at 1.60 Ga, with the Georgetown Inlier accreted to the Mount Isa Inlier, possibly along the Empress Suture Zone during the final Nuna assembly.

[1] A Pourteau *et al.*, *Geology*, 46(11), 959 (2018).

[2] M Greenwood (2018).

[3] C Roger (2014).

[4] JL Maher (2008).

[5] JL Maher (2009).

[6] D Champion (2013).

Palaeomagnetism argue against a stable supercontinent during the Archaean–Proterozoic transition

Liu, Yebo¹, Mitchell, Ross N.^{2,1}, Li, Zheng-Xiang¹, Kirscher, Uwe^{1,3}, Pisarevsky, Sergei A.^{1,4}, & Wang, Chong^{1,2,5}

¹Earth Dynamics Research Group, The Institute for Geoscience Research (TIGeR), School of Earth and Planetary Sciences, Curtin University, Bentley, Western Australia 6102, Australia; ²State Key Laboratory of Lithospheric Evolution, Institute of Geology and Geophysics, Chinese Academy of Sciences, Beijing 100029, China; ³Department of Geosciences, University of Tübingen, Sigwartstr. 10, 72076 Tübingen, Germany; ⁴Institute of the Earth's Crust, Siberian Branch of the Russian Academy of Sciences, Irkutsk 664033, Russia; ⁵Department of Geosciences and Geography, University of Helsinki, Helsinki, Finland

Many Archaean cratons exhibit Proterozoic rifted margins, implying they were pieces of some ancestral landmass(es). The idea that such an ancient continental assembly represents an Archaean supercontinent has been proposed but remains to be justified. Starkly contrasting geological records between different clans of cratons have inspired an alternative hypothesis where cratons were clustered in multiple, separate “supercratons”. A new palaeomagnetic pole from the Yilgarn Craton of Australia, when compared with available coeval poles globally, is compatible with either two successive but ephemeral supercontinents, or two stable supercratons across the Archaean–Proterozoic transition. Neither interpretation supports the existence of a single, long-lived supercontinent, suggesting that Archaean geodynamics were fundamentally different from subsequent times (Proterozoic–present), which were influenced largely by supercontinent cycles.

The emergence of eclogites linked to global arc chemistry change at 2 Ga

Tamblyn, Renée, Hasterok, Derrick, Hand, Martin, & Gard, Matthew

Department of Earth Sciences, the University of Adelaide, SA, Australia

The thermal state of the solid Earth determines the interactions between the mantle and the crust. The only way to probe the thermal conditions of the ancient Earth is from the mineralogical and geochemical record of thermally driven processes, i.e., metamorphism and magmatism. The generally accepted model for the thermal budget of the Earth balances heat accumulated from accretion and the decay of heat producing elements and indicates an overall cooling trend from ca 3 Ga to present, encompassing the emergence of modern plate tectonics. The geological record however indicates this simple cooling model may not hold true. Thermally sensitive metamorphic mineral assemblages, such as eclogites, emerge in the rock record transiently from 2.2–1.8 Ga, and disappear again until ca 0.8 Ga. Coincident with this transient emergence of eclogite, the global record of arc granite chemistry also shows significant step changes, most notably decreased Sr and Eu and increased Y and rare earth element concentrations, from 2.0–1.8 Ga, both of

which point to a global increase in thermal gradients that intersected granite genesis. We suggest these changes occurred as the secular cooling of the mantle and crust was reversed by a net increase in the spatial extent of continental crust between 2–1.8 Ga, resulting in thermal insulation of the mantle. The following 1.2 billion years on Earth was dominated by a warm, insulated mantle and crust, maintained by stable continental volumes, which eventually cooled to allow the second emergence and widespread preservation of eclogites from ca 0.8 Ga until present. While novel, this idea combines unrelated global petrological and geochemical datasets to explore the sensitivity of switches in the thermal evolution of the solid Earth.

When did Australia's Cratons come together?

Gorczyk, Weronika, Tyler, Ian, Aitken, Alan, & Kohanpour, Fariba

Centre of Exploration Targeting, School of Earth Science, University of Western Australia, Perth, Australia

Assembly of Australian cratons as part of Nuna assembly has been a subject of debates for decades. Especially within Australian geoscience community the timing and style of Western Australia Craton (WAC) with Northern Australian Craton (NAC) collision causes a lot of controversy. The dispute arises mostly due to sparsity of data available. As the Proterozoic knowledge of Australian cratons, as well as others grew new models for Nuna assembly were proposed, and the literature became overcrowded with variable models, based on localised and limited data.

Here, without presenting any new data, an attempt is made to analyse existing models in an unbiased style, questioning and correlating all the tectonic and sedimentation events across WAC, NAC and SAC (Southern Australia Craton). The position and interactions with Laurentia and North China – which are believed to be proximal to Australia at the time of paleo-meso Proterozoic, as also considered.

To achieve this task, plate reconstruction software (GPlates) is used. Publicly available geological data that describe tectonic and sedimentary events affecting WAC, NAC and SAC, as well as paleomagnetic data to be taken into account to support or contradict conceptual models. The immense advantage of this approach is continuous space and time visual representation of the plate interactions and occurrence of events.

Three (with variations) time models of WAC and NAC collision are shown with different subduction polarity: (1) 1800–1765 Ma, (2) 1590–1550 Ma, (3) ca 1300 Ma. Essentially, in the first model one can correlate all the tectonic events across WAC and NAC and SAC with one another post-collision, but spatial problem arises between the cratons and events that follow. In the second model the collision of WAC and NAC can be correlated with metamorphic and magmatic events in Arunta region, as well as in Mt Isa, but does not allow for correlation of previous events across WAC and NAC. The third model with subduction under WAC combines the tectonic evolution of Paterson region, Wankanki Arc and Stage I of Albany Fraser in a very elegant way, but again keeps WAC on a separate plate prior 1300 Ma and does not allow for correlation of events across the cratons of with similar styles and

timings. Pros and cons for all models will be presented, and the verdict will be left to you.

Detrital zircon record of Proterozoic strata in the Priest River region of western Laurentia: Evaluating “SWEAT” relationships for supercontinents Nuna and Rodinia

Brennan, Daniel T.¹, Li, Zheng-Xiang¹, Link, Paul K.², & Johnson, Tim³

¹*Earth Dynamics Research Group, School of Earth and Planetary Sciences, Curtin University, WA, Australia;* ²*Department of Geosciences, Idaho State University, Pocatello, ID, USA;* ³*School of Earth and Planetary Sciences, The Institute for Geoscience Research (TIGeR), Curtin University, WA, Australia*

Correlation of rocks across purportedly paired margins, such as Proterozoic strata (notably the Belt-Purcell and Windermere Supergroups) of western Laurentia with coeval rocks and/or magmatic sources in and around the Gawler Craton, have long been used as a key piercing point for SWEAT-like reconstructions of supercontinents Nuna and Rodinia. Here we evaluate the nature and timing of the proposed correlations through U–Pb and Lu–Hf analysis of detrital zircon (DZ) from the Proterozoic Gold Cup Quartzite, Belt-Purcell Supergroup, Deer Trail Group, and Buffalo Hump Formation of the Priest River region, northwestern USA.

The <1.7 Ga Gold Cup quartzite contains mostly ca 2.6 and 1.8 Ga DZ grains, indicating it is likely a western equivalent of the Neihart Formation. Lu–Hf values from these grains suggest that the younger ca 1.8 Ga population ($\epsilon_{\text{Hf}_t} = -9$ to -3) resulted from a reworking event on the ca 2.6 Ga crust involving juvenile mantle input ($\epsilon_{\text{Hf}_t} = -2$ to 4). This is consistent with the sediments being sourced from proximal Neoproterozoic Laurentian terranes such as the Clearwater/Medicine Hat block, that were intruded by Paleoproterozoic magmatism associated with the collision of the Wyoming and Medicine Hat blocks. Thus, these units do not require a SWEAT configuration (or the existence of Nuna) at ca 1.7 Ga. In the overlying western (ca 1.48–1.37 Ga) Belt Supergroup units, significant juvenile ($\epsilon_{\text{Hf}_t} = 2$ to 8) ca 1.6 Ga DZ grains are present. These grains fall within the North American Magmatic Gap and likely indicate provenance from the Gawler Craton, supporting a proto-SWEAT configuration for Nuna during ca 1.5–1.4 Ga as in most Nuna reconstructions. The overlying <1.3 Ga, fine-grained and carbonate Deer Trail Group is interpreted as a passive margin succession and contains mostly ca 1.9–1.65 Ga DZ grains with a wide range of Lu–Hf values ($\epsilon_{\text{Hf}_t} = -6$ to 9), notably ca 1.6 Ga DZ grains are absent. This provenance shift could be indicative of Nuna breakup, removal of the Gawler Craton from its Nuna position along western Laurentia, and a southwestern Laurentia provenance or recycling from underlying rocks of the Lemhi group of the Belt-Purcell Supergroup.

Coarse, locally conglomeratic, rocks of the Buffalo Hump Formation unconformably overly Deer Trail group strata. Prior small-n DZ study of the Buffalo Hump Formation identified a ca 1.1 Ga youngest DZ population, which was suggested to record deposition at ca 1.0 Ga during Rodinia amalgamation. However, our large-n study of the Buffalo Hump Formation

identified for the first time a minor (~1%) yet significant ca 760 Ma DZ population, which constrains the maximum age of deposition. These geochronology results redefine the onset of Rodinia rift-related sedimentation to after ca 760 Ma in this region. Additionally, the Buffalo Hump Formation lacks any ca 900–790 Ma DZ grains. Such a DZ age-spectrum, and inferred rift history, is difficult to reconcile with an immediate neighbourhood between Laurentia and Australia in Rodinia as the latter had an earlier start of continental rifting (with ca 830–750 Ma rifting and syn-rift magmatism).

Review of SHRIMP zircon ages for the Eastern Succession of the Mount Isa and Etheridge Provinces and their provenances

Withnall, Ian

Geological Survey of Queensland, Brisbane, Australia

The migration of zircon geochronology data collected by Geoscience Australia (GA) and Geological Survey of Queensland (GSQ) from the Mount Isa Province into the Online Geochron Delivery System, an important repository maintained by GA, provided an opportunity to review the data and replot it using a consistent approach. This included data for which only preliminary plots of had been available to GSQ and never published.

The review highlighted that the main magmatic events that would have contributed zircon to the Eastern Succession sedimentary rocks occurred at 1850–1870 Ma, 1790–1800 Ma, 1780 Ma, 1760 Ma, 1735–1745 Ma, 1725 Ma, 1705–1715 Ma and 1670–1680 Ma and volumetrically smaller events at 1770 Ma, 1755 Ma, 1655–1660 Ma and 1650 Ma.

The Soldiers Cap Group in the easternmost part of the Mount Isa Province and extending under cover to the east is younger than most of the eastern succession. It consists of Llewellyn Formation, Mount Norna Quartzite and Toole Creek Volcanics in ascending stratigraphic order. The Kuridala Group comprises the Starcross Formation and Hampden Slate.

Samples of the two lowermost units of the Soldiers Cap Group and Starcross Formation have similar maximum depositional ages. A closer comparison has been made of their respective provenances by pooling analyses for units in each group. These provenances are similar, indicating a minor, very old source around the Archean–Proterozoic boundary and then almost none up to ca 1900 Ma (the Barramundi Orogeny). Except for minor components from the Kalkadoon–Leichhardt basement (1850–1870 Ma) and Argylla Formation (1780 Ma), by far the major sources appear to be the Wonga–Burstall–Gin Creek plutonic suites at ca 1740 Ma and Fieri Creek Volcanics or Weberra Granite at ca 1710 Ma. They also both have a significant younger component (slightly older in the Soldiers Cap Group at ca 1685 Ma, and ca 1675 Ma in the Starcross Formation). Pooling analyses from the Hampden Slate indicates that apart from the youngest component being ca 1655 Ma, other components are almost identical to those in the Starcross Formation.

By contrast the provenance of the Toole Creek Volcanics is dissimilar to the other units. It shows an ca 1795 Ma, ca 1850 Ma, and ca 2680 Ma.

Comparing the provenance spectra of the lower part of

the Soldiers Cap and Kuridala Groups with those of the lower part of the Etheridge Group in the Etheridge Province (Georgetown region) suggests that they were probably deposited at about the same time, but the provenance patterns are strikingly different. The Etheridge Group shows a large Archean component as well as almost continuous spread of data points throughout the Paleoproterozoic including peaks around 1900–2000 Ma. This dissimilarity has been cited as evidence that the Georgetown rocks were not distal to Mount Isa and were part of Laurentia until welded to the Australian craton during the assembly of Nuna. The provenance of the upper part of the Etheridge Group, however, is like that of the Toole Creek Volcanics.

Partial melting, granulites, retrogression and their control on late orogenic exhumation processes

Kenki-Tok, Bénédicte^{1,2}, Rey, Patrice F.², & Arcay, Diane¹

¹*Géosciences Montpellier, Université de Montpellier, CNRS, 34095 Montpellier Cedex 5, France;* ²*Earthbyte Research Group, School of Geosciences, University of Sydney, NSW 2006, Sydney, Australia*

Orogenesis drives the differentiation of the continental crust through metamorphic and magmatic processes, the exhumation of deep metamorphic terranes and the concomitant formation of sedimentary basins. A major consequence of prograde metamorphism following a typical orogenic thermal gradient is the dehydration and partial melting of buried rocks leading to the formation of migmatites and granulites. Partial melting and granulitisation are often intertwined and primarily linked to the availability of fluids. Here, we consider the thermal and mechanical consequences of coupled partial melting, granulitisation and strain-rate dependent retrogression during the orogenic cycle, in particular during the recovery phase when the crust's thickness and geotherm re-equilibrate. We explore through 2D thermo-mechanical modelling how the interplay between mechanical weakening due to partial melting and mechanical strengthening due to granulitisation impacts the formation and preservation of crustal roots, the exhumation of the partially molten crust in gneiss domes, the formation of HT/UHT terranes and the partitioning of deformation through the crust.

Our results show that the survival of granulites, which strengthen the lower crust and decrease its capacity to flow under gravitational stresses, impedes the formation of migmatite-cored gneiss domes, and controls the formation and preservation of thick and strong granulitic roots. These are strong enough to stay immune to gravitational stresses and persist over hundreds of million years. These can be actually compared with stable intracontinental regions where the presence of localized crustal roots explains the remarkable variability – from 25 to 65 km – of crustal thickness. Finally, our results highlight the importance of an elevated radiogenic heat production in the upper crust in order to form the long-lived HT/UHT terranes often resulting from supercontinents amalgamation. Our experimental results explain as well why some ancient orogenic domains expose at the Earth's surface dominantly granulitic terranes (e.g., South India, Sri

Lanka, Madagascar, Antarctica, Baltica), whereas others (Variscides) expose dominantly migmatitic and granitic crust.

Mantle refertilization from 3.2 billion years ago points to an early start of plate tectonics

EL Dien, Hamed Gamal¹, Doucet, Luc-Serge¹, Murphy, J. Brendan^{1,2}, & Li, Zheng-Xiang¹

¹*Earth Dynamics Research Group, The Institute for Geoscience Research (TIGeR), School of Earth and Planetary Sciences, Curtin University, GPO Box U1987, Perth, WA 6845, Australia;* ²*Department of Earth Sciences, St. Francis Xavier University, Antigonish, Nova Scotia, Canada*

Progressive mantle melting during the Earth's earliest evolution led to the formation of a depleted mantle and a continental crust enriched in highly incompatible elements. Re-enrichment of Earth's mantle can occur when continental crustal materials begin to founder into the mantle by either subduction or, to a lesser degree, by delamination processes, profoundly affecting the mantle's trace element and volatile compositions. Deciphering when mantle re-enrichment/refertilization became a global-scale process would reveal the onset of efficient mass transfer of crust to the mantle and potentially when plate tectonic processes became operative on a global-scale. Here we document the onset of mantle re-enrichment/refertilization by comparing the abundances of petrogenetically significant isotopic values and key ratios of highly incompatible elements compared to lithophile elements in Archean to Early Proterozoic mantle-derived melts (i.e., basalts and komatiites). Basalts and komatiites both record a rapid change in mantle chemistry around 3.2 billion years ago (Ga) signifying a fundamental change in Earth geodynamics. This rapid-change is recorded in Nd isotopes and in key trace element ratios that reflect a fundamental shift in the balance between fluid-mobile and incompatible elements (i.e., Ba/La, Ba/Nb, U/Nb, Pb/Nd and Pb/Ce) in basaltic and komatiitic rocks. These geochemical proxies display a significant increase in magnitude and variability after ca 3.2 Ga. We hypothesize that rapid increases in mantle heterogeneity indicate the recycling of supracrustal materials back into Earth's mantle via subduction. Our new observations thus point to a ≥ 3.2 Ga onset of global subduction processes via plate tectonics.

The role of isostasy in the evolution and structural styles of fold and thrust belts

Ibrahim, Youseph, & Rey, Patrice
University of Sydney, Sydney, Australia

Fold and thrust belts (FTB) are highly deformed regions that form as the crust accommodates shortening. The evolution of FTB's records the dynamic interplay between crustal and surface processes, in conjunction with the rocks' intrinsic properties. The stacking of thrust sheets and mass transfer of sediment during orogenesis imposes a load on the lower crust and the mantle underneath, inducing isostatic adjustment and a flexural response, which may also contribute to the overall architecture of FTB's. The tempo at which a fold and thrust belt forms is a consequence of plate kinematics. The tempo of the isostatic response,

however, is reliant on the rheology of the mantle and the elastic thickness of the crust. Here, we focus on the role isostasy plays in controlling structural style in FTB's. We run two-dimensional, coupled thermal and mechanical, numerical experiments using the Underworld framework to explore the interplay between the rate of compression and the rate of isostasy on the structural evolution of FTB's.

The numerical model runs in a cartesian domain by solving the conservation of energy, mass, and momentum equations. The numerical domain is 42 km wide and 16 km tall, with a grid resolution of 80 m. From top to bottom, the model consists of 'sticky air', 4 km of sediment that alternates in competence at 500 m intervals, a 3 km thick basement, and a virtual basal layer, which allows us to implement a local 'pseudo-isostasy' boundary condition. Models are run with varying compressional velocities and isostatic rates.

Our suite of models demonstrates the relationship between tectonic and isostatic rates. When the tectonic rate is greater than the isostatic rate, subsidence or flexure is post-tectonic mainly, and therefore isostasy is unlikely to play a role in the development of the FTB, however, it may modify its architecture post-loading. Alternatively, when the tectonic rate is slower than or equal to the isostatic rate, subsidence will keep pace with tectonic loading. In this scenario, isostasy plays an important role in the development of FTB's, influencing the topographic elevation generated, the outward extent of the FTB, and thrust fault angles.

Structural evolution of a 1.6 Ga orogeny related to the final assembly of the supercontinent Nuna: coupling of episodic and progressive deformation

Volante, S.^{1,2}, Collins, W. J.¹, Pourteau, A.¹, Li, Z.-X.¹, Li, J.¹, & Nordsvan, A. R.^{1,3}

¹*Earth Dynamics Research Group, Australian Research Council Centre of Excellence for Core to Crust Fluid Systems (CCFS) and The Institute for Geoscience Research (TIGeR), School of Earth and Planetary Sciences, Curtin University, Perth, Australia;* ²*Institute of Geology, Mineralogy and Geophysics, Ruhr-Universität Bochum, Bochum, Germany;* ³*Department of Earth Sciences, University of Hong Kong, Pokfulam, Hong Kong*

The poly-deformed Georgetown Inlier (GTI) in NE Australia has recently been suggested to record a 1.60 Ga orogenic event related to final Nuna assembly. However, the structural evolution of the inlier has remained poorly constrained at the regional-scale, and major tectonothermal events occurred at ca 1.55 Ga. The GTI is the type-region for conceptualisation of crenulation cleavage development and where the foliation intersection axes (FIAs) approach has been applied. We re-evaluated both concepts by combining a multiscale petrostructural analysis with recent petrological and geochronological data. Three main deformation events (D1, D2, D3) and associated composite fabrics (S1, S2, S3) are identified in the GTI. The original NE-orientation of 1.60 Ga D1 compressional structures is preserved in the low-grade western domain, and the associated composite S1 fabric is retained as microstructural relicts within ca 1.55 Ga D2 low-strain domains to the east. Extensional D2 structures, characterised by a pervasive, high-grade,

composite S2 foliation throughout the central and eastern domains, are interpreted as the footwall of a regional N–S-trending, W-dipping crustal-scale detachment zone. Syn-D2 S-type granites formed at 1.55 Ga as the detachment evolved. D1 stage was associated with Nuna assembly, whereas D2 represents post-collisional extension. Progressive foliation development occurred twice in the GTI, at 1.60 Ga (D1) and 1.55 Ga (D2), but the previous FIA analysis only records the 1.60 Ga event and cannot be easily reconciled with the regional structural analysis. This study highlights that a multiscale and multi-disciplinary approach is required to unravel the structural history of orogenic belts.

Development of William's Ridge, Kerguelen Plateau, and Broken Ridge: tectonics, hotspot magmatism, microcontinents, and Australia's extended continental shelf

Coffin, Millard F.¹, Whittaker, Joanne¹, Daczko, Nathan², Halpin, Jacqueline¹, Bernardel, George³, Picard, Kim³, Gardner, Robyn², Gürer, Derya⁴, Brune, Sascha⁵, Gibson, Sally⁶, Hoernle, Kai⁷, Koppers, Antonius⁸, Storey, Michael⁹, Uenzelmann-Neben, Gabriele¹⁰, Magri, Luca¹ Neuharth, Derek⁵, Christiansen, Sascha Høegh⁹, & Easton, Laura³

¹Institute for Marine and Antarctic Studies, University of Tasmania, Hobart, Australia; ²Macquarie University, Sydney, Australia; ³Geoscience Australia, Canberra, Australia; ⁴University of Queensland, Brisbane, Australia; ⁵GFZ German Centre for Geosciences, Potsdam, Germany; ⁶University of Cambridge, Cambridge, United Kingdom; ⁷GEOMAR Helmholtz Centre for Ocean Research Kiel, Kiel, Germany; ⁸Oregon State University, Corvallis, United States of America; ⁹Natural History Museum of Denmark, Copenhagen, Denmark; ¹⁰Alfred Wegener Institute for Polar and Marine Research, Bremerhaven, Germany

William's Ridge, a ~300-km-long salient extending southeast from the Central Kerguelen Plateau, and Broken Ridge are conjugate divergent margins in the southern Indian Ocean that separated at ca 43 Ma. In early 2020, scientists aboard Australia's Marine National Facility, RV *Investigator*, acquired multi-channel seismic reflection (MCS), sub-bottom profiling, multibeam bathymetry, and gravity data on these margins, as well as dredged rock samples, on a 57-day voyage. The research project constitutes the first-ever case study of conjugate oceanic plateau end-member tectonic plates, with the goal of advancing knowledge of lithospheric rifting, breakup, and initial plate separation processes. The first-ever dedicated multibeam mapping of William's and Broken ridges encompassed ~52 000 km² and ~43 000 km², respectively. Four new RV *Investigator* MCS profiles (500 line-km) across William's Ridge complement one legacy RV *Rig Seismic* and three new RV *Sonne* MCS profiles, five new RV *Investigator* MCS profiles (603 line-km) across the conjugate portion of Broken Ridge are the first to be acquired on that feature. Multibeam bathymetry and MCS transects of William's Ridge show multiple linear ridges and troughs interpreted as horst and graben. In contrast, multibeam bathymetry and MCS transects of Broken Ridge show a prominent E–W scarp (Diamantina Escarpment) with a complex morphology of emanating en echelon crustal blocks

and depressions at the base of the scarp. Prominent angular unconformities (middle Eocene hiatus?) characterize the sedimentary section on some ridges, and dipping reflection sequences within interpreted igneous basement suggest subaerial basalt flows. Rock dredges on the facing conjugate margin fault scarps targeted all stratigraphic levels exposing basement rocks. Nine on William's Ridge yielded both oceanic and (*in situ*?) continental rocks, eight on Broken Ridge yielded solely oceanic rocks. The new geophysical data and geological samples may justify a new or revised submission to the United Nations Commission on the Limits of the Continental Shelf to extend Australia's marine jurisdiction on and around William's Ridge under the United Nations Convention on the Law of the Sea.

Linking supercontinents to a convective mantle framework

Martin, Erin L.^{1,3}, Cawood, Peter A.¹, & Murphy, J. Brendan^{2,3}

¹School of Earth, Atmosphere and Environment Science, Monash University, Clayton, Australia; ²Department of Earth Sciences, St Francis Xavier University, Antigonish, Canada; ³Earth Dynamics Research Group, The Institute for Geoscience Research (TIGeR), School of Earth and Planetary Sciences, Curtin University, Perth, Australia

The amalgamation of continental fragments into supercontinents can occur by processes of introversion, involving the closure of interior oceans, extroversion, in which the exterior ocean closes, or orthoversion, entailing formation 90° from the centroid of the previous supercontinent. However, individual supercontinents are often defined as forming by contradictory mechanisms, for example, Pangea has been argued as forming by introversion and by extroversion. Conflicting interpretations arise, in part, from attempting to define an ocean as interior or exterior based on paleogeography, or the age of oceanic crust relative to the time of supercontinent breakup. We argue that interior and exterior oceans should be defined relative to the peripheral subduction ring and its associated accretionary orogens that surround the amalgamated supercontinent. The subduction ring broadly divides the Earth into two cells, which conform to the spherical harmonic degree-2 structure of the mantle: one associated with supercontinent assembly, and therefore dominated by continental crust with only minor oceanic crust, and the other containing almost exclusively oceanic crust, which is subducted to create peripheral accretionary orogens at the margin of the supercontinent. All oceans within the cell that contains continental blocks are interior oceans, as they are interior to the continental cell of the degree-2 planform. By contrast, the exterior ocean is the oceanic cell antipodal to the continental cell, separated by the subduction ring. Interior oceans close following asymmetrical subduction and collisional orogenesis. However, for the exterior ocean to close, the subduction ring must collapse upon itself, leading to the juxtaposition of long-lived accretionary orogens within the core of the supercontinent. Employing this geodynamic definition for interior and exterior oceans, Rodinia formed by extroversion, but all other supercontinents formed by introversion which cannot occur without orthoversion.

Distinct formation history for deep mantle domains reflected in geochemical differences

Doucet, Luc S.¹, Li, Zheng-Xiang¹, El Dien, Hamed Gamal^{1,2}, Pourceau, Amaury¹, Murphy, J. Brendan^{1,3}, Collins, William J.¹, Mattielli, Nadine⁴, Olierook, Hugo K. H.^{5,6}, Spencer, Christopher J.^{1,7}, & Mitchell, Ross N.^{1,8}

¹Earth Dynamics Research Group, TIGeR, School of Earth and Planetary Sciences, Curtin University, Perth WA 6845, Australia; ²Geology Department, Faculty of Science, Tanta University, 31527 Tanta, Egypt; ³Department of Earth Sciences, St. Francis Xavier University, Antigonish, Nova Scotia, B2G 2W, Canada; ⁴Laboratoire G-Time, Université Libre de Bruxelles, ULB, CP 160/02, Av. FD Roosevelt, 50, Brussels 1050, Belgium; ⁵Timescales of Mineral Systems, Centre for Exploration Targeting – Curtin Node, Curtin University, GPO Box U1987, Perth, WA 6845, Australia; ⁶John de Laeter Centre, Curtin University, GPO Box U1987, Perth, WA 6845, Australia; ⁷Department of Geological Sciences and Geological Engineering, Queen's University, Kingston, Ontario K7L 2N8, Canada; ⁸State Key Laboratory of Lithospheric Evolution, Institute of Geology and Geophysics, Chinese Academy of Sciences, Beijing 100029, China

The Earth's mantle is currently divided into the African and Pacific domains, separated by the circum-Pacific subduction girdle and each domain features a large low shear-wave velocity provinces (LLSVPs) in the lower mantle. However, it remains controversial as to whether the LLSVPs have been stationary through time or dynamic, changing in response to changes in global subduction geometry. Here we compile radiogenic isotope data on plume-induced basalts from ocean islands and oceanic plateaus above the two LLSVPs which show distinct Pb, Nd and Sr isotopic compositions for the two mantle domains. The African domain shows enrichment by subducted continental material during the assembly and breakup of the supercontinent Pangaea, whereas no such feature is found in the Pacific domain. This deep-mantle geochemical dichotomy reflects the different evolutionary histories of the two domains during the Rodinia and Pangaea supercontinent cycles and thus supports a dynamic relationship between plate tectonics and deep mantle structures.

Coupled evolution of plate tectonics and basal mantle structure

Cao, Xianzhi^{1,2}, Flament, Nicolas³, & Müller, R. Dietmar²

¹Frontiers Science Center for Deep Ocean Multispheres and Earth System, Key Lab of Submarine Geosciences and Prospecting Techniques, Ministry of Education, College of Marine Geosciences, Ocean University of China, Qingdao 266100, China; ²EarthByte Group, School of Geosciences, The University of Sydney, Sydney, NSW, Australia; ³GeoQuEST Research Centre, School of Earth and Environmental Sciences, University of Wollongong, Northfields Avenue, NSW 2522 Australia

The relationships between plate motions and mantle flow remain poorly understood over the life cycle of supercontinents and superoceans. Contrasting models propose that the structure of the deep Earth may have

remained stable over time, or that it could be linked to the aggregation and dispersal of supercontinents. Here we investigate the evolution of mantle flow driven by synthetic end-member plate tectonic models extending back one billion years. We implement a tectonic scenario in which supercontinent breakup and reassembly occurs by introversion and consider three distinct reference frames that result in different net rotation of the lithosphere with respect to the mantle. Our flow models predict a dominant degree-2 mantle structure most of the time, which is similar to the present-day structure of the lower mantle that is dominated by two antipodal Large Low Shear Velocity Provinces (LLSVPs). We analyse the relationship between imposed tectonic velocities and deep mantle flow, and find, as expected, that at spherical harmonic degree 2, the maxima of lower mantle poloidal flow and temperature follow the motion path of the maxima of surface divergence. We show that a time lag of up to 250 Myr can occur between major changes surface kinematics and the motion of long-wavelength basal mantle structures when (1) the lower mantle is reorganised by sinking slabs sinking onto basal thermochemical structures, and/or (2) slabs stagnate in the transition zone, for instance due to fast trench retreat. Basal thermochemical structures move at less than 0.6 degree/Myr in our models, with a temporal average of 0.16 degree/Myr when net lithospheric rotation is removed from the reconstruction, and between 0.20–0.23 degree/Myr when net lithospheric rotation exists and partial introduced into the lower mantle. Our results suggest that basal thermochemical structures are not stationary, but rather linked to global plate motions, indicating that the lithosphere and the entire mantle constitute a co-evolving dynamic system.

What is under the Antarctic ice: An integrated study of U–Pb, O and Lu–Hf isotopes

Chen, Bei, & Campbell, Ian

Research School of Earth Science, Australian National University, Canberra, ACT 2601, Australia

Antarctica is the central piece in the Gondwana jigsaw, connecting Australia, India and Africa. Little bedrock is exposed in Antarctica with over 98% of the continent covered by ice. Its geology can provide new insights into the relationship between Antarctica and its neighbours and elucidate its role in the amalgamation and breakup of the Gondwana supercontinent.

Detrital zircons separated from IODP holes drilled around Antarctica have been analysed for U–Pb, O and Lu–Hf isotopes. U–Pb results show major detrital zircon crystallization peaks at ca 250, 550, 950 and 1200 Ma, with a minor peak at 1600 Ma. They broadly correlate with younger peaks in the Australian detrital zircon population, but the older Australian peaks are missing. By far the largest peak, at ca 550 Ma, is interpreted to represent zircons derived from the Transgondwana Supermountain formed by the collision between East and West Gondwana. Unlike previous studies, based on ⁴⁰Ar/³⁹Ar dating from hornblende and biotite, our data show a significant ca 250 Ma peak, indicating that Antarctica was affected by an event of Pangaea age.

Oxygen isotope in zircons display a step increase at the end of the Archean, consistent with the temporal evolution of zircon $\delta^{18}\text{O}$ as recognized by Valley *et al.* (2005). $\delta^{18}\text{O}$ values of ca 500 Ma group from Antarctica

cover a large range (4.9–11‰), similar to the range of $\delta^{18}\text{O}$ in ca 500 Ma detrital zircons from Australia. Interestingly, zircons of ca 100 Ma from West Antarctica are unusual in having $\delta^{18}\text{O}$ less than the mantle value, implying crystallization from a felsic magma produced by melting wet basalt. Lu–Hf isotopes of these detrital zircons show that they were derived from juvenile crust, which formed around 100 Ma. ϵHf values of the ca 550 Ma zircons show the largest variation (–18 to 10), and in this respect are similar to zircons of the same age from Australia. Arc Mantle Hf model ages reveal three major periods of growth of Antarctic continental crust: 300–500, 1200–1600 and 2000–2300 Ma, and indicate that the growth of the Antarctic continental started to form after the Archean. An unexpected outcome of this study is that it showed that Antarctica is younger than the other continents we have investigated both in terms of its model ages, and the orogenic events that have affected it.

Valley, J. W., Lackey, J. S., Cavosie, A. J., Clechenko, C. C., Spicuzza, M. J., Basei, M. A. S., ... & Peck, W. H. (2005). 4.4 billion years of crustal maturation: oxygen isotope ratios of magmatic zircon. *Contributions to Mineralogy and Petrology*, 150(6), 561–580.

Paleomagnetic constraints on formation of the Manning Orocline, far-field effects of Pangea-B to -A transformation and breakup?

Klootwijk, Chris

Research School of Earth Sciences, ANU, Canberra, Australia

The Myall blocks of the southeastern Tamworth Belt (TB), southern New England Orogen (SNEO), have been studied for paleomagnetic control on evolution of the Manning Orocline, focussing on ignimbritic rocks which best retain primary magnetisations despite pervasive overprinting. Paleomagnetic, rock magnetic and magnetic fabric results from upper lower Carboniferous to lower Permian successions cover 64 forearc basin, arc-fringe and arc sites from across the western Myall block and 16 forearc basin sites from the westernmost eastern Myall block. Thermal demagnetisations show a widely present low-temperature weathering overprint, intermediate-temperature primary and overprint components confined to the Nerong Volcanics (ca 340 Ma), and high-temperature primary and overprint components. Overprinting is far more prevalent in the Myall blocks than in other TB blocks studied, with five phases dated tentatively from mid Carboniferous to mid Triassic.

Myall blocks results are interpreted against the Carboniferous SNEO polepath based on Rocky Creek, Werrie, Rouchel and Gresford blocks data, against a Permian polepath for the Australian craton, and against a Triassic Indian polepath transferred to Australia within Gondwana. Comparison of the Myall blocks primary and overprint poles against these reference polepath segments shows counterclockwise rotations that increase from 20°–45° for the main part of the western Myall block and from 30°–90° for its southwestern margin, to 80°–110° for the eastern Myall block. Rotations likely started with the Tablelands phase (ca 305 Ma, L2 loop on SNEO polepath) and ended during the late Permian (ca 270–260 Ma) initial pulse of the Hunter-Bowen phase of the Gondwanide Orogeny. The southwestern margin of the western Myall block also shows a mid Triassic, or later, clockwise rotation,

increasing from ~50° near the Williams River Fault to ~110° for the Port Stephens arc complex.

Deformation of the SNEO is attributed customarily to changes in Paleopacific subduction, less so to changes in global plate movements as proposed herein. Comparison of the SNEO Carboniferous polepath with a Carboniferous polepath for the European Variscan massifs (Edel, 2003, Edel *et al.*, 2018) shows comparable mid to late Carboniferous (ca 330–305 Ma) segments, spanning large arcs (~130° between poles defining the L2 and L3 loops on the SNEO polepath, ~105° between the Cp and A1 poles on the Variscan polepath). Euler pole matching of these polepath segments, representing antipodal fringes of Gondwana, relocates “Armorica” as a northern spur of Gondwana in a Pangea-B configuration.

This novel, significant, finding opens avenues for interpretation of Australian mid Carboniferous to mid Triassic tectonics as primarily driven by the African, rather than Pacific, LLSVP-centred mantle upwelling, acknowledges the “Hercynian unconformity” as a late Carboniferous Gondwana-wide uplift reflecting heat accumulated beneath Pangea from the African upwelling, identifies the L3 loop (ca 305 Ma) on the SNEO polepath as the start of the Pangea-B to -A transformation displacing Gondwana westward along an equatorial shear, interprets the early to mid Permian Pangea-wide extension – including eastern Australia – as a reflection of that transformation by dispersing accumulated heat, and argues for development of the Manning Orocline as driven primarily by changes in movement of Gondwana rather than the Paleopacific.

Geophysical investigation of the evolution of William’s Ridge and Broken Ridge, Kerguelen Plateau

Magri, Luca¹, Whittaker, Joanne M.¹, Coffin, Millard F.¹, & Gürer, Derya^{1,2}

¹*Institute for Marine and Antarctic Studies, University of Tasmania, TAS 7004, Australia;* ²*School of Earth and Environmental Sciences, The University of Queensland, QLD 4072, Australia*

The Kerguelen Plateau is the second largest submarine plateau on Earth and is composed of both oceanic and continental crust. Its presumably dominant oceanic crust is commonly attributed to the Kerguelen mantle plume, probably interacting with mid-ocean ridges, and ranges in age from ca 120 Ma in the south to ca 35 Ma in the north. *In situ* continental rocks recovered to date from the Kerguelen Plateau (Elan Bank) are Proterozoic in age and bear affinities with similar rocks in once-nearby East Antarctica, eastern India, and Western Australia. Extending for ~300 km southeast from the ca 100 Ma Central Kerguelen Plateau is William’s Ridge, which separated at ca 43 Ma from its conjugate ca 95 Ma Broken Ridge by seafloor spreading along the nascent Southeast Indian Ridge.

In early 2020, a 57-day voyage was undertaken in the Southern Indian Ocean, aboard Australia’s Marine National Facility, the RV *Investigator* to expand our knowledge of lithospheric rifting, breakup, and initial separation processes between William’s Ridge and Broken Ridge. Multichannel seismic reflection (MCS), sub-bottom profiling, multibeam bathymetry/backscatter, and gravity data were acquired, along with dredged rock samples.

We present initial results from the post-expedition analysis of MCS acquired from the conjugate features. Using these profiles, we aim to better understand their formation and evolution during breakup of the once-contiguous Kerguelen Plateau and Broken Ridge. Using the newly acquired MCS data, we investigate the depositional and tectonic history of the two conjugate divergent margins. By defining the main stratigraphic and structural characteristics of the margins, we reveal the relationships that exist between the pre-rift, syn-rift, and post-rift sequences, determine the margin structural domains, and the dominant deformation processes related to each domain.

Timescales of continental subduction: Constraints from ultrahigh-pressure metapelites in the Western Gneiss Region, Norway

March, Samantha¹, Tamblyn, Renée¹, Hand, Martin¹, Carvelho, Bruna² & Clark, Chris³

¹Department of Earth Sciences, the University of Adelaide, Australia; ²Dipartimento di Geoscienze, Università degli Studi di Padova, Italy; ³School of Earth and Planetary Sciences, Curtin University, Australia

The Western Gneiss Region (WGR), Norway is an archetypal continental ultrahigh-pressure (UHP) terrane with an extensive metamorphic history, recording the subduction and subsequent exhumation of continental crust to depths exceeding 120 km. The vast bulk of past work within the WGR has focused on mafic eclogites. In this study, data from rare garnet–kyanite metapelites in (UHP) domains of the WGR is presented. U–Pb geochronology and trace element compositions in zircon, monazite, apatite, rutile and garnet were acquired, and *P–T* conditions were calculated by mineral equilibria forward modelling and Zr-in-rutile thermometry. The Ulsteinvik metapelite defines a prograde path that traverses through ~600–710 °C and ~11–14 kbar. Minimum peak conditions are ~750 °C and ~2.9 GPa in an inferred garnet–kyanite–coesite–omphacite–muscovite–rutile–quartz–H₂O assemblage. Plagioclase–biotite–quartz inter-growths developed after omphacite–phengite–rutile breakdown on the early retrograde path, followed by cordierite–spinel–plagioclase symplectites after garnet–kyanite–biotite, defining a retrograde *P–T* point at ~740 °C and ~7 kbar. Late Ordovician–Early Silurian (*ca* 470–440 Ma) zircon and rutile age data in Ulsteinvik pre-dates the major Scandian UHP subduction episode in the WGR, interpreted as recording early Caledonian subduction within the Blåhø nappe. Monazite and apatite U–Pb geochronology and trace element data suggest exhumation occurred at *ca* 400 Ma. The Fjørtoft meta-pelite is a constituent of the Blåhø nappe. Minimum peak *P–T* conditions are ~1.8 GPa and ~750 °C, with poor peak mineral fidelity attributed to extensive retrograde deformation. Negative Eu anomalies in *ca* 423 Ma monazite suggest retrograde conditions were reached by *ca* 423 Ma. Ulsteinvik and Fjørtoft may have experienced pre-Scandian subduction together within the Blåhø nappe but record dissimilar histories after this. Two potential scenarios are presented: (1) Ulsteinvik resided within the mantle for 20 million-years longer than Fjørtoft during Scandian subduction, or (2), the samples were exhumed at different times during pre-Scandian subduction of the

Blåhø nappe. The preservation of prograde zoning within Ulsteinvik garnets precludes a long-term residence within the mantle and suggests the latter option. In this scenario, the subducting Blåhø nappe experienced a degree of slab tear and partial underplating of the upper plate during the early stages of continental underthrusting. Discrete pieces may have later reattached to the lower plate at different times, partially exhumed, and then subducted to mantle-depths during the Scandian.

Refining tectonic models of the Rayner Complex in the Rodinia supercontinent

Morrissey, Laura¹, Halpin, Jacqueline², Hand, Martin³, & Payne, Justin⁴

¹Future Industries Institute, University of South Australia, Adelaide, Australia; ²Institute for Marine and Antarctic Science, University of Tasmania, Hobart, Australia; ³Department of Earth Sciences, University of Adelaide, Adelaide, Australia; ⁴UniSA STEM, University of South Australia, Adelaide, Australia

The Mesoproterozoic Rayner Complex, Antarctica, and the Eastern Ghats Province, India, belong to a single terrane that records some of the highest known temperatures for regional metamorphism on Earth. This formerly contiguous terrane separates Archean cratons of India and Antarctica, and the ultra-high temperature metamorphism is thought to record the collision between cratonic India and Antarctica. The timing of ultra-high temperature metamorphism at *ca* 1000–900 Ma corresponds to the timing of Rodinia amalgamation, making the Rayner–Eastern Ghats terrane one of the largest known Rodinia-aged belts and a key constraint in Rodinia reconstructions. However, the position of the Rayner–Eastern Ghats terrane in the Rodinia supercontinent is debated, with the most recent reconstructions suggesting the Rayner–Eastern Ghats terrane may have been isolated from main Rodinia supercontinent. One of the challenges of placing the Rayner Complex into a supercontinent construct relates to the paucity of information about the protoliths and geodynamic setting of this region prior to ultra-high temperature metamorphism.

Mac.Robertson Land in East Antarctica provides a transect through the Mesoproterozoic Rayner Complex into the Archean–Paleoproterozoic crust of cratonic East Antarctica. Outcrops extend from the Mawson Coast in the north, through the northern Prince Charles Mountains (nPCM) and Fisher Terrane, to the Archean southern Prince Charles Mountains (sPCM). New Lu–Hf isotopic data from magmatic protoliths in the Fisher Terrane shows that this region contains the some of the oldest and most isotopically juvenile protoliths in the Rayner Complex. Magmatic rocks in the Fisher Terrane are *ca* 1300 Ma calc-alkaline rocks that were reworked at *ca* 1020–980 Ma. The *ca* 1300 Ma rocks have $\epsilon\text{Hf}(t)$ of +6 to +10, and the younger granites have $\epsilon\text{Hf}(t)$ of +2 to +5.5. In contrast, limited data from 990–950 Ma granites and charnockites from the nPCM suggests these are more evolved, with $\epsilon\text{Hf}(t)$ of –5 to 0. Previously published data from *ca* 1100–980 Ma magmatic protoliths along the Mawson Coast have even more evolved $\epsilon\text{Hf}(t)$ values of –10 to +2.

The isotopically juvenile nature of the calc-alkaline rocks in the Fisher Terrane suggest that it was an arc built on highly extended, juvenile crust with little input

from evolved sources. The shift to more evolved ϵ_{Hf} values from south to north may confirm models that place the Rayner Complex in a highly extended back arc setting off the margin of cratonic India. This setting involved nearly continuous magmatism from ca 1490–950 Ma, with peak metamorphic temperatures reached between ca 970–900 Ma. Importantly, there is no evidence of magmatism after ca 950 Ma and the terrane is characterised by extremely slow cooling. Tectonic models that place the Rayner Complex in an isolated setting during Rodinia amalgamation must account for the fact that there is no evidence for continued consumption of oceanic crust after 950 Ma.

Understanding continental processes with low temperature thermochronology

Thermochronology frontiers in Australia

McInnes, Brent I. A.

John de Laeter Centre, Curtin University, Perth, Australia

The field of thermochronology in Australia has seen a significant increase in both capability and capacity development over the last decade. New labs have sprung up at University of Adelaide, the University of Queensland and Curtin University, which augment the University of Melbourne lab which has been a research powerhouse for almost half a century. These lab developments are one of many positive outcomes of informal meetings organised by geochemistry labs around the country via TANG³O (Thermochronology and Noble Gas Geochronology and Geochemistry Organisation).

Most labs now take an integrative approach using multiple radiometric dating techniques (e.g., U–Pb, Ar–Ar, U–He, fission-track) to generate geothermochronology data sets which provide a complete cooling history for any given rock sample. Repeating this process for multiple samples at scale allows researchers to detect differences in thermal history models that reflect major tectonic events in crustal evolution (e.g., continental breakup and collision, mountain-building and basin formation). Computational inversion of geothermochronology datasets are also becoming more sophisticated and allow the 4D thermal evolution of the crust to be imaged, providing a more detailed understanding of tectonic processes as well as predictive capability in the search for mineral and energy resources.

Another promising development is the increasing collaboration between research labs and geological surveys across Australia to address significant geoscience questions, such as: (1) mapping out thermal events across the continent (e.g., National Argon Map project led by Geoscience Australia), (2) demarcation of the end of orogenic events (Hall *et al.*, 2016, Quentin de Gromard *et al.*, 2020), and (3) regolith geochronology (Wells *et al.*, 2019). Continued cooperation will lead to the training of a cadre of young geoscientists skilled in being able to provide a “biography” of a geological unit rather than just its “birth date”.

Challenges remain however in understanding the crystal chemistry factors that produce inaccurate or

irreproducible thermochronology ages in Archean and Proterozoic lithologies. The *in-situ* U–Th/Pb–He microanalysis approach (Danisik *et al.*, 2017), which generates grain-scale zircon He maps and quantifies intragrain He distribution, can be used by researchers to exclude problem areas in grains with anomalous He concentrations due to crystal defects or inclusions. The potential adoption of *in situ* microanalysis in thermochronology can be viewed similarly to the paradigm shift experienced by the geoscience community when SHRIMP became available in the 1990’s, an event which led to orders of magnitude increase in zircon U–Pb data production and fundamental changes to the design of geological maps and our understanding of the planet.

Danišik, M. *et al.* (2017). Seeing is believing: Visualization of He distribution in zircon and implications for thermal history reconstruction on single crystals. *Science Advances*, 3(2), e1601121. <https://doi.org/10.1126/sciadv.1601121>

Hall, J. W. *et al.* (2016). Exhumation history of the Peake and Denison Inliers: insights from low-temperature thermochronology. *AJES*, 63(7), 805–820. <https://doi.org/10.1080/08120099.2016.1253615>

Quentin de Gromard, R. *et al.* (2019). When will it end? Long-lived intracontinental reactivation in central Australia. *Geoscience Frontiers*, 10, 149–164. <https://doi.org/10.1016/j.gsf.2018.09.003>

Wells, M. A. *et al.* (2019) (U–Th)/He-dating of ferruginous duricrust: Insight into laterite formation at Boddington, WA. *Chemical Geology*, 522, 148–161. <https://doi.org/10.1016/j.chemgeo.2019.05.030>

AusGeochem and the future of big data in low-temperature thermochronology

Boone, Samuel C.¹, Kohlmann, Fabian², Theile, Moritz², Noble, Wayne², Kohn, Barry¹, Glorie, Stijn³, Danišik, Martin⁴, & Zhou, Renjie⁵

¹University of Melbourne, School of Earth Sciences, Melbourne, Australia; ²Lithodat Pty. Ltd., Melbourne, Australia; ³University of Adelaide, Centre for Tectonics, Resources and Exploration, Department of Earth Sciences, School of Physical Sciences, Adelaide, Australia; ⁴Curtin University, John de Laeter Centre, Perth, Australia; ⁵University of Queensland, School of Earth and Environmental Sciences, Brisbane, Australia

The AuScope Geochemistry Network (AGN) and Lithodat are developing AusGeochem, a novel cloud-based platform for Australian-produced geochemistry data from around the globe. The open platform will allow laboratories to upload, archive, disseminate and publish their datasets, as well as perform statistical analyses and data synthesis within the context of large volumes of publicly funded geochemical data aggregated by the AGN. As part of this endeavour, representatives from four Australian low-temperature thermochronology laboratories (University of Melbourne, University of Adelaide, Curtin University and University of Queensland) are advising the AGN and Lithodat on the development of low-temperature thermochronology (LTT)-specific data models for the relational AusGeochem database and its international counterpart, LithoSurfer.

Adopting established international data reporting best practices, the LTT expert advisory group has designed database schemas for the fission track and (U–Th–Sm)/He techniques, as well as for thermal history modelling results and metadata. In addition to recording the parameters required for LTT analyses, the schemas include fields for reference material results and error

reporting, allowing AusGeochem users to independently perform QA/QC on data archived in the database. Development of scripts for the automated upload of data directly from analytical instruments into AusGeochem using its open-source Application Programming Interface are currently under way.

The advent of a LTT relational database heralds the beginning of a new era of structured Big Data in the field of low-temperature thermochronology. By methodically archiving detailed LTT (meta-)data in structured schemas, intractably large datasets comprising 1000s of analyses produced by numerous laboratories can be readily interrogated in new and powerful ways. These include rapid derivation of inter-data relationships, facilitating on-the-fly age computation, statistical analysis and data visualisation. With the detailed LTT data stored in relational schemas, measurements can then be re-calculated and re-modelled using user-defined constants and kinetic algorithms. This enables analyses determined using different parameters to be equated and compared across regional- to global scales. Indeed, Australian thermochronologists are already using the new AusGeochem LTT data model as a novel research tool to perform intra- and inter-laboratory experiments and continental-scale tectono-thermal imaging of the upper crust.

Development of a digital apatite fission-track analysis training module

Chung, Ling, Boone, Samuel C, Gleadow, Andrew, McMillan, Malcolm, & Kohn, Barry

School of Earth Sciences, the University of Melbourne, Melbourne, VIC, Australia

We report the development of a digital fission-track analysis training module that delivers a traditionally labour-intensive laboratory training routine to the analyst's computer, making it more practical, accessible and efficient. The module is made possible by Fission Track Studio, a cross-platform dual software suite that is specialized for microscope control and image acquisition (TrackWorks) and analysis (FastTracks), developed by the Melbourne Thermochronology Research Group. Using high-resolution photomicrograph stacks of fission tracks in a range of mica and apatite samples pre-captured in TrackWorks, the module aims to equip researchers with the confidence and skill to produce reliable and reproducible External Detector Method (EDM) and LA-ICP-MS/Digital Fission Track (LAFT) analyses using FastTracks.

The module comprises a series of step-by-step training exercises focused on acquiring the various skills involved in digital fission track analysis, including identifying fission tracks, choosing appropriate grains for analysis, selecting intragrain regions of interest, using FastTracks' semi-automated counting, c-axis and Dpar functions and measuring confined track lengths. An additional sub-module teaches trainees how to employ FastTracks' built-in EDM function for the split-screen analysis of apatite-mica sample pairs, as well as allow them to calculate their own user-specific zeta-calibration through analysis of co-irradiated external detectors from standard glasses. The training image sets include the two most commonly used apatite reference materials, Fish Canyon Tuff and Durango, as well as a further six apatites with distinct chemical compositions and track length distributions obtained

from a variety of geological settings. Trainees are able to evaluate their progress by comparing their data with expert-reviewed solution files on a grain-by-grain and track-by-track basis.

The digital fission track analysis training module is cloud-stored, allowing for easy access worldwide. Module material includes fission track age and confined track length image sets of well-characterized apatites, expert determined analytical solutions, and a list of recommended reading material and online resources. In collaboration with two international laboratories, the module is being tested on both experienced conventional fission track analysts and untrained students and augmented for improved usability.

Development of this novel training module will empower geoscientists to become remotely trained to perform digital fission track analysis at low cost without face-to-face tutelage or specialised equipment. This enables a new coordinated digital fission track analysis stream, whereby researchers can outsource sample preparation and image capture to laboratories equipped with suitable equipment. Captured image stacks and parent isotope concentrations, in the case of the LA-ICP-MS technique, would then be returned electronically to the newly trained researcher for digital fission track analysis and interpretation. This advance will enhance the accessibility and affordability of this powerful technique and make digital fission track analysis achievable for geoscientists globally.

Thermal annealing of implanted ²⁵²Cf fission-tracks in monazite

Jones, Sean, Gleadow, Andy, & Kohn, Barry
University of Melbourne, Australia

Monazite ((Ce, La, Nd, Sm)PO₄), a rare-earth element (REE) phosphate mineral, is found as an accessory mineral in a variety of rock types. Suitable uranium and thorium content make it a useful mineral for isotopic and chemical dating using the (U-Th)/He and U-Th-Pb methods. However, unlike other uranium-bearing minerals such as apatite, zircon and titanite, apart from a few reconnaissance studies, its potential for fission-track dating has not been systematically investigated. These earlier studies produced very young ages suggesting that fission tracks may be annealed at very low temperatures. This study further assesses its potential for thermochronology studies by determining its thermal annealing properties via a series of isochronal heating experiments.

²⁵²Cf fission-tracks were implanted into Harcourt Granodiorite (Victoria, Australia) monazite crystals on polished surfaces oriented parallel and perpendicular to {100} prismatic faces. Tracks were annealed over 1, 10, 100 and 1000 hour schedules at temperatures between 30 °C and 400 °C. Track length measurements were made on captured digital image stacks, and then converted to calculate mean lengths of equivalent confined fission tracks. In all annealed samples, the mean equivalent confined track length was always less than that in unannealed control samples. As annealing progresses, the mean track length is reduced and monazite fission-track lengths also appear to be anisotropic, as is the case for apatite, with tracks oriented perpendicular to the crystallographic c-axis annealing faster than those oriented parallel. To investigate how the mean track lengths decreased as a

function of annealing time and temperature, one parallel and two fanning models were fitted to the empirical dataset. The temperature limits of the monazite partial annealing zone (MPAZ) were defined as length reductions to 0.95 (lowest) and 0.5 (highest) for this study. Extrapolation of the laboratory experiments to geological timescales indicates that for a heating duration of 107 years, estimated temperature ranges of the MPAZ are -44 to 101 °C for the parallel model and -71 to 143 °C (both ± 6 – 21 °C, 2 standard errors) for the best fitting linear fanning model ($T_0 = \text{¥}$). If a monazite fission-track closure temperature is approximated as the mid-point of the MPAZ, then these results, for tracks with similar mass and energy distributions to those involved in spontaneous fission of ^{238}U , are consistent with previously estimated closure temperatures (calculated from substantially higher energy particles) of <50 °C and perhaps not much above ambient surface temperatures. Based on our findings it is estimated that the closure temperature (T_c) for fission tracks in monazite ranges between ~ 45 and 25 °C over geological timescales of 106–107 years, making this system potentially useful as an ultralow temperature thermochronometer.

Integrating thermochronology with numerical plate-tectonic models: A case study for Central Asia

Glorie, Stijn¹, Zahirovic, Sabin², & Kohlmann, Fabian^{1,3}

¹*The University of Adelaide, Department of Earth Sciences, Adelaide, Australia;* ²*The University of Sydney, School of Geosciences, Sydney, Australia;* ³*Lithodat Pty. Ltd., Melbourne, Australia*

The low-temperature thermal history of Central Asia has been extensively studied over the last decade. The exhumation history of this intracontinental deformation zone, derived from thermochronological studies, is often linked to far-field effects associated with discrete tectonic events at the former (Meso-Cenozoic) continental margins. While these links are often speculative, the development of numerical plate-tectonic models, with deformable plate-margins, now allows a more detailed evaluation of how tectonic processes at the margins might have propagated into the Eurasian interior. In this contribution, we present a comprehensive dataset of apatite fission track thermal history models for Central Asia. For over 400 sample locations, published thermal history models have been digitised and standardised, and the time-integrated cooling gradient for each sample has been calculated for each 1 Ma increment between 250 Ma and present day. These data are plotted on the latest GPlates model to reveal how the Eurasian interior responds to modelled plate-tectonic processes. The results show how cooling related with intracontinental deformation propagates from the Tian Shan to the Altai during the Mesozoic in response to roll-back processes in the Tethys Ocean. Cenozoic cooling in the Tian Shan starts at ca 55 Ma and accelerates at ca 30–25 Ma, which provides constraints on the timing of strain propagation from the India–Eurasia collision.

Revisiting the break-up evolution of the SE Australian rifted margin: new perspectives from larger data sets

Gleadow, Andrew, McMillan, Malcolm, Boone, Samuel, & Kohn, Barry

School of Earth Sciences, The University of Melbourne, Parkville, VIC 3010, Australia

Studies of the apatite fission track (AFT) thermochronology of the SE rifted margin of NSW in the early 1980s were amongst the first to show a relationship between low temperature thermochronology (LTT) and the processes of continental rifting. Similar studies have followed in other parts of the world. Several studies on the SE Australian margin have centred on a transect across the Bega Batholith from Nimmitabel via Bega to Tathra-Bermagui on the coast. Like many rifted margins, this area shows an uplifted plateau of low relief separated by a major erosional escarpment near Brown Mountain from a broad coastal plain of moderate relief to the present Tasman Sea coast.

Apatite fission track ages along this transect fall into three zones, the first on the uplifted plateau with AFT ages of ca 270–300 Ma, mean track lengths (MTL) of ~ 13 μm and unimodal length distributions. The second, from the escarpment towards the coast, with AFT ages of 150–250 Ma and broader, often bimodal, length distributions with means of 10–12 μm . The third zone, within ~ 10 km of the coast, has AFT ages of 90 ± 10 Ma with narrow length distributions and long MTLs of ~ 14 μm . These zones define the original 'boomerang' trend of MTL with AFT age where the MTL reaches a minimum for the intermediate ages and represent the progressive replacement of an older age on the plateau (~ 300 Ma) by a younger cooling event (~ 90) near the coast representing samples that must have been at temperatures $>100^\circ\text{C}$ prior to rapid cooling in the mid Cretaceous. Similar patterns, with some significant variations, have been found on rifted margins in other parts of the world, but are by no means universal.

The tripartite zoning in the AFT data approximately coincides with the principal geomorphic elements of this area which has long suggested that the two records are related. Denudation from around the time of Tasman Sea rifting has been invoked to explain exposure of relatively deeper levels along the coast with much older ages preserved on the plateau. Important corollaries of this interpretation are that the boomerang trend and the youngest ages must always lie below the erosional escarpment, and that the youngest ages should approximately date at least the onset of denudation.

Much larger regional scale AFT data sets now show, however, that the particular relationship between the AFT zones and the escarpment observed around Bega is atypical and probably fortuitous. Further north the boomerang trend diverges inland and crosses the escarpment implying that the underlying thermal history, tied to the ca 90 Ma cooling event, must pre-date formation of the escarpment and be independent of the subsequent post-breakup landscape evolution. The minimum of the boomerang trend closely parallels the western margin of the Sydney Basin and we propose that the AFT thermal history relates largely to Cretaceous erosion of a formerly more extensive Permo-Triassic sedimentary cover. Evolution of the present-day landscape is poorly constrained by the

thermochronology and may be of substantially younger age, probably Cenozoic.

Distal footprints of the Alice Springs Orogeny preserved in Paleoproterozoic northern Australia: An application of multi-kinetic thermochronology in the Pine Creek Orogen and Arnhem Province

Nixon, Angus L.¹, Glorie, Stijn¹, Collins, Alan S.¹, Whelan, Jo A.², Reno, Barry L.², Danišik, Martin³, Wade, Benjamin P.⁴, & Fraser, Geoff⁵

¹*Mineral Exploration Cooperative Research Centre, Department of Earth & Environmental Sciences, School of Physical Sciences, The University of Adelaide, SA 5005 Australia;* ²*Northern Territory Geological Survey, Department Industry Tourism and Trade, Darwin, NT 0801, Australia;* ³*John de Laeter Centre, Curtin University of Technology, Perth, WA 6845, Australia;* ⁴*Adelaide Microscopy, The University of Adelaide, Adelaide, SA 5005, Australia;* ⁵*Minerals Energy and Groundwater Division, Geoscience Australia, GPO Box 378, Canberra, ACT2601, Australia*

The Precambrian Pine Creek Orogen and Arnhem Province represent two of the oldest basement terrains in northern Australia and are often considered to be devoid of major tectonic or deformational activity since the cessation of regional metamorphism in the Paleoproterozoic. A major caveat in the current hypothesis of long-lived structural inactivity is the absence of published low-temperature thermochronological data and thermal history models for this area. This study presents the first apatite U–Pb, fission track and (U–Th–Sm)/He data for igneous samples from both the Pine Creek Orogen and Arnhem Province, complemented with apatite geochemistry data acquired by electron microprobe and laser ablation mass spectrometry methods, and presents detailed multi-kinetic low-temperature thermal history models. Low-temperature thermal history models for the Pine Creek Orogen and Arnhem Province reveal a distinct phase of denudation coeval with the Paleozoic Alice Springs Orogeny in central Australia, suggesting that this orogenic event impacted a larger area of the Australian crust than previously perceived. Low-temperature perturbations observed in northernmost Australia are consistent with widespread mid-Paleozoic denudation is preserved across both the North Australian Craton and South Australian Craton, indicative of a cratonic scale thermal event during north–south shortening via the Alice Springs Orogeny. Additionally, minor localised Mesozoic thermal perturbations proximal to the Pine Creek Shear-Zone record evidence for Mesozoic reactivation contemporaneous with modelled mantle-driven subsidence and the onset of sedimentation in the Money Shoal Basin, while the Arnhem Province samples demonstrate no evidence of Mesozoic thermal perturbations.

The uplift history of the Nyika Plateau, Malawi: A long lived paleo-surface or a contemporary feature of the East African Rift?

McMillan, Malcolm¹, Boone, Sam¹, Kohn, Barry¹, Gleadow, Andy¹, & Chindandali, Patrick²

¹*The University of Melbourne, Melbourne, Australia;*

²*Geological Survey of Malawi, Zomba, Malawi*

The Malawi Rift is the southern-most expression of the magma-poor western branch of the East African Rift. A noticeable feature belonging to Malawi is the Neogene Lake Malawi (Nyasa), occurring directly above the main locus of the Malawi Rift. Lake Malawi hosts a series of half-grabens of alternating polarity with elevated shoulders. In the northern region of Lake Malawi, just ~10 km west of the largest border fault system, the Nyika Plateau rises ~2100 m above the surrounding landscape. Nyika is a Paleoproterozoic (Ubendian) granitic intrusion, surrounded by Neoproterozoic Pan-African metamorphic complexes with sparse Permian Karoo sediments outcropping to the north and east of the plateau. Similar elevations to Nyika occur in the area, on the Mozambiquan side of Lake Malawi above the Livingstone border fault and to the north of Lake Malawi, in the Oligocene Rungwe Volcanic Province (RVP).

Since King¹ it has been contentiously hypothesized that such high-relief plateaux, like Nyika and the Livingstone mountains, are long-lived “Gondwana surfaces” and are largely unrelated to the modern-day Malawi Rift. However, recent seismic evidence² suggests a zone of thinned lithosphere beneath the RVP persists broadly beneath the Nyika Plateau and the Livingstone Mountains, and may indicate that higher elevations in the surrounding region are actively supported by rising asthenospheric mantle, resulting in relatively rapid, recent, tectonic uplift.

Low-temperature thermochronology typically provides thermal history constraints on the upper ~3–7 km of the crust, using radiometric dating techniques sensitive to changes in the thermal regime, from events such as rapid uplift causing denudation or changes in the geothermal gradient. Here, we use apatite fission track (AFT), apatite (U–Th–Sm)/He (AHe), and zircon (U–Th)/He (ZHe) thermochronology to further investigate the uplift history of the Nyika Plateau and the surrounding region from 25 samples collected with help from the Geological Mapping and Mineral Assessment Project (GEMMAP) and Malawi’s Geologic Survey Department.

We found consistently Permo-Triassic AFT apparent ages with moderate mean track lengths ranging from ~11.2–12 µm. AHe ages are largely dispersed in all but two samples, which show consistent mid-Cretaceous apparent ages. ZHe ages are consistently Devonian. AFT and AHe ages are consistent with ages previously reported along the Livingstone Mountains^{3,4}. Thermal history models suggest that the Nyika Plateau is not a direct feature of modern-day rifting and has largely cooled slowly through the partial annealing zone since at least the late Mesozoic. The youngest AFT age (*ca* 70 Ma) occurs off the plateau to the north, directly adjacent to a Permian Karoo sequence. Using this Karoo deposition as a thermal history constraint indicates the area may have been completely covered by Karoo deposition, up to ~2 km (considering moderate geothermal gradients), that may have blanketed Nyika and the surrounding region in the Permo-Triassic.

¹ King, 1962. *The Morphology of the Earth*, Oliver and Boyd, Edinburgh and London, 29.

² Njini *et al.*, 2019. Lithospheric Structure of the Malawi Rift: Implications for Magma-Poor Rifting Processes. *Tectonics* 38, 3835–3853.

³ van der Beek *et al.*, 1998. Denudation history of the Malawi

and Rukwa Rift flanks (East African Rift system) from apatite fission track thermochronology. *J. African Earth Sciences* 26, 363–385.

⁴Mortimer *et al.*, 2016. Spatio-temporal trends in normal-fault segmentation recorded by low-temperature thermochronology: Livingstone fault scarp, Malawi Rift, East African Rift System. *Earth and Planetary Science Letters* 45, 65–72.

Detachment fault and metamorphic core complex at the distal continental margin of the northern South China Sea

Deng, Hongdan¹, Ren, Jianye¹, Rey, Patrice², & McClay, Ken³

¹College of Marine Science and Technology, China University of Geosciences, Wuhan, 430074, China;

²Earthbyte Research Group, Basin Genesis Hub, School of Geosciences, The University of Sydney, Sydney, NSW 2006, Australia; ³Australian School of Petroleum, Adelaide University, North Terrace, Adelaide, SA 5000, Australia

Detachment fault and metamorphic core complex (MCC) are widely documented structures in extensional environment where continental lithosphere has been thermally weakened. The North American Cordillera and Aegean Sea have a widespread deformation of extension (up to 1000 km) and are regions that exemplify detachment fault and MCC development in natural exposures. However, how these structures evolve from wide extended terrane to continental break-up remains enigmatic because there are a few exposed continental margins that preserved these types of deformation. In addition, thick package of sedimentary units on the passive margin could obscure the imaging of low-angle fault and dome structures at depth. Here we use high-resolution 2D and 3D seismic data together with International Ocean Drilling Program (IODP) result and industry wells to show that Eocene extension across the northern margin of the South China Sea records large detachment fault (displacement >100 km) and MCCs at the highly extended (<15 km), distal continental margin. The South China Sea has wide continental margins that span a width of up to 1000 km and 500 km in the north and in the south. On the basis of high-resolution seismic data, we document the presence of dome structures, a corrugated and grooved detachment fault, and subdetachment deformation involving crustal-scale nappe folds and magmatic intrusions, which are coeval with supradetachment basins. On the distal continental margin, we conclude that the thermal and mechanical weakening of this broad continental domain allowed for the formation of metamorphic core complexes, boudinage of the upper crust and exhumation of middle/lower crust through detachment faulting. The structural architecture of the northern South China Sea continental margin is strikingly similar to the broad continental rifts in the North American Cordillera and in the Aegean domain, and further indicates that detachment faulting and the development of metamorphic core complex play an important role in controlling continental break-up.

Exhumation of the Indus-Yarlung Tsangpo Suture Zone (NW India): New constraints from low-temperature thermochronology

Zhou, Renjie, & Aitchison, Jonathan C.

School of Earth and Environmental Sciences, The University of Queensland, St Lucia, QLD 4072, Australia

The Indus-Yarlung Tsangpo Suture Zone (IYTS) is the zone of original contact between two colliding masses of continental lithosphere, the Indian subcontinent and Eurasia. It extends for several thousand kilometres and is well exposed in NW India, southern Tibetan Plateau, and near the border between India and Myanmar. The rock record in the IYTS contains information regarding evolution of the now vanished Tethyan Ocean, its closure, and the on-going growth of the Himalaya. In the NW Himalaya, the IYTS zone is well exposed in the Zaskar River valley and incorporates an array of sedimentary rock units collectively referred as the Indus Basin. On its northern side, the Indus Basin is in depositional contact with the Ladakh Batholith, the exhumed 'root' of the Trans-Himalayan continental arc that developed along the southern margin of Eurasia in association with subduction of Tethyan oceanic lithosphere. To the south, the Indus Basin contains rock units that are in faulted contact with rocks that represent the former margin of the Indian continent.

We present new low-temperature thermochronologic data produced by apatite U–Th/He, apatite fission-track and zircon fission-track methods. Samples were taken from the southern edge of the Ladakh Batholith where the depositional contact between the batholith and the Indus Basin (the Indus Molasse) is observed. A series of samples was also taken from the Indus Basin along river gorges that traverse the IYTS. Previous apatite fission track (AFT) ages from across the Ladakh Batholith are generally young along its northern flank (as young as ca 5–6 Ma) while AFT ages from the south are older, spanning from ca 22 to 35 Ma. We further constrain exhumation of the northern Indus Basin and southern Ladakh Batholith by applying geologic constraints to our thermal models, yielding evidence for two episodes of rapid exhumation in the late Eocene and Miocene. Preliminary AFT ages from the Indus Basin indicate exhumation at around 15 Ma, consistent with the second cooling episode observed along the southern Ladakh Batholith.

Recent advances in the geology and mineral potential of the eastern Australian Tasmanides

New constraints on the tectonic and metallogenic history of Lachlan Orogen

Meffre, Sebastien, Leslie, Chris, Wells, Tristan, Habib, Umer, & Schaap, Thomas

CODES. Centre for Ore Deposits and Earth Sciences, University of Tasmania, Private Bag 79, Hobart, TAS 7001, Australia

The Lachlan Orogen has a long and complicated geological history involving:

- Cambrian collision and orogenesis
- Ordovician continental-derived sediment

deposition

- Ordovician island arc development formation of porphyry and epithermal deposits
- Silurian orogenesis and extension and formation of volcanic-hosted massive sulphide deposits
- Devonian orogenesis and formation of granite-related deposits

This geological framework is well-supported by data from many previous studies. However, the exact plate configurations responsible for these geological events remain poorly constrained. These constraints are required to make predictions about the location of ore deposits and to gain a better understanding of the structure and composition of the continental crust.

New data acquired throughout the Lachlan orogen over recent years combined with data from previous studies have helped to improve scientific knowledge showing that:

- During the earliest geological history of the Lachlan Orogen there was at least 2 Cambrian arcs: one continental and the other oceanic. The continental arc extended along the western edge of the orogen. The intra-oceanic island was dismembered after it collided with the Selwyn Block and Tasmania.
- Geochemical and geochronology data from the Melbourne zone and the Selwyn block in Victoria show that most of this zone is likely underlain by crust containing juvenile components rather than thick Mesoproterozoic continental crust.
- The intra-oceanic Macquarie Arc began approximately 10 Ma after the end of the Cambrian magmatism and was active for a further 40 million years.
- Magmatism in Macquarie Arc began to be contaminated by continental material starting at 450 Ma in the Molong area. Continental contamination and porphyry development occurred at different times within the magmatic history of the arc.
- The Lachlan Orocline model explains much of the tectonic evolution of the area from the latest Ordovician through to Devonian periods.

Although these constraints are useful in refining the tectonic models, many details remain unresolved and uncertain.

Devonian–Carboniferous regional deformation in the northeastern Lachlan Orogen, southeastern Australia

Fergusson, Chris¹, & Colquhoun, Gary²

¹*School of Earth, Atmospheric and Life Sciences, University of Wollongong, Wollongong, Australia;*

²*Geological Survey of New South Wales, Mining, Exploration & Geoscience, Department of Regional NSW, Maitland, Australia*

The timing of the regional deformation of the turbiditic Silurian–Devonian Hill End Trough in the northeastern Lachlan Orogen has been a contentious issue with one view ascribing the regional north–south folds and axial planar foliation to Middle Devonian basin inversion. Alternatively, it has been argued that given the low-angle discordance between Lower and Upper Devonian

units on the Capertee and Molong highs, and the development of a dominant episode of folding mapped from the Hill End Trough into the adjoining highs, the major regional deformation is latest Devonian to early Carboniferous and predates intrusion of Bathurst-type granites at 358–314 Ma. We have approached the problem by analysing the gentle, upright, southeast-trending folds and deformation patterns in Devonian units of the northern Capertee High (Cudgegong area), drawing a cross-section across the Hill End Trough and reviewing the structure of two areas in the Molong High (west of Orange, and south of Wellington). Upper Devonian units on the highs are affected by fold patterns that extend into the underlying successions and have been interpreted as continuous into the central Hill End Trough, confirming the extent of the latest Devonian to early Carboniferous regional deformation in the northeastern Lachlan Orogen. Constraints from timing of deposition and radiometric ages are ambiguous and imply deformation was overlapping with sedimentation, as has also been inferred from sedimentary features of the Upper Devonian succession. Steeply dipping faults along the highs predated the Late Devonian and were probably formed in extension during formation of the Hill End Trough and were reactivated during basin inversion and potentially during Upper Devonian sedimentation. Our conclusion is that the simplest hypothesis is that the regional north–south deformation was latest Devonian to early Carboniferous age, although poorly understood basin inversion occurred in the Middle to Late Devonian.

Substrate of the Macquarie Arc: geophysical evidence and implications for tectonic setting

Musgrave, Robert

Geological Survey of New South Wales, Department of Regional NSW, Maitland, Australia

Ordovician to early Silurian calc-alkaline volcanic-, associated intrusive-, and shallow-marine sedimentary rocks comprise the Macquarie Arc, the principal arc system in the Lachlan Orogen. Although Pb-isotope ratios and positive ϵNd suggest intraoceanic origins, there are competing hypotheses regarding the arc's tectonic setting. The range of proposed tectonic models include:

1. simple intraoceanic models, in which subduction initiated in the Ordovician over a west-dipping subduction zone, an east-dipping zone that later reversed polarity, or a south-dipping zone within a back-arc that later rotated anticlockwise,
2. two-stage intraoceanic models, in which the Ordovician arc developed on an earlier intraoceanic Cambrian arc,
3. the Lachlan Orocline model, which suggests the Macquarie Arc arose close to the Cambrian convergent margin of Gondwana, and
4. or in a very different viewpoint, the Macquarie 'Arc' may have been an extensional system in a back-arc, far behind the frontal arc located outboard of the New England Orogen.

Seismic reflection and refraction surveys across the Macquarie Arc, with corresponding potential-field models, were previously interpreted to indicate a MORB-like substrate, consistent with proposed tectonic

models of type 1 and (arguably) 4. However, petrophysical parameters yielded by these potential-field models are inconsistent with this interpretation. Long-wavelength, deeply sourced signals from a variety of geophysical techniques can clarify the composition of the basement, and these differing datasets show remarkable agreement. Long-wavelength aeromagnetic features qualitatively indicate a basement of low magnetic susceptibility. Quantitative modelling limits this to values typical of intermediate intrusive rocks characteristic of either mature arc or continental basement. Seismic velocity from the AuSREM model maps out a belt of low p-wave velocity, consistent with an intermediate chemistry, in the mid- to lower crust, which corresponds closely to the areas of magnetic susceptibility lows. Long-wavelength, long period MT signals recorded by the AusLAMP array map out conductivity highs that continue from mid (10 km) to lower (40 km) crustal depth and broadly correspond to the Macquarie Arc.

Petrophysical interpretation of an intermediate composition in the middle and lower crust below the Macquarie Arc is incompatible with a MORB-like composition and requires the basement of the Macquarie Arc to be either a pre-existing arc, a continental fragment, or a very thick arc in which little of any original MORB remains in situ. Tectonic models of types 1 and 4 are therefore ruled out. Recently reported magmatic Cambrian zircons from Macquarie Arc rocks are consistent with models of either type 2 or 3, but Pb isotope links between the Macquarie Arc and the forearc of the Cambrian Mount Wright Arc on the Gondwana margin suggest support for a version of model type 3, the Lachlan Orocline model. The Eocene to Recent forearc to rear-arc system of the Izu-Bonin Arc, south of Japan, shares geochemical, geophysical and scale similarities with the Macquarie Arc. This analogy suggests a genetic linkage between the Macquarie Arc, the Cambrian boninite–tholeiite–calc-alkaline belts in Victoria and offshore NSW, and the Cambrian Ponto Group on the margin of the Delamerian orogen in northwest New South Wales.

Life cycle of the Ordovician Macquarie Arc, Lachlan Orogen, eastern Australia

Zhang, Qing^{1,2}, Nutman, Allen¹, & Buckman, Solomon¹

¹*School of Earth, Atmospheric and Life Sciences, University of Wollongong, Wollongong, Australia;*
²*State Key Laboratory of Lithospheric Evolution, Institute of Geology and Geophysics, Chinese Academy of Sciences, Beijing, China*

The Ordovician intra-oceanic Macquarie Arc is preserved in a tectonostratigraphic terrane, faulted to the west and east against coeval, quartz-rich turbidites of the Adaminaby Group, within the Lachlan Orogen of eastern Australia. Debates exist concerning the allochthoneity of the Macquarie Arc, the polarity of its related subduction and the nature and exact timing of collision with Gondwana. These key problems are addressed by the integrated application of field observations, petrography, zircon U–Pb–Hf isotopes and whole rock geochemistry to key units within the Macquarie Arc stratigraphy. By these approaches, it has been possible to answer (i) the timing and juvenility of the arc initiation, (ii) the timing of arc-continent collision, and (iii) the allochthoneity and emplacement

mechanism of the Macquarie Arc onto the eastern edge of Gondwana. The new results confirm that the Macquarie Arc was initiated far from the continent with no continental contamination, most likely via outboard (eastward) subduction at high dip angle. The arc started colliding with the eastern Gondwana during the Late Ordovician (ca 456 Ma), indicated by the trench-fill sedimentary protoliths of the Triangle Formation. Preservation of juvenile island arc on continental margins is aided by outboard subduction that results in emplacement of the arc complex as a klippe in an upper plate position on top of the passive margin sequence, instead of an autochthon extending deep to the mantle, amalgamated with the continent through a back-arc closure.

These results enriched the knowledge of continental growth of eastern Gondwana that it involved the episodic addition of juvenile oceanic terranes via east-dipping subduction and emphasized that the detrital zircon ages could record the process. By establishing the arc chronology via these zircons is a major contribution to understanding the geodynamic setting of this Paleozoic arc-related copper mineralization along the Pacific margin.

Unravelling the Tumut Trough: A Middle Ordovician age for the Brungle Creek Metabasalt, eastern Lachlan Orogen

Bruce, Michael, Percival, Ian, Zhen, & Yong, Yi

Geological Survey of New South Wales, W.B. Clarke Geoscience Centre, Londonderry, Australia

Alpine-type ultramafic bodies are exposed in numerous localities throughout the Lachlan Orogen of New South Wales. Despite the tectonic significance of such oceanic lithosphere to the development of the orogen, few studies on the genesis of these bodies have been documented.

The Coolac Serpentinite is an Alpine-type ultramafic intrusion that marks the eastern edge of the Tumut Trough in the eastern Lachlan Orogen. Recent petrological, geochemical and geochronological studies into the massive harzburgite (Bruce 2018) that makes up most of this body reject any ophiolitic association with rocks of the North Mooney Complex. These rocks are traditionally 'lumped in' as part of the proposed Coolac Ophiolite Suite, largely because of their physical location and resemblance to a layered, crustal ophiolitic sequence. Instead, a 2-stage melting model is proposed for the origin of the Coolac harzburgites with a late Cambrian latest melting event inferred from an allochthonous block (501 ±2.6 Ma, U/Pb zircon) with petrological links to the harzburgites.

The 'block' has been incorporated into the Silurian Jackalass Slate within the trough, which was previously thought to be simple sedimentary trough fill but is now partly interpreted as a sedimentary-matrix melange incorporating much older blocks. This interpretation is supported by blocks of chert found within the Jackalass Slate that contain conodont elements (*Periodon aculeatus*) of late Darrivilian to early Gisbornian age. Slightly older conodont assemblages with diagnostic elements of *Periodon hankensis*, indicating a late Dapingian to early Darrivilian age, are also found within chert lenses of the structurally underlying Brungle Creek Metabasalt.

Chert blocks within the Jackass slate and chert lenses

within the Brungle Creek Metabasalt show near-identical, REE chondrite normalised abundances and patterns as well as evidence of significant terrigenous mafic volcanic and hydrothermal input. This implies that the Brungle Creek Metabasalt is coeval with chert deposition and is thus early Middle Ordovician in age (465–468 Ma). The presence of Cambrian basement, widespread cataclastite in and around the Brungle Creek Metabasalt and structurally underlying Bullawyarra Schist, and identical chert units in the Brungle Creek Metabasalt and younger Jackalass Slate, as well as lenses of chert–volcanic clast conglomerate within the Brungle Creek Metabasalt, all support the structural interpretation of Stuart-Smith (1990), who suggested uplift, collapse and extension along a low-angle detachment fault. In addition, it is suggested that older, collapsed blocks have later been re-sedimented into younger Silurian basin strata.

Bruce M.C. 2018. Petrology, geochemistry and a probable Cambrian age for harzburgites of the Coolac Serpentinite, New South Wales, Australia. *Australian Journal of Earth Sciences*, 65, 335–355.

Stuart-Smith P.G. 1990. Evidence for extensional tectonics in the Tumut Trough, Lachlan Fold Belt, NSW, Australia. *Australian Journal of Earth Sciences*, 37, 147–167.

Orogenesis terminated by mafic underplate delamination at prior passive rift margins: The Delamerian-Ross example.

Foden, John, Tappert, Ralph, Todd, Angus, & Segui, David

Department of Earth Sciences, University of Adelaide, Australia

Stretching from southern Africa to north east Australia the Late Neoproterozoic to Late Cambrian aged Delamerian–Ross Orogen formed at the rifted Rodinia break-up margin, facing the newly opened Pacific. The orogenic history of this margin reflected initiation of subduction of the Pacific plate. At the end of the Cambrian, along the entire belt, active convergent orogenesis was terminated abruptly by rapid exhumation, uplift and cooling. This event is recorded as a widespread regional Upper Cambrian unconformity from southern Africa across Antarctica and into Tasmania. Rapid erosion that resulted from this event produced latest Cambrian to Early Ordovician proximal and distal siliciclastic sediment deposits including conglomerates and fluvial sandstones as well as marine turbidites. These deposits include the South African Cape Supergroup, the Ross Orogen Carryer and Douglas Conglomerates, the Tasmanian Jukes and Owen Conglomerate and the western Victorian turbidites.

In South Australia Jurassic aged kimberlite intruded the Delamerian Orogen and transported an abundant population of mafic xenoliths ranging from garnet–pyroxenite (*eclogite*) to pyroxenite and mafic granulite. Mineral assemblages include, Cpx–Gt–Rt, Cpx–Gt–Amp–Rt, CPX–Gt–Amp–Ky, Plag–Cpx–Gt ± Amp, Ky, Il. These were sampled from lithospheric mantle recording pressures in the range 8 to 25 kbar. Exsolution of garnet and kyanite from Cpx provides evidence for cooling at constant or increasing pressure. Whole rock Nd isotopes yield an imprecise Late Neoproterozoic external isochron and their geochemical composition indicate that parental mafic magma was anorogenic rift-related tholeiite. Importantly the suite of samples forms

clear compositional trends that show igneous 'gabbroic' pyroxene + plagioclase fractionation control even though many samples are now plagioclase-free.

The conclusion is that these were magmas produced during Rodinian rifting and breakup and formed underplated gabbros at Moho depth. Subsequent cooling to produce plagioclase-free, garnet and pargasite-bearing assemblages lead to increasing density and subsequent delamination resulting in buoyant crustal uplift and probably coupled with slab roll back led to orogenic termination. The common occurrence of high pressure pargasitic amphibole may implicate the role of hydrous flux from the subducting Pacific plate in catalysing high pressure cooling reactions in the mafic underplate. Critical to their density increase, P–T modelling of the pyroxenite bulk compositions indicates that at Moho depths (9 kbar) cooling of the Neoproterozoic magmatic underplate would cross the garnet and pargasite-in reactions at 1000 °C and the plagioclase-out reaction at 750 °C. The time taken for initial mafic magmatic intrusions at 1350 °C to cool to cross these important density increasing reactions at a Moho T of ~600 °C is of the order of 5–15 My. Delamination may also promote local thermal convection leading to anomalous asthenospheric ascent and the production of post-tectonic magmas.

The style of orogenic termination described here forms a distinctive class and reflects subduction at the rift magma-rich margins of continental fragments formed during break-up of earlier continents. This orogenic style seems common to many belts formed during Gondwanan accretion.

Apatite as an indicator of porphyry fertility in the Northparkes district

Wells, Tristan¹, Meffre, Sebastien¹, Cooke, David R.^{1,2}, Steadman, Jeffrey A.¹, & Goemann, Karsten³

¹CODES. Centre for Ore Deposits and Earth Sciences, University of Tasmania, Private Bag 79, Hobart, TAS 7001, Australia; ²ARC Industrial Transformation Research Hub for Transforming the Mining Value Chain – TMVC, Private Bag 79, University of Tasmania – Hobart, TAS 7001; ³Central Science Laboratory, University of Tasmania, Hobart, TAS 7001

The resistate nature of apatite in the weathering profile, combined with its potential to record physical and chemical information about magmatic and hydrothermal systems, makes it a useful mineral for assessing magmatic fertility. Magmatic apatite trace element compositions can reflect the degree of fractionation, sulphur content and oxidation of the host rock, whereas hydrothermal or recrystallised apatite also has the potential to record hydrothermal fluid evolution.

Apatite from the Northparkes district, NSW were analysed by colour cathodoluminescence, scanning electron microscopy, electron micro-probe and laser ablation inductively coupled mass spectrometry. Colour cathodoluminescent imaging of apatite from Northparkes highlights complex zonation and differing luminescent colours that are linked to variations in mineral trace element abundance and crystal origins. At Northparkes, magmatic apatites have a lavender or blue luminescent colour, whereas apatites that have complex internal geometries and a yellow-green to brownish luminescent colour are associated with

hydrothermal alteration and proximity to mineralised centres. Magmatic and hydrothermal apatite have similar crystal forms, making them virtually indistinguishable from each other without the aid of colour cathodoluminescence. Depletion of light rare earth elements in apatite is associated with hydrothermal alteration across the Northparkes district. Hydrothermally altered apatite from the mineralising intrusions at the Endeavour 26 deposit have pronounced LREE depletion and MREE enrichment, concurrent with a strong positive Eu anomaly. The detection of apatite with these characteristics can be used to infer the proximity to mineralization in porphyry systems in the Northparkes district.

Evolution of the Lachlan Orogen in the East Riverina region, NSW: Insights from 100 new SHRIMP dates

Bodorkos, S.¹, Gilmore, P. J.², Eastlake, M. A.², Bull, K. F.², Blevin, P. L.², Trigg, S. J.², Campbell, L. M.², & Waltenberg, K.¹

¹*Minerals, Energy and Groundwater Division, Geoscience Australia (GA)*; ²*Geological Survey of New South Wales (GSNSW), Department of Regional NSW*

The southern part of the central Lachlan Orogen in NSW is prospective for intrusion-related tin–tungsten (e.g., Ardlethan), porphyry-style copper–gold, and orogenic gold mineralisation, however, the regional geological framework has long been poorly understood. GSNSW's 2014–2018 East Riverina mapping project (spanning the area between West Wyalong and the Murray River, east to Cootamundra and Adelong, and west to Narrandera and the Murray Basin) updated large areas of 1960s–1990s geological mapping, to support mineral prospectivity studies. The project included a collaborative GA–GSNSW geochronology program that generated nearly 100 new U–Pb SHRIMP zircon dates, to establish a regional chronology of felsic and intermediate magmatism, and to understand the depositional history of the intervening basin successions. Some highlights include:

1. Sheared 493 Ma and 489 Ma granites of the Belimebung Igneous Complex confirm previous LA-ICPMS dating of the first Cambrian igneous rocks identified within the Gilmore Fault Zone. They were intersected in drillcore beneath the early Silurian Gidginbung Volcanics north of Barmedman and indicate a possible latest Cambrian age for NW-trending magnetic lineaments near the Gilmore Fault.
2. The propylitically altered 439 Ma Cooba Monzonite southeast of Junee extends the known distribution of 'Phase 4' Macquarie Volcanic Belt rocks (prospective for porphyry copper mineralisation) to the south.
3. Tholeiitic andesites of the 432 Ma Junawarra Volcanics and related rocks host gold mineralisation at Dobroyde, northeast of Junee. These are geochemically distinct from, and significantly younger than, the shoshonitic 439–436 Ma Gidginbung Volcanics to the northwest and establish two separate associations of Silurian gold-bearing volcanic rocks in the region.
4. More than 20 S-type plutons of the 432–427 Ma Koetong Supersuite have been dated, as far north

as Nymagee, east to Young and Tumut, and west under Murray Basin cover to Borellan and Howlong.

5. The predominantly mid-Silurian 'Wagga Batholith' is transected and flanked by NW-trending belts of Early Devonian (420–412 Ma) plutonic rocks linked to intrusion-related mineralisation. S-type granites associated with tin–tungsten mineralisation include the 418 Ma Burrandana Granite and the de-silicated 417 Ma Ryan Granite in the south and fractionated 415–413 Ma granites near Ardlethan in the north. Contemporaneous I-type rocks include the cassiterite-bearing Yithan Rhyolite at Ardlethan, diorite associated with gold mineralisation at Mount Adrah, and intrusions east and south of Tarcutta and Holbrook.
6. Regional Early Devonian volcanism encompasses the expanded 419–416 Ma Gurrugong Group in the Cargelligo-Ardlethan area, and the newly-defined Culcairn Group (comprising the 415–413 Ma S-type Budginigi Ignimbrite and the 413–411 Ma Wallandoo Ignimbrite and Hickory Hill Diorite) in the Culcairn-Henty-Walbundrie area. These volcanic units constrain the timing of pre-eruptive siliciclastic sedimentation and influence the detrital signatures of post-eruptive sediments.
7. I-type plutonism is youngest in the southwestern East Riverina. Early Devonian (414 Ma and 411 Ma) Leeton Igneous Complex granites stitch the unexposed northwestern extension of the Kancoona Fault. Northeast and north of Albury, the 407–402 Ma Mullengandra Monzodiorite and Jindera Granite appear to be associated with Central Victorian granites of similar age.

Structure of the Silurian Quidong Basin: new observations on a microcosm of Eastern Lachlan Orogen tectonic and metallogenic problematica

Hood, David I. A.¹, Durney, David W.², & Parkes, Ross A.²

¹*ARDEX Australia R&D Dept. Seven Hills, NSW 2147*; ²*Department of Earth and Environmental Sciences, Macquarie University, NSW 2109.*

The Quidong Basin is a small (~20 km²) structural basin made up of sediments of Wenlock to Ludlow age within the in-faulted Ordovician–Silurian Tombong Block in the Delegate area of far southeastern New South Wales. It is a true microcosm of several contested tectonic and metallogenic problems that are common to other parts of the Lachlan Orogen of New South Wales. (1) It displays an angular unconformity with older Silurian sediments attributed to a localised convergent orogeny: the "Quidongan Orogeny". (2) There have been competing syngenetic and thrust-related models for the origin of stratbound and faultbound massive sulphide mineralisation in the Basin. (3) It is affected by complex superposed folding and cleavage development whose sequence has not been resolved in the published literature. (4) Interpreted time relations between folding and prominent faulting in the area have been ambivalent. (5) The area lacks a direct time constraint on the age of the convergent fold deformation.

A better understanding of the deformational structures and how the unconformity may have formed is also

important for palaeogeographical reconstruction and stratigraphical correlation of fossil horizons in the faulted and folded sediments. It was for this purpose that DH carried out field observations and analysis of structures at selected sites in the area in support of palaeontological and sedimentological work by Ross Parkes for his PhD study at Macquarie University in the early 2000s.

We have since reviewed the structural data of DH to examine their implications for the broader questions listed above. These data have the benefit of being observational and detailed. The methods of analysis are well known but not often used in rocks of similar age elsewhere in the Orogen: *domain analysis* of fold directions and whether a time sequence can be determined in individual superposed folds, and *incremental strain-axis analysis* of kinematically significant minor fault, vein and stylolite associations. We also describe a new type of structure—*incoherent fault-related folds* (DD)—which provides unambiguous criteria to determine the time relation between sub-parallel faults and minor folds.

From these observations and analyses we report (a) the time relation between at least two of the three known fold systems in the area, (b) the same three fold systems above and below the unconformity, which argues against a convergent deformation origin of the unconformity, (c) minor thrust and wrench kinematic data consistent with sinistral wrench reactivation of prominent NNW faults, (d) pre-fold normal movement on the prominent NNW faults, (e) a pre-fold or syngenetic origin of the massive-sulphide mineralisation, (f) no detected map-scale thrusts or inversions and (g) regional correlations which suggest a post-Late Devonian or Kanimblan age of the multiple folding.

Approaches to structural history in areas of weak to moderate upright folding

Durney, David W.

Earth & Environmental Sciences, Macquarie University, Australia

A particular style of convergent deformation in upper crustal sedimentary basins in many parts of Australia is gentle to close *upright folding* on *multiple trends*, typified by dome-basin interference patterns. This style occurs widely in Siluro-Devonian continental back-arc sedimentary and volcanic strata of the Lachlan Orogen (LO) in New South Wales (NSW). Several hypotheses have been suggested for folding in that region, most notably up to four successive extensional and 'orogenic' events.

As conventional methods of structural analysis have limited applicability, the present talk aims to outline the basis of the approach used by Hood *et al.* at this conference in their analysis of this style in the mildly deformed Quidong Basin in NSW.

The basis is both geological and mechanical. It is geological in the sense that:

1. the area is one of very-low grade metamorphism where the geologically observable solution-transfer/pressure-solution deformation mechanism is known to be prominent in many sedimentary rocks, and
2. extensional deformation is acknowledged in the

formation of the basin.

It is mechanical in the sense that:

- the theoretical rheology of solution-transfer deformation is approximately linear-viscous, meaning slow deformation can occur under very low stress,
- because of that, ductile rather than brittle deformation is prominent and
- viscous buckling theory applies to layered strata under horizontal compression.
- As a separate matter, equilibrium of horizontal forces is recognised as a constraint on likely structural combinations at any given time over broad regions of continental upper crust.

It is suggested that these points also limit the range structural hypotheses that are applicable to such regions.

Briefly, the methods have been selected to emphasise short-period incremental deformations: (1) identification of separate fold directions, (2) application of buckling theory to infer associated shortening directions and their relative timing in upright Ramsay Type 2 or 'banana' refolds, (3) correlation of incrementally sensitive mesoscopic spaced cleavages in limestones with the folds, (4) use of outcrop-scale kinematic indicators to establish the 3D character of the deformations, (5) use of buckling theory to explain "fault-related minor folds" and (6) application of force equilibrium to infer regional distribution.

Late Cambrian–Middle Ordovician extension of the northern Tasmanides: thinned crust that facilitated intense Silurian (Benambran) shortening deformation

Henderson, Robert¹, Fergusson, Chris², & Withnall, Ian³

¹*Department of Earth and Environmental Sciences, James Cook University, Townsville, Australia;* ²*School of Earth, Atmospheric and Life Sciences, University of Wollongong, Australia;* ³*Geological Survey of Queensland, Brisbane, Australia*

The Charters Towers and Greenvale Provinces of the Thomson Orogen provide the most extensive exposure of early Paleozoic rocks in the northern Tasmanides. Upper crust represented by the Charters Towers Province developed a thick, Proterozoic passive margin, sedimentary assemblage with a minor contribution from mafic igneous rocks. This assemblage was subsequently overprinted by active margin tectonism commencing in the mid Cambrian (ca 510 Ma), reflecting a broad scale Tasmanide regime change of that age. The overprinting regime generated thick (>15 km) basinal infill, inclusive of a substantial intermediate to silicic volcanic complement, of the upper Cambrian–Middle Ordovician Seventy Mile Range Group and other upper Cambrian basinal relicts identified for the Charters Towers and Argentine Metamorphics. Magmatic arc plutonism is widely developed as the Ravenswood Batholith and Fat Hen Creek Complex. Regional metamorphism and penetrative fabric development of Early Ordovician age overprinted all of the Proterozoic passive margin assemblage and part of the Cambrian basin fill, with structural analysis favouring its association with

extensional strain. Coeval basin formation, plutonism and metamorphism across the province reflects an enduring episode of crustal extension.

The Greenvale Province consists largely of meta-volcanic and metasedimentary tracts with protoliths of Early Ordovician age. Lower Ordovician granites are also represented and in broad aspect, rock units of the province both resemble, and are correlative with, the active margin assemblages of the Charters Towers Province. Structural analysis shows a deformation history matching that of the Charters Towers Province with the dominant foliation similarly attributed to extensional strain. Development of the province represents thick basinal infill developed on thinned crust of a continental margin. Contrary to earlier publications, no rocks older than Ordovician are known for the province. Amphibolite and ultramafic units interleaved with metasediments on its eastern (outboard) side suggest it may have developed on oceanic crust.

For both provinces thin crust had developed by the Middle Ordovician, weakening its resistance to subsequent Benambran contraction. Cambro-Ordovician rock assemblages of both provinces were affected by structural/metamorphic overprint with local generation of mylonite in wide shear zones. Contraction is dated as Silurian by Ar–Ar mineral ages, by fabric development in deformed granites of known age and by the age of overlap strata. Tight upright folds and accompanying foliation, generated by shortening, deformed tracts affected by Ordovician extensional strain, steepening previously formed fabrics. Basin fill represented by the Seventy Mile Range Group was inverted. For the Greenvale Province, widespread amphibolite grade metamorphism indicates that much of it has been exhumed from considerable crustal depth (>15 km). In contrast exhumation of the Charters Towers Province was heterogeneous, ranging from <5 km (unmetamorphosed Seventy Mile Range Group) to >15 km (amphibolite facies metamorphism and local migmatite). Silurian structural trends, considered by some authors as registering an orocline, are attributed to strain partitioning consequential on oblique convergence.

Regional scale folding in the Arthur Metamorphic Complex: structural constraints for the Keith River–Lyons River area, NW Tasmania

Cumming, G.¹, Jackman, C.¹, Everard, J. L.¹, & Gray, D.²

¹*Geological Survey Branch - Mineral Resources Tasmania - Geological Survey Branch, Rosny Park, Australia;* ²*Consultant Structural Geologist for Mineral Resources Tasmania - Geological Survey Branch, Rosny Park, Australia*

New geological mapping in the Keith River–Lyons River area in NW Tasmania has provided insight into the structural framework of the northern Arthur Metamorphic Complex (AMC) in NW Tasmania. The AMC is flanked to the east by the Oonah Formation and to the west by the Rocky Cape Group. The main lithological units of the AMC share transitional metamorphic, interpreted low angle fault, and both conformable and unconformable contacts. At a regional scale a significant north-plunging synform, or a large

north-tilted block, is contained within the high-strain core of the AMC. Five deformation episodes can be observed throughout the area at outcrop-scale. Three early deformational episodes are likely related to the Middle Cambrian Tyennan orogeny, manifested as early, high strain events which caused isoclinal folding and development of schistose axial planar fabric. A rotational shear component, apparent as shear bands, suggests north over south or sinistral transport. Subsequent D3 deformation within the AMC occurred during the later stage of the Tyennan Orogeny. This event folded and tightened the various stacked lithostratigraphic units to form non-cylindrical asymmetric folds. These were later subject to generally northwest-directed, potentially Devonian compression (D4) and tilting. At a regional scale, late-stage north-plunging folds are inferred along the highest strain zone of the northern AMC. This area is a locus for Mesozoic or early Cenozoic faults, and a half-graben also extends along this zone, which is also in the core of the AMC. A late stage (D5) folding event may be partly related to Devonian compression, although the timing and nature of this folding event is largely unclear.

Evidence for fire fountaining at Skillion Hill, southern Tasmania

Cumming, G.¹, Orth, K.², Bottrill, R.¹, Everard, J.¹, & Vicary, M.¹

¹*Geological Survey Branch - Mineral Resources Tasmania - Geological Survey Branch, Rosny Park, Australia;* ²*School of Earth Sciences, University of Tasmania, Hobart, TAS, Australia.*

Skillion Hill, in Southern Tasmania, is a flat-topped hill at the southern edge of a 2.5 km long zone of Cenozoic mugearite/basalt flows and basaltic breccias. The linear volcanic centre is positioned at the northern edge of a north-northeast-trending line of volcanic centres that span from Droughty Hill (to the south). The volcanic centres consist of strongly evolved alkaline rocks, which generally occur as small plugs, explosive vents, diatremes and scoriaceous flows elsewhere in southern Tasmania. The area has been recently excavated for a building subdivision, enabling the observation of fresh exposures. New geological mapping and textural analysis of samples has revealed a wide variety of volcanic features comparable to eruptive products formed from fire fountaining.

Exposures of “hackly” basalt display an almost clastic appearance owing to a fine network of thin, wispy-lenticular structures (< 0.1 mm thick). These features are parallel to the stratification observed in the scoria deposits above and below. The basalt contains very fine grained, mostly altered, olivine, clinopyroxene, pseudobrookite, magnetite and plagioclase crystals, in an altered glassy groundmass. It is locally xenolith-rich, containing clasts of underlying sedimentary and igneous rocks, anorthoclase–pyroxene, enstatite xenocrysts and some partly fused quartz clasts. An isolated zone within the basalt also contains fluidal ribbon-like clasts. The “hackly” basalt is interpreted to have formed from spatter clasts that underwent agglutination and coalescence during fire-fountaining to form a lava-like appearance. These features indicate rapid accumulation during the eruption, allowing immediate coalescence of hot impacting clasts (as detailed in Sumner *et al.*, 2004).

Fluidal to ropy and blocky scoria breccia occurs above, beneath and within the “hackly” basalt. The breccia is poorly sorted, coarse grained, massive and generally monomictic with elongate, vesicular, variably flow banded, fluidal lenticular or ribbon shaped clasts (>10 cm across). The breccia contains clasts with distinct morphologies similar to volcanic bombs and the bulk of the material is interpreted as deformed and flattened spatter, which may have started as completely fluid clasts that agglutinated (or partly agglutinated) on impact during deposition. Abundant bread-crust and spindle-shaped clasts with smooth cores are commonly found in the newly excavated trenches and are also interpreted as once partly fluidised volcanic bombs.

Poorly sorted, crudely stratified scoria breccia with alternating finer grained granule rich matrix-supported layers contain fairly oxidised, ragged, angular to blocky shaped clasts which overlie and are intercalated with the “hackly” basalt and scoria breccia. The crude stratification may have been caused by changes in eruption dynamics, such as eruption column height, fragmentation processes or changes in dispersal patterns during the eruption (McPhie *et al.*, 1993).

Structural measurements of flow banding and the stratification in the scoria breccia facies, along with the incidence of proximal spatter piles or fountain-fed lavas (formed in an inner-fountain setting) suggest that Skillion Hill represents a partly dissected edifice of a fissure vent or scoria cone. Eruptions likely involved alternating or contemporaneous low viscosity, less volatile rich magma with high effusion rates (to form coalesced spatter), and eruptions with high volatile content and high explosivity (to form agglutinated spatter and volcanic bombs).

McPhie J., Doyle M., Allen R., Allen R. L., 1993. *Volcanic textures: a guide to the interpretation of textures in volcanic rocks*. Centre for Ore Deposit and Exploration Studies, University of Tasmania, Hobart

Sumner J. M., Blake S., Matela R. J., Wolff J. A., 2005. Spatter. *Journal of Volcanology and Geothermal Research*, 142, 49–65.

Geochronology of various fault bound units at Savage River: a melange of different terranes

Cumming, G. V.¹, Bottrill, R. S.¹, Calver, C.², & Meffre, S.²

¹Geological Survey Branch - Mineral Resources Tasmania - Geological Survey Branch, Rosny Park, Australia; ²School of Earth Sciences, University of Tasmania, Hobart, TAS, Australia.

To support geological mapping of the poorly dated Arthur Metamorphic Complex (in the Savage River Area), the detrital zircon provenance of some major geological units were characterised. Detrital zircon was obtained from several units within the Ahrberg Group, Timbs Group (including Bowry Fmn. & Fulfords Ck Schist), Armstrong Ck schist and Keith Schist. All samples were dated by the U–Pb method using laser ablation inductively coupled mass spectrometry (LA-ICPMS).

Results from the Donaldson Formation (basal Ahrberg Group) indicate that deposition occurred after ca 1343 Ma. The detrital zircon age spectra are comparable to those previously obtained from the Forest Conglomerate (Rocky Cape Group) and Oonah Formation and support a previously suggested

correlation with these units (Mulder *et al.*, 2015). However, this age is much older than the youngest zircons obtained from the Oonah Formation and correlatives elsewhere (ca 734 Ma). Our results from the Bernafai Volcanics (upper Ahrberg Group) indicate deposition occurred after ca 569 Ma which, along with field relationships, supports a correlation with the Kanunnah Subgroup of the Togari Group.

In contrast, samples from the Bowry Formation (Timbs Group) cannot be easily related to other units in Tasmania (based purely on the zircon spectra alone). A 717 ±18 Ma age (with 2σ error) of albitised meta-sediment gives a revised maximum age for the Bowry Fmn. Four age assemblages have been characterised from the Bowry Fmn. Two of these have restricted ages, and the remainder show complex and varied age spectra. Samples with restricted age profiles between 780 and 750 Ma were most likely deposited during Neoproterozoic rifting, and sediments with diverse components were probably derived from intraplate sedimentation during these rifting events. Furthermore, samples from the Timbs Group cannot be easily correlated with the Ahrberg Group, an idea proposed by previous workers (Turner & Crawford 1993). The western section of the Timbs Group was interpreted by Holm and Berry (2002) as a parautochthonous slice of the Ahrberg Group, and they referred to it as the ‘eastern’ Ahrberg Group, yet this relationship was not confirmed by detrital zircon geochronology due to the paucity of zircon in this group. However, there are strong peaks of 1400 and 1700 Ma zircons in additional units in the Timbs Group (Armstrong Creek Schist and Fulfords Creek Schist). These peak ages are comparable with the Keith Schist, and ‘upper’ and ‘lower’ Rocky Cape Group lithologies.

The varied zircon age spectra in samples from Savage River is foreseeable, given that they were obtained from narrow fault-enclosed blocks in a melange zone, in the highest strain portion of the Arthur Metamorphic Complex. The Timbs Group likely represents an assemblage of fault bounded allochthonous fragments of Meso to Neoproterozoic siliclastic, carbonate rich and rifted intra-plate basins. These fragments were deformed, albitised and faulted together during the Early–middle Cambrian collisional event and emplaced against the Late Neoproterozoic Bernafai Volcanics.

Holm, O. H., & Berry, R. F., 2002. Structural history of the Arthur Lineament, northwest Tasmania: an analysis of critical outcrops. *Australian Journal of Earth Sciences*, 49, 167–185.

Mulder, J. A., Halpin, J. A., & Daczko, N. R., 2015. Mesoproterozoic Tasmania: Witness to the East Antarctica-Laurentia connection within Nuna. *Geology* <https://doi.org/10.1130/G36850.1>

Turner, N. J., & Crawford, A. J., 1993. General features and chemical analyses of mafic and other rocks, Corinna geological map quadrangle. *Report Mineral Resources Tasmania* 1993/23

Early Tasmanides evolution: passive to convergent margin history in New South Wales, Australia

Greenfield, John, Gilmore, Phil, & Musgrave, Robert
Geological Survey of New South Wales, Department of Regional NSW, Maitland, Australia.

Initial development of the Tasmanides in southeastern Australia involved Early Neoproterozoic rifting/break-up of the Rodinian supercontinent, expressed as tholeiitic

dyke swarms and continental rifting in the Adelaide Rift Complex of eastern South Australia. This left highly extended, transitional crust between the Gawler Craton and Curnamona Province, which became the depocentre for extensive platform carbonate and shallow marine clastic sedimentation. By ca 700 Ma, a passive margin developed east of the Curnamona Province which saw the initiation of the palaeo-Pacific Ocean. A final NE–SW phase of rifting in the Late Neoproterozoic was associated with shallow marine platform sedimentation and alkaline magmatism (Mount Arrowsmith Volcanics), further attenuating the eastern Curnamona Province crust and presenting an angular continental salient towards the nascent ocean to the east.

This crustal configuration profoundly influenced the palaeogeography and tectonism that followed during the Delamerian Cycle, as passive margin clastic deposition in the early Cambrian gave way to west-facing subduction in the mid Cambrian. Elements of the resulting Cambrian volcanic arcs (Mount Wright and Loch Lily–Kars) are now immediately adjacent to the Curnamona Province margin. However, regional geological mapping in the Koonenberry Belt has shown that the Mount Wright Arc developed in a rift zone within the Curnamona Province that probably initiated during the last phase of Rodinia break-up in the Late Neoproterozoic. In contrast, the strike-equivalent Loch Lily–Kars Arc was developed in an intra-oceanic setting. Mapping, drillhole and geophysical data shows that this arc segment, along with forearc volcanic rocks of the Ponto Group, were oroclinally folded clockwise almost 90°, and thrust against the southeastern Curnamona Province margin during the Late Cambrian Delamerian Orogeny. If the original arc segments were part of a linear belt, it would have extended southeast from the oroclinal hinge at the Grasmere Knee Zone. Recently acquired and modelled AusLAMP magnetotelluric data show a strong lower crustal conductive anomaly aligned along this trend.

The Delamerian Orogeny caused strong ductile deformation of rocks deposited in the Delamerian Cycle. Areas that were highly attenuated during break-up suffered tight upright folding and oroclinal bending, which may also have been affected by clockwise rotation of the Curnamona Province. Proterozoic Olarian Cycle metamorphic rocks along the margins of the Curnamona Province and the eastern edge of the Gawler Craton also suffered upright open to tight folding during the Delamerian, with σ_1 perpendicular to the outboard margin. In the Broken Hill Domain, early southwest-directed fold-thrusting switched to northwest-directed fold-thrust and strike-slip deformation at the end of the Delamerian Orogeny in the Early Ordovician.

Clearly the switch to a convergent setting, with arc accretion and terminal deformation in the Delamerian Orogen, caused extensive shortening of a highly attenuated margin that had been in extension for ca 300 Ma. The Curnamona Province, although acting as a salient in the early Delamerian Orogeny, was itself deformed and could not insulate the distal-foreland Flinders Ranges from deformation late in this event. This had cumulative effects on the ensuing cycles of subduction roll-back, extension and contraction that defined the Tasmanides throughout the Palaeozoic.

CRUST, SURFACE & COSMOS

Carbonates as archives of the past

Trace element distributions in carbonate rocks: a sedimentologist's perspective on sample targeting versus technique

Webb, Gregory E.

The University of Queensland, Brisbane, Australia

Trace element geochemistry is useful increasingly in ancient and not so ancient carbonate rocks where it provides the basis for radiometric dating and many palaeoenvironmental proxies. High precision U–Th and U–Pb analyses in carbonate samples are converging to close the 'undatable' window past 500 ka. A variety of palaeothermometers are used commonly (e.g., Sr/Ca, Mg/Ca, U/Ca, etc.) and rare earth elements (REEs) inform the source of ancient water masses, water quality and redox states. Other elements (e.g., Ba, Mn, V, etc.) provide proxies for biological processes and palaeoproductivity as well as terrestrial processes, including firing. Redox sensitive elements (e.g., Mo, V, U, etc.) inform complex oxygenation scenarios in Precambrian seas. Trace elements are providing an ever-increasing tool kit for sedimentologists, stratigraphers and palaeoenvironmentalists.

However, a variety of pitfalls accompany the expanding use of trace element geochemistry in carbonate rocks. As carbonate minerals are metastable at the Earth's surface, sedimentologists are highly attuned to the problem of diagenetic alteration. Effective sample vetting is crucial, but new core scanning technologies and SEM approaches are easing sample selection. Regardless, many samples are complex mixtures of sources with differing elemental concentrations and distributions that require detailed understanding of the sample, which elements are being targeted for analysis and the reservoir for which they are meant to serve as proxies. For example, trace elements in marine precipitates are sourced from ambient seawater, but depending on the sample, elements also may reflect siliciclastic detritus (contamination) and organic components, which may or may not cause fractionations or enrichments. Additionally, analysed element distributions may record local micro-environments rather than the ambient water masses in which they occur. Where ambient water chemistry is targeted, elemental contributions of all other sources must be identified and removed. For bulk samples (dissolution ICP-MS), contaminants can be removed post-analysis using mixing lines to quantify contamination in each sample. Alternately, sequential etching may attempt to analyse separate sources independently during dissolution. Increasingly, laser ablation (LA) ICP-MS combined with LA mapping can be used to identify and sample increasingly small, specific targets while avoiding contaminants. Other elemental mapping approaches (e.g., synchrotron-based x-ray fluorescence, SEM electron dispersive spectroscopy) also aid sample vetting and targeting of appropriate sources. The source of the proxy elements is critical.

Although ICP-MS is increasingly common, significant technical issues remain past adequately low blanks and high count rates. As sample size decreases (e.g., LA

analysis), low sample volume exacerbates low element concentrations leading to poor data quality. However, even apparently 'low quality' data for some elements, like the REEs, provide useful information owing to their self-normalising behaviour. Cohesive REE data suggest adequate precision to carry information, regardless of calculated detection limits and groups of less cohesive data can be analysed statistically to provide some information.

Overall, successful interpretation of trace element proxies requires more than a good geochemical laboratory, it requires knowledge of the finite relationship between the targeted proxy elements and the sample being analysed (i.e., context) along with application of the most appropriate technique for the job.

Neoproterozoic carbonates as archives of paleo-redox conditions on early Earth: Insights from metal isotope analyses of the Tumbiana Formation, Pilbara, WA

Farkas, Juraj¹, Kläebe, Robert¹, Scarabotti, Liam¹, Stormberg, Jessica², & Spinks, Sam²

¹*Metal Isotope Group (MIG), Department of Earth Sciences, University of Adelaide, SA, Australia;*
²*CSIRO, Division of Mineral Resources, Perth, WA, Australia*

The redox conditions of the earth's surface environments are intimately linked to past changes in the atmospheric O₂ levels, and thus to the long-term evolution of photosynthetic life on our planet. It is generally believed and accepted that Archean Eon is characterised by extremely low levels of atmospheric O₂ concentrations with predominantly anoxic / euxinic marine and terrestrial environments, where the first significant rise in atmospheric O₂ levels is documented much later during the Paleo-Proterozoic period at around 2.4 to 2.1 billion years (Byr) ago, the latter also called the Great Oxidation Event (GOE). This study aims to further constrain paleo-redox conditions during Neoproterozoic times by analysing selected metal isotope tracers and elemental concentrations in carbonate-rich samples from the Tumbiana Formation of the Fortescue Group in the Northern Pilbara Craton in WA, dated at ca 2.7 Byr, which thus represent unique archives of paleo-environmental and redox conditions on early Earth. Here we analysed stable chromium isotopes ($\delta^{53/52}\text{Cr}$ variations), coupled with REEs and elemental Zn/Fe ratios, to infer past changes in redox conditions during the deposition of the Tumbiana Formation, and radiogenic strontium isotopes ($^{87}\text{Sr}/^{86}\text{Sr}$ ratios) were used to test marine versus continental / lacustrine origin of the studied Neoproterozoic carbonates from the Fortescue Group. Interestingly, acquired results strongly support non-marine and thus likely lacustrine origin of the Tumbiana Formation carbonates, and more importantly our pilot data from redox-sensitive proxies ($\delta^{53/52}\text{Cr}$ and Zn/Fe ratios) point to an active redox cycling of Cr isotopes during the deposition of the Tumbiana Formation at ca 2.7 Byr, thus challenging the prevalent views of strictly anoxic conditions during the Neoproterozoic. In addition, the above geochemical/isotope evidence for an active redox cycling (i.e., oxidation–reduction) of chromium and iron is documented in horizons with abundant stromatolitic carbonates, perhaps suggesting that local production of

O₂ via photosynthesizing microbial communities in restricted lacustrine settings could be partly responsible for the observed paleo-redox signals recorded in $\delta^{53/52}\text{Cr}$ and Zn/Fe tracers in carbonates from the Tumbiana Formation. We will discuss broader implications of the above findings for paleo-redox studies in deep times, including possibilities that predominantly anoxic and O₂ depleted Archean earth's surface environments could also harbour localised 'oxygenated oasis' in very specific depositional settings.

Descending into the “snowball”: Improving interpretations of Tonian palaeoenvironments with multi-proxy elemental and isotopic geochemistry

Virgo, Georgina^{1,2}, Collins, Alan², Farkas, Juraj³, Blades, Morgan², Amos, Kathryn¹, & Lloyd, Jarred²

¹*Australian School of Petroleum and Energy Resources, the University of Adelaide, SA 5005, Australia;* ²*Tectonics and Earth Systems (TES) and Mineral Exploration CRC, Department of Earth Sciences, the University of Adelaide, SA 5005, Australia;* ³*Metal Isotope Group (MIG), Department of Earth Sciences, the University of Adelaide, SA 5005, Australia*

The Tonian–Cryogenian transition represents a period of significant physiochemical change in Earth history. It involved variations in oceanic and atmospheric oxygenation, significant changes in the biosphere, tectonic reorganisation, and the onset of the global 'Sturtian' glaciation. Tonian and Cryogenian sedimentary rocks in the Adelaide Superbasin, South Australia (SA), represent some of the most well-exposed, continuous and thick sections of this interval globally, recording major environmental shifts through distinct variations in lithology and isotope chemistry. Although this transition is geologically significant, it remains enigmatic due to a distinct lack of comprehensive, contemporary Tonian–Cryogenian research in South Australia.

We present robust palaeoenvironmental interpretations for a complete pre- to post- Sturtian glacial succession near Copley in the northern Flinders Ranges, SA. During fieldwork, a ~3 km sedimentary log was measured for facies and sequence stratigraphic analyses, and 350 samples were collected for elemental and isotopic geochemical analyses. Our study reveals multiple regressive–transgressive cycles, recorded by deltaic rippled and cross-stratified sandstones, through lagoonal intra-clastic magnesite and stromatolitic carbonates, to sub-tidal laminated siltstone and platform carbonates. These pre-glacial formations are unconformably overlain by subglacial to ice contact pebbly diamictites with quartzitic and dolomitic interbeds, which grade into proglacial laminated mudstone and sandstone with dropstones. We suggest that these facies reflect glaciomarine conditions. The post-glacial formation consists of subtidal laminated shales and carbonates, reflecting widespread transgression after the glaciation.

Elemental chemistry, along with C- and Sr-isotope signatures were analysed to determine primary basin water chemistries or palaeoseawater compositions, and to further constrain the depositional setting. Results demonstrate a nearshore/restricted, dysoxic setting

with indications for moderate hydrothermal input, which supports the sedimentological data. Furthermore, there is an inverse relationship between ¹³C and ⁸⁷Sr/⁸⁶Sr data, ranging from 7.37 ‰ to –6.68 ‰ and 0.7088 to 0.7182, respectively. In addition, the studied carbonates also exhibited relatively light ⁸⁸Sr values (≤0.211 ‰). These isotopic observations could reflect a drop in relative sea level, increased weathering of carbonates and sufficient input of continental material, which is consistent with sequence stratigraphic interpretations. Such settings might be analogous to the modern Coorong depositional environment, SA, where interaction of seawater with brackish continental waters facilitate precipitation of primary dolomite and magnesite. Insights into the water chemistry and isotope signatures of these primary Mg-rich carbonates will assist with interpretations of isotope data collected from the studied Tonian dolomites and magnesites. This multi-proxy study presents new palaeo-environmental insights into a key Tonian–Cryogenian succession, which sheds light in our understanding of how the world descended into one of the most severe glaciations ever recorded.

Deep water cusped stromatolites in the Cryogenian Trezona Formation, South Australia

O'Connell, Brennan, Wallace, Malcolm W., Hood, Ashleigh & Rebecchi, Luke

University of Melbourne, Australia

Deep water stromatolite horizons are well developed in the Cryogenian Trezona Formation and were deposited in an open marine, mid- to outer-ramp setting. Stromatolite horizons predominantly occur in association with shales that contain intraclastic horizons interpreted as mass flow deposits and are associated with iron oxides and irregular surfaces of erosion. These stromatolite horizons—developed as elongate structures with cusped mm-scale laminae—are interpreted as condensed sections in sediment starved settings. Documentation of these deep-water stromatolites adds to a small collection of deep water stromatolites, which appear to be largely represented by cusped forms. Deep water stromatolites could be linked to specific redox environments such as anoxic/suboxic ferruginous waters, and/or may be related to carbonate saturation, sediment starvation, or other factors.

Characteristics and diagenesis of the Upper Permian Beekeeper Formation from the Perth Basin, Western Australia

Adhari, Muhammad Ridha, & Wilson, Moyra E. J.

School of Earth Sciences, The University of Western Australia, Perth, Australia

The Upper Permian Beekeeper Formation is a proven reservoir in the Woodada field, Perth Basin, Western Australia, yet the nature and sedimentary features of this formation are not well understood. The Beekeeper Formation is about 20 km wide and 70 km long and the thickness of this sedimentary unit is up to 134 m. This formation is interpreted to be deposited in a cool-water ramp setting and has been identified not only in the Woodada field, but also in the Beharra Spring field, Perth Basin. This study aims to better understand the

characteristics of the Beekeeper platform and the diagenetic processes that occurred during its evolution. Sixty metres of conventional cores are available from five wells from the Perth Basin and 127 thin sections were made from those cores. Sedimentary logging, acetate peels, thin section petrography, and acid digestion have been conducted on the available dataset. Results from this study show that the Beekeeper Formation is a mixed carbonate-siliciclastic system, with both coeval and reciprocal mixing during sequence development. Bryozoas, brachiopods, and crinoids are the main bioclasts in packstones, grainstones, and rudstones. Primary matrix porosity is minimum in the Beekeeper Formation, but the secondary fracture porosity is of the highest quality. The fracture system is interpreted to be generated through tectonic activity on the basis of the relative timing of the paragenetic events, offset along the fractures, common sub-vertical fracture orientations, multi-size and multi-episode fracture development, and multi-phase fracture cements. The main diagenetic processes affecting the Beekeeper Formation include micritisation, boring, mechanical compaction, syntaxial overgrowth, granular-blocky calcite cementation, chemical compaction, dolomitisation, recrystallisation, and replacement, whereas bioclast and calcite vein dissolution are as minor features. These findings are expected to advance our understanding of this Upper Permian mixed carbonate-siliciclastic system and reservoir.

Quantifying the dolomite problem and its impacts on Mg/Ca change through time

Opdyke, Bradley

The Australian National University, Australia

Global dolomite deposition has declined globally throughout the Cenozoic. While the volumes of other sedimentary rocks increase from the Paleocene to the Holocene. This anomaly has been called the 'dolomite problem' and recognized since the time of Darwin. Recently my team discovered that crustose coralline algae (CCA) does precipitate calcium-magnesium carbonate with a dolomite chemistry. CCA is not as abundant on immature reefs as mature reefs, in fact CCA 'crusts' only become thick and widespread once a significant portion of the reef flat has been located within the tidal zone for many thousands of years. In a world where sea level is moving up and down like a Milankovitch driven yo-yo it is rare for these algal facies to become established, hence dolomite precipitation is rare. Recent sea level studies and compilations of stable isotope records from the Eocene to the Holocene allow us to model the probable trajectory of dolomite deposition over this time interval and calculate the probable Magnesium-Calcium ratio change in sea water. At the present time we only have a few 'tie points' for the Mg/Ca over this time. Using the stability of sea level as a driver of dolomite production we can predict more precisely how the Mg/Ca ratio has increased from 2.5 at the Eocene/Oligocene boundary to 5.1 in modern sea water.

On the foundering of carbonate platforms and reefs

Wilson, Moyra E. J.¹, Arosi, Hamed, A.¹, Loche, Marco¹, & Webster, Jody²,

¹*School of Earth Sciences, University of Western Australia, Perth WA;* ²*University of Sydney, Sydney, Australia*

Carbonate systems and coral reefs build amongst the largest edifices on the planet, are able to keep-up with most tectonic or glacio-eustatic induced sea-level rises and consequently the foundering of many platforms is often enigmatic. The cause of demise of platforms and the deposition of potential overlying seal units are critical for understanding thresholds for carbonate platform survival as well as petroleum systems evaluations in better understanding relationships between reservoirs and caprocks.

The paradox of foundering of carbonate platforms has been variously linked to 'drowning' via (1) fast glacio-eustatic sea-level rise, (2) tectonic induced sea-level rise, (3) nutrient and/or clastic poisoning and (4) subaerial exposure, shut-down of the carbonate factory and a subsequent inability to 'catch-up' on subsequent reflooding. Despite better understanding of the foundering of carbonate platforms being critical for their survival, evaluations of the sedimentary, geochemical and petrophysical signatures of each of the potential causes for demise remain understudied.

This study will evaluate the sedimentary, geochemical and diagenetic signatures across key outcrop analogue sections and subsurface reservoirs to understand the impacts of different causes of foundering on reservoir and caprock development. The research investigates: (1) both short- and longer-term (~> 1 Ma) transgressive drowning successions of carbonate platforms, (2) nutrient/or and clastic influenced land-attached, nearshore carbonate foundering, (3) carbonate platforms affected by karstification prior to drowning, and (4) volcanogenic smothered systems.

Rafted benthic microfossils as proxies of Neogene ocean current history in the Bass Strait seaway, southeastern Australia

Warne, Mark, & McDonald, Abbey

School of Life and Environmental Sciences, Deakin University, Melbourne, Australia

Cenozoic marine strata along the southeast Australian coastline contain a record of Southern Ocean evolution over geological time. A significant aspect of this oceanic evolution is the development and interplay of surface currents such as the East Australian Current, Leeuwin Current and Antarctic Circumpolar Current. These, and other ocean currents, have substantially shaped marine biological diversity along the southern Australian continental margin, and have left distinctive stratigraphic markers within the marine sedimentary rock record.

Traditionally, proxy records of past surface ocean currents have been derived from fossils of marine microplankton preserved in deep ocean and continental shelf sediments. However, in life, zooplankton often exhibit variation in depth distribution, which complicates relationships with surface ocean currents. In contrast, and paradoxically, shallow marine benthic microfossils associated with floating macroalgae, such as epiphytal ostracods and foraminifera, can provide more direct evidence of changes in global patterns of surface ocean circulation, because dispersal only occurs at the sea surface. The dispersal mechanism for these benthic micro-organisms is via attachment to seaweed, ripped up from shallow marine environments by coastal storms, and sent drifting vast distances across oceans on surface currents, until colonization occurs in new, distant shallow marine realms.

Key Neogene rafting-related ostracod migration and extinction events apparent in carbonate and siliciclastic marine strata along the southern Victorian coastline, and which defined broad phases in the oceanographic history of Bass Strait, are as follows:

Strong warm plumes of East Australian Current waters entering eastern Bass Strait (around 16.4, 5.8 and 3.2 million years ago), as evidenced by fossil occurrences of warm water, western Pacific *Neohornibrookella* species. Increases in the influence of East Australian Current waters in the Bass Strait region around 3 Ma, also likely facilitated the expansion of Pacific *Ambostracon* spp (*pumila* group species) into SE Australian coastal shallow and marginal marine realms.

Sporadic incursions of Antarctic Circumpolar Current waters entering western Bass Strait between approximately 9 and 5 million years ago, as evidenced by the influx of mid to high latitude *Tasmanocypris* (*darnalli* group) species.

The inception of warm Leeuwin Current (aka Zeehan Current) waters entering western Bass Strait (4.4 million years ago), which created a confluence with East Australian Current waters. This is evidenced by an east–west biogeographic differentiation of shallow marine ostracod faunas across this seaway. Notable is the widespread disappearance of *Neohornibrookella* and *Tasmanocypris* (*darnalli* group) species from warm shallow marine ostracod faunas west of Cape Otway, during the early Pliocene.

Widespread extinction of warm SW Pacific derived marine ostracod taxa across the entirety of Bass Strait

(e.g., *Neohornibrookella* species) due to the inception of the cold winter Bass Cascade current (1.8 to 2.2 million years ago), which led to winter water temperature minima too cold for these taxa. The inception of the Bass Cascade was associated with an early Quaternary northward shift in the position of the southern hemisphere, mid latitude westerly wind belt.

Holocene microbialite records of terrigenous influence on water quality for the offshore southern Great Barrier Reef

Salas-Saavedra, Marcos¹, Webb, Gregory E.¹, Sanborn, Kelsey L.², Zhao, Jian-Xin¹, Webster, Jody M.², Nothdurft, Luke D.³, & Nguyen, Ai¹

¹*School of Earth and Environmental Sciences, The University of Queensland, QLD 4072, Australia;*

²*Geocoastal Research Group, School of Geoscience, University of Sydney, NSW 2006, Australia;* ³*School of Earth and Atmospheric Sciences, Queensland University of Technology, GPO Box 2434, Brisbane, QLD 4001, Australia*

Anthropocene climate change and water quality degradation represent unprecedented challenges to modern coral reef ecology. Projected trends for the Great Barrier Reef (GBR) suggest continuing declines in reef health. Although declining reef health after European colonization is well documented around the world and increased terrigenous sediment flux is known to have terminated deglacial reefs in the GBR, longer-term patterns of water quality are poorly understood. Without historical data, it is difficult to disentangle natural and anthropogenic reef behaviour to better model anthropogenic effects. Here we present the first proxy-based long-term Holocene water quality reconstruction for any reef. The geochronological framework provided by rotary coring on Heron and One Tree reefs (offshore, southern GBR) allowed reconstruction of offshore water quality from 8200 to 1800 years before present (BP) using centennial resolution microbialite-based geochemical proxies. Microbialites, which form part of growing reef framework, contain a robust proxy record of water quality through incorporation of trace elements (e.g., rare earth elements-REEs, Zr, Th, etc.) from ambient seawater. Trace elements associated with terrigenous flux were measured in dated microbialites as well as poorly consolidated Pleistocene limestone and palaeosol formed at the Pleistocene–Holocene unconformity at Heron and One Tree reefs. Paleosol samples have REE patterns similar to the Queensland based shale proxy Mud of Queensland (MuQ) consistent with local soil formed on exposed reefal limestone. Framboidal pyrite within the palaeosol suggests anoxic soil conditions during initial inundation. Younger microbialite-hosted REE and yttrium (REY) normalised to MuQ (subscript SN) have seawater-like patterns (e.g., light REE–LREE depletion and high Y/Ho ratios) but with a well-defined, non-linear trend of changing water quality through the ensuing Holocene.

Immediately following reef initiation (>8300 yrs BP) data suggest increasing terrigenous influence to 8000 yrs BP on the basis of coordinated, more mud-like microbialite proxies, including reduced LREE depletion (e.g., (Nd/Yb)_{SN} > 0.4) and lower Y/Ho ratios (< 53) with higher concentrations of lithophile elements. Proximal seawater became 'cleaner' from ca 7000 years ago,

with opposing REY trends reflecting seawater with less terrigenous influence but showed marked mid-Holocene variability related to changing regional climatic factors. The strong fluctuation between intervals of high and low relative terrigenous sediment influence correlates well with particular regional and more global climate records, such as, the Indian-Australian Summer Monsoon (IASM) strength, high turbidity periods at 7.0, 5.4, and 2.7 ka BP with dampened El Niño Southern Oscillation (ENSO) frequency and fluctuations in local relative sea level. Water quality improved significantly after 3200 yrs BP.

The new microbialite geochemical record provides a fully independent new water quality proxy and a means to interpret reef growth dynamics in relation to changing water quality associated with climate evolution at centennial to millennial scales. Such records provide valuable context for predictions of modern reef behaviour in a changing world where coastal water quality is more likely to decline than to improve.

Insights into palaeo-hydrology of the Coorong Lagoon, South Australia, based on Strontium Isotope Tracers ($^{87}\text{Sr}/^{86}\text{Sr}$ and $\delta^{88/86}\text{Sr}$) in fossil carbonates

Shao, Yuexiao^{1,2}, Woolston, Zara¹, Farkaš, Juraj^{1,2}, Chamberlayne, Briony¹, Tibby John³, Haynes, Deborah¹, & Tyler, Jonathan¹

¹Department of Earth Sciences, School of Physical Sciences, University of Adelaide, Australia; ²Metal Isotope Group (MIG), University of Adelaide, Australia; ³Department of Geography, Environment and Population, School of Social Sciences, University of Adelaide, Australia

The Coorong lagoon, as part of the wetland system at the terminus of the River Murray, is recognised not only for its ecological importance but also for its unique geomorphology and salinity gradient that ranges from fresh/brackish (< 35 PSU) in the North Lagoon to hypersaline (> 70 PSU) in the South Lagoon. The lagoon hydrology is controlled by seawater-continental water mixing processes that are traceable via the radiogenic Strontium (Sr) isotopes ($^{87}\text{Sr}/^{86}\text{Sr}$ ratios). The hypersaline South Lagoon, being more geomorphologically restricted, is known for high degree of evaporation, which leads to ongoing calcium carbonate precipitation, which also acts as a sink for dissolved inorganic carbon (DIC) [1]. These processes involving carbonate formation and a local inorganic carbon cycling are traceable via the novel stable Sr isotope ($\delta^{88/86}\text{Sr}$), which is particularly sensitive to mass-dependent isotope fractionation linked to carbonate precipitation / dissolution. Importantly, the South Lagoon has seen dramatic hydrological and ecological changes over the last ca 200 years (since the European settlement), which is evident from geochemical and diatom records of the Coorong sediment cores [2] and has implications for water resource management and future strategies for the recovery of local ecosystem to more natural conditions [3]. In order to reconstruct paleo-hydrology of the Coorong before and after the European settlement, this study calibrated the $\delta^{88/86}\text{Sr}$ fractionation between recent aragonitic bivalve shells (*Arthritica helmsi* species) and local water in the modern Coorong lagoon, and a constant difference of $\delta^{88/86}\text{Sr}$ between

the shells and the local water $\Delta^{88/86}\text{Sr}$ ($\delta^{88/86}\text{Sr}_{\text{solid}} - \delta^{88/86}\text{Sr}_{\text{water}}$) = -0.92 ‰ was discovered. Such calibrations, coupled with $^{87}\text{Sr}/^{86}\text{Sr}$ and $\delta^{88/86}\text{Sr}$ analyses of fossil *A. helmsi* shells from a sediment core in the South Lagoon, are complemented by radiocarbon dating and elemental concentration data, to better constrain (i) variability in the mixing of water sources in modern Coorong and over the last ca 2500 years, and (ii) to reconstruct palaeosalinity changes and associated carbonate precipitation/dissolution processes. Primary results based on $^{87}\text{Sr}/^{86}\text{Sr}$ of shells indicated the source of water in the South Lagoon were never purely marine, however, according to $\delta^{88/86}\text{Sr}$ of the shells, the the South Lagoon in the past ca 2500 years was probably less evaporated than it has been in recent times (i.e., post European settlement).

[1] Shao *et al.* (2018), *Geochimica et Cosmochimica Acta*, 239, 90–108.

[2] McKirdy *et al.* (2010) *Organic Geochemistry*, 41, 96–110.

[3] Brookes *et al.* (2018). Goyder Institute for Water Research Technical Report Series No. 18/04, Adelaide, South Australia. ISSN: 1839–2725.

Variations in mid- to late Holocene nitrogen supply to northern Great Barrier Reef *Halimeda* macroalgal bioherms

McNeil, Mardi¹, Nothdurft, Luke¹, Erler, Dirk², Hua, Quan³, & Webster, Jody M.⁴

¹Queensland University of Technology, Brisbane, Australia; ²Southern Cross University, Lismore, Australia; ³ANSTO, Lucas Heights, Australia; ⁴The University of Sydney, Australia

The northern Great Barrier Reef (GBR) *Halimeda* bioherms have accumulated on the outer continental shelf from calcium carbonate algal sediments over the past ca 10 000 years and cover >6000 km² of shelf area. As such, *Halimeda* bioherms play a key role in the shallow marine carbon cycle over millennial timescales. The main source of nitrogen (N) to these bioherms is thought to be westward transport of upwelled NO₃⁻-rich water from the Coral Sea. However, the primary N source has not been traced geochemically, and we have no understanding of any temporal variation. Here, we reconstruct patterns of N supply to *Halimeda* bioherms in the GBR since the mid-Holocene using the ¹⁵N/¹⁴N ratio of skeletal-bound organic N ($\delta^{15}\text{N-SOM}$) in modern and fossil *Halimeda* sediment cores.

Average *Halimeda* skeletal $\delta^{15}\text{N-SOM}$ was 6.28 ± 0.26‰, consistent with $\delta^{15}\text{N-NO}_3^-$ from western tropical South Pacific (WTSP) thermocline waters. Thus geochemically validating shelf-break upwelling of an oceanic N source that appears to regulate the *Halimeda* bioherm spatial distribution. *Halimeda* $\delta^{15}\text{N-SOM}$ decreased by 1–2 ‰ from 5000 to 2000 cal. yr BP, reaching a minima of 5.5‰ that persisted for almost 1000 years. The *Halimeda* $\delta^{15}\text{N-SOM}$ variation reflects mid- to late Holocene changes in regional climate and intensified El Niño activity that likely facilitated elevated N₂ fixation in the WTSP, thereby lowering thermocline $\delta^{15}\text{N-NO}_3^-$. Thus, *Halimeda* skeletal material provides a valuable high-resolution geochemical archive of past oceanographic and climatic processes over centennial to millennial timescales, complementing existing paleoclimate proxy records.

Solution pipes and focussed vertical water flow in carbonates with matrix porosity

White, Susan¹, Lipar, Matej², Szymczak, Piotr³, & Webb, John¹

¹*Environmental Geoscience, Department of Ecology, Environment and Evolution, La Trobe University, Melbourne, Bundoora, VIC 3086, Australia;* ²*Anton Melik Geographical Institute, Research Centre of the Slovenian Academy of Sciences and Arts, Gosposka ulica 13, SI-1000 Ljubljana, Slovenia;* ³*Institute of Theoretical Physics, Faculty of Physics, University of Warsaw, Pasteura 5, 02-093 Warszawa, Poland*

Focused vertical flow is one of the distinctive features of karst processes within porous calcareous media with matrix porosity, especially in calcarenites, and forms distinctive features termed solution pipes. These are vertical cylindrical voids of variable diameter and depth predominantly in the vadose (epikarstic) zone. Although dissolutional in origin, the initial trigger that focuses the water flow in the host rock matrix is poorly understood, although they appear to be related to vegetation and rock heterogeneities.

Measuring of the morphology of pipes e.g., pipe diameter, depth, density and shape, is common but has not resolved the problem and neither has a 2D statistical data based on 5 x 5 m area in Australia which included inside and outside diameter of the pipes, their elongation, the thickness of cemented rim, and distance and direction to nearest neighbour. The stratigraphy, mineralogy, fabric and geochemistry of the surrounding rock and pipe rims and fills provide insights into pipe formation but do not address the issue of focussed flow. Thin section and X-ray diffraction has been used to distinguish between rim and host rock fabric. Stable isotope analysis partly correlated with host rock age indicates that the dissolutional process is under vadose conditions. Dating of the rim cement has not been successful due to the minute size of the carbonate cement samples. And the rock clasts of the host rock are obviously older.

Triggers to flow include lithological irregularities e.g., cracks in calcrete, surface geomorphology e.g., potholes and vegetation e.g., stem flow, buried tree trunks. If these are not present the instability of the wetting front infiltrating into the unsaturated zone breaks advances into unsaturated host rock as self-organised fingers. This fingered flow, a non-uniform accelerated transport of sinking water, through the porous material due to an unstable wetting front, is particularly favoured if the media is water repellent, which causes uneven infiltration.

The roles of dynamic instabilities and self-organisation in the emergence of focusing patterns and the various challenges, especially in the vadose zone, can probably be only resolved with modelling, conjunction with field data. From the numerical point of view, modelling of solution pipe formation requires solving the coupled equations for the groundwater flow, chemical transport and porosity evolution. The ground-water system may be either saturated, or partly or completely unsaturated. Morphologically similar pipes seem to develop under both conditions. Pipes formed in deglaciated Miocene sediments in Poland can be modelled using Darcian flow equations. However, the pipes found in unglaciated areas e.g., Cape Bridgewater, Victoria, were clearly

formed by dissolution in the unsaturated (vadose) so this model is inappropriate. However, the Richards equation applies a continuity requirement resulting in a general partial differential equation describing water movement in unsaturated non-swelling media. This appears to be the best option for modelling water flow in the vadose zone

As most solution pipes form under vadose conditions and show potential as palaeoclimatic indicators, further understanding of their formation and behaviour is important.

Quantifying the Dolomite problem and its impacts on Mg/Ca change through time

Opdyke, Bradley

Global dolomite deposition has declined globally throughout the Cenozoic. While the volumes of other sedimentary rocks increase from the Paleocene to the Holocene. This anomaly has been called the 'dolomite problem' and recognized since the time of Darwin. Recently my team discovered that crustose coralline algae (CCA) does precipitate calcium-magnesium carbonate with a dolomite chemistry. CCA is not as abundant on immature reefs as mature reefs, in fact CCA 'crusts' only become thick and widespread once a significant portion of the reef flat has been located within the tidal zone for many thousands of years. In a world where sea level is moving up and down like a Milankovitch driven yo-yo it is rare for these algal facies to become established, hence dolomite precipitation is rare. Recent sea level studies and compilations of stable isotope records from the Eocene to the Holocene allow us to model the probable trajectory of dolomite deposition over this time interval and calculate the probable Magnesium-Calcium ratio change in sea water. At the present time we only have a few 'tie points' for the Mg/Ca over this time. Using the stability of sea level as a driver of dolomite production we can predict more precisely how the Mg/Ca ratio has increased from 2.5 at the Eocene/Oligocene boundary to 5.1 in modern sea water.

Paleoatmospheric CO₂ oscillations through a cool mid-Late Cretaceous recorded from pedogenic carbonates in Africa

Orr, Theresa J.¹, Roberts, Eric M.², Wurster, Christopher M.¹, Singleton, Russell E.¹, Lawrence, L.², & Mtelega, Cassy³

¹Department of Geosciences, James Cook University, Cairns, Australia; ²Department of Geosciences, James Cook University, Townsville, Australia; ³Department of Geosciences, University of Dar es Salaam, Dar es Salaam, Tanzania

Pedogenic carbonates are valuable terrestrial climate archives of past atmospheric, climatic and environmental conditions. The stable isotope composition of pedogenic carbonates preserves a record of ancient atmospheric CO₂ concentration and temperature at the time of mineral precipitation. While pedogenic carbonates have been used extensively as proxies to reconstruct past climates, few studies have been conducted on the climate of mid-Late Cretaceous Africa. The paucity of paleoclimate data from the region represents a significant obstacle in interpreting past climate change, and thus our ability to predict future changes. The preservation of pedogenic carbonates in the Galula Formation of southwest Tanzania provides an opportunity to enhance our understanding of the paleoclimatic conditions of the mid-Late Cretaceous. The Cretaceous Galula Formation is a fossiliferous continental sedimentary succession of braided fluvial deposits that are well-exposed in the river drainages of the Rukwa Rift Basin. This study presents the first estimated atmospheric CO₂ concentrations for the mid-Late Cretaceous derived from pedogenic carbonates from Africa. Paleosol carbonate nodules were sampled from seven Bk-horizons located throughout ~500 m of the Galula Formation stratotype section, including four from the lower Mtuka Member (Aptian–Cenomanian) and three from the upper Namba Member (Cenomanian–Campanian). Oxygen isotope values averaged -5.6‰ and -7.2‰ VPDB for the Mtuka and Namba members, equating to mean annual temperatures of 14.5 °C and 11.2 °C, respectively. Using the stable isotope composition of pedogenic carbonates from the Mtuka Member, an average pCO₂ of 1390 ppm was estimated for the Aptian–Cenomanian, before declining to an average of 740 ppm in the Namba Member, during the Cenomanian–Campanian. Atmospheric pCO₂ fluctuated through the mid-Cretaceous, rising to a peak of 1900 ppm, before falling to the lowest concentration of 990 ppm, corresponding to the cool greenhouse period that spanned the Aptian–Albian. The gradual decline in pCO₂ (930 ppm to 620 ppm) recorded in the paleosols of the Namba Member occurred during Late Cretaceous cooling following the Cretaceous Thermal Maximum. This work indicates that the mid-Late Cretaceous was not a continuous greenhouse climate, and that an episodic climate mode prevailed, rather than a monotonic increase or decrease in pCO₂ and temperature throughout the geologic period.

Sedimentary deposits: Earth and planetary processes

Preservation of ancient eolian landscapes beneath flood basalt: an example from the Officer Basin, Western Australia

Haines, Peter

Geological Survey of Western Australia, Perth, Australia

Eolian landscapes should be common on planets with an atmosphere and were presumably more widespread on Earth before the evolution of land plants. However, preservation of intact ancient eolian landscapes from this time period are rare. The Ediacaran to middle Cambrian succession of the Western Australian (WA) Officer Basin is dominated by eolian sandstone with interbedded alluvial fan, fluvial and playa deposits. Outcrops of this succession near the western end of the basin (McFadden Formation) include eolian foresets on a massive scale, possibly exceeding 60 m in height. Farther east, the broadly equivalent concealed Lungkarta Formation displays steeply dipping single foresets up the 30 m in thickness in drill core, and other sedimentary features confirming an eolian mode of deposition. In the central Officer Basin in eastern WA this eolian sandstone succession is overlain by the basaltic Table Hill Volcanics (THV), a component of the widespread ca 511 Ma (middle Cambrian) Kalkarindji Large Igneous Province of flood basalts and associated intrusions. Although rarely exposed, the distribution of the flat-lying THV can be mapped from drill hole intersections and aeromagnetic datasets. In one area the aeromagnetic patterns indicate that the basalt flowed over and entombed an active dune field. Near the southern margin of the flood basalt the flows thinned to be thinner than the height of the dune crests, allowing the dunes (relatively non-magnetic) to be clearly distinguished from the interdune corridors (filled with magnetic basalt). The resulting aero-magnetic patterns, enhanced by viewing the first vertical derivative of the total field data, indicate south-southwest-trending compound linear dune ridges, each separated by parallel interdune corridors. The parallel basalt flows terminate southward along an irregular north-northwest-trending boundary that was likely controlled by an inflection in the paleoslope. Details of dune morphologies indicate east-northeast directed prevailing winds, somewhat oblique to the east-southeast migration direction the overall composite linear dune crests. Modern analogues can be found in extremely arid vegetation-free dune areas such as the Rub' Al-Khali sand sea of southern Saudi Arabia. A particularly good match is found in the east of this extensive sand sea (near 21°N, 54°E). This area likewise shows compound linear dune ridges moving obliquely to the prevailing wind direction indicated by the orientation of smaller scale dune components, although the interdune corridors are broader than the Officer Basin example. Coincidentally, the ancient Officer Basin dune crest spacing (1–1.5 km) is similar to that of the modern vegetation-stabilised longitudinal dunes of the Great Victoria Desert in the same area today, although dune type is different and inferred crest heights are significantly greater in the ancient deposit. Apart from revealing the morphology of an ancient eolian landscape, the relationship with the dated basalt

can now be used to infer a precise date for the top of this previously poorly dated succession, as the dunes were apparently active at the time of entombment in the middle Cambrian. Similar burial of eolian and fluvial landscapes are suggested by aeromagnetic patterns elsewhere in the Kalkarindji Large Igneous Province.

Correlation of stratigraphic sequences to evaluate downstream transitions within the Wonoka canyon at Umberatana syncline, South Australia

Giles, Sarah M., & Christie-Blick, Nicholas

Lamont-Doherty Earth Observatory of Columbia University, Palisades, NY 10964, USA

Mid-Ediacaran (ca 580 Ma) paleocanyons as much as 1 km deep in the Wonoka Formation of South Australia are associated with the largest carbon-isotope excursion in Earth history, the Shuram anomaly. Widely interpreted as submarine, the canyons are thought by many to be comparable to those found at modern continental margins. New data from the northern Flinders Ranges reinforce an alternative hypothesis: that the Wonoka canyons were subaerially incised as a result of evaporative drawdown in a temporarily isolated marine embayment at the onset of the Gaskiers glaciation. Critical supporting evidence has emerged in the canyon-fill at Umberatana syncline, where four oblique cross-sections interpreted as a single sinuous canyon are being independently analyzed. The three incisions studied so far are characterized at the base by ~30-m-thick conglomerate-based cycles that are bounded by laterally persistent erosion surfaces and fine upwards into sandstone, siltstone, and minor carbonate (canyon-marginal tongues). Nine such cycles are confidently correlated between the first two incisions (Fortress Hill and Mt. Curtis), and at least plausibly related to seven cycles identified in the third incision (Muccabaloona south) on the basis of 168 measured sections and high-resolution physical stratigraphic mapping. Our correlation of cycles is based on similarities in facies stacking and stratigraphic position. Greater variability in cycle thickness at Muccabaloona south is attributed to facies changes within some cycles in the direction of sediment transport from channelized boulder conglomerate to pervasively rippled sheet-like sandstone and siltstone event layers, as well as a northward increase in structural complexity. The local erosional relief at cycle boundaries is comparable across the three outcrops: 3–6 m at Fortress Hill, 5–10 m at Mt. Curtis, and 3–7 m at Muccabaloona south. The observed stratigraphic organization and details of the facies lead us to interpret the diffusely stratified, channelized conglomerates as fluvial, and the prevalently rippled and laminated tabular sandstones/siltstones as deltaic. The lack of dish structures and nested channels in the sandstone facies, as well as the apparent absence of classical turbidites interstratified with hemipelagic mudstone further supports our fluvial-deltaic interpretation rather than a deep marine interpretation. An upward transition to primarily siltstone event layers interstratified with cm-scale carbonate couplets and monolithologic breccias is interpreted to represent canyon drowning. New field work is planned at the fourth incision (Muccabaloona north) to further test our model. We expect fewer conglomerate-based cycles, and additional fining

overall. The correlation of stratigraphic cycles across all four incisions will allow us to evaluate the length scale of downstream facies transitions, which we expect to be much more abrupt in the subaerial incision model than the deep marine canyon interpretation.

Quantifying lateral and distal variability within hybrid beds, case studies from Central and Northern Italy

Brooks, Hannah L.¹, & Steel, Elisabeth²

¹School of Earth Sciences, 253-283 Elgin St, University of Melbourne, Carlton VIC, Australia; ²Department of Geological Sciences and Geological Engineering, Bruce Wing/Miller Hall, 36 Union Street, Queen's University, Kingston, Ontario, Canada.

Hybrid beds or linked debrites are deposits that form under bi- or tri-partite flow conditions, involving both turbulent and laminar flow conditions. Often, hybrid beds occur with distal or lateral flow transformation following significant entrainment of a muddy substrate and/or declining turbulent energy. Hybrid beds have been noted to make up significant proportions of deposits within basin floor setting worldwide, most commonly within the distal fringes of lobe systems. The study examines dip and lateral variations in facies and architecture in hybrid beds using detailed facies analysis of selected sections within the Castagnola, Marnoso-Arenacea and Gottero formations, deposited within three different basins within central and northern Italy. Sections within these systems were selected where hybrid beds could be traced out laterally or down-dip for several metres to several kilometres. In total 407 samples were taken for laser-diffraction grain-size analysis. Samples were selected through beds at 20 cm intervals and across/ down-dip at 10's of metre to several kilometre intervals. Layers within beds were classified into facies divisions which were ran through 'EMMA 'End Member Modelling Analysis, this splits beds into an optimum number of end members that when combined create the trends found within the dataset. This method is utilized to establish patterns of changes within beds laterally and down-dip which are otherwise difficult or too complex to be quantified from field data alone.

This detailed study of facies, architectural and grain-size changes within the targeted deposits will help to establish how flow processes varied as flows spread laterally and moved downstream. Through quantifying the amount of mud within the matrix and clasts at any one time within the flow it is possible to interpret how and when turbidites and hybrid beds erode and incorporate sediment from underlying substrate. Initial results from EMMA indicate that using three end members for each formation is an optimum number for observing basal trends within beds. These end members constitute a sand-rich unimodal end member, a silt-rich unimodal end member, and a bimodal poorly sorted end member, interpreted to represent a high-density turbidite, a low-density turbidite and a debrite respectively. Recognised trends within the data include a decrease laterally in the sand-rich unimodal end member within the Marnoso-Arenacea section, interpreted as an increased distance from the flow input or the presence of a lateral basin slope. Through application of this methodology in basins with well-established bed correlation it is possible to provide

novel understanding that will significantly augment traditional field techniques. It is evident that laser diffraction grain-size analysis and EMMA are vital tools in furthering our understanding of process sedimentology and should be applied more widely.

Reviewing stratigraphic units defined in the ACT

Marais-van Vuuren, Christo, Brown, Catherine, & Jarrett, Amber

Geoscience Australia/GSA ACT and External Territories Stratigraphy Subcommission, Canberra, Australia

The usual role for Australian Stratigraphy Commission members in most of Australia is to assist geologists writing up unit definitions or redefinitions, in areas of recent study <http://www.ga.gov.au/data-pubs/datastandards/stratigraphic-units/unit-definition-form>. The situation in the ACT is a bit different. Although there has been recent mapping work in surrounding areas of NSW, and recent geochronology done on 9 units in the ACT, there has been no new mapping or revision of geological units in the ACT since Bob Abell's (1991) Geology of the Canberra 1:100 000 sheet area, which only covers the northeastern part of the ACT. Geological mapping over the rest of the ACT (Brindabella, Tantangara and Michelago sheets) is even older. Many of the original unit descriptions and definitions were done by Armin Opik in 1958. Some of these have never been revised.

Prior to self-government in the Australian Capital Territory (ACT), the Bureau of Mineral Resources had an engineering geology and mapping role in the Territory, but that role has not been maintained at either local or federal level. So, given the urban development and other landscape modifications in the ACT, the ACT Stratigraphy Subcommission has decided it would be useful to review the type section locations of units defined in the ACT. The initial aim is to make it easier to find most of them, but we will also need to consider replacement type sections/type areas, in cases where the original is no longer accessible, and possibly some additional reference sections too.

There are 78 current stratigraphic units identified in the ACT, many of them also extending into NSW. At least 22 of those units have been defined/redefined in the ACT. All of the type sections or type areas need locations revised to a modern, known co-ordinate system (GDA 2020). It is already clear that locating some of the type sections will involve some historical research and comparison of old maps with modern ones. We have also identified that some of the original locations are no longer accessible due to road realignments, modification or 'treatments' of road cuttings, flooding (creation of artificial lakes) etc. Where type or reference sections have been nominated in drill core, we need to ascertain whether or not the core is still accessible, as well as the location of the hole.

The project is in the early stages and has started with a review of the information available through the Australian Stratigraphic Units Database <http://www.ga.gov.au/data-pubs/datastandards/stratigraphic-units> and information in other Geoscience Australia and ANU databases. We expect the review will lead to some local field trips and hope that our work may encourage further review of

ACT geology generally, to improve edge-matching with more recent geological work by the Geological Survey of New South Wales, in particular.

Ultimately this work will represent a major update to type section understanding and definitions of stratigraphic units in the ACT, which is decades overdue. If it also encourages some other old definition reviews, that would be a bonus.

A Pb isotope regolith map of Australia

Desem, Candan¹, Maas, Roland¹, Woodhead, Jon¹, Carr, Graham², & de Caritat, Patrice³

¹The University of Melbourne, Parkville, Australia; ²CSIRO, North Ryde, Australia; ³Geoscience Australia, Canberra, Australia

The lead (Pb) isotopic composition of the regolith reflects contributions from bedrock geology, mineralisation, wind-blown dust and anthropogenic contamination (industry, transport, agriculture, residential, waste handling). Evaluating the relative roles of each contribution is critical to many studies ranging from attempts to capture the history and extent of Pb pollution through to mineral resource exploration programs. To this end we have produced the first Pb isotope map of Australia's regolith at a continental scale. Catchment outlet (~ floodplain sediment) samples collected for Geoscience Australia's National Geochemical Survey of Australia (NGSA) program, with an average sampling density of 1 site/5200 km² and covering ~ 81% of the Australian continent, were utilised here. The coarse grain-size fractions (<2 mm) of the top outlet sediment (0–10 depth) samples were selected.

A number of acid leaching protocols have been devised to separate loosely bound Pb (e.g., aerosol from anthropogenic contamination) from Pb structurally bound in minerals (from the underlying geology, mineralisation, or their weathering products). We utilised a sequential leach protocol with ammonium acetate followed by aqua regia (HNO₃–HCl), originally developed by Mike Korsch and Graham Carr at CSIRO. Ammonium acetate is expected to extract loosely bound Pb sourced from windblown dust (including anthropogenic contributions) or from shallow groundwater interaction. Pb extracted using the more aggressive aqua regia step represents the underlying geological signature. Pb isotope compositions were acquired using a sector-field ICP-MS, which provided 'fit for purpose' levels of precision/accuracy and the high throughput required in order to process large sample sets – more than 1500 samples in this case.

Our research program aims to (i) compare the Pb isotope signatures released by the two leach protocols, (ii) examine if soil Pb isotope mapping can identify underlying geology and metallogenic provinces, and (iii) investigate anthropogenic signals across the continent. Preliminary analysis of the data obtained for the aqua regia leachates shows clear and distinct trends reflecting the underlying bedrock geology. For example, the Archaean rocks of the Yilgarn and Pilbara Cratons are marked by regolith with more radiogenic Pb isotope compositions, while regolith samples from younger geological provinces (e.g., Tasmanides of eastern Australia) have less radiogenic Pb isotope signatures. Other geological elements (e.g., Gawler Craton, Curnamona Province) are also clearly distinguished.

Preliminary Pb isotope maps of the continent will be presented.

Ediacaran stratigraphy in the western part of the Northern Territory Amadeus Basin, central Australia

Verdel, Charles, Donnellan, Nigel, Normington, Verity, & Simmons, Jack

Northern Territory Geological Survey, Alice Springs and Darwin, Australia

Neoproterozoic stratigraphic nomenclature has historically differed between the eastern and central to western parts of the Amadeus Basin, leading to issues in basin-wide correlation and evaluation of potential lateral facies changes. In the more extensively described eastern part of the basin, the major Ediacaran lithostratigraphic units are (in ascending order) the basal Ediacaran cap carbonate of the Olympic Formation, Pertatataka Formation, Julie Formation, and latest Ediacaran lower Arumbera Sandstone. New mapping has revealed that most of these units correspond with parts of the informal and historical “Winnall beds” of the central and western Amadeus Basin. The new, formally defined Winnall Group spans Ediacaran to perhaps Cambrian time and consists of five formations: in ascending order, the Breaden, Gloaming, Froud, Liddle, and Puna Kura Kura formations. In the westernmost part of the Northern Territory Amadeus Basin (i.e., the region stretching from approximately Watarrka (Kings Canyon) National Park to the Western Australia border), the main part of the Winnall Group that is exposed is the Liddle Formation, a succession of cross-bedded sandstone that reaches a thickness of approximately 500 m. Lithostratigraphic comparison with the eastern Amadeus Basin suggests that the Liddle Formation is partly or entirely correlative with carbonate of the Julie Formation, and extensive detrital zircon U–Pb data from the Liddle Formation are permissive of a mid to late Ediacaran age assignment. The Liddle Formation may be a stratigraphic counterpart of the late Ediacaran Bonney Sandstone in the Adelaide Superbasin of South Australia.

Allocyclic controls on shoreface sedimentation from the Late Cretaceous to Miocene, Gippsland Basin, SE Australia

Mahon, Elizabeth, & Wallace, Malcolm

University of Melbourne, Melbourne, Australia

Shoreface deposits can act as excellent proxies for basinal conditions, recording relative sea level fluctuations and tectonic episodes as changes in sediment type, and depositional architecture. The Gippsland Basin contains a continuous succession of amalgamated clastic shoreline deposits from the Cretaceous to present day. This basin has experienced a number of major tectonic, eustatic, climatic and oceanographic events during the Cenozoic. From the Late Cretaceous to the Miocene, stacked shoreface deposits display progradational to transgressive geometries. Despite a range of significant allocyclic events, these shoreface deposits are predominantly transgressive, and strong basinal subsidence appears to be one of the major driving forces controlling shoreline behaviour.

Paleoflora and environment of the Surat Basin at the time of the JK transition

Cooling, Jennifer¹, Esterle, Joan¹, & McKellar, John²

¹*School of Earth and Environmental Sciences, University of Queensland, Brisbane, Australia;*

²*Department of Natural Resources, Mines and Energy, Brisbane, Australia*

The Westbourne Formation to Mooga Sandstone interval of the Surat Basin contains the most complete record of deposition from Queensland from the time of the Jurassic–Cretaceous transition. As relatively few botanical macrofossils have been reported from this interval, and few of those have been well described, palynological studies, such as the one presented here, provide the best window into the region’s flora just before the arrival of the angiosperms. Palynological samples taken from three stratigraphic boreholes that intersected this interval produced a diverse, but relatively stable, microflora of 218 taxa. Fern spores are the most abundant component of assemblages, averaging 51 percent of all samples, in particular those of the Osmundaceae and Matoniaceae. Spores produced by the Dicksoniaceae, Gleicheniaceae, Horsetails, Marattiaceae, Schizaeaceae, Pteridaceae and Polypodiaceae are also represented. Averaging 20 percent of all assemblages the spores of the lycopods were the second most abundant group and were the most taxonomically diverse. Conifer pollen averaged 17 percent of all assemblages with that produced by the Araucariaceae being the most common of these. Pollen from the Cheirolepidaceae, Podocarpaceae, Pinaceae and Taxodiaceae is also recorded in these samples. Pollen produced by the seed ferns averaged five percent of all samples, while spores produced by bryophytes averaged less than two percent and the monocolpate pollen that may have been produced by some combination of cycads, ginkgoes and gnetales less than one percent of all assemblages. While the link between palynoflora and macrofloral abundances is not a direct one, being influenced by sedimentological and taphonomic effects, some broad conclusions about the parent flora can be made. The Surat Basin flora of the mid-Tithonian to early Hauterivian was a diverse one, with a floodplain (from where these samples were taken) flora dominated by members of the Matoniaceae and Osmundaceae along with numerous other species of ferns, lycopods and bryophytes. The somewhat drier upland flora is represented by the Araucariacean conifers with the seed ferns and the Podocarpacean and Cheirolepidacean conifers producing much of the remaining upland palynoflora assemblage.

With their high proportion of fern spores to conifer pollen, the majority of the samples from this project can be recognized as coming from a backswamp or floodplain facies. This paleoenvironmental interpretation supports the view that the Westbourne Formation to Mooga Sandstone sequence was, like much of the Australian Late Jurassic sequence, deposited in a highly fluvial environment of meandering and braided streams, shallow lakes and swampy floodplains. This interpretation is further supported when the contributions of different palynomorph ecogroups (PEGs) to the assemblages are considered and the results of polytopic vector analysis (PVA) of the assemblages.

High-resolution rapid thermal neutron tomographic imaging of fossiliferous cave breccias from Southeast Asia

Smith, Holly Ellen¹, Bevitt, Joseph², Garbe, Ulf², Zaim, Jahdi³, Rizal, Yan³, Aswan, Puspaningrum³, Mika Rizki³, Trihascaryo, Agus³, Price, Gilbert J.⁴, Webb, Gregg⁴, & Louys, Julien¹

¹*Australian Research Centre for Human Evolution, Environmental Futures Research Institute, Griffith University, Brisbane, Queensland 4111, Australia;* ²*Australian Centre for Neutron Scattering, Australian Nuclear Science and Technology Organisation, New Illawarra Rd, Lucas Heights, NSW 2234;* ³*Geology Study Program, Institut Teknologi Bandung, Jawa Barat 40132, Indonesia;* ⁴*School of Earth and Environmental Sciences, Faculty of Science, University of Queensland, Brisbane, Queensland 4001, Australia*

Tomographic imaging is gaining importance amongst palaeontologists as a non-invasive approach to studying fossil remains. Traditional methods of preparing a fossil risks damage to the specimen and destroys contextual evidence in the surrounding matrix. CT imaging can reveal the internal composition and structure of buried fossils and consolidated sediment matrices before any destructive mechanical or chemical preparation. Neutron tomography (NT) discerns denser matrices impenetrable to CT imaging, however, this approach remains relatively under-utilised in palaeontology. We employ high-resolution rapid thermal neutron tomographic imaging to visualise internal diagnostic features of dense fossiliferous breccia from three Pleistocene cave localities in Sumatra, Indonesia. We demonstrate that these seemingly homogeneous breccia are an excellent source of data to aid in determining taphonomic and depositional histories of complex depositional sites such as tropical caves. The breccia subsamples retain excellent details of site formation history and results suggest the primary agents in the formation of the breccia and concentration of incorporated vertebrate remains are several rapid depositional phases of water and sediment gravity flow. This study highlights the potential for analyses of breccia deposits in palaeontological studies in Southeast Asian caves in the future.

How the zebra rock got its stripes: origin of hematite banding in East Kimberley siltstones

Coward, Andrew J.¹, Slim, Anja C.¹, Brugger, Joël¹, Wilson, Siobhan A.², Pillans, Bradley J.³, & Williams, Tim⁴

¹*School of Earth, Atmosphere and Environment, Monash University, Clayton, VIC 3800, Australia;* ²*Department of Earth and Atmospheric Sciences, University of Alberta, Edmonton, AB T6G 2R3, Canada;* ³*Research School of Earth Sciences, Australian National University, Canberra, ACT 0200, Australia;* ⁴*Monash Centre for Electron Microscopy, Monash University, Clayton, VIC 3800, Australia*

Zebra rock is an Ediacaran paleosol unique to the East Kimberley region of Western Australia, renowned globally for its highly regular and unusual red and white banding. The underlying mechanisms behind the self-organisation of zebra rock patterns has remained an

enduring question ever since the first scientific studies of the ornamental stone in 1926 and continues to fascinate geologists to this day. Many theories have been proposed to explain the formation of these unique patterns, including the infilling of ripple beds, Liesegang banding, and ferronematic liquid crystals, but no definitive consensus has yet been reached, in part due to the lack of supporting chemical and mineralogical analysis.

Twenty-five zebra rock samples were analysed from five different outcrops across the Lake Argyle region using a variety of analytical techniques, including XRD, SEM, TEM, LA-ICP-MS and X-Ray CT imaging. The principle pigment of zebra rock was found to be exclusively hematite in all cases, a result consistent with previous studies. Within the dark banding, hematite manifested as large (1–10 µm) aggregates of nanoscale (200–500 nm) hexagonal platelets distributed within the interstitial spacing between larger quartz and kaolinite grains. Large (100 µm), polycrystalline hematite was also observed within the white bands, although at significantly reduced abundance (<1 wt%). Hexagonal platelets and needle-like crystals of hematite were observed in the overlying, iron-rich host shales, while the comparatively iron-poor, underlying shales exhibited a random arrangement of large iron-oxide nodules and dissolution voids.

Zebra rock mineralogy was found to be highly variable on a regional scale. Across the five deposits examined, four distinct mineralogical assemblages were identified, each defined by the absence or presence of one or more of alunite, muscovite and dickite as major phases. Each of these four assemblages contained key indicator minerals suggestive of argillic and advanced argillic hydrothermal alteration, most prominently dickite, kaolinite, alunite and, in low amounts, svanbergite and pyrophyllite. All four mineral assemblages can each be correlated with a different degree of argillic and advanced argillic alteration, suggesting a gradual neutralisation of acidic hydrothermal fluids as they progressed laterally along permeable bedding. On a local, outcrop scale, zebra rock mineralogy was found to be largely homogeneous, with no mineral phase other than hematite exhibiting consistent concentration gradients between the dark and light bands. Trace elements followed a similar pattern, with no consistent concentration gradients outside of significant enrichment in the dark banding of V⁵¹, Cr⁵², Mn⁵⁵, Co⁵⁹, Ni⁶⁰ and Mo⁹⁵, elements all known to strongly adsorb to hematite. Curiously, no HREE enrichment was detected, as might otherwise be expected in hydrothermal systems.

On the basis on the above findings, we propose two alternative hypotheses to explain the development of zebra rock patterns: (1) high temperature, argillic hydrothermal alteration in conjunction with the formation of the 510 Ma Kalkarindji large igneous province or (2) low temperature acid-sulphate weathering in anoxic, waterlogged soils during the Ediacaran. Dating techniques, such as paleomagnetic analysis and stable O isotopes, are required to determine which of these two mechanisms is responsible for the hematite patterns of zebra rock.

Understanding the nature transition of the Late Jurassic formations of the Surat Basin through borehole image logs using cumulative dip plots

de A V Filho, Claudio Luiz¹, Sobczak, Kasia², Holl, Heinz-Gerd², Hurter Suzanne², & Vasconcelos, Paulo¹
¹*School of Earth and Environmental Science, the University of Queensland, Brisbane, Qld, Australia;*
²*UQ Centre for Natural Gas, the University of Queensland, Brisbane, Qld, Australia*

The Surat Basin located on the border of Queensland and New South Wales is one of the most prominent coal-bearing basins in Australia. Over the past decade, the basin has become one of Australia's largest and most productive coal seam gas (CSG) provinces, with major reservoirs discovered in the Middle–Late Jurassic Walloon Coal Measures.

The Walloon Coal Measures are directly overlain by the Late Jurassic Springbok Sandstone, which has been characterised as a regional aquifer. This raises major environmental concerns regarding the connectivity between the two formations and potential impact of coal seam gas exploration and production from the Walloon Coal Measures on local groundwater reservoirs in the Springbok Sandstone. Therefore, there is a pressing need for a good understanding of the relationship between the two formations, and accurate modelling of reservoir interconnectivity. Despite the growing interest in the Springbok Sandstone, however, the nature of the boundary between the two formations remains unclear. Thus, this study aims to better characterise the Walloon–Springbok contact using high-resolution image log analysis in five wells in the northeastern Surat Basin. Measured bedding-plane orientations are presented on cumulative dip plots that allow precise location of shifts in dip directions and angles related to unconformities, sequence boundaries and structural features.

The analysis revealed the presence of a distinct inflection point on the cumulative dip plot between the Walloon Coal Measures and the Springbok Sandstone in only one of the analysed wells. This inflection point reflects a shift in bed orientation that may indicate an unconformity. Conversely, the remaining four wells did not show a significant change in dip magnitude and azimuth at the base of the Springbok Sandstone, suggesting that there is no major or regional unconformity, contrary to previous studies. Additionally, several significant inflection points were observed in the Walloon Coal Measures in all five wells, indicating possible major time gaps in sediment accumulation within the formation, rather than at the formation boundary. These findings largely support recently published depositional ages from U–Pb zircon dating of tuffs that suggest the presence of an unconformity within the Walloon Coal Measures.

The image log analysis used in this study provides new constraints on depositional continuity and unconformity distribution in the CSG-producing formations of the Surat Basin. A more extensive application of this approach across the basin in the future will allow assessing the magnitude and regional extent of the identified unconformities.

Cryogenian syn-glacial carbonates and implications for a snowball Earth

Hood, Ashleigh¹, Penman, Donald², Lechte, Maxwell³, Wallace, Malcolm¹, Giddings, Jonathan¹ & Planavsky, Noah²

¹*School of Earth Sciences, University of Melbourne, Parkville, Australia;* ²*Department of Geology and Geophysics, Yale University, New Haven, USA;* ³*Department of Earth and Planetary Sciences, McGill University, Montreal, Canada*

Perhaps the most extensive ice age in Earth's history, the Neoproterozoic was host to two globally extensive glaciations from ca 717–635 Ma. There has been ongoing debate as to the extent of ice coverage over the oceans during this time. The 'snowball Earth' theory suggests that during this time the Earth's surface was completely frozen, with marine ice sheets that sealed off the Earth's oceans from its atmosphere (Hoffman *et al.*, 1998, *Science*, 281, 1342–1346). A central tenet of this hypothesis is that carbonate could not precipitate from syn-glacial seawater due to a lack of alkalinity influxes into ice-covered, isolated oceans. These oceans would instead be dominated by chemical exchange with mid-ocean ridge volcanic systems, developing low pH (resulting in carbonate dissolution) and low Mg/Ca ratios (Hoffman *et al.*, 1998).

However, carbonate sediments are present in both of the Neoproterozoic (Sturtian and Marinoan) ice ages in global glacial successions. Further, Sturtian sediments of the Adelaide Fold Belt, South Australia have sedimentological evidence for dolomite precipitation from syn-glacial seawater. Discrete beds of dolomite and dolomitic silt (with a carbonate content of up to 72%) are present throughout the Sturtian Yudnamutana Subgroup, including in horizons over one kilometre stratigraphically below post-glacial strata. These carbonates may be deformed by sedimentary processes (e.g., dropstone emplacement) demonstrating their syn-sedimentary precipitation. Euhedral dolomite crystals appear to replace detrital (silicate) minerals and show no evidence of a detrital core, indicating an authigenic origin for the dolomite. The mid-Sturtian Warcowie Dolomite Mb. shows increasing carbonate content towards the upper bed surface, suggesting a seawater source for the dolomitising fluid.

The dolomite mineralogy of these syn-glacial sediments, as well as the post-glacial 'cap carbonates', is inconsistent with 'snowball Earth' Mg-poor glacial ocean conditions and implies that magnesium cycling (i.e., continental weathering) must have been active during the ca 57 million year Sturtian glaciation. Based on these observations, a recent Precambrian geochemical model (PreCOSCIIOUS) was modified to test the links between Sturtian carbonate mineralogy and environmental conditions. We found that around 9% of present continental chemical weathering during glaciation (i.e., not fully isolated oceans) is consistent with sedimentological observations and further supports the long timescale of glaciation.

Seismic-scale soft sediment deformation associated with subaqueous dewatering: an example from the continental shelf of the Otway Basin

Niyazi, Yakufu¹, Warne, Mark², & Ierodiaconou, Daniel¹

¹*School of Life and Environmental Sciences, Deakin University, Warrnambool, Australia;* ²*School of Life and Environmental Sciences, Deakin University, Burwood, Australia*

Soft-sediment deformations (SSDs) are created in unconsolidated sediments and are relatively common in finer-grained depositions. Numerous natural processes can induce the SSDs, including seismicity, glaciation, thermal activity, rapid deposition etc. And the deformation often occurs rapidly, close to the surface, during or shortly after burial. The SSDs have been documented as micro-scale under the microscopes to meter-scale in the field outcrops. Here we show an example of seismic-scale SSD that might have associated with the subaqueous dewatering processes.

The Plio-Pleistocene Whalers Bluff Formation of the offshore Otway Basin is composed of mixed siliciclastic-carbonate sediments. In seismic cross-section, this formation includes an interval that is formed of alternating depressional ponds and raised ridges. This interval is shallowly buried and lies between 40–150 ms two-way travel time below the present-day seafloor. The ponds are expressed as densely packed, circular to polygonal, and in some cases, hexagonal-shaped features in time slice maps. The ponds are 200–800 m in diameter and are separated by ~20 m wide ridges. The distribution and organization of these enigmatic features closely resemble the previously documented honeycomb-like structures (HSs). In our study area, they cover an area of 760 km², and some of them, especially those in the NE of the study area, are aligned strongly along the NW–SE trend-lines. The HSs or similar features have been documented by many studies and are related to the formation of the carbonate build-ups, polygonal faults, focused-fluid escape pipes, paleo-karsts, or soft sediment contraction accompanied by diagenetic processes. Seismic geomorphological and geospatial analysis indicate that the HSs might have been resulted from the bulk contraction of soft sediment, associated with shallow burial diagenesis processes such as subaqueous dewatering of the fine-grained successions within the Whalers Bluff Formation.

Reconstructing environmental conditions in a ca 2.4 Ga microbialite reef using Si isotope and trace element analyses

Soares, Georgia^{1,2}, Van Kranendonk, Martin^{1,2}, Scicchitano, Maria³, Nomchong, Brendan^{1,2}, & Barlow, Erica^{1,2}

¹*Australian Centre for Astrobiology, School of BEES, UNSW, NSW, Sydney, Australia;* ²*ARC Centre of Excellence for Core to Crust Fluid Systems, Macquarie University, NSW, Sydney, Australia;* ³*WiscSIMS Laboratory, Department of Geoscience, University of Wisconsin, Madison, USA*

Approximately 2.4 billion years ago during the Great Oxidation Event (GOE), following a series of

glaciations, a microbialite reef complex was deposited within the Turee Creek Group (TCG) in Western Australia. This reef is unique because it is well-preserved and contains an abundance of diverse types of both microbial and more cryptic life. The world's oldest known phosphorite made up of microbial mats, the first appearance of thrombolites and a complex deep water microfossil assemblage containing novel forms of life are a few examples of the diverse array of life within the reef [1, 2, 3]. This diversity has been linked to the influx of oxygen and nutrients in the oceans during the GOE. However, it is difficult to establish whether oxygenated, nutrient-rich conditions actually prevailed within the reef at the time of deposition. Sedimentary cherts are good preservers of geochemical signals that are related to primary environmental conditions because they form rapidly and often early, before burial. Silica is present throughout the carbonate-dominated microbialite reef complex in many forms including, as euhedral quartz crystals within phosphorous-rich peloids, micro-crystalline quartz in thrombolites, and black chert lenses preserving deep water microfossils [1, 2, 3]. Known examples of primary and secondary cherts were compared using silicon isotope analysis, as well as major and trace element analysis to reconstruct the environment during the deposition of the reef from shallow to deeper waters. Isotopic data spanned a wide range, with $\delta^{30}\text{Si}$ from -2.8 to 4.1‰ , which is typical of Precambrian cherts [4, 5, 6]. The isotopic data was correlated with major element data to show that the primary quartz textures were seawater precipitates (e.g., $\text{Al}_2\text{O}_3 < 0.5 \text{ wt\%}$ and $\delta^{30}\text{Si} > 0\text{‰}$) and that the secondary precipitates had a greater hydrothermal influence (e.g., $\text{Al}_2\text{O}_3 < 0.5 \text{ wt\%}$ and $\delta^{30}\text{Si} < -0.5\text{‰}$). Rare earth element data showed that the more primary quartz textures had patterns typical of riverine (shallow water precipitates) to oceanic sources (deep water precipitates) (i.e., $\text{La/La}^* = 0.81\text{--}3.78$, $\text{Gd/Gd}^* = 0.48\text{--}2.42$, $\text{Y/Ho} = 14.37\text{--}50.18$). This data also showed that there is evidence of oxygen in the shallow waters of the reef (i.e., $\text{Ce/Ce}^* = 0.4\text{--}1.1$) and that there are relatively high levels of nutrient elements (e.g., P up to 7000 ppm) in shallow water precipitates. By linking isotopic data to trace and rare earth element data, as well as petrography, it has been established that: the shallow waters of the reef had a greater continental/ riverine influence and were oxygenated with an increase of nutrients (P), and that the deeper waters had a greater oceanic influence and were anoxic. The presence of oxygen and nutrients within the microbialite reef complex may provide a reason for the abundance and diversity of life preserved.

[1] Soares *et al.*, 2019. *Precambrian Res.*, 320, 193–212.

[2] Nomchong & Van Kranendonk, 2020. *Precambrian Res.*, 338.

[3] Barlow & Van Kranendonk, 2018. *Geobiology*, 16, 449–475.

[4] Zheng *et al.*, 2019. *Geochim. Cosmochim. Acta*, 253, 267–289.

[5] Stamm *et al.*, 2019. *Geochim. Cosmochim. Acta*, 255, 49–68.

[6] Heck *et al.*, 2011. *Geochim. Cosmochim. Acta*, 75, 5879–5891.

Using macrofossils to interpret peatland facies of Miocene brown coals, Gippsland Basin, southeastern Australia

Tosolini, Anne-Marie P.¹, Korasidis, Vera A.², Wallace, Malcolm W.¹, Wagstaff, Barbara E.¹, & Hill, Robert S.³

¹*School of Earth Sciences, The University of Melbourne, VIC 3010, Australia;* ²*Department of Paleobiology, National Museum of Natural History, Smithsonian Institution, Washington D.C. 20013, U.S.A.;* ³*Environment Institute, University of Adelaide, SA 5005, Australia*

Coals rarely preserve fossil leaves due to catabolic, fungal, bacterial, and/or root disturbance mechanisms that degrade leaf material deposited on the surface of swamps. Well-preserved leaf macro- and meso-fossils (cuticles) have, however, been recovered from the Miocene Morwell 1 brown coal seams in the Gippsland Basin, southeast Australia. Three separate mechanisms of preservation facilitated the accumulation of these floral Lagerstätten, with the unifying condition for all mechanisms that plant material is delivered directly to the anaerobic catotelm and avoids the degrading aerobic acrotelm. Well-preserved leaf material found in these coals is, thus, derived from leaf litter that falls into low-energy acidic and anoxic water-filled depressions that lie below the water table.

Cyclic successions within individual coal seams reflect repeated lithotype cycles in the peat swamps that represent peatland aggradation and record relative drying or terrestrialization events. Six facies occurring within the cycles are defined by colour, texture, gelification and weathering: laminated dark, dark, medium dark, medium light, light and pale. A full lithotype cycle was located within both the lower M1B and upper M1A seams in the Loy Yang Open Cut Mine, Latrobe Valley, where each facies was sampled, analysed for macrofossils where present, which yielded leaves, wood and seeds, then macerated for mesofossils, which yielded leaf cuticles.

Laminated dark facies contain abundant rushes (Typhaceae/Restionaceae), common coral-ferns (Gleicheniaceae) and a high abundance of charcoal (but lack recognisable cuticles), suggesting deposition in open, well-lit, inundated, emergent to meadow marsh environments. Dark facies contain abundant Kauri leaves (Araucariaceae: *Agathis yallournensis*) and Blue Quandong endocarps (Elaeocarpaceae: *Elaeocarpus*), cuticle assemblages are dominated by gymnosperms (abundant *Agathis yallournensis*, common Podocarpaceae: *Dacrycarpus*, *Dacrydium*). These arborescent taxa suggest deposition in periodically inundated environments of a forested bog. Medium dark and medium light facies are dominated by angiosperms: abundant *Elaeocarpus* endocarps and *Oleinites*, common *Agathis yallournensis* and Myrtaceae leaves, and abundant cuticles of Proteaceae (*Banksia laevis*, possible *Orites*) and lilly pilly (Myrtaceae: *Syzygium*), and notably contain tawheowheo (Parachryphiaceae: *Quintinia*). Deposition of these facies was in an angiosperm-dominated forested bog environment. Light and pale facies contain abundant Casuarinaceae leaves and cuticles (and rare *Quintinia*) that represent shallowing upwards and drying of the swamps into ombrogenous forest bog, with some open canopy areas, and finally to the formation of oxidised soils.

The macro- and mesofossil elements of these six different facies within repetitive cycles in the M1B and M1A brown coals, thus, represent changing floral composition as a direct result of changes in substrate wetness during peatland aggradation and the evolution of wetland/peatland systems through the Early to Middle Miocene. Facies progression reflects development of the peatland from fire-prone marsh environments to an angiosperm-dominated, ombrogenous forested bog and supports previous palynological, sedimentological and charcoal analyses. These multidisciplinary analyses have overturned previous theories that charcoal represents the driest facies, whereas in fact, charcoal forms from the burning of fire-tolerant and flammable species in the marsh environments. Modern peat swamp analogues of these cyclic facies successions are found on the South Island of New Zealand and support the “dry-light”, shallowing upwards, facies model.

Investigating the origin of organic matter in Archean chert

Zepeda, Vanessa K.

School of Earth and Atmospheric Sciences, Queensland University of Technology

The origin of organic matter from the 3.43 billion-year-old Strelley Pool Formation (SPF), Pilbara Craton, Western Australia has been heavily debated. The region has an extensive history of diverse hydrothermalism induced by thrusting granitoid complexes which underlie the protocontinent. In consequence, hundreds of siliceous chert dike systems rich in carbonaceous material cross-cut Archean sedimentary rocks. Hydrothermal systems have the potential to synthesize organic molecules abiotically by a process called Fischer Tropsch Synthesis, particularly in the presence of certain metal catalysts. Conversely, a recently proposed hydrothermal pump hypothesis suggests that organic matter in anoxic waters could have been incorporated and redistributed to significant depths due to the higher geothermal gradients in hydrothermal systems. Differentiating between abiotic and biological sources becomes increasingly difficult because both processes induce fractionation effects on ¹³C that are significantly depleted. The author aims to address the questions regarding the origin of organic matter in the SPF by exploring the distribution of metal catalysts that could stimulate abiotic synthesis, as well as utilizing fine-scale geological and geochemical techniques to form paleoenvironmental interpretations of the ancient hydrothermal system. Developing new investigative methods and corroborative lines of evidence from ancient systems like the SPF is likely to yield new insights into the origin and early evolution of life on Earth, as well as other bodies in our solar system such as Mars.

Understanding basin formation and evolution from a plate-tectonic perspective

Mapping and modelling a future passive margin in Afar, East Africa

Zwaan, Frank^{1,2}, Corti, Giacomo³, Keir, Derek^{1,4}, Sani, Federico¹, Muluneh, Ameha⁵, Illsley-Kemp, Finnigan⁶, & Papini, Mauro¹.

¹University of Florence, Florence, Italy; ²University of Bern, Bern, Switzerland; ³National Italian Research Council, Florence, Italy; ⁴University of Southampton, Southampton, United Kingdom; ⁵Addis Ababa University, Addis Ababa, Ethiopia; ⁶Victoria University Wellington, Wellington, New Zealand

This multidisciplinary research project (Zwaan *et al.*, 2020a, 2020b) focuses on the tectonics of the Western Afar Margin (WAM), which is situated between the Ethiopian Plateau and Afar Depression in East Africa. The WAM represents a developing passive margin in a highly volcanic setting, thus offering unique opportunities for the study of rifting and (magma-rich) continental break-up so that our results have both regional and global implications.

We show by means of earthquake analysis that the margin is still deforming under a *ca* E–W extension regime (a result also obtained by analysis on fault measurements from recent field campaigns), whereas Afar itself undergoes a more SW–NE extension (Zwaan *et al.*, 2020a). Together with GPS data, we see Afar currently opening in a rotational fashion. This opening is however a relatively recent and local phenomenon, due to the rotation of the Danakil microcontinent modifying the regional stress field (since 11 Ma). Regional tectonics is otherwise dominated by the rotation of Arabia since 25 Ma and should cause SW–NE (oblique) extension along the WAM. This oblique motion is indeed recorded in the large-scale *en echelon* fault patterns along the margin, which were reactivated in the current E–W extension regime. We thus have good evidence of a multiphase rotational history of the WAM and Afar.

Furthermore, analysis of the margin's structural architecture reveals large-scale flexure towards Afar, likely representing the developing seaward-dipping reflectors that are typical for magma-rich margins. Detailed fault mapping and earthquake analysis show that recent faulting is dominantly antithetic (dipping away from the rift), bounding remarkable marginal grabens, although a large but older synthetic escarpment fault system is present as well.

By means of analogue modelling efforts (Zwaan *et al.*, 2020b) we find that marginal flexure indeed initially develops a large escarpment, whereas the currently active structures only form after significant flexure. Moreover, these models show that marginal grabens do not develop under oblique extension conditions. Instead, the latter model boundary conditions create the large-scale *en echelon* fault arrangement typical of the WAM. We derive that the recent structures of the margin could have developed only after a shift to local orthogonal extension. These modelling results support the multiphase extension scenario as described above.

Altogether, our findings are highly relevant for our understanding of the structural evolution of (magma-rich) passive margins. Indeed, seismic sections of such margins show very similar structures to those of the WAM. However, the general lack of marginal grabens, which are so obvious along the WAM, can be explained by the fact that most rift systems undergo or have

undergone oblique extension, often in multiple phases during which structures from older phases affect subsequent deformation.

Zwaan, F., Corti, G., Sani, F., Keir, D., Muluneh, A., Illsley-Kemp, F., Papini, M. 2020a. Structural analysis of the Western Afar Margin, East Africa: evidence for multiphase rotational rifting. *Tectonics*. <http://doi.org/10.1029/2019TC006043>

Zwaan, F., Corti, G., Keir, D., Sani, F., 2020b. An analogue modeling study of marginal flexure in Afar, East Africa: implications for passive margin formation. *Tectonophysics*. <https://doi.org/10.1016/j.tecto.2020.228595>

Dynamics of arc–continent collision: the role of crustal–mantle dynamics on controlling the formation of basins in continental margins

Rodriguez-Corcho, Andres^{1,2}, Móron-Polanco, Sara^{1,2}, Farrington, Rebecca¹, Beucher, Romain³, Moresi, Louis³, & Montes, Camilo⁴

¹The University of Melbourne, Melbourne, Australia;

²The University of Sydney, Sydney, Australia;

³Australian National University, Canberra, Australia;

⁴Universidad del Norte, Barranquilla, Colombia

Arc–continent collision is the process by which intra-oceanic arc crust is accreted to continental margins. It is a process which commonly occurs in the tectonic-cycle and the most important mechanism that enables the growth of the continental crust since Phanerozoic times. We use numerical visco-plastic mechanical models to explore how compositional density contrasts and crustal–mantle dynamics control the formation of basins in continental margins during arc–continent collision. We performed a series of simulations only varying the thickness of the arc as it has been suggested to control the density profile (buoyancy) and rheology of intra-oceanic arcs and therefore the dynamics of collision. Modelling results show that arc–continent collision can evolve into two mechanisms: (i) arc transference in dense arcs (15–31 km in thickness), where the middle–lower arc crust is at least 2.1% denser than the adjacent continental crust–lithosphere, and (ii) slab break-off in buoyant arcs (32–35 km in thickness), where the density contrast between the middle–lower intra-oceanic arc crust and the adjacent continental crust–lithosphere is lesser than the 2.1%. In turn, these two mechanisms trigger the partition of stress into extension in the continental margin and compression towards the subducting plate. We interpret that the partitioning in stress into compression and extension in all simulations is caused by a gravity-driven flow that equilibrates the contrasts in gravitational potential energy (GPE) stored in the lithosphere during arc–continent collision and episodes of lithospheric thickening. We argue that this gravity-driven flow applies a horizontal gravitational force directed from the collided arc towards the subducting plate (compressional) and the continental margin (extensional). This simultaneous occurrence of compression and extension in an active plate boundary allows the formation of basins in the continental margin without the need of the fore-arc or back-arc extension mechanisms. Finally, we conclude that the large-scale mantle return flow emerged from crustal–mantle dynamics (slab-anchoring) facilitates the stress partitioning by enhancing: (i) compression and lithospheric thickening, and (ii) the contrast in GPE between the accreted arc and the continental margin

during collision.

A late Tonian plate reorganization event revealed by a full-plate Proterozoic reconstruction

Collins, Alan S.¹, Blades, Morgan L.¹, Merdith, Andrew S.², & Foden, John D.¹

¹*Tectonics and Earth Systems (TES), Department of Earth Sciences, The University of Adelaide, Adelaide, SA 5005, Australia;* ²*EarthByte Group, School of Geosciences, The University of Sydney, Sydney, Australia*

Plate reorganization events are a characteristic of plate tectonics that punctuate the Phanerozoic. They fundamentally change the lithospheric plate-motion circuit, influencing the planet's lithosphere–mantle system and both ocean and atmospheric circulation through changes in bathymetry and topography. The development of full-plate reconstructions for deep time allows the geological record to be interrogated in a framework where plate kinematic reorganizations can be explored. Here, we interpret the geological record of the one of the most extensive tracts of Neoproterozoic crust on the planet (the Arabian-Nubian Shield) to reflect a late Tonian plate reorganization at ca 800–715 Ma that switched plate-convergence directions in the Mozambique Ocean. This caused Neoproterozoic India to move towards both the African cratons and Australia-Mawson, instigating the closure of the intervening ocean and the future amalgamation of central Gondwana ca 200 million years later. This plate kinematic change is coeval with constraints on break-up of the core of Rodinia between Australia-Mawson and Laurentia and Kalahari and Congo.

Reconstructing the Mesoproterozoic palaeogeography of northern Australia through coupled detrital thermo- and geochronometers

Yang, Bo¹, Collins, Alan^{1,2}, Blades, Morgan¹, & Jourdan, Fred³

¹*Tectonics and Earth Systems Research Group, Mawson Centre for Geosciences (MCG), Department of Earth Sciences, The University of Adelaide, SA 5005, Australia;* ²*Mineral Exploration Cooperative Research Centre (MinEX CRC), WA 6151, Australia;* ³*Western Australian Argon Isotope Facility, Department of Applied Geology, Curtin University, Perth, WA 6845, Australia.*

This study presents detrital muscovite ⁴⁰Ar/³⁹Ar data from the Mesoproterozoic Roper Group and the overlying latest Mesoproterozoic to early Neoproterozoic unnamed successions in the Beetaloo Sub-basin, northern Australia. Detrital muscovite chronology, compiled with the previous detrital zircon data, is used to identify basin source regions, providing integrated thermo- and geo- constraints on the basin provenance. The coupled detrital thermo- and geochronometers illustrate a dynamics tectonothermal history of the North Australia Craton (NAC) through the Mesoproterozoic.

Data show that the Bessie Creek Sandstone, the oldest analysed formation from the Roper Group, provenance from multiple sources, whereas the overlying formation

(the Velkerri Formation) consists of detritus from a dominant source. The predominant ca 1.48 Ga muscovite and ca 1.60 Ga zircon analyses seen in the Velkerri Formation closely match the published data from the exposed basement rocks to the southeast of the basin (e.g., Mt Isa Region, South Australia Craton (SAC), and the palinspastically adjacent Georgetown Province). These southeast source regions are located along the eastern margin of the Proterozoic Australia, and would have been uplifted, as rift-shoulders, during the separating between the Proterozoic Australia and the Laurentia at ca 1.45 Ga. The uplifted southeast sources then became the most significant topographic highs, and subsequently swamped the basin with ca 1.47 Ga detrital muscovite grains as well as the ca 1.60 Ga detrital zircon grains, as those seen in the Velkerri Formation. The successions overlying the Velkerri Formation exhibit a gradually increased introduction of southern sources derived detritus. Data show that the Kyalla Formation, the youngest analysed formation from the Roper Group, was predominately sourced from the southern sources (e.g., Aileron Province and Tanami Region). The coeval absence of ca 1.47 Ga detrital muscovite and ca 1.60 Ga detrital zircon grains indicates the Kyalla Formation received little contributions from the southeast sources. Further, detrital muscovite ⁴⁰Ar/³⁹Ar data show that the cumulated lag time of the Kyalla Formation is distinctly longer than the underlying formations. This is interpreted to reflect a different exhumation mechanism within source regions corresponding to a changed tectonic setting. The change in provenance and tectonic background is interpreted to relate to the closure of an ocean basin during the period 1.35–1.25 Ga, which resulted in uplift of the southern margin of the North Australia Craton.

The latest Mesoproterozoic to early Neoproterozoic sandstone successions overlying the Roper Group provenance from the Musgrave Province. Coupled detrital zircon and muscovite data imply a rapid cooling at ca 1.20–1.15 Ga that is interpreted to reflect a syn-orogenic exhumation during the Musgrave Orogeny. This quick exhumation is temporally consistent with the syn-orogenic cooling and exhumation in the Albany-Fraser Orogen. The synchronous orogenic exhumation events, seen in the Albany-Fraser Orogen and the Musgrave Province respectively, might represent a coeval collision of the West Australia Craton with the combined NAC and SAC, at ca 1.20 Ga.

Reconstruction of the North China Craton within the Meso–Neoproterozoic supercontinents: evidence from large igneous provinces and rift sediments

Zhang, Shuan-Hong¹, Pei, Jun-Ling¹, Zhou, Zai-Zheng², Yang, Zhen-Yu³, Zhao, Yue¹, Cai, Yuhang¹, Zhang, Qi-Qi¹, Hu, Guo-Hui¹, & Zhuo, Sheng-Guang⁴

¹*Institute of Geomechanics, Chinese Academy of Geological Sciences, Key Laboratory of Paleomagnetism and Tectonic Reconstruction, Ministry of Natural Resources, Beijing 100081, China;* ²*College of Earth Sciences and Engineering, Shandong University of Science and Technology, Qingdao 266590, China;* ³*College of Resources, Environment and Tourism, Capital Normal University, Beijing 100048, China;* ⁴*College of Resources and Materials,*

Northeastern University at Qinhuangdao, Qinhuangdao 066004, China

Large igneous provinces (LIPs) and rift sediments can provide robust tools for paleogeographic reconstructions of Precambrian supercontinents. In this presentation, we use correlations of the Meso–Neoproterozoic LIPs and magmatism and sedimentation in continental margin rift basins in North China Craton (NCC) and other continents, combined with the previously published paleomagnetic data, in order to give better constraints on paleopositions of the NCC within the Nuna (Columbia) and Rodinia supercontinents. Our results show that the NCC was adjacent to Siberia, Laurentia, Baltica, North Australian Craton (NAC) and India in the Nuna (Columbia) supercontinent, and the northern–northeastern margin of the NCC was connected with the northern margin of the NAC during the early–middle Mesoproterozoic period. Global spatial distributions of the 1.4–1.3 Ga LIPs and rift sediments and paleogeographic reconstructions suggested existence of a 1.4–1.3 Ga continental rift system between Laurentia, Siberia, Baltica, NAC and NCC, which resulted in breakup of the Nuna (Columbia) supercontinent. Interestingly, the ca 1.30 Ga Bayan Obo world’s largest REE deposit and carbonatites in the northern NCC and the ca 1.38–1.33 Ga Mountain Pass world’s second largest REE deposit and carbonatites in western margin of Laurentia are distributed in this rift system and are most likely related to 1.4–1.3 Ga continental rifting in the Nuna (Columbia) supercontinent.

New detrital zircon U–Pb and Hf isotopic data from the late Mesoproterozoic to Neoproterozoic sedimentary rocks in the eastern–southeastern NCC combined with paleomagnetic data suggest that during the late Mesoproterozoic to early Neoproterozoic period, the eastern–southeastern margin of the NCC was most likely connected to the western–southern Australian cratons in the Rodinia supercontinent. Breakup of the eastern–southeastern margin of the NCC from the western–southern Australian cratons occurred during 0.92–0.89 Ga as suggested by the Sariwon-Liaodong-Xuhuai mafic LIP in rifting basins in the eastern–southeastern NCC. During “Earth’s Middle Age” from 1.7 Ga to 0.75 Ga, the core of the Nuna (Columbia) and Rodinia supercontinents (including Laurentia, Siberia and Baltica) remains stable and these long-lived connections between Laurentia, Siberia and Baltica as the core of both Nuna and Rodinia suggest that the transition from Nuna to Rodinia was much less dramatic than the subsequent transition from Rodinia to Gondwana and Pangea, which is consistent with relatively lithospheric stability in “Earth’s Middle Age” that contrasts with the dramatic changes in preceding and succeeding eras.

Reconstruction of a Paleoproterozoic greenstone belt and tectonic implications (Toumodi Greenstone Belt, West Africa)

Hayman, Patrick¹, Asmussen, Pascal¹, Senyah, Gloria¹, Tegan, Eudes², Coulibaly, Inza³, Denyszyn, Steven⁴, & Jessell, Mark⁴

¹Queensland University of Technology, Brisbane, Australia; ²Institut National Polytechnique Felix Houphouët Boigny, Yamoussoukro, Côte d’Ivoire; ³Université Nangui Abrogoua, Abidjan, Côte d’Ivoire; ⁴University of Western Australia, Perth, Australia

Despite many similarities between late Archean and Paleoproterozoic greenstone belts, volcanological, compositional, temporal and geometric variations reflect differences in lithospheric strength and geodynamics. We present new field, geochemical and geochronological (U–Pb LA-ICPMS and ID-TIMS) data of the Toumodi Greenstone Belt (Ivory Coast, West Africa) to reconstruct the stratigraphic, paleo-depositional environment and structural history of a well-preserved greenstone belt that represents one of the first post-Archean supracrustal sequences. We then compare and contrast results with a typical 2.7 Ga greenstone belt (Agnew, Western Australia) and highlight some important differences across the A–P boundary. The Toumodi Belt is 130 km long and >5 km wide and preserves a sequence 5–10 km thick, for which there is no evidence of pre-existing continental basement. The stratigraphy consists of three main stages: (I) an initial (ca 2.35–2.30 Ga) tholeiitic lava flow and sill succession intercalated with minor cherts and black mudstones, representing a mafic event in an open, anoxic and deep-water setting (mid-oceanic ridge basalt or oceanic island?), (II) a diverse volcano-sedimentary package (ca 2.30–2.15 Ga) of basalt/andesite lavas and turbidites that formed in deep water, as well as pyroclastic (scoria/tuff cones) and epiclastic deposits, including debris avalanche flow deposits, that formed in a subaerial setting, and (III) an uppermost (ca 2.15–2.05 Ga) sequence of felsic pyroclastic and epiclastic rocks that formed in a subaerial setting, as well as coeval and distal turbidites. Stages II and III form a synclinal sequence, while stage I forms only on the western edge of the belt. Similarities with 2.7 Ga greenstones include transitions from mafic to felsic volcanism and subaqueous to subaerial environments. Important differences include the protracted history (>250 vs 70 Myrs), belt asymmetry, and abundance of emergent stratigraphy (especially during stage II) that reflect multiple thermal events, accretionary tectonics, and stiffer continents, respectively.

Building a boundary – processes, products, and consequences of Neogene collisional geodynamics in eastern Indonesia

Geology of the Mutis Complex, Miomaffo, West Timor

Berry, Ron¹, Goemann, Karsten², & Danyushevsky, Leonid¹

¹CODES, University of Tasmania, Hobart, Australia; ²Central Science Laboratory, University of Tasmania, Hobart, Australia

Mesozoic accretionary assemblages are widespread across Indonesia and these can be seen in the overthrust terranes on Timor. The oldest rocks in the allochthonous Mutis Complex, West Timor are Jurassic melange containing blocks of N-MORB basalt (194 ±5 Ma), amphibolite (metamorphism at 175 Ma), garnet and actinolite bearing schists, arkosic sandstone and volcanogenic material. The sedimentary component is sourced from Mesozoic island arc along the southern margin of Indonesia (ca 200 Ma based on detrital zircon). Prehnite is common as a late metamorphic

mineral in the matrix. The accretionary material is complexly deformed with a dominant foliation and cataclastic zones. This sequence is intruded by calc-alkaline andesitic dykes (possibly in the Eocene). To the west of the melange is a transition to high strain greenschist facies rocks (isoclinal folding and transposition layering) where the block in matrix texture can no longer be recognised, but the range of bulk composition is the same. Further west across several faults is an amphibolite facies metamorphic province. Amphibolites have the same N-MORB composition as the basalt in the east. The peak metamorphic conditions are 600–720°C, 0.6–1.1 GPa. This area has the same bulk composition as the melange including detrital zircon ages. The metamorphic assemblages overprint low T isoclinal folds. Peak metamorphism occurs at 38 Ma reflecting an event within the active margin of Sundaland. At about 5 Ma, NW Australia collided with this margin and the Mutis Complex was thrust over Timor. A late generation of cataclastic faults zones cuts all the pre-existing lithologies but is largely a result of extensional collapse. The complex is cut by a younger fault zone that affects the underlying unconsolidated sedimentary rocks and contains evidence of both strike slip and normal fault movement. The Mutis Complex is an excellent example of the complex geological history of rocks along the boundary between Indonesia and Australia.

Cenozoic affinity of the Gondwanan rocks of eastern Timor: evidence from geothermochronometry

Duffy, B.¹, Lew, B.¹, Boland, K.¹, Kohn, B.¹, Matchan, E.¹, Maas, R.¹, Dixon, D.¹, Pedro, L.², de Carvalho, P.², & Sandiford, M.¹

¹The University of Melbourne, Australia; ²Instituto do Petróleo e Geologia, Dili, Timor-Leste

Timor occupies a critical position within Wallacea and within the Indonesian throughflow, but its tectonic history remains poorly constrained compared to other parts of the region. Tectonic models typically divide the island into (1) Australian affinity rocks, including a thick sequence of Paleozoic and Mesozoic rocks and metamorphosed equivalents, and (2) Asian affinity rocks, made up of predominantly Cretaceous and Paleogene rocks and their metamorphosed equivalents, known as the Lolotoi Metamorphic Complex (LMC). New field mapping shows that the type-area of the LMC is pre-Permian basement exposed in an erosional window. Much of the previously mapped LMC is actually overlying alkaline Permian basalt. LA-ICPMS U–Pb ages for zircons, apatites and titanites from the LMC type-area are Precambrian and consistent with those from Gondwanan continental slivers that now form the basement of eastern Java and West Sulawesi. Such basement ages are also identified in peaks from inherited zircons from the LMC elsewhere in Timor. Basement faults separating the LMC from Triassic and Jurassic sediments contain white micas yielding Ar–Ar ages of ca 38 Ma, which are within the age range of white micas from the Asian affinity Mutis metamorphic complex of West Timor. Zircon and apatite (U–Th)/He thermochronometric data and low vitrinite reflectance values across much of the study area do not support previous models suggesting Cenozoic overthrusting. However, close to the basement fault the

thermochronometric data indicate rapid Eocene–Oligocene cooling and like the white mica ages, this is consistent with the thermal history of the Mutis complex of West Timor. On the basis of these data, we revive Barber's (1978) interpretation that almost all of the pre-Neogene exhumed rocks of eastern Timor, including the Gondwanan rocks, resided in Sundaland during the Cenozoic. This finding strongly supports hydrocarbon prospectivity onshore in Timor and has implications for the geodynamics of the Banda Arc, reconstructions of Wallacea, and the Neogene paleogeography of the Indonesian Throughflow.

Oblique plate convergence drives deformation, uplift of coral reefs and earthquakes in the eastern Bird's Head Peninsula, West Papua, Indonesia

Saputra, Sukahar Eka, Fergusson, Chris, Dosseto, Anthony, Murray-Wallace, Colin, Nutman, Allen, & Dougherty, Amy

School of Earth, Atmospheric, and Life Sciences, University of Wollongong, Wollongong, Australia

Plate motions result in the Bird's Head Peninsula of northwestern New Guinea undergoing oblique convergence from the northeast driven by westward motion of the Pacific-Caroline Plate and northward motion of the Australian Plate. The Bird's Head Peninsula is part of a northwestern extension of the Australian Plate and has a basement of a Paleozoic to early Mesozoic orogenic belt containing mid Paleozoic accretionary turbidite successions and Devonian to Triassic granites. This basement is overlain by a Mesozoic passive margin succession with rifting in the Jurassic. Subsequent development reflects complex Cenozoic tectonics with island arcs colliding with the northern margin of New Guinea. The Kemum High, the northern mountainous spine of Bird's Head, was caused by major uplift in the Pleistocene. Further to the northeast the hilly terrain around Manokwari has been more recently uplifted. The northern and north-eastern part of Bird's Head are cut by two major strike-slip faults, the Sorong and Ransiki faults, respectively.

The present-day tectonics reflects the oblique plate convergence with partitioning of plate motion into normal convergence across the Manokwari Trough/New Guinea Trench and sinistral strike-slip along the Sorong and Yapen faults. Abundant earthquakes immediately north of Bird's Head have first motion solutions that indicate south-dipping, east-southeast-trending, thrust faults and are consistent with underthrusting along the Manokwari Trough. On land much of the Sorong Fault is aseismic although offshore to the east the Yapen Fault is associated with earthquakes that have first motion solutions indicating east-southeast-trending, sinistral strike-slip movement. A cluster of earthquakes is associated with the junction of the north-northwest-trending Ransiki Fault and the east-southeast-trending Yapen Fault. First motion solutions, aftershocks and earthquake damage, including fissures, cracks, faults, sand flows, and subsidence, are indicative of dextral movement on the Ransiki Fault and sinistral movement on the Yapen Fault.

In the Manokwari region in the northeastern part of the Bird's Head north-northeast convergence is reflected in Pleistocene contractional deformation and uplift of Pliocene to Pleistocene shallow marine sediments and

coral reefs. Earlier uplift of parts of the Kemum High is indicated by provenance (rock types and detrital zircon ages) of conglomeratic/sandy units in the Pliocene to lower Pleistocene Befoor Formation. The Miocene Maruni Limestone and Pliocene to lower Pleistocene Befoor Formation are affected by east-southeast-trending, upright to steeply inclined, folds that decrease in interlimb angle from north to south reflecting buttressing against the uplifted basement rocks of the Kemum High. The deformation occurred within the Pleistocene as shown by an angular unconformity with weakly deformed overlying uplifted coral reefs of the Pleistocene Manokwari Limestone. Upraised coral reefs have U series coral ages of 65–130 ka at elevations up to 100 m asl. Fissures filled with coral debris (coral gravel dykes) are indicative of paleoseismicity and occur in the Befoor Formation and also in Manokwari Limestone. They are near-vertical with east-southeast and north-northeast trends consistent with stress directions shown by the first motion solutions of earthquakes.

Seismic Imaging of the subducted Australian continental margin beneath Timor and the Banda Arc Collision Zone

Zhang, Ping, & Miller, Meghan S.

Research School of Earth Sciences, Australian National University, Canberra, Australia

The active arc–continent collision in the Banda Arc is a result of convergence of the Indo-Australian plate with the Eurasian plate in Southeast Asia. There, the subduction of the Cretaceous to Jurassic age Indian Ocean lithosphere along the Sunda Arc transitions to the recent arc–continent collision at the Banda arc while the NW Australian continental margin and the active volcanic arc converge. Such complicated convergent tectonics leads to pronounced structural heterogeneity and complexity of both vertical and lateral extents along to the convergent margin. Therefore, understanding detailed knowledge of deep structure in the area is key to unravelling the dynamic processes that occur. In this study, we image detailed crustal and uppermost mantle structure utilizing *ca* 4-years of broadband seismic data recently collected in the Timor-Leste and Nusa Tenggara Timor region of Indonesia. We apply three techniques, ambient noise tomography, teleseismic P-wave receiver function and coda autocorrelation, to resolve a 3-D Vs model and Moho structure. Our tomographic images show low-velocity anomalies (<30 km) beneath the outer arc island of Timor related to the underthrust Gondwana Sequence from the incoming Australian plate, which are vertically offset by the high-velocity backstop of the Banda forearc terrane. The structure progressively changes along strike, reflecting different collisional stages developed as a result of the oblique convergence and incoming plate heterogeneity. At greater depth, we detect seismically fast lithospheric mantle (>30 km) and the arc-ward dipping Moho beneath Timor, both interpreted to be from the incoming Australian plate. Our findings provide direct seismic structural evidence of the subducted Australian continental margin at lithospheric depths beneath the Banda Arc collision zone.

A kinematic model of the northeast Australian Plate boundary zone

Zhao, Siyuan¹, McClusky, Simon¹, Koulali, Achraf², Cummins, Phil¹, & Miller, Meghan¹

¹*The Australian National University, Canberra, Australia;* ²*Newcastle University, Newcastle upon Tyne, United Kingdom*

The northeast Australian plate boundary zone encompasses a complex tectonic environment, characterised by the rapid convergence of the Pacific, Australian, Philippine Sea plates and the Sunda Block. The mechanism driving the oblique convergence in this region and the activity and partitioning of fault slip rate within this deformation zone have hitherto been conjectural. In this study, we perform a simultaneous inversion of 500 earthquake slip vectors and 236 GPS velocities to quantify the kinematics of block bounded faults within the deformation zone spanning the Sunda-Banda Arc, Irian Jaya region and Papua New Guinea. Our best fitting kinematic block model comprises 23 elastic blocks, for which we estimate the rotation rates, uniform horizontal strain rate tensor, and block boundary slip rates. The compressional component of the convergence between the Sunda Block and Australian Plate is largely accommodated by the Sunda-Banda forearc and back-arc, and ~34% of the shear component is transferred to the eastern back-arc through the Semau Fault. The Bird's Head block is rotating 2.642 ± 0.070 °/Myr anticlockwise with respect to the Australian plate, resulting in average 44.3 mm/yr motion across the Seram Trough and the formation of the Cendrawasih Bay sphenochasm. The relative slip vectors across the New Guinea Fold-and-Thrust Belt indicate a transition in the regime of the block boundary from predominately thrust faulting at its western segment with an average convergence rate ~13.6 mm/yr, to the predominately left-lateral strike-slip in the middle segment with a slip rate of 7–8 mm/yr, then again to thrust in the eastern segment of New Guinea Highlands with an average convergence rate up to 10.0 ± 0.5 mm/yr. In the western part of the New Guinea Highlands, the fault-parallel slip rate decreases from 27.8 ± 0.7 mm/yr to 19.8 ± 0.6 mm/yr, and the average fault-parallel slip rates in the western New Guinea Highlands is greater than that of in the eastern segment (23.3 mm/yr and 5.5 mm/yr, respectively), which implies some of the subsidiary movement of the highly active sinistral Tarera-Adiuna Fault may be accommodated within the Highlands thrust belt. The available GPS measurements of crustal motion suggest interseismic strain accumulation associated with normal faulting along the Banda detachment, and the low subsidence rates observed in the outer arc are consistent with weaker strain accumulation in the fold-and-thrust belt. In our model, the New Guinea Highlands thrust belt accommodates less than 13% of convergent and 17% of left lateral motion between the Australian and Pacific plates, and the rest of the convergence is largely accommodated by the New Guinea Trench with a slip rate up 84.2 ± 2.5 mm/yr. Our best-fit model also reveals 2.195 ± 0.117 °/Myr anticlockwise rotation of the Woodlark crustal block relative to the Australian Plate, which produces a seafloor spreading rate of 28.9 mm/yr in the Woodlark Basin and 15.9 mm/yr of extension in the continental rift in the Papuan Peninsula. Multiple normal structures located in the D'Entrecasteaux Islands accommodate the extensional

deformation, slipping at high rates around 17.7 mm/yr.

The Proterozoic Earth system and plate tectonics—correlations and causation?

Extending whole-plate tectonic models into deep time: linking the Neoproterozoic and the Phanerozoic

Merdith, Andrew¹, Collins, Alan², Williams, Simon³, Tetley, Michael¹, Mulder, Jacob⁴, Blades, Morgan², Young, Alexander⁵, Armistead, Sheree⁶, Cannon, John⁷, Zahirovic, Sabin⁷ & Müller, Dietmar⁷

¹UnivLyon, Université Lyon 1, Ens de Lyon, CNRS, UMR 5276 LGL-TPE, F-69622, Villeurbanne, France;

²Tectonics and Earth Systems Group (TES), Dept of Earth Sciences, The University of Adelaide, Adelaide, SA 5005, Australia; ³Northwest University, Xi'an, China;

⁴School of Earth, Atmosphere and Environment, Monash University, Clayton, VIC 3168, Australia;

⁵GeoQuEST Research Centre, School of Earth, Atmospheric and Life Sciences, University of Wollongong, Northfields Avenue, NSW 2522, Australia;

⁶Geological Survey of Canada, 601 Booth Street, Ottawa, Ontario, Canada & Metal Earth, Harquail School of Earth Sciences, Laurentian University, Sudbury, Ontario, Canada; ⁷Earthbyte Group, School of Geosciences, University of Sydney, Sydney, NSW 2006, Australia

Recent progress in plate tectonic reconstructions has seen models move beyond the classical idea of continental drift by attempting to reconstruct the full evolving configuration of tectonic plates and plate boundaries through time. These advances are an essential step in quantifying the role plate tectonics has had in the evolution of Earth-surface systems, including the biosphere, atmosphere and hydrosphere, as well as palaeogeographies and the evolving shape of the Earth surface (palaeobathymetry and topography). Previous work has resulted in a number of full-plate reconstructions spanning the last 1 Ga. However, so far these models cover discrete time periods, meaning that a complete model with a consistent set of plate motions and boundaries is not yet available to the Earth Science community. This is a particular problem for the Neoproterozoic and Cambrian, as it means that many existing interpretations of geological and palaeomagnetic data have remained disconnected from younger, better-constrained periods in Earth history. Here we present a continuous full-plate model spanning 1 Ga to the present-day, that is focused on a revised and improved model for the Neoproterozoic–Cambrian (1000–520 Ma) but connects with models of the Phanerozoic and opens up pre-Gondwana times for quantitative analysis and further regional refinements. The model is presented in a purely palaeomagnetic reference frame, and is otherwise geologically derived, based on preserved data from past-plate boundaries. This is a first step in the direction of a detailed and self-consistent tectonic reconstruction for the last billion years of Earth history.

The impact of Snowball Earth Glaciation on ocean water $\delta^{18}\text{O}$ values

Defliese, William F.

School of Earth and Environmental Sciences, The University of Queensland, St Lucia, QLD, Australia

It has been long recognized that glacial episodes can affect the $\delta^{18}\text{O}$ value of ocean water, where preferential storage of ^{16}O in ice changes the $^{18}\text{O}/^{16}\text{O}$ ratio of the ocean. However, these effects are generally thought of as transient, as Cenozoic glaciation has had neither the magnitude nor duration to cause long-term change with ocean water buffered to values close to $0 \pm 2 \text{‰}$ VSMOW by tectonic processes. The Snowball Earth glaciations of the Cryogenian have the potential to cause much larger changes in ocean water $\delta^{18}\text{O}$ values due to their increased ice volume and long duration relative to Cenozoic glaciation, but these effects have not been previously investigated.

Here, I use a numerical box model to investigate ocean water $\delta^{18}\text{O}$ values over the Proterozoic and Phanerozoic. The model simulates various temperature and tectonics dependant fluxes of ^{18}O , while also incorporating a zero-dimensional climate model and ice volume component to model glacial cycles. Monte Carlo simulations of the Sturtian and Marinoan glaciations reveal that these had the potential to alter ocean water $\delta^{18}\text{O}$ values for hundreds of millions of years after the termination of glaciation, providing a mechanism for secular change in the $\delta^{18}\text{O}$ value of ocean water. This occurs as a very large volume of ice (presumably, but not necessarily ^{18}O depleted) is sequestered from the ocean, causing the ocean to become enriched enough in ^{18}O for exchange at mid-ocean ridges to remove ^{18}O from the ocean and slowly change the overall ocean water $\delta^{18}\text{O}$ value. If Snowball Earth ice volumes were as large as proposed (~28–32% of ocean volume), present day values of ice $\delta^{18}\text{O}$ would cause significant secular change in ocean water $\delta^{18}\text{O}$ extending into the Phanerozoic. An additional finding of this work is that the duration of the Sturtian glaciation required a very low CO_2 degassing rate on the order of ~2 Tmol/year, significantly less than that estimated from most other mass balance approaches for the Phanerozoic.

Redefining the basement architecture of the southern Mount Isa Inlier

Brown, D. D.¹, Bultitude, R. J.¹, Simpson, J. M.¹, Purdy, D. P.¹, Connors, K. A.², & Sanislav, I. V.³

¹Geological Survey of Queensland; ²University of Queensland; ³James Cook University

The Paleoproterozoic Kalkadoon-Leichhardt belt (KLB) forms the major basement block to a series of Paleoproterozoic Superbasin sequences of the Mount Isa Inlier. The basement sequences of the Mount Isa Inlier have a broad two-fold division comprising: (1) the Leichhardt Volcanics and the Kalkadoon Granodiorite (ca 1865 Ma) formed during the Barramundi Orogeny, and (2) a series of pre-1870 Ma units which are restricted in distribution to the KLB and margins of the Western Succession (Kurbayia Metamorphic Complex, Yaringa Metamorphics, and Saint Ronans Metamorphics).

The eastern portion of the KLB is overlain by and

complexly faulted with the Mary Kathleen Domain (MKD). The MKD is dominantly comprised of calcareous and siliciclastic metasedimentary units belonging to the Paleoproterozoic Leichhardt Superbasin (ca 1790–1740 Ma) and igneous rocks of the Wonga and Burstall suites (ca 1740 Ma). At the southern outcropping extent, several intrusive units had previously been included in either the Burstall Suite (Saint Mungo Granite), Wonga Suite (Birds Well Granite, Bushy Park Gneiss) or correlated with ca 1740 Ma magmatism (Tick Hill Complex) and thus included in the Mary Kathleen Domain.

New SHRIMP and LA-ICP-MS U–Pb geochronology shows that some units in the southern MKD are much older and form part of the basement (KLB). The Bushy Park Gneiss and Birds Well Granite form part of the KLB with crystallisation ages consistent with the Barramundi portion of the KLB. Hafnium isotope studies indicate these units to have ϵ_{Hf} which closer to CHUR whereas the previously analysed Barramundi portion of the KLB has uniform ϵ_{Hf} values of ~ -4 which indicates some heterogeneity in the southern portion of the inlier.

This is confirmed by interpretation and reinterpretation deep seismic lines CF3 and M6, which reveal an extensive basement package in the subsurface of the Southern Mount Isa inlier and throughout the Eastern Sub province. This package appears to be a controlling factor for deformation and basin development from 1865 Ma.

Detrital zircon age and provenance of the Tonian–Cryogenian of the Adelaide Superbasin

Lloyd, Jarred C.^{1,2}, Van Der Wolff, Erica¹, Blades, Morgan L.¹, Virgo, Georgina M.^{2,1}, Collins, Alan S.¹, & Amos, Kathryn J.²

¹*Tectonics and Earth Systems Group, Mawson Centre for Geoscience, The University of Adelaide, Adelaide, SA 5005, Australia, and MinEx CRC;* ²*Australian School of Petroleum and Energy Resources, The University of Adelaide, Adelaide, SA 5005, Australia*

The Adelaide Superbasin is a vast Neoproterozoic to middle Cambrian sedimentary basin in southern Australia that initiated due to the break-up of central Rodinia and evolved into the Australian passive margin on edge of the Pacific Basin. We present over 2000 new detrital zircon analyses from more than 20 Tonian–Cryogenian formations of the central Adelaide Rift Complex of the Neoproterozoic–middle Cambrian Adelaide Superbasin. These new data focus on understudied formations from within the Burra and Umberatana Groups that were identified in Lloyd *et al.* (2020, Precambrian Research, doi:10.1016/j.precamres.2020.105849). Building on the >7500 data previously published we now consider that we are getting an adequate idea of the spatial variation of detrital zircon populations for time-equivalent formations within this large basin. The same statistical method of Lloyd *et al.* (2020) is applied to this dataset. Samples of Burra and Umberatana Groups from the Mount Lofty Range region in the south of the superbasin, preserve local sources (Barossa Complex/Gawler Craton, ca 2500–1560 Ma), suggesting local derivation. This contrasts time-equivalent formations from the north of the of basin (central and northern Flinders Ranges), where zircon

sources include distal regions (Musgrave Orogen, ca 1550–1050 Ma) and suggest axial transport through the Willouran Trough. Samples in the south then show increasing zircon source diversity up sequence, similar to, although not as pronounced as, the progression seen in the north of the basin. All areas are then punctuated by the Sturtian Cryogenian ice-transported deposits. Post-Sturtian glacial deposits preserve younger zircon sources (ca <1000 Ma), potentially from southern sources (Antarctica?). Notably ca 980–950 Ma zircon populations are more common in the samples from the south of the basin than in the north of the basin. These observations and interpretations are suggestive of a progressive southward opening of the Superbasin, consistent with the current interpretation of lithostratigraphy.

In-situ Rb–Sr dating of Precambrian sediments

Subarkah, Darwinaji¹, Blades, Morgan L.¹, Collins, Alan S.¹, Farkas, Juraj¹, Gilbert, Sarah², & Lloyd, Jarred C.¹

¹*Tectonics and Earth Systems (TES) Group and Mineral Exploration CRC, Department of Earth Sciences, University of Adelaide, Adelaide, SA 5005, Australia;* ²*Adelaide Microscopy, University of Adelaide, Adelaide, SA 5005,*

Sedimentary rocks make up only 5% of the Earth's crust and yet represents the primary archive of the planet's biogeochemical cycles. As such, precise depositional age constraints of sedimentary sequences are critical to our understanding of how these systems have evolved through time. Here we present from a novel application of in-situ Rb–Sr dating and elemental analyses using laser ablation-inductively coupled plasma-mass spectrometry (LA-ICP-MS/MS) on a set of sedimentary rocks across the Precambrian under different geological settings. A reaction gas is introduced between two quadrupoles in the system, allowing for the online separation of ⁸⁷Sr and ⁸⁷Rb. Three case studies were investigated using this method. Roper Group shale samples in proximity with the Derim Derim Dolerite intrusion were sampled from the UR5 drill hole in the Proterozoic McArthur Basin, northern Australia. These samples yielded ages extremely radiogenic initial ⁸⁷Sr/⁸⁶Sr values analogous to the dolerite sample taken from the same well. These time constraints are consistent with the crystallisation age of the igneous suite (ca 1313 Ma) located elsewhere in the basin. We propose that these samples recorded an alteration event instigated by the intrusion that reset the Rb–Sr chronometer and geochemistry of the surrounding sediments. On the other hand, a sample from the intrusion-absent UR6 borehole has been interpreted to reflect the depositional history of the Roper Group instead. Multiple analyses on glauconitic sediments from the Doomadgee Formation in the South Nicholson Basin gave two main outcomes. One set of results gave an age ca 1300 Ma and retained a very high initial Sr isotopic ratio. On the other hand, another sample gave an age of 1607 ±28 Ma, which overlaps with a tuff age interbedded within the same formation. Furthermore, this sample's initial ⁸⁷Sr/⁸⁶Sr ratio was within error of contemporary seawater. Lastly, a calcareous shale from the Neoproterozoic Tapley Hill Formation in Arkaroola yielded an age of 664 ±28 Ma with initial ⁸⁷Sr/⁸⁶Sr value overlapping with their coeval

seawater during time of deposition. Together, our study demonstrates the capabilities of this technique to date Precambrian sediments and evaluate the nature of fluids that their isotopic system was in equilibrium with by coupling laser-derived Rb–Sr and geochemical data. This approach thus allows for a rapid and accurate discrimination of depositional and alteration histories of sedimentary sequences and has potential to be a powerful dating tool for these archives through deep time.

Did Neoproterozoic (Ediacaran) regional sea-level drawdown trigger extensive allochthonous salt breakout and incision of the Wonoka paleocanyons, Flinders Ranges, South Australia?

Giles, Sarah M.¹, Giles, Katherine A.², Rowan, Mark G.³, Christie-Blick, Nicholas¹, & Lankford-Bravo, David F.²

¹Lamont-Doherty Earth Observatory of Columbia University, Palisades, NY 10964, USA; ²University of Texas, Department of Geological Sciences, El Paso, TX 79968, USA; ³Rowan Consulting, Inc., Boulder, CO 80302, USA

Passive salt diapirs can be triggered to spread subhorizontally (allochthonous flow) as a result of contractional tectonics, a marked decrease or cessation in sediment accumulation over the diapir, or from the removal of significant overburden. In the Flinders Ranges of South Australia, salt diapirs sourced from the ca 802–777 Ma Callanna Group have risen passively through much of the later Neoproterozoic to Cambrian interval and spread allochthonously at discrete stratigraphic levels. One such level of appreciable allochthonous salt breakout has previously been placed near the contact between the Ediacaran-age Bunyeroo and Wonoka formations. However, recent chemostratigraphic results suggest that the level of allochthonous breakout could be more accurately placed within the lower Wonoka. Constrained near that same stratigraphic level is a regional unconformity associated with incision of ~1 km deep paleocanyons (the Wonoka canyons), which have an origin debated between deep-water or subaerial incision. Research in progress continues to favor subaerial erosion hypothesized to have resulted from an evaporative drawdown event corresponding with the onset of the Gaskiers glaciation. In the absence of clear-cut tectonic and accumulation-related explanations for allochthonous salt breakout across the Flinders Ranges, we offer an alternative: that breakout may have been triggered by the sea-level drawdown thought to have been responsible for subaerial incision of the Wonoka canyons due to the removal of overburden. There is evidence for tens of meters of stratigraphy having been removed regionally at canyon shoulders.

Our timing constraints are based upon preliminary carbon isotope chemostratigraphy and geologic mapping that indicate allochthonous salt flow and canyon incision initiated near the same stratigraphic level. We plan to collect a more robust chemostratigraphic dataset and to develop a physical stratigraphic framework for the Patawarta, Pinda, and Beltana allochthonous salt sheets, in order to constrain the level of allochthonous salt breakout with respect to the paleocanyons at Umberatana syncline,

Oodnanapicken, and Beltana. The breakout of allochthonous salt possessing sedimentary inclusions and associated with carbonate caprock could have facilitated a short-lived pulse of organic carbon into the seaway in which the Wonoka Formation was deposited, potentially bearing on the local expression of the Shuram carbon isotope anomaly and the emergence of the Ediacara biota.

Sedimentology and geomorphology of dryland continental systems

Australian drylands depositional environments: local news, globally relevant

Wakelin-King, Gresley A.

Wakelin Associates, Melbourne, Australia

Landforms and sediments of continental drylands are relevant to the rock record and to sustainable land management. Globally, many strata were deposited in dryland settings, and modern landscapes are used as analogues for conceptual models of depositional processes. In the present day, ~40% of the world's land is drylands, and it houses >30% of the people, Australian drylands are ~80% of the main continent and contain communities, industries and biodiversity. Understanding how drylands work is clearly desirable. Globally, drylands have highly variable rainfall, highly to extremely variable flow regimes, and a moisture deficit: attributes which govern biota life strategies and create characteristic sedimentary deposits.

Previously, modern analogues focussed on northern hemisphere examples, typically from coarse-clastic, tectonically vigorous, high gradient catchments with flashy hydrology. Australia's context is different: low-relief, low-gradient, subtly expressed neotectonism, a blanket of regolith, and ephemeral rivers capable of big floods and sustained flows. Few Australian drylands sediments have been well-documented, other similar drylands (Thar desert, India, sub-Saharan Africa) may also be under-represented in (English-language) literature or under-utilised as modern analogues.

This presentation journeys through some Australian continental sedimentary landscapes.

Mud-Aggregate Floodplain, Massive Mudrock

Mud aggregate floodplains are the modern analogue for massive mudrock. The current modern analogues (both located in Australia) are vertic soils transported as sand/ silt-sized bedload. Cooper Creek's floodplain has black muds deposited/reworked in braid-like bars, Fowlers Creek is a cut-and-fill floodplain with vertically accreted red muds.

Low-Angle Alluvial Fans

In Australia downstream-diverging fluvial networks are common, usually as low-angle alluvial fans. Channel systems range from coeval multithread to ~single channels sequentially moving across a depositional surface. Fine sediments transported by low-energy flows create broad low-gradient fans. Diverse topographic and climatic contexts lead to a range of sedimentary deposits, most of which are undocumented. Two examples are the mud-dominant Lodden Fan in semi-arid grassland, and the complex aeolian and fluvial sands in the Cooper Creek Fan (Strzelecki Desert).

Floodouts: a Fluvial Process

Floodouts are unchannelised river reaches (flow path is 100% floodplain). Declining discharge during development of Cenozoic aridity means that many Australian drylands rivers are underfit, or their flows no longer extend down the length of the network. Episodic and incomplete sediment transport promotes floodout formation, typically where flow emerges from lateral constriction and loses sediment transport capacity. Floodouts occur in range-front plains, macrochannels, and valley confluences, they are valuable in land management. Some floodout bedding sequences could be identifiable in the rock record.

Flashy Flow Events, Froude Numbers, and Flat Bedding

Sedimentary fluvial rocks from a drylands setting may include planar-bedded sands. Comparison with the standard bedform diagram may lead to an interpretation of deposition during the high-energy ($F = 1$) flood peak of a "typical" flashy desert flow. However, bedforms in modern drylands rivers demonstrate more complex conditions including widespread subcritical ($F < 1$) planar bedding, and low-energy gravel imbrication. Bedforms are governed by grain size and flow velocity, but also by flow depth and sediment composition, this leads to intriguing bedform combinations in rivers with rapid flood recession.

Circadian rhythm of dune-field activity

Gunn, Andrew¹, Lancaster, Nicholas², Edmonds, Douglas³, Ewing, Ryan⁴, & Jerolmack, Douglas¹

¹University of Pennsylvania, Philadelphia, United States; ²Desert Research Institute, Reno, United States; ³Indiana University, Bloomington, United States; ⁴Texas A&M University, College Station, United States

Wind-blown sand dunes are both a consequence and a driver of climate dynamics, they arise under persistently dry and windy conditions, and are sometimes a source for airborne dust. Dune fields experience extreme daily changes in temperature, yet the role of atmospheric stability in driving sand transport and dust emission has not been established. Here we report on an unprecedented multi-scale field experiment at the White Sands Dune Field (New Mexico, USA), where we demonstrate that a daily rhythm of sand and dust transport arises from non-equilibrium atmospheric boundary layer convection. A global analysis of 45 dune fields, including those in Australia, confirms the connection between surface wind speed and diurnal temperature cycles, revealing an unrecognized land-atmosphere feedback that may contribute to the growth of deserts on Earth and dune activity on Mars

Lacustrine littoral landforms in drylands: diversity and significance with examples from Quaternary megalakes of Africa and Australia

Schuster, Mathieu¹, May, Jan-Hendrik^{2,3}, & Nutz, Alexis⁴

¹CNRS & Université de Strasbourg, Strasbourg, France; ²School of Geography, University of Melbourne, Melbourne, Australia; ³GeoQuest, University of Wollongong, Wollongong, Australia;

⁴CEREGE, Aix-Marseille Université, Aix-en-Provence, France

Due to the scarcity of water that defines dryland continental systems, the superficial processes (erosion, transport and deposition) are dominantly controlled by wind and intermittently by water. As such, sedimentologists and geomorphologists working in drylands expect to find there a great diversity of landforms, bedforms and surfaces related to aeolian and alluvial-fluvial environments. However, it is not rare to also identify abandoned landforms which are quite exotic for drylands, such as beach ridges-and-swailes, spits, cusped forelands, barrier islands, wave-ravinement surfaces, or lobate-cusped deltas. These typical shore-related morpho-sedimentary structures evidence past more humid events or periods that have culminated in the development of large lakes. As for their marine counterparts, these littoral landforms provide key geomarkers to restore the trajectory of the shorelines through time, and to understand the cross-shore and alongshore redistribution of clastics by waves and currents.

To illustrate the diversity of the lacustrine littoral landforms that can be preserved in drylands and to explain their significance for climate, environments and hydrodynamics, we focus here on a selected number of remarkable very large paleolakes which developed over Quaternary times in continental deserts from both hemispheres. These are Megalakes Chad, Eyre Kati-Thanda and Frome (Cohen *et al.*, 2012, May *et al.*, 2015, Schuster *et al.*, 2005).

According to both the physiography of the lake basins and the importance of the associated littoral landforms marking their shorelines, these megalakes can be considered as wind-driven waterbodies (Nutz *et al.*, 2018), a category of lakes for which sedimentation is dominated by wind-wave-related processes and basin-scale wind-induced hydrodynamics.

Cohen *et al.*, 2012. doi:10.1016/j.palaeo.2011.06.023

May *et al.*, 2015. doi:10.1016/j.yqres.2014.11.002

Nutz *et al.*, 2018. doi:10.1007/s10933-016-9894-2

Schuster *et al.*, 2005. doi:10.1016/j.quascirev.2005.02.001

Late Holocene landscape dynamics and sediment cycling around Lake Callabonna, Central Australia

May, J.-H.^{1,2}, Marx, S.², Cohen, T.², Schuster, M.³, & May, S. M.⁴

¹School of Geography, University of Melbourne, Melbourne, Australia; ²GeoQUEST Research Centre, University of Wollongong, Wollongong, Australia; ³Institut de Physique du Globe, University of Strasbourg, France, ⁴Institute of Geography, University of Cologne, Cologne, Germany

Lake Callabonna is one of four large, connected playa lakes northwest of the Flinders Ranges in South Australia. These lakes are now mostly dry but would have joined to form mega-lake Frome that existed until ca 45 ka. Although interrupted by major highstands, lakes declined in size since then and became successively disconnected. While this would significantly alter lake hydrology over time, the pronounced variability in lake levels also must have had a profound impact on the ways in which sediment were (i) supplied to the lakes by fluvial processes, (ii) distributed and deposited in various parts of the lake

basin by lacustrine and coastal processes, or (iii) re-activated to be exported from the playa lake system by aeolian processes. In this spatially and temporally highly dynamic system, source-bordering lunettes play a particularly significant role by linking these different depositional and erosional environments. Despite the important clues these landforms may therefore hold in assessing mechanisms, timescales and controls on landscape-scale sediment flux in drylands, existing models of lunette formation are still very limited and often oversimplified. To contribute new data and discussions towards a better understanding the dynamically evolving landscapes around dryland playa lakes, we therefore explore the use of 'source-to-sink' perspectives in unravelling the palaeoenvironmental potential of desert lunettes, and specifically discuss geomorphic, sedimentary and geochronological data from Lake Callabonna in South Australia.

Multiple lunettes were identified around Lake Callabonna and occur in various shapes, sizes and orientations reflecting significant variability in sediment source and/or aeolian transport processes over time. We here present new data from a small km-scale lunette adjacent to the Moppa-Colina delta in the northwestern corner of the lake. Lunette texture is dominantly sandy and implies depositional processes analogous to coastal foredunes. Sedimentary architecture, however, is characterized by laterally continuous and finely interbedded intercalations of well-sorted fine and loamy sands, respectively. These observations are inconsistent with foredune formation, and rather point to processes of frequent and alternating processes of extensive aeolian sand accretion (i.e., draping) across the landscape. Our topographic and new chronological constraints suggest that sustained sediment supply in a late Holocene seasonally active deltaic environment at the interface between fluvial, lacustrine, coastal and aeolian process domains may best explain the observed morphostratigraphic data. In contrast to its growth over more than two millennia, the lunette has been actively eroding over the last few centuries from the combined effects of wind and water. In combination, our observations and preliminary results imply that in addition to variations in wind speed and direction, or the source and supply of sandy sediment, changes in vegetation cover (e.g., pre vs post-European land use) have to be considered when discussing the depositional and post-depositional mechanisms involved in sandy lunette formation as well as their potential for recording late Quaternary palaeoenvironmental conditions and pathways of sediment transport in drylands.

Dryland deltas of Western Australia – analogues for mixed-influenced fluvial-deltaic depositional systems

Lang, Simon¹, Paumard, Victorien¹, O'Leary, Mick¹, Goodwin, Ian¹, Cousins, Victoria¹, Lebec, Ulysse¹, Jian, Andy¹, Holbrook, John², Smith III, Pomeroy², Hasiotis, Stephen³, Vakarelov, Boyan⁴ & Krapf, Carmen⁵

¹Centre for Energy Geoscience, School of Earth Science, University of Western Australia, Perth, Australia; ²Texas Christian University, Dallas, Texas, USA; ³Kansas University, Lawrence, Kansas, USA; ⁴Sedbase, OOD, Sophia, Bulgaria; ⁵Geological Survey

of South Australia, Department of Energy and Mining, Adelaide

Marine deltas are controlled by the dominance of fluvial outflow (F) relative to the influence of waves (W) and tides (T) that control facies distribution. However, in dryland deltaic systems, the rivers typically flow only following ephemeral or seasonal flooding events (i.e., a few weeks of the year either following cyclones or winter storms).

This study focusses on the influence of increasing tidal range and wave power on the coastal geomorphology of three coastal deltas along the arid to semi-arid coast of Western Australia (Gascoyne, Ashburton, and de Grey river deltas), and the role of distributary channel avulsion that build large distributary fluvial systems. Satellite image-derived bathymetry, dGPS transects, digital elevation models, ground penetrating radar, auger holes and outcrops are used for facies mapping of the surficial stratigraphy. Initial results show internal geometries and facies distribution of channel bar forms (dominated by coarse- and medium grained downstream and lateral accretion macroforms), alluvial and delta plain silt- and mud-prone oxidised overbank facies, sandy and silty coastal plain tidal-flats, tidal channels, well-sorted fine-grained sandy strandplain beach ridges, and fine-medium grained distributary mouth bars.

Fluvial distributary channels undergo upstream avulsion and new fluvial mouth-bars grow, and alluvial flood deposits accrete or are eroded on the upper and lower delta plain. Most of the year, the mouth-bars are reworked by waves and tides to build asymmetric, mixed-influenced deltas, and aeolian processes rework the delta/coastal plain. As the tidal range increases from micro-tidal to meso- and macro-tidal, the individual mouth-bar elements become amalgamated into a very broad sand-prone delta front, increasing sand connectivity. Tidal reworked sands are pumped up the distributary channels in the lower delta plain, especially in the dry seasons, where they are highly bioturbated, and homogenized. Laterally, waves generate highly elongate beach-ridges accreting up-drift from the mouth-bars and becoming moulded by aeolian processes. Down-drift, tidal flats pre-dominate, stabilised by mangroves that also line the mud-prone tidal creeks.

High evaporation rates lead to high salinity in the delta plain distributary channels, coastal lagoons and salinas. Calcareous ooids in foreshore deposits are preserved in some of the beach-ridges.

The 2D and 3D geometry and spatial juxtaposition of facies has implications for the range of uncertainty in subsurface reservoir/aquifer modelling of dryland fluvial-deltaic reservoirs.

Cenozoic channel deposits of the Bowen Basin, Queensland

Yu, Tianjiao, Dube, Kudzai, Moss, Patrick, Abylgazina, Adiya, Cooling, Jennifer, & Esterle, Joan

School of Earth and Environmental Sciences, University of Queensland

During the Late Cretaceous through Cenozoic, uplift and weathering in the northern Bowen Basin region, created a series of deep (up to 150 m) channels that filled with sediments and lava flows. The Australian

Cenozoic was a time of great climatic and tectonic change. From the Late Cretaceous as Australia and Antarctica separated and the Australian plate moved northwards, the climate became warmer and drier, and the characteristic modern Australian flora developed. These paleochannels provide an important record of these changes, however their development, age of deposition and the impact of changing weathering conditions are poorly understood. Analysis of core samples confirm that the channel sediments host palynofloras identified as Late Cretaceous to Eocene and record a change from a fire prone environment to a warm and wet high-density rainforest by the Paleogene. Aridification followed from the Neogene into the Quaternary. Lithological and mineralogical analysis of basaltic lavas from the area indicate they were deposited both as subaerial pahoehoe and subaqueous pillow lavas, suggesting that inland lakes covered the landscape at the same time as the volcanisms occurred. These lakes also form carbonaceous mudstones and lignite.

Some channels also floored by tens of metres of breccia that contain angular clasts of underlying Permian strata which fine upwards to conglomerates and sandstones, and also exhibit soft sediment deformation and sedimentary injection features. These are interpreted as alluvial fans initiated by extensional faulting that may have been seismically active during deposition and contributed to subsidence resulting in the inland lakes. Here thick (2 to 4 m) lignites alternating with kaolinite-rich white clays and heavily altered claystones complete the sedimentary sequence that is then capped by basaltic lava flows. The kaolinite-rich clays can have a number of different origins. It may be primary, or weathering products of intrusive quartz rich rhyolite, tuff, or other sediments subjected to hydrothermal alteration beneath the basalts or stripped by humic acids from the lignites. The origins and timing of kaolinite development is being investigated.

Sedimentology and geomorphology of Lake Yamma Yamma – a long-lived structurally controlled playa lake of the Lake Eyre Basin

Mann, Sandra, & Amos, Kathryn

The University of Adelaide, Adelaide, Australia

This poster details the sedimentology and geomorphic evolution of a modern structurally controlled lake, with an emphasis on dryland lake-delta deposits and paleo shorelines. Lake Yamma Yamma, off Cooper Creek, sits ~750 km upstream and ~90 m higher than the ultimate base level of the basin at Kati Thanda-Lake Eyre. Satellite imagery, inundation frequency maps, hydrological data and digital elevation data, along with modern sediment observations and descriptions are used to interpret sedimentary processes, depositional elements and the evolution of the playa lake. Results suggest that Lake Yamma Yamma is long lived and evolution is primarily structurally controlled with the lake delta aggrading to the northwest over time, and that paleoshorelines to the north of the lake may be remnant features of a prior climate regime. This poster is for those interested in the sedimentology and geomorphology of dryland continental systems for applications such as landscape evolution, environment, natural resource management.

Scientific results of the International Ocean Discovery Program: A decade of success

The isotopic footprint of a submarine mineral system: Cr and Sr isotopes in the Iheya North hydrothermal field, Okinawa Trough (IODP expedition 331)

McGee, Lucy¹, Burke, Thomas¹, Farkas, Juraj¹, Cave, Bradley¹, & Yeats, Chris²

¹*Department of Earth Sciences, University of Adelaide, Adelaide, Australia;* ²*Geological Survey of New South Wales, Department of Regional NSW, Maitland, Australia*

'Black smokers', or submarine hydrothermal vents, represent sites of intense hydrothermalism. Such chimneys transport metals into the ocean where they precipitate as Fe, Pb, Zn and Cu sulfide minerals. However, the spatial footprint of these high-temperature processes transporting metals in marine environments is not well constrained. Legacy material from the 2011 IODP expedition 331 to the Iheya North hydrothermal field in the Okinawa Trough provide a unique opportunity to investigate the isotopic footprint of key metals in the hydrothermal system. The sample set is based on the analysis of four cores: one situated at the foot of an actively forming massive sulfide mound, one drilled at a background site located 1km away from the hydrothermal vents and two cores sampled between these sites, representing a high temperature vent and a lower temperature vent. Samples taken at various depths from the four cores represent a wide range of material, from unaltered distal marine clays, through hydrothermally altered clays and volcanic material, to massive sulfides.

Bulk digestions on 30 samples give a suite of trace element analyses which show large variations, particularly in transition metal element concentrations. SEM-MLA mapping of key samples show important interactions between sulfide phases and the presence of gypsum/anhydrite shows oxidation and reduction in the same sample. The large variation between magmatic and seawater endmembers in ⁸⁷Sr/⁸⁶Sr isotopic ratios provide an excellent opportunity to investigate the magmatic 'footprint' of the metalliferous hydrothermal system in marine settings and how far into the background this can be detected. Stable Cr isotopes have the potential to show important redox interactions during anticipated oxidation of hydrothermal Cr(III) species in marine settings into oxidised Cr(VI), and possible back-reduction to Cr(III).

East Antarctic meltwater influx from the Wilkes Subglacial Basin since the Last Glacial Maximum as determined by beryllium isotopes

Behrens, Bethany^{1,2}, Miyairi, Yosuke¹, Sproson, Adam D.¹, Yamane, Masako³, & Yokoyama, Yusuke^{1,2,4}

¹*Atmosphere and Ocean Research Institute, University of Tokyo, Kashiwa, Japan;* ²*Graduate Program on Environmental Science, University of Tokyo, Komaba, Japan;* ³*Institute for Space-Earth Environmental Research, Nagoya University, Furocho, Japan;* ⁴*Department of Earth and Planetary Science, Graduate*

School of Science, University of Tokyo, Hongo, Japan

The West Antarctic Ice Sheet (WAIS) and East Antarctic Ice Sheet (EAIS) contain an amount of ice equivalent to 3–5 m and 53 m sea level rise, respectively (1). The WAIS, as a largely marine-based ice sheet, is susceptible to changes in ocean temperatures and prone to retreat. Recent research has revealed that areas of the EAIS situated below sea level are also very sensitive to atmospheric and oceanic temperature changes and vulnerable to retreat (2, 3). The two largest subglacial basins in East Antarctica, the Wilkes and Aurora basins, hold a total ice mass equivalent to 28 m sea level rise (4), demonstrating that even a partial collapse of the EAIS would have a major effect on global sea level.

While we know the general timing of post-LGM glacial retreat around Antarctica, there is scarce data on specific locations with detailed, high-resolution records of ice sheet dynamics during the Holocene. Here we present meteoric beryllium-10 (^{10}Be) analysis of a marine sediment core from the Adélie Basin, located on the continental shelf offshore the Wilkes Basin, extracted during IODP Expedition 318. Our record covers the most recent period of major Holocene ice sheet retreat, sea level rise, and increased atmospheric CO_2 since the Last Glacial Maximum ice sheet retreat (5). The beryllium isotope data suggest oceanic or climatic changes occurred at ca 9.8 ka, ca 6.3 ka, and from ca 4.1 ka. From prior research, we can conclude our high meteoric ^{10}Be values at ca 9.8 ka and ca 6.3 ka are attributed to an open marine environment created by the retreat of grounded ice along with an increased influx of meltwater (6–8). The elevated concentration and frequency variation of meteoric ^{10}Be values starting from ca 4.1 ka indicate a change in regime, possibly linked to changes in climate.

- (1) Wilson DJ, Bertram RA, Needham EF, van de Fliedert T, Welsh KJ, McKay RM, *et al.* Nature. 2018, 561(7723): 383–6.
- (2) Hansen MA, Passchier S. Geo-Marine Letters. 2017, 37(3): 207–13.
- (3) DeConto RM, Pollard D. Nature. 2016, 531:591.
- (4) Shen Q, Wang H, Shum C, Jiang L, Hsu HT, Dong J. Scientific Reports. 2018,8(1): 4477.
- (5) Yokoyama Y, Esat TM, Thompson WG, Thomas AL, Webster JM, Miyairi Y, *et al.* Nature. 2018, 559(7715): 603–7.
- (6) Yokoyama Y, Anderson JB, Yamane M, Simkins LM, Miyairi Y, Yamazaki T, *et al.* Proceedings of the National Academy of Sciences. 2016, 113(9): 2354.
- (7) Valletta RD, Willenbring JK, Passchier S, Elmi C. Paleoceanography and Paleoclimatology. 2018, 33(9): 934–44.
- (8) Behrens B, Miyairi Y, Sproson AD, Yamane M, Yokoyama Y. Journal of Quaternary Science. 2019, 34(8): 603–8.

85 000 years of polar front, warm current variability, and ice rafting in contourites off southwest Ireland

Westgård, Adele¹, Gallagher, Stephen J.¹, Monteys, Xavier², Foubert, Anneleen³, & Rüggeberg, Andres³

¹The University of Melbourne, Melbourne, Australia; ²Geological Survey of Ireland, Beggars Bush, Haddington Road, Dublin 4, Ireland; ³Department of Geosciences – Geology, University of Fribourg, Chemin du Musée 6, CH - 1700 Fribourg, Switzerland

Integrated Ocean Drilling Program Expedition 307 Site U1318B cored a 90 m thick Quaternary contourite sequence in the Porcupine Seabight in 423 m water

depth to understand paleoenvironmental conditions of cold-water coral carbonate mound growth initiation. Two warm contour currents flow northwards in the Porcupine Seabight: the Eastern North Atlantic Central Water (ENACW, ~600 m) and the Mediterranean Outflow Water (MOW, ~1000 m). However, while much work has been carried out on the carbonate mound province in the area the palaeoenvironmental context of the surrounding contourites has received scant attention. This work analysed planktonic foraminiferal assemblages and ice rafted debris (IRD) variability in the upper 30 m of Site U1318B to interpret oceanographic variability related to contourite sedimentation and interpret the extent and timing of the British Irish Ice Sheet (BIIS) over the last 85 000 years.

Samples from Site U1318B were processed for foraminiferal analysis. Planktonic foraminiferal assemblages (>150 μm fraction) were used to interpret sea surface temperatures (SST). The presence of the polar front (SST <8 °C) in the region was characterised by >80% *Neogloboquadrina pachyderma* (%NPS). IRD (>150 μm) abundance was counted and plotted by source area. An age model was developed using a ^{14}C date, a nannofossil datum (*Emiliana huxleyi*/*Gephyrocapsa caribbeanica*) and regional correlation to MD01-2461 using %NPS and magnetic susceptibility data and to the Lisicki & Raymo (LR2004) stack.

The upper 30 m of Site U1318B is typified by alternations of dark brown-grey, occasionally laminated mud and medium to coarse sand facies with erosional bases. Muddy sand layers, sand lenses and dropstones are common. Planktonic foraminiferal data suggests that in the last 85 ka the polar front was south of Site U1318B (>80% NPS) ca 24 ka, ca 28 ka, from 35 to 37 ka, 40 to 66 ka and ca 68 ka. %NPS reached 70–79% on several times suggesting intermittent polar conditions. Subtropical taxa are rare when NPS are common. Maxima (<12%) of subtropical taxa occur several times in the last 35 ka suggesting intermittent ENACW influence. The IRD are predominantly sourced from the BIIS area. Increased IRD yield coincides with decreased %NPS. IRD maxima do not coincide with %NPS maxima since ice rafting was related to melting. IRD concentration gradually decreased after the last glacial maximum (LGM) (ca 20 ka).

Presence of subtropical taxa in contourite facies suggest increased current activity during warm periods. These currents likely slowed/shut down in association with the North Atlantic Meridional Overturning Circulation during cold periods. Periods of increased IRD concentration suggest BIIS extent reached the SW continental margin of Ireland from late MIS 5 (ca 80 ka) to MIS 2 (ca 20 ka). Significant decrease in IRD concentration suggests the BIIS started to retreat from the Porcupine Seabight following the LGM at around 20 ka.

Hydrocarbons in a new early Paleocene sedimentary section recovered from the Campbell Plateau, south of New Zealand, by IODP Expedition 378

George, Simon C.¹, Ausin, Blanca², Childress, Laurel B.³, Röhl, Ursula⁴, Thomas, Deborah J.⁵, Hollis, Christopher J.⁶, and the IODP Expedition 378 Science Party

¹Department of Earth and Environmental Sciences, Macquarie University, Sydney, Australia; ²Department

of Geology, University of Salamanca, Spain; ³International Ocean Discovery Program, Texas A&M University, USA; ⁴MARUM, University of Bremen, Germany; ⁵College of Geosciences, Texas A&M University, USA; ⁶GNS Science, New Zealand

The Cenozoic era in the South Pacific is poorly known through rather sparse drilling. International Ocean Discovery Program (IODP) expedition 378 “South Pacific Paleogene Climate” took place offshore New Zealand from January to February 2020. Expedition 378 recovered the first continuously cored, multiple-hole Paleogene sedimentary section from the southern Campbell Plateau at Site U1553. This high-southern latitude site builds on the legacy of Deep Sea Drilling Project (DSDP) Site 277, a single, partially spot cored hole, providing a unique opportunity to refine and augment existing reconstructions of the past ca 66 My of climate history. Multiple cored intervals were likely recovered from the Eocene–Oligocene transition (EOT), the Middle Eocene Climatic Optimum (MECO) and other Eocene Thermal Maximum events, and the Paleocene–Eocene Thermal Maximum (PETM). Expedition 378 also discovered a new expanded Paleocene siliciclastic formation (Unit V) that had never been drilled before, with an unknown basal age.

Coring at Site U1553 reached a maximum depth of 584.3 mbsf and recovered a 581.16 m long sedimentary succession of deep-sea pelagic sediment of Pleistocene and Oligocene to early Paleocene age from the Campbell Plateau. The recovered sections comprise five lithostratigraphic units. About 4 m of Pleistocene foraminifer-rich nannofossil ooze (Unit I) overlies an expanded sequence (~200 m thick) of late Oligocene–early Oligocene nannofossil ooze with foraminifers (Unit II). The nannofossil ooze in Unit II gradually transitions into nannofossil chalk in Unit III over 50 m from ~175 to 225 mbsf. Lithification of carbonates continues downcore and results in limestone, categorized as Unit IV. Finally, the bottom ~100 m of the sediment column contains siliciclastic Unit V, characterized by alternating mudstone, sandy mudstone, and very fine to medium-grained sandstone.

Headspace gas analyses for the uppermost 480 m of Site U1553 indicated very low hydrocarbon concentrations, suggesting the lack of biogenic and/or thermogenic gas production or their upward migration. A sudden increase in methane concentration occurred at the transition from Unit IV to Unit V. The methane increase was accompanied by the detection of thermogenic hydrocarbons (C₂, C₃ and C₄), suggesting *in situ* methane production, possibly by microbial activity, and upward migration of thermogenic gas. Additionally, the deeper Unit V cores had a strong hydrocarbon odour on the catwalk and after core splitting and fluoresced under UV light. A sample of the deepest core in Hole D was placed in a glass vial immediately after on-board core splitting and covered with acetone, to obtain a signature of these hydrocarbons. This solvent mixture was analysed by gas chromatography-mass spectrometry, which has revealed the presence of a bimodal distribution of n-alkanes (maxima at n-C₁₄ and n-C₂₀). The sample also contains methylalkanes, isoprenoids, alkylcyclohexanes, alkylbenzenes, alkyl-naphthalenes, alkylphenanthrenes, other polycyclic aromatic hydrocarbons, and high molecular weight biomarkers including hopanes and steranes. The distribution of these compounds is

consistent with a mixed signature, from firstly a mature migrated hydrocarbon phase, and secondly from indigenous immature hydrocarbons from the rock matrix.

A microbial mayhem in the Chicxulub crater

Schaefer, Bettina¹, Grice, Kliti¹, Coolen, Marco J. L.¹, Summons, Roger E.², Cui, Xingqian², Bauersachs, Thorsten³, Schwark, Lorenz³, Böttcher, Michael E.^{4,5,6}, Bralower, Timothy, J.⁷, Lyons, Shelby, L.⁷, Freeman, Kate H.⁷, Cockell, Charles S.⁸, Gulick, Sean S.⁹, Morgan, Joanna V.¹⁰, Whalen, Michael T.¹¹, Lowery, Christopher, M.⁹, & Vajda, Vivi.¹²

¹Western Australian - Organic and Isotope Geochemistry Centre (WA-OIGC), School of Earth and Planetary Sciences, The Institute for Geoscience Research, Curtin University, Perth WA, Australia; ²Department of Earth, Atmospheric and Planetary Sciences, Massachusetts Institute of Technology, Cambridge, MA, USA; ³Department of Organic Geochemistry, Institute of Geoscience, Christian-Albrechts-University, Kiel, 24118, Germany; ⁴Geochemistry & Isotope Biogeochemistry Group, Department of Marine Geology, Leibniz Institute for Baltic Sea Research, 18119 Warnemünde, Germany; ⁵Marine Geochemistry, University of Greifswald, 17489 Greifswald, Germany; ⁶Department of Maritime Systems, Interdisciplinary Faculty, University of Rostock, 18059 Rostock, Germany; ⁷Department of Geosciences, Pennsylvania State University, University Park, PA, USA; ⁸School of Physics and Astronomy, University of Edinburgh, Edinburgh, UK; ⁹Institute for Geophysics, Jackson School of Geosciences, University of Texas, Austin, TX, USA; ¹⁰Department of Earth Sciences and Engineering, Imperial College London, UK; ¹¹Department of Geosciences, University of Alaska, Fairbanks, AK, USA; ¹²Department of Palaeobiology, Swedish Museum of Natural History, Stockholm, Sweden

The Chicxulub crater (Yucatán Peninsula, Mexico) was formed by an asteroid impact 66 Ma ago and is thought to have caused the Late Cretaceous mass extinction event (e.g., Schulte *et al.*, 2010; Hildebrand, 1991), which led to 76% loss of species world-wide including non-avian dinosaurs (Sepkoski, 1986). Also, a collapse in phytoplankton productivity in the world's oceans occurred due to a lack of sunlight (Zachos & Arthur, 1986). In 2016, the peak ring of the Chicxulub crater core was recovered by the International Ocean Discovery Program and International Continental Drilling Program Expedition 364 (“Chicxulub: Drilling the K-T Impact Crater”). Samples from this core were extracted and analysed for lipid biomarkers and stable isotopes.

Lipid biomarker profiles were used to reconstruct the origin, recovery and development of non-fossilized microbial life forms and the associated paleo-environmental conditions in the crater from the days after the impact to up to 4 million years. A tsunami that flooded the crater within a day after the impact (Gulick *et al.*, 2019) deposited the upper part of the suevite sequence and carried debris containing cyano-bacteria, archaea, dinoflagellates and all types of anaerobic photosynthetic sulfur bacteria, likely originating from microbialites that inhabited the coast of the carbonate platform prior to impact site. The redeposited coastal

cyanobacteria predominantly were diazotrophic heterocystous bacteria of the order Nostocales, as evidenced by their characteristic C₂₆-glycolipids. The coastal anaerobic sulfur bacteria were composed of Chlorobiaceae and Chromatiaceae, revealed by the presence of their specific biomarkers from carotenoid pigments (Schaefer *et al.*, 2020). In addition, re-deposited terrestrial organic matter was degraded *in situ* in the tsunami layer by fungi, as evidenced by enhanced concentrations of perylene (cf. Grice *et al.*, 2009).

As tsunami energy declined, land-derived material and nutrients fed the crater's microbial ecosystem for the following ca 30 kyr and led to non-heterocystous pelagic cyanobacterial blooms, recognized by the presence of 2a-methylhopanes. A major change towards an oligotrophic sea occurred 200 kyr after impact supporting nitrogen-fixing heterocystous cyanobacteria (Schaefer *et al.*, 2020). The cyanophyte community structure by then had changed and diversified, as recognized by the occurrence of C₃₂-heterocystous glycolipids, abundant in cyanophytes of the order Stigonematales. About 300 kyr after the impact with the onset of the Danian-C2 hyperthermal event (ca 65.7 Ma ago) during deposition of hemipelagic limestones abundant carotenoid biomarkers of photosynthetic sulfur bacteria suggests that the water-column in the crater became episodically stratified allowing for the development of photic zone euxinia.

The microbial life near the Chicxulub crater recovered quickly under harsh conditions post impact and subsequently continued to experience rapid changes in environment.

Gulick, S., *et al.*, 2019. First Days of the Cenozoic. *PNAS*, 116, 19342–19351.

Grice *et al.*, 2009. New insights into the origin of perylene in geological samples. *Geochimica et Cosmochimica Acta*, 73, 6531–6543.

Hildebrand, A. R. *et al.*, 1991. Chicxulub crater: a possible Cretaceous/Tertiary boundary impact crater on the Yucatan Peninsula, Mexico. *Geology*, 19, 867–871.

Schaefer, B., *et al.*, 2020. Microbial life in the nascent Chicxulub crater. *Geology*, 48, 328–332.

Schulte, P., *et al.*, 2010. The Chicxulub Asteroid Impact and Mass Extinction at the Cretaceous–Paleogene Boundary. *Science*, 327, 1214–1218.

Sepkoski, J. J., 1996. In: *Global events and event stratigraphy in the Phanerozoic*. pp. 35–51, Springer.

Zachos, J., Arthur, M., 1986. Paleocyanography of the Cretaceous/Tertiary boundary event: inferences from stable isotopic and other data. *Palaeogeography & Palaeoclimatology*, 1, 5–26.

investigations through this sequence. At Site U1512 offshore of southern Australia, IODP Expedition 369 recovered a 690 m thick succession of lower Turonian to upper Santonian silty claystone with only a few thin beds of glauconitic and sideritic sandstone (<32 cm thick). This core provides the most comprehensive record of depositional and paleoenvironmental events obtained from the Bight Basin. Clay-rich sedimentary facies and a dominance of agglutinated benthic foraminifera suggest the succession was rapidly deposited by hyperpycnal and hypopycnal flows in a marine prodelta setting, presumably in response to high terrestrial runoff. Organic geochemical and palynofacies data indicate sustained fluvial input into the basin with increases in delivery of plant-derived material. Marine-algal input slowly increases from the Turonian into the Santonian as indicated from C₂₇/C₂₉ steranes ratios between 1 and 1.5. Pristane/phytane ratios (1.73 to 0.13) in conjunction with common glauconite and pyrite reveal the basin became more dysoxic and restricted during Turonian and Coniacian times before slowly opening up during the Santonian. This was possibly due to the combined effect of a eustatic lowstand during the late Turonian, unstable patterns in oceanic circulation and increasing continental influence. Provenance studies from analysis of detrital zircons from the Coniacian part of the succession show that sediment was derived from similar sources determined for the Santonian to Maastrichtian succession in the nearby Gnarlyknobs 1A well. Sediment was not only derived from the Whitsunday Large Igneous Province (ca 125–95 Ma) and the New England Fold Belt (ca 300–200 Ma) to the northeast, but also from the Albany-Fraser Orogen (ca 1.3–1.0 Ga) to the west. The gradual switch in sedimentary provenance during the Late Cretaceous was likely related to exhumation and erosion of these regions during the rifting of Zealandia off southeastern Gondwana. Evidence from Site U1512 suggests the basin was fed by two or more large transcontinental rivers that entered the restricted basin that were present before the break-up of Australia and Antarctica. These records offer a new understanding of Gondwanan paleogeography and our understanding of marginal marine settings in the southern high latitudes during the Cretaceous Greenhouse.

Late Cretaceous turmoil in the southern high latitudes: a story of environmental stress, basin restriction and deltaic sedimentation from IODP Site U1512, Bight Basin, Australia

Wainman, Carmine C., & McCabe, Peter J.

Australian School of Petroleum and Energy Resources, University of Adelaide, Adelaide, Australia

The Bight Basin is a relatively poorly explored basin that developed during the break-up of Australia and Antarctica. The basin hosts a 15 km thick deltaic succession deposited during the height of the Cretaceous Greenhouse. Although there have been extensive seismic investigations and a few provenance studies from cuttings in the region, there is little well data and core material to undertake detailed

CORE TO CRUST

The Australian Lithosphere in 2021: What do we know and future challenges

Goelectric structure of Tasmania from multi-scale magnetotelluric data

Ostensen, Thomas^{1,2}, Reading, Anya², Cracknell, Matthew², Roach, Michael², McNeill, Andrew³, Duffett, Mark³, Bombardieri, Daniel³, Thiel, Stephan⁴, Robertson, Kate⁴, Duan, Jingming⁵, & Heinson, Graham⁶

¹*Solve Geosolutions, Level 5, 24 Davey Street (Hobart City Council Building), Hobart, Australia;* ²*School of Natural Sciences (Earth Sciences), Private Bag 79, University of Tasmania, Hobart, Australia;* ³*Mineral Resources Tasmania, Department of State Growth, 30 Gordons Hill Road, Rosny Park, Australia;* ⁴*Geological Survey of South Australia, Level 7, 101 Grenfell St, Adelaide, Australia;* ⁵*Geoscience Australia, Cnr Jerrabomberra Ave and Hindmarsh Drive, Symonston, Australia;* ⁶*School of Physical Sciences (Earth Sciences), The University of Adelaide, Adelaide, Australia*

The current understanding of Tasmania's enigmatic tectonic history has been informed by geological information observed or sampled at the Earth's surface coupled with geophysical data sets sensitive to magnetic, density and seismic properties of the rocks forming the crust and mantle beneath. With the completion of the Tasmanian portion of the Australian Lithospheric Architecture Magnetotelluric Project (AusLAMP), new 3D and 2D geophysical models describing the electrical properties of the Tasmanian lithosphere at different spatial scales have been derived to compliment these data.

At the whole-of-state scale, 3D inverse models of the long period magnetotelluric (MT) data have illuminated the electrical structure of the mid-crustal to lithospheric mantle depths. This model images the full extent of the Tamar Conductivity Anomaly, a crustal-scale conductor extending from northern to southern Tasmania along the boundary between eastern and western Tasmanian geologic terrains.

In the west of the state, a 2D inverse model transecting the Cambrian Mount Reid Volcanics brings the electrical structure of the upper- to mid-crustal depth range in this economically important part of the state into sharper focus. The model images west-dipping conductive structures spatially coincident with major faults and associated copper mineralisation near Queenstown.

Finally, in the central east of Tasmania, a joint inversion incorporating legacy broadband MT data with newer AusLAMP MT data using the whole-of-state scale model as a priori goelectric structure was conducted. Inversion results demonstrate a potential use case for regional scale AusLAMP models to improve higher resolution goelectric structure modelling, with the joint inverse model imaging the Lemont geothermal field at higher resolution while simultaneously mapping geologically feasible 3D resistivity structures.

New insight into the Carpentaria Conductivity Anomaly from high resolution MT data in the Cloncurry region

Simpson, J. M.¹, Brown, D. D.¹, Duan, J.², & Kyi, D.²

¹*Geological Survey of Queensland, Brisbane, Australia;* ²*Geoscience Australia, Canberra, Australia*

The electrical structure of Queensland is dominated by the Carpentaria Conductivity Anomaly (CCA). It stretches hundreds of kilometres from the Gulf of Carpentaria in the north, possibly extending as far south as Birdsville. It is present in the crust and extends down into the mantle. The CCA is of great interest as it underlies significant mineral deposits in the Eastern Succession of Mount Isa such as Ernest Henry. Modelling of existing broadband and long period MT data has been used to suggest the CCA may be associated with collisional tectonics along the Gidyea Suture during the Proterozoic.

A new MT survey in the Cloncurry region offers insight into the crustal portion of this anomaly. The survey offers over 500 new MT sites at 2 km station spacing and was collected in 2020. Conductive anomalies are imaged by the new data which are associated with both the Mount Margaret and the Quamby/Fountain Range Faults. The conductive response occurs from approximately 2 km depth and extends into the deep crust. These are both major structures that have accommodated significant crustal movements throughout the complex history of Mount Isa. Mount Margaret Fault is related to the Gidyea Suture, while different interpretations of deep crustal seismic data in the area suggests that the Quamby/Fountain Range Fault extends either into the mid-crust or is full crustal thickness structure.

The presence of conductive anomalies along such major structures suggests that they could be functioning as more localised fluid pathways from the deeper part of the conductive anomaly. The presence of conductive anomalies along both these structures, rather than just along the Gidyea Suture associated Mount Margaret Fault suggests that the CCA is not simply a suture related feature.

Next-generation model of the Australian crust from synchronous and asynchronous ambient noise imaging

Chen, Yunfeng^{1,2}, & Saygin, Erdinc¹

¹*Deep Earth Imaging, Future Science Platform, CSIRO, Perth, Australia;* ²*Department of Physics, University of Alberta, Edmonton, Canada*

The proliferation of seismic networks in Australia has laid the groundwork for improved probing of the continental crust. Despite ever-growing seismic instrumentation across the country, the last major effort of mapping continental-scale structures with seismic ambient noise was conducted more than a decade ago, thereby demanding a new appraisal of its crustal structure. In this study, we develop a new crustal model of the Australian continent using a large dataset that consists of nearly 30 years (1992–2019) of continuous seismic recordings from over 2200 stations. This unprecedented dataset is further exploited with the recently developed ambient noise imaging workflow of Chen & Saygin (2020) that integrates results from

temporary seismic arrays deployed at different times. We compute two sets of noise correlation functions (NCFs) between (1) synchronous stations with the conventional ambient noise correlation (i.e., C1) and (2) asynchronous pairs with the high-order correlation technique (i.e., C2) based on correlational and convolutional types of source–receiver interferometry. The C2 approach enables extracting 1–3 times more NCFs than available from using C1 alone, and the combined dataset leads to over 200 000 high-quality NCFs to image the crustal structures, significantly improved upon the most recent model constructed from 7500 measurements. We invert the Rayleigh wave arrival times for group velocities between 4–40 sec using a trans-dimensional inversion. This non-linear inversion approach adopts an adaptive parameterization and Bayesian inference to account for unbalanced data sampling and allows assessment of the model uncertainties. The final 3D shear velocity model reveals fine-scale structure in the Australian crust. The low velocities at shallow depths (<10 km) are in excellent agreement with the distribution of known sedimentary basins and also hint at the presence of unreported basins/sub-basins in previously poorly explored areas, for example, northern Australia. At lower crustal depths (30–40 km), our model delineates the boundaries of major Archean blocks such as the Yilgarn and Pilbara cratons in Western Australia. High-velocity structures also characterize the lower crust/uppermost mantle of the Phanerozoic New England Orogen near the eastern continent margin. In conclusion, this study provides significantly improved constraints on the shear velocity structures and builds a new basis for the next-generation crustal model of the Australian continent.

Recent progress in laboratory studies of seismic wave attenuation relevant to the Earth's upper mantle

Qu, Tongzhang¹, Jackson, Ian¹, David, Emmanuel C.^{1,2}, & Faul, Ulrich H.^{1,3}

¹Research School of Earth Sciences, Australian National University, Canberra, ACT, Australia; ²Now at Department of Earth Sciences, University College London, London, United Kingdom; ³Department of Earth, Atmospheric and Planetary Sciences, Massachusetts Institute of Technology, Cambridge, Massachusetts, USA

The Earth's upper mantle is being imaged with increasing fidelity with the various methods of modern seismology. However, such images are of limited value without laboratory-based models for their robust interpretation in terms of the many factors (e.g., chemical composition, temperature, and partial melting) that influence the seismic properties of mantle materials. Over decades, we have developed a unique capability for measurement of seismic properties of rock cylinders by forced oscillation at seismic periods (1–1000 s) rather than the much shorter periods (ns– μ s) of laboratory wave-propagation methods. Sustained application of these methods has documented grain-size sensitive viscoelastic relaxation, responsible for frequency dependence (dispersion) of the shear modulus and hence wavespeed and related strain-energy dissipation in polycrystalline olivine, as well as the influence of partial

melting and dislocation density, and more recently, of oxidizing/hydrous conditions.

Here we report new measurements on olivine–orthopyroxene mixtures. For temperatures reaching 1200 °C and seismic periods, the strain-energy dissipation and shear modulus dispersion are generally similar to those for essentially pure olivine, but somewhat diminished and slightly more temperature-sensitive with increasing orthopyroxene concentration from 5% to 95%. The viscoelastic behaviour is of the high-temperature-background type without any evidence of the superimposed dissipation peak reported by others for a melt-bearing specimen of otherwise similar composition. It is concluded that our olivine-based model for seismic wave dispersion and attenuation will require only modest modification to accommodate the role of orthopyroxene.

In order to further refine our methodology, we are also addressing the effect of uncertainty in the mechanical behaviour of the enclosing mild-steel jacket arising from the transition between the austenite and ferrite phases on cooling across the interval 900–700 °C. Variations of its microstructure and hence viscoelastic behaviour have the potential to mask the seismologically important onset, within this temperature range, of appreciably viscoelastic behaviour of upper-mantle materials. Accordingly, we have previously conducted a study in which a specimen of polycrystalline olivine is jacketed instead within a copper sleeve which retains its face-centred-cubic (fcc) structure throughout the range of the measurements – limited to 1050 °C maximum by the proximity of the melting point. Here we report new measurements to higher temperature (1200 °C) in which we employed austenitic (fcc) stainless steel (SS) as an alternative jacket material. Prior measurement of the mechanical properties of the SS jacket material allowed subtraction of its contribution to the torsional stiffness of the SS-jacketed specimen. The resulting dissipation spectrum for the olivine specimen consists of a monotonic background dissipation with a superimposed peak located within the 1–1000 s period range for temperatures between 900 and 1050 °C. The dissipation peak and associated shear modulus dispersion, potentially attributable to elastically accommodated grain-boundary sliding, display an Arrhenius dependence upon temperature – moving systematically to shorter periods with increasing temperature. Comparison of the results obtained for synthetic Fo₉₀ olivine specimens enclosed within the alternative mild-steel, copper, and stainless-steel jackets is providing new insight into the nature of the seismologically important transition between the elastic and anelastic regimes.

Provenance of late Cambrian–Ordovician sedimentary rocks in western, northeastern Tasmania and southern Victoria: constraints from U/Pb dating, zircon geochemistry and ϵ Hf isotope

Habib, Umer, Meffre, Sebastien, Kultaksayos, Sitthinon, & Berry, Ron

Centre of Ore-Deposit Geology and Earth Sciences, University of Tasmania, Hobart, Australia

The sedimentary sequences in western, northeastern Tasmania and southern Victoria preserves an excellent record of distinctive Cambrian to Ordovician deposition

environments and sediment provenance. Here we integrate new and already published U/Pb detrital age data, field observations, zircon geochemistry, and Hf isotope data to establish the sediment source and tectonostratigraphic history of these rocks. Overall, the detrital age spans from 2.6 Ga to 0.476 Ga, which includes some major Precambrian and Cambrian age peaks. The 1.8–1.2 Ga peaks for Western Tasmania are consistent with derivation from the Tyenna region which incorporate sediments derived from granitoids in Laurentia (North America) and Baltica. A small population of detrital ages from 1.5–1.1 Ga from northeastern Tasmania and southern Victoria is suggested to have Grenville provenance, possibly from central Australia or other parts of the Grenvillian Orogen. The 850–545 Ma detrital ages occur in all sedimentary rocks and are from the widely represented Pacific-Gondwana Phanerozoic sediments of south eastern Australia. These 850–545 Ma detrital ages are rare in the Owen Group, relative to the overlying Middle–Late Ordovician Pioneer Sandstone, implying a sharp shift in provenance in western Tasmania in the Early Ordovician. The Pioneer Sandstone is very similar to Early Ordovician sandstones from Waratah Bay in southern Victoria and Ordovician sandstone from eastern Tasmania. Also present in the samples are 480–520 Ma zircons. However, the proportions of these in the sedimentary rocks are variable. The Th/U ratios from the Cambrian zircons in western Tasmania support a proximal source from the Mt Read Volcanics. The Cambrian zircons in eastern Tasmania and southern Victoria have much lower Th/U ratios, implying a different provenance. The ϵ_{Hf} isotope signatures and statistical analysis, along with sedimentological and paleocurrent data from previous studies, support a local derivation from Precambrian and Cambrian detrital sources for the western Tasmanian rock units, indicating deposition in a segmented basin-margin fault system. The eastern Tasmanian and southern Victorian sandstone were deposited in a basin offshore from the Tyennan-Delamerian Orogen during the Ordovician.

Lapstone Structural Complex and uplift of the Blue Mountains, tectonic backdrop to western Sydney, Australia

Fergusson, Chris¹, & Hatherly, Peter²

¹*School of Earth, Atmospheric and Life Sciences, University of Wollongong, Wollongong, Australia;*
²*Lavender Bay, Sydney, Australia*

The eastern margin of the Blue Mountains uplift is well defined by the Lapstone Structural Complex (LSC) with elevations typically of 150 to 200 m but locally up to 600 m at Kurrajong Heights. While it has been suggested that the LSC is related to normal faulting associated with passive margin development, this suggestion is inconsistent with a west-dipping reverse fault with minimal fault damage development (the Bargo Fault) we have found in the southern part of the LSC. We prefer the alternative view that the LSC consists of east-facing monoclines and reverse faults that dip both east and west. The underlying controlling structure could be a west-dipping thrust and the surface expression is due to the formation of a triangle zone. Further support for our interpretation is found in the northern part of the LSC where there are gravels (Rickabys Creek Gravel) and clay (Londonderry Clay) which are draped along

the front of the monocline. Their position indicates that they were folded during development of the LSC. Thus the gravels do not occur in a series of terraces as was previously considered. Unfortunately, no direct age of the Rickabys Creek Gravel and the Londonderry Clay has been determined but their unconsolidated state is consistent with a Neogene age thereby constraining formation of the LSC to the Neogene. Ongoing seismic activity associated with the LSC indicates neotectonic activity along the structure. The higher parts of the Blue Mountains are at elevations of over 1000 m and overall rock units of the Sydney Basin slope to the east at an angle of ca 1.5°. We consider that the latest phase of uplift in the Blue Mountains was associated with formation of the LSC and other structures including the Mt Tomah Monocline. Given earlier phases of uplift associated with formation of the eastern highlands it is problematic to identify the limits of this younger phase of Blue Mountains uplift particularly in the west where it apparently merges with the Central Tablelands. The enduring debate about the cause of the uplift of the Great Dividing Range of eastern Australia has become increasingly centred on the importance of mantle upwelling. We consider that the younger phase of uplift of the Blue Mountains associated with formation of the LSC was related to Australia's setting west of the Southwest Pacific convergent margin rather than mantle upwelling.

Disorientation control on trace element segregation in fluid-affected low-angle boundaries in olivine

Tacchetto, Tommaso^{1,2}, Reddy, Steven^{1,2}, Saxey, David², Fougereuse, Denis^{1,2}, Rickard, William², & Clark, Chris¹

¹*School of Earth and Planetary Sciences, Curtin University, Perth, Australia;* ²*Geoscience Atom Probe, Curtin University, Perth, Australia*

The interfaces between minerals (grain boundaries *s.l.*) play a critical role in controlling the rheological behaviour of rocks and the ability of fluids to penetrate them in the deep crust. However, the role of chemical segregation in controlling the behaviour of mineral interfaces remains largely unexplored. In this work, we combined electron backscattered diffraction (EBSD) and atom probe tomography (APT) to assess the relationship between deformation-related low-angle boundaries in naturally deformed olivine and the degree of trace element segregation to those boundaries. The sample studied comes from the Bergen Arcs (Norway), where high-grade, dry, metamorphic rocks of the lower crust have been overprinted by fluid-present high-pressure metamorphism during the Caledonian tectonic subduction between 430 and 410 Ma. EBSD orientation mapping of deformed olivine is used to characterise the slip systems associated with deformation and the misorientation relationships within different parts of the microstructure. APT has then been used to systematically target grain boundaries of different misorientation angle (up to 8°).

The analysed boundaries formed by sub-grain rotation recrystallisation associated with {100}<001> slip system developed during the fluid-catalysed metamorphism. APT data show that olivine trace elements segregated to the low-angle boundaries during this process. Boundaries with < 2° degrees show

marked enrichment associated with the presence of multiple, non-parallel dislocation types. However, at increased misorientation ($>2^\circ$), the interface becomes more ordered with dislocation geometries defined by linear concentrations of trace elements, and which are consistent with the EBSD data. These boundaries show a systematic correlation of increasing trace element segregation with misorientation angle. In particular, elements are generally more enriched at higher degrees of distortion, where variations are mostly significant for Ca (from 0.07 up to 0.6 at%) and Cl (up to 0.3 at%). Elements that are segregated to the low-angle boundaries (Ca, Al, Ti, P, Mn, Fe, Na, Mg and Co) are here interpreted to be captured and accumulated by dislocations as they migrate to the sub-grain boundary interfaces. However, the exotic trace elements Cl and H, also enriched in the low-angle boundaries, likely reflect a small but significant contribution of an external fluid source during the fluid-related deformation. In particular, since the occurrence of H in olivine is strongly attributed to Ti defects, the segregation of Ti to grain boundaries is consistent with the detected enrichment of hydrogen in the low-angle interfaces.

The observed compositional segregation of trace elements to low-angle boundaries have significant implications for the deformation and transformation of olivine at mantle depth, the interpretation of geophysical data and the redistribution of elements deep in the Earth. Furthermore, the nanoscale correlation between heterogeneous distribution of elements like Ti and the diffusion of H along boundary interfaces within olivine might have the potential to yield important implication for the understanding of the hydrogen distribution in the upper mantle and its consequences for the rheological properties of mantle-rocks during deformation.

Age constraints on the formation and emplacement of Cambrian Ophiolites along Heathcote, Dookie, and Governor fault zones, Central Victoria

Habib, Umer¹, Meffre, Sebastien¹, & Bottril, Ralph²

¹Centre of Ore-Deposit Geology and Earth Sciences, University of Tasmania, Australia; ²Mineral Resources Tasmania, Rosny Park, Hobart, Australia

The preservation of dismembered ophiolites in major fault zones of the central Lachlan Orogen suggests complex oceanic crust formation along the East Gondwana margin during the Early to Late Cambrian. The ophiolite sequences exposed at Heathcote, Dookie and along the Governor Fault zone in Victoria, are multiply deformed and preserve spectacular examples of fault propagation duplex systems with accretion of oceanic crust. Understanding when they were formed and emplaced is crucial for understanding the evolution of the Lachlan Orogen to constrain when sea-floor spreading and terrane accretion occurred. In this study LA-ICPMS (U/Pb) zircon ages are used to get detailed age information for the Lachlan ophiolite sequences. Ophiolitic layered, structurally complex gabbro from Tatong gave an age of 518 ± 4.1 Ma. Gabbro samples from Dookie yielded ages of 513 ± 4.4 and 515 ± 4.0 Ma. These are similar to the 516 ± 0.9 Ma age calculated for the Mclvor Hill gabbro from the Mt Read Volcanic belt in Tasmania from a previous study. Detrital zircons in cherts from the Dookie

complex are 8 million years younger at 508 ± 4.6 Ma. Detrital zircons from the Knowsley East shales from the northern part of the Heathcote Cambrian volcanic rocks were 18 million years younger at 490 ± 4.3 Ma. These new data, combined with previously published zircon ages, suggest a 2-stage evolution (ca 518–505 Ma and 502–490 Ma) for Central Victorian ophiolites.

Lithospheric structure of the Kidson reflection seismic line 18GA-KB1 from 2D multi-constrained gravity inversion

Moro, Polyanna¹, Giraud, Jérémie^{1,2}, Ogarko, Vitaliy³, & Jessell, Mark^{1,2}

¹Centre for Exploration Targeting, School of Earth Sciences, The University of Western Australia, Perth, Australia; ²Mineral Exploration Cooperative Research Centre, School of Earth Sciences, The University of Western Australia, Perth, Australia; ³International Centre for Radio Astronomy Research, Faculty of Engineering and Mathematical Sciences, The University of Western Australia, Perth, Australia.

We performed 2D gravity inversions along the reflection seismic line 18GA-KB1, crossing the Eastern Pilbara Craton, the Paterson Orogen, and the Kidson sub-basin, based on the Alternating Direction Method of Multipliers (ADMM). We aimed to reduce the uncertainties in defining properties and the Moho in the region to better understand its lithospheric signature. These arise from the weak constraints imposed by seismic tomography models at such depths, given the poor seismic coverage in parts of the basin, and the ambiguity between structure and mass variation of unconstrained gravity inversions.

In our inversion scheme, densities are allowed to vary within a set of predefined intervals defining bounds at each location, in conformity with geologically reasonable petrophysical distributions (based on global datasets, with densities varying at depth as a function of pressure, temperature, and compositional changes). We used geological interfaces interpreted from the reflection seismic line as hard constraints and density iso-surfaces from a preceding seismic-gravity study as soft constraints to restrict bounds locally, thus reducing uncertainty and narrowing the model search space. The interfaces from the reflection seismic included the depths of the basin and the Moho. These were retrieved by assigning constant P wavespeeds of 6 km/s for the crystalline crust and 3.7 km/s for the basin. During the “picking” of the Moho, a bounding ribbon around this interface was ascribed to an “ambiguous” or transitional zone. From the ADMM constraints, densities were allowed to vary laterally and vertically throughout inversion, while remaining within, or as close as possible to, the values assigned to each interpreted geologic unit. The permitted densities within the “ambiguous” zone comprised the intersection between values termed for the lower crust and upper mantle.

Inversions were performed using distinct a priori models. These included upper mantle densities derived from the AuSREM model and an alternative homogeneous upper mantle model of 3300 kg/m^3 . Notwithstanding the different choice of priors, resulting models converged to a similar endmember, indicating consistency between results obtained in different fashions. These results suggest that, while the initial model is sensitive to the mantle density model, its

influence is resolved within the bounds of the inverted models.

Our results corroborate with the physical characteristics suggested by previous seismic models in the region, with a low uppermost mantle density of $\sim 3280 \text{ kg/m}^3$ within the Paterson Orogen and low uppermost mantle densities ranging from 3240 to 3260 kg/m^3 within the Canning Basin. The eastern margin of the Pilbara Craton shows a bulk crustal density that is lower than the adjacent tectonic provinces, such as expected for Archean cratons, with a high-density lower crust of $\sim 3145 \text{ kg/m}^3$ and a complementary uppermost mantle density of 3320 kg/m^3 . The bulk crust of the Paterson Orogen and southern Kidson sub-basin is denser than the adjacent crustal domains and may be a result of convergent tectonics and subsequent magmatic additions to the lower crust related to Proterozoic–Cambrian LIPs in the region. This interpretation is supported by the reflectivity patterns at the crust–mantle boundary observed in the reflection seismic section.

Advances in volcanic and magmatic processes

Shallow conduit and vent processes during the 1886 basaltic Plinian eruption at Tarawera, New Zealand

Moore, Hannah¹, Carey, Rebecca¹, Houghton Bruce², Jutzeler, Martin¹, & White, James³

¹*School of Natural Sciences and CODES, University of Tasmania, TAS, Australia;* ²*Department of Earth Sciences, University of Hawaii at Mānoa;* ³*Department of Geology, University of Otago*

The 1886 eruption of Tarawera, New Zealand, is one of four known examples of basaltic Plinian eruptions. During the climactic phase, a high Plinian eruption column was produced, fed by vents in four segments along an 8-km-long fissure across Mt Tarawera. This eruptive activity was simultaneous with other adjacent vents across the mountain that were in a low-intensity style of eruption. Here we present a detailed re-examination of microtextures from pyroclasts to constrain the ascent and degassing histories of the magma which influenced the Plinian versus low intensity styles of eruption along the Mt Tarawera portion of the fissure. With this study, we aim to understand how this basaltic magma erupted at such high mass eruption rates. Scoria clasts and ash particles selected from stratigraphy proximal to the vent represent (1) a widespread endmember, sedimented from the Plinian column margin and (2) a localised endmember, sedimented from low intensity explosions, representing the lowest mass eruption rates. We also study clasts from a medial section, from which clasts were absolutely entrained into the Plinian plume and represent the highest mass eruption rates. The main differences in scoria clasts from different sites along the fissure segment are in microlite crystallinities: these are low within the proximal localised material (35–55%), high within the proximal widespread material (95–99%), and intermediate within the medial material (69–84%). We suggest that, for vents erupting at Plinian intensity, there was a strong parabolic velocity profile across the conduit, which ensured that magma near conduit

margins ascended slower, cooled faster and became more viscous than magma along the axis, leading to longer residence times and therefore more advanced degrees of outgassing and crystallisation. The highly viscous magma at the margins may have reduced permeability and therefore outgassing from magma along the axis, causing a build-up of pressure within the conduit, driving higher eruption rates, and leading to a Plinian eruption. Eruption products sedimented into the widespread proximal environment represent the collar of cooler, more crystallised magma, whereas products entrained into the high plume and sedimented into the medial location represents magma from the central axis. For vents erupting at low intensities, there were transient discrete explosions, where the most intense explosive eruptions cleared out the shallow conduit. These episodic explosions allowed efficient outgassing from magma in the shallow conduit, but viscosity remained relatively low compared to Plinian magma.

Trace element sector zoning in clinopyroxene as a function of undercooling: an experimental evaluation in trachybasaltic magmas

MacDonald, Alice¹, Ubide, Teresa¹, Masotta, Matteo², Mollo, Silvio³, & Pontesilli, Alessio⁴

¹*The University of Queensland, Brisbane, Australia;* ²*University of Pisa, Pisa, Italy;* ³*Sapienza University of Rome, Rome, Italy;* ⁴*University of Otago, Dunedin, New Zealand*

Clinopyroxene chemistry is increasingly being utilised to investigate magmatic processes, due to its ability to record an extensive history of physiochemical changes in the host magma. However, clinopyroxene chemistry is not only influenced by pressure, temperature, and magma composition, but also by kinetic effects that may generate compositional zoning, such as sector zoning. Previous experimental work has highlighted the role of undercooling ($\Delta T = T_{\text{liquidus}} - T_{\text{system}}$) on crystal morphology and major element chemistry of sector-zoned clinopyroxene. In this regard, the spatial distribution of trace elements in clinopyroxene remains relatively underexplored.

Here we present trace element data collected by laser ablation ICP-MS mapping of experimental sector-zoned clinopyroxenes crystallised from a trachybasalt melt representative of one of the most primitive magmas ever erupted at Mt Etna volcano (Italy). Experiments were conducted an isobaric pressure of 400 MPa, and a range of temperatures (1050–1200 °C) and H₂O contents (0–4 wt%). Undercooling was attained by cooling the experiments from a starting temperature (1300 °C) above the clinopyroxene liquidus at a rate of 80 °C/min to a resting temperature (T_{system}) resulting in a range of ΔT (23–173 °C).

Our results indicate that clinopyroxene crystals show different styles of zoning across the entire range of ΔT , where zones enriched in Al are also enriched in HFSEs and REEs. At $\Delta T < 40$ °C, clinopyroxene is sector-zoned with distinct Al-poor hourglass and Al-rich prism sectors. At $\Delta T = 75$ –123 °C, skeletal morphologies dominate as crystal growth transitions from interface controlled to diffusion limited. These crystals are comprised of Al-rich skeletons and Al-poor overgrowths. At $\Delta T = 123$ –173 °C, clinopyroxene is primarily dendritic, with subtle Al zoning.

The overall correlation between Al and trace element composition is attributed to charge-balancing mechanisms. Highly charged cations are favourably incorporated into the M1 and M2 sites with increasing Al, to compensate for the substitution of Si for Al in the tetrahedral site.

Thermodynamic modelling of lattice strain parameters for 3+ cations in the M2 site (REEs + Y) illustrates that the strain-free partition coefficient (D_0) is strongly correlated with ΔT . Conversely, the optimum radius (r_0) and Young's modulus (E), remain constant across our dataset.

The application of trace element calibrations to natural samples from Mt Etna supports the growing conception that sector zoning in clinopyroxene is related to low degrees of ΔT , whereas microlites crystallised at moderate degrees of ΔT . Our new experimental data could bring crucial new insights into magmatic processes which occur under polythermal and polybaric crystallisation regimes, in the lead up to volcanic eruptions.

Timescales of magma ascent recorded by olivine zoning patterns from Mount Leura and Mount Noorat, Newer Volcanics Province, Australia

Didonna, Rosa¹, Handley, Heather¹, Cas, Ray², Fidel, Costa³, & Murphy, Timothy¹

¹*Department of Earth and Environmental Sciences, Macquarie University, Sydney, NSW, Australia;* ²*School of Earth, Atmosphere and Environment, Monash University, Clayton, VIC, Australia;* ³*Earth Observatory of Singapore, Nanyang Technological University, Singapore*

Intraplate continental basaltic volcanic provinces (ICBVPs) occur on all continents, but the timescales of magmatic processes that lead to eruption in such settings are poorly understood due to the temporal infrequency and lack of spatial pattern in eruptions. Therefore, unravelling the timescale of magma ascent is a critical aspect to advance our understanding of volcanic hazard and risk. Here we focus on the Newer Volcanics Province (NVP) of SE Australia is an active intraplate basaltic province that contains over 400 volcanic centres. Volcanic landforms include maars, tuff rings, scoria cones, lava fields along with more complex eruption centres and the rate of activity has varied in space and time. Despite a large number of studies on the bulk-rock geochemistry and physical volcanology of the deposits (e.g., stratigraphy, eruption styles), few constraints are available on the timescales of magma ascent in the province.

We have investigated the olivine crystals within entrained mantle xenoliths and as individual crystals within the groundmass of basaltic volcanic rocks using compositional X-ray maps, backscattered electron (BSE) images and electron microprobe analyses (EMPA). We focus on NVP samples from Mount Leura (Lehurra kang) and Mount Noorat (Knorart) to shed a light on the dynamic processes that lead to the eruption and the relative timescales of magma ascent. Olivine crystals in mantle xenoliths are mainly unzoned with Mg#90 ($Mg\# = 100 \times Mg/[Mg+Fe]$) with few crystals normally zoned (<Mg#75 rim). Olivine grains in the groundmass are commonly up to 1 mm in size and are mainly skeletal, with significant variation in Mg#, CaO,

MnO and NiO content from core to rim. Olivine grains in the Mount Noorat samples are largely normally zoned with crystal interiors characterised by >Mg#90 and rims by <Mg#75. Olivine crystals from Mount Leura contain complexly zoned olivines suggesting a more complex crystallisation and transport history (Mg#77–79 cores and rims up to Mg#85). We model the chemical zonation patterns in olivine crystals that reveal a short time of magmatic processes before the eruption. The insight of magma storage, ascent and the pathway to the surface at NVP is a crucial information in understanding the volcanic hazard and mitigation risk in the region for which too little consideration is still given at the present.

Geophysical and geochemical constraints on the formation of Holocene intraplate volcanism in East Asia

Ward, Jack F.¹, Rosenbaum, Gideon¹, Ubide, Teresa¹, Wu, Jonny², Caulfield, John T.^{1,3}, Sandiford, Mike⁴, & Güerer, Derya¹

¹*School of Earth and Environmental Sciences, The University of Queensland, Brisbane, Australia;* ²*Department of Earth and Atmospheric Sciences, University of Houston, Houston, USA;* ³*Central Analytical Research Facility, Institute for Future Environments, Queensland University of Technology, Brisbane, Australia;* ⁴*School of Earth Sciences, University of Melbourne, Melbourne, Australia*

East Asia contains many Holocene volcanic centres, several of which are located far (between 600 and 1500 km) from the Pacific and Philippine Sea plate subduction zones. The origin of these intraplate volcanoes, which include Jeju, Ulleungdo, Tianchi, Jingbohu, Erkeshan and Wudalianchi, remains enigmatic. Geodynamic processes proposed to explain the occurrence of the East Asian Holocene intraplate volcanoes include mantle plume activity, subduction processes with slab fluid involvement, and subduction processes without slab fluid involvement. Here, we evaluate a variety of geophysical datasets and a compilation of geochemical data to assess the feasibility of these mechanisms. High-resolution tomography data provide no evidence for the rise of deep-seated mantle plumes. Instead, the tomographic and seismic data highlight the stagnation of the Pacific slab at the 660 km discontinuity below Tianchi, Longgang, Jingbohu, Erkeshan and Wudalianchi. The geophysical data also provide evidence for the stagnation of the Philippine Sea slab at the 410 km discontinuity below Jeju and Ulleungdo. Although the intraplate volcanoes appear to be located above subducted slabs, the geochemical data do not provide evidence for melt generation due to slab metasomatism. Instead, the intraplate volcanoes are alkaline in composition and display primitive mantle normalised trace element characteristics comparable to those shown by ocean island basalts. In light of the absence of evidence for plume activity or slab metasomatism, we suggest that convective upwellings occurring at the edges of the Pacific and Philippine Sea slabs may be responsible for Holocene intraplate volcanism in East Asia. Because it is likely that the Pacific and Philippine Sea slabs have been stagnant in the mantle transition zone for millions of years, we speculate that slab-edge convection and volcanism may be driven by regional-

scale tectonic events. We conclude by discussing possible Neogene–Quaternary tectonic events that may have contributed to the occurrence of East Asian Holocene intraplate volcanism.

Volcanic stratigraphy and eruption mechanisms from the last remaining outcrops at Wiri Mountain, Auckland Volcanic Field, New Zealand

Foote, April¹, Németh, Károly², & Handley, Heather¹

¹*Department of Earth and Planetary Sciences, Macquarie University, Sydney, Australia;* ²*Institute of Agriculture and Environment, Massey University, Palmerston North, New Zealand*

Dispersed volcanic fields (commonly labelled as monogenetic volcanic fields) are of great interest in volcanology as they provide a relatively simple volcanic architecture to study regarding magma source to surface processes, edifice growth and subsequent destructions. The Auckland Volcanic Field (AVF) in New Zealand is among the few hundred documented dispersed volcanic fields worldwide that were active through the Holocene and can broadly be defined as a mafic intraplate monogenetic volcanic field. Recent research has highlighted that the transition between monogenetic and polygenetic volcanism is far more continuous than was originally thought, where volcanoes traditionally viewed as monogenetic are commonly found to have had multiple eruptions and complex magmatic plumbing systems.

This study focuses on the last remaining outcrops of Matukutūru, or Wiri Mountain, one of the southernmost volcanic centres in the AVF. Wiri Mountain presents a unique situation where despite the large extent to which deposits have been removed, the remaining spectacular outcrops allow a clear picture to be formed, including analysis of stratigraphy and facies, vent location and extent of deposits, fragmentation depth, eruptive styles and their transitions and the eruption history of the volcanic centre.

Wiri Mountain has had a complex eruption history, beginning with a pre-existing tuff ring/maar landscape. An initial basal tuff ring was deposited by predominantly pyroclastic density currents with ballistic curtain deposits and some pyroclastic fall, through a debris filled vent that widened mostly at depth through the course of the eruptions. At least two smaller, satellite tuff rings were then deposited on the outer flanks of the first by a combination of pyroclastic density currents and pyroclastic fall, with a transition from phreatomagmatic to Strombolian eruptive style. A central scoria cone was then deposited within the initial tuff ring, followed by lava spatter and lava flows that covered the tuff rings, the scoria cone, and the surrounding area. This complex eruption history highlights the range and transition of eruptive styles leading to the production of multiple types of eruptive products and deposits that can be typical for the AVF.

The small magma volumes typical of monogenetic volcanism allow for significant influence of fragmentation and eruptive products by external water, resulting in a wide variety of volcanic landforms. However, based on the results of this study, volcanic activity at Wiri Mountain and the surrounding area of the southern end of the AVF was potentially more complex than would typically be expected from the textbook

definition of monogenetic activity, with a large enough eruptive volume to allow a complex eruptive evolution over time, multiple satellite cones, and potential connections to nearby centres, highlighting the grey area on the concept boundary of monogenetic volcanism.

Transitions in Eruptive Style During the 2012 Deep Submarine Silicic Eruption of Havre Volcano, Kermadec Arc, New Zealand

Clark, Acacia¹, Carey, Rebecca¹, Jutzeler, Martin¹, & Mitchell, Samuel²

¹*University of Tasmania, Hobart, Australia;* ²*University of Bristol, Bristol, United Kingdom*

Submarine eruptions are poorly understood compared to their subaerial counterparts due to challenges accessing and observing them. The 2012 silicic submarine eruption of Havre Volcano in the Kermadec Arc was the largest deep ocean eruption (~900–1220 meters below sea level) ever recorded.

The main vent transitioned in eruption style during the event. The current eruption framework describes the onset of magma disruption on the seafloor at high (107 kgs⁻¹) eruption rates, which produced a large pumice raft (~1 km³) accompanied with a giant pumice seafloor deposit. This phase transitioned to an intermediate phase of unknown intensity that produced an ash-lapilli-block (ALB) deposit proximal to the vent. The final eruptive phase was low intensity (104 kgs⁻¹) effusive magma emplacement that produced a 250 m-high dome complex (Dome OP) over the vent. Previous studies have focused on microtextures of these main phases to understand shallow conduit processes.

We have identified lobe deposits around Dome OP which stratigraphically sit above the ALB deposit but were emplaced prior to the end of the effusive phase. These deposits represent a transitional phase between high to low eruption rates. Detailed micro-textural studies were conducted on four representative clasts from in-situ Dome OP together with three clasts from surrounding lobe deposits, and two dense end-member ALB clasts not previously studied.

Microlites of the same crystal types and habits are present in lobe deposits and in-situ Dome OP clasts, where they are most abundant. ALB clasts are microlite free with almost spherical vesicles. Clasts from lobe deposits have elongated vesicles with round edges and in-situ Dome clasts have elongated and flattened vesicles. ALB clasts have the highest vesicle number density, followed by lobe deposits and then in-situ Dome clasts. Rounded vapor-phase cristobalite is present in lobe deposits and in-situ Dome O clasts, whereas in-situ Dome P clasts contain an abundance of oblong cristobalite crystals that exist entirely within the groundmass. No discernible correlation could be made between vesicle size and cristobalite crystal size. Silicic submarine domes are morphologically and texturally similar to subaerial domes, indicating hydrostatic pressure has a minor role in outgassing and emplacement processes of lava domes.

Zircon trace element geochemistry as an indicator of magma fertility in iron oxide–copper–gold provinces

Wade, Claire^{1,2}, Payne, Justin³, Barovich, Karin², Gilbert, Sarah⁴, Wade, Benjamin⁴, Crowley, James⁵, Reid, Anthony^{1,2}, & Jagodzinski, Elizabeth¹

¹*Geological Survey of South Australia, Adelaide, Australia;* ²*Department of Earth Sciences, University of Adelaide, Australia;* ³*UNISA STEM, University of South Australia, Australia;* ⁴*Adelaide Microscopy, University of Adelaide, Australia;* ⁵*Department of Geosciences, Boise State University, Boise, USA*

The trace element signatures of zircon from Phanerozoic porphyry-related magmatic rocks and their mineralising systems have recently been applied as a means to assess potential magmatic suite fertility. The iron oxide–copper–gold (IOCG) and iron oxide–apatite (IOA) deposit family share some genetic attributes with porphyry Cu deposits, including subduction-modified magmatic sources, association with calc-alkaline to mildly alkaline magmas, and highly oxidised magmas. The observed relationship between magma fertility and zircon chemistry in porphyry Cu deposits raises the possibility that the trace element signature of zircon could also be used to assess the fertility of magmatic systems associated with IOCG and IOA systems.

Significant IOCG deposits in southern Australia (Gawler Craton) and IOA deposits in the south-central USA are associated with extrusive and intrusive felsic rocks formed as part of silicic large igneous province magmatism. Zircons from early rhyolitic and granitoid rocks coeval with IOCG mineralisation in the Gawler Craton are distinguished from younger rhyolite and granitoid zircons by their higher Eu/Eu*, Ce/Ce* and Ti values and separate magma evolution paths with respect to Hf. Higher zircon Ce/Ce* and Eu/Eu* correspond to more oxidising magmatic conditions and lower degrees of fractionation and/or crustal assimilation, respectively. Higher zircon Ti contents correspond to higher magmatic temperatures in the magma coeval with mineralisation. In this respect, we consider higher oxidation state, lower degrees of fractionation and higher magmatic temperatures to be features of fertile magmas in southern Australian IOCG terrains.

Similar zircon REE characteristics are shared between Australian IOCG magmatic rocks and IOA rhyolites from the St Francois Mountains, Missouri. IOCG and IOA magmatic rocks have high Ce/Ce* and high Dy/Yb ratios in zircon, which are indicative of oxidised and dry magmas, respectively. Syn-mineralisation IOCG and IOA magmatic rocks are distinguished from unmineralised ones by their higher Eu/Eu* zircon signature, and higher magmatic temperatures. Zircon Dy/Yb are generally higher and Eu/Eu* are generally lower in IOCG and IOA magmatic rocks when compared with fertile porphyry Cu deposit magmatic rocks. The dry and more fractionated nature of the IOCG and IOA associated magmas contrast with the hydrous and unfractionated nature of fertile porphyry Cu deposit magmas, highlighting differences in setting and magma formation of porphyry Cu deposits and the IOCG-IOA deposit family. As indicated by high zircon Ce/Ce* ratios, the oxidised nature of mineralised IOA magmatic rocks coupled with lower degrees of fractionation and higher magmatic temperatures, are

akin to fertile IOCG magmatic rocks and considered to be key elements in magma fertility in IOCG-IOA terrains.

Newly identified mafic and felsic tuffs of the Shoalhaven and Talaterang Groups, southern Sydney Basin: their volcanic significance and palaeoecological impacts

Bann, Glen¹, Graham, Ian², & Jones, Brian¹

¹*School of Earth, Atmosphere and Life Sciences, University of Wollongong;* ²*University of NSW, Kensington, Australia*

A suite of newly identified mafic and felsic tuffs are described from the Shoalhaven and Talaterang Groups of the southern Sydney Basin. This includes the Clyde Coal Measures, Wasp Head, Pebbly Beach and Snapper Point Formations, Wandrawandian Siltstone, Nowra Sandstone, Berry Siltstone and the lower Broughton Formation. The tuffs are readily observed from outcrops in the field however, so far, have proved very difficult to discern in drill cores.

The mafic tuffs commonly comprise abundant biotite and muscovite grains, which are often deformed, K feldspar, plagioclase, volcanic quartz, with embayments, quartz shards and rare euhedral zircons. The felsic tuffs contain abundant volcanic and metamorphic quartz, plagioclase, more common pumaceous material, less micas and very rare or absent, shards. All tuffs contain carbonaceous material of various amounts and both are commonly reworked, although a lack of abrasion on the phenocrysts in the mafic tuffs suggests that the material has not travelled far from its source. Numerous dropstones of the same tuff material are common throughout the sequence, with volcanic types dominating in the east and metamorphic cratonic types in the west.

The Koo Lee Tuff Member, the largest of the mafic eruptions with a maximum thickness of almost 3 m, is stratigraphically located within the lower Broughton Formation and due to its explosiveness and volume, has been deposited across a large area of the basin, hence outcrops in a number of locations. This provides the opportunity to identify eruption and emplacement mechanisms plus lateral changes in the deposit as well as providing a chronological time line through the southern Sydney Basin.

Volcanic detritus from island volcanoes to the southeast inundated sediment derived from the craton to the west during this period. Evidence from the presence of predominantly Cruziana ichnogenera and glendonites throughout the succession, in addition to wavy contact surfaces beneath coarser sands and sporadic volcanic derived clasts suggest deposition was dominated by episodic storm activity in cold climate conditions with periodic coastal ice sheets depositing the clasts, or dropstones. Very fine-grained carbonaceous horizons indicate that deposition was also periodically dominated by extended low energy conditions. These deposits represent small or distant components of much larger volcanoclastic aprons surrounding a series of vents to the southeast. Evidence suggests a proximal source from island volcanoes ranging from mild Strombolian to the violently explosive Vulcanian or Plinian phreatomagmatic type eruptions. The association with the Late Permian Gerringong Volcanics and these earlier

eruptions is presently unclear. The felsic eruptions are more distal, possibly associated with a large felsic provenance in the Zealandia craton to the south east.

The tuffs are often associated with trace fossil escape burrows, both successful and unsuccessful, and marine body death assemblages, commonly within the tuffs themselves but also found both below and above the tuffs. The effects of the eruptions and the tuffs on the local biota at the time will include changes in pH and Eh, elevated water and substrate temperatures, chemical toxicities such as Hg and As, during and post eruption, and an increase in turbidity. Effects will impact different species, with the more significant eruptions impacting everything. The more proximal eruptions, such as the Koo Lee Tuff, will also destroy habitat, displacing the animals.

It is therefore apparent that volcanism was controlling and dominating the deposition and conditions during early stages of the formation of the southern Sydney Basin.

U–Pb ages and aluminium concentrations of colourful sapphire-related zircon megacrysts from Far North Queensland: Merlot, Rosé and Champagne

Allen, Charlotte M.¹, Porter, Erica J.¹, & DeBruyn, Mitchell²

¹Central Analytical Research Facility, Institute for Future Environments, Queensland University of Technology, Brisbane; ²School of Mechanical, Medical and Process Engineering, Faculty of Science, Queensland University of Technology, Brisbane

Detrital sapphires are commonly found with megacrystic zircon but it is only co-location that links these free grains. If related, zircon can constrain the circumstances by which nature creates corundum. Trail and co-workers suggested that zircons from high-Al-activity magmas (peraluminous ones) have Al contents >4 ppm, a step-jump up from Al contents from zircons from metaluminous magmas. Aluminium is generally not considered to crystallize in zircon because of radius and charge but was included in the 24 isotopes analytical list. Twenty-seven 25 micron laser ablation spots were targeted on 3 colour groups from detrital zircon megacrysts associated with sapphires of Scot's Camp near Undara National Park, a Lava Plains locality. Three spots on each of three grains in each colour group were analysed by Agilent 7900 ICPMS. Zircons were cathodoluminescence and backscatter imaged. Reported dates are concordant ²⁰⁶Pb/²³⁸U ages using Temora as calibrant with no Th-disequilibrium correction. Trace element concentrations (TE) are based on NIST 610 with Si as internal standard and assumed 15.22 wt% concentration.

Champagne grain #1, wholly, proved to be older than the rest at 2716 Ma (1 stdev, n = 3) but its cathodoluminescence, morphology and TE are not distinctive. Two other Champagne spots gave 5.5 and 4.1 Ma, ages older than Merlot grains, which are consistent at 2.60.2 Ma (n = 7). Rosé grains give the same age (2.90.5 Ma, n = 5).

TE among the 9 grains has somewhat grain-specific compositions which is true of aluminium. Merlot, Rosé and Champagne have average Al contents of 98, 2619 and 3323 ppm (1 stdev), respectively. The 271 Ma grain

(Champagne#1) contains variable Al (4 to 78 ppm) whereas #2 is consistent at 812 ppm (n = 3). Compare these averages to our reference zircons and sources: Temora (quartz-monzodiorite), Plešovice (alkalic granulite), and 91500, a detrital megacryst provisionally associated with syenite (?). Respectively, they give 1.81.0, 8935 and 7.72.4 ppm Al. The Lava Plains megacrysts, indeed, were generated from Al-rich sources.

Sapphire-associated zircons tend to be TE-poor as in a 13.6 Ma example from Mt Weldborough, NE Tasmania. Uranium is <100 ppm in Champagne and Rosé but Merlot has U from 200 to 1250 ppm save one and thus gives the more precise age. Except for Al and P, Merlot has greater TE contents. Zircon classification based on Yb, U, and Hf indicate these are continental and/or kimberlitic zircon types. Features of note are small to zero Eu anomalies and positive Ce anomalies of 100–300 for Merlot and Rosé but 10s for Champagne (method after Blundy & Wood). These Lava Plains zircons are decidedly not-mantle-like, particularly in their Zr/Hf (>>37, the chondritic value).

The dominant age of 2.6 Ma is in the range of the oldest Lava Plains eruption ages, however, to find a morphologically non-distinctive Permian megacryst among them means that nature has repeated herself in providing the odd conditions to generate both sapphire and zircon megacrysts, crystals that have been brought to the surface by alkalic basalts of similar or much younger age. Permian is a common age among Queensland sapphire-related zircons.

Corundum conundrum

Raffan, Nick
University of NSW

Volcaniclastics and basalts are widely spread across the Anakie Gemfields in Central Queensland, Australia. A principal elevator of sapphires to the surface is widely believed to have been eruptions from Hoy Province volcanoes, followed by disintegration and release of sapphire from lava flows. However, it is noteworthy that volcaniclastic rocks are usually associated with areas where intensive sapphire mining has taken place. Although corundum has been reported from some Hoy plugs, it is extremely rare but is more commonly found by miners in volcaniclastics (called clinker by local miners). Crucially, although numerous basalt clasts of various textural types occur within the mined gravels, despite a hundred years of mining miners have not found any corundum within these clasts. The volcaniclastics from this field vary widely in mineralogy, texture, and chemistry. A surprising result is that some samples comprise over 50% dolomite, with some containing much higher amounts of around 70%. The volcanic origin of these is supported by anomalously high levels of zirconium and titanium. In addition, these alkaline rocks some-times contain abundant small equant-shaped flakes of biotite, now altered to clays. This raises an important question: were the dolomite-rich volcaniclastics erupted from one or more carbonatite-type volcanos? And were these also the source for the corundums? Also, what were the sources for the diverse suites of zircons and spinels found in the gem gravels? The timing of events is complicated by the range in ages of Hoy plugs from 67 Ma to 14 Ma. The most likely scenario is that lavas flows initially

protected earlier volcanoclastics from erosion. After removal of the flows, the volcanoclastics were free to release corundum to the waterways. Trace element geochemistry for seven plugs and four volcanoclastic samples suggests that they are genetically related. Matters are complicated by an undocumented basalt field high in the Drummond Range, west of the sapphire fields where clinker was also observed, along with possible volcanoclastics immediately below the basalt flows.

QEMSCAN and PGE geochemistry to track sulfide saturation, magmatic evolution and fertility of porphyry suites (on the example of Mount Hagen, Papua-New Guinea)

Misztela, Monika, & Campbell, Ian

Research School of Earth Sciences, Australian National University, Canberra, Australia

Sulfide saturation is believed to play an important role in porphyry systems fertility. It can also determine the type of ore in an economic deposit. During the early stages of magma evolution Cu, Au and Pd behave incompatibly, and they are concentrated in the melt by fractional crystallisation. If sulfide saturation occurs early, the chalcophile elements are trapped in sulfide phases and locked in an underlying magma chamber, where they are able to enter the fluid phase, which results in a barren system. However, if sulfide saturation occurs later, after or shortly before volatile saturation, the metals are able to enter the fluid phase and form an economic deposit.

Platinum Group Elements are sensitive indicators of sulfide saturation due to their high partitioning into immiscible sulfide melts. Cu and Au also partition into sulfide melts but with lower partition coefficient, so that PGE are more sensitive to any changes in the system. Furthermore, their solubilities in hydrothermal fluids are lower, they are less mobile than Cu or Au, so their concentration in rocks reflect magmatic rather than hydrothermal processes.

QEMSCAN (Quantitative Evaluation of Materials by Scanning Electron Microscopy) can provide valuable information when studying magmatic suites. It provides high-resolution maps and images of mineral and elemental distributions, porosity structure maps, the density of samples and most importantly, quantitative mineral and elemental analyses.

Mount Hagen is an arc system that could potentially be related to a porphyry deposit. Its favourable location and proximity to other deposits was the initial motivation for undertaking this project. Eighteen samples, covering a compositional range from 2 to 11.5 wt% MgO, were analysed for the PGE. Thirteen rocks were selected for detailed petrological description and mineral quantification by QEMSCAN. Quantitative reports were used to plot the cumulative abundance of major mineral phases as a function of whole-rock MgO. The results show that significant changes occur at ~ 6 wt% MgO. Hornblende appears as a primary phase, which is attributed to major input of wet magma into the system at that time. Analysis of olivine cores revealed a reversal in their compositional trend at 6 wt% MgO, which confirmed this hypothesis. Pd, Pt and Au analysis showed that concentrations of these elements initially increase, up to about 8.5 wt% MgO, followed by a decrease. The change at 8.5 wt% Mg is interpreted to

mark the start of sulfide saturation, and it correlates well with the similar change in the Cu trend. At about 6 wt% MgO there is a reversal of the trend, followed by a second decline, which can also be explained by a new magma influx to the system.

Mount Hagen was an open system, with at least one major magma recharge into the chamber. The magma experienced early sulfide saturation, which makes it unlikely that this system produced economic mineralisation.

Mineralisation around Mount Adrah, New South Wales: new observations by the Geological Survey of NSW

Wang, Yamei, Forster, David, Cronin, Dan, Montgomery, Karen, & Blevin, Phil

Geological Survey of New South Wales, Department of Regional NSW, Maitland, Australia

This study summarises previous exploration in the Mount Adrah area and presents the results of new petrographic, sulfur isotopic and HyLogger™ hyperspectral analyses of intrusion-related gold mineralisation centred on the Hobbs Pipe intrusion at Mount Adrah, New South Wales. The work was conducted as part of the five-year East Riverina Mapping Project, which improved geological understanding to aid mineral exploration and enable informed land use decisions in the region.

The Hobbs Pipe deposit contains about 770 000 oz of gold and is interpreted to be an intrusion-related gold deposit. Two main styles of mineralisation are present: disseminated pyrite–gold, developed within a cylindrical, zoned intrusion (Hobbs Pipe), and narrow, high-grade gold reefs located nearby. Drill hole GHD009 (total depth 1312 m) provides a representative section through the Hobbs Pipe deposit and associated rocks.

Reconnaissance petrology was undertaken on twenty thin sections collected from drill hole GHD009. Three main phases have been identified: a felsic monzogranite core, an intermediate quartz monzodiorite to diorite outer core, and an intermediate–mafic diorite to gabbro rim. Disseminated pyrite–gold mineralisation in the Hobbs Pipe deposit is mainly hosted in the felsic monzogranite core.

Twenty-eight sulfur isotope results were obtained, twenty-seven from drill hole GHD009 and one from White Deer Reef, intersected in drill hole GHD011. $\delta^{34}\text{S}$ results mainly fall within a relatively narrow range and suggest a single, magmatic-dominated source of sulfur.

HyLogger™ hyperspectral analysis of drill hole GHD009 was conducted at the WB Clarke Geoscience Centre, Londonderry, New South Wales. Chlorite, white mica and dark mica type all show mineralogical changes near lithological contacts and/or alteration which relates to gold mineralisation.

The geology and alteration assemblages in conjunction with new petrology, hyperspectral data and sulfur isotopes suggest that both the disseminated mineralisation within the core of the intrusive stock and the distal high-grade gold-bearing reefs are related to the same mineralising event, and probably the same fluid source.

A penecontemporaneous intrusion into marine sediments of the lower Shoalhaven Group and significance to the volcanic history of the southern Sydney Basin

Bann, Glen

School of Earth, Atmosphere and Life Sciences, University of Wollongong

This paper describes a dolerite intrusion and stratigraphy located at Kinghorn Point, just to the north of Jervis Bay, within the upper Wandrawandian Siltstone of the lower Shoalhaven Group of the southeastern Sydney Basin. Approximately half of the intrusion is a bifurcating dyke <1 m wide whilst the other half is a sill <1.2 m thick. Bedding dips gently to the east and comprises grey siltstone beds up to 3 m thick (mainly <25 cm) with thin interbedded buff coloured, fine-grained sandstone beds up to 30 cm thick (mainly 2–5 cm). Geochemical and mineralogical analyses performed indicate that the dyke/sill complex is an olivine micro-dolerite which can be massive to highly vesiculated,

Evidence for penecontemporaneous emplacement into wet unconsolidated shallow marine sediments includes, destruction of primary sedimentary structures with extensive interaction and intermingling between the sedimentary and igneous materials, including the formation of peperite with the injection of the magma into the sediments forming brecciated contacts and with angular and rounded basalt and trachyte clasts, from microscopic spherical 'droplets' to decimetres in size, fluidization and entrainment of the sediments into the magma, the presence of tube-like flow features in the sill causing loading and deformation of the underlying sediments, hyaloclastite and baked sediments along the contact margins, cooling and flow fractures in the magma filled with fluidized sediment and sliding, slumping and load structures in the sediments, fumaroles, and vesicles within both the sediment and magma. High vesiculation is characteristic of intrusion near the surface, possibly extrusion at the sediment water interface.

Sediments were deposited in the deeper part of a coastal seaway characterised by northward-directed palaeocurrents and a Cruziana ichnofacies. Abundant glendonites, crinoid stem fossils and cross-bedding in a few sandstone beds exhibit a preferred palaeocurrent direction to the north. Periodic storm deposits or tempestites, thin (generally 2–5 cm thick) fine-grained sandstone beds comprising widely scattered unaltered euhedral prismatic plagioclase and strongly perthitic K-feldspar grains, predominantly volcanic quartz although metamorphic quartz is also present, uncommon quartz shards, with detrital muscovite and biotite. Zircon crystals are also present. These sandier, lighter coloured beds are tuffaceous and were derived from volcanic edifices, probably island volcanoes to the southeast, indicating that regional volcanism was pervasive during this period.

The mineralogy, especially key element ratios of the HFSE and major and trace element geochemistry of the intrusion are very different to the shoshonites of the Gerringong Volcanics, suggesting they are unrelated, rather, they are similar to the Karuah dykes in the far north of the Sydney Basin, which have been dated as Mid Permian, suggesting that the Kinghorn Point intrusion may have formed part of an early intermediate

phase of the Gerringong Volcanics, or it may be distinctive and unrelated.

Evidence therefore indicates that regional mafic volcanism was occurring and well evolved in the southern Sydney Basin during sediment deposition by the mid-Permian.

Gem sapphires and zircons in a basalt diatreme, northeastern Tasmania

Bottrill, Ralph¹, Everard, John¹, Duncan, David⁴, Sutherland, Lin⁵, Meffre, Sebastien², & Matchan, Erin³

¹*Geological Survey, Mineral Resources Tasmania, Rosny Park, Australia;* ²*School of Earth Sciences, University of Tasmania, Hobart, TAS, Australia;* ³*School of Earth Sciences, University of Melbourne, Parkville, VIC;* ⁴*Kingston, TAS;* ⁵*Australian Museum, Sydney, NSW*

Many notable occurrences of gem sapphire are known in Tasmania, mostly in the extensive alluvial tin-bearing deposits in the northeast (Yim *et al.*, 1985; McGee, 2005; Sutherland & Webb, 2007; Bottrill & Baker, 2008). The alluvial sapphires are typically associated with coarse-grained, ferroan (pleonaste) spinel and zircons, but except for the spinel, these are rarely seen within any host rock, although a basaltic source is commonly suspected (Sutherland & Webb, 2007).

Source rocks for these sapphires have recently been determined at a site on Logans Road in the Priory sapphire field, east of St Helens, where a small diatreme or breccia pipe has been emplaced within Devonian granite. The diatreme consists mainly of basanite clasts containing abundant, partly disaggregated, spinel lherzolite xenoliths, but also contains altered granite xenoliths within the diatreme. This area is undisturbed by tin mining.

Nearby, sapphires occur as detrital grains in the surrounding headwater drainage together with pleonaste spinel, zircon, pyroxenes and olivine, which mostly appear to derive from the diatreme. The mineral grain shapes are rather irregular and angular with little or no transport abrasion and thus obviously adjacent to source. The creeks also contain variably weathered basanite boulders and pebbles, with soft brown weathered surfaces revealing many emergent mineral grains. A single subrounded/subangular blue to grey sapphire, 7 mm across with a distinct parting with a distinct parting, was found partly exposed in an a weathered, inclusion-rich pebble by a prospector, Michael Lloyd (Duncan & Lloyd, 2013). It was confirmed with gemmological tests, indicating at least some of the Tasmanian sapphires have a basaltic source.

Fresh volcanic glass from the basanite diatreme was separated and dated using Ar/Ar multi-collector mass spectrometry to reveal a 42.0 (±0.1)–47.2 (±0.1) Ma (2σ) age for this basanite diatreme.

Coarse red-brown gemmy zircons are present with the alluvial sapphires, although they were not identified within the basanite itself, and these were dated by the U–Pb method using laser ablation inductively coupled mass spectrometry (LA-ICPMS). Two populations were found, one between ca 42–44 (±4) Ma and one between 233–247 (±4) Ma.

The younger zircon date probably records partial resetting by the basanite host, as it closely matches its Ar/Ar date, the older date probably records an

unknown, underlying Triassic intrusive source.

There is a 233 ± 5 Ma (K/Ar) alkali basalt flow near St Marys (Calver & Castleden, 1981) and a 214 ± 1 Ma (K/Ar) age from “felsic tuff” near Bicheno (Bacon & Green, 1984). Rhyolite clasts occur in the upper Triassic near St Marys, and may have a proximal source (Forsyth, 1989). No in situ Triassic felsic lavas or intrusives have been found in Tasmania, however.

The site at Logans Road helps to explain the origin of gem sapphires and zircons, in this district, although their ultimate origin is enigmatic.

- Bacon, C. A. & Green, D. C., 1984. A radiometric age for a Triassic tuff from eastern Tasmania. *Tasmanian Geological Survey, Unpub. Rept.* 1984/29
- Bottrill, R. S. & Baker, W. E., 2008. A Catalogue of the Minerals of Tasmania. *Bull.* 73. Tasmanian Geological Survey
- Calver, C. R., & Castleden, R. H., 1981. Triassic basalts from Tasmania. *Search*, 12, 0–41
- Duncan, D. McP., & Lloyd, M., 2013. The discovery and exploration of the Priory Sapphire Field. Unpublished Report for RG Prospecting.
- Forsyth, S. M., 1989. Upper Parmeener Supergroup. *Geology and Mineral Resources of Tasmania*. Geol. Soc. Aust., Spec. Pub. 15.
- Khin Zaw, Sutherland, F. L. Dellapasqua, F., Ryan, C.G., Yui, Tzen-Fu, Mernagh, T. P., & Duncan, D. McP., 2006. Contrasts in gem corundum characteristics, eastern Australian basaltic fields: Trace elements, fluid/melt inclusions and oxygen isotopes. *Mineralogical Magazine*, 70(6), 69–687
- Matchan, E., 2020. $^{40}\text{Ar}/^{39}\text{Ar}$ step-heating analysis of basanite groundmass sample R013378/NJ449 Report UM20-0801.
- McGee, B. M., 2005. Characteristics and origin of the Weldborough sapphire, NE Tasmania. Unpub Hons thesis, U.Tas.
- Sutherland, F. L., & Webb, G. B., 2007. Australian Sapphires and Rubies. *Rocks & Minerals*, 82(2), 116–139.
- Tasmania Department of Mines, 1970 *Occurrences of gemstone minerals in Tasmania*. Mineral Resources Tasmania.
- Yim, W. W.-S., Gleadow, A. J. W. & Van Moort, J. C., 1985. Fission track dating of alluvial zircons and heavy mineral provenance in North-east Tasmania. *J. Geol. Soc. Lond.*, 142, 351–356.

Pompeii to Stabiae: downwind versus substrate-induced variations of the AD 79 Vesuvius fall deposits and their impact on human settlements

Chiominto, Giulia¹, Scarpati, Claudio¹, Perrotta, Annamaria¹, Sparice, Domenico², Fedele, Lorenzo¹, Santangelo, Ileana¹, Muscolino, Francesco², Rescigno, Carlo³, Silani, Michele³, & Massimo, Osana²

¹*Department of Earth, Environmental and Resources Sciences, University of Napoli Federico II, Napoli, Italy;*
²*Parco Archeologico di Pompei, Pompei, Italy;*
³*Dipartimento di Lettere e Beni Culturali, Università della Campania Luigi Vanvitelli, Santa Maria Capua Vetere, Italy*

The AD 79 Vesuvius eruption destroyed the famous towns of Pompeii and Herculaneum located 5 and 10 km from the vent, respectively. A more distant town, Stabiae, where Pliny the Elder found his death, was also buried by pyroclastic material. Recent excavations carried out in collaboration with the Archaeological Park of Pompeii, both in Pompeii and in the imposing Stabian villas, have shown the products of the AD 79 eruptive sequence that covered these Roman settlements. During the excavation phases, ephemeral sections are exposed and then removed as the excavation proceeds. The presence on the excavation sites of a team of volcanologists allows the acquisition and

evaluation of all stratigraphic and sedimentological data. The discovery of thick sequences of reworked material accumulated during previous excavations, testifies for the presence of underground tunnels dug for the Royal House of Bourbon. The deposit of pumice lapilli which forms the lower part of the pyroclastic succession, was studied in detail to define the downwind variations of its sedimentological features and how these were influenced by urban structures. At Pompeii, the AD 79 fall deposit consists of a lower white to grey pumice lapilli bed (units A and B) showing a remarkable thickness variation ranging from 0 to 4.5 metres. Two ash layers (units C1 and C2) are interstratified at the top of unit B. The internal structure of the pumice lapilli fall deposit is weakly stratified, showing sub-horizontal layering when observed in open areas (peristyles), or appearing strongly stratified with coarse to fine layering when the pumice lapilli deposit forms piles with steep layers. At Stabiae, this deposit ranges in thickness from 0 to 2 metres and is not interstratified by ash horizons. Its internal structure shows the same types of stratification observed at Pompeii. Several roofing-tiles, either intact or in fragments, were recovered at various stratigraphic heights in the lapilli deposit at Pompeii and Stabiae. This study shows that downwind variations in lapilli fall deposits are strongly influenced by an articulated substrate like that of urban structures. During the first phase of the AD 79 eruption, several roof collapses occurred, as evidenced by abundant debris and tiles found in the lapilli fall deposit. The presence of steep roofs allowed the falling pumice clasts to roll and slide down and then accumulate in the impluvium areas and in the alleys, attaining greater thicknesses with respect to deposits accumulated in open areas. This rolling produced a selection by size and density of the pyroclasts, thus forming a well-stratified deposit. At the same time, under the canopies the fall deposit thins dramatically towards the sheltered corridors. It is evident that the urban structures affect the structure of the deposit much more than the variations induced by the increase in the distance from the eruptive vent.

Does the St Marys Porphyrite represent a super eruption in eastern Tasmania?

Gallagher, Till, Bottrill, Ralph, Carey, Rebecca, Cumming, Grace, & Orth, Karin
University of Tasmania, Hobart, Australia

In the Eastern Tasmania Terrane (ETT), the southernmost extent of the Lachlan Fold Belt, the St Marys Porphyrite (SMP) is thought to represent the only incidence of Devonian volcanism south of mainland Australia. The lack of volcanic succession contrasts with Victoria and New South Wales, where Devonian magmatism is associated with numerous caldera-related volcanic successions.

Turner (1986) described tell-tale textures thought to be volcanic in origin and interpreted the SMP as a dacitic, welded ash-flow tuff. He considered it to be an extrusive equivalent of the hornblende–biotite granodiorite plutons of the Blue Tier Batholith. He interpreted highly welded zones and devitrification textures, but perplexing extrusive and intrusive contact relationships, and granophyric-like crystallisation textures have puzzled subsequent workers. The application of modern volcanology techniques aims to re-evaluate

past conclusions and introduce new knowledge and evidence to develop a revised emplacement model for this enigmatic unit.

The distribution and characteristics of texturally diverse polymictic lithic clasts are used to identify variations within the SMP. Several different clast types and a number of textural features have been identified. The most abundant clast type observed throughout the internal part of the SMP is described as 'white igneous lenticular domains' or WILDS. The WILDS are tentatively interpreted to represent phenocryst rich relict pumiceous domains and or possible cognate igneous inclusions which form a fabric visible on weathered surfaces. These domains appear to dip consistently to the southwest. This study estimates the original eruption volume of the SMP by using the aspect ratio of both fiamme, WILDS and the surface area of the unit (based on new and previous geological mapping by Turner (1986).

The interpretation of a volcanic ignimbrite and measurements of the flattening ratios for both fiamme and WILDS enable us to calculate pre-compaction thicknesses of the SMP. Thickness coupled with the area of emplacement enables us to calculate a minimum eruption volume of 920+ km³. It is likely that pre-erosion volumes of the SMP is far greater, as work to understand the geometry of the unit is ongoing. Preliminary volume estimates are speculative but suggest, if the SMP is of a volcanic origin, that it could represent the product(s) of a super eruption (>1000 km³ erupted material). Further calculations to estimate the original volume of the SMP are warranted and will assist us to estimate the eruption magnitude related to the emplacement of the unit.

Understanding the eruption and emplacement processes of the SMP expands our understanding of the Devonian upper crustal architecture of eastern Gondwana and provide insight into the plumbing system of eastern-Tasmanian granites.

Magma ascent in Australian Intraplate basaltic volcanic provinces

Handley, Heather¹, Cas, Ray², England, Tom¹, Didonna, Rosa¹, & Ezad, Isra¹

¹*Department of Earth and Environmental Sciences, Macquarie University, Sydney, Australia;* ²*School of Earth, Atmosphere and Environment, Monash University, Clayton, Australia*

Basaltic intraplate volcanic fields, those located within tectonic plates, occur on every continent, often in close proximity to large population centres and yet they are amongst the least well-understood volcanic systems on Earth. In this study we use textural and chemical information stored within minerals from two of the youngest volcanic eruptions in northeast and southeast Australia to investigate magmatic plumbing systems and magma ascent in intra-plate volcanic fields. Volcanic rock samples from the three main eruptive phases at Mt Schank volcano in the Newer Volcanics Province, South Australia, reveal textural and mineralogical differences throughout the evolution of the eruption that correspond to variations in eruption style and the availability of external water. Crustal xenoliths (e.g., quartz and limestone) are abundant in the middle, maar-forming phase of the eruption. The lack of mantle-derived xenoliths and xenocrysts

throughout the eruption, olivine compositions and sector and oscillatory zoned, euhedral clinopyroxene suggest a more stalled ascent pathway of magma compared to the mantle xenolith-bearing volcanoes in parts of the Victorian sector of the province. Skeletal olivine crystals and dendritic clinopyroxene microlites indicate moderate degrees of undercooling at Mt Schank during magma ascent. In northeast Queensland, interaction of magma with a mantle xenolith (pyroxenite) is used to determine magma ascent dynamics. Disequilibrium and quench textures and chemical zoning patterns in olivine, clinopyroxene, orthopyroxene and spinel on xenolith margins and within host glass reveal a detailed and complex history of magma ascent.

Pompeii to Stabiae: downcurrent versus substrate-induced variations of the AD 79 Vesuvius pyroclastic current deposits and their impact on human settlements

Santangelo, Ileana¹, Scarpati, Claudio¹, Perrotta, Annamaria¹, Sparice, Domenico², Fedele, Lorenzo¹, Chiominto, Giulia¹, Muscolino, Francesco², Rescigno, Carlo³, Silani, Michele³, & Massimo, Osanna²

¹*Department of Earth, Environmental and Resources Sciences, University of Napoli Federico II, Napoli, Italy;* ²*Parco Archeologico di Pompei, Pompei, Italy;* ³*Dipartimento di Lettere e Beni Culturali, Università della Campania Luigi Vanvitelli, Santa Maria Capua Vetere, Italy*

The AD 79 Vesuvius eruption buried the Roman towns around the volcano under several metres of pyroclastic materials. The destruction of these Roman towns allows volcanologists to build models that can provide valuable information on the extent and type of damage that a future Plinian eruption could cause in urbanized areas. In order to fully understand these phenomena, volcanologists need to observe the sequence of volcanic layers (stratigraphic reconstruction) that buried the city during the AD 79 eruption and which of these layers are associated with damage and victims. This study reports the results of a collaboration between the Archaeological Park of Pompeii and the University of Naples Federico II to document the stratigraphic sequence and the distribution of damage and victims unearthed by new excavations in the archaeological sites of Pompeii and Stabiae. A systematic survey of all exposed pyroclastic sequences allowed us to study in detail the distribution and lateral facies variations of the different stratigraphic units. The deposit of stratified ash forming the upper part of the pyroclastic succession, was studied in detail to define the downcurrent variations of its sedimentological features and how these were influenced by urban structures. Pronounced lateral variations are observed in the upper part of the sequence at Pompeii, mainly consisting of a pyroclastic density current (PDC), stratified ash deposit, that ranges in thickness from few tens of centimetres to two metres. In this case, thin, massive ash layers can be traced laterally into thick, poorly sorted, ash and lapilli layers, with well-developed sedimentary structures. All PDC layers, except the lowermost, are dispersed across the entire Pompeii area, although some are missing locally as a result of the erosive action of the following PDC. The layer associated with the most destructive impact on the Roman buildings shows a

strong lateral variation in thickness (0 to 330 cm) and sedimentary structures. Where it is less than 30 cm thick, the deposit is fine-grained and thinly stratified. Where it thickens, the lower part is rich in coarse pumice lapilli and locally shows well-developed stratifications, while the upper part shows an internal arrangement of alternating layers of fine and coarse ash forming progressive dunes. Upwards, ash deposits show rare pumice lapilli clasts and diffuse accretionary lapilli. This ash sequence is interstratified with four well-sorted, thin lithic-rich layers that exhibit mantling structures of fall deposits. At Stabiae, the ash PDC deposit ranges in thickness from 70 to 160 centimetres. Its internal structure shows the same types of stratification observed at Pompeii. Ash layers thicken and show lateral lithofacies variations where the pumice deposit thins and close to standing walls. It is proposed that the urban structures affect the structure of the deposit much more than the variations induced by the increase in the distance from the eruptive vent.

autopew: Microanalytical Coordinate System Transforms

Williams, Morgan, & Schoneveld, Louise

CSIRO Mineral Resources, Australian Resources Research Centre, Kensington, WA, Australia

autopew is an open-source Python package designed for coordinate system transformation which enables easy transfer of analysis points between microanalytical equipment sample stages and/or images. This software supports rapid and repeatable sample targeting over multiple instruments and analytical techniques (e.g. electron microprobe and laser ablation) which maximises instrument time available for data collection, rather than sample navigation, spot location and naming consistency. The ability to record and precisely relocate sample analyses with *autopew* allows reproducible integration of multiple microanalytical point-sampling and imaging datasets.

autopew allows for arbitrary transformation between planar cartesian coordinate systems (including images) using two-dimensional affine transforms. The package provides methods for import and export of sample coordinates in a variety of file formats, allowing for direct import of coordinates for a selection of instruments. Networks of coordinate transformations between multiple images and instrument stages are readily constructed, allowing cross-referencing between images and stage coordinates. The coordinate transforms between images and sample stages can be archived with completed analytical datasets for future reference and data quality assurance and quality control (QA/QC) where needed.

Where high resolution images are acquired (e.g., via light or electron microscopy), *autopew* records the micro-spatial context of each in-situ analysis. This will support new insights into the micro-environmental effects and spatial dependence of mineral and glass geochemistry and allow for more reliable inference across scales, i.e., from well-characterised in-situ microanalysis to macroscale geological processes.

The package is currently under active development, for more information on features and how to participate see <https://autopew.readthedocs.io/>

Where will Australia's next volcano erupt?: wider perspectives

Sutherland, Frederick L.¹, & Graham, Ian T.²

¹*Geosciences, Australian Museum, 1 William Street, Sydney, NSW 2010, Australia;* ²*School of Biological Earth and Environmental Sciences, University of New South Wales, Sydney, NSW 2052, Australia.*

East Gondwanan Cretaceous late Mesozoic thermal rifting initiated near-continuous Australian intraplate basaltic volcanism that inevitably will continue. Researchers mostly expect that the next eruption will likely occur within the young SW Victoria–SE South Australia or NE Queensland basalt fields. These areas preserve many eruptive features, although the southern fields seem past peak activity, while the northern fields seem closer to peak activity. This presentation looks beyond these areas and examines isolated eruptive events within the last 5 Ma elsewhere throughout Eastern Australia. These sites forecast that a new volcano may well erupt in an unexpected area.

Queensland: Young isolated basalt sites include 3.7 Ma nephelinites at Silver Plains, over 200 km NW of the main NE Queensland basalt provinces. These fields have been linked to a cryptic mantle plume below the adjacent Coral Sea floor. The isolated South Barnard offshore islands are ca 1 Ma old pyroclastic cones and intrusive dykes, SE of the main Atherton basaltic field. A further eruption there would create shallow marine explosive activity. Mount St Martin, northern Bowen Basin, is a unique isolated 2.4–3.1 Ma lava-capped pyroclastic vent of hybrid basanite–trachyte, much younger than adjacent basalts and rhyolites of the Nebo Province. In western Qld, in the Winton–Longreach region, ³He/⁴He and ⁸⁷Sr/⁸⁶Sr studies on ground water discharges and an underlying slow seismic anomaly suggested sub-surface cooling basaltic intrusions. In SE Qld, an age-decreasing trend of isolated young basaltic fields extends 200 km SW from Bundaberg to Brigooda. It predicts potential further eruption to the SW, but this may depend on the lithospheric depth.

New South Wales: Young 2–5 Ma reset zircon megacrysts eroded from basaltic eruptives fringe outskirts of older basaltic areas in several regions. In rare cases they occur in diatremes, as at Gloucester River, SW of Barrington Tops shield volcano. Otherwise, they concentrate in alluvial deposits on the eastern flank of that volcano. In Tobins Camp lead SE of Yarrowitch, 2.7 Ma zircons in the isolated deposit are 40 Ma younger than adjacent Yarrowitch basalts. At Oban and Uralla, 2–3 Ma zircons are ca 20 Ma younger than adjacent basalts. In SW NSW, bentonite ash beds in 1.6–2.4 Ma Murray Basin strata at Arumpo seem linked to proximal eruptive sites.

Victoria: In eastern Victoria, the Uplands basalts include 2 and 4 Ma flow events, while to the NW near Toombullup alluvial deposits contain 2 Ma reset zircons.

Tasmania–West Tasman Sea: Mantle CO₂ discharges in NW Tasmania and seismic activity east of Flinders Island and in the Central Tasman Sea floor mark predicted dormant plume positions for the East Australian plume array. Recent research voyages have now located young sea mounts at the predicted plume nodes for the Tasmantid and Lord Howe seamount chains.

Summary: These widespread young activities offer a

complex dynamic scenario for future eruptions.

Tracking plumbing system architecture in age-progressive intraplate volcanoes in Eastern Australia.

Tapu, Al-Tamini, Ubide, Teresa, & Vasconcelos, Paulo
School of Earth and Environmental Sciences, The University of Queensland, Brisbane, Australia

Cenozoic age-progressive volcanism in eastern Australia crops out as the longest age-progressive continental track of shield volcanoes that extends for ~2000 km. The so-called 'central volcanoes' show a southward-younging trend that has been related to the motion of the Australian plate over one or several stationary mantle plumes. Central volcanoes developed in regions of contrasting lithospheric thickness and have distinct eruptive volumes, however, the relationships between regional context and extent of volcanic activity remain poorly constrained.

Here we apply a high-resolution geochemical-geochronological approach to investigate differences in the time spans of volcanism and the architectures of the magma feeder systems at depth. We investigate central volcanoes Ebor, Nandewar, and Canobolas, located in regions of different lithospheric thickness and with varied volumes of magma from 50 to 300 km³.

The rocks are porphyritic to aphyric basalts to trachytes and rhyolites, including 5–40 vol% phenocrysts of plagioclase, clinopyroxene, and minor olivine. Clinopyroxene-melt thermobarometry indicates crystallization at 10–3 kbar (25–10 km depth) and 800–1150 °C. Rhythmic-oscillatory zonation in plagioclase (An₅₅) and clinopyroxene (Mg#₇₀) suggest steady-state growth in deep reservoirs undergoing continued magma supply and differentiation of compositionally similar magmas. K-feldspar and green-clinopyroxene (Mg#_{25–45}) are interpreted as antecrysts recycled from pockets of fractionated melts. Successive mafic magma influx before eruption generated growth of mafic mineral zones (plagioclase An₆₅, clinopyroxene Mg#₇₅) over partially resorbed, sieved, and/or patchy cores (An_{35–50} and Mg#_{55–65}, respectively). ⁴⁰Ar/³⁹Ar geochronology indicates that the volcanoes were episodically replenished over timescales of ca 0.1 Ma, and the eruptive activity lasted for ca 3–1.5 Ma.

The combined geochemical and geochronological studies suggest three spatially separated but genetically linked volcanoes were fed through comparable plumbing system architectures. Rhythmic mafic recharge and fractionation controlled the lifespans and tempos of eruptive activity.

Geochemical data analysis workflows with *pyrolite*

Williams, Morgan, & Schoneveld, Louise
CSIRO Mineral Resources, Perth

The availability and accessibility of instrumentation to rapidly acquire large volumes of geochemical data has steadily increased over recent decades. However, the geochemical community as a whole is only beginning to embrace the flexibility and relative power of adopting high-level programming languages (e.g., Python) to process, summarise and visualise this data. This emerging shift provides opportunities to address

scientific reproducibility concerns, increase the comparability of geochemical datasets, and develop transferable digital skills within the research community. Taking a declarative programmatic approach to data processing and analysis makes these tasks more repeatable, particularly when compared to multi-stage workflows based on extensive user interface interaction where steps are often only descriptively documented. When combined with versioning and environment management, this approach enables reproducible workflows which can be shared such that others can effectively examine, compare and re-use existing code as needed. To address the relative scarcity of geochemistry-focused tools and support adoption of a programmatic approach to geochemical data analysis we've developed *pyrolite* – an open-source Python package for working with geochemical data. In this presentation we'll provide an overview of a series of short examples demonstrating some of the advantages of adopting a programmatic approach to geochemical data analysis workflows and highlighting some of *pyrolite*'s key features.

pyrolite aims to allow new users to get off the ground quickly by providing 'batteries included' functionality for transforming, analysing and visualising geochemical and compositional data. The package contains a suite of functions commonly used in geochemical data workflows, including log-transforms for working with compositional data in a robust manner, scaling between units and simple element-oxide conversion. *pyrolite* also implements several common geochemical visualisations and plot templates and provides easy access to data-density based visualisation methods better adapted to larger multivariate datasets with hundreds to hundreds of thousands of samples. Beyond providing foundational functionality, *pyrolite* also provides a framework to encode and document relevant algorithms recently introduced to the geochemistry community (e.g., *lambdas* for parameterising rare earth element profiles, bootstrap resampling methods) and also link geochemical data to common machine learning frameworks (e.g., *scikit-learn*). The package is built upon and exposes the API of commonly used scientific Python packages, including *matplotlib* and *pandas*, allowing a greater degree of interoperability and familiarity for new users.

The package and related tools continue to be actively developed, and the package has recently been peer reviewed and [published](#). Future development is planned to include support for interactive visualization and will expand the set of examples and tutorials within the [documentation suite](#). The project is being developed for and by the geochemistry community, and we encourage new users to get involved. We hope to foster a growing community of users and contributors to ensure the long-term sustainability and usefulness of the project, all forms of contribution to the project are welcome.

Architecture, composition and geodynamic history of cratons and craton

Contrasting growth of the Pilbara and Yilgarn cratons from hafnium and neodymium isotopes

Kemp, Tony

School of Earth Sciences, University of Western Australia, Perth, WA 6009

Long-lived radiogenic isotope systems such as ^{147}Sm – ^{143}Nd and ^{176}Lu – ^{176}Hf suggest that large volumes of the Earth's continental crust formed in the Archean Eon (>2.5 Ga). The onset of substantial continent stabilization in the geological record is marked by the distinctive 'granite-greenstone' terranes that are the hallmarks of Archean crustal blocks. Yet, to what extent generation of the buoyant, silica-rich (i.e., continental) components in these terranes involved the re-melting of pre-existing, primordial crust as opposed to rapid differentiation of new mantle additions, remains uncertain. Establishing the composition of the mantle source from which early crust was extracted, and comparing this with the compositions of felsic crust, is key to this question. The geochemical signatures of ancient, unambiguously mantle-derived rocks are, however, susceptible to modification by later metamorphism. Here, hafnium and neodymium isotope data are reported for well-preserved mafic–ultramafic and felsic igneous rocks of the Pilbara and Yilgarn Cratons, Western Australia. Comparing the mantle and crustal records of Archean continent formation in these cratons reveals a striking isotopic link that endured over 500 million years. In the Pilbara Craton, this linkage is interpreted to reflect the efficient transformation of new mafic inputs from the mantle into felsic continental crust throughout the history of the craton. In contrast, broadly coeval rocks in the Yilgarn Craton formed by remelting older rocks, although the crustal evolutionary records of both cratons converge in the Neoproterozoic. The possible reasons for the cratonic contrasts are considered.

Records of the Earth's early crust from apatite inclusions in zircon – development and applications of *in situ* $^{87}\text{Sr}/^{86}\text{Sr}$ analysis by SIMS

Gillespie, Jack¹, Kinny, Pete¹, Martin, Laure², Kirkland, Christopher¹, Nemchin, Alexander¹, & Cavosie, Aaron¹

¹The Institute for Geoscience Research (TIGeR), School of Earth and Planetary Sciences, Curtin University, Perth, WA 6845, Australia; ²Centre for Microscopy, Characterisation and Analysis (CMCA), University of Western Australia, 35 Stirling Highway, Perth, WA 6009, Australia

Rb–Sr isotopes in geological materials provide a system for tracing crustal differentiation processes and insights into the evolution of planetary bodies. The ingrowth of radiogenic ^{87}Sr from the decay of ^{87}Rb leads to increased $^{87}\text{Sr}/^{86}\text{Sr}$ over time, and due to the strong relationship between the Rb/Sr and SiO_2 contents of igneous rocks, this provides a time-integrated window into the evolution of geochemical reservoirs. However, the high geological mobility of both Rb and Sr in whole rocks during metamorphism and fluid alteration means that this record becomes progressively less reliable in older rocks that have experienced post-crystallization geological events.

Strontium is easily substituted into the crystal lattice of

apatite, occurring as a trace element in concentrations ranging from less than a hundred parts per million to several weight percent. In contrast, apatite nearly entirely excludes Rb (<1 ppm) resulting in negligible radiogenic ingrowth of ^{87}Sr , and consequently the initial $^{87}\text{Sr}/^{86}\text{Sr}$ ratio of the melt from which an apatite crystallizes is faithfully recorded by the mineral. Inclusions of apatite within magmatic zircons are particularly valuable as they are armoured by the more robust host mineral, allowing them to survive subsequent events that might otherwise cause isotopic reset or recrystallization. However, the typically very small size of apatite inclusions in zircon and the complex isobaric interferences on the isotopes of Sr during *in-situ* mass spectrometry have previously limited the information that can be obtained from this archive.

Our recent development of a method to measure the $^{87}\text{Sr}/^{86}\text{Sr}$ ratio in apatite by SIMS with a spot size appropriate for accessing typical mineral inclusions in zircon (<15 μm) makes it possible to routinely analyse the commonly occurring inclusions of apatite in zircon. We have applied this method to determine the initial $^{87}\text{Sr}/^{86}\text{Sr}$ ratios of various Eo–Meso Archean igneous rocks by analysing the Sr isotope composition of apatite inclusions. High resolution SEM imaging and EPMA analysis illustrate the primary nature of these inclusions. Combining the measured $^{87}\text{Sr}/^{86}\text{Sr}$ of apatite inclusions with the U–Pb age and Hf isotopic composition of the co-genetic zircon host allows for the 'triangulation' of the Rb/Sr necessary for the ingrowth of radiogenic strontium over the crustal residence interval calculated from the crystallization and Hf model ages. Examples from SW Greenland and the Narryer Gneiss Terrane of Western Australia suggest that these rocks were derived from the melting of ancient crustal material that was on average of intermediate–felsic rather than mafic composition.

Neodymium and oxygen isotope maps of Western Australia

Lu, Yongjun¹, Smithies, R. H.¹, Champion, D. C.², Wingate, M. T. D.¹, Johnson, S. P.¹, Martin, L.³, Jeon, H.⁴, Pujol, M.⁵, Zhao, J.⁶, Maas, R.⁷, & Creaser, R. A.⁸

¹Geological Survey of Western Australia, 100 Plain Street, East Perth, WA 6004; ²Geoscience Australia, GPO Box 378, Canberra ACT 2601; ³Centre for Microscopy, Characterisation, and Analysis, University of Western Australia, Perth, WA 6009; ⁴Swedish Museum of Natural History, Box 50 007, SE-104 05 Stockholm, Sweden; ⁵Univ Rennes, CNRS, Géosciences Rennes - UMR 6118, 35000 Rennes, France; ⁶Radiogenic Isotope Facility, School of Earth Sciences, The University of Queensland, Brisbane, QLD 4072, Australia; ⁷School of Earth Sciences, University of Melbourne, Parkville, VIC 3010, Australia; ⁸Dept. Earth & Atmospheric Sciences, University of Alberta, Edmonton, Alberta, Canada

Multi-isotope maps can characterise lithospheric architecture through time, play an increasingly important role in predictive exploration targeting, and are consequently sought-after datasets by industry. We present the first zircon oxygen isotope map and an updated whole-rock Sm–Nd isotope map of Western Australia. These shed new light on crustal evolution and

mineral system distributions. The isotope maps were generated from datasets that are subject to ongoing updates as new data are generated and compiled.

Median zircon $\delta^{18}\text{O}$ values for about 125 igneous rocks have been spatially visualized so far, and coverage currently extends across the Pilbara and Yilgarn Cratons, the Capricorn, Paterson, and Albany-Fraser Orogens and the Eucla basement (Madura and Coompana Provinces). The Pilbara and Yilgarn Cratons are dominated by mantle-like $\delta^{18}\text{O}$ values (4.7–5.9 ‰), consistent with reworking of igneous material that had not been exposed at the surface. A ca 3.47 Ga diorite, four ca 3.3 Ga hornblende-bearing granitic rocks, and a ca 2.95 Ga hornblende monzogranite in the Pilbara Craton exhibit weakly elevated zircon $\delta^{18}\text{O}$ values (5.9–6.5 ‰), which together with trace element enrichment were attributed to hydrous sanukitoids or to derivation from a sanukitoid-enriched source. The Capricorn, Paterson, and Albany-Fraser Orogens and the Eucla basement also contain rocks with elevated $\delta^{18}\text{O}$ values (6.6–9.9 ‰), suggesting significant reworking of upper crustal material during magma genesis. Zircons with sub-mantle $\delta^{18}\text{O}$ values (<4.7 ‰) were found for granitic rocks of ca 3.55 Ga in the Sylvania Inlier, of ca 3.44 Ga in the northern Pilbara Craton, and of ca 3.0 and 2.67 Ga in the South West Terrane, suggesting recycling of crustal material subjected to high-temperature hydrothermal alteration, such as observed in post-Archean rift systems or calderas.

Sm-Nd isotopes for about 1120 felsic igneous rocks provide regionally extensive images of crustal architecture. The map of two-stage depleted mantle model ages (T_{DM^2}) highlights the distinction between Archean cratons ($T_{\text{DM}^2} > 2.6$ Ga) and Proterozoic orogens ($T_{\text{DM}^2} < 2.2$ Ga), and isotopic boundaries correlate well with most existing proposed terrane boundaries. However, the isotopic boundary between the South West Terrane and the Youanmi Terrane appears to be about 100 km west of the previously proposed boundary, but correlates well with magnetic and gravity anomaly zones and the distribution of gold mineralization. The crustal residence map highlights predominantly short residence times (<0.5 Ga) for the Pilbara and Yilgarn Cratons, and much longer crustal residence times (>0.8 Ga) in the Paterson, Albany-Fraser, Pinjarra and Capricorn Orogens, suggesting decreased juvenile crust generation in these orogens.

These maps are directly applicable to metallogeny. For example, most giant gold deposits in WA are located on or near significant isotopic boundaries and tectonic structures. Interestingly, Telfer, Plutonic and giant gold deposits in the Murchison are aligned along a north-east-trending isotopic boundary. Similar boundaries occur between the eastern and western parts of the Pilbara Craton and between the Yilgarn Craton and the Albany-Fraser Orogen. These isotopically defined discontinuities may be important clues to the earliest architectural elements in Western Australia.

Way out west – does the Arunta Orogen continue westward beneath the Canning Basin?

Kelsey, David E.^{1,3}, Spaggiari, Catherine V.¹, Wingate, Michael T. D.¹, Lu, Yongjun¹, Fielding, Imogen O. H.¹, & Finch, Emily G.^{1,2,3}

¹Geological Survey of Western Australia, 100 Plain St,

East Perth, WA 6004, Australia; ²University of South Australia, 101 Currie St, Adelaide, SA 5001, Australia; ³MinEx CRC

Crystalline basement lies beneath the southeastern margin of the Canning Basin and immediately west of the exposed Arunta Orogen, although whether that basement is the continuation of the Arunta Orogen is unknown. The major bounding fault of the Canning Basin coincides with the inferred trace of the Lasseter Shear Zone, which truncates dominant east-trending structures of the orogen and potentially also terminates it. The Top Up Rise prospect is located above a distinct northeast-trending gravity anomaly bound by northeast-trending shear zones coincident with the Lasseter Shear Zone. Five co-funded Exploration Incentive Scheme diamond drillcores from Top Up Rise contain partially melted or melt-injected upper-amphibolite to low-granulite facies basement rocks. These are currently the only drillcores that intersect the Canning Basin basement in this region and provide a means to test its tectonic affinity, and the significance of the Lasseter Shear Zone.

Petrography of granitic gneiss and paragneiss indicates distinctly higher metamorphic grade than is observed in exposed rocks of the west Arunta Orogen, consistent with their separation by a significant shear zone. SHRIMP U-Pb zircon geochronology of several granitic gneiss samples has so far revealed a single magmatic protolith crystallization age of ca 1875 Ma, which is distinctly older than known magmatic rocks in the Arunta Orogen. Maximum deposition ages of 1877–1822 Ma for the metasedimentary rocks are similar to or younger than the magmatic protolith ages of the granitic gneiss, suggesting that emplacement of granitic rocks predated deposition of at least some of the sedimentary rocks. Zircon rims in both granitic gneiss and paragneiss samples record high-grade metamorphism at 1622–1604 Ma. Although metamorphism of this age is unknown in the west Arunta Orogen, thermal events of similar age may have occurred in the central Arunta Orogen (Alessio *et al.*, 2020, *Lithos*, [doi:10.1016/j.lithos.2019.105280](https://doi.org/10.1016/j.lithos.2019.105280)), and granitic magmatism occurred at this time in the Haast Bluff Domain of the Warumpi Province (NTGS Special Publication 5, 2013).

The granitic protolith ages of ca 1875 Ma from Top Up Rise are different to those of granitic suites in the Lamboo Province and Granites-Tanami Orogen, however, felsic volcanic rocks of the lower Halls Creek Group have been dated at ca 1880 Ma (Phillips *et al.*, 2016, GSWA Report 164) and ca 1880 Ma granitic rocks are known in the Arnhem Province (NTGS Record 2017-008). In contrast, detrital zircon age components at ca 1875 Ma are widespread and form significant age components in the Lander Rock Formation of the Arunta Orogen, the Marboo Formation and Tickalara Metamorphics of the Halls Creek Orogen, as well as in Top Up Rise paragneisses. Hence, the newly identified granitic basement in the Top Up Rise drillcores may be representative of a major source component that fed detritus into turbidite fan systems that included the Lander Rock Formation. This basement could represent part of the 'missing' Arunta basement, which would support interpretations that the Arunta does continue westwards, or it could be part of a previously unrecognized Proterozoic crustal element that underlies the Canning Basin.

Multiple ages of rutile from a single sample of granulite

Durgalakshmi¹, Williams, Ian S.¹, & Sajeev, K.²

¹Research School of Earth Sciences, Australian National University, Canberra, Australia; ²Centre for Earth Sciences, Indian Institute of Science, Bengaluru, India

Rutile (TiO₂) is a common accessory mineral in hydrothermal and metamorphic rocks that is stable across a wide range of P–T conditions. It can incorporate up to 200 ppm of U, and has a lower closure temperature than zircon, making it a reliable mineral with which to date retrograde metamorphism and low- to medium-grade metamorphic events by the U–Pb technique. Further, Pb and Th are incompatible in rutile, so corrections for its small initial Pb can be made accurately using its ²⁰⁸Pb content.

During prograde metamorphism, rutile forms following the breakdown of biotite or ilmenite as part of a continuous reaction. During retrogression, rutile can be replaced by ilmenite and titanite. Secondary rutile can be formed by hydrothermal alteration, oxidation or exsolution. In high-grade metamorphic rocks, rutile occurs as single crystals in the matrix and/or as inclusions in other minerals such as garnet, pyroxene and amphibole. In low- to medium-grade rocks it usually occurs as needles or polycrystalline aggregates. Using an ion microprobe (SIMS), rutile can be dated in its textural context in thin section, providing age information directly linked to metamorphic reactions. Dating and trace element analysis of separated rutile grains have a wide range of applications from sedimentary provenance studies to dating vein mineralisation and granitic pegmatites that host mineral deposits.

In the Neoproterozoic Southern Granulite Terrane, India, rutile preserves a record of the late thermal history that is not provided by other datable minerals such as zircon or monazite. One studied sample of granulite grade felsic gneiss contains at least three distinct generations of rutile that preserve a range of Neoproterozoic to early Palaeozoic U–Pb ages. The zircon from the same sample is Neoproterozoic, with no evidence of a younger component. The rutile occurs as single ~ 0.5–0.8 mm crystals in the matrix, some of which are rimmed by titanite. Rutile-forming reactions, which can be linked to the metamorphic conditions, have been dated, contributing to unravelling the polymetamorphic and tectonic history of this complex terrane.

Geodynamic influences on volcanological, paleoenvironmental and tectonic evolution of the Archean Kalgoorlie Terrane LIP, Western Australia

Cas, R.A.F.¹, Hayman, P.C.², Squire, R. J.³, Campbell, I. H.⁴, Wyche, S.⁵, Sapkota, J.⁶, & Smithies, H.⁷

¹School of Earth, Atmosphere and Environment, Monash University, Vic 3800, Australia; ²Queensland University of Technology, Brisbane, QLD 4074, Australia; ³School of Earth, Atmosphere and Environment, Monash University, Vic 3800, Australia; ⁴Research School of Earth Sciences, Australian National University, ACT 4074, Australia; ⁵Geological Survey of Western Australia, Perth and Kalgoorlie, WA, Australia; ⁶Geological Survey of Western Australia,

Perth & Kalgoorlie, WA, Australia; ⁷Geological Survey of Western Australia, Perth & Kalgoorlie, WA, Australia

The stratigraphy of the late Archean (>2.7 Ga to 2.658 Ga) Kalgoorlie Terrane Large Igneous Province, in the Eastern Goldfields Superterrane, Yilgarn Craton, Western Australia, preserves an evolution of magmas, eruption processes paleo-environments, sediment provenance, and deformation that are inconsistent with a plate tectonic setting. An initial, deep submarine LIP komatiite and basaltic succession several kms thick (Stage 1 ca 2.72–2.69 Ga) of lavas, hyaloclastite breccia and sills, with intercalated chert, black mudstones and minor felsic volcanics, extends > 600km along strike. It represents a widespread mantle plume event during regional extensional (D1) rift volcanism. Eruptions occurred in an open, anoxic, deep-water setting with no evidence of nearby emergent continents. Hydrostatic pressure suppressed all explosive activity.

From ca 2.69 to 2.67 Ga (Stage 2) felsic TTG magmatism was dominant, represented by submarine lavas, hyaloclastite, monomictic tuffaceous megaturbidites, polymictic volcanogenic turbidite and conglomeratic mass flow deposits, and contemporaneous high-level granitoid intrusions. A major mafic event at ca 2.80 Ga indicates mantle heat likely caused felsic crustal magmatism. The felsic volcanics and volcanoclastics represent marine intra-basinal felsic volcanoes (lava domes, strato-volcanoes?), some of which grew into shallow water and became emergent, were explosive under low ambient pressures, and produced the submarine tuffaceous megaturbidites. The Stage 2 volcanic conglomerates, including some granitoid clasts, were not generated by orogenic deformation and uplift, but were derived exclusively from the intra-basinal volcanic centres and sub-volcanic plutons, and from Stage 1 komatiite and mafic stratigraphy that was up-domed by diapiric granitoids. Ongoing plume buoyancy and contemporaneous local granitoid diapirism caused regional and local uplift (D2') and shallowing of basins during ongoing regional extension (D1).

From ca 2.67 Ga a transition into more widespread subaerial paleoenvironments is represented by felsic tuffaceous volcanic sediments deposited in fluvial braid-plain, alluvial fan, shallow marine, and local deep-water settings (Stage 3A). At < 2.658 Ga "late basin" polymictic, alluvial fan – fan delta conglomerates and sandstones represent major, regional crustal compression, uplift (D2/D4', depending on scheme), emergence of large landmasses, and far-field sediment provenance (Stage 3B). There is no geological evidence of a plate tectonic regime prior to 2.658 Ga (i.e., no ophiolites, accretionary prisms, blueschist belts, uplifted orogenic belts, mountainous continents). A long-lived mantle plume caused partial melting of thick metasomatized mafic crust causing uprise of TTG plutons, leading to plutonic diapiric updoming, and changing paleo-environments and eruption styles from Stages 1 to 3 (ca 50 Myr). Widespread TTG magmatism does not signify a subduction setting, but widespread anatexis of a lid-like crust/lithosphere.

On the destructive tendencies of cratons: 3D geodynamics modelling of cratons and subduction

Farrington, Rebecca¹, Cooper, Katie², & Miller, Meghan³

¹*School of Earth Sciences, The University of Melbourne, Melbourne, VIC 3010, Australia;* ²*School of the Environment, Washington State University, Pullman, Washington 99164, USA;* ³*Research School of Earth Sciences, The Australian National University, Canberra, ACT 2600, Australia*

Subduction of lithosphere at convergent plate boundaries drives large-scale mantle flow patterns. When in the vicinity of craton margins this mantle flow can provide the potential for craton destruction. Examples of this setting can be seen along the northern margin of South America and northwestern Africa where active subduction zones occur adjacent to craton margins. We present a 3D numerical geodynamic study exploring the interaction between subducting lithosphere and craton margins. We propose that subducting slabs can direct flow along craton margins, a process that may shape and carve these margins and impact the overall stability of the craton.

An isotopic Atlas of Australia: foundational data for integrated geoscience through time and space

Fraser, Geoff, Waltenberg, Kathryn, Jones, Sharon, Huston, David, Champion, David, & Bodorkos, Simon
Geoscience Australia, Canberra, Australia

Australia has been, and continues to be, a leader in isotope geochronology and geochemistry. This has included fundamental contributions to instrumentation, method development and geological applications. While new isotopic data is being produced with ever increasing pace and diversity, there is also a rich legacy of existing high-quality age and isotopic data, most of which have been dispersed across a multitude of journal papers, reports and theses. Where compilations of isotopic data exist, they tend to have been undertaken at variable geographic scale, with variable purpose, format, styles, levels of detail and degree of completeness. Consequently, it has been difficult to visualise or interrogate the collective value of age and isotopic data at continental-scale. Contrast this situation with the almost ubiquitous use of national-scale geophysical data coverages, such as magnetic and gravity compilations. Age and isotopic patterns at continental scale can provide intriguing insights into the temporal and chemical evolution of the continent, and an opportunity to add additional geological meaning to such geophysical coverages.

As national custodian of geoscience data, Geoscience Australia has addressed this challenge by developing an Isotopic Atlas of Australia, which so-far consists of national-scale coverages of five widely used age and isotopic data-types, as follows:

- Sm–Nd whole-rock analyses of granites and felsic volcanics
- Lu–Hf analyses of zircon
- Pb–Pb of ore-related minerals – primarily galena and pyrite

- U–Pb mineral ages from magmatic, metamorphic and sedimentary rocks (typically zircon but also including monazite, titanite, baddeleyite...)
- K–Ar and ⁴⁰Ar–³⁹Ar analyses of minerals and whole rocks.

Several of these isotopic coverages are now freely available as web-services for use and download from the GA Portal (www.portal.ga.gov.au). While there is more legacy data to be added, and a never-ending stream of new data constantly emerging, the provision of these national coverages with consistent classification and attribution provides a range of benefits:

- it vastly reduces duplication of effort in compiling bespoke datasets for specific regions or use-cases
- data density is sufficient to reveal meaningful temporal and spatial patterns
- a guide to the existence and source of data in areas of interest, and of major data gaps to be addressed in future work
- facilitates production of thematic maps from subsets of data. For example, a magmatic age map, or K–Ar mica cooling age map
- sample metadata such as lithology and stratigraphic unit is associated with each isotopic result, allowing for further filtering, subsetting and interpretation.

The GA Portal also contains a great diversity of other geological, geophysical and geographic coverages. This provides the opportunity to conveniently overlay age and isotopic patterns with geological maps, major structural and province boundaries, crustal and lithospheric thickness, seismic velocity images, electrical conductivity maps, and many more. There is much to be explored in these comparisons and correlations.

The Isotopic Atlas of Australia will continue to develop via the addition of both new and legacy data to existing coverages, and by the addition of new data coverages from a wider range of isotopic systems and a wider range of geological sample media (e.g., soil, regolith and groundwater).

Chasing lower crustal tectonic domains in the Yilgarn Craton

Gessner, Klaus, Smithies, R. Hugh, & Lu, Yongjun
Geological Survey of Western Australia, East Perth, WA 6004, Australia

The Yilgarn Craton has been divided into six tectonic domains, of which the South West Terrane, in the southwest of the craton, remains the least studied and understood. Several geological, geophysical and geochemical observations suggest a fundamental geological difference between the South West Terrane and the Archean terranes to the east. Whereas the boundary between the South West Terrane and the Youanmi Terrane is largely hypothetical, a distinct NNW-oriented boundary between the Youanmi Terrane and the Eastern Goldfields Superterrane is recognizable in regional geophysical, geochemical, geochronological and isotopic datasets.

We use whole-rock geochemical analyses of Archean granitic rocks in the South West Terrane as a proxy to

test whether crustal melts were sourced from spatially distinct lower crustal source domains. We divide the granitic rocks into four groups according to their source composition (K_2O/Na_2O , sodic if <1 , potassic if >1) and depth of melting (Sr/Y , high = >40 , low = <40) and also consider variations in trace element characteristics and in whole-rock initial $^{206}Pb/^{204}Pb$ ratio. As variation in these proxies for melting-pressure shows no spatial relationship with a gravity anomaly identified within the South West Terrane, we propose that this anomaly does not directly relate to Archean felsic magmatism, but more likely relates to the Proterozoic or Phanerozoic evolution of the West Australian Craton.

The spatial distribution of the granitic rocks defines a NE-trend that is independent of the NNW-trend of the eastern boundary of the South West Terrane and may even extend into the western part of the Eastern Goldfields Superterrane. This spatial geochemical trend is consistent with the interpretation of large wavelength geophysical data including gravity and magnetic anomaly data, is a prominent feature of Nd model age distributions and also appears to be reflected in the spatial distribution of earthquakes. The results of statistical analyses of the geochemical data relative to NE-trending geophysical domains supports our hypothesis that spatially distinct populations exist. We conclude that these NE-trends relate to basement domains that existed before the younger (post-2.73 Ga) terrane boundaries were imposed.

Archean craton formation and plate tectonics evolution: A new model evoked by discoveries in the Yilgarn Province of Western Australia.

Lascelles, D. F.

An alternative model of Archean tectonics suggests that early (before 2.5 Ga) crustal plate collisions may have resulted in folding of the thin ocean crust into upright folds with a total amplitude of up to 50 km instead of subduction beneath ocean plates or continental masses. The folded crust would be deeply depressed into the mantle by isostatic compensation with consequent partial melting at depth forming a felsic melt and a dense ultramafic restite. Anatectic replacement of the down-folded ocean crust by granite and extended erosion of the upper parts of the folds resulted in the formation of an Archean granite and greenstone style craton with an ultimate thickness of around 30–35 km.

The collision of two cratons folded the intervening mafic crust, including sediment deposited on the ocean floor, to form a new craton that combined the cratons into a continent. Uplift and erosion of continents during the late Archean deposited sediments on the thinner margins of the continents forming extensive continental margin basins. The subduction of ocean crust did not occur until the formation of deep sedimentary accumulations on the sea floor beyond the margins of the continents depressed the ocean crust and was able to subduct the oceanic plate beneath the continental margin. The subducting ocean crust caused compression of the sedimentary basin and the formation of modern style orogenic fold belts and volcanic arc systems that were not present during the Archean era.

Composition and evolution of the southern African lithosphere from combined xenocryst and magnetotelluric data

Özaydin, Sinan, & Selway, Kate

Department of Earth and Environmental Sciences, Macquarie University, Australia

Cratons provide us sparse clues about their composition and evolution through xenoliths and the few geophysical methods that can penetrate the cratonic lithosphere. Alone, these methods do not provide enough information to fully understand cratons so it is vital that they be interpreted together so that the fullest possible understanding of cratons can be developed.

In this talk, we focus on the southern African lithosphere, which is arguably the most well-studied cratonic region on Earth. Comparatively voluminous kimberlite magmatism has produced large quantities of mantle xenoliths and xenocrysts that have been used to interpret the composition and evolution of the southern African cratons. However, questions remain about whether these exhumed mantle rocks are representative of the wider lithospheric mantle.

To address the question of cratonic composition, we compare the southern African mantle xenolith and xenocryst data with new, 3D magnetotelluric (MT) models produced from the SAMTEX dataset. Detailed comparisons between the geochemical and MT data around the Jagersfontein and Kimberley kimberlite pipes show that modal mineral compositions and water content measurements from the xenoliths generally agree with those we would interpret from the geophysical data, subject to uncertainties in the geotherm and experimental constraints. However, the water contents interpreted from the MT data and those from the xenoliths do not agree uniformly, suggesting that the region has experienced some localised metasomatism at the scale of the kimberlite pipes that has not affected the mantle more regionally.

In addition to the detailed comparisons around kimberlite pipes, we also consider the broader implications of the MT model for southern African lithosphere composition. As has been observed for most cratonic regions, the MT model over the southern African cratons shows considerable heterogeneity, showing that cratonic compositions must also be heterogeneous. These conductivity contrasts do not generally follow the surface expressions of tectonic boundaries and are more likely to reflect metasomatic enrichment and melting depletion events than lithospheric architecture related to continental assembly. Outcropping kimberlite pipes avoid the regions of highest mantle conductivity, suggesting an interplay between the processes of mantle metasomatism, which produce the strong mantle conductors, and kimberlite magmatism.

Joining the dots: insights into the magmatic nickel sulphide potential of the western Gawler Craton

Reid, Anthony^{1,2}, & Pawley, Mark¹

¹*Geological Survey of South Australia, Department for Energy and Mining, 11 Waymouth St, Adelaide, SA 5001, Australia;* ²*Department of Earth Sciences,*

University of Adelaide, SA 5005, Australia

Nickel is back in high demand, with the result that the risk equation for greenfield exploration is significantly improved. Of Australian Proterozoic terranes, the Gawler Craton in South Australia stands out as a terrane with a perceived lack of nickel potential. But is this really the case, or is the current prospectivity telling us more about a lack of data, than a lack of metals?

Recent exploration drilling in the western Gawler Craton intersected over 200 m (down-hole length) of nickel and copper bearing sulphides hosted by a pyroxenite intrusive. This greenfields discovery by Western Areas in JV with Iluka Resources is highly encouraging. While previous drilling has intersected mafic and ultramafic intrusions with minor sulphide, this has been the first drilling to demonstrate that significant sulphide mineralisation is present in the region.

A review of the geological and geophysical features of the western Gawler Craton demonstrates why this intersection is unlikely to be the last. Key features of the western Gawler Craton include:

1. Curvature of the lithosphere–asthenosphere boundary upwards towards the western edge of the craton.
2. Topography on the Moho, with up to 5–10 km offsets across major structures imaged in crustal reflection seismic.
3. Trans-lithospheric conductivity zones imaged in magnetotelluric data that correspond to major structures in regional aeromagnetic data.
4. A complex network of anastomosing shear zones, with evidence for poly-metamorphism and syn-deformation intrusion.
5. The localisation of different magmatic events into specific regions, with the boundaries between these magmatic domains corresponding to major structural boundaries in the region.
6. Variation in (admittedly sparse) radiogenic isotope composition of these magmatic rocks suggesting variation in composition of the deep crust across the region.
7. Geochemistry of mafic and ultramafic rocks suggests an enriched mantle source coupled with crustal interaction and assimilation.
8. A metasedimentary component to the region, including an Archean to earliest Paleoproterozoic succession (Mulgathing Complex) and sedimentary rocks deposited at ca 1700 Ma and ca 1660 Ma.
9. Variable depth of exhumation across the region, with upper crustal lithologies juxtaposed against lower crustal granulites across major structures.

Joining the dots along these lines of evidence suggests a broad geological setting that is comparable to other terranes with proven nickel–copper–PGE resources. In the Gawler Craton melting of previously fertilised lithospheric mantle produced mafic and ultramafic magmas that were able to ascend towards the crust. Assisted by trans-lithospheric structures and complex deformation these magmas were likely focused into the crust during one or more tectonothermal events, where they underwent crustal assimilation. Variation in exhumation depth across the region as a result of the complex anastomosing shear zone network means

magma chambers, magma transfer zones and the root zones are likely present in different parts of the region providing opportunities for the formation and preservation of sulphide accumulation zones. Future work in this region including mapping of sparse outcrop, geophysical interpretation, systematic geochronology and ultimately further exploration drilling will assist to better understand this mineral system.

Evidence for a 3.2–3.1 Ga accretionary orogeny along the southeastern edge of the Kaapvaal Craton: a regional setting for late-stage gold mineralisation in Barberton

Taylor, Jeanne

Department of Earth Sciences, Stellenbosch University, South Africa and Institute of Geoscience, Goethe University Frankfurt am Main, Germany.

The Barberton Granite-Greenstone Belt (BGGB) of South Africa is one of only a few exceptionally preserved Paleo- to Mesoarchean terranes in the world able to advance our understanding of tectonic processes operating on the early Earth. Together with the Pilbara Craton of Western Australia, it has fuelled the debate of uniformitarian (modern-style subduction-accretion) *versus* non-uniformitarian (vertical) geodynamic models for Archaean crustal evolution. Barberton is also known for its world-class lode-gold deposits, which formed late in its tectonic evolution during at least two episodes, at 3080 Ma and at 3040–3015 Ma. However, the thermal-tectonic processes responsible for gold mineralisation remain somewhat cryptic.

The Ancient Gneiss Complex (AGC) of Swaziland constitutes a fragment of pristine 3.7–2.7 Ga continental crust in direct contact with the southeastern margin of the BGGB and represents a unique opportunity to interrogate contrasting tectonic models. A large body of recent data from 3.23–3.22 Ma granitic rocks, and high-grade, aluminous clastic meta-sediments deposited at 3.53–3.43 Ga and ca 3.2 Ga, is largely inconsistent with a non-uniformitarian geodynamic model. Granulite-facies meta-sedimentary rocks display extraordinarily complex metamorphic histories within single hand-samples, which have been deciphered by high-resolution, in situ dating of accessory phases. These rocks seemingly experienced an early thermal episode at 3.43–3.40 Ga, followed by two granulite-facies events at 3.23 Ga and 3.15–3.05 Ga. Peak metamorphic conditions of 830–875 °C and 6.5–7.6 kbar were reached by 3.11–3.07 Ga, accompanied by extensive in situ partial melting. A final retrograde thermal overprint took place at 2.73 Ga involving rehydration and further decompression. Syn- to post-peak metamorphic (i.e., 3.11–3.07 Ga) deformation fabrics in the granulites (NW–SE directed compression and synchronous NE–SW extension) are similar in character, and coaxial with large-scale deformation features in Barberton and the surrounding 3.23–3.07 Ga AGC granites.

Detrital zircon U–Pb age spectra from clastic meta-sediments deposited at ca 3.2 Ga display patterns comparable to those found in modern convergent margin settings (after Cawood *et al.*, 2012), in particular, trench and fore-arc basin environments. Significantly, detrital zircon ϵ_{Hf} isotope signatures indicate that these (meta)-sediments were largely

derived from an isotopically distinct (i.e., younger, more juvenile) source terrane compared to the BGGB or the AGC, such as a ≤ 3.32 Ga primitive island arc. Detrital zircon age data, combined with in situ dating of metamorphic monazite inclusions in the cores of high-grade garnets (from the same samples), further testify to the rapid, deep burial of these meta-sediments soon after their deposition to ± 25 – 30 km crustal depths by ca 3.10 Ga. In combination, the AGC data provide strong evidence for a long-lived ca 3.2–3.1 Ga accretionary margin (involving northwestward subduction) along the southeastern edge of the proto-Kaapvaal Craton and support the idea that gold mineralisation in Barberton was linked to late orogenic, transtensional tectonics following terrane accretion. Further connections can be made with long-lived southward subduction and tectonic accretion in the Pietersburg Block (the northernmost terrane of the Kaapvaal Craton), during a comparable time interval between 3.15 and 2.97 Ga.

Crustal-scale controls on the evolution of the Yeneena Basin

Tyler, Ian, Kohanpour, Fariba, & Gorczyk, Weronika
Centre for Exploration Targeting, School of Earth Sciences, University of Western Australia, Perth WA 6009, Australia

The Neoproterozoic (<911 Ma to >655 Ma) Yeneena Basin is exposed at the northeastern margin of the West Australian Craton, deposited on extended crust of the Archean Pilbara Craton and the Proterozoic Capricorn Orogen. It is deformed and metamorphosed within the Proterozoic Paterson Orogen and hosts the world-class Telfer Au–Cu mine. The recent Winu Cu–Au discovery is focussing exploration interest under Canning Basin cover.

An understanding of the tectonic setting and geodynamic history of the Yeneena Basin can be derived from published data, enhanced by new information extracted from key exploration and stratigraphic drillholes held in the Geological Survey of Western Australia Core Library, including rock properties, structural analysis and petrography, geochemistry, geochronology, isotope geology, sedimentology and sequence stratigraphy. When integrated with geophysical imagery, including gravity, magnetics and passive and active (reflection) seismic surveys, it can form the basis of a consistent crustal-scale 3D map, which can be used as a framework to understand the geodynamic evolution of the basin and its mineral systems.

In the Yeneena Basin, the lower Throssell Range Group occurs between the Vines Fault, and the Southwest Thrust to the west and the Parallel Range Thrust to the east. The basal Coolbro Sandstone, which has a low magnetic signature, unconformably overlies the 1.8 to 1.3 Ga crystalline basement of the Rudall Province, and is overlain by the Broadhurst Formation, a sequence of carbonaceous and sulfidic shale, sandstone and dolomite that extends beneath shallow cover to the northwest. The overlying Isdell Formation is predominantly carbonate and is overlain in the Parallel Range Thrust zone by the Lamil Group comprising the Malu Formation (quartz sandstone), the overlying Puntapunta Formation (carbonate, sandstone, shale and siltstone) and the Wilki Formation (quartz

sandstone and shale).

The Tarcunyah Group in the adjacent North West Officer Basin is part of the 850–700 Ma Supersequence 1 of the Centralian Superbasin. It includes a basal siliciclastic package, which unconformably overlies the Archean Fortescue Group west of the Vines Fault, and an overlying shallow-water shelf evaporate-carbonate package, which contains distinctive stromatolite assemblages. In magnetic images, a transition can be seen from the non-magnetic evaporate-carbonate package across the Southwest Thrust and into the non-stromatolitic and magnetic sedimentary rocks of the Broadhurst Formation. This is consistent with the Throssell Range Group comprising deeper water, basin floor deposits, laterally equivalent to Supersequence 1.

The sediment-hosted Nifty Cu deposit has been dated at 823–791 Ma and can be linked to 830 Ma mafic intrusions emplaced during basin extension. Inversion of the basin by southwest verging thrusting and associated dextral strike-slip faulting took place during the Miles Orogeny at 655 Ma. Au–Cu and W mineralisation is associated with intrusions of the 650–610 Ma Mount Crofton Granite east of the Parallel Range Thrust. To the north and east of Telfer, the upper Lamil Group is buried by less than 300 m of Phanerozoic sedimentary rocks deposited in the overlying Canning Basin. Important elements for Au–Cu mineralisation targeting can be identified in geophysical images.

GEOSCIENCE IN SOCIETY, EDUCATION & ENVIRONMENT

Natural hazards and engineering geology

Tasmanian landslide fatalities and some implications for landslide risk

Roberts, Nicholas

Mineral Resources Tasmania, Rosny Park, Australia

Tasmania experiences frequent, diverse landslides ranging from extremely slow failures that gradually damage structures to extremely fast ones capable of claiming lives. Their impacts in recent decades might give the false impression that Tasmanian landslides threaten only infrastructure and not lives. However, life-loss risk is poorly constrained – and generally under appreciated – because the state's landslide fatalities have not been fully inventoried. Details from a growing catalogue of Tasmanian landslide fatalities (excluding underground failures) show that deaths, although sporadic, do occur and were surprisingly common during the nineteenth and earliest twentieth centuries. Landslides have injured at least 23 people in the last 100 years. Fourteen of the injuries and four of the five confirmed landslide fatalities from that period occurred in 2001 when a road shoulder collapsed under the weight of a bus. Although sometimes conflated with mass movement, the rainfall-triggered burst of a rock-filled concrete dam above Derby in 1929 that claimed 14 lives was unrelated to landsliding. Tasmania's at least eight landslide fatalities prior to 1920 provide additional insight into life-loss potential. Deadly landslides occurred during construction of Port Arthur's Convict Church (ca 1836), quarrying in Hobart (1848) and Queenstown (1905), railway expansion through Kelly Basin (1889), and open-pit mining at Mount Bischoff (1900). All but the 1848 failure, which killed four, were single-fatality events, providing a stronger historical basis for calibrating quantitative estimates of individual risk compared to group risk. Commonalities between these early events highlight settings and processes of particular concern as well as a population of elevated exposure. Each failure affected very recently excavated slopes, involved extremely rapid sliding and flow of soil-strength materials, and exclusively claimed lives of workers (convicts before 1850, employees thereafter). Coronial Inquests into each of the events from 1848 to 1905 provide more detail about failure metrics and behaviour than is commonly available for landslides of that era. All eight deaths were ruled accidental despite knowledge that many sites were failure prone. Several close calls prior to 1920 highlight risks of members of the public being engulfed by debris flows or impacted by landslides at home. However, fatalities from hazardous phenomena that commonly influence (bushfires) or accompany landslides (flash flooding) remain more common. Although Tasmanian landslide fatalities superficially appear to have decreased, determining and explaining trends in these records is complicated by data sparsity. Advances over the past century in engineering, workplace safety, and regulation undoubtedly affect risk levels, but evaluating other possible influences such as long-term drought-rain cycles requires further work.

Decreases in per-capita landslide fatalities elsewhere are attributed to progressive improvements (e.g., British Columbia) or drastic reforms (e.g., Hong Kong) in local risk management, circumstances in Tasmania are closer to the former, although the low number of deaths complicates comparisons. Notwithstanding these challenges, it is noteworthy that fatal landslides in Tasmania show several commonalities, are generally underestimated, and are possible in the future, particularly as population and development increase.

Real-time tracking of the 2019 pumice raft in the southwest Pacific

Jutzeler, Martin¹, Van Sebille, Erik² & Marsh, Robert³

¹*Centre for Ore Deposit and Earth Sciences, University of Tasmania, Australia;* ²*Institute for Marine and Atmospheric Research, Utrecht University, Netherlands;* ³*School of Ocean and Earth Science, University of Southampton, UK*

Pumice rafts can be hazardous to maritime traffic due to their ability to clog engine water intakes, block harbours and divert maritime traffic for weeks. On 7 August 2019, a 195 km² pumice raft was produced at an unnamed submarine volcano in the Tonga Islands (Southwest Pacific Ocean). The raft quickly expanded in size and got segmented into multiple smaller rafts that reached the Lau and Fiji Islands over the following weeks. Yachts that crossed the raft as early as two days post-eruption sent an alert to the Rescue and Co-Operation Centre New Zealand (RCCNZ), the Maritime Safety Authority of Fiji, who relayed us the information. The coupling of real-time satellite observations with weather reports and oceanographic Lagrangian simulations allowed near-real time forecasting of raft dispersal. The abundance of satellite images allowed us to contrast virtual particle tracking methods with ocean model currents to explore the relative influence of surface currents, wind, and wave action on pumice flotsam dispersal. We produced bi-weekly hazard maps to RCCNZ and key local individuals for dissemination to the yachting, shipping and fishing communities via social media and word of mouth. This strategy successfully prevented further vessels from encountering the pumice raft and facilitated contact with sailing crews for information on the raft and samples. The dispersal models built for this pumice raft can be used for global maritime hazard mitigation.

Displacement of mega-boulders across and up coastal rock platforms south of Sydney, Australia, by big storm waves generated by East Coast Lows

Bann, Glenn¹, & Lau, Annie²

¹*School of Earth, Atmosphere and Life Sciences, University of Wollongong;* ²*School of Earth and Environmental Sciences, University of Queensland*

This research reports on a number of large boulders, or blocks, displaced across coastal rock platforms between Kiama and Snapper Point, south of Sydney, Australia. All boulders are derived from underlying fine to coarse-grained sandstones. A boulder described previously (Bann, 2012), weighing ~10 tonnes, had been transported 42m across the rock platform and rotated 110° from its original *in-situ* position. Before and after photos show evidence of more recent movements,

~1 m sideways and rotating it back 50° in 2016, coinciding with an 'East Coast Low' that impacted the whole NSW shoreline in June 2016. It was moved again in 2017 a further 30° and ~30 cm sideways with one end lifted ~15 cm to rest it on a ledge, then in July 2020 following another East Coast Low, another 10° rotation and ~20 cm movement occurred off and away from the ledge. Three smaller boulders nearby of ~1 to 2 tonne each also get tossed around with these events. Two other much larger boulders weighing ~100 and ~180 tonnes also reported movement previously from 2016 (Bann *et al.* 2018), to the north of Jervis Bay moved ~10 m upslope and rotated ~15 degrees for the smaller one and a few metres up slope for the larger one. The smaller boulder has also been flipped over at some stage given by reversed cross-bedding and inverted sedimentary grading. Slight movement of these two has also been detected since 2016. Examples from other localities include the placement of blocks weighing a few tonnes onto an elevated rock platform, then removed at a later date, a block weighing about 1 tonne lifted and moved onto a higher ledge on a cliff about 20 m from the platform sea edge and 5 m elevation, and a boulder weighing about 10 tonnes on a rock platform lifted with tree logs emplaced and wedged firmly beneath it before settling on them. Satellite imagery was used to identify approximate movement times and then correlated with storm wave data obtained from wave buoys located offshore at Port Kembla and Batemans Bay. This provided timing in addition to wave heights, allowing approximate wave height constraints for wave height formulas. None of the boulders appear to have been pushed or slid across the actual platform, rather, all boulders show evidence of being lifted during displacement, hence by saltation or suspension. Calculations suggest that waves of considerable height and wave length are required to displace these boulders across the platform, either in the one event, or in incremental steps, larger than the actual heights from the wave buoy data show. The findings indicate that large storm waves are capable of shifting very large boulders, such as those generated by East Coast Lows which frequent the coast during the winter months. Although a few previous authors use boulder movements as evidence that the east coast experiences occasional large tsunamis, tsunamis are not required to transport these large boulders on coastal platforms. Clearly, coastal lowland environments south of Sydney are prone to occasional very large storm waves and needs to be prioritized in coastal hazard and sustainable management plans, particularly applicable to climate change and future sea level rise.

Structural analysis of wavecut platform structures, Shellharbour, New South Wales

Lennox, Paul¹, Goff, James^{1,2}, Edwards, David¹ & Coates, Ashlie^{1,3}

¹*School of Biological, Earth and Environmental Sciences, UNSW Sydney, NSW, 2052, Australia;*
²*School of Ocean and Earth Science, University of Southampton, UK;*
³*Department of Industry, Innovation and Science, 10 Binara St., Canberra, ACT 2601, Australia*

Bedrock-sculptured features on the wavecut platform south of Shellharbour, NSW have been structurally assessed as some consider they have been formed by

a southeast to northwest directed (mega)tsunami. These features have formed within the up to 120 m thick, Late Permian Upper Bumbo Latite unit of the Gerringong Volcanics.

The research focused on two subareas, the southern side of Bass Point (Bushranger Bay) where apparent s-forms due to tsunami-sculptured rock platforms expose so called "muschelbruche" having a relief of decimetres to several metres and Atcheson Rock one kilometre to the southwest. At Atcheson Rock the orientation of the channel and the so-called vortex nearby, a semi-circular depression with raised internal feature were assessed with respect to the orientation of the local jointing, layering and flow foliation.

The muschelbruche vary in size from a few metres across to tens of metres across. The orientation of bedrock-sculptured features south of Bushranger Bay display various relationships to the flow foliation and jointing. In some cases, the sides or raised back of the "muschelbruche" are aligned subparallel to either the flow foliation, joint strike or some combination. The long axis of the muschelbruche is not predominantly aligned northwest-southeast as expected if they were generated by a single (mega)tsunami from the southeast.

The cross-cutting? Cenozoic dyke at Atcheson Rock weathers to a channel in the basalt and is along strike of a similar eroded dyke and channel on the coastline south of Bushranger Bay. The strike of this dyke is subparallel to the strike of flow foliation and the dominant jointing in the basalt. Some assert that the canyon containing this dyke is not structurally controlled. Normal coastal erosion of this dyke has caused Atcheson Rock headland to almost be cut off from the mainland. The Cenozoic dyke has intruded subparallel to the dominant northeast to southwest striking joints and flow foliation in this region. Some consider that the vortex pit on the south side of Atcheson Rock was eroded by a tsunami from the southeast causing a whirlpool over 10m wide and characterised by a central plug of bedrock 5 m high. The presence of a rounded but north-south elongated depression in the basalt ("vortex") can be explained by weathering related to the pervasive localised NNE-SSW and ~NW-SE striking jointing, gently southeast-dipping layering in this locality but not the NE-SW or NW-SE striking flow foliation.

The orientation, scale and development of various coastal erosional features including channels, scour-like structures (muschelbruche) and depressions near Shellharbour, NSW can be explained through normal coastal processes without the necessity to invoke (mega)tsunami-related scouring from the southeast.

Rock stress in Tasmania

Hills, Peter

Pitt & Sherry Operations Pty Ltd, Hobart, Australia

Rock stress can have a profound impact on underground excavations in mining and civil space. Rock stress measurement was first undertaken in Tasmania to inform the design of excavations for the Poatina Power Station in 1960 and led to an innovative trapezoidal section to the crown of station cavern in near horizontal Permian sediments. Since that time stress measurements have been undertaken at 15 sites across western and northern Tasmania and this has

provided a database, which in addition to assisting in the management of individual assets, has allowed a number of more general observations to be made.

Rock stress is the result of tectonic forces and overburden pressures. The former creates a background stress condition that is widely evident within a given geological terrane. All Tasmania's stress measurements have been undertaken in the Western Tasmanian Terrane and indicate a major principal stress (σ_1) orientation striking WSW–ENE which is an anticlockwise rotation from that observed in Victoria where measurements have largely been undertaken in rocks of the Lachlan Fold Belt. This is thought to reflect upon the key location of Tasmania during the accretion of Gondwanaland and the eventual separation from Antarctica. The latter typically reflects depth below surface with the magnitude of the stress generally increasing with depth. In most cases in Australia, and it is the case in Tasmania, that the orientation of the minor principal stress (σ_3) steep and consequently the intermediate principal stress (σ_2) is relatively flat. The general stress condition in Tasmania can be described in terms of orientation and magnitude as follows:

$$\begin{aligned}\sigma_1, 23^\circ/261^\circ & (0.039 \times \text{depth}) + 10.7 \text{ MPa} \\ \sigma_2, 15^\circ/164^\circ & 0.035 \times \text{depth MPa} \\ \sigma_3, 62^\circ/043^\circ & 0.023 \times \text{depth MPa}\end{aligned}$$

Local geological and geomorphological setting can significantly impact the stress locally. At Cethana Power Station the stress measured in the crown of the station prior to excavation of the cavern was found to be four times the expected magnitude. However, it is readily explained by its location in the steep sided Forth River Gorge which was rapidly cut through the Fossey Mountains during relatively recent glaciation. At Hellyer Mine the magnitude of the measured stress is more-or-less consistent with the depth of the measurements beneath the Waratah Plateau, but the orientation of the shallower measurements is strongly influenced by the orientation of the nearby Southwell River Gorge. Renison Mine provides a further example where the orientation of the stress field is strongly influenced by the orientation of the Federal-Bassett Fault and the associated Pine Hill Horst.

Stress measurement in Tasmania has been undertaken for direct engineering construction as in the case of the John Butters Tunnel where it was specifically directed at determination of the length of tunnel lining required. It has also been used extensively to understand the orientation and magnitude of the stress condition in deep mines at Mount Lyell, Renison, Rosebery and Beaconsfield and assist with excavation, and particularly, stope design. Stress change due to extraction has also been monitored at those mines as well as Dolphin and Cleveland.

Hills, P B, 2020. Tasmanian rock stress. *Australian Geomechanics*, 55(1), 77–111.

Structural integrity and Liesegang rings

Hills, Peter

Pitt & Sherry Operations Pty Ltd, Hobart, Australia

Many will be familiar with nature's abstract paintings generated by the formation of Liesegang rings.

The often-spectacular features illustrated in vibrant yellows, oranges and browns cross cutting the bedded fabric of the strata are a feature of the Tasmanian

landscape in many areas, particularly, but not exclusively, in outcrops of the Ross Sandstone. Those near the former settlement of Darlington on Maria Island, the Painted Cliffs, are a frequent feature in tourism brochures, with good reason.

The railway tunnel at Rhyndaston, 45 km due north of Hobart passes a distance of 943 m through the same strata as that hosting the Painted Cliffs, the Liesegang rings and other solution features displayed in the largely unlined tunnel are no less spectacular. However, they have also played a role in preserving the structural integrity of the civil asset.

The Rhyndaston Tunnel was originally excavated in the 1870's when the Main Line between Hobart and Launceston was established. A small tunnel, it was inadequate to meet the late 1950's watershed development in global freight that was heralded by the creation of the standard shipping container. Consequently, the tunnel was enlarged in 1964/65 using a tunnel boring machine (TBM). That TBM was the first to have been used in Australia, boring the tailrace and sections of the headrace tunnels for the Poatina Power Station development over the previous three years. Rhyndaston became the third bored tunnel in Australia by several years (Stack, 1982).

The profile of the tunnel is circular affording a clear opportunity to monitor dilapidation of the exposed rock mass. At an elevation of 400 m A.S.L. the environment in the tunnel is often cold and the air moving through it is frequently moist. The rockmass presents in three facies, a competent coarse grained yellow-brown sandstone displaying strong current bedding, a white silty sandstone usually displaying laminar bedding, and occasional thin micaceous shale bands. The yellow-brown sandstone which is the dominant facies, shows little sign of dilapidation, with the radial marks of the TBM cutters still clearly visible after 56 years. The TBM head was 4.93 m diameter and the average tunnel diameter in the yellow-brown sandstone is less the 4.95 m. Much of the 20 mm difference is due to the gauge of the TBM cutters. However, in the white silty sandstone, the tunnel diameter is as much as 5.01 m, some 60 mm more. In comparison to tunnels in similar sandstones in Sydney where erosion rates of <2 mm/yr have been recorded (Nash *et al.*, 2019), the effective erosion rate of ~0.5–0.9 mm/yr is favourable. However, Liesegang rings within that sandstone are no more eroded than the yellow-brown sandstone and the TBM cutter marks remain clearly visible. It is posited that the Liesegang rings are serving to protect the silty white sandstone from greater erosion than might otherwise have been the case.

The shale bands, which are confined within the yellow-brown sandstone are of insignificant dimension, and while they are prone to severe slaking, they do not pose a significant threat to tunnel integrity.

Stack, B, 1982. *Handbook of Mining and Tunnelling Machinery*, 742 p., John Wylie & Sons: Chichester.

Nash, T., Bertuzzi, R. & de Ambrosis, A., 2019. Deterioration of sandstones and shales in Sydney tunnels, in *Proceedings of the 13th Australia New Zealand Conference on Geomechanics*, pp. 877–882. Australian Geomechanics Society: Sydney.

Communication for disaster prevention culture: The Cusco-PATA Case (Cusco, Peru)

Piscoya, Juan Carlos^{1,3}, Reupo, Palmira¹, & Villacorta, Sandra^{2,3}

¹Pedro Ruiz Gallo National University, Lambayeque, Peru; ²Charles Darwin University, Casuarina, Darwin, Australia; ³Peruvian Section of International Association for Promoting Geoethics, Peru

This article presents an application of the communication strategy developed by the project Paleoseismology, Active Tectonics, Archeoseismology in Cusco (Cusco-PATA) in the village of Huasao, (Cusco, Peru). The project began in 2016 and involves a group of researchers from Peru, France and the United Kingdom which investigate the active and archaeo-seismological faults as well as their effects in Machu Picchu and other nearby Inca sites.

The communication strategy developed has explored methods to address the problems of growing countries like Peru, where authorities do not usually rely on scientific research for the formulation and execution of infrastructure projects. Likewise, the impact of high levels of misinformation on citizens due to the limited dissemination of scientific and technical content related to disaster prevention and geosciences.

The research was carried out throughout surveys and interviews with authorities, researchers and population. According to the results of this project, the Huasao community is almost exclusively dedicated to agriculture. There is a majority of male (51%) over the women (49%) and the 18–25 age group is a 24% of the total, the same amount as the inhabitants with completed high school. More than 60% of the community access content on disaster prevention through radio, television and newspapers. The rest of them find out through talks and workshops organized by local and private entities, as well as through social networks. Regarding the knowledge of the stakeholders on geological hazards, a reduced amount of population has poor knowledge about the causes of these events in the study area, while a significant group of residents is completely unaware of them. It is important to note that around 30% of the Huasao population believes that disaster is looming and cannot be averted. This is room for improving the knowledge of geosciences. On the other hand, those who believe that prevention is effective are willing to participate in prevention exercises. For the latter, activities aimed at reinforcing prevention awareness should be designed.

This experience has helped to verify how a population with little knowledge acts in a crisis. Although it is necessary to carry out an analysis of the appropriate social media and actors in the scientific communication process, it is possible to conclude that dissemination and awareness are essential to avert the geological risks.

It has also been identified that communication plans for geoscientific research developed by researchers without communication skills do not give the same results as those monitored and executed with the support of professionals in communication sciences. Within this framework, the entities involved in disaster prevention projects should manage scientific communication and strengthen the culture of prevention, incorporating specialists in the media and communication.

Finally, it is recommended to design specific content that is tailored to meet the specific needs of the target population. For example, it is clear that in the case of Huasao, the high-risk areas due to the reactivation of the Pachatusan and Tambomachay faults needs to be widely disseminated in the population.

Natural or green infrastructure to face the effects of extreme events, benefits and proposal of application in Chosica, Lima, Peru

Villacorta, Sandra¹ Evans, Ken^{1,2}, Prendes, Nicanor³, Villanueva, Ignacio⁴, & Abad, Cesar⁵

¹Charles Darwin University, Casuarina, Darwin, Australia; ²Surface Water & Erosion Solutions, Casuarina, Darwin, Australia; ³Ministry for Ecological Transition (MITECO), Spanish Office of Climate Change, Madrid, Spain; ⁴Independent Consultant, Zaragoza, Aragon, Spain; ⁵Presidency of the Council of Ministers, Lima, Peru

In Peru, some initiatives have been launched recently to create a more favourable environment to prevent deforestation and subsequent environmental hazard development. Moreover, mechanisms to encourage investments linked to "Natural or Green Infrastructure" have been developed. For example, "Sembramos Agua" funding of the Water and Sewerage Service of Lima, has created a platform to encourage compensation mechanisms for ecosystem services and the natural infrastructure is currently recognized within the framework of investment by the Peruvian government. At the implementation level in Peru, such other growing countries, this kind of initiatives are in progress.

Local and national authorities in the Latin American region have limited knowledge of the benefits of using green technology to address geodynamic problems, such as flood and debris flow, that impact the region year after year. It should be noted that natural infrastructure for flood mitigation is one that is configured under an approach based on the conservation of ecosystems to increase resilience to floods and at the same time contributes to the improvement of a self-sustainable community. In this context, it also contributes to the improvement of the quality of life of communities (Benedict, 2006). However, although there has been created regulations, precise methodologies for targeting these interventions are needed.

This approach was tested empirically by professionals of the National Engineering University of Peru in Chasquitambo (Ancash, Peru) in 2017. It experienced by the first time the effectiveness of this kind of infrastructure in debris-flows prevention during the rainy season produced by the "Coastal El Niño" phenomenon of that year. This alternative is based on the concept that a hydrographic basin is a flow management system that "resembles" the structure of a leaf. Leaf vein development models have been used in landform evolution models of river basin (Willgoose, 1989) and the method requires the efficient use of debris-flow energy using a series of constructed drains similar to that dendritic pattern.

In this framework, this article presents the proposal to apply this option in the Carossio stream basin in the Chosica district (Lima, Peru). It is planned to use

pedraplens (handcrafted rock embankments) which distribution will be designed using numerical modelling of non-Newtonian events which involve a friction formulation. This exercise will hopefully contribute to the debris flows assessment, the application of recent trends to develop sustainable environmental solutions to future crises and to promote resilient and self-sufficient cities in Peru.

Geoscience education

Coping with COVID – using virtual geological objects for on-line Earth Science Education

Roach, Michael, Orth, Karin, & Scott, Robert

Discipline of Earth Sciences, University of Tasmania, Hobart, Australia

Restrictions due to the global COVID pandemic have meant that most tertiary Earth science education has had to rapidly transition from face-to-face to primarily on-line delivery. Teaching Earth science in on-line environments has special challenges due to the 'hands-on' nature of typical practical and field-based programs. Fortunately, rapid improvements in visualisation methods and technology now allow educators to incorporate diverse, intuitive, immersive virtual objects into on-line education programs. Virtual objects can never fully replace the visual and tactile experience of visiting an outcrop or touching a specimen but they can augment and enrich traditional education programs and facilitate more effective on-line student experiences.

At the University of Tasmania, we have generated the world's most comprehensive open-access collection of geological visualisations and have made extensive use of these objects in our undergraduate and postgraduate education programs. We have generated over 4000 photo-realistic three-dimensional geological models, together with thousands of full spherical panoramas and deep zoom images of significant outcrops and hand specimens. These visualisations have been integrated to produce virtual tours and virtual practicals that were used in our education programs prior to COVID and which have been crucial for recent on-line delivery. Student feedback on the use of virtual educational material has generally been very positive.

This presentation will showcase some of our recently developed resources and illustrate how we have utilised digital visualisations in our undergraduate and postgraduate educational programs. We will also discuss both student and educator perceptions on the efficacy of these new teaching resources and provide suggestions for how visualisations may be effectively integrated into future conventional educational programs when physical distancing limitations are removed.

The real work of virtual teaching: Learnings from EESO Summer School 2021 development

McNamara, Greg, Almborg, Leslie, & Carr, Ruth

Australian Science Innovations, Australia

The Australian Earth and Environmental Science Olympiad (EESO) program selects 24 high-ability high school students from Years 9, 10 and 11 to attend a Summer School program in each January.

The EESO Summer School program, delivered annually at RSES-ANU, provides a life-changing educational experience for the students. The residential camp is an intense two weeks of Earth & Environmental Science learning combined with the fun of spending time with like-minded peers and participating in associated social activities.

In 2020, the EESO Summer School was postponed due to the extreme smoke conditions on campus, with the majority of the theory progressively placed online through February and March. Students were given an opportunity to engage with teachers in a weekly Q&A session via SLACK. An on-campus practical session planned for April was cancelled due to COVID-19 concerns, with the final assessment – based on the online theory materials – delivered via Moodle to all students across the country.

Here we discuss the lessons learned from this rapid-response on-line teaching program and how we applied them to the 2021 EESO Summer School program to avoid the pitfalls of poor content quality, ineffective engagement and inadequate assessment. The aim of the 2021 program was to deliver the same content we provide in the face-to-face environment in an engaging, rewarding and socially beneficial manner. The additional aim is to utilise virtual teaching tools developed for the 2021 event in future face-to-face events.

Plans include: time-managed online delivery of synchronous and asynchronous theory content, limited, but essential, hands-on content based on materials supplied to each student, and supplementary online 3D simulations of materials and field locations. In addition to content, we plan to provide socially engaging opportunities via games, team challenges, and digital and physical rewards.

The Q&A during the AESC will provide an opportunity to discuss how these plans panned out within the context of the programme delivered in January 2021 to 30 students by a team of three senior staff and ~8 program alumni.

Earth Science Education after 2020

Blewett, Shona & Przeslawski, Rachel

Geoscience Australia, Canberra, Australia

Many people fondly remember assembling their first rock collection or exploding a baking soda volcano as a child. These experiences can be a great gateway into the Earth sciences, but a more tailored and modern approach will ensure future generations are geoscience-literate and eventually able to contribute to the workforce. In this presentation, we use the Geoscience Australia (GA) Education Program as a case study of changing approaches to Earth science education and engagement.

For over 20 years, the remit of the GA Education Program has been to engage and inspire school students and teachers in geoscience. Before 2020, over 10 000 students visited the Education Centre each year. The physical facilities, curriculum-based programs and the dedicated staff were central to the ongoing success of the school-age education programs.

However, with the cessation of all school visits during 2020 due to the pandemic, the program shifted its focus

to digital engagement, including a series of short educational videos, virtual visits with classes and webinars for teachers. This in turn has raised challenges such as transferring a tactile experience to the virtual setting and the sometimes, overwhelming flood of digital resources and virtual fatigue common after 2020. In parallel there has also been increasing emphasis on education about emerging geoscience topics that receive limited attention in schools (e.g., earth observation, positioning, critical minerals).

Moving forward, we will continue efforts to develop topical virtual educational experiences, particularly for remote or disadvantaged schools unable to visit our building. When we resume face-to-face experiences, a major challenge will be to juggle the demands of on-site and digital engagement to make our products and facilities available for all.

100 iconic rocks for a proof-of-concept display at the National Rock Garden

Pillans, Brad

Research School of Earth Sciences, The Australian National University, Canberra, Australia

The economic cost of the COVID-19 pandemic will make it extremely difficult to fund the published masterplan for the National Rock Garden (NRG). As a result, the NRG cannot expect substantial financial support from Federal or State Governments, or from the corporate sector, in the foreseeable future.

Early in 2020, the NRG Steering Committee recognised the desirability of a “Proof-of-Concept” display of approximately 100 iconic rocks. This display would incorporate 10 themed rock clusters, linked by a meandering path, with appropriate explanatory signage. It would entail negligible excavation work, and no building construction, facilitating both works approval and reduced funding requirements.

The main financial outlay would be the cost of transportation of large (10–20 tonne) specimens, especially from distant locations. Transportation costs for individual rocks are expected to range between \$2000 and \$12 000, which could be achieved with corporate support or by individual donations. NRG State Rock Selections Sub-Committees are fine-tuning their key targets to enable a small number of rocks to be delivered during 2021.

The “Proof-of-Concept” display will clearly demonstrate the goals of the National Rock Garden and encourage modest levels of financial support. The proposed “Proof-of-Concept” display would also enable the Rock Garden to be opened to the public much sooner than could possibly occur with the original highly ambitious masterplan

The Steering Committee has recognised the desirability of developing strong links with the other national institutions in Canberra, including the National Museum of Australia, Questacon, the National Dinosaur Museum and the National Arboretum Canberra.

We also support establishment of a Natural History Museum, though this has not progressed beyond the 2018 parliamentary report which recommended that a business case be examined.

Proposed rock cluster themes for the NRG Proof-of-Concept display:

1. Indigenous welcome feature
2. Early Earth (Archean) – laying Australia’s foundations
3. Building Australia and its resources (Proterozoic)
4. Australia grows eastwards (Paleozoic)
5. Gondwana breakup (Mesozoic) – the Great Artesian Basin forms
6. Shaping the Australian landscape (Cenozoic)
7. Peopling Australia (Late Pleistocene/Holocene) – linking cultural and geological heritages
8. The Australian region – from New Guinea to Antarctica
9. Geoscience knowledge – building our future
10. The Federation Rocks – celebrating our nation

Geology comes alive for high school students with fieldwork near Yass, NSW

Price, Colin¹, Bradshaw, Marita², & Smith, Mike²

¹Daramalan College P.O. Box 84, Dickson, ACT 2602, Australia; ²National Rock Garden, Suite 8, Level 2, 141 Peats Ferry Road, Hornsby, NSW 2077, Australia

Daramalan College provides Earth and Environmental Science (EES) students with direct exposure to the challenges of geological analysis by conducting practical field excursions. One excursion takes Year 11 students to a field northwest of Yass where there is a prominent exposure of a volcanic ash flow, an ignimbrite, which is overlain by a sequence of various sedimentary rocks. All of the units dip at about 20 degrees to the west, enabling students to walk across the rocks and so recognise and describe the layered sequence of sandstone, siltstone and limestone. The exposures are in creek beds and on gently undulating sheep pasture.

The students describe what they can see and then interpret the depositional environment for each rock unit, noting the progressive changes in that environment from the older rocks to the younger rocks. The sequence records a marine transgression, from volcanics on land to shallow water with coral patches, and then deep water as the shales were deposited by settling of fine particles. The students experience the reality of fieldwork, contrasting the poor to non-existent outcrop of the fine-grained units to the thrill of finding fossils in the limestones. The most common fossils are tabulate and rugose corals, crinoid ossicles and stromatoporoids that help bring alive a picture of what life was like in an ancient shallow tropical sea.

The rocks are part of the Silurian (Wenlock) section of the Yass Syncline in the Lachlan Foldbelt, from the Laidlaw Volcanics up into the Bowspring Limestone Member, Silverdale Formation, Hattons Corner Group. Radiometric dating of the volcanics and a biostratigraphic age from a conodont in the limestone indicates that the sequence the students investigate represents about 3 million years of earth history.

By examining the remains of a volcanic chain and an ancient seabed now found as rocks outcropping in the paddocks near Yass, the students have a rich educational experience and get a sense of the environmental changes that can occur over an interval of geological time. Science staff at Daramalan College are also enthusiastic about the capacity of the National

Rock Garden to help teachers to engage with young people studying the rock cycle in Year 8, plate tectonics in Year 9 and those undertaking the Year 11/12 EES course. In one place they can view a great variety of lithologies from all over Australia, displayed in large and interesting rock specimens with polished areas that provide a window to view in detail igneous and metamorphic textures, sedimentary structures, and fossils.

How do we attract the next generation of Earth Scientists?

Selway, Kate¹, Condon, Jo², Przeslawski, Rachel³, Tiddy, Caroline⁴, Underwood, Narelle⁵, & Cohen, David⁶

¹*Department of Earth and Environmental Sciences, Macquarie University, Australia;* ²*Marketing and Communications, AuScope;* ³*Discovery and Engagement, Geoscience Australia;* ⁴*Future Industries Institute and MinEx CRC, University of South Australia;* ⁵*NSW Surveyor-General and Chair, NSW Surveying Taskforce;* ⁶*School of Biological, Earth and Environmental Sciences, University of New South Wales and Australian Geoscience Council*

Join us to discuss how we might collectively and effectively promote pathways to diverse, exciting and meaningful Earth Science careers to late high school students across Australia.

Earth Science education in Australia is facing critical challenges. University Earth Science departments face low numbers of undergraduate student enrolments, which in some cases are threatening their viability. These low undergraduate enrolments reflect weak interest in Earth Science at the high school level, and result in insufficient skilled graduates to meet industry needs. This is bad for Australia, which needs skilled geoscientists for its environmental and economic future, bad for industry, which needs skilled graduates to continue to innovate, and bad for the students themselves, who miss out on fulfilling careers.

In this presentation we discuss efforts to promote Earth Science to students in late high school. We consider this to be a key focus within broader strategies to improve Earth Science education more generally. Students at this level are actively considering their university study options and many have little exposure to Earth Science or have negative perceptions of the field. University-level Earth sciences in Australia typically boast a higher than average retention of students from first year to subsequent years. Therefore, successful programs that attract more high school students into Earth Science could substantially increase graduate numbers even on a five-year time frame.

Many existing programs, run by government, industry, and academic groups, are already aiming to promote Earth Science pathways to high school students and in this presentation we will summarize some of these programs. Any successful program must be student-focussed and respond to the students' own priorities, as illustrated by the increasing numbers of students studying climate science. Therefore, we will also summarize some of the broader data surrounding the attitudes and priorities of late high-school students. We consider the attributes of programs in other fields, most notably surveying, that have successfully produced

measurable increases in high school student engagement and higher education enrolments. We present this analysis in the hope that it will help guide the discussion on how we can most effectively ignite the interest of late high-school students in pursuing Earth Science.

Geoscience education challenges and opportunities – an industry perspective

Terry, Jillian
BHP, Melbourne, Australia

The resources industry is transforming due to technology application, discovery and extraction of increasingly deep and complex orebodies, a changing future-facing commodity and energy mix and environmental and social value commitments.

At the same time, an ageing and experienced technical workforce is contemplating retirement, early career geoscientists require upskilling, universities face severe financial challenges, breadth of Geoscience career options is not understood and resources industry perception is at an all-time low. These factors are contributing to unprecedented low numbers of enrolments in Geoscience degrees.

Australia needs a consistent supply of diverse, quality geoscience graduates and access to workforce development programs to meet forecast industry and societal demand.

This paper will propose collaboration opportunities for educators, government, and industry to inform, influence and support students to build careers in geoscience.

Supporting the 3 Rs of earth science education – rocks, relevance and rapture!

Meakin, Simone¹, & Filan, Susan²

¹*Geological Survey of New South Wales, Department of Regional NSW, Maitland, Australia;* ²*Australian Earth Science Education, Londonderry, Australia*

In 2018, the New South Wales (NSW) high school curriculum for Earth & Environmental Science was overhauled. There is new emphasis on both renewable and non-renewable resources, exploration techniques including sampling and geophysical surveying, and rehabilitation after mining. In response to the need for new teaching materials, the Geological Survey of NSW (GSNSW) expanded its outreach to educators. A range of general interest publications, hands-on activities, display sets, events and workshops have been delivered, and self-guided geotrails developed.

GSNSW also investigated the engagement of an education officer to support educators in NSW. It sought guidance from teachers and groups such as Earth Science Western Australia (ESWA), a successful industry-sponsored organisation that has supported teachers in WA for 15 years by providing teacher training, school incursions and excursions, and a wide range of high-quality teaching resources. In 2020, ESWA expanded to establish Australian Earth Science Education (AusEarthEd) and recruited an education officer in NSW, based at the GSNSW's WB Clarke Geoscience Centre at Londonderry, western Sydney. Ongoing collaboration between the organisations has enabled targeting of some products and resources to

address the curriculum, thereby better supporting teachers.

The widespread lockdown associated with the COVID-19 pandemic has had a significant impact on geoscience outreach and education activities. Many activities and projects were moved online, and teachers relied heavily on online resources. The launch of the Newcastle Coastal Geotrail and a supporting app by the GSNSW in August 2020 was accompanied by a series of videos and a webinar that presented geological information in a new and engaging way. This had unprecedented reach, attracting over 400 attendees to the webinar and over 100 000 views of the video on social media. A significant number of teachers have since made use of the NSWGeoTour app that features a self-guided tour of the geological features and historical context of the area. AusEarthEd also mapped the geotrail content against the Year 1–12 curriculum in Science, History and Geography, suggesting real and virtual excursions for teachers.

It is helpful to map educational resources to the curriculum so that teachers can immediately see relevance to the curriculum. For discoverability, resources must be delivered through accessible websites that teachers use regularly. Ongoing collaboration between geoscientists and teachers, including enhanced creative development of online teaching resources, will be vital to meet the evolving demands of teachers and students.

Squiggly lines, mountains, organised chaos or Forrest Gump. What is the image of a geoscience career?

Tiddy, Caroline¹, Andrahannadi, Upekha^{2,3}, Perera, Sanjeewa^{2,3}, & Sardeshmukh, Shruti^{2,3}

¹*Future Industries Institute, University of South Australia, SA 5000, Australia;* ²*UniSA Business, University of South Australia, SA 5000, Australia;* ³*Centre for Workplace Excellence (CWeX), University of South Australia, SA 5000, Australia*

Diversity at strategic levels is recognised as a key to improved organisational performance and innovation. Diversity takes many forms. Gender diversity (male and female for simplicity) is the focus of this research.

STEM fields struggle with gender equality, with fewer women in senior roles (SAGE, 2019). Geoscience is no exception. More than 80% of the mining workforce is male, with even fewer women in leadership positions (WEGA, 2018). In academia, 35.4% of Level A (Research Associate) and only 8.7% of Level E (Professor) academic appointments in Earth Sciences are female (ERA 2018 FoR 04: Earth Sciences). Numerous organisations that undertake geoscience-related activities have taken steps to correct this imbalance. Many have achieved Science in Australia Gender Equity (SAGE) Athena SWAN Bronze Award Accreditation

(<https://www.sciencegenderequity.org.au/>). Senior male figures within geoscience-related organisations identify with the *Male Champions of Change* group who are committed to acting on gender inequality (<https://malechampionsofchange.com/>).

We present results of an interview-based study of 60 geoscientists from junior through senior levels from academia, government and industry and that provide

insights into geoscientists' career perceptions. Perceptions are powerful and shape how we approach our careers, therefore gender differences in perceptions may explain underlying reasons for gender inequality. Interviews examined participants' career from undergraduate studies to their current position. Towards the interview conclusion, respondents were asked to provide a visual metaphor (e.g., an image, movie or cartoon character) describing their career and then the career of the opposite gender. Metaphors were used as they are a playful exercise that can provide structure and organisation to our perceptions of a complex topic, in this case perception of careers.

Data analysis highlights that irrespective of gender, geoscientists viewed their career as non-linear. Women geoscientists' career metaphors include dimensions of being challenging and incomplete (e.g., "squiggly line always moving forwards and progressing", "a mountain and a little person not at the top"), whereas men often see their careers as being rewarding and having achieved (e.g., "Forrest Gump – not the smartest guy in the room but somehow always landed on his feet", "spiralling nebular with kind of order... sort of a chaos... But also, it's all worked").

Perceptions of the opposite gender are contrasting. Women geoscientists often described male geoscientists' careers as having overcome challenges, achieved a pinnacle and used dominating figures such as silverback gorillas and the Incredible Hulk. Ideologies with negative connotations were expressed in some perceptions with women describing men as being within a "boys' club" or as "old, white men with a beard". Male geoscientists described women as "starting to find their voice", "not as appreciated" and "incredibly capable" where their career path is more challenging than that of a male (e.g., "uphill battle", "getting over a big mountain").

This study provides a spirited way to identify perceptual barriers to women in geosciences. The overt masculine perception of geosciences belies the broad range of positive experiences women geoscientists report. Our research goal is to identify enablers to women's careers, which will help remove these perceptions and attract talented people to geoscience careers.

Gamification – A pathway into Earth Science and Resources career awareness

Urbaniak, Suzy

CoRE Learning Foundation, Perth, Australia

Have you ever wondered how to make your Earth Science curriculum interesting, relevant, and loaded with 21st-century enterprising skills such as leadership, communication, and collaboration whilst engaging in an interdisciplinary and assessable format? The answer is gamification. It is a well-known fact that young students' interest lies in being active, problem-solving learners, who want to explore and discover their learning experience in real-time and be an integral and informed member of an innovative and creative situation.

Australia's resources industry is a key driver of our economic growth, however student understanding and progression into the industry are at an unprecedented low point. It's never been more important for Australia's future to create this awareness and expose our students to the beauty of earth science and the diverse,

STEM career pathways into the resources industry.

The resources industry recognises that meaningful K-12 engagement highlighting its 'innovation and contribution to mainstream society is vital to strengthening STEM capabilities across the sector. To appreciate and develop an understanding and career passion for the resources industry, learning needs to commence early and be engaging, continuing, purposeful and applicable.

The scope and sequence of this proposal begins in Year 5 and continues through middle school to Year 10, assessable, and correlating with the ACARA (Australian Curriculum, Assessment & Reporting Authority) curriculum. This opportunity creates and delivers sustainable, engaging, and impactful 3D resources-based gamification learning products, utilising an Earth Science context but also integrating and extending other scientific disciplines, data literacy and science, the design and digital technology, and social value through the humanities curriculums.

Gaming technology is hands-on, interactive learning which is both available and enjoyable to engage both the educator and the student, taking them on a #therealclassroom journey, with immersive, real-world experiences. More importantly, gamification learning has the potential to reach the full spectrum of remote and regional communities in which the resources industry operates, thereby helping to ensure that the learning experiences are inclusive and representative of the industry's footprint.

The proposal for a Year 6 and a Year 8 pilot program is progressing from concept through to development and is scheduled for release in semester two 2021 for trialling, nationally through pilot schools. Educating the educator through this student-centred, project-based learning scenario is a priority for the project team. Unlike, other STEM initiatives that tend to be extracurricular or 'bolt-ons', this gamification initiative is integrated and aligned with the national curricula. Its STEM learning format encompasses the ACARA's General Capabilities, Aboriginal Framework, and Cross-Curricula priorities.

Integrative geologic event class activity: a case for Taal Volcano Eruption of 2020 in the Philippines

Emralino, Francis¹ & Emralino, Blaisie²

¹*Physics Unit, Curriculum and Instruction Division - Philippine Science High School CALABARZON Region Campus, Batangas City, Philippines;* ²*High School Department - Laguna College, San Pablo City, Laguna Philippines*

While various geologic events disrupt activities in populated areas, they offer an opportunity for educators in the earth sciences to integrate them in their classroom teaching. This paper presents an integrative geologic event class activity which incorporates details relating to the recent 2020 eruption of the Taal Volcano in the Philippines. The first part of the lesson design format consists of experiential narrative that will come from the student participants and is correlated with highlight events from the eruption. This part allows the learners to own the activity as they are engaged in the event which they directly or indirectly experienced. The second part proceeds to involve the students

scientifically in terms of analysing samples (in this case, collected volcanic ashes) from the eruption. Sub-activities here include recording of naked-eye observations of the sample, feature analysis and comparison using a loupe and a portable optical microscope, and tabletop physical characterizations. This in-class or laboratory activity is designed to accommodate actual and remote conduct. It is envisioned that early integrated science educators can use the design format to fit their activities based on the geologic events they experience in their respective places.

In Australasia, gender is still on the agenda in geosciences

Handley, Heather^{1,2}, Hillman, Jess^{2,3}, Finch, Melanie^{2,4}, Ubide, Teresa^{2,5}, Kachovich, Sarah^{2,6}, McLaren, Sandra^{2,7}, Petts, Anna^{2,8}, Purandare, Jemma^{2,9}, Foote, April^{1,2}, & Tiddy, Caroline^{2,10}

¹*Macquarie University, Sydney, Australia;* ²*Women in Earth and Environmental Sciences Australasia (WOMEESA) Network, Sydney, Australia;* ³*GNS Science, Avalon, New Zealand;* ⁴*Monash University, Clayton, Australia;* ⁵*University of Queensland, Brisbane, Australia;* ⁶*International Ocean Discovery Program, Texas, USA;* ⁷*The University of Melbourne, Melbourne, Australia;* ⁸*Geological Survey of South Australia, Adelaide, Australia;* ⁹*Griffith University, Southport, Australia;* ¹⁰*University of South Australia, Adelaide, Australia*

Diversity and inclusion in the workplace optimize performance through the input of a range of perspectives and approaches that drive innovation and invention. However, gender inequity is prevalent throughout society and females remain under-represented in geoscience careers. This study provides the current status of gender equity in geosciences throughout Australasia within the context of broader gender equity policy, frameworks and initiatives and suggests additional solutions and opportunities to improve gender equity and the retention of women in the geoscience workforce. At an individual institutional level in academia, females make up between 23%–52% of the total geoscience departmental or school staff in Australia, 26%–39% of the total staff in New Zealand, 29% of total staff at the University of Papua New Guinea and 18% at the University of the South Pacific. Significant gender imbalance exists at more senior levels, with disproportionately more males than females, a pattern typical of many Science Technology Engineering and Maths (STEM) disciplines. Gender inequity is prevalent within the general membership, committee roles and in award recipients of Australasian geoscience professional associations. Within the Geological Society of Australia and Geoscience Society of New Zealand, only 4% (n = 47) and 18% (n = 161), respectively of past award recipients for national and general awards were female. All past awards considered in this study that are named in honour of a person were named in honour of a man (n = 9). In recent years, women-focused networks have begun to play an invaluable role to support the retention and promotion of women in geosciences and provide a supportive mentoring environment to discuss challenges and share advice. The improved visibility of women in the geoscientific community is an ongoing issue that can in part be addressed through the

development of public databases of women geoscientists. These provide a list of women geoscientists that encourages and supports the achievement of gender balance of invited talks, job shortlisting and on panels, as well as in the media. This work highlights that more must be done to actively reduce and eliminate sexual harassment and assault in university and field environments. We emphasise that particular efforts are required to make geoscience careers more inclusive and safer, through the establishment of specific codes of conduct for field trips. Shared learning of best practices from evidence-based approaches and innovative solutions will also be of value in creating positive change. Greater engagement from the wider geoscientific community, and society in general, is required for the success of gender equity initiatives. Identified solutions and opportunities must target all levels of education and career development. Additional data in future should be collected to look beyond gender to monitor and assess intersectionality. Improved efforts to understand why women leave STEM careers will help to address the “leaky pipeline” and determine the initiatives that will be most effective in creating long term sustainable change.

Geotourism: enriching the visitor experience

Immersive virtual reality in geotourism

Raimondo, Tom

UniSA STEM, University of South Australia, GPO Box 2471, Adelaide SA 5001

Project LIVE (Learning through Immersive Virtual Environments) is a cross-disciplinary initiative at the University of South Australia to embed immersive virtual and mixed reality experiences across the entire teaching program of UniSA STEM. This is achieved using techniques such as Remotely Piloted Aircraft (drone) surveying, 3D photogrammetry, gigapixel photography, terrestrial laser scanning (LiDAR), 360-degree panoramic photos and videos, and location-based mobile learning apps. The Project LIVE team has recently developed a flexible template for the efficient production of high-quality virtual tours, where users can easily substitute images, videos, 3D models and narrative components such as voiceovers and text descriptions to adapt the experience to new field locations. Our platform opens up significant opportunities for the creation of a suite of engaging, authentic and impactful VR geotourism experiences. This presentation will demonstrate a proof of concept using the Hallett Cove Geological Heritage Site in Adelaide, South Australia. Entitled *Beyond the Ice*, the virtual tour incorporates several complementary elements including an immersive VR experience, web-based geotour, mobile learning game and 360 street view walking trail, all of which are freely available at: <https://www.projectlive.org.au/beyond-the-ice>. Further examples from other major geosites across Australia will be shown, concluding with a discussion of the future geotourism opportunities to be explored.

Augmenting the geotourism experience through new digital technologies

Robinson, Angus M.¹, James, Pat², & Ng, Young³

¹ *Australian Geoscience Council, Carlton South, Australia* ² *University of South Australia, Adelaide, Australia* ³ *Danxiashan UNESCO Global Geopark, Shaoguan City, China*

In developing a National Geotourism Strategy for Australia, the Australian Geoscience Council Inc has recognised that state-based geotourism maps can be supplemented by publications, as well as consideration of new digital technologies (e.g., smartphones, 3D visualisation, augmented reality and virtual reality) and GIS technologies as a cost-effective means of accessing and better communicating geological content. This approach is encapsulated in the first strategic goal of the Strategy i.e., ‘to deliver and interpret for the traveller, quality natural heritage content, highlighting geology and landscape’.

Several groups have formed in Australia to trial these technologies with a view of realising some commercial opportunities with geotourism in mind.

In South Australia (SA,) the local Division of the Geological Society of SA has developed Field Guides for many areas of outstanding geological significance e.g., including Hallett Cove, the Flinders Ranges, and Victor Harbor amongst the set of 10 guides produced so far which are available online https://www.gsa.org.au/Public/Publications/Field_Guides/

The Geological Survey of SA is likewise producing interactive, online Google Earth-based, Discovery Trails as virtual geotours <https://discoverytrails.sarig.sa.gov.au/> while at the University of SA, the Project LIVE (Learning through Immersive Virtual Environments) (<https://www.projectlive.org.au/wicked-witchelina>) initiative is highlighting some significant outback areas with interactive virtual geotours, including drone and field video recording, 360 degree GigaPan panoramas and a range of other interpretive materials.

The current pursuit in SA for World Heritage status for the northern Flinders Ranges is also encouraging many strands of geotourism activity and development. These ranges approximately 500km north of Adelaide provide a window into deepest past geological time and abound with significant natural, cultural, historic and scenic values. As well as this, they provide geological and chronological records of one of the world’s greatest ancient super-basins, evidence of the earliest global glaciations, and widespread debris from Australia’s mightiest, extra-terrestrial Acraman meteor impact, and not least evidence of the evolution of the Ediacaran, earliest and multicellular complex life on Earth. It is also very fortunate that the many (so far more than 50) geosites located within this region are already documented and illustrated within the sophisticated compendium of State registered Geoheritage sites (formerly geological monuments) published by the SA Division of the GSA.

Current and planned real, augmented and virtual reality geotourism developments within the Flinders Ranges, include underground and above ground geotrails and mine tours at Blinman, new Ediacara interpretation centres and trails at Nilpena, aerial overflights of

Wilpena, Brachina Gorge and Arkaroola landscapes and the sensational Jeff Morgan Panorama gallery at Hawker. Virtual and augmented technologies are thus being applied to create unique visitor experiences and world class interpretation in this unique Australian geotourism region.

Danxiashan UNESCO Global Geopark of China has been working closely with DJI Technology, the world's largest manufacturer of aerial photography systems, in applying drones to locate, identify, map and monitor geohazards, bush fire, illegal land use, forest clearance and vegetation growth in the geopark. It is cost and time effective particularly in the preliminary survey of a large area.

These technologies will impact on future geotourism product development.

Geotales and geotrails – collaborative geotourism initiatives and implications for new visitor experiences in regional NSW

Fleming, Guy¹, & Boyd, Ron²

¹*Geological Survey of New South Wales, Department of Regional NSW, Maitland, Australia;* ²*University of Newcastle, Newcastle, Australia*

Geotrails provide an excellent opportunity to create new, place-based visitor experiences in regional locations that are self-guided, have low environmental or infrastructure impact, and are ideally suited to the social-distancing requirements of our post-COVID world. Several new geotrails have been successfully developed by the Geological Survey of New South Wales (GSNSW) in highly collaborative partnerships with the University of Newcastle, other local stakeholders and site custodians, with a longer-term aim of creating a network of geotrails across the state.

Geotourism is defined as tourism that focuses on an area's geology and landscape as the basis of fostering sustainable tourism development. Geotrails provide this geotourism experience through visitor engagement, learning and enjoyment using an earth science approach. GSNSW's geotrails are delivered in the form of free, self-guided apps for mobile devices, brochures, web content and signage (if supported by site custodians). Additional high-quality digital content such as spoken word audio, video, virtual and augmented reality imagery and podcasts can provide even richer content to support the geotrail.

Geotrails also provide an opportunity to incorporate complementary information, such as Aboriginal or European heritage, mining heritage and ecological features that have a relationship to the geology and landscape at a place. Integration of complementary information also adds greatly to visitor engagement and buy-in from local stakeholders or site custodians and can act as an enabler at relatively under-developed sites.

Best-practice geotrails are constructed around existing tourist routes that provide a logical and safe journey, incorporate local biodiversity and culture, meet the needs of visitors and local stakeholders, and allow for co-design and collaboration with local community and stakeholders during production. Recently completed GSNSW geotrails at Port Macquarie, Newcastle and Warrumbungle National Park illustrate a best-practice approach for successful design and development

based on practical experience.

Building the Darwin City Geotrail. Reflections, experiences and lessons

Asendorf, Mark

Marmel Enterprises

The Darwin City Geotrail evolved over a period of 4 years shortly after the authors return to his hometown, Darwin. A 16-year journey and experiences through Alice Springs, Roxby Downs, and Adelaide and through multiple industries has influenced the formation of the Geotrail with many familiar places seen through a new lens, and appreciation of things previously hidden in ignorance.

Darwin city hosts some interesting geological features, with some stories are literally written in stone. However, there is more to the history and evolution of Darwin than the landscape. The Darwin City Geotrail is about telling some of those stories.

The journey into Geoheritage and Geotourism can be enriching and rewarding, and Darwin has an interesting story to tell, extending back over 1.8 billion years. It is a story that many non-geoscientists are not aware of, yet it captures their attention and interest when stated.

The Darwin City Geotrail (DCG) was launched in August 2020, within the resourcing and time constraints of its author. Several ambitious components were descope from the launch due to these constraints but remain firmly on the enhancements pipeline.

The DCG has already triggered a few alternative responses – positive, neutral, and negative. Some were anticipated but many others have launched new endeavours and rethinking of some aspects of the Geotrail.

Discussion will include the technical aspects on the Darwin City Geotrail, the issues and concerns encountered, and next steps in enhancing the Geotrail for future users.

Larapinta Trail, Tjoritja/West MacDonnell National Park, central Australia – a potential geotrail

Weisheit, Anett

Northern Territory Geological Survey, Department of Industry, Tourism and Trade, Alice Springs, Australia

The Larapinta Trail extends from Alice Springs Telegraph Station in the east along the West MacDonnell Ranges to the summit of Mount Sonder/Rwetyepme 230 km to the west. This renowned hiking trail is divided into 12 sections (graded moderate to very hard), each section takes one or two days to walk. The Larapinta Trail is managed by the Northern Territory Government Parks and Wildlife, who provide detailed access and hiking information, and maps. General information about flora, fauna, landscape, geology, and culture is also available through various published guidebooks and trail maps.

The rocks comprising the spectacular scenery along the trail are well exposed and easily accessible. They include orthogneisses, metasedimentary rocks, and igneous rocks of two Palaeoproterozoic basement provinces (Aileron and Warumpi), and sedimentary rocks of the Neoproterozoic–Devonian Amadeus Basin.

Cenozoic consolidated and non-consolidated sediments occur as colluvial and alluvial regolith. Rock types and textures exposed along the trail are therefore varied with occurrences of interesting minerals (eg garnet, staurolite) and fossils (stromatolite). There are also excellent exposures of rock relationships such as intrusive and tectonic contacts, unconformities, bedding and layering, and alteration and brecciation zones. Additionally, many of the rocks preserve evidence for ductile and brittle deformation, for instance, mylonitic shear zones, faulting, fracturing, and centimetre- to 100 metre-scale folding.

This variability of lithologies and rock structures profoundly influenced the morphology of the West MacDonnell Ranges. Deep valleys formed by shear zones, alternating ridges and valleys of sedimentary layers 10s of km long and rolling hills of granitic rocks are some of the characteristic geomorphological features that can be seen along the trail. The rocks and their associated landscape developed over ca 1.8 billion years, including episodes of metamorphism and magmatism, terrestrial and marine sedimentation, mountain building, and erosion. They also span the time of emergence and development of early life and preserve impact structures and palaeosurfaces.

Central Australia's unique geology and climate support a multitude of fauna and flora, of which some can be seen along the trail. Climate in particular, but also flora, fire, and termites have in turn affected the exposed rocks leading to distinctive weathering and regolith.

The West MacDonnell Ranges are home to the Arrente People, whose ancestors lived in this country for at least 35 000 years. Some evidence of this cultural heritage, as well as remains of early European settlement can be visited along the trail, and there are excellent museums and heritage sites in Alice Springs.

A geological trail guide available in a convenient format — a small-printed book, booklets, or digital data — would greatly enhance the hiker's experience of the West MacDonnell Ranges. It would provide many benefits of geotrails outlined by the Australian Geoscience Council Inc, and others. These include, but are not limited to, ease of access along an established tourism track, provision of visitor engagement, learning and enjoyment, and promotion of conservation.

Geological logging of a proposed 305-km recreational geotrail in SE Queensland

D'Arcy, Bill, & Winter, George

Member (Retired), Geological Society of Australia

The 161-km Brisbane Valley Rail Trail (BVRT) and the 88-km Kilkivan-Kingaroy Rail Trail (KKRT) were established along disused branch lines of the railway network of SE Queensland, linking them together is the 55-km Yarraman-Kingaroy Link Trail (YKLT). We logged the geology along this 305-km recreational trail on behalf of the Geological Society of Australia (GSA) – Qld Division. Tectonic terrains encountered include a Late Paleozoic accretionary complex formed during westward subduction of the proto-Pacific under the eastern margin of the Australian proto-continent, and Carboniferous to Triassic volcanic and plutonic rocks of an associated volcanic arc, these are elements of the New England Fold Belt, and form a basement to the Esk Basin, a half-graben overfilled with Triassic volcanics

and volcanoclastic sediments. The above-mentioned units in turn are partially overlapped from the south by Mesozoic elements of the terrestrial Clarence-Moreton Basin, which overlies the Ipswich Basin, host to formerly important coal measures around Ipswich (but not exposed on the trail route). Extensive Paleogene (probably Oligocene) terrestrial basalt flows are crossed along some northern segments of the route. Cenozoic units are mostly alluvium deposited in the modern river network, and minor swamp and lake sediments.

GSA member Warwick Willmott has condensed our detail logs of the BVRT and KKRT to concise brochures compatible with the *Rocks and Landscape Notes* series, which can be downloaded without charge from the GSA website. We have begun work on compiling the geological features along the YKLT (logged in mid-2020), for inclusion in this series of brochures. The brochures were written for readers with little or no formal geological education and describe outcrop-scale features exposed along the route, as well as the regional-scale geological factors that influence the landscape, including the evolution of the fluvial drainage network to its current configuration. We also describe a few localities that are close to the trail and have significant geological interest. Copies of the BVRT and KKRT brochures were delivered in July 2020 to Municipal Visitors' Information Centres, and cafes popular with trail-users along the route.

Telling the Earth's stories

Boswell, Russell

In a world muddled by fantasy, fake news and marketing hyperbole, the stories of the earth provide people with a core reality and true sense of perspective.

Our increasing understanding of our world, from core to cosmos, should be shared with a wide range of audiences and celebrated to build the understanding and engagement of tourists, students and local community custodians.

However, storytelling is challenging. The complexity and span of earth sciences is daunting to the lay person and simplifying concepts and terminology can blur meaning.

The science of storytelling provides some insights into how this can be approached. Linking earth's processes to our audience's life experiences, harnessing emotion and description, and finding interactive ways to stimulate synapses in the brains of our listeners can provide pathways to understanding and memorable lessons.

Savannah Guides is a network of over 500 tour guides and tourism operators around Australia, the "Protectors and Interpreters of the Outback", including the Undara Lava Tubes, Capricorn Caves, El Questro Station, Cobbold Gorge and other geological wonders. The organisation provides training and professional development at field schools and through online platforms, provides linkages to Protected Area Managers, researchers and Traditional Owners, and delivers workshops on guiding skills including interpretation and storytelling.

Savannah Guides has worked since 1988 to build the geotourism message and connect more people with their world. It is now engaged with the National Geotourism Strategy and its associated stakeholders

and has ongoing involvement in supporting several regions to develop their geoscience stories.

This presentation will provide examples of these collaborations and some of the storytelling techniques that have captivated guests, as well as providing examples of how geoscientists can better connect with the wider community through tourism.

Geotourism in Tasmania

Vicary, Mike, Cumming, Grace, & Bottrill, Ralph¹

Geological Survey Branch - Mineral Resources Tasmania - Geological Survey Branch, Rosny Park, Australia

Tasmania is one of world's most geodiverse places on the planet, with rocks ranging in age from Proterozoic to Recent. The geology has been subjected multiple episodes of deformation, felsic and mafic magmatism, rifting, erosion and weathering, reflecting changes in tectonic setting and climate with time.

The UNESCO world heritage area (WHA) forms the greater part of the 30% of Tasmania that is occupied by National Park or reserve. The WHA is one of only two areas in the world which satisfies at least seven of the ten criteria required for listing. Importantly, four of these criteria are directly related to the WHA's unique geology and landscape.

Significant geological features include folded and metamorphosed Proterozoic basement, Cambrian ophiolites, Cambrian to Devonian sedimentary rocks, Permian to Triassic sedimentary sequences with widespread Jurassic dolerite intrusive sills, karst features, Cenozoic glacial and periglacial landforms, fluvial and coastal landforms and extensive blanket bogs. These features help to define the World Heritage status and are also widespread across Tasmania. Together with the Mt Read Volcanics, extensive Tertiary sequences with basaltic volcanic centres, the Ordovician to Devonian sequence of NE Tasmania, Devonian granite intrusions and rare gems, minerals and fossils, they make Tasmania an ideal place for geotourism.

Tasmania receives about 1.3 million visitors/year with the majority visiting the State to enjoy a holiday in the natural environment. Many current tourist operations provide a basic level of geological information. DPIPW provides interpretation in the WHA and National Parks through its website, visitors centres and track signage. Tour operators conduct boat trips in the Freycinet, Tasman Peninsula, Bruny Island and the Gordon River areas, wilderness flights to Melaleuca in the WHA and guided cave tours. The Wilderness Railway provides commentary on the mining history in the Queenstown area. There are first class rock displays at many of the local museums, especially Zeehan.

The tourist operations are supplemented by three Geotrains, which provide the tourist with a greater level of geological interpretation. The 'Created from Chaos' Geotrail was developed to highlight the complex Proterozoic–Palaeozoic sequences and Cenozoic geology along the northwest coast. The West Coast ('Living Earth') Geotrail has been developed, including the southern part of the Cambrian Mt Read Volcanic belt, with sites highlighting aspects of the Cambrian to Ordovician rift development, Devonian granite magmatism, mining history and the Cenozoic

landscape development. A third Geotrail on the Furneaux Islands highlights the Palaeozoic to Cenozoic evolution of Bass Strait.

Other notable geotourism projects completed include the production of an excursion guide to King Island (Calver, 2016), a non-technical book on the geological evolution of Tasmania (Corbett, 2019) and a pamphlet highlighting the geological features of the Tasman Peninsula (Mineral Resources Tasmania, 2019). A new book describing Tasmanian Fossils by Peter Manchester is due for completion in 2021.

Calver C.R. 2016. A guide to the Geology of King Island. King Island Natural Resource Management Group.
Corbett, K.D. 2019. Child of Gondwana: The geological making of Tasmania. FortySouth Tasmania Mineral Resources Tasmania 2019. Geological Features of the Tasman Peninsula).

Driving Australia's National Geotourism Strategy through the AGC

Robinson, Angus M F AusIMM (CP)

Coordinator, Australian Geoscience Council Inc, Carlton South, Australia

The Australian Geoscience Council Inc (AGC) has set up a National Geotourism Strategy Reference Group (NGSRG) which includes representatives of other key active stakeholders (e.g., the Geotourism Standing Committee of the Geological Society of Australia), and under the guidance of this reference group, other key stakeholder groups will be best placed to help deliver different parts of a National Geotourism Strategy (NGS).

This NGS is being designed to support the orderly development of major geotourism projects and activities in line with overseas trends and domestic regional development imperatives. The AGC sees the articulation of a strategy with a staged and incremental approach as being essential to ultimately gain government endorsement at all levels. The development of a National Ecotourism Strategy in 1994 and subsequent state/territory-based initiatives is considered as a particularly useful precedent and guide. Of significance internationally is the development of geotourism in Australia that lags many countries' approach, notwithstanding the fact Australia has taken the initiatives in several areas in development of the concepts underpinning geotourism.

The pursuit of geotourism offers the potential for new industries and employment opportunities through the development of major projects within Australia. Also, very significantly from a strategic perspective, the AGC recognises that the development of geotourism may be one of the best ways to communicate the value of geoscience to the broader Australian community. The AGC considers that this improved profile for geoscience is likely to have a positive impact in other areas of strategic importance, most notably the need for continuing tertiary enrolments in geoscience, which is required to meet Australia's needs for highly qualified geoscience graduates and researchers into the future.

The NGS will be based on a number of strategic goals based on the following themes.

1. Consideration of new digital technologies (e.g., delivered through smartphones and in visitor interpretation centres – 3D visualisation, AR & VR) as a cost-effective means of accessing and better

communicating and interpreting content for travellers.

2. Consideration of establishing a national set of administrative procedures for 'georegional' assessment to provide for potential geopark nomination at state and national levels, and as approved by governments, at a UNESCO Global Geopark level.
3. Compilation from existing sources, including the various state-based geoheritage inventories, of a national register of geosites that are suitable for promotion as geotourism sites.
4. New geotrail development – local, regional and national engagement to open up dialogue with existing walking, biking and rail trail interest groups and operators to highlight the availability of quality natural heritage data.
5. Mechanisms for developing mechanisms for collaboration with providers of other areas of natural (bioregion) and cultural heritage content, inclusive of mining and resource industry heritage (e.g., mining companies, geological and mining museums, historical societies, as well as specialist groups with interests in flora and fauna etc. has been identified as an opportunity for the Australian mining industry.
6. Strengthening Australia's international geoscience standing through geotourism excellence.
7. Professional development opportunities for geoscientists wishing to develop content interpretation and tour guiding skills for enhanced interaction with the public, and engagement with the Savannah Guides and the professional group Interpretation Australia.

Myths and perceptions about Geoparks in Australia challenged

Briggs, Alan

Geoparks WA, Perth, WA

Stakeholders hold the key to establishing geoparks in Australia. There has been a shift in community thinking about geoparks. The effect of the 2009 Environment Protection and Heritage Council communique recommending geoparks not be supported in Australia is waning. It is now possible, that if State governments show support for geoparks, the Federal government will assist in recommending aspiring geoparks to UNESCO for recognition as Global Geoparks. However, despite the success of geoparks internationally (161 in 44 countries), there remain negative perceptions and myths about geoparks in Australia. Australia remains the only continent that does not have a geopark. Global geoparks attract UNESCO branding with associated marketing and promotion. Geoparks are community-led and achieve geoheritage protection through education and sustainable development. Geotourism is the key driver for economic returns for geoparks.

Research in the Wheatbelt of Western Australia has shown that stakeholders hold the perception that geoparks represent a sound strategy for revitalising rural areas through geotourism. Research findings indicate that stakeholders consider geoparks as a positive way of growing rural businesses and creating employment in rural areas, and they are prepared to support geoparks as a sustainable tourism strategy. Other research findings included consideration of the myths about geoparks such as the perceived green veneer of UNESCO, confusion about the word "park" and clashes with grazing and mining industries.

This presentation will outline the findings of this research and challenge the perceptions and myths associated with geoparks.

The Murchison GeoRegion – A Potential Aspiring Geopark, Western Australia

Dowling, Ross

Edith Cowan University, Perth, Australia

Whilst geoparks exist around the world including 161 UNESCO Global Geoparks in 44 countries, there are none in Australia. However, in Western Australia GeoparksWA is working on establishing a number of aspiring geoparks, with the intention of later nominating all or part of these to become UNESCO Global Geoparks.

The Murchison Region of Western Australia is approximately 250 000 sq km making it about the same size as New Zealand but larger than the United Kingdom. It lies approximately 600 km north of Perth and comprises the seven Shires of Cue, Meekathara, Mount Magnet, Murchison, Sandstone, Wiluna and Yalgoo. In 2009 WA's Forum Advocating Cultural & Eco Tourism (FACET) held a tourism conference in the town of Mount Magnet and since then there has been a growing interest in fostering geological tourism. In 2016 the WA Government's Mid West Development Commission created a 'development blueprint' for the region which included the goal of establishing tourism based on the region's unique geology.

Since then, the Shires have worked together to create

the Murchison GeoRegion and in September 2020 the Murchison GeoRegion was launched. The GeoRegion would now form the basis of WA's first Aspiring Geopark with the ultimate aim of applying for recognition as a UNESCO Global Geopark. A website and app have been created supplemented by a Trail Booklet under the banner of 'Discover Ancient Lands, Brilliant Skies'. The booklet describes 21 geological sites along a GeoRegion Trail which highlights the abiotic, biotic and cultural features to encourage visitors to find a deeper understanding of and connection with the land they are travelling through. These geological sites will be added to with others focussing on biotic or cultural attractions. Other areas in Western Australia are now working with *GeoparkWA* to create Aspiring Geoparks so it is hoped to have a network of geoparks established across the state in the near future.

Geoheritage and geoconservation

Three decades of geoconservation in retrospection

Díaz-Martínez, Enrique^{1,2,3}, & Brocx, Margaret^{3,4,5}

¹Geological Survey of Spain (IGME), Madrid, Spain; ²Geological Society of Spain (SGE); ³European Association for the Conservation of Geological Heritage (ProGEO); ⁴Murdoch University, Perth, Australia; ⁵Geological Society of Australia (GSA)

During the last 30 years, geoconservation has seen an accelerated evolution and advancements, but there are also a few steps backwards. We herein provide a summary from the perspective of three points of view: Spain, The United Kingdom, and globally. Both the United Kingdom and Spain had an active geological survey by the mid-19th century and began work on geoconservation in the 1970s, but an acceleration of achievements began in the 1990s with The European Association for the Conservation of Geological Heritage (ProGEO) as a catalyser for inventories, legislation, conferences, publications, and later on (2009) a peer reviewed journal (*Geoheritage*). ProGEO promoted the Global Geosites Programme (GGP) with support from IUGS and UNESCO, starting a list of geological sites of international relevance. After the establishment of World Heritage criterion viii for geological heritage (1972), the first international conference on geoheritage was held in Digne, France (with the Declaration of the Memory of the Earth in 1991), followed by the Global Geoparks Programme (2004), the definition of the scope and scale of geoheritage including indigenous heritage (2007), and the first inclusion of geoheritage within IUCN resolutions (2008, 2012 and 2016). This was followed by the establishment of a Geoheritage Specialist Group within IUCN's World Commission on Protected Areas, the inclusion for the first time of geoconservation in a World Parks Congress (2014), and of a specific chapter on geoconservation in the 2015 revised edition of IUCN's book on *Protected Area Governance and Management*.

Currently, the United Kingdom, Spain, and Portugal are the only countries in the world having fulfilled the GGP, and after China, Spain has the second highest number of UNESCO Global Geoparks (15 in 2020). The withdrawal of official support for the GGP by IUGS and UNESCO in 2003, left the programme orphaned. In its quest for an international standard that would force the

Spanish government to inventory and protect its geoheritage, the Geological Society of Spain (SGE) became a member of IUCN in 2008, and that same year managed to pass resolution WCC-2008-RES-040 obliging to include geoconservation in the IUCN agenda and for all its members. ProGEO joined IUCN in 2011 and, for the first time in the history of IUCN, the 5th WCC (2012) saw many geoconservation-related activities, including resolution WCC-2012-RES-048 recommending the use of inclusive terms to refer to nature, natural heritage and natural diversity (it's not all biodiversity!), as well as IUCN's support to the GGP.

This presentation will further explore nodal points in the history of geoconservation on the global platform, lessons learnt, and Spain as a case study of a country that has worked towards establishing a national inventory of sites of geoheritage significance for the purpose of geoconservation.

Geoheritage significance of the deltas of the Pilbara Coast, northwestern Australia

Semeniuk, T. A.¹, & Semeniuk, V.^{2,3}

¹Western Sydney University, The College, Quakers Hill, NSW 2763; ²V & C Semeniuk Research Group; ³Notre Dame University, Fremantle

The Pilbara Coast, one of the most arid coasts in the world, has a consistent ENE orientation. It has a diverse hinterland geology and a sharp rainfall gradient on the landward side and progressing south to north a distinct progressively microtidal to macrotidal, wave-dominated oceanographic setting. On the seaward front, processes are wave-dominated, and interior to the deltas, processes are tide dominated. Along this unique coastal stretch, a large number of rivers discharge to the sea. This gives rise to an array of deltas, having variable size, shape, and active processes, and variable occurrence of barriers, lagoons, and landforms on the deltaic plain. They represent a plethora of delta types that can be characterised as active deltas, and inactive deltas. The largest drainage systems, such as the Ashburton River and De Grey River, build large classic active deltas, reflecting their large catchments and large supplies of terrigenous sand and mud that interfaces with a wave-dominated environment. Shorter rivers, such as the Robe River, have largely inactive deltas, which are heavily reworked by marine processes. Inactive deltas with shoreline retreat leave a line of shore-parallel ridges in their wake and, with beach-rock cementation, result in a series of cemented ridges that form nearshore shore-parallel rocky ridges. The Fortescue delta and the Yannarie delta represent a special case in the region, the former being a reworked edge of an alluvial fan system, and the latter where fluvial discharges interact with a dune field, forming unique deltaic elements. The arid tropical setting of these deltas gives rise to several distinct sediment facies, including low tidal sand flat sheets, dune sand or beach-ridge ribbons, mangrove-structured sand sheets and muddy sand sheets, muddy ribbons and high tidal mud sheets. The range of traditional and non-traditional, active and inactive delta types along this arid coast makes it globally unique ensemble of deltas and a globally significant set of deltas from a geoheritage perspective.

Geoheritage significance of the Holocene Yanrey Delta, Pilbara Coast, Western Australia

Semeniuk, V.^{1,2}, & Brocx, M.³

¹V & C Semeniuk Research Group, Warwick, WA;

²School of Arts & Sciences, Notre Dame University, Fremantle, WA; ³Environmental and Conservation Sciences, Murdoch University, Perth, WA

From a geoheritage perspective, the Holocene Yanrey Delta of the southern Pilbara Coast, Western Australia is a unique arid-zone delta of international significance. It provides a deltaic model unlike any established deltaic forms documented elsewhere globally. The delta in the discharge zone of the Yanrey River is located on the eastern shore of a semi-protected large embayment (Exmouth Gulf) in an arid climate. With limited rainfall in the hinterland, the Yanrey River floods episodically and, over the Holocene, has built a triangular deltaic plain. In its east to west orientation (normal to the coast) the river traverses a linear red-sand dune field of northerly-oriented dune. As such, instead of building a classic wave-, tide-, or fluvially dominated delta form, the Yanrey Delta has geomorphically and sedimentologically interacted with the dune field developing a complex of arid-zone dunes interspersed with deltaic deposits, the latter composed of sand and mud. In its migration and switching of channels from north to south over the Holocene, the delta in combination with regional winds has transformed the originally coarsely spaced northerly-oriented linear dunes to more finely spaced northerly-oriented linear dunes. While there is a sand-and-mud component to the deltaic deposits on the delta plain, the inter-dune swales also are being filled with floodplain red mud to form scattered (isolated) mud lenses. As such the deltaic sequences is a mixture of deltaic sediments *sensu stricto*, deltaic sediments admixed with reworked red sand dune sediments, and patches of reworked red sand dune sediments. At its seaward edge, the Yanrey Delta is tidal, and the deltaic sediments are tidal flat in character but, in addition, they also interfinger with and overlie pre-existing earlier tidal flat deposits. The Yanrey Delta adds an extra delta form to the existing suite of delta types.

Geoconservation of ancient Pilbara stromatolite fossils as a multifunctional landscape

Fletcher, Clare¹, Van Kranendonk, Martin J.², Metternicht, G.³, & Walter, M. R.⁴

¹University of New South Wales, Sydney, Australia;

²Australian Centre for Astrobiology, Sydney, Australia;

³University of New South Wales School of Biological, Earth and Environmental Science, Sydney, Australia;

⁴Emeritus Professor, Macquarie University, Sydney, Australia

The ancient (3.48 billion year old) stromatolite fossils of Western Australia's Pilbara region constitute the oldest convincing evidence of life on Earth found to date. These fossils offer a unique insight into the origin of life on Earth and elsewhere in the universe. There are six key sites for ancient life in the Pilbara, mostly concentrated around the North Pole Dome geological region. Since the discovery of such ancient and well-preserved stromatolite fossils in 1980, they have become a sought-after item for indiscriminate collectors to the point where the original site (Dunlop) no longer exists.

Due to this indiscriminate collection, various methods of conservation have been recommended over the years. In 1987 a Geological Survey of WA report recommended that the North Pole Dome fossils were placed on the Register of National Estate (henceforth RNE) (now the National and Commonwealth Heritage Lists). The site was also placed on an indicative list for UNESCO World Heritage listing in 1996. Whilst the sites of Buick and Awramik were registered on the RNE, the Register was closed in 2007, and so the legal conservation status of these sites was lost, and they were once again left unconserved.

Currently the six sites are State Geoheritage Reserves vested in the Minister for Mines and Petroleum. While this affords some protections such as requiring approval before visiting these sites, it has not prevented collection of material from the sites. Mining licenses can also be granted for the collection of materials from these sites. The conservation of these sites is complicated by the surrounding lands being either Crown Land or pastoral lease (depending on the site). Other stakeholders include the Nyamal people, the community of Marble Bar, NASA, the European Space Agency, the Japanese Space Agency, and others.

The vision for these sites is both geoconservation and on-the-ground management that prevents further theft of the fossils and facilitates learning and tourism in the area. We have petitioned the Department of Biodiversity Conservation and Attractions to add the North Pole Dome sites to Meentheena for consideration under the WA Government's Plan For Our Parks initiative which works concurrently with an Indigenous Ranger program. Our vision also includes a combined scientific research and ranger station, that can be used for site visits by space agencies, universities, schools, and potentially become a visitor information and discovery centre combining science on the origin of life and Indigenous history and tellings.

The type of conservation effort to be pursued is yet to be determined. While both National Heritage listing and World Heritage listing are appropriate for the site because of its universal importance, the timeframe of

achieving either of these as well as the additional legal protections afforded need to be considered before committing to either effort. Public-private partnerships are also to be considered alongside conservation efforts. While different conservation avenues are being explored public-private partnerships will allow for the vision for geoconservation of the North Pole Dome stromatolite fossils to be realised.

Geoheritage values of Beenyup Swamp, in the Yellagonga Regional Park, Western Australia

Unno, Joy

V & C Semeniuk Research Group

Beenyup Swamp in the southern part of Yellagonga Regional Park on the Swan Coastal Plain in Western Australia is a Holocene wetland with geoheritage values. It is part of the chain of linear wetlands belonging to the Yanchep Wetland Suite that is located between limestone ridges of the Spearwood Dunes near the boundary of the quartz-sand-dominated Bassendean Dunes. Instead of being dominated by calcilutite as are other wetlands in this Suite, Beenyup Swamp is a basin stratigraphically dominated by peat. As such, in contrast to other basins in the Yanchep Wetland Suite that are mostly calcilutite-filled, Beenyup Swamp has a stratigraphy of thick homogeneous peat, with stratigraphic evidence of fire scarring including buried lumps of charcoal, and ubiquitous diagenetic products of acidic groundwater. The sequence of peat in this region of the Yanchep Wetland Suite dates back to 8000 years BP and contains a diagenetic record of plant organic matter grading from fibrous peat to organic gel. The stratigraphy, the Holocene fire history, the acidic water diagenesis providing a model of peat accumulation and peat diagenesis at Beenyup Swamp is a geological ensemble of geoheritage significance.

The status of geoheritage and geoconservation in Australia

Cresswell, Ian

University of Newcastle, Callaghan NSW

The protection of Australia's natural heritage has been ongoing since the 1870s in every state and territory, however, efforts to identify and conserve important sites of geoheritage significance have had limited success. This presentation reviews the policies and legislation governing geoheritage and geoconservation in all Australian jurisdictions and shows that there are inconsistencies and inadequacies in the processes to identify and protect areas of geoheritage significance. Each state and territory has differing emphases on geoconservation and different degrees of success in achieving geoconservation goals. In 2015 the Australian Government released the Australian Heritage Strategy as the overarching framework for the identification, management, and protection of Australia's heritage across all levels of government and community. While in recent years there have been a few *ad hoc* successes related to national heritage or to state heritage, it is not clear the strategy is working. There is an urgent need for a nation-wide systematic approach to identifying representative geoheritage sites, and to enact processes for their protection.

A geoheritage treasure – a case study of the Hornsby Diatreme

Semeniuk, T. A.

Western Sydney University, The College, Quakers Hill, NSW 2763

The quarrying for bluestone at the Hornsby Quarry Site exposed a > 40 m-deep cross-section of a volcanic diatreme, showing a volcanic neck extruding through Sydney Basin sediments, complete with volcanic features visible at many scales, with post-volcanic features related to magma and gas extrusion at various depths, and with different host rocks. Globally, there are very few instances of such excellent exposure, revealing a full range of macroscale to microscale features in three dimensions. It is arguable that this exposure alone, makes it a site of international geoheritage significance. Using the Geoheritage Toolkit, applied at various scales shows that this diatreme is internationally to nationally significant. For example, at the macroscale, there dish beds in all orientations of the quarry walls are visible, giving a three-dimensional picture of its structure, reflecting its volcanic accretion and later caldera collapse. At the mesoscale, where breccia beds, bombs, and surge layers are visible, these show how the magma interacted with various host rocks and other post-volcanic processes that occurred prior to solidification. Finally, at the microscale, lapilli (including accretionary lapilli), chilled margins and carbon-rich xenoliths are evident in hand specimen. As such, this Quarry is a unique site worldwide. In fact, the Quarry, exposing the volcanic pipe of the Hornsby Diatreme, offers a snapshot in time of the Sydney Basin, preserving its volcanic and post-volcanic history on the quarry walls.

Recognising and preserving mineral diversity: An updated catalogue of type mineral specimens in Victoria's State collections

Oskar Lindenmayer

Museums Victoria, Melbourne, Australia

Type mineral specimens are designated by the International Mineralogical Association (IMA) as the physical standards by which newly discovered mineral species are defined. They represent the benchmarks against which the world's mineral diversity can be recognised and studied. Each type-mineral specimen is a globally significant element of movable natural heritage and forms an irreplaceable resource for researchers in the fields of mineralogy, crystallography and materials science. Despite their importance, the management of these specimens has historically lacked transparency.

Museums Victoria holds approximately half of the type-mineral specimens in Australian institutions. The most recent edition of the global catalogue of type-mineral specimens, prepared under the direction of the IMA Commission on Museums, lists 98 specimens as lodged with Museums Victoria, of which 45 are from Australian localities and 53 are from overseas localities. This catalogue also lists the whereabouts of 12 specimens from Australian localities as unknown. In contrast to the global catalogue, Museums Victoria's internal catalogue includes 125 type mineral

specimens, of which 59 are from Australian localities and 66 are from overseas localities. There are also a number of discrepancies between the two catalogues for specimens that appear on both, including type status (i.e., whether the specimen is a holotype, cotype or neotype) and registration number.

To resolve these issues, a review of the information available in publications, Museums Victoria records and correspondence, and minutes from meetings of IMA Commissions has been undertaken for each specimen. Where necessary and practical, authors of new mineral descriptions have been contacted for further information. A methodology has been developed to identify legitimate type specimens and appropriately categorise them by their type status. In a departure from previous attempts to document type mineral specimens in Victoria's State collections, areas of uncertainty or missing information for specimens are flagged and explicitly discussed.

The sources of the majority of the discrepancies between the global and internal catalogues were found to be either publicly undocumented transfers from other institutions or incomplete information having been given in the original publications of new mineral descriptions. Amongst the discrepancies resolved was the identification of Museums Victoria as the lodging institution for five of the type specimens listed as having unknown whereabouts in the global type catalogue. In the absence of a formal mechanism for reviewing details or reporting transfers of type mineral specimens, periodical review and publication of catalogues by the institutions that hold them is necessary for the ongoing management of these most significant parts of mineral collections. It is hoped that by undertaking this review in a transparent manner, and making the results and methodology publicly available, other institutions will be encouraged to do the same.

Patina: a microscopic feature of palaeo-environmental and geoheritage significance

Clifford, Penelope¹, & Semeniuk, Vic^{1,2}

¹*Notre Dame University, Fremantle;* ²*V & C Semeniuk Research Group*

Patina is an ultra-thin crust of silica or silica and carbonate that is developed on glass and, while it best developed on anthropogenic glass, it provides important information on products and processes associated with weathering of glasses in general. It is common in modern environments, though variable in expression dependent on environmental setting, and it has been recorded on pre-Mediaeval and Mediaeval artefacts. Anthropogenic glass is geochemically unstable and, as such, it corrodes relatively rapidly (within years), generating a variety of weathering crusts of different thicknesses, and various internal structures. The type of patina that is developed depends on the glass composition, the type of soil it is embedded in, the hydrochemistry of the soil water, climate setting, and whether the glass is located in an inland vadose zone or phreatic zone, a maritime coastal zone, or a submarine environment. The patina crusts are < 10 µm up to 100 µm, thickening with age. The solutinal relationship of the patina to the glass varies from straight, undulating, irregular, to cusped and, internally, shows structures of colloform to undulating lamination, parallel lamination, massive to mottled patterns, micro-

brecciation, shrinkage cracks, and infiltrated dust-sized minerals, all reflecting and recording a history of solution and precipitation, and variation in climate. For vadose environments, the main agent in the patination is alternating wet and dry vadose conditions, and alternating acid and alkaline vadose conditions that result in precipitation of an amorphous silica 'gel' that forms silica laminae, its layer-parallel shrinkage, and the precipitation of calcite laminae. While modern patina and historic patina have been documented from the various climate, hydrochemical, and pedogenic environments, the results are widely applicable to understanding and unravelling the weathering of natural materials such as obsidian, chert, and volcanic glasses – in this context, it conforms to the geoheritage category of 'modern processes' and provides a record of modern processes and products in the weathering of natural glass and glass-like materials.

Geoheritage significance of three contiguous Holocene wetlands 161, 162 and 163 in the Becher Wetland Suite, southwestern Australia

Semeniuk, Christine¹, & Semeniuk, Vic^{1,2}

¹*V & C Semeniuk Research Group;* ²*Notre Dame University, Fremantle*

The Becher Wetland Suite comprises a series of wetland basins located in inter-dune depressions on a Holocene prograded beach-ridge plain. With progradation, the wetlands formed by the regional water table naturally rising into the inter-dune depressions. As beach-ridge progradation is westerly, the inter-dune depressions (becoming wetland basins) generally young towards the west, with the oldest basins some 4500 years old, and the youngest < 900 years old. Through the Becher region, the insertion of wetlands on the prograded beach-ridge plain, through generally younging westwards, in detail, is staggered because of the uneven topography of the depressions along their length. For instance, wetlands 161, 162 and 163, the subject of this paper, all occur along an inter-dune depressions located on the 4500-year beach-ridge isochron (the oldest part of the beach-ridge plain) and, as such, ideally should be the same age and show the same history. However, they have a staggered history, with wetland 161 commencing accretion some 4350 years ago, wetland 162 commencing 4110 years ago, and wetland 163 commencing 2920 years ago. All three basins filled with calcilutite. However, with different ages and longevity of accretional history, and subject to differing small-scale temporal climate changes (in the order of 100 years or less) they exhibit different sedimentary history in terms of thickness of calcilutite, the relationship of calcilutite to underlying sand, diagenetic effects (such as dissolution of underlying carbonate sand, dissolution of *Chara* and sponge spicules, and patchy cementation of calcilutite), and the responses to fire. This sequence of wetlands illustrates the complexities of wetland basin sedimentation. As such, the contiguous wetlands 161, 162 and 163 are a system of international geoheritage significance.

Six disused quarries tell of a much earlier Canberra geoheritage story

Finlayson, Douglas

Canberra

In the central part of Canberra there are six disused quarries that illustrate various aspects of the Silurian tectonic setting of the eastern Lachlan Origin. These quarries were developed for engineering and construction purposes during the building of the nation's capital city. They are located around Black Mountain, Mount Ainslie, Red Hill, Mount Mugga Mugga, Yarralumla brickworks and Acton Peninsula.

Among this group of central Canberra quarries the outcrops can demonstrate a shallow marine environment about 438–433 Ma, dacitic ignimbrite volcanism at 428–424 Ma, a second eruptive history about 424–422 Ma, limestone deposition in a warm shallow marine environment near the equator at 428–425 Ma, Silurian fossils in a tuffaceous sandstone, siltstone, mudstone marine environment at 424–423 Ma, and later metamorphism by a northern pluton of the Bega Batholith about 417 Ma.

Together these quarry rock outcrops backup paleogeographic reconstructions that indicate that during the early part of the Paleozoic era Australia was part of the Gondwana supercontinent and largely surrounded by warm waters north of the Equator. The Paleo-Pacific Ocean lithospheric plate was colliding with Gondwana and there were subduction zones, with associated island arc volcanoes and earthquakes, dipping under its embryonic Australian margins.

Geological Surveys now and into the future

Mapping the geology that matters – the role of Australia's geological surveys in supporting mineral discovery in the 21st century

Yeats, Chris

Geological Survey of New South Wales, Department of Regional NSW, Maitland, Australia

During the late 20th century, Australia's geological survey organisations (GSOs) completed 1:250 000 scale surface geological mapping of the continent. This work provided a framework for mineral exploration that led to the discovery of most of the surface and near-surface deposits in areas of outcropping basement that form the basis of the country's current mineral production. From the 1970s, geological mapping was augmented by regional geophysical data and from the mid-1990s increased geochronological analysis, which supported a second generation of higher resolution mapping under the National Geoscience Mapping Accord into the early 21st century. However, this second wave of mapping, which often focused on areas of good quality outcrop with known mineral potential, did not lead to many significant discoveries and over 80% of the country's current mineral production now comes from deposits discovered prior to 1980.

In order to provide a framework for mineral discovery in the 21st century, Australian GSOs need to change the search space and provide the exploration industry with

the data they need to successfully explore deeper and step out into the 75% of the Australian continent where prospective basement is buried under younger, non-prospective cover. Essentially, GSOs must map "the geology that matters" – defining the structural architecture, temporal evolution and lithologies of potentially prospective geological terranes, regardless of whether they are exposed at the surface, or not.

This work has already started in New South Wales (NSW), with the NSW Seamless Geology providing an interpreted lithotectonic framework for the state, based primarily on surface mapping and potential field geophysical data. However, further geological data is required to support this model, particularly in undercover terranes. As participants in the ten-year MinEx CRC National Drilling Initiative (NDI), Australia's GSOs will generate new precompetitive geoscientific data over several underexplored, undercover regions across the continent. Equally importantly, the NDI will support development of cheaper, faster drilling technologies, real-time sensing technologies and new concepts and decision-making tools that will aid mineral exploration in deep and/or covered terranes, thereby making large parts of the continent more accessible to mineral exploration.

Concurrently, Australia's GSOs are deploying new technologies to augment existing national datasets. The ~55 km-spaced stations of the collaborative Australian Lithospheric Architecture Magnetotelluric Project (AusLAMP) is delivering a lithospheric-scale conductivity model that can be used to define areas of anomalous fluid flow for further investigation. Completion of the AusAEM electromagnetic survey across Australia over the next four years will deliver a near-surface conductivity model that can be used to define depth to basement, as well as potential for mineral and groundwater resources. New geochemical and isotopic datasets are also being used to define fluid sources and crustal evolution at a continental scale.

As we enter the third decade of the 21st century, Australia's GSOs face a watershed moment. We must and are transitioning from mapping the surface geology, to mapping prospective geology and delivering new types of data, to create a framework for the discovery of the new deposits needed to support Australia's mineral industry into the second half of the century.

How the GSNSW is helping to preserve data from the NSW infrastructure boom

Adewuyi, David

Geological Survey of New South Wales, Department of Regional NSW, Maitland, Australia

Geotechnical data provide information about rock/soil characterisation, strength and stability and subsurface hazard identification that is critical to infrastructure planning, design and construction, and asset protection and maintenance. These data also provide information about the volume and quality of construction materials that, when enough data is collated, can be used to assess available resources for possible extraction. Due to the vast recent and forecast increase in public construction infrastructure spending, including a New South Wales (NSW) Government commitment of \$93 billion over four years to 2022–23, responsible NSW agencies that procure geotechnical services have been tasked with maintaining the integrity of their

geotechnical data assets. Keeping a corporate record of geotechnical reports and re-using the information has been a key challenge for these agencies.

In January 2020, the NSW Department of Planning, Industry and Environment (including the Geological Survey of NSW (GSNSW), Sydney Water and Public Works Advisory NSW) signed a Memorandum of Understanding (MoU) with Transport for New South Wales (comprising Sydney Metro, Sydney Trains, and Roads and Maritime Services) and the Australian Rail Track Corporation, to collaborate in the development of a whole-of-government single repository for NSW geotechnical information – the Government Geotechnical Report Database (GGRD). Presently, there are over 3450 Public Works reports available in the GSNSW's DiGS document archive and geo-located in the online spatial viewer, MinView. Industry professionals in both the private and public sector have attested to the usefulness of the database in the initial planning stages of projects for informing desktop studies, gaining preliminary understanding of subsurface conditions and identifying potential risks while scoping geotechnical investigations, which enables a more robust estimation of project costs.

To demonstrate how the geotechnical data can be used, GSNSW is working on the construction of a 3D geotechnical model as a proof-of-concept planning tool for the Western Sydney Aerotropolis area. As well as modelling the strength of the subsurface, the project will also give insights on the extraction potential of construction resources in the area.

The GGRD will also support the ongoing digital transformation in NSW that is being applied in the creation of a NSW Spatial Digital Twin, launched by NSW Spatial Services in early 2020. The NSW Spatial Digital Twin will provide 3D and 4D digital spatial models of built and natural environments. It allows visualisation of amenities even before construction begins to enable better planning of infrastructure and communities in the state.

Enhancing NSW statewide geophysics with high resolution company data

Matthews, Sam

Geological Survey of New South Wales, Department of Regional NSW, Maitland, NSW, Australia

The Geological Survey of New South Wales (GSNSW) has released an updated suite of magnetic grids and imagery which improve the existing images through the inclusion of high-resolution, open-file company data. The foundation of this product comprises over 60 regional government surveys flown at 200 to 400 m line-spacings. The addition of about 150 private company surveys flown at 50 to 200 m line-spacings increases the resolution of the grids in these areas. The higher-resolution surveys also allow the data to be gridded with a 25 m cell size rather than the previous 50 m, which provides better definition of anomalies.

The project commenced with the quality assurance (QA) of about 650 airborne magnetic surveys flown in New South Wales since the late 1950s. An algorithm was derived to quantitatively assess each survey on the merits of the survey metadata. The algorithm applied a weighted score to various parameters such as line-spacing, flight height, sampling interval, and survey

area. A baseline score was calculated for the previous statewide merge based on the regional government surveys, which became the cut-off for the company data. All surveys falling below that score were excluded. A final manual QA of the remaining surveys was performed to ensure only the best data filtered through the algorithm before being included in the new merges.

The boundaries of each survey were placed into a shapefile and where any overlap occurred, the survey with the lower score from the algorithm was clipped using the boundaries of the higher scoring survey. An external buffer of 500 m was added to the survey boundaries, creating a small overlap to allow the software to align features when merging. After clipping, all surveys were re-sampled and re-projected into a unified grid cell size and projection. A base layer of total magnetic intensity (TMI) for the merge was created using the regional government surveys, which were levelled to the Australia-wide 70 km spaced magnetic traverses (AWAGS) to retain the long spatial wavelengths. Holes were clipped into this grid and buffered to the shapes of the company surveys. The final merge with the company data was then performed to create the high resolution statewide TMI grid.

The TMI grid became the foundation to create a series of enhancements. Reduction to the Pole, First and Second Vertical Derivative, and Tilt Angle filters were applied to the TMI data, which were then reprojected into a suite of projections relevant for NSW. The final high-resolution imagery is now available on MinView, the GSNSW web-based data portal. The improvements are immediately visible, with far higher resolution of magnetic anomalies across the state, especially in regions with extensive company surveys. The additional resolution provides precise definition of geophysical signatures and geological structures at all scales and will lead to improved image interpretation for geological mapping and exploration targeting.

The urban geochemical baseline of Canberra: does it provide dirt on criminals?

Aberle, Michael¹, de Caritat, Patrice^{2,1}, McQueen, Ken¹, & Hoogewerff, Jurian¹

¹National Centre for Forensic Studies, Faculty of Science and Technology, University of Canberra, Canberra, Australia; ²Geoscience Australia, GPO Box 378, Canberra, Australia

Topsoil is a common material that may be transferred to people and objects prior to, during, or after perpetrating a criminal activity. Traditionally the use of soil material in law enforcement operations involves one-to-one comparison of recovered soil evidence with reference samples collected from known areas of interest. In casework and intelligence applications where this contextual information is not available, properties of the recovered evidence may be used to triage geographical regions as areas of low and high interest. If sufficient relevant spatial information is available, this approach may provide forensic intelligence to better focus operational resources on areas of interest. Here, spatial variability is both a strength and a weakness, with research required to determine (1) which parameters are sufficiently discriminatory at the chosen spatial scale, and (2) the effect of contributing anthropogenic and geogenic sources on forensic soil provenancing applications.

To investigate these issues, a high-density (1 site/km²) geochemical survey has been conducted to map the compositional variation of ~700 urban topsoil (0–5 cm depth) samples across Canberra, Australian Capital Territory. As a study location, Canberra represents a large city (population > 450k) with a system of urban open green spaces and bushland reserves, as well as minimal heavy industrial activity. Thus, in addition to law enforcement applications, the effect of urbanisation on the environment can be studied without significant masking by industrial pollutant sources. Using standard protocols for urban geochemical surveys, including extensive quality control measures, the samples have been prepared in a fusion flux matrix and characterised for bulk elemental geochemistry using X-Ray Fluorescence and Inductively Coupled Plasma-Mass Spectrometry analysis of total acid digests. Bulk mineralogy has been determined on a subset of samples using powder X-Ray Diffraction.

The results demonstrate that the geochemistry of the topsoils is strongly influenced by the dominant lithological units of the underlying bedrock. While the concentrations of known anthropogenic elements are mainly below thresholds for health-based investigation (with 1 or 2 sites marginally at threshold), there is evidence of diffuse anthropogenic contributions, particularly in older suburbs and light industrial areas.

For provenancing applications, a number of different approaches have been suggested to 'match' a recovered sample to a map. Typically, these involve comparing the properties of the recovered sample to those in each 'target' survey grid cell and attributing statistical significance to some measure of 'overlap' at an arbitrary inclusion/exclusion threshold (e.g., 95%). By instead comparing each grid cell to a series of questioned samples from within and outside the survey boundary and weighing each probability by the probability of observing the grid cell value in the total dataset in a likelihood ratio approach, we have demonstrated that regions of interest may be reduced in a more conservative manner better suited to forensic provenancing than previous approaches.

Further merits and challenges of provenancing topsoil from urban environments will be presented, notably the significance and impact of displacement and introduction of topsoil material from other areas on developing forensic soil surveys, as well as determining the source of questioned samples.

EARTH OBSERVATIONS & MODELS

Data-driven and computational methods to reveal hidden or changing surfaces

Bayesian inversion of 3D groundwater flow within the Sydney-Gunnedah-Bowen Basin

Mather, Ben¹, Müller, Dietmar¹, O'Neill, Craig², & Moresi, Louis³

¹*EarthByte Group, School of Geoscience, The University of Sydney, Camperdown, NSW, Australia;*

²*Department of Earth and Environmental Sciences, Macquarie University, North Ryde, NSW, Australia;*

³*Research School of Earth Sciences, Australian National University, Canberra, ACT, Australia*

In the driest inhabited continent on Earth, aquifers of the Sydney-Gunnedah-Bowen Basin are essential for Australian agriculture production, yet they experience progressively declining water level trends. In addition, groundwater discharge from the basin into the coastal ocean, a process now widely recognised as being important for providing significant inputs of nutrients and solutes to the oceans, has never been modelled. We have constructed a 3D Bayesian numerical groundwater flow model spanning the entire width and depth of this continent-scale basin. Our model assimilates groundwater recharge rates from water chloride concentrations, and borehole temperature measurements to constrain hydrothermal flow within the basin. We show that inland aquifers exhibit slow flow rates of 0.5 cm/day, resulting in a groundwater residence time of approximately 383 thousand years. In contrast, coastal aquifers have flow rates of approximately 30 cm/day, and a groundwater residence time of just 182 years. Our open-source modelling approach can be extended to any basin and help inform policies on the sustainable management of groundwater. In the future, our approach will enable time-dependent modelling of groundwater flow in response to uplift, erosion and climate change.

Mapping subglacial sedimentary basin distribution in Antarctica using Random Forest method

Li, Lu, Aitken, Alan, Lindsay, Mark, & Jessell, Mark

The School of Earth Sciences, The University of Western Australia, Perth WA, Australia

Antarctica preserves the largest ice sheet in the world, which has a potential contribution to future sea-level rise up to 60 m. Understanding subglacial sedimentary basin distribution is essential for studying ice sheet behaviour, as it forms an important basal boundary condition for ice sheet dynamics. It also records the geological history for tectonic evolution and past ice sheet behaviour. However, the subglacial sedimentary basin distribution is poorly known in Antarctica. A map of sedimentary basin distribution is a prerequisite to improving understanding of current and past ice sheet behaviour, aiding to project future ice sheet change and sea-level rise.

In this study, we present a sedimentary basin distribution likelihood map for Antarctica using the supervised machine learning method Random Forest. We apply this to generate a model based on the current understanding of Antarctica bedrock type distribution. We label the sedimentary basin and crystalline basement distribution driven from sparse rock outcrops, seismic imaging, and potential field data interpretation. Evidence layers are chosen from the available continental-scale geophysical datasets. By applying variable importance selection, we remove the unimportant and highly correlated evidence layers. After that, a strata sample process ensured a balanced class of each bedrock type during the training process. A sedimentary basin distribution map is then spatially predicted. The model accuracy is evaluated based on block cross-validation to overcome the underestimate of prediction error in the spatial correlated geophysical data.

Our results confirm the existence of previously documented subglacial sedimentary basins in Antarctica, and in general define the margins and extents of sedimentary basins in more detail. Specifically, in West Antarctica Rift System, the model delimits boundaries between sedimentary basins and volcanic rocks. We find a potential sedimentary basin preserved in Byrd Subglacial Basin, which is highly likely contributing to the currently fast flow in Thwaites Glacier. Further, our model shows more widely distributed subglacial sedimentary basins in East Antarctica than been previously recognized. Properties of geophysical and remote sensing data in Recovery Glaciers suggest a high probability of sedimentary basin preservation.

The AuScope Geochemistry Network and AusGeochem

Dalton, Hayden¹, Prent, Alexander M.², Boone, Samuel C.¹, Florin, Guillaume³, Greau, Yoann³, McInnes, Brent I. A.², Gleadow, Andrew¹, O'Reilly, Suzanne Y.³, Kohn, Barry P.¹, Matchan, Erin L.¹, Alard, Olivier³, Rawling, Tim⁴, Kohlmann, Fabian⁵, Theile, Moritz⁵, & Noble, Wayne⁵

¹*School of Earth Sciences, University of Melbourne, Melbourne, VIC 3010, Australia;* ²*John de Laeter Centre, Curtin University, Bentley, WA 6102, Australia;*

³*Department of Earth and Planetary Sciences, Macquarie University, NSW 2109, Australia;* ⁴*AuScope, University of Melbourne, Melbourne, VIC 3010, Australia;* ⁵*Lithodat Pty Ltd, Melbourne, VIC 3030, Australia*

In 2019, [AuScope](#), in response to a national expression of need for better organisation and coordination of geochemistry laboratories and data, established the AuScope Geochemistry Network (AGN). The AGN aims to foster and coordinate a national geochemistry laboratory infrastructure that incorporates earth science institutions across Australia in order to solve the national challenges of today and tomorrow. The AGN's goals include (but are not limited to): (i) promotion of capital and operational investments in new, advanced geochemical infrastructure, (ii) endorsing existing geochemical capability and supporting increased end user access to laboratory facilities across Australia, (iii) fostering collaboration and professional development via online tools, training courses and workshops, and

(iv) developing and maintaining a [FAIR](#) Australian geochemistry data ecosystem capable of hosting a diverse suite of geochemistry and geochronology data ([AusGeochem](#)). The AGN is led out of Curtin University with partner 'nodes' currently comprising The University of Melbourne and Macquarie University. The AGN actively encourages all Earth Science institutions from government, academia and industry, to [register their interest](#) in becoming a data contributing partner of the network and collaborate towards a national geochemistry infrastructure.

The AGN and collaborator [Lithodat](#) are making significant progress towards the goal of developing the AGN's data repository and platform, AusGeochem, to become the interface between the institutional, collaboration and public domains, facilitating laboratory data upload and dissemination. Using AusGeochem, institutes and geoscientists will be able to upload, disseminate and publish their datasets while maintaining data privacy control and plot and synthesise their data within the context of a wealth of publicly funded geochemical data aggregated by all data contributing partners.

The AGN is working with a number of Expert Advisory Groups (EAGs) to build common technique specific interlaboratory metadata templates and data models, currently for SHRIMP U–Pb, LA-ICP-MS U–Pb and Lu–Hf, Ar/Ar, fission track and (U–Th–Sm)/He, with expansion to more data types on the horizon. Comprising geochemical specialists from across Australia, the EAGs are providing invaluable advice regarding data reporting best practices, data quality assessment and visualisation tools to be incorporated into AusGeochem. The AGN has also been teaming up with the Australian Research Data Commons ([ARDC](#)) to integrate [International Geo Sample Number](#) (ISGN) minting capabilities into AusGeochem, allowing users to simultaneously mint their samples when uploading their data into the platform.

The AGN plans to grow its network and to continue engagement with the geoscience community through its [monthly webinar series](#) and hosting national workshops to share best practice and foster new collaborations across Australia.

Resolving multidisciplinary challenges of seamless integration of data on people, business, and the environment through applying a Discrete Global Grid System Framework

Crossman, Shane

Geoscience Australia, Canberra, Australia

Increasingly, crisis situations require the ability to rapidly integrate diverse data from many sources: this is essential for timely and effective delivery of complex solutions to enable effective decision and policy making. Solutions commonly have to simultaneously cover multiple diverse use cases (e.g., social, environmental and economic) and be transparent, verifiable and trusted. The 2020 Australian bushfire crisis and the global COVID-19 pandemic are examples of these complex crisis events.

The unifying factor for these events is location: everything is happening somewhere at some time. Inconsistent representation of location (e.g.,

coordinates, statistical aggregations and descriptions) and the use of multiple techniques to represent the same data creates difficulty in spatially integrating multiple data streams often from independent sources and providers. A Discrete Global Grid System (DGGs) is developed through OGC emerging cutting-edge technology. It provides a common framework capable of integrating very large, multi-resolution and multi-domain datasets together, and is a very efficient way of handling multiple data streams. The DGGs is changing the way how spatial data are enabled leading to an endless range of diverse and powerful data integration possibilities.

The DGGs aims to greatly increase the amount of location intelligence by flexibly linking big and small data in multiple formats, types and structures, and provides a framework for quick, reliable, repeatable, reusable infrastructure and codes. It fosters cross community collaboration and facilitates quick responses to stakeholder needs and for multiple use cases.

This paper will outline how Geoscience Australia and its partners implement the DGGs to address cross-portfolio needs around location-based data to provide a consistent way for seamless integration of data on people, business, and the environment. Two use cases will be highlighted:

1. Providing a good analytical basis to understand the environmental health issues such as human vulnerability during extreme natural events such as heatwaves, and
2. Allowing for rapid and repeatable analysis of cross-portfolio information and decision making in response to devastating events of the 2020 Australian Bushfires.

FAIR Metadata as a tool for consistent data findability and access

Bastrakova, Irina¹

Geoscience Australia, Canberra, Australia

In the era of overwhelming amounts of data and information being readily available over the web and other media sources it is vitally important to adopt machine-to-machine readable techniques that enable quick, reliable and repeatable resource discovery and then based on rules and definitions, facilitate determination as to whether the data and information are relevant and fit for purpose. Quality metadata can provide such a tool as:

- It allows the creation of multiple discipline specific metadata profiles based on international generic standards to improve data management and interoperability
- Through cross-walks to other community defined standards, it can be easily translated and used by multiple communities
- It enables the user to understand the data, its purpose, suitability and usability by capturing the history of acquisition and subsequent transformations, the description and evaluations of data quality, and the data dictionaries used
- It helps improve data discoverability on the web and also trace its usage and incorporation in derivative products

- It records and explains how to access and use data by related services, APIs and other tools

Australian and New Zealand Metadata Working Group (ANZ MDWG) has been working on development consistent methods of implementing such tool across disciplines, communities and sectors to facilitate a conversation, support a wider understanding and consistent application. The current focus of the group is on development of improving interoperability and consistency of data management and description through developing discipline specific profiles and ontologies.

This presentation will examine how FAIR Metadata can assist data managers and users to resolve challenges of data findability, accessibility, interoperability and reusability.

Building foundation spatial data

Crossman, Shane

Geoscience Australia, Canberra, Australia

The national mapping function within Geoscience Australia is undergoing significant change as it positions itself for the future. This is driven by the need to deliver on the Geoscience Australia 2028 Strategy, changes in technology and a need to deliver Foundation Data more consistently and efficiently to our users. The 2019–2020 Bushfires and the 2020 COVID-19 Pandemic have also emphasised the need for improvements in common operating pictures throughout government to enable faster and smarter planning, decision making and recovery support in times of crisis. These changes will help us provide the data and tools to facilitate this more effectively.

Geoscience Australia key outcomes for a foundation spatial data will include,

- Geoscience Australia to develop a nationally consistent common operating picture for Location Information.
- Supports Australia's national challenges, such as bushfires and global pandemic.
- Internal changes to focus resources on the challenge, fundamental changes to the way we source and store data.
- Improve the way we inform the users of ANZLIC's Foundation Spatial Data Framework in terms of quality and accessibility (Findable, Accessible, Interoperable and Reusable FAIR principal).
- Program to initially focus on Transport and Physical Infrastructure.

Digital regolith mapping from integrated sources of LiDAR data and historical imagery – a case study in Hong Kong

Hou, Wenzhu¹, Tsui, Wing Sum Regine¹, & Hart, Jonathan Roy¹

GeoRisk Solutions Ltd., Sheung Wan, Hong Kong

Knowledge of regolith types and distribution forms a key component of a geomorphological model. For engineering projects in Hong Kong, conventional methods widely used for regolith mapping include aerial photograph interpretation (API) together with ground 'truthing' by direct field observations. However, these

techniques can be time consuming, and information obtained in the field is constrained by cost and accessibility. Regolith mapping from API is highly subjective, being dependent on the interpreter's experience, and is constrained by photo quality, vegetation cover, cloud cover and shadow. Furthermore, although there are significant aerial photograph resources available in Hong Kong, in many countries this is not the case.

This paper describes an alternative method of regolith mapping for a landslide hazard assessment project in Hong Kong, using the latest available digital resources on an ArcGIS platform. A number of digital resources, particularly a territory-wide airborne LiDAR survey, are now available in Hong Kong and are being used increasingly to enhance conventional methods. However, the DEM derived from LiDAR only provides spatial information and lacks spectral information needed for ground modelling. Therefore, an integrated approach combining spectral and spatial data is used to establish a preliminary geomorphological model, which can be done quickly and at minimal cost at an early stage of a project. This digital method maps regolith automatically using image classification tools in ArcGIS, and is based on a multiband raster, including a raster from greyscale aerial photos, and rasters from the DEM.

The Hong Kong Government recently completed high-accuracy georeferencing of photos taken in 1963 when the vegetation cover in many parts of the territory was extremely low, providing an excellent record of the surface conditions. This monochromatic imagery was used as one band in the multiband raster. A territory-wide, airborne LiDAR survey was carried out in 2010 and a DEM of 0.5 m resolution or better is available from this survey. Under the alternative method described in this paper, three spatial rasters (slope gradient, surface roughness ^[1] and landform classification), were generated from the DEM, and combined with the first band to form the multiband raster. The slope gradient raster is used as an indicator of regolith type given that steep slopes reflect transportational processes whereas gentle slopes reflect depositional processes. An enhanced topographic position index method was adopted for landform classification ^[2]. Five regolith categories (rock, saprolite, slope colluvium, valley colluvium and taluvium), based on limited field knowledge, were annotated on the multiband raster for training the classifier. The multiband raster was then classified to automatically map regolith using this trained classifier. The results were extremely encouraging despite relatively limited training samples. By combining spectral and processed spatial rasters, the alternative method produced a good regolith model closely matching that developed using conventional methods. The method can be tested elsewhere with different digital resources to develop good quality, cost-effective, early-stage geomorphological models.

[1] Garriss, R. N. (2019). Modeling Surface Roughness as an Indicator of Age and Landslide Susceptibility, and the Spatial Inventory of Prehistoric Landslides: Green River Valley, Washington. <https://doi.org/10.15760/etd.7051>

[2] De Reu, J., Bourgeois, J., Bats, M., Zwertvaegher, A., Gelorini, V., De Smedt, P., ... & Van Meirvenne, M. (2013). Application of the topographic position index to heterogeneous landscapes. *Geomorphology*, 186, 39–49.

Parallel coordinate visualisations for knowledge generation in the geosciences

Reading, Anya^{1,2,3}, Morse, Peter^{2,3}, & Staal, Tobias^{2,3}

¹*School of Natural Sciences (Physics), University of Tasmania, Hobart, Australia;* ²*School of Natural Sciences (Earth Sciences, CODES), University of Tasmania, Hobart, Australia;* ³*Institute for Marine and Antarctic Studies, University of Tasmania, Hobart, Australia*

Parallel Coordinate Visualisations (PCVs) are a powerful means of exploring multivariate, high-dimensional, numerical datasets. Their great strength is the ability of such plots to reveal relational patterns in data that would be hard to identify using conventional geostatistical tools such as scatter plots. Although high-dimensional datasets are commonplace in the geosciences, PCVs have had limited previous usage for addressing questions related to the Earth and environment. Practical considerations such as the ordering of axes, and the need to change and experiment with such ordering, leads to difficulties in usage with PCVs as static plots. A productive way forward is to make use of interactivity, now enabled in many plotting environments. Thus, PCV plots can be handled in a dynamic way, enabling the exploration of data through high dimensions as originally intended.

This presentation illustrates the process of knowledge generation using PCVs for geoscience examples at two scales. In the first example, a dataset produced by a rock sample map generated by Laser Ablation ICP-MS analysis is explored. We show that while some patterns shown in the PCV are evident in the maps for individual masses (elements) the PCV also reveals previously unseen patterns. In the second example, a large-scale dataset, a multilayer geophysical compilation from Antarctica relational patterns are shown that can be taken forward from this reconnaissance analysis to more detailed study by conventional means. Interactive PCV plots may be manipulated on a conventional desktop display screen, however, extended reality (XR, immersive) platforms may also be used. We review the benefits of using this technology, and in particular the types of datasets for which the (relatively small) additional investment might be useful. We find that interactivity is vital to the successful use of PCVs. Up to 3–4 most evident data relations are readily revealed by interactive desktop displays and the XR platforms enable reconnaissance of up to twice that number of relational patterns, should they be present in the data. In summary, PCVs are a useful addition to the geoscientific tool box provided the analyst can make use of an interactive desktop display. The use of XR may be indicated if there is a need to identify more subtle relations in the presence of other dominant relational patterns.

Geophysical inversion through ensemble optimization

Scheiter, Matthias, Valentine, Andrew, & Sambridge, Malcolm

Research School of Earth Sciences, Australian National University, Canberra, Australia

In geophysics, most inverse methods fall into one of two categories: optimization, where a single solution is found through gradient descent, or ensemble inversion

methods such as Markov chain Monte Carlo, where one or more best-fitting regions in model space are identified. Both of these classes have their drawbacks: optimization algorithms often find local rather than global optima, and ensemble methods are known for their high computational cost. In this presentation, we devise a new framework for geophysical inversion in which an ensemble of solutions is produced through optimization.

Our framework consists of three building blocks: a generator function that proposes models, either deterministically or probabilistically, a forward operator that simulates synthetic data for those models, and a discriminator function that somehow assesses the similarity of synthetic and observed data – either by comparing individual examples, or by looking at the overall properties of ensembles. The generator and discriminator can have adjustable parameters that are optimized with traditional gradient descent methods. After convergence, the generator can be used to sample an arbitrarily large number of models, forming regions in model space that explain the observed data and their uncertainty. The discriminator can be any pre-defined or evolving misfit measure.

In the simplest case, the generator could be identified as a function returning a single model, and the discriminator could be a L2 misfit measure. In this way, established optimization methods can be seen as a special case of this framework. As another example, the generator and discriminator can be neural networks and trained in an adversarial manner, as in generative adversarial networks. This provides a large degree of flexibility to find a meaningful model ensemble representing the solution of the inverse problem. The new framework combines the merits of finding an ensemble of solutions with the computational efficiency of optimization algorithms.

Data-driven tectonic regionalization of Antarctica: appreciate the similarity

Stål, Tobias^{1,2}, Reading, Anya M.^{1,2}, Cracknell, Matthew J.¹, Halpin, Jaqueline A.², Latto, Rebecca B.¹, Morse, Peter E.¹, Turner, Ross J.¹, & Whittaker, Joanne M.²

¹*School of Natural Sciences, University of Tasmania, Hobart, Australia;* ²*Institute for Marine and Antarctic Studies, University of Tasmania, Hobart, Australia*

Antarctica is the continent with the least constrained lithospheric architecture. Geophysical and geological data are sparse, and often associated with larger uncertainties than elsewhere. Such limitations have challenged the robustness of global tectonic regionalization models and schematic continental scale geological maps in Antarctica. Some published crustal models simply exclude high latitudes.

We collect an ensemble of robust datasets that covers the Antarctic continent. We match those Antarctic observables with global compilations to detect the most similar geological and tectonic setting. Most datasets are derived from satellite potential field surveys, seismic surface wave tomography and geological observations. We aim to take advantage of all and any existing data for Antarctica with a reasonable coverage and quality, and with a global equivalent reference observable.

The degree of similarity between Antarctic locations and global reference locations is used to generate a similarity rating map. We use this map to extract the suggested segment type classes from a number of published global tectonic regionalization models. The uncertainty of classification is expressed as information entropy for each location in Antarctica.

We present a number of tectonic regionalization models for Antarctica that can replace or extrapolate the global counterpart for high latitudes. Reference global models used include legacy studies, seismic segmentation, and lithological maps.

Compressive inversion in an overcomplete basis

Turunçtur, Buse, Valentine, Andrew, & Sambridge, Malcolm

Research School of Earth Sciences, Australian National University, Canberra, Australia

The concept of compressive sensing has promised a revolution in data collection. Rather than a traditional sampling of a temporal or spatial signal with uniformly distributed samples, compressive sensing enables an exact recovery of the signal with fewer but randomly chosen samples. Provided that the target signal is 'sparse', i.e., has only a few non-zero Fourier components, it can be recovered with high fidelity using inversion algorithms designed to minimize the L_1 norm of the recovered solution. Compressive sensing allows signal recovery beyond the Nyquist limit, allowing high-frequency information to be recorded using relatively few samples.

We aim to adapt this concept to suit inverse problems of the form commonly encountered in geophysics. To guarantee that models have a sparse representation, we employ an 'overcomplete' basis, comprising a complete set of functions with global support, and

another complete set with local support. We compare results for L_1 - and L_2 -regularised inversion in synthetic examples and show that the former enables excellent recovery of input models. We suggest that this concept has a variety of promising applications in geophysics, including low-artefact imaging of systems containing features at multiple scale lengths, and image denoising.

Detrital zircon facies of the Amadeus Basin, central Australia

Verdel, Charles

Northern Territory Geological Survey, Alice Springs, Australia

The Amadeus Basin of central Australia has one of the most well-characterised detrital zircon records in the world. Detrital zircon samples span not only the full stratigraphic range of the basin but are also distributed across its areal extent. These data therefore capture both stratigraphic variability in zircon age populations that may arise from, for example, orogenic uplift and erosion, as well as lateral variability related to proximity to basement exposures of different age (in the case of the Amadeus Basin, the adjacent Musgrave Province to the south, and the Aileron and Warumpi provinces to the north). New detrital zircon results from the Northern Territory Geological Survey have been combined with previous data to generate detrital zircon facies maps of the Amadeus Basin that illustrate both stratigraphic and spatial variability in detrital zircon age distributions. Comparison with data compilations from other basins highlight some of the key features of the Australian detrital zircon record.

Next generation 3D geological modelling – development and applications

LoopStructural 1.0: Time aware geological modelling

Grose, Lachlan¹, Ailleres, Laurent¹, Laurent, Gautier², & Jessell, Mark³

¹*School of Earth Atmosphere and Environment, Monash University, Melbourne 3800, Australia;*

²*Université d'Orléans, CNRS, BRGM, ISTO, UMR 7327, Orleans France;* ³*Mineral Exploration Cooperative Research Centre, School of Earth Sciences, UWA, Perth, Australia*

LoopStructural is a new open-source 3D geological modelling python package (www.github.com/Loop3d/LoopStructural). Geological features are encoded into the geological model using a time aware approach where the relative timing of different deformation features is used to help construct complicated geometries. We use structural frames which are curvilinear coordinate systems based around the major structural feature (e.g., fold axial surfaces, fault surfaces), structural direction (e.g., fold axis, fault slip direction) and where necessary an intermediate direction (e.g., fault extent). This allows for folds and faults to be integrated into the description of the geological features in the implicit models. In this contribution we will use *map2loop* to automatically extract and augment input data from open access geological datasets from Geological Survey of Western

Australia from the Hamersley Basin. The model area will include consists of upright refolded folds of Archean and Proterozoic stratigraphy over-lying an Archean basement. The folded stratigraphy is overprinted by NW–SE-trending faults. In the model the fault network is modelled first using observations of the fault trace using the estimated displacements from the geological map. The folded stratigraphy is then modelled by building a fold frame that characterises the geometry of the axial surface and the fold axis direction. The fold geometry is modelled by fitting curves representing the fold axis geometry in the axial surface and the fold geometry looking down plunge. We show that by using the fold constraints the geometry of the modelled folds are consistent with the geometries drawn in cross sections.

LoopResources – reducing the mining footprint

Ailleres, Laurent¹, Grose, Lachlan¹, Caumon, Guillaume², & Jessell, Mark³

¹*School of Earth, Atmosphere and Environment, Monash University, Melbourne, Australia;* ²*RING, Université de Lorraine, Nancy, France;* ³*CET, University of Western Australia, Australia*

Loop is a OneGeology initiative, initiated by Geoscience Australia and funded by Australian Territory, State and Federal Geological Surveys, the ARC and the MinEx CRC with the participation of BHP, Anglo American, GSWA and Micromine. The project is led by Monash University and involves research groups from the University of Western Australia, the RING consortium at the Université de Lorraine, Nancy, France and RWTH Aachen in Germany. In-kind research is also provided by Natural Resources Canada (Geological Survey of Canada), Geoscience Australia, the British Geological Survey and the BRGM.

We have implemented the use of all structural geological data (e.g.: fault kinematics, fold axial surfaces, fold axes, deformational overprinting relationship) in the modelling process. We have automated the building of 3D geological models from geological survey served geological data including automatic geological map topological analysis and geological history building. As a proof of concept, users can now draw a polygon on a map and generate 3D models in just a few minutes using the `map2loop` and `LoopStructural` libraries. (github.com/Loop3D/LoopStructural & github.com/Loop3D/map2loop-2)

We are integrating geophysical constraints and modelling as early as possible in the modelling workflow. Model uncertainty is characterised and an integral part of the modelling process. We are in the process of generalising the use of Bayesian modelling to 3D structural geological modelling.

The main outcome of the development of the structural modelling method (`LoopStructural`) is the definition of structural frames. A structural frame is interpolated throughout the entire modelled volume and is associated to each structural event or object and their corresponding finite strain axes. Each fault has a structural frame (Fig. 1) based on the geometry of the fault (faults are not necessarily planar) and the damage zone defined by an ellipsoid representing the decay of the offset in all directions (slowest decay along the

throw direction). A fold event has a structural frame defined by a direction normal to the axial surface foliation, a direction parallel to the fold axis and the last axis is parallel to the extension direction. Combining these different events, in a time-aware manner, is the essence of `LoopStructural`.

`LoopResources` will be the property estimation library for the Loop platform. During modelling, the time-aware application of structural frames results in the implicit definition of a curvilinear rectangular coordinate system everywhere in the model and conformable to geological layering. Using this deformed cartesian coordinate system, we propose to adapt geostatistical and interpolation methods (e.g., kriging) to curvilinear coordinate systems. This will ensure that lithological anisotropies are enforced during resource estimation and property modelling.

The proposed outcomes improve significantly on current capabilities and will provide a machine-supported decision system for (1) improved domaining, (2) optimal definition of ore blocks of consistent ore grades, geotechnical properties, and crushing requirements, (3) optimal extraction, crushing and processing costs, and (4) increased recovery rates.

In essence, building a much better digital-twin representing the geology, distribution of resources, the geometallurgical and geotechnical characteristics of a mine will ensure better mining of deposits and ultimately better mine footprint.

Reproducible 3D model construction using `map2loop`

Jessell, Mark¹, Ogarko, Vitaliy², Lindsay, Mark¹, Joshi, Raneer¹, Piechocka, Agnieszka^{1,5}, Grose, Lachlan³, de la Varga, Miguel⁴, Fitzgerald, Des⁶, Aillères, Laurent³, & Pirot, Guillaume¹

¹*Mineral Exploration Cooperative Research Centre, Centre for Exploration Targeting, School of Earth Sciences, UWA, Perth, Australia;* ²*International Centre for Radio Astronomy Research, UWA, Perth, Australia;* ³*School of Earth, Atmosphere and Environment, Monash University;* ⁴*Computational Geoscience and Reservoir Engineering, RWTH Aachen, Germany;* ⁵*CSIRO, Mineral Resources – Discovery, ARRC, Kensington WA, Australia*

The advent of digital geological maps has not been matched by an uptake of analysing the structural data contained within. At the regional scale, the best predictor for the 3D geology of the near-subsurface is often the information contained in a geological map. This remains true even after recognising that a map is also a model, with all the attendant hidden biases 'model' status implies. The difficulty in reproducibly preparing input data for 3D geological models has created a demand for increased automation in the model building process. The information stored in a map falls into three categories of geometric data: positional data such as the position of faults, intrusive and stratigraphic contacts, gradient data, such as the dips of contacts or faults and topological data, such as the age relationships of faults and stratigraphic units.

We present two Python libraries (`map2loop` and `map2model`) which combine all these observations with conceptual information, including assumptions regarding the subsurface extent of faults and plutons to

provide sufficient constraints to build a reasonable 3D geological model. These algorithms allow automatic deconstruction of a geological map to recover the necessary positional, topological and gradient data as inputs to different 3D geological modelling codes. This automation provides significant advantages: it significantly reduces the time to first prototype models, it produces reproducible models for the same source data, it clearly separates the primary data from subsets produced from filtering via data reduction and conceptual constraints, and provides a homogenous pathway to sensitivity analysis, uncertainty quantification and Value of Information studies. We use examples of the folded and faulted terrains across Australia to demonstrate a complete workflow from data extraction to 3D modelling using three different 3D modelling engines: *GemPy*, *LoopStructural* and *3D GeoModeller*.

We acknowledge the support of the MinEx CRC and the Loop: Enabling Stochastic 3D Geological Modelling (LP170100985) consortia. The work has been supported by the Mineral Exploration Cooperative Research Centre whose activities are funded by the Australian Government's Cooperative Research Centre Programme. This is MinEx CRC Document 2020/48.

Propagation of data and algorithmic uncertainty based on borehole calibration and perturbation – a sensitivity analysis

Pirot, Guillaume¹, Lindsay, Mark¹, Grose, Lachlan², de La Varga, Miguel³, & Jessell, Mark¹

¹Centre for Exploration Targeting, The University of Western Australia, Crawley, Australia; ²School of Earth, Atmosphere and Environment, Monash University, Clayton, Australia; ³Institute for Computational Geoscience and Reservoir Engineering, RWTH Aachen University, Aachen, Germany

Subsurface modelling is a challenge because we have a limited access to direct observations of the desired quantities of interest and because we have an imperfect understanding of geological processes. Thus, each model realization is quite uncertain. This is why we need to consider both our sources of errors and alternative modelling schemes. In order to avoid uncertainty underestimation when the purpose of modelling is decision-making, uncertainties related to observations, algorithms and conceptual representations should be propagated in the generation of stochastic geological realization ensembles.

Here, we focus on the sensitivity of data and algorithmic uncertainties on the resulting geological uncertainty. Indeed, it might not make sense to compare a pie with a cake or a mousse. This is why we leave conceptual uncertainty aside and in the hands of model selection techniques. While data errors can be estimated by repeating some measurements, algorithmic uncertainties might be more complex to define and are not always accessible. To handle that, we propose to rely on the use of pilot-stick perturbations, which consists in adding fictive drill-holes complying with the assumed stratigraphy and the presence or absence of surface geological information.

To illustrate the method, we perform a sensitivity analysis of the perturbations on a synthetic case, based on a Precambrian basin setting, with three different geological modelling engines. The resulting geological

uncertainty is analysed with different indicators based on the cardinality, entropy, connectivity, topology and geostatistics of both lithological formations and their underlying scalar-fields. Preliminary results show the pre-dominant importance of pilot-stick perturbations and their ability to mitigate the smoothing resulting from implicit modelling, in particular at locations where no surface data is available.

This work is supported by the ARC-funded Loop: Enabling Stochastic 3D Geological Modelling consortia (LP170100985) and DECRA (DE190100431) and by the Mineral Exploration Cooperative Research Centre whose activities are funded by the Australian Government's Cooperative Research Centre Programme. This is MinEx CRC Document 2020/46.

Morphological gravity inversion to refine geological models

Giraud, Jeremie Eugene Cyril^{1,2}, Lindsay, Mark^{1,2}, & Jessell, Mark^{1,2}

¹Centre For Exploration Targeting, School of Earth Sciences, University of Western Australia, Crawley, Australia; ²Mineral Exploration Cooperative Research Centre, School of Earth Sciences, University of Western Australia, Crawley, Australia

We present a geophysical inversion technique designed for the recovery of the geometry of rock units in 3D. It relies on the iterative adjustment of the location of interfaces between homogenous rock units implicitly defined by the signed-distance to each contact. We formulate the inverse problem using a generalized level-set method capable of dealing with any number of rock units. Our implementation uses a deterministic least-squares inversion framework. It is flexible and allows the incorporation of prior geological information such as the location, shape and aspect ratio of rock units in the regularisation function and to adjust the thickness of the interface between them. While the utilisation of this algorithm focuses on adjusting pre-existing geological models to honour geophysical data it also supports topological changes during the inversion. We first explore the capabilities of the proposed inversion approach using noisy synthetic gravity data and perform the proof-of-concept. We then model field gravity data from the northeastern part of the Yerrida Basin (Western Australia) to model the geometry of a prospective greenstone belt that previous studies highlighted as requiring further investigation.

The synthetic example demonstrates the capability of the proposed method to improve the recovery of the geological bodies' geometry and to change the initial geological model's topology to honour the geophysical measurements. The application to real world data allows suggests revision of the accepted tectonic setting and structure is required. In particular, results suggest that the undercover mafic greenstone belt may be shallower and thinner than predicted by surface geology alone, perhaps influenced by previously unidentified deep-penetrating structure.

We acknowledge the support of the MinEx CRC and the Loop: Enabling Stochastic 3D Geological Modelling (LP170100985) consortia. The work has been supported by the Mineral Exploration Cooperative Research Centre whose activities are funded by the Australian Government's Cooperative Research Centre Programme. This is MinEx CRC Document 2020/xx.

LoopStructural 1.0: Time aware geological modelling

Grose, Lachlan¹, Ailleres, Laurent¹, Laurent, Gautier², & Jessell, Mark³

¹*School of Earth Atmosphere and Environment, Monash University, Melbourne 3800, Australia;* ²*Université d'Orléans, CNRS, BRGM, ISTO, UMR 7327, Orleans France;* ³*Mineral Exploration Cooperative Research Centre, School of Earth Sciences, UWA, Perth, Australia*

LoopStructural is a new open-source 3D geological modelling python package (www.github.com/Loop3d/LoopStructural). Geological features are encoded into the geological model using a time aware approach where the relative timing of different deformation features is used to help construct complicated geometries. We use structural frames which are curvilinear coordinate systems based around the major structural feature (e.g., fold axial surfaces, fault surfaces), structural direction (e.g., fold axis, fault slip direction) and where necessary an intermediate direction (e.g., fault extent). This allows for folds and faults to be integrated into the description of the geological features in the implicit models. In this contribution we will use *map2loop* to automatically extract and augment input data from open access geological datasets from Geological Survey of Western Australia from the Hamersley Basin. The model area will include consists of upright refolded folds of Archean and Proterozoic stratigraphy over-lying an Archean basement. The folded stratigraphy is overprinted by NW–SE-trending faults. In the model the fault network is modelled first using observations of the fault trace using the estimated displacements from the geological map. The folded stratigraphy is then modelled by building a fold frame that characterises the geometry of the axial surface and the fold axis direction. The fold geometry is modelled by fitting curves representing the fold axis geometry in the axial surface and the fold geometry looking down plunge. We show that by using the fold constraints the geometry of the modelled folds are consistent with the geometries drawn in cross sections.

Automated subsampling of geological maps as inputs of 3D geological multiscale modelling: Yalgoo–Singleton Greenstone Belt example

Joshi, Ranee^{1,2}, Jessell, Mark^{1,2}, Lindsay, Mark^{1,2}, & Ivanic, Tim, J.³

¹*Centre of Exploration Targeting, School of Earth Sciences, University of Western Australia, 35 Stirling Highway, Crawley, WA 6009, Australia;* ²*Mineral Exploration Cooperative Research Centre (MinEx CRC), School of Earth Sciences, University of Western Australia, 35 Stirling Highway, Crawley, WA 6009, Australia;* ³*Geological Survey of Western Australia, Mineral House, 100 Plain Street, East Perth WA 6004, Australia*

To maximize the meaningful geological information provided by three-dimensional (3D) geological models, we propose producing dynamic geological models that allow data to be subsampled and dynamically

visualized to better answer specific scale-dependent geological questions. Given that most geological questions are scale-dependent, building a multiscale geological model would seem to be desirable. Achieving this aim requires developing workflows that properly subsample various forms of geoscientific data (e.g., lithology, stratigraphy, structure, geophysics) and dimensionalities (0D: point observations, 1D: drilling data, 2D: lines and polygons on maps and sections) to be able to use them appropriately as inputs for 3D geological modelling.

In this contribution, we present the preliminary results of subsampling 1:500 000 knowledge-rich geological data and their resulting multiscale models. The geological data, in the form of geological maps and structural measurements, were generated from recent regional geologic mapping of the western Youanmi Terrane, Yilgarn Craton, Western Australia by the Geological Survey of Western Australia (GSWA). The case study area for this work covers the Yalgoo–Singleton Greenstone Belt (YSGB), a mineralized, lithologically diverse and structurally complex area with regions of sparse and clustered data. The multiscale models are built through systematically subsampling the geological maps (ESRI shapefile format), to ensure 3D samples were representative and preserved heterogeneity. The geological maps are subsampled based on a combination of the stratigraphic hierarchy (derived from the GSWA Explanatory Notes System), prospective units and petrophysical contrasts. The polygonal features are upscaled by simplifying the geometry however, preserving the crucial vertices critical to preserving the shape and topology. The structural measurements (GSWA WAROX database) are subsampled depending on the scale of interest.

The resulting subsampled data is used as inputs into modelling applications. Multiple 3D geological models were built, 1:2 500 000 using craton/terrane information, 1:500 000 using rock group and suite levels and at 1:100 000 using rock units. These models show that stratigraphic filters maintain meaningful information at most scales. However, we show that particular combinations of filters is desirable. The suite of scaled models show that vertex simplification with a point reduction of up to 86% on the polygons maintains the geometric and geological constraints of the greenstone belts and plutons. The scaled geological models were built with minimal user-provided input and stayed true to the digital geoscientific inputs that describe the geology at all three scales. Our results from the 1:2 500 000 scale model indicate a need for additional depth constraints in the southwestern Youanmi Terrane (e.g., deep-reflection seismic data).

Preliminary results show the proof-of-concept that this workflow of subsampling geological vector maps effectively selects and identifies relevant geological features, aggregates features into hierarchical stratigraphic groups, simplifies 2D vectors by vertex reduction and extracts topological information, basal and intrusive contacts. The tools developed to subsample geological inputs for multiscale modelling are compiled as a part of the Python package *map2loop*.

We acknowledge the support of the MinEx CRC and the Loop: Enabling Stochastic 3D Geological Modelling (LP170100985) consortia. The work has been supported by the Mineral Exploration Cooperative

Research Centre whose activities are funded by the Australian Government's Cooperative Research Centre Programme. This is MinEx CRC Document 2020/42.

The New South Wales 3D wireframe model

Spampinato, Giovanni

Geological Survey of New South Wales, Department of Regional NSW, Maitland, Australia

Since 2014, the Geological Survey of New South Wales (GSNSW) has developed a series of interlocking 3D models of orogenic provinces, basins, major faults and depth of post-Carboniferous cover across the state. The aim of the program is to deliver an integrated, seamless 3D model that represents the fault architecture, major tectonic zones and the boundaries, structure and stratigraphy of orogenic provinces and basins. In June 2020, GSNSW released the first statewide New South Wales (NSW) 3D Wireframe Model.

The NSW 3D Wireframe Model illustrates the distribution of orogens together with associated tectonic domains and major faults that define the basement architecture of the state. Creating the model has drawn together and consolidated previous large-scale geological and structural interpretations. Constraining datasets include surface geological mapping, geological cross-sections, well data, digital elevation models, seismic, gravity and magnetic data, 3D models and 2D forward models.

The NSW 3D Wireframe Model establishes a fundamental statewide geological framework that will provide context for future 3D models. For example, the wireframe model will provide an upper crustal framework that will help inform and connect to deeper geological modelling of the lithosphere using geophysical data gained from the AusLAMP magnetotelluric and WOMBAT passive seismic surveys. At the smaller scale, in-fill 3D geological modelling will benefit from the regional baseline constraints provided by the wireframe model in much the same way that traditional detailed geological mapping is given context by regional geology.

This NSW 3D Wireframe Model will also serve as a template for a 3D printed physical model of the geology of NSW. This will be used as a hands-on educational tool for scientists, students, decision-makers and the general public.

The NSW 3D Wireframe Model is available for download via the GSNSW MinView web mapping application.

A new approach to integrate passive seismic HVSR depth models in magnetotelluric (MT) 1D inversion to characterize the cover-basement interface

Suriyaarachchi, Nuwan^{1,2}, Giraud, Jeremie^{1,2}, Seille, Hoel³, Jessell, Mark^{1,2}, Lindsay, Mark^{1,2}, Hennessy, Lachlan⁴, & Ogarko, Vitaliy⁵

¹Centre of Exploration Targeting, School of Earth Sciences, University of Western Australia, 35 Stirling Highway, Perth WA 6009, Australia; ²Mineral Exploration Cooperative Research Centre (MinEx CRC), School of Earth Sciences, University of Western Australia, 35 Stirling Highway, Perth, WA 6009,

Australia; ³CSIRO Deep Earth Imaging FSP, Australian Resources Research Centre, 26 Dick Perry Avenue, Kensington, WA 6151, Australia; ⁴Anglo American, Group Discovery and Geosciences, 201 Charlotte Street, Brisbane, QLD 4000, Australia; ⁵International Centre for Radio Astronomy Research, University of Western Australia, 35 Stirling Highway, Perth, WA 6009, Australia

Electromagnetic methods are useful tools to understand cover-basement interface in many aspects. They could provide valuable information to exploration targeting, mineral prospectivity mapping and in some cases. They can also provide volume constraints for groundwater and energy resource estimates with a fraction of the cost of drilling. In this study, we use passive seismic Horizontal to Vertical Spectral Ratios (HSVR) to reduce the uncertainties of detecting cover-basement contact in Magnetotelluric (MT) depth-resistivity models.

We invert MT apparent resistivity and phase using Occam's inversion algorithm to obtain resistivity-depth model. Generally, Occam's inversion produces the smoothest model that fits the observations (data) with a certain target misfit. But the smoothest model may not fully describe a realistic resistivity structure, such as thin resistivity layers and sharp resistivity contrasts (eg. impermeable basement), which is critical to identify the cover-basement transition and thus interface. For this study, we expect to control the MT depth-resistivity model smoothness (or roughness) without producing unrealistic models. For that, we brought forward the importance of detection of cover-basement interface prior to 1D MT inversion. Our approach is to use a prior interface-depth model to support interface prediction by adjusting the model roughness values in Occam's 1D inversion. This prior interface-depth model is generated from co-located or reasonably placed passive seismic-HVSR models, which give robust results to detect possible interfaces up to 1500 m depths.

To test our approach, we created a synthetic homogenous two-layer cover-basement case with 20 Ω m cover resistivity, 1000 Ω m basement resistivity and a cover-basement interface at 1000m depth. The 1D forward response (from 10^4 to 10^{-3} Hz) was calculated and 5% random noise was added to the synthetic data. Firstly, a cover-basement interface depth interval is estimated using synthetic HVSR model data. Then we performed 1D MT inversions. The inversions are regularized using a series of roughness penalty values ranging from 0 (no penalty) to 1.00 (maximum penalty) within this hypothetical cover-basement transition depth interval. Thinner MT depth mesh was used at the HVSR derived cover-basement interface region to identify accurate resistivity variations.

Preliminary results on the synthetic test show that the depth roughness penalty values between 0.05–0.25 reveal sharp resistivity contrasts consistent with the true depth to cover basement interface. We tested a spectrum of cover-basement depths and cover basement resistivity scenarios. We expect to test the procedure further for multi-layer synthetic cases and analysed the results statistically to validate our approach. Additional priori information, such as borehole data and stratigraphy data will be used to improve the HVSR-based constrain for the 1D MT (real data) inversion.

We acknowledge the support of the MinEx CRC and the

Loop: Enabling Stochastic 3D Geological Modelling (LP170100985) consortia. The work has been supported by the Mineral Exploration Cooperative Research Centre whose activities are funded by the Australian Government's Cooperative Research Centre Programme. This is MinEx CRC Document 2020/xxx.

IAN MCDUGALL SYMPOSIUM

Timescale of events around the Cretaceous–Paleogene Boundary: Links between the Chicxulub impact, Deccan volcanism, and the Cretaceous–Paleogene mass extinction

Sprain, Courtney J.¹, Renne, Paul R.^{2,3}, Clemens, William A.³, Wilson, Gregory P.⁴, Self, Steve³, Vanderkluisen, Loyc⁵, Pande, Kanchan⁶, Fendley, Isabel⁷, & Mittal, Tushar⁸.

¹University of Florida, Gainesville, FL, USA; ²Berkeley Geochronology Center, Berkeley, CA, USA; ³University of California-Berkeley, Berkeley, CA, USA; ⁴University of Washington, Seattle, WA, USA; ⁵Drexel University, Philadelphia, PA, USA; ⁶Indian Institute of Technology, Mumbai, India; ⁷University of Oxford, Oxford, UK; ⁸Massachusetts Institute of Technology, Cambridge, MA, USA

The Cretaceous–Paleogene boundary (KPB) mass extinction is one of the most important biotic turnover events in Earth history. This event is important to study for several reasons, the most relevant being its implications on our understanding of the effects of abrupt climate change. Although the temporal coincidence between the Chicxulub crater and the KPB has strongly implicated the impact as the main player in the mass extinction, the eruption of the Deccan Traps (DT) cannot be dismissed as a possible contributor. The timing of DT eruptions spans the KPB and, furthermore, the onset of DT volcanism roughly coincides with Late Cretaceous records of environmental change. Both the Chicxulub impact and DT volcanism have similar environmental forcing mechanisms, albeit acting on different timescales. Until recently, insufficient geochronology has made it difficult to tease apart effects from either agent.

To better understand the effects of both the Chicxulub impact and the DT in the KPB crises, we developed a high-precision chronologic framework that outlines the temporal sequence of biotic and climatic changes, and proposed perturbations, around the KPB using ⁴⁰Ar/³⁹Ar geochronology and paleomagnetism. This work was primarily conducted in two areas: the Hell Creek region of NE Montana, USA and the Deccan Traps, India. The Hell Creek region is one of the best-studied terrestrial KPB sites in the world. We developed a high-precision chronostratigraphic framework for fluvial sediments within the Hell Creek, using ⁴⁰Ar/³⁹Ar dating, magnetostratigraphy, and chemical finger-printing. This work constrained the timing of terrestrial faunal decline and recovery while calibrating North American Land Mammal Ages biostratigraphy. The coupling of our magnetostratigraphic sections and high-precision ⁴⁰Ar/³⁹Ar ages further allowed for calibration of the circum-KPB polarity chron (C29r) at unprecedented precision, enabling correlation of our record to other KPB records around the globe. To better understand the role of the DT in the KPB extinction, we developed high precision ⁴⁰Ar/³⁹Ar ages for >20 lavas ranging the entire DT stratigraphy.

Tying all of this work together, we are able to determine: (1) the decline in terrestrial faunas began between 400 ka and 150 ka pre-KPB, (2) terrestrial disaster faunas are constrained to the first ca 25 ka of the Paleogene, and recovery occurred gradually over the next 850 ka,

(3) over 90% of the DT volume was erupted in < 1 Ma, with 50–75% emplaced post-KPB, (4) the onset of volcanism is approximately coincident with the onset of pre-KPB warming, but despite this (5) pre-KPB records of climate change coincide temporally with the eruption of the smallest DT phases, suggesting that if the DT are the source of pre-KPB climate change, the release of climate-modifying gases cannot be directly related to eruptive volume as previously assumed. Overall, our new work highlights the close temporal relationship between the Chicxulub impact, Deccan volcanism, and the KPB. But more work is needed, specifically addressing Deccan volatile release and eruption tempo, in order to fully understand the impact of the DT on the Earth system and its role in the mass extinction.

Bitterroot and Anaconda Core Complexes: Cretaceous ductile flow and Eocene detachment faulting in the northern U.S. Rocky Mountains defined by Ar/Ar thermochronology

Foster, David A.

Department of Geological Sciences, University of Florida, Gainesville, Florida 32611, U.S.A.

The Bitterroot and Anaconda metamorphic core complexes of western Montana and central Idaho, U.S.A. were exhumed by Eocene extensional detachment faulting between about 53 and 38 Ma. The rocks in the lower plates of these core complexes include highly sheared Proterozoic to Palaeozoic metasediments, Cretaceous granitoids, and Eocene felsic plutonic rocks. Early exhumation of the core rocks occurred after crust of in the Montana hinterland was dramatically thickened (forming the “Montanaplan”) between about 130 and 80 Ma. By Late Cretaceous time the middle crust of the orogenic pile was plastically deforming, resulting in large-scale nappes and shear zones. Voluminous intermediate to felsic igneous rocks intruded the shear zones and formed sheet-like plutons at thrust ramps. Plastic flow led to ductile thinning of the middle crust coincident with out-wedging in the Montana fold and thrust belt. Rocks exposed in these two core complexes experienced about 5–10 km of exhumation in the Late Cretaceous on the basis of metamorphic assemblages, reconstruction of sections, and thermochronology of upper plate rocks. Eocene extension began in the Northern Rockies about 53 Ma and resulted in linked extensional detachments and magmatism in both core complexes. The Bitterroot complex underwent as much as 15 km of additional exhumation along a ductile to brittle detachment system that initiated with amphibolite facies mylonite. The Anaconda complex underwent about 10–12 km in the deepest part and records greenschist facies mylonite overprinted by transitional brittle-ductile fabrics, and brittle deformation. Ar/Ar mica cooling ages from both detachments decrease from west to east and constrain the rates of fault slip and unroofing. Exhumation of the middle crustal rocks was at least a two-stage process with significant Cretaceous–Paleogene thinning by ductile flow, followed by unroofing beneath the east-rooted detachment systems. Thermochronology data indicate that both detachment systems developed as composite structures with shallower crustal levels and less exhumation in the west rooting to about 10-km deeper to the east. The hanging wall of the Anaconda

complex includes the less-deformed Cretaceous Boulder batholith and related volcanic rocks, while hanging wall rocks of the Bitterroot complex, in the Sapphire Range, record Cretaceous exhumation and more limited Eocene unroofing.

⁴⁰Ar/³⁹Ar geochronology of syn-kinematic phengite reveals the tectonic history of underthrust European crust (W Alps): a synthesis

Yann, Rolland

EDYTEM, Université de Savoie Mont Blanc– CNRS, UMR 5204, Le Bourget du Lac, France.

The major problem of ⁴⁰Ar/³⁹Ar geochronology applied to deformation is often to find sufficiently large crystals that grew in a clear relationship to the deformation context, and that have been preserved in the following tectonic history.

The dating of white mica syn-kinematic fibres (phengite) in complement to their PT conditions (obtained by combined mineralogical mapping for instance) allows the dating of deformation stages at a depth constrained by PT calculations and along certain geothermal conditions. Kinematics of related shear zones provide the polarity of tectonic motions. The integration of such data into the tectonic framework of a geodynamic zone allow deciphering along-belt variations, which relate to strain propagation and changes in the stress field through time and space.

The External Crystalline Massifs (ECM) of the Alps provide a nice case example of a crustal domain in which this technique was successfully applied to the dating of brittle-ductile motions at mid-crustal levels (10–15 km). The Western Alps are a curved mountain belt that accommodated tectonic motions related to subduction dynamics in the Mediterranean domain after a brief period of continent–continent collision of the Apulian microblock with Eurasia. Subsequently, the timing and the along-belt variations of deformations has been progressive through time.

In this presentation, I propose a synthesis of analyses conducted at the External Alps scale to investigate the timing of shear zone deformation since the onset of Eocene–Oligocene collision. The data include ⁴⁰Ar/³⁹Ar stepwise dating of synkinematic phengites, the associated shear zone kinematics and thermo-barometric constraints on the depth and temperature of deformation. The advent of new dating approaches, based on U–Pb dating of syn-kinematic allanite, of hydrothermal vein monazite, and more recently, of calcite from veins and fault gouges, do confirm the timing of deformation suggested by the obtained ⁴⁰Ar/³⁹Ar ages on micas.

These dating constraints are used to discuss the timing of deformation of underthrust European crust related to changes in tectonic modes during the Alps tectonic history. These changes are related, at the larger scale, to the evolution of the Mediterranean domain, i.e., to the rapid underthrusting of the external part of European plate, dated in the ECM at 35–32 Ma, followed by the onset a mainly dextral strike-slip context. This strike-slip context is controlled by the anticlockwise rotation of Apulia, notably driven by the Apulian roll-back.

High resolution ⁴⁰Ar/³⁹Ar geochronology in continental margin settings – the Aegean plate margin as a natural laboratory for subduction processes

Wijbrans, Jan, Uunk, Bertram, de Paz Álvarez, Manuel, Huybens, Rosanne, & Brouwer, Fraukje

Department of Earth Sciences, Vrije Universiteit Amsterdam, the Netherlands

Time scales of tectonic and metamorphic processes in the greenschist–blueschist domain are essential to better understand the dynamics of accretionary wedges. However, such time scales are difficult to obtain because the number of geochronometers available to us is limited. For these geochronometers only partial setting, or resetting, of the isotopic clocks can be expected at temperatures reached in the blueschist and greenschist facies, whilst shear zone deformation may not cause full recrystallization. New, or more refined geochronological approaches, can thus shed additional light on the processes in accretionary wedges.

The Aegean subduction complex has emerged over the years as a key natural laboratory to study subduction processes. Our focus in recent years has been on the subduction related processes as experienced by the rocks of Syros and Sifnos islands. Here, we report (1) our efforts to further refine dating approaches: ⁴⁰Ar/³⁹Ar by dating of suites of single phengite crystals on an outcrop to section scale, and (2) our work exploring new approaches of dating of minerals free of lattice-bound potassium such as garnet, amphiboles and epidotes by dating the signal derived from the fluid inclusions by stepwise crushing.

Dating complete 100+ m sections by single grain phengite dating has the added benefit that all available lithologies in the section contribute to a histogram or PD-plot. Where previously a multigrain average from a single rock specimen was obtained, now is revealed that different units record an age range often as much as 10 Myrs wide, the oldest ages recording crystallization and the younger resetting following crystallization. Dating fluid inclusions by stepwise crushing allows the identification of multiple fluid reservoirs that contribute to the obtained signal sequentially. Typically, the first crushing steps reveal a reservoir that contains large amounts of excess ⁴⁰Ar, whereas following exhaustion of this reservoir other distinctly different sources of argon are revealed. Age signals thus obtained are interpreted as documenting periods of increased fluid mobility during and following mineral crystallisation.

Combination of these two approaches provides new insights into the tectonic processes during deep subduction and subsequent exhumation to shallower depths.

Sub-solidus replacement of rapakivi textures during high-temperature potassium metasomatism of the Mannum Granite

Goswami, Naina^{1,2}, Forster, Marnie^{1,2}, Reid, Anthony³, & Lister, Gordon¹

¹Research School of Earth Sciences, Australian National University, Canberra ACT 2601; ²MinEx CRC, Canberra ACT 2601; ³Geological Survey of South

Australia, Adelaide SA 5001

The Mannum Granite is a high-temperature A-type granitoid emplaced during the late stages of the Delamerian Orogeny in South Australia. It has attracted considerable research interest over past decades because it is a porphyritic A-type granite that displays well-developed rapakivi structures and has been linked to the process of magma-mingling above deep-seated mafic igneous bodies. It contains many mafic enclaves of varied sizes and textures including potassium feldspar and quartz porphyroblasts with disseminated sulphides. The alkali feldspar cores of the rapakivi textures are lobate and overgrow the plagioclase rims, suggesting alkali feldspars are younger.

We conducted $^{40}\text{Ar}/^{39}\text{Ar}$ geochronology in conjunction with ultra-high-vacuum (UHV) step heating ^{39}Ar diffusion experiments on K-feldspar and biotite from the Mannum granite. Conjoint inversion of data from the UHV ^{39}Ar diffusion experiments using the *Wunderkind* program applied to data from the K-feldspar experiment demonstrates the presence of highly retentive core domains capable of retaining radiogenic argon even to temperatures in excess of 600 °C. Inversion of the geochronology data using the *MacArgon* program produces a temperature-time history that suggests that the K-feldspar in the core of the rapakivi texture formed as the result of sub-solidus solid state replacement and/or metasomatism at ca 443 Ma, and then cooled rapidly at ca 440 Ma. Since biotite spectra which define a plateau age at ca 472 Ma are relatively undisturbed, the temperature excursion associated with the metasomatic event would have to have been limited in its magnitude (<~500°C) and duration (<< 1 Ma).

The biotite age (ca 473 Ma) is close to the previously determined early Ordovician crystallisation ages for the granites in this belt. In addition, the biotite appears to be highly retentive, with closure temperature for cooling at 20°C/Ma determined as the result of the UHV ^{39}Ar diffusion experiment at ~485 °C. These are thus exceptionally retentive biotite, which correlate with the fact that they are iron-rich and fluorine-rich, and fluorine-rich biotite typically exhibits higher argon retentivity. Overall, this short/sharp thermal pulse may have occurred in consequence of fluid movement associated with the Old Teal Flat Shear Zone to the east, which contains fabrics dated in this study at ca 445 Ma.

Microstructural analysis shows sericite and calcite precipitated along grain boundaries, fractures and exsolution lamellae. The presence of interpenetrating grain boundaries, sericite, calcite and secondary K-feldspar is attributed to the infiltration of an acidic hydrothermal agent hydrolysing primary K-feldspar to produce secondary sericite and quartz, further reacting with Ca-rich plagioclase and quartz to produce secondary K-feldspar phase(s) and calcite. Microstructures thus confirm the presence of a potassium-rich metasomatic event at Mannum leading to fluid-assisted *in-situ* replacement of K-feldspars with concomitant precipitation of secondary mineral phases.

The work has been supported by the Mineral Exploration Cooperative Research Centre whose activities are funded by the Australian Government's Cooperative Research Centre Program. This is MinEx CRC presentation.

The implications of muscovite sub-spectra in phengitic white mica on the theory and practice of argon geochronology

Forster, Marnie, & Lister, Gordon

Research School of Earth Sciences, Australian National University, Canberra 2601, Australia

This study illustrates a new method for the quantitative determination of the timing of movement in ductile shear bands formed in mylonites, or in strongly stretched metamorphic tectonites. The method is of particular use where phengitic white mica is involved, since interlayering in this mineral is usually so fine as to preclude the application of laser methods. In any case, laser methods as they are currently applied, do not have the capability of extracting exact and detailed age-temperature spectra. Laser methods also fail to achieve the multitudinous steps of the age spectrum evident from our high-definition UHV diffusion experiments. Laser methods also lose all information in terms of the low-volume early release of argon that is essential for the recognition of sub-spectra. Computer modelling and simulation shows that such detail in the age spectrum is essential in terms of being able to accurately infer the timing and duration of metamorphic events.

Here we show that high-definition ultra-high-vacuum (UHV) ^{39}Ar diffusion experiments using phengitic white mica are routinely able to extract muscovite sub-spectra in the first 10–30% of ^{39}Ar gas release during $^{40}\text{Ar}/^{39}\text{Ar}$ geochronology. A critical factor is that the recognition of muscovite sub-spectra requires Arrhenius data in order to recognise the steps dominated by release of ^{39}Ar from muscovite. In turn this requires precise measurement of temperature during each heating step. The muscovite sub-spectrum is distinct and separate to the main spectrum, which is itself dominated by mixing of gas released from phengite as well as muscovite. The muscovite sub-spectra allow consistent estimates of the timing of the formation of microstructural shear bands in various mylonites, as well as allowing quantitative estimates of temperature variation with time during the tectonic history of shear zones.

Our new data reveals hitherto unsuspected variation in the timing of exhumation of individual slices of the eclogite-blueschist belt, caused by Eocene and Miocene detachment-related shear zones. With excellent outcrop, the eclogite-blueschist belt exposed in the Cycladic archipelago in the Aegean Sea, Greece, offers a spectacular natural laboratory in which to decipher the structural geology of a highly extended orogenic belt and to ascertain the history of the different fabrics and microstructures that can be observed. Using phengitic white mica we demonstrate a robust correlation of age with microstructure, once again dispelling the myth that $^{40}\text{Ar}/^{39}\text{Ar}$ geochronology using this mineral, produces cooling ages alone. Previous work in the Cycladic eclogite-blueschist belt has incorrectly assumed that the diffusion parameters for phengitic white mica were the same as for muscovite. Arrhenius data suggest this is not the case, and that phengitic white mica is considerably more retentive of argon than muscovite. Previous workers have also erred in dismissing microstructural variation in age as an artefact, supposedly as the result of the

incorporation of excess argon. This has led to inconsistencies in interpretation, because phengite is able to retain argon at temperatures that exceed those estimated using metamorphic mineral parageneses.

The argon system has been treated as a thermochronometer. However, we demonstrate a robust correlation between microstructure and age, down to the detail present in complex tectonic sequence diagrams produced during fabric and microstructural analysis of individual thin sections. This points to new strategies being required in terms of the theory and practice of argon geochronology.

Hydrous polymetamorphic crustal rocks in an eclogite-bearing terrane record post-peak recrystallisation during arc–continent collision

Brown, Dillon¹, Hand, Martin¹, & Morrissey, Laura^{2,1}

¹Department of Earth Sciences, University of Adelaide, Adelaide, SA, Australia; ²Future Industries Institute, University of South Australia, Mawson Lakes, SA, Australia

Ultrahigh- and high-pressure terranes are identified based on the occurrence of mafic eclogite-facies mineral assemblages, which effectively record burial and subduction metamorphic conditions. In such terranes however, mafic mineral assemblages are volumetrically minor compared to the continental rocks that host them, which typically preserve anhydrous quartzo-feldspathic amphibolite-facies mineral assemblages. Continued debate centres around two hypotheses accounting for the petrology of the continental rocks: (1) the protoliths to the continental rocks did not respond to burial and subduction, and (2) the continental rocks developed high-pressure mineral assemblages which were subsequently overprinted during exhumation. However, less is known about continental rocks that preserve hydrous amphibolite-facies assemblages and schistose fabrics, which are also documented in high-pressure rock systems. In western Tasmania, southeast Australia, eclogite-facies mafic boudins with previously constrained subduction metamorphic conditions of 18–21.5 kbar and 650–700°C are hosted by weakly foliated to mylonitic metapelitic continental rocks preserving hydrous amphibolite-facies assemblages dominated by siliceous muscovite, quartz, and garnet. Weakly foliated metapelites preserve relict kyanite and two possible textural generations of garnet, moderately foliated metapelites record evidence of partial melting, and mylonitic metapelites contain sillimanite within the rock fabric. Monazite LA–ICP–MS U–Pb geochronology documents two instances of monazite growth in the metapelites: a possible Mesoproterozoic growth event at ca 1385 Ma and a younger, yet poorly constrained growth event in the Cambrian. Rutile LA–ICP–MS U–Pb geochronology more precisely constrains Cambrian-aged metamorphism in the metapelites between 520–505 Ma. Monazite–garnet petrochronology reveals that Mesoproterozoic-aged monazite formed in a system with little or no influence of garnet whereas Cambrian-aged monazite formed in the presence of garnet during subduction. Metamorphic mineral equilibrium modelling of Cambrian subduction indicates that the weakly foliated metapelites best approximate peak metamorphism, recording

metamorphic conditions of 13–17 kbar and 600–720 °C. Migmatitic metapelites record lower pressure conditions of 8–13 kbar and 660–740 °C and mylonitic metapelites equilibrated at 3.5–7 kbar and 590–680 °C. We infer that the amphibolite-facies metapelites record different stages of Cambrian-aged exhumation and, unlike their mafic counterparts, do not record burial or subduction. We attribute the inferred eradication of peak subduction mineral assemblages in the metapelites to the influence of fluid and localised deformation.

Evaluation of the ⁴⁰Ar/³⁹Ar technique for kimberlite geochronology: three case studies from Finland

Dalton, Hayden¹, Phillips, David¹, Matchan, Erin¹, Giuliani, Andrea^{1,2}, Hergt, Janet¹, Maas, Roland¹, Woodhead, Jon¹, & O'Brien, Hugh³

¹School of Earth Sciences, The University of Melbourne, Parkville, VIC 3010, Australia; ²Institute of Geochemistry and Petrology, Department of Earth Sciences, ETH Zurich, Clausiusstrasse 25, Zurich 8092, Switzerland; ³Geological Survey of Finland, P.O. Box 96, Espoo, Finland

Kimberlites are enigmatic, volcanic rocks of both great economic and scientific importance due to acting as the primary host-rock to diamonds and being the deepest-derived continental magmas on Earth. Despite this significance, there remains debate concerning the sources of kimberlites and what triggers mantle melting to form these rocks. Robust determination of the timing of kimberlite eruption is a crucial prerequisite if we are to unravel the presence of any spatiotemporal relationships between kimberlite emplacement and large-scale tectonic processes, super-continental cycles or mantle plumes.

Despite the benefit of the remarkably high precision achieved with modern ⁴⁰Ar/³⁹Ar analytical techniques, and the presence of K-bearing groundmass phlogopite in many kimberlites, this technique has seldom been applied to kimberlites and related rocks. Early utilisation of this method revealed issues related to the presence of extraneous argon in mica macrocrysts and phenocrysts which yields anomalously old or maximum emplacement ages. Nonetheless, apparently reliable age results have been obtained on magmatic mica from kimberlites and related rocks. In this study we compare new, precise ⁴⁰Ar/³⁹Ar ages with other independent age constraints (e.g., Rb/Sr, U/Pb) on three clusters of kimberlites and related rocks from Finland to rigorously assess the instances where ⁴⁰Ar/³⁹Ar dating produces older apparent ages.

Our results indicate that sample selection and groundmass mica (phlogopite or kinoshitalite) separation needs to be extremely judicious prior to analysis. Where fresh mica phenocrysts are available for ⁴⁰Ar/³⁹Ar analyses we recommend that plateau results are interpreted with caution. Age spectra which are entirely flat, such that an age plateau includes 100% of the gas are likely the most accurate and precise reflection of the emplacement age of a kimberlite. In contrast, aliquots that yield younger apparent ages for heating steps preceding the plateau may reflect argon recoil redistribution resulting in anomalously older high temperature/plateau ages when compared with independent age constraints. In cases where such

discordance exists, we recommend that total-gas ages give a better approximation of the emplacement age and one which agrees more closely with ages from other geochronometers.

The KBS Tuff Controversy fifty years on: new ultra-precise ages for the KBS tuff and correlates, Omo-Turkana Basin, Kenya

Phillips, David, & Matchan, Erin

School of Earth Sciences, The University of Melbourne, Parkville, VIC 3010, Australia

Archaeological expeditions by the National Museum of Kenya to east Lake Turkana (formerly Lake Rudolf) in 1968 and 1969 led to the discovery of remarkable stone artefacts and hominin fossils, associated with volcanic tuffs, including the famous KBS (Kay Behrensmeyer Site) tuff.

Initial attempts to date the KBS tuff proved unsuccessful due to fluvial deposition of most tuffs and contamination by older material. Early $^{40}\text{Ar}/^{39}\text{Ar}$ dating of pumice feldspar grains from the KBS tuff yielded a reported age of 2.61 ± 0.26 Ma, which was soon disputed on the basis of faunal correlations, thereby precipitating a controversy that played out in Nature publications for the next decade. In 1975, the Berkeley geochronology laboratory published K–Ar ages of 1.60 and 1.8 Ma for two KBS localities, with the former age later attributed to laboratory error. The Cambridge geochronology laboratory then reported a range of $^{40}\text{Ar}/^{39}\text{Ar}$ ages (0.52–2.61 Ma) and revised the age of the KBS tuff to 2.42 ± 0.02 Ma, in accord with preliminary zircon fission track ages. Subsequent geochemical correlations with the H2 (= KBS) tuff in Ethiopia, dated at ca 1.8 Ma by the K–Ar method, heightened the controversy. Later K–Ar and $^{40}\text{Ar}/^{39}\text{Ar}$ dating analyses by Ian McDougall at the Australian National University largely resolved the debate, with reported ages of 1.89 ± 0.01 Ma and 1.88 ± 0.02 Ma, coincident with a revised fission track age of 1.87 ± 0.04 Ma. More recent analyses of single feldspar crystals from KBS pumice clasts produced a weighted mean age of 1868 ± 14 ka – but with significant scatter, suggesting the presence of inherited grains or extraneous argon.

New ultra-precise $^{40}\text{Ar}/^{39}\text{Ar}$ data obtained for single feldspar pumice crystals from several tuff localities across the Omo-Turkana Basin, including the KBS tuff, show variably complex age distribution patterns even within single pumice clasts. Based on co-irradiated A1T and FCT sanidine aliquots and a Bayesian statistical analysis approach, we calculate astronomically calibrated ages for several tuff horizons at precision levels approaching $\ll 0.1\%$. The KBS and correlated H2 tuff give an astronomically calibrated, weighted mean age of 1879.2 ± 1.3 ka (0.069% 95%CI). The stratigraphically younger Malbe (= H4) tuff, which was originally misidentified as the KBS tuff, gives a Bayesian eruption age of 1837.75 ± 0.86 (0.047%, 95%) ka. These results enable effective stratigraphic correlations across the Basin and reveal paleoclimate and paleo-environmental variability at millennial timescale resolution.

This study is dedicated to the memory of Ian McDougall and Frank Brown, who worked tirelessly to unravel the magmatic and geological history of the Omo-Turkana Basin.

Dating the timing of motion in major ductile shear zones

Lister, Gordon, & Forster, Marnie

Research School of Earth Sciences, Australian National University, Canberra 2601, Australia

There is confusion in the argon geochronology world as to what allows movement in a ductile shear zone to be dated. Some assert that all that is necessary is to date mica and to obtain a 'plateau'. But this is not at all sufficient to make the argument. $^{40}\text{Ar}/^{39}\text{Ar}$ geochronology (like all radiometric dating techniques) does not have the ability to date movement. It is the microstructural modification of existing grains that must be dated, e.g., growth or regrowth during movement. Otherwise, it may be that the fabric forming minerals are remnant: namely, relicts of an earlier formed mineralogy, and the ages obtained not at all relevant to the timing of movement in a later shear zone.

An ideal circumstance would be clear and unambiguous demonstration that growth of a particular mica had taken place immediately prior to or during the operation of a ductile shear zone, and that mineral separation (or laser spots) had focussed on those volumes during measurement. An example would be sudden growth of mica porphyroblasts that were then rotated and aligned in a developing shear zone fabric, as occurs in retrograde shear zones in the Cycladic Eclogite-Blueschist Belt. Movement has not been dated, but an estimate has been obtained as to the timing of growth during or immediately preceding movement. Another optimal circumstance would be if the operation of the ductile shear zone had shredded mica, progressively reducing its diffusion dimension. This behaviour leads to staircase spectra characteristic of fractal diffusion. Such age spectra appear to be able to allow the distinction of the start and the end of shear zone operation. In some cases, the age of relict mica microstructures is also evident, e.g., in mica from the Main Central Thrust of the Himalaya.

A more difficult circumstance occurs when age spectra from fabric forming minerals appear to be unrelated to the timing of movement, e.g., for mica from greenschist facies ductile shear zones in the Cap de Creus, Spain. We inverted data from $^{40}\text{Ar}/^{39}\text{Ar}$ geochronology step-heating experiments, using potassium feldspar, after conjoint inversion of data from simultaneous ultra-high-vacuum (UHV) ^{39}Ar diffusion experiments. The resultant temperature-time curves imply that these mylonites formed in Eocene to Oligocene time, and therefore that they are not Variscan or Jurassic, as previously argued. Their tectonic significance is likely to be as right-lateral strike-slip shear zones formed in transfer faults accommodating roll-back of the Tethyan subduction zone as it dragged Sardinia and Corsica away from the Palaeo-European margin during opening of the Gulf of Lyon.

These examples suggest caution needs to be exerted in the dating of movement in ductile shear zones. Laser-step heating (or laser spot analysis) is not suited for this purpose, since this method provides no information in respect to Arrhenius data. In consequence the retentivity of relevant minerals in respect to argon diffusion cannot be assessed. In addition, laser methods do not produce consistent detail in age spectra. In contrast, robotic methods applied to resistance-furnace step-heating experiments offer a

cheap, efficient, and reliable way to obtain the detailed age spectra that are necessary (in conjunction with Arrhenius data) to characterise the pattern of argon release.

ARGA SYMPOSIUM

Regolith and landscape evolution

Australia and Brazil: contrasting weathering and erosion histories but similar cratonic landscapes

Vasconcelos, Paulo

School of Earth and Environmental Science, the University of Queensland, Brisbane, Qld, Australia.

Australia is sparsely vegetated and the flattest, hottest, most tectonically stable but fastest latitudinally moving continent on Earth, it has migrated from high to low latitudes in ca 50 Ma. In contrast, Brazil is a densely vegetated, wet, high relief cratonic terrane that has moved slowly longitudinally along the Equator for the past ca 70 Ma. Despite these contrasting underlying geological and geographical characteristics, landscapes in these two regions are remarkably similar, share analogous ancient weathering histories, and are marked by plateaus surrounded by dissected plains that erode similarly and at equivalent rates. In situ cosmogenic isotopes show that plateaus eroded at less than 2 m.Ma⁻¹, while dissected plains erode at 5–20 m.Ma⁻¹. Cosmogenic isotope concentrations in sediments show greater erosion rates, suggesting that erosion focusses preferentially along escarpments. ⁴⁰Ar/³⁹Ar geochronology on Mn-oxides and (U–Th)/He–⁴He/³He geochronology on goethite show that ancient weathering profiles blanketing plateaus in both continental areas are as old as ca 90–70 Ma. These results are substantiated by in situ cosmogenic ³He concentrations in hematite. Geochronological results for the surrounding plains, on the other hand, indicate that the dissected areas are typically younger than ca 30 Ma. Weathering profiles in both continental areas, on opposite sides of the planet, host supergene mineral populations that record analogous and often contemporaneous events of water-rock interactions through time. Importantly, these plateaus have been continuously emergent throughout their entire histories, hosting in the weathering profiles underneath minerals precipitated under contrasting climatic conditions through time. Interestingly, the analogous weathering histories of the two continental areas are mostly recorded in oxides, hydroxides, and clay mineral assemblages. The distribution and abundance of sulphates, carbonates, and silica-minerals, on the other hand, mark significant contrasts between the two landmasses. The most striking contrast is weathering under water deficient conditions in Australia while Brazil weathered under pronounced oversupply of rainwater. It is remarkable that such differences in climatic conditions produced such similar resulting landscapes. This is only possible because in Brazil, iron oxyhydroxides and ferricretes provided the landscape scaffolding that is provided in Australia by silica minerals and silcretes.

A fresh look at the stratigraphy of the Lefroy Palaeodrainage System, Eastern Goldfields, WA

Lynham, Leah

James Cook University, Townsville, Australia

Buried palaeovalley sediments within the Lefroy and Cowan palaeodrainage systems and other palaeodrainage systems in the wider Eastern Yilgarn craton contain economically viable deposits of alluvial gold (Oxenburgh *et al.*, 2017). The Lefroy Palaeodrainage System and other, parallel systems are said to have formed pre-Jurassic (Clarke, 1994), potentially from glacial scouring during the Late Palaeozoic (Eyles and de Broekert, 2001), before a depositional regime led to ~100 m of buried fluvial, marginal marine and marine sediments being deposited in the buried palaeovalleys. Little is known about the geological controls on the activation of the system, the origin of the basal placer deposits or the sedimentary controls on the channel infill. Unravelling the geological controls on the incision of the palaeovalley network and infill of the palaeochannel sediments within the Lefroy palaeodrainage System could have positive implications for future alluvial gold exploration within the area.

Previous studies have suggested that the Lefroy and Cowan systems became separated due to uplift along the Jarrahwood axis prior to Eocene deposition (eg (Clarke, 1994, de Broekert and Sandiford, 2005), although studies disagree on how far North the Jarrahwood Axis transects the Cowan System. Building on the foundations of already completed work, new palaeocurrent data from field observations, and new stratigraphic data from the Neptune Open pit, and diamond drill cores from the area help to refine the stratigraphy of the Lefroy Palaeodrainage System, and the palaeoenvironment leading to the deposition of the Lefroy Palaeodrainage System sediments.

Clarke, J. D. A. 1994. Evolution of the Lefroy and Cowan palaeodrainage channels, Western Australia. *Australian Journal of Earth Sciences*, 41, 55–68.

De Broekert, P. & Sandiford, M. 2005. Buried Inset-Valleys in the Eastern Yilgarn Craton, Western Australia: Geomorphology, Age, and Allogenic Control. *The Journal of Geology*, 113, 471–493.

Eyles, N. & De Broekert, P. 2001. Glacial tunnel valleys in the Eastern Goldfields of Western Australia cut below the Late Paleozoic Pilbara ice sheet. *Palaeogeography, Palaeoclimatology, Palaeoecology*, 171, 29–40.

Oxenburgh, S., Falconer, M., Douth, D., Edmonds, P., Foley, A. & Jane, M. 2017. Kambalda – St Ives goldfield. In: PHILIPS, N. (ed.) *Monograph 32 – Australian Ore Deposits*. The Australasian Institute of Mining and Metallurgy.

(U–Th)/He-dating of iron oxides: Towards establishing a temporal framework for landscape evolution and regolith development in southwest Western Australia

Wells, M. A.¹, González-Álvarez, I.^{2,3}, & Danišik, M.⁴

¹John de Laeter Centre (JdLC), Curtin University, Perth, WA 6102, Australia; ²CSIRO, Mineral Resources, Discovery Program, Perth, Australia; ³University of Western Australia, Centre for Exploration Targeting, Perth, Australia; ⁴John de Laeter Centre for Isotope Research, Applied Geology, Curtin University, Perth, Australia

Understanding the temporal formation of iron oxides can provide important clues for understanding landscape evolution, weathering processes and past climatic conditions. Recent application of (U–Th)/He-dating to iron oxide assemblages in iron ore deposits¹ and in weathering systems in Western Australia, analysed in the John de Laeter Center (JdLC) GeoHistory Facility, have demonstrated the efficacy of the technique for the geochronological analysis of iron oxide-rich systems. Hence, the iron oxide-rich duricrust, capping the deeply weathered regolith of the Darling Range in the southwest of Western Australia, provides a suitable geochronological proxy that provides a time-integrated record of the weathering processes that have shaped regolith formation.

Despite numerous studies focused on laterite formation in the Darling Range, there is a paucity of data pertaining to the age or timing of laterite formation. The exceptions are for exposures of lateritic duricrust at two sites along the Darling Scarp. Early work on lateritic duricrust near Toodyay (50 km northeast of Perth), yielded (U–Th)/He ages of 10.0–7.5 Ma (Late Miocene) and more recently, findings arising from a pathfinder JdL-GSWA project, measured comparable Late–Miocene/Early Pliocene, to possible Early–Pleistocene (U–Th)/He ages of 5.7–1.3 Ma for pisolithic and fragmental duricrust in lateritic profiles at the Boddington Gold Mine (100 km southeast of Perth).

Further east, in the central Yilgarn, a recent JdL-CSIRO pilot study also measured Late Miocene/Pliocene ages (7.9–3.5 Ma) for nodular duricrust exposed near the Blue Haze Au mine, Forrestania (120 km southeast of Southern Cross). An exception in this study was an Early Oligocene age (34.8 ± 3.8 Ma) for one example of nodular duricrust. Given the small number of samples examined in this study, an explanation for the much older age is currently open to interpretation. However, the generally comparable (U–Th)/He ages for lateritic duricrust across these widely spread locations in southern WA, suggest that the processes of regolith formation and/or modification were, broadly, regionally synchronous. These initial findings help to underscore and provide the impetus in establishing a temporal framework for duricrust formation, which may also provide a record of past processes that have helped in shaping landscape evolution in the broader, Southwest Western Australia.

Acknowledgements: The authors would like to thank Classic Minerals for their support and permission in publishing the Forrestania dating work. The Boddington dating results derive from a project funded by the Geological Survey of Western Australia (GSWA) from the Exploration Incentive Scheme. Martin Danišik acknowledges the support of a Curtin Senior Research

Fellowship.

Mapping landscape domains in Western Australia: developing a tool to link geology, geochemistry and landscape variability at large scales

González-Álvarez, I.^{1,2}, Albrecht, T.³, Klump, J.¹, Pernreiter, S.⁴, Heilbronn, K.⁵, & Ibrahimi, T.¹

¹CSIRO, Mineral Resources, Discovery Program, Perth, Australia; ²University of Western Australia, Centre for Exploration Targeting, Perth, Australia; ³Department of Mechanical and Aerospace Engineering, Monash University, Melbourne, Australia; ⁴Institute of Geology, University of Innsbruck, Innsbruck, Austria; ⁵Geosciences, College of Science and Engineering, James Cook University, Townsville, Australia.

Landscapes contain essential information related to the geochemical footprint of ore deposits at depth. Variable surface topographical features can be grouped to define and classify unique landscape domains. Climatic conditions, tectonic activity, geological features, biological activity, and sedimentary dynamics are fundamentally linked to landscape variability. Consequently, the study of landscapes can reveal the link between surface features and geological processes at depth. Ore deposits and mineral systems can have dispersed or enhanced geochemical footprints, depending on how the landscape evolved. Geochemical dispersion halos penetrating through cover can be detected by selecting suitable landscape regimes and appropriate sampling media. Cataloguing landscape variability and understanding their evolution at a regional scale can be challenging. The primary difficulty is associated with the selection of the geographic extension of surficial features. In the past, landscape variability mapping relied on field observations along transects. However, a constraint on this approach lies in the uncertainty related to the extrapolation of field observations, especially when attempting to extrapolate them to regional scales. Such extrapolation can be unreliable due to the complexity and variability of landforms, the paucity of data availability, and the difficulty in defining quantitative criteria that discriminate diverse landscape types. Modern data analytics technology and advanced satellite data provide access to large data sets that can assist in characterizing landscape features and their distribution at regional scales. The ability to accurately map landscape variability domains may reveal a vector that links the geochemistry and geology at depth with the architecture of the cover. Such an approach will result in more efficient means to detect and constrain geochemical footprints and dispersion processes at large scales.

Planetary regolith and regolith in mineral exploration

Martian regolith: from cryolithosphere to atmosphere

Caprarelli, Graziella

Centre for Astrophysics, School of Sciences, University of Southern Queensland, Toowoomba, QLD 4350, Australia

Regolith is: “everything, from fresh rock to fresh air” [1]. The term indicates the layers of loose material that mantle bedrock, although there is disagreement among regolith experts between the camp that subscribes to the broad definition given above, and the camp that discriminates between the material formed in place as a product of weathering, and sediments formed elsewhere, transported and deposited on bedrock which was not the parent material [2]. We now know that regolith mantles the surface of all rocky bodies in the solar system: on many of these objects there are no geological processes leading to sedimentary erosion and deposition such as on Earth. Thus, here I use the term in its broader sense.

Mars is a hyperarid planet [3], with water stored as ice in its polar caps and in the ground. The uppermost layers of the martian crust are thus termed the ‘cryolithosphere’. Meteoritic “gardening” since early Noachian times (ca 4.0 Ga) has produced the thick layer of broken rocky material covering Mars’s surface globally. Wind erosion and mass wasting also act on a global scale, while chemical processes have led to the deposition of hydrous minerals in the soil. The martian regolith thus comprises dust, sandy soils and sediments, pebbles, rocks, secondary minerals, and may include water ice at mid- to high latitudes, where permafrost landforms are observed [4], and where additional disintegration of bedrock occurs owing to thaw/freeze cycles. Aeolian processes move solids across the martian surface: dust particles (< 10 mm) may remain in suspension indefinitely, dust and silt (< 60 mm) are lifted and may be deposited at great distance by atmospheric currents, sand particles (up to a few hundred mm) move by saltation, breaking into smaller fragments that may then be lifted, coarse grained material (1–5 mm in size) is dragged or accumulates as lag deposits. A way to study the distribution of these materials is through satellite thermophysical data: mapping based on thermal inertia and albedo classification [5] shows links between type of material and geology.

My colleagues and I have investigated the spatial distribution and vertical composition of the martian cryolithosphere through impact processes [6] and by ground penetrating radar [7]. Here, I show and discuss the main outcomes of our work in relation to: (a) the spatial distribution of the martian regolith and its composition, (b) ground ice and regolith, (c) the link between cryolithosphere and atmosphere. These aspects underpin part of the geological and climatological history of the planet, with far reaching implications about the selection of landing sites and possible future human missions to Mars.

[1] Eggleton, R. A., Ed. (2001). CRC LEME, ISBN 0-7315-3343-7, 144 pp.

[2] Pain & Ollier (1996). *AGSO J Austral Geol Geophys* 16(3), 197–202.

[3] Baker V. R. (2001). *Nature*, 412, 228–236.

[4] Lasue *et al.* (2013). *Space Sci Rev*, 174, 155–212.

[5] Jones *et al.* (2014). *Remote Sensing*, 6, 5184–5237.

[6] Jones *et al.* (2016). *JGR Planets*, 121, 986–1015.

[7] Orosei *et al.* (2017). *JGR Planets*, 122, 1405–1418.

Inverted Hunder dune swales, Ladakh, India

Clarke, J. D. A.¹, & McGuirk, S^{1,2}

¹Mars Society Australia, c/o 43 Michell St Monash, ACT 2904; ²Fenner School, Australian National University, ACT 0200

Introduction

The Hunder Dunes are one of a series of small dune fields in the Shyok and Nubra valleys of the Ladakh region of northwestern India. The dune fields are composed of mostly barchanoid and transverse dunes and are composed of sand reworked from the seasonally exposed beds of these rivers. Wind directions are strongly unimodal in orientation and controlled by valley orientation (McGuirk 2017). The Hunder Dunes occur at an altitude of 3083 m in the Nubra valley and cover an area of about 1500 x 700 m. The area is a popular tourist location because of the visual impression of the dunes against the background of the Karakorum Range rising to over 6000 m, and the presence of a small herd of Bactrian camels. No scientific investigation of the dunes has been previously made. During a 2016 expedition to the area (Pandey *et al.*, 2019) we noticed the presence of numerous inverted swale deposits. Inverted swales have not, to our knowledge, been described in the literature. We here present a brief description of them and discuss their formation and possible significance.

Location

The Hunder Dune field occurs in the Nubra valley and are centred at 77°29'47.60"E and 34°34'49.00"N. The dune fields are composed of mostly barchanoid at the present time, although the evidence from Google Earth imagery shows that they have been dominated by transverse bedforms in the past. The dunes lie on the south bank of the Nubra River. The Hunder Dunes occur at an altitude of 3083 m in the Nubra valley and cover an area of about 1500 x 700 m (Figure 1).

Climate

The climate of the Hunder Dunes is arid with warm summers and cold winters, temperatures falling below zero. The area corresponds with zone IV of Hewett (1989). Valley floors experience strong winds, the dominant wind vector responsible for the dunes is from the northwest. No rainfall data exists for Hunder, but the city of Leh in the valley of the Indus, which is the next valley to the south, has an annual rainfall of 104 mm (Climate data 2018).



Figure 1: Hunder dunes.



Figure 2. Concave upward wedding cake mesas formed by inversion of flooded swale deposits at Hunder dunes.

Morphology and stratigraphy

The features interpreted as inverted swales consist of small (10–20 m long, 5–10 m wide, and up to 1.5 m high), ellipsoidal mesas exposed in the swales between active dunes. Most of the mesas have a tiered, wedding cake appearance, due to the presence of stacked cycles of sediment (Figure 2). Individual cycles range from 40 to 50 cm in thickness and are composed of a repeated succession of lithologies (Table 1), forming cycles. Not all units are present in each cycle, unit A is only present only at the base of the mesa and is not always exposed. Only one of the rippled units B and C may be present, and rarely the muddy unit D is absent. Some swales are partly buried by dune migration, some others are being exposed by the same process.

Table 1. Repeating cyclic units in mesas

Unit	Grain size	Structures	Interpretation	Figure
D	Mud	Mud drape over ripples, desiccation cracks, vertebrate footprints	Desiccated pond	Figure 3
C	Sand	Symmetrical ripple cross-laminae	Pond	Figure 4
B	Sand	Asymmetrical ripple cross-laminae	River flooding	Figure 4
A	Sand	Parallel slightly upwards bedding	Aeolian dunes	Figure 4

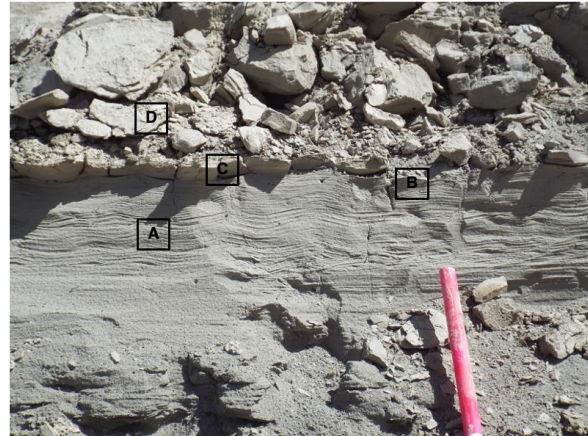


Figure 3. Unit 4 desiccation-cracked mud (unit A) at top of swale flood cycle showing cloven hoof prints.



Figure 4. Complete cycle exposed inside of mesa, units A, B, C, and D shown.

Interpretation

As shown in Table 1, the cyclic units are interpreted as showing the flooding of dune swales by muddy river waters, followed by their desiccation. The convex-upward basal unit A represents the aeolian swale deposits. The convex upward geometry of the swale is propagated ward through each cycle. The asymmetric cross-laminated unit B represents the influx of river flood water carrying sand and mud. The symmetric cross-laminated unit C represents wind-driven wave sand deposition water flood recession as isolated the sales into ponds. Interference patterns between ripple sets are visible on the upper surfaces of the topmost cycles exposed in the mesas. The uppermost unit C represents settling out of suspended mud in the final phases of drying out of the pond in the swales. The muddy unit is often desiccation cracked and may preserve vertebrate footprints. Multiple cycles of flooding and desiccation form the swale deposits.

The deposits are very weakly indurated following deposition by precipitated carbonate. This allows them to withstand deflation to form the mesas. The muddy unit C is also slightly more resistant than the sands to erosion, so form overhanging caps. The mesas show small scale landforms showing wind erosion, including polished surfaces and ventifacts (Figure 5).

Discussion

Several swales in the Hunder dunes were flooded at the time of our visit. These ponds lacked mud, however, so we interpret the water as being due to either a raised groundwater table, or rainfall runoff, or both. The sale flooding from the river would carry mud, as the suspended sediment load of the Nubra River is

B

substantial.

While the dune swales can be flooded by the Nubra River we expect the deposits to accrete to the height of the river flood. When isolated from the river by dune migration, erosion of the swale deposits can begin, leading to formation of the concave upward wedding cake inverted mesas.

Acknowledgements: The data from Hunder was collected during Mars Society Australia's NASA Spaceward bound India expedition in August 2016. The expedition was funded in-part by a grant from Tata Motors, India. We also acknowledge the support of the Birbal Sahni Institute of Palaeosciences, the Department of Science and Technology, the Chief Wildlife Warden of Ladakh, and Inspired Journeys Ltd. Craig Strong¹ and Frank Mills ANU supervised the project at ANU.



Figure 5. Complex ventifact formed by wind erosion of mud drape (unit D)

Climate Data.org 2018. Leh. Address when accessed <https://en.climate-data.org/location/24802/>

Hewitt, K. 1989. The altitudinal organization of the Karakorum geographic processes and depositional environments. *Zeitschrift für Geomorphologie Supplement* 76, 9–32.

McGuirk, S. 2018. Do synoptic scale atmospheric processes drive surface winds in the valleys of Ladakh, in the northern Himalaya? BSc Honours thesis in the Fenner School of Environment and Society, Australian National University, Canberra, unpublished, 68 p.

McGuirk, S. L., Clarke, J., Strong, C. L., and Mills, F. 2018. Remote sensing of valley winds in the Northern Himalaya. *Proceedings of the 18th Australian Space Research Conference*, Sydney, Australia

Pandey S *et al.* (2019). Ladakh: diverse, high-altitude extreme environments for off-earth analogue and astrobiology research. *International Journal of Astro-biology* 1–21. <https://doi.org/10.1017/S147355041900011>

Regolith-hosted ferrihydrite: a forgotten sorbent in the search for REEs?

Bamforth, Tobias^{1,2}, Tiddy, Caroline¹, Gonzalez-Alvarez, Ignacio^{2,3}, Whittaker, Eric⁴, & Faulkner, Leon⁵
¹Future Industries Institute (FII), University of South Australia (UniSA), Adelaide, Australia; ²CSIRO, Mineral Resources Discovery Programme, Kensington, Perth, Australia; ³CET, University of Western Australia, Crawley, Perth, Australia; ⁴Terramin Australia Ltd., Adelaide, Australia; ⁵Environmental Copper Recovery Ltd., Adelaide, Australia

The negatively charged surfaces of clay minerals demonstrate an excellent capacity for the adsorption of rare-earth elements (REE's) in regolith. Often, this is

observed during the formation of secondary phases such as kaolinite and halloysite (Borst *et al.*, 2020. *Nat. Comm.*), though alternate clay minerals display a similar capacity for REE sorption across low-temperature environments. For instance, ferrihydrite ($5\text{Fe}_2\text{O}_3 \cdot 9\text{H}_2\text{O}$) is an amorphous clay mineral that is widely acknowledged as an excellent REE sorbent in hydrospheric systems. Thus far, evidence for its potential in association with high-grade REE accumulation has been limited, however, new data from the Kapunda Cu mine, South Australia, suggests that even in the presence of co-existing kaolinite, ferrihydrite may act as a principal sorbent during lanthanide fixation.

Petrographic analysis of weathered vein samples from the Kapunda mine, which exhibit total rare-earth oxide (TREO) concentrations of 17.1 wt%, demonstrate that interstitial aggregates of REE phases monazite and rhabdophane are spatially associated with ferrihydrite particulates. In comparison, a negative correlation is observed between REE minerals and crystalline phases of goethite, hematite and kaolinite. Ferrihydrite formed during the acidic dissolution of primary pyritic minerals, which is evidenced by cubic void spaces throughout the sample. In addition, geochemical evidence from Ce/U valency modelling suggests that weathering fluids were highly acidic (pH 1–3) and moderately oxidising (Eh 0.7–0.9) in nature. REE mobilisation was likely facilitated by the formation of sulphate complexes, which is supported by geochemical whole-rock profiles that exhibit low chondrite-normalised La/Yb ratios (Migdisov *et al.*, 2016, *Chem. Geol.*). Chondrite-normalised plots also exhibit $\text{Pr} > \text{Nd} > \text{Ce} > \text{La}$ enrichment, which compliment previous conclusions on the ability of ferrihydrite to selectively adsorb the valuable REE's Pr and Nd (Bau, 1999, *Geochim. Cosmochim. Acta*). Phosphate ions were sourced from primary sedimentary apatite, which is evidenced by the pseudomorphic replacement of hexagonal crystals by secondary REE-bearing phases. This advocates for the role of ferrihydrite as a catalyst following the co-adsorption of REE's and PO_4^{2-} (Arai & Sparks, 2001, *J. Colloid Interface Sci.*), and explains the observed spatial boundaries of lanthanide accumulation, as apatite is not expressed in notable quantities throughout the bulk of the Cu deposit.

Results demonstrate the potential of ferrihydrite as a principal sorbent for economic REE mineralisation, when considering: (1) its relative pervasiveness across global regolith profiles, (2) its crystal structure, surface area and adsorption capacity and, (3) its potential ability to selectively adsorb the valuable light rare-earth elements Nd and Pr. Additionally, this work emphasises the importance of apatite as a phosphate source in REE-mineralising systems, and advocates for the increased consideration of ferrihydrite as a potential catalyst for REE accumulation as the demand for these critical metals escalates under the development of renewable technologies.

Hydrogeochemistry to explore the Georgina Basin's phosphate potential

Schroder, Ivan, & de Caritat, Patrice
Geoscience Australia, Canberra, Australia

With the increasing need to extend mineral exploration

under cover, new approaches are required to better understand concealed geology, and to narrow the mineral prospectivity search-space. Hydrogeochemistry is a non-invasive exploration technique based on the premise that groundwater interacting with a deposit or supergene alteration can cause anomalous elemental and isotopic signatures down-gradient. Water chemistry can reflect mineralisation directly but can also reveal other key components of a mineral system, including fluid-flow pathways (e.g., fault/fracture zones), evidence for mineral system traps (e.g., evaporites, shales), or metal sources (e.g., mafic rocks).

The Northern Australia Hydrogeochemical Survey (NAHS) was a multiyear regional groundwater sampling program that aimed to understand the regional mineral potential within the Tennant Creek to Mt Isa area (Schroder *et al.*, 2020). This presentation will explore the application of NAHS for investigating mineral potential of a region and present a workflow for establishing spatial or lithological baselines to evaluate hydrogeochemical anomalies.

The Georgina Basin is well known for its phosphate potential, with several >1 Mt deposits discovered in recent years such as Amaroo and Wonarah, however, the basin has been largely unmapped in terms of phosphate distribution under cover. This work focuses on a subset of 162 NAHS samples collected within two predominant aquifers of the Cambrian Georgina Basin (and time equivalents in the Wiso Basin). This focus restricts us to samples which experience a similar climate, recharge conditions, and aquifer compositions, reducing the hydrogeochemical variation that can mask intra-aquifer anomalies.

Elevated concentrations of P (used as a proxy for PO_4^{3-} and normalised to HCO_3^- or Cl^-) is observed in the groundwater on the eastern margin of the Georgina Basin. This region is known for Cambrian phosphorite deposits, with sampled bores proximal to a number of near-surface Georgina Basin phosphorite deposits. Additionally, several other subgroups within the Georgina Basin were identified with elevated P, corresponding to areas of greater cover and without known phosphorite deposits nearby.

Because the solubility of phosphate minerals depends on many factors – including groundwater physico-chemical parameters (pH, T etc.), groundwater chemical composition, and phosphate mineral composition (such as degree of CO_3^{2-} substitution) – a high (or low) P concentration is not a definitive indicator of the presence (or scarcity) of phosphates in the aquifer or recharge area. Thus, our data analysis focused on minor (i.e., F) and trace (i.e., U, V) elements commonly substituting in phosphate mineral structures or typically enriched in phosphorites, to evaluate these elements' relationships with P concentration as a tool for recognising dissolution of phosphate-bearing minerals. When normalised to Cl^- on log-log scatterplots, clear linear relationships between selected minor/trace elements and P concentrations become apparent in several of the identified subgroups that cannot be attributed to other water-rock interactions. This observation supports the implication that there is further undiscovered regions of the Georgina Basin with potential for hosting phosphorites.

Schroder, I. F., Caritat, P. de, Wallace, L., *et al.*, 2020. Northern Australia Hydrogeochemical Survey: Final Data Release and Hydrogeochemical Atlas for EFTF.

Mineral exploration in and through the critical zone

Application of indicator minerals in mineral exploration

Salama, Walid, Le Vaillant, Margaux, Schoneveld, Louise, Schlegel, Tobias, & Anand, Ravi

CSIRO Mineral Resources, Kensington, Perth, WA

Mineral exploration in weathered and covered terrains has given preference to geophysical and geochemical methods over mineralogical analyses. Airborne and ground geophysical surveys identify magnetic, electromagnetic and gravitational anomalies and allow the rapid delineation of exploration targets. However, the methods don't indicate whether a target is mineralised or not. Geochemical surveying, based on the analysis of soils, vegetation, termites or calcrete are well-established techniques for locating and identifying variable types of mineralisation. However, their application in areas of deep cover is limited. Indicator minerals, useful for exploration in the weathered and covered terranes, are those that (1) resist chemical weathering in weathered profiles, (2) undergo chemical changes to form secondary minerals in the weathering profile, (3) precipitate within organic-rich sediments during diagenesis, and (4) resist physical weathering during erosion, transportation and deposition.

Mineral explorers are interested in knowing the fertility of a mineral system, in minerals indicating the presence or absence of mineralisation and in vectors towards mineralisation. Within the CSIRO Discovery Program, research projects continue to focus on the identification and characterisation of indicator minerals. Examples of such studies are the potential use of trace element zoning patterns in pyroxenes as fertility indicators for magmatic Ni–Cu–Co–(PGE) deposits, white mica composition in hydrothermal alteration halo as a vector toward Au mineralisation, trace element composition of chromite and arsenide as exploration tools for Ni and Au deposits, and the REE composition of fluorite which reflect the fluid type involved in IOCG mineralisation.

In weathered terrains, rutile, gahnite and cassiterite with base metal sulfide inclusions are residually enriched in the leached and lateritic zone over the Scuddles massive sulfides forming Bi, Sb and Pb anomalies. The use of heavy indicator minerals is also a practical exploration tool in areas of Quaternary glacial till in Canada and Fennoscandia and in the Permian glacial diamictites in Australia. In Australia, the diamictites deposited immediately above the Permian unconformity are largely unweathered and contain detrital sulfides. The distance that indicator minerals disperse from the source depends mainly on the topography of the unconformity between the cover and the bedrock. In northeast Yilgarn Craton, the Permian diamictites were deposited on a rough topography and indicator minerals are expected to be derived from proximal source rocks. Iron, Cu, Zn, As, Ni and Co sulfides were identified at the base of the Permian cover above mafic–ultramafic rocks and used as vectors toward Au mineralisation at Agnew and Lancefield in Western Australia.

In summary, trace element contents of indicator minerals are used to vector toward mineralisation and the source fluids involved in its formation. Residual and supergene indicator minerals in weathered profiles can indicate mineralised bedrock underneath the cover. Detrital and diagenetic indicator minerals in transported cover are a potential vectoring tool for various types of mineral deposits.

Regional cover characterisation of the Central Gawler – clipping regolith–plant associations to better constrain geology and prospectivity

Petts, Anna¹, Noble, Ryan², & Reid, Nathan²

¹*Geological Survey of South Australia, Department for Energy and Mining, Adelaide, Australia;* ²*CSIRO, Mineral Resources, Discovery Program, Perth, WA*

Basement rocks and basin sediments seem far detached from surface features such as soils, landform features and plant assemblages. Regolith research in the last 50 years in Australia and abroad has proven many times that the types of assemblages of plants seen across a landscape is in fact well connected to the underlying geology, however, and therefore may be used to demarcate different regolith and landform features for mapping and for cover charactering. Also, these same plants will be linked to the geochemistry of the cover and underlying geological units through plant-nutrient cycling and groundwater uptake and therefore present a suitable, available and sometimes widespread sampling media for exploration geochemistry surveys and mining rehabilitation studies.

This concept has been tested in a regional survey across the Central Gawler Craton, of South Australia. The Geological Survey of South Australia (GSSA) has collected 212 native plant samples as part of a wider collaboration with CSIRO Minerals. The biogeochemical analysis will be used in conjunction with over 150 CSIRO UltraFine+ (UF) soil results to constrain complex plant-soil chemical relationship as well as test exploration geochemistry applications for plants as regional sampling media. Biogeochemical surveys are becoming increasingly popular first-pass techniques for mineral exploration companies and the GSSA has identified the need to provide relevant regional datasets to assist with identification, analysis and interpretation of plant major and trace element levels. This will enable better confidence when using similar techniques as well as provide improved data reporting standards.

The availability of select plant species (including Bladder Saltbush *Atriplex vesicaria*, Pearl bluebush *Maireana sedifolia*, Black bluebush *Maireana pyramidata*, Mulga *Acacia aneura* and Mallee) for sampling and mapping purposes has not been widely recorded analysed. Also the regolith-plant associations of the Central Gawler region, utilising current statewide and newly available regional regolith-landform map products, shows useful relationships and will contribute to accurate promotion of best biogeochemical practice in this region. The most widespread plant assemblage in the Central Gawler Craton UF survey area is chenopod shrubland, with the top two plant species sampled being Pearl Bluebush (47%) followed by Bladder Saltbush (39%) – based on data collected during fieldwork.

Airborne electromagnetics for regional cover thickness mapping

Roach, Ian C., Wong, Sebastian, Ley-Cooper, Yusen, Brodie, Ross C., & Wilford, John

Geoscience Australia, GPO Box 378, Canberra ACT 2601, Australia

Geoscience Australia applies airborne electromagnetic (AEM) surveying to map regional geology and the architecture of mineral, energy and groundwater systems. Most recently, Geoscience Australia has engaged in very large area, very wide line spacing AEM data acquisition as part of the AusAEM program. In this, we acquire ~20 km line spacing data to broadly characterise the electrical conductivity of wide swathes of Australia in the world's largest (by area) AEM surveys.

Results from regional AEM surveys demonstrate the efficacy of the AEM method for mapping regolith and sedimentary cover over basement rocks, as well as for mapping large hydrostratigraphic systems. Data commonly also reveal conductivity features associated with potential ore host rocks and alteration systems. Airborne electromagnetic data are especially effective when interpreted in combination with other datasets including boreholes and potential fields. The AusAEM data are being combined with other data to develop 3D cover thickness and stratigraphic surface models either by manual interpretation or by using a machine learning approach.

As an example, in the Paterson Province of Western Australia, 2 km and 6 km spaced AEM lines and industry boreholes were used to develop a 3D depth to Proterozoic basement model. This, together with newer, more detailed AEM acquired by explorers, is now being used by industry as a first-pass risk reduction dataset for locating new Au, Cu and base metal resources in Neoproterozoic rocks of the Anketell Shelf under the Canning Basin. The AEM data have also been used in this area to map groundwater systems within the palaeodrainage systems, which can be used to model the sources and sinks of potash-bearing brines.

Soil geochemistry imaging gold prospectivity in the South West Terrane of Yilgarn Craton, Western Australia

De Souza Kovacs, Nadir, & Lu, Yongjun

Geological Survey of Western Australia, Perth

The South West Terrane of the Yilgarn Craton is prospective for a number of important commodities such as gold, nickel and lithium, however, the region remains poorly geologically understood. The South West Terrane is one of the focus areas of the Geological Survey of Western Australia's Accelerated Geoscience Program, 2020–21. This terrane is often associated with farming land, viticulture and grain growing, nevertheless it also hosts several world-class mineral deposits such as those at Boddington (Au–Cu), Greenbushes (Li–Ta) and Ravensthorpe (Ni). The geology of these deposits known from open-file statutory exploration reporting (stored in the Geological Surveys MINEDEX and WAMEX databases) provide a wealth of knowledge, that when combined with other publicly available geoscientific data compiled by the

survey, data are providing new insights into the geological and mineralisation histories of the terrane.

The gold assay results from 84157 soil samples covering the South West Terrane were extracted from WAMEX and were spatially visualized and evaluated. The distribution of high-grade gold samples (0.53 to 1.37 ppm) cluster along several regional faults, including the Newdegate, Darkan, Manjimup, Tenterden, Koolanooka, Hyden, Pingaring, Dumbleyung Faults and other prominent but unnamed regional faults. By contrast, low-grade gold (<0.001 ppm) samples occur in areas without major faults. The regolith-landform map shows that the southern part of the Lockhart Paleovalley follows the strike of the Newdegate Fault and coincident structures on regional-scale magnetic images. The spatial distribution indicates that gold in soils is genetically linked to the regional faults, which are likely to have acted as fluid pathways during gold mineralization.

One particularly interesting feature is that high-grade gold in soils clustering along the north-trending Newdegate Fault also coincide with the isotopic boundary imaged by whole-rock neodymium isotopes of felsic igneous rocks. This isotopic boundary also correlates well with gravity and magnetic anomaly zones and has been suggested to be the terrane boundary between the South West Terrane and the Youanmi Terrane (Lu *et al.*, 2021; AESC). This correlation is supported by the spatial distribution of gold deposits including Griffins Find, Tampia and Edna May, which are located on or close to this isotopic boundary. It indicates that gold anomalism in soils might be potentially useful for ranking deep crustal structures.

The spatial distribution of gold in soils in the South West Terrane is closely associated with regional faults. Through integration with other data, such as isotopic mapping or regional geophysical compilations, the regional scale gold in soil datasets can assist in prioritising the most prospective areas for exploration.

Understanding the cover in the Gawler Craton, South Australia: combining landscape variability, linear structures, and regolith mapping to assist mineral exploration

González-Álvarez, Ignacio^{1,2}, Krapf, Carmen³, Kelka, Uli¹, Martínez, Cericia¹, Albretch, Thomas⁴, Ibrahimi, Tania¹, Pawley, Mark³, Irvine, Jonathan³, Petts, Anna³, & Klump, Jens¹

¹CSIRO, Mineral Resources, Discovery Program, Perth, WA, Australia; ²University of Western Australia, Centre for Exploration Targeting, Perth, WA, Australia; ³Geological Survey of South Australia, Department for Energy and Mining, Adelaide, Australia; ⁴Department of Mechanical and Aerospace Engineering, Monash University, Melbourne, Australia

Successful mineral exploration in Australia has sharply decreased over the past few decades. With >75% of South Australia's land surface covered by transported regolith material, exploration is a significant challenge. Regolith integrates the expression of geology, climate, groundwater, topography, and geomorphological processes. Landscape domains and their stratigraphy record the 4D architecture of the overburden and capture the relationship of the surface and cover to the

underlying basement geology. To understand regolith composition and distribution, as well as the landscape variability, surface mapping can potentially be a cost-effective and powerful exploration tool. To date, this has involved traditional field-mapping techniques accompanied by remote sensing and geophysical data.

The Archean basement in South Australia has numerous major structures that are expressed at surface as lineaments, landforms and possibly as boundaries between different landscape domains. Several studies on neotectonic features highlighted the potential significance of these structures as geochemical pipelines that connect basement rocks with the surface.

In this study, we integrate regolith mapping, linear surface features, and landscape variability in the central Gawler Craton, South Australia. We aim to enhance the understanding of how basement structures such as faults and shear zones may affect present-day landscapes and surface lineaments. We also explore if the integration of landscape variability, surface lineaments, basement features and regolith domains, can provide sample areas that may efficiently record geochemical footprints from underlying basement rocks.

This project tests the conceptual variability of landscape domains across the study area and offers insights into possible geochemical dispersion pathways from depth through cover to surface.